CODING PROPERTIES IN INVERTEBRATE SENSORY SYSTEMS

EDITED BY: Sylvia Anton, Anders Garm and Berthold G. Hedwig
PUBLISHED IN: Frontiers in Physiology

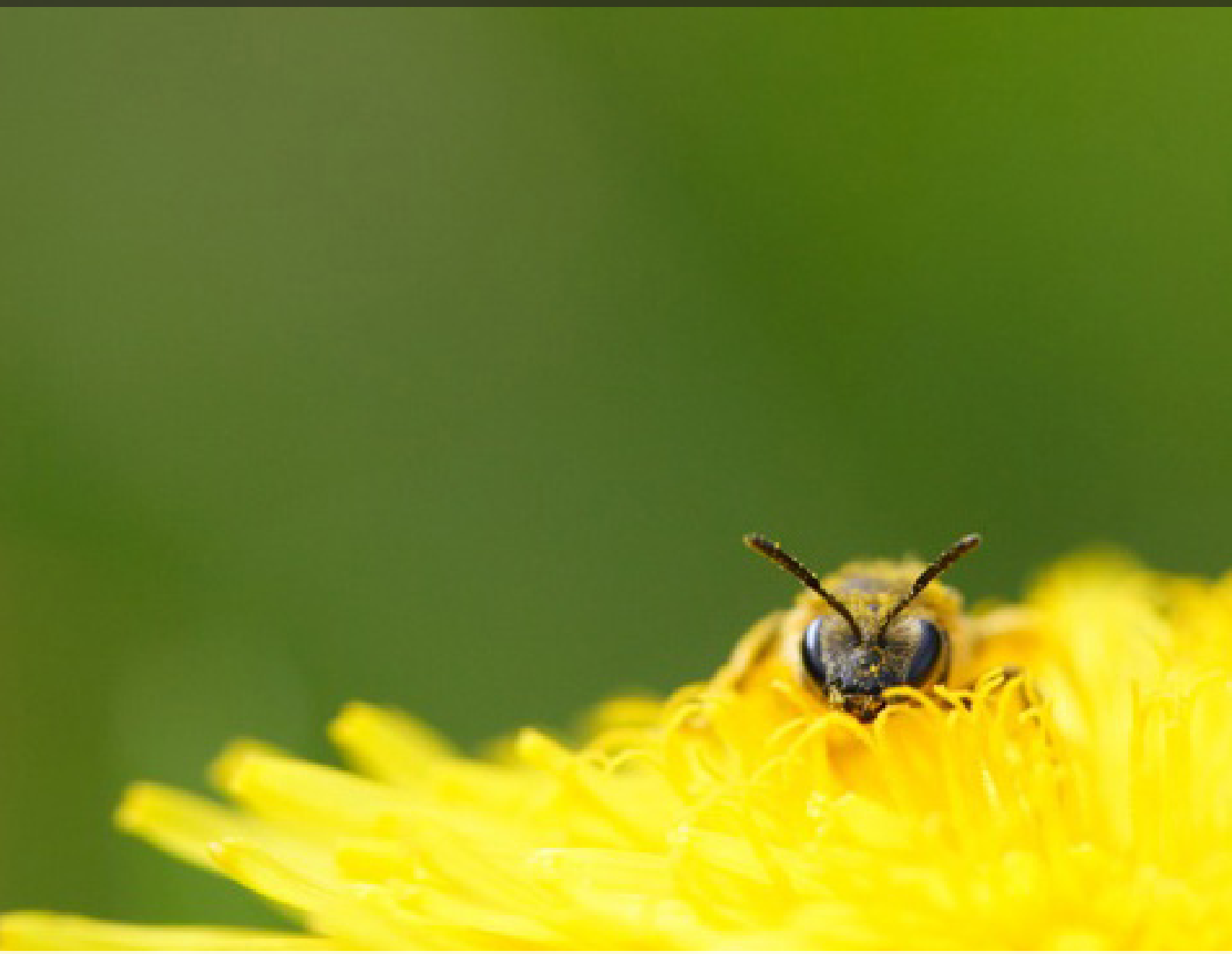

frontiers Research Topics

frontiers

ISSN 1664-8714
ISBN 978-2-88945-106-7
DOI 10.3389/978-2-88945-106-7

About Frontiers

Frontiers is more than just an open-access publisher of scholarly articles: it is a pioneering approach to the world of academia, radically improving the way scholarly research is managed. The grand vision of Frontiers is a world where all people have an equal opportunity to seek, share and generate knowledge. Frontiers provides immediate and permanent online open access to all its publications, but this alone is not enough to realize our grand goals.

Frontiers Journal Series

The Frontiers Journal Series is a multi-tier and interdisciplinary set of open-access, online journals, promising a paradigm shift from the current review, selection and dissemination processes in academic publishing. All Frontiers journals are driven by researchers for researchers; therefore, they constitute a service to the scholarly community. At the same time, the Frontiers Journal Series operates on a revolutionary invention, the tiered publishing system, initially addressing specific communities of scholars, and gradually climbing up to broader public understanding, thus serving the interests of the lay society, too.

Dedication to Quality

Each Frontiers article is a landmark of the highest quality, thanks to genuinely collaborative interactions between authors and review editors, who include some of the world's best academicians. Research must be certified by peers before entering a stream of knowledge that may eventually reach the public - and shape society; therefore, Frontiers only applies the most rigorous and unbiased reviews.
Frontiers revolutionizes research publishing by freely delivering the most outstanding research, evaluated with no bias from both the academic and social point of view.
By applying the most advanced information technologies, Frontiers is catapulting scholarly publishing into a new generation.

What are Frontiers Research Topics?

Frontiers Research Topics are very popular trademarks of the Frontiers Journals Series: they are collections of at least ten articles, all centered on a particular subject. With their unique mix of varied contributions from Original Research to Review Articles, Frontiers Research Topics unify the most influential researchers, the latest key findings and historical advances in a hot research area! Find out more on how to host your own Frontiers Research Topic or contribute to one as an author by contacting the Frontiers Editorial Office: **researchtopics@frontiersin.org**

CODING PROPERTIES IN INVERTEBRATE SENSORY SYSTEMS

Topic Editors:
Sylvia Anton, INRA-Agrocampus Ouest-Rennes 1 University, France
Anders Garm, University of Copenhagen, Denmark
Berthold G. Hedwig, University of Cambridge, UK

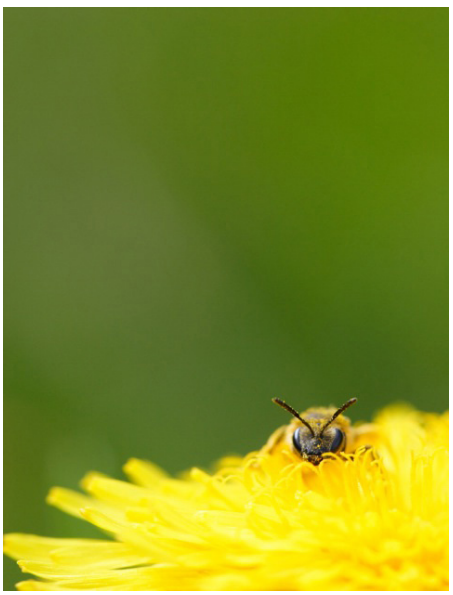

Foraging honey bee exposed to olfactory, visual and mechanosensory cues while visiting a flower (Copyright Antoine Abrieux)

Animals rely on sensory input from their environment for survival and reproduction. Depending on the importance of a signal for a given species, accuracy of sensory coding might vary from pure detection up to precise coding of intensity, quality and temporal features of the signal. Highly sophisticated sense organs and related central nervous sensory pathways can be of utmost importance for animals in a complex environment and when using advanced communication systems. In sensory systems different anatomical and physiological features have evolved to optimally encode behaviourally relevant signals at the level of sense organs and central processing. The wide range of organizational complexity, in combination with their relatively simple and accessible nervous systems, makes invertebrates excellent models to study general sensory coding principles. The contributions to this e-book illustrate on one hand particular features of specific sensory systems, and on the other hand indicate not only common features of sensory coding across invertebrate phyla, but also similar processing principles of complex stimuli between different sensory modalities. The chapters show that the extraction of behaviourally relevant signals from all environmental stimuli, as well as the detection of low intensity signals and the analysis of temporal features can be similar across sensory modalities, including olfaction, vision, mechanoreception, and heat perception.

Citation: Anton, S., Garm, A., Hedwig, B. G., eds. (2017). Coding Properties in Invertebrate Sensory Systems. Lausanne: Frontiers Media. doi: 10.3389/978-2-88945-106-7

Table of Contents

frontiers in Physiology

EDITORIAL
published: 10 January 2017
doi: 10.3389/fphys.2016.00688

Editorial: Coding Properties in Invertebrate Sensory Systems

Anders Garm[1], *Berthold G. Hedwig*[2] *and Sylvia Anton*[3]*

[1] *Marine Biological Section, Department of Biology, University of Copenhagen, Copenhagen, Denmark,* [2] *Department of Zoology, University of Cambridge, Cambridge, UK,* [3] *Neuroéthologie-RCIM, Institut National de la Recherche Agronomique-Université d'Angers, Beaucouzé, France*

Keywords: sensory signal extraction, temporal coding, neuro-ethology, olfaction, vision, mechanoreception, heat detection

Editorial on the Research Topic

Coding Properties in Invertebrate Sensory Systems

Animals adapt their behavior according to the environment and their specific needs in a given situation. In order to do so in an appropriate way, they need to detect, analyze, and code the relevant sensory cues. This task is handled by sensory systems and their associated parts in the central nervous system. With few exceptions, the amount of information present in the environment and thus in principle available to sensory systems, is close to infinite. It is impossible and not desirable to encode and process all the information. Therefore, the first and most important task of any sensory system is to filter and select only the essential information—information, which potentially will improve the fitness of the bearer. Differences in sensory information processing occur between animals of different organization levels. Sensory coding in invertebrates and vertebrates relies on multiple stages of processing to extract information relevant to the survival of the individual. The wide range of organizational complexity, in combination with their relatively simple and accessible nervous systems, makes invertebrates excellent models to study general sensory coding principles. In addition, many invertebrate species are of socio-economic importance as pollinators, crop pests, or as disease vectors or elicitors. Therefore, understanding their communication systems and sensory biology is important for the development of insect management or plant protection strategies.

In the present Research Topic in Frontiers in Invertebrate Physiology we present a series of original papers and reviews illustrating the current directions of this field. The different contributions indicate not only common features of sensory coding across invertebrate phyla, but also similar processing features of complex stimuli between different sensory modalities. This is interesting, because the characteristics of the different types of sensory stimuli are inherently different, and require different types of detectors and potentially different ways of integration in nervous systems. The majority of the papers treat the coding of olfactory information with its multidimensionality, which was supposed to function under different operational constraints than other sensory modalities, and has been a field of high research activity over the past years. However, the articles of this Research Topic show that the extraction of behaviourally relevant signals from all incoming environmental stimuli, as well as the detection of low intensity signals and the analysis of temporal features can be similar across different sensory modalities, including olfaction, vision, mechanosensation, and heat perception.

The papers treating the coding of olfactory information include work on temporal processing and signal extraction in complex environments, and its behavioral outcomes as a function of physiological state, as well as potential applications of the findings to control harmful insects.

OPEN ACCESS

Edited by:
Xanthe Vafopoulou, York University, Canada

Reviewed by:
Wolfgang Rössler, University of Würzburg, Germany
Andrew Dacks, West Virginia University, USA

***Correspondence:**
Sylvia Anton
sylvia.anton@inra.fr

Specialty section:
This article was submitted to Invertebrate Physiology, a section of the journal Frontiers in Physiology

Received: *01 December 2016*
Accepted: *23 December 2016*
Published: *10 January 2017*

Citation:
Garm A, Hedwig BG and Anton S (2017) Editorial: Coding Properties in Invertebrate Sensory Systems. Front. Physiol. 7:688. doi: 10.3389/fphys.2016.00688

One of the major challenges for olfactory systems is to extract behaviourally relevant information from highly complex and dynamic signals. Hellwig and Tichy propose in a perspective article that olfactory receptor neurons in cockroaches, which signal sudden changes in the concentration of olfactory stimuli as compared to a constant background stimulation, might be used for tracking behaviourally relevant odor plumes. The fact that OFF neurons code better for falling concentration changes than ON neurons suggests, that they play a role in alerting a loss of an odor plume. The paper by Brill et al. shows that parallel processing of olfactory information via two antennal lobe output tracts in the honey bee comprises coincident activation patterns of projection neurons within and across parallel tracts. The results from simultaneous recordings of olfactory projection neurons in both tracts support the role of spike timing in coding olfactory information (temporal code). Another physiological property of the insect antennal lobe, which is potentially important in temporal coding of insect olfaction, is the afterhyperpolarization-phase of the projection neurons. Lei et al. show in their paper, through pharmacological experiments and modeling, some of the control mechanisms of the afterhyperpolarization phase, and confirm the involvement in temporally resetting the system for further odor-specific responses.

Another challenge for olfactory systems is the extraction of a highly relevant signal from an odor background, such as detection of moth sex pheromones in a rich background of plant volatiles. Whereas the common belief was that sex pheromone and plant odors are processed and encoded by two distinct pathways in the insect brain, Rouyar et al. show for the first time that a structurally dissimilar plant-derived odorant is able to activate the pheromone specific pathway and thus might influence pheromone processing. Badeke et al. demonstrate, however, that even though high concentrations of single plant odors can influence female tracking in the male noctuid moth *Heliothis virescens,* sex pheromone-guided behavior is not influenced by plant odors at natural concentrations.

Sensory processing and integration of different stimuli in higher brain centers ultimately leads to adequate motor output. The review by Namiki and Kanzaki addresses the function of the lateral accessory lobe in the insect brain, which is at the interface between multimodal sensory input and locomotor output. This brain area is believed to be an important output region of the brain for the control of locomotion. In a comparative approach, structure and function of lateral accessory lobe neurons in different insect species are discussed.

Because olfaction is widely used by many insect species, it has become also an important model for sensory ecology and is exploited to develop alternative methods to control harmful insects. Reisenman and Riffell review the neurobiology of host plant selection in the moth *Manduca sexta* in an ecological context. Reisenman et al. evaluate how results from the field of neuroethology can be used to elucidate how harmful insects, be it crop pests or insects transmitting diseases, trace the odors of their host plants or animal hosts. They summarize the current knowledge on the use of semiochemicals, and how results from applied studies improve our knowledge on detection and processing of olfactory signals.

The tracking of host plants sometimes changes between different life stages, and Wu et al. show that one of the odorant binding proteins (OBPs), binding to attractant semiochemicals, is upregulated in mated females of a pest fruit fly. This upregulation possibly accounts for an increased attraction to their host plant. The role of OBPs in chemosensory detection and coding is also addressed by Sun et al. Although OBPs are often found to be necessary for odor discrimination, the authors show that the function of homologous OBPs in bugs can change between species to binding of non-volatiles in the gustatory system.

The visual system basically counts the number of photons from a certain direction during a defined time period, and potentially also measures their energy (color) and their polarity. The challenges here are to extract behaviourally relevant information under limiting environmental conditions. Two papers of this Research Topic deal with coding in the visual system under low light conditions. Two strategies to enhance vision in darkness are through temporal and/or spatial summation of the photons, which will increase sensitivity on the cost of temporal and spatial resolution, respectively. Nocturnal bees enhance sensitivity through optical specializations but not through temporal summation, which would probably hamper their flight control at night (Baird et al.). Garm et al. examine vision in a nocturnal box jellyfish, which enhances sensitivity by having both a low temporal and spatial resolution. This visual system seems to be optimized to code only one highly specific information, the direction of bioluminescent flashes indicating high prey densities.

Two papers in this Research Topic deal with different forms of heat perception. The molecular actors of heat perception have been very little investigated so far. Junca and Sandoz tested the association of a heat shock with aversive olfactory conditioning of the sting extension response, and show that the TRP channel HsTRPA may be involved in heat detection in honeybees. Infrared (IR) sensing has been considered as either a specialized type of vision or thermoreception. In Jewel beetles, Schneider et al. propose a theory, which would allow bimodal photomechanic sensilla housed in IR organs to increase sensitivity to weak IR signals during flight, by making use of muscular energy coupled out of the flight motor. This mechanism could explain the capacity of these beetles to detect wood fires over distances of more than 100 km, allowing to find the resources for larvae developing in fire-killed trees.

Two contributions deal with different aspects of processing and coding of mechanosensory information. Hedwig reviews how a series of filters at different levels of the auditory pathway is used to process and code the male song by the female cricket. Carrier frequency, pulse duration and the pulse pattern are serially processed and finally tune the female phonotactic behavior to the characteristic properties of the male calling song. The other paper examines touch sensing in leeches. Kretzberg et al. show that touch- and pressure-sensitive cells in the skin, converging on common interneurons, both use quantitative and temporal elements to encode the precise location of tactile stimuli in order to elicit minimal, but precise avoiding behavior.

Altogether the work presented in this Research Topic shows the advantage of studying coding of behaviourally active sensory stimuli in invertebrates of different phyla as it reveals common features in the processing of complex sensory signals and different modalities.

AUTHOR CONTRIBUTIONS

All authors listed, have made substantial, direct and intellectual contribution to the work, and approved it for publication.

Conflict of Interest Statement: The authors declare that the research was conducted in the absence of any commercial or financial relationships that could be construed as a potential conflict of interest.

frontiers in Physiology

PERSPECTIVE
published: 01 March 2016
doi: 10.3389/fphys.2016.00063

Rising Background Odor Concentration Reduces Sensitivity of ON and OFF Olfactory Receptor Neurons for Changes in Concentration

*Maria Hellwig and Harald Tichy**

Department of Neurobiology, Faculty of Life Sciences, University of Vienna, Vienna, Austria

The ON and OFF ORNs on cockroach antennae optimize the detection and transfer of information about concentration increments and decrements by providing excitatory responses for both. It follows that the antagonism of the responses facilitates instantaneous evaluations of the odor plume to help the insect make tracking decisions by signaling "higher concentration than background" and "lower concentration than background". Here we analyzed the effect of the background concentration level of the odor of lemon oil on the responses of the ON and OFF ORNs to jumps and drops of that odor, respectively. Raising the background level decreases both the ON-ORN's response to concentration jumps and the OFF-ORN's response to concentration drops. Impulse frequency of the ON ORN is high when the concentration jump is large, but for a given jump, frequency tends to be higher when the background level is low. Conversely, impulse frequency of the OFF cell is high at large concentration drops, but higher still when the background level is low. Analyses of this double dependence revealed that the activity of both types of ORNs is raised more by increasing the change in concentration than by decreasing the background concentration by the same amount. This effect is greater in the OFF ORN than in the ON ORN, indicating a bias for falling concentrations. Given equal change in concentration, concentration drops evoke stronger responses in the OFF ORN than concentrations jumps in the ON ORN. This suggests that the OFF responses are used as alert information for accurately tracking.

Keywords: odor concentration coding, ON and OFF responses, asymmetric sensitivities, effect of background concentration, gain of responses

OPEN ACCESS

Edited by:
Sylvia Anton,
Institut National de la Recherche Agronomique, France

Reviewed by:
Silke Sachse,
Max Planck Institute for Chemical Ecology, Germany
Martin F. Brill,
Howard Hughes Medical Institute, USA

****Correspondence:***
Harald Tichy
harald.tichy@univie.ac.at

Specialty section:
This article was submitted to Invertebrate Physiology, a section of the journal Frontiers in Physiology

Received: *26 November 2015*
Accepted: *11 February 2016*
Published: *01 March 2016*

Citation:
Hellwig M and Tichy H (2016) Rising Background Odor Concentration Reduces Sensitivity of ON and OFF Olfactory Receptor Neurons for Changes in Concentration. Front. Physiol. 7:63. doi: 10.3389/fphys.2016.00063

INTRODUCTION

An insect tracking a turbulent odor plume to its source perceives the odor signal as a sequence of pulses of high concentration interspersed with the surrounding medium containing gaps of low or zero concentration (Moore and Atema, 1991; Zimmer-Faust et al., 1995; Vickers, 2000). Key features pertaining to the location of an odor source are the timing of concentration jumps and concentration drops as well as the level of odor concentration between these changes, referred to here as background concentration. The effect of the background value on the responses of ORNs

to superimposed concentration pulses was first investigated in the lobster (Borroni and Atema, 1988) and more recently described in the housefly (Kelling et al., 2002). Those experiments tested single synthetic compounds, and the analysis was limited to the concentration jump at the onset of the pulse. While with increasing background level the response of lobster ORNs to concentration jumps gradually diminished, the response of housefly ORNs was enhanced to small jumps and reduced to large jumps. The response enhancement was interpreted as the result of depolarization or diminution of the resting membrane potential due to the presence of the background odor. The response reduction was attributed to competition between stimulus and background molecules for membrane receptors (Borroni and Atema, 1988; Kelling et al., 2002).

Based on these studies, two statements can be made. The first is that ORNs are detectors for the relative rather than the absolute concentration. The second is that the higher the background level, the weaker the responses to rapidly increasing odor concentration. An animal tracking a turbulent odor plume will therefore perceive the same concentration jump progressively weaker the closer it approaches the source. However, weak responses signify less sensory evidence than strong responses. Such constraint has been described in the neural circuits implementing the binary decision about the direction of a motion stimulus, which determines saccadic eye movement in the rhesus monkey (Roitman and Shadlen, 2002; Bogacz et al., 2009). The speed of decision is associated with integrator neurons in pre-motor brain areas which gradually increase their discharge rate by accumulating the inputs of sensory neurons over time. With decreasing difference between the baseline activity of these integrator neurons and the response threshold of non-integrator neurons, decisions are prone to errors. Simply sampling of information sequentially facilitates accurate detection and decision-making under uncertain conditions (Heitz and Schall, 2012; Heitz, 2014). However, sampling as little as possible will save time and effort (Drugowitsch and Pouget, 2012). In view of the situation of the olfactory system, it would be a possible economical alternative to create a separate system of ORNs with a different coding mechanism. Such a strategy of sensory coding and information processing seems to be realized in the ON and OFF ORNs on the cockroach's antennae: they produce opposite responses to changes in odor concentration (Hinterwirth et al., 2004; Tichy et al., 2005; Burgstaller and Tichy, 2011, 2012). The discharge rate of the ON ORNs is increased by raising odor concentration and decreased by lowering it, and the discharge rate of the OFF ORNs is increased by lowering odor concentration and decreased by raising it. During moment-to-moment contact with the odor signal, the activity of the ON ORN increases when the odor concentration jumps to a higher value when contact is made with an odor pulse. Conversely, the activity of the OFF ORN increases when odor concentration drops to a lower value after encountering an odor gap. A recent study reveals a bias for concentration drops, suggesting a bias for detecting the loss of contact with the odor signal (Burgstaller and Tichy, 2011).

In this study, we quantified the simultaneous dependence of the ON and OFF ORNs on the background level and the superimposed concentration jumps or drops of the same odor, respectively. We used the complex odor of lemon oil emanating from citrus fruits as odor stimulus and we determined the gain of response for the background concentration and for the jumps or drops in concentration. In particular we asked: (i) what is the difference between the two gain values in each type of ORN, and (ii) what is the difference between the two types of ORNs? A falling-concentration bias results in overestimation of concentration drops relative to jumps. In terms of accuracy, a drop would be perceived by the cockroach as being larger than it actually is. We examined whether the disparity between the ON and OFF responses to equal concentration jumps and drops depends on the amplitude of the change and the background level. A disparity for larger concentration changes at higher background levels would be an advantage for receiving information about large jumps at the lateral edges of the plume than small jumps within the odor plume. Asymmetry in the neural coding of concentration jumps and drops is at the root of understanding what characteristics of the odor signal are important for tracking a turbulent odor plume.

MATERIALS AND METHODS

An adult male cockroach was anesthetized with CO_2 and fixed on a Perspex holder with strips of Parafilm wrapped around the holder. The antenna was fastened with adhesive tape and dental cement on a Perspex stage projecting from the holder. Action potentials were recorded extracellularly with electrolytically sharpened tungsten electrodes. One electrode was placed lengthwise into the tip of the antenna and the other was inserted into the base of the sensillum. The recorded signals were amplified (NPI, SEC-05X) and filtered (0.1–3 kHz), passed through a CED 1401plus (Cambridge Electronic Design, Cambridge, UK; 12 bit, 10 kHz) interface connected to a PC for on-line recording. Spikes were detected and classified off-line using commercial software (spike2, version 6). Impulse frequency (imp/s) is the per-second impulse count for fixed periods of 0.2 s.

The gain of response is defined as the ratio of output to input and given by the slopes of the regression planes that approximate the relation between impulse frequency, background concentration and concentration change ($F = y_0 + aC + b\Delta C$; where F is the impulse frequency and y_0 the height of the regression plane, a is the background concentration and b the concentration change). The R^2 coefficient of determination indicates how well the regression plane approximates the real data points.

The odor of lemon oil (Art. 5213.1; Carl Roth GmbH + Co.KG; Karlsruhe, D) was applied by an air stream merging at 2 m/s from a glass tube 7 mm in diameter. An air dilution olfactometer was used to control odor concentration (Burgstaller and Tichy, 2011). Compressed clean air was divided into two streams and their flow rates were controlled by passing them through mass flow meters. Each stream was led through a 25-l tank; the first tank contained the liquid odorant and the second tank was empty. After flowing out from the tank, each air stream was passed through an electrical proportional valve (Kolvenbach KG, KWS 3/4) and

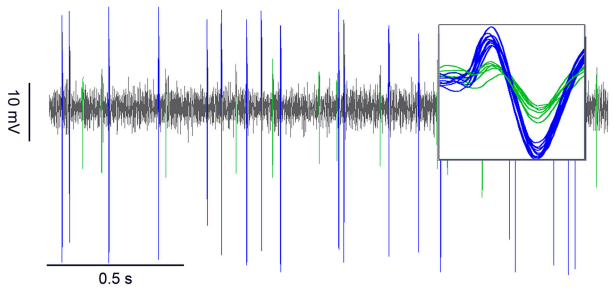

FIGURE 1 | Simultaneously recorded discharge rates of a pair of ON and OFF ORNs from a single sensillum exposed to the odor of lemon oil at constant concentration of 20%. The ON ORN (green) displayed smaller impulse amplitudes than the OFF ORN (blue). *Inset* The waveform sensitive template mechanism (spike2) was used to identify and sort action potentials from ON and OFF ORNs.

an air flow sensor (AMW 3000; Honeywell). The two streams were then combined. In order to hold the total flow rate of the combined air stream constant, the phase of the control voltages of the proportional vales was shifted by 180°. Instantaneous odor concentration was determined by the flow rate ratio of the odor-saturated air to clean air and indicated by the percentage of saturated air in the air steam playing on the antenna. The amplitude of the concentration change was described by the difference between the background level and concentration of the odor pulse. A positive value ($+\Delta C$) indicates a concentration jump and a negative value ($-\Delta$) a concentration drop. After adaptation for 30 s to a constant background level, there followed a series of concentration changes to various higher or lower concentrations, each of which was maintained for 1 s before the return to the background value. The steps were presented every 30 s. This paradigm enabled testing at least four series of concentration jumps or concentration drops from different background levels on each of 13 ON and OFF ORNs, respectively.

RESULTS

The ON and OFF ORNs occur together in short, slightly curved hair-like sensilla on the distal margin of each antennal segment. Both ORNs were encountered simultaneously by penetrating the recording electrode gently into the sensillum base. The recordings usually contained the impulses from both ORNs, which could be easily separated by their amplitudes (**Figure 1**). The impulse trains were sorted into the responses of the ON and OFF ORNs by using a waveform-sensitive template matching mechanism (**Figure 1**, inset).

The experiment shown in **Figure 2** illustrates some of the parameters determining the responses of the ON and OFF ORNs. The experiment involved four different background levels of the lemon oil odor (0, 40, 60, and 100%) as well as two 60% jumps and two 60% drops in the concentration of that odor. The ON ORN responded to the concentration jumps with a phasic increase in impulse frequency followed by a decline during the 1-s pulse period. The frequency of the ON ORN was higher at the low (**Figure 2A**) than at the high background level (**Figure 2B**). The OFF ORN fell silent for the pulse period. The impulse frequency of the OFF ORN, in contrast, rose rapidly at an odor gap, followed by a decline during the 1-s gap period. Similarly to the ON ORN, the frequency of the OFF ORN was higher at the low (**Figure 2D**) than at the high level (**Figure 2C**). The ON ORN ceased discharging during the gap period.

To quantify the effect of the background on the ON-ORN's response to concentration jumps, four concentration series were tested at different levels in the 0–40% range. Frequency increased with the amplitude of the jump, but more rapidly the lower the background. As the equal-frequency line in **Figure 3A** illustrates, it takes a 60% concentration jump to elicit 10 imp/s at 40% level, but only a 13% jump at 0% level.

The effect of the background on the OFF-ORN's response to concentration drops was described by testing four concentration series at different levels between 40 and 100%. The data obtained resembled those from the ON ORN, inasmuch as frequency of the OFF ORN increased with the amplitude of the drops. The increase in frequency was more rapid the lower the background. This relationship is exemplified in **Figure 3B**. The equal-frequency line indicates that it takes a 64% concentration drop to elicit 30 imp/s at 100% level, but only a 26% drop at 40% level.

Multiple regressions ($F = y_0 + aC + b\Delta C$; where F is the impulse frequency and y_0 the height of the regression plane) were calculated to determine the simultaneous effect of the background concentration (a–slope) and the jump or drop in concentration (b–slope) on the frequency of the ON and OFF ORN, respectively. The slopes demonstrate the three properties that characterize both types of ORNs: (*i*) the sign of the a–slope is negative for the ON and OFF ORNs—that is, a decrease in the background raises the frequency of both ORNs to concentration changes; (*ii*) the sign of the b–slope is positive for the ON ORN and negative for the OFF ORN—that is, an increase in concentration jumps raises the frequency of the ON ORNs and an increase in concentration drops raises the frequency of the OFF ORNs, and (*iii*) the slopes are steeper for the OFF than for the ON ORN—that is, changes in both the background and in the size of the change have stronger effects on the frequency of the OFF than on that of the ON ORN with due consideration of the sign.

In all 13 examined ON ORNs and 13 OFF ORNs the coefficients of determination of the multiple regressions show a strong linear relationship between impulse frequency, the background level and the concentration change ($R^2 > 0.95$ in **Figures 3C,D**). The slopes of the regression planes emphasize the gain of responses for the background concentration (a–slope) and the concentration change (b–slope). In the ON ORN, the mean gain for jumps was 0.2 imp/s per Δ%, and the mean gain for the background was −0.1 imp/s per %. Frequency can be raised more by increasing the jump by yet another percent than by decreasing the background by 1%. Thus, an increase of 1 imp/s can be elicited either by a 5% increase in the concentration jump or by a 10% decrease in the background.

In the OFF ORN, the mean gain for concentration drops was 0.4 imp/s per $-\Delta$% and the mean gain for the background was −0.2 imp/s per %. Frequency can be raised more by increasing the concentration drop by still another percent than by changing

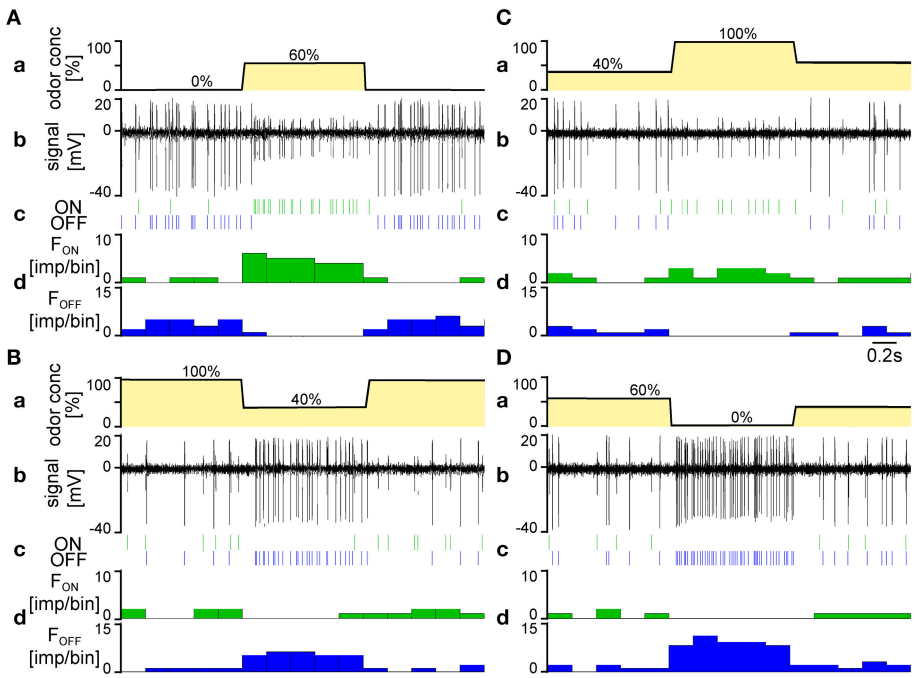

FIGURE 2 | Simultaneously recorded responses of an ON ORN and an OFF ORN during the final 1-s of a 30-s presentation of different constant background concentration of the lemon oil odor, followed by a 1-s presentation of higher or lower odor concentrations and a return to the initial background value. (A,B) Concentration jumps (+60Δ%) from 0 to 40% background level, respectively. **(C,D)** Concentration drops (−60Δ%) from 100 to 60% background level, respectively. *a* time course of odor concentration. *b* extracellular recorded action potentials; the OFF ORN displayed larger impulse amplitudes than the ON ORN. *c* action potentials represented as raster plots. *d* responses ORNs represented as time histograms (bin width, 0.2 s).

the background by 1%. Thus, an increase of 1 imp/s can be elicited either by a 2.5% increase in the concentration drop or by a 5% decrease in the background. The sensitivity of the OFF ORNs for concentration changes superimposed on the background level is twice as high as that of the ON ORNs.

DISCUSSION

ON and OFF ORNs responding antagonistically to increments and decrements of the same odor have been described so far only in the cockroach (Hinterwirth et al., 2004; Tichy et al., 2005; Burgstaller and Tichy, 2011, 2012). This may be due to technical reasons. First, the odor stimulus used by the cited authors was provided by means of an air dilution olfactometer. This set-up allowed continuous presentation of odor-loaded air and enabled conditioning the OFF ORN to high concentration levels before dropping to low or zero concentration values. Second, a natural odor was used for stimulation instead of single compounds. We do not know, however, which compounds contained in the odor of lemon oil are responsible for eliciting the antagonistic responses.

In the lobster (Borroni and Atema, 1988) and the housefly (Kelling et al., 2002), increasing the background level reduced the responsiveness of ORNs to concentration jumps (Kelling et al., 2002). A similar effect has been observed for the ON ORN of the cockroach (Burgstaller and Tichy, 2011). Furthermore, the OFF ORNs fit well with this observation because the response to concentration drops decreases with increasing background. However, the responses of the ON and OFF ORNs are not mirror images. The responses of the latter span a larger frequency range than the former, which means that the OFF ORNs respond with higher frequencies to concentration drops than the ON ORN to equivalent jumps (Burgstaller and Tichy, 2011).

In this study we determined the gain of responses of the ON and OFF ORNs for background concentration and superimposed changes of the same odor. In the OFF ORNs, the gain values are twice as high as in the ON ORNs. Thus, falling concentration holds greater salience than rising concentration. Furthermore, with increasing background, the disparity between rising and falling values becomes grater. Notwithstanding this difference, the relationship between the gain values for background concentration and for concentration changes are similar in the ON and OFF ORNs: the value for changes in both types of ORNs is twice as high as the value for the background concentrations.

The stronger gain for changes vs. background reflects the significance of the dynamic aspect of the stimulus. Since the dominance of the gain for concentration change increases with the amplitude of the change and decreases with falling background level, the magnitude of response of an ORN cannot be predicted by simply adding background to change values. This conclusion was drawn from the regression functions in **Figures 3C,D**. By direct comparisons, an ON ORN will respond to an end-value of 80% attained by a 60% jump from a 20%

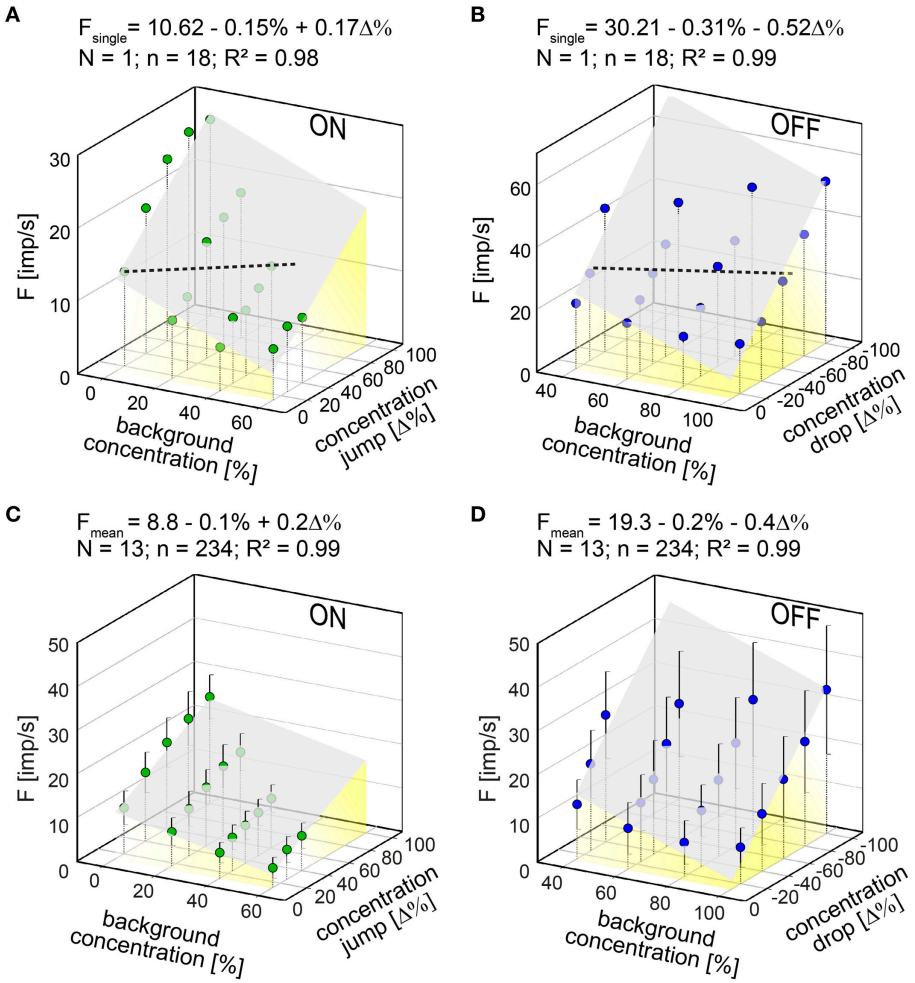

FIGURE 3 | (A,B) Responses of a single ON ORN **(A)** and a single OFF ORN **(B)** plotted as a function of background concentration and jumps or drops in odor concentration, respectively. Dotted horizontal lines: equal frequency line at 10 imp/s for the ON ORN and 30 imp/s for the OFF ORN. **(C,D)** Mean responses of 13 ON ORN **(C)** and 13 OFF ORN **(D)** plotted as a function of background concentration and jumps or drops in odor concentration, respectively. Error bars represent SEM. Multiple regressions which utilize 3-dimensional planes ($F = y_0 + aC + b\Delta C$; where F is the impulse frequency, and y_0 the height of the regression plane) were calculated to determine the gain for background concentration (a slope) and the concentration change (b slope) on the response. Note that the sign of the concentration axis in **(A,C)** is oriented in different direction than in **(B,D)**. N number of ORNs, n number of points used to calculate regression plane **(A,B)** or mean responses **(C,D)**, R^2 coefficient of determination.

background with 18.8 imp/s, but to the same end-value of 80% attained by a 20% jump from an 80% background with 4.8 imp/. An OFF ORN will respond to an end-value of 20% attained by an 60% drop from a 80% background with 27.3 imp/, but to the same end-value of 20% attained by a 20% drop from a 40% background with 19.3 imp/s.

Another conclusion from **Figures 3C,D** is that the background concentration set limits to the dynamic responses of both types of ORN. With increasing background concentration, equal increments in jumps or equal decrements in drops do not cause equal increments in the rate of discharge of the ON and OFF ORNs. Instead, the increments in the discharge rate of both ORNs become progressively smaller. This compressed scaling has some advantages. An ON ORN whose sensitivity to concentration jumps is best at low backgrounds, and decreases as the background from which the jump to be detected increases, provides strong sensory evidence when the cockroach encounters an odor plume. At low backgrounds it will be important to have available a wider dynamic frequency range in order to differentiate between small-amplitude jumps. The same small differences at high backgrounds could be trivial. Conversely, an OFF ORN whose sensitivity to concentration drops is best at low backgrounds, and decreases as the background from which the drop to be detected increases, provides strong sensory evidence at large concentration decreases, when the cockroach approaches the lateral edge of the plume or even leaves the plume. At low backgrounds it will be important to have available a wider dynamic frequency range in order to distinguish between small-amplitude drops. The same small differences at high backgrounds may be less important. Nonetheless, small-amplitude differences

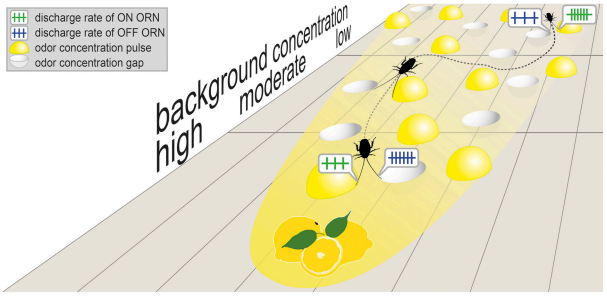

FIGURE 4 | Schematic representation of turbulent plume features proposed as potentially relevant to plume tracking, including odor pulses and odor gaps separated by the background odor concentration that gradually increases with decreasing distance to the source (lemon fruits). A cockroach walking toward the source will perceive the spatial distribution of odor concentration as temporal concentration change. By using simultaneous or successive sampling strategies, concentration differences determined by bilateral comparison of the responses of ON and OFF ORNs on both antennae will guide the cockroach to move forward or return to the previous position. Response bias for equal-amplitude concentration drops relative to jumps enhances detection of low concentration change with rising background level. Therefore, the OFF responses are used as alert information for accurately tracking motion.

may bear a vital message too. Therefore, there must be some mechanism to secure the information conveyed by responses which become progressively weaker and prevent loss of contact with the odor signal. Such a mechanism seems to be realized by the bias of the antagonistically responding ON and OFF ORNs.

Classical concepts of odor plume tracking use spatial and temporal sampling to explain the mechanisms underlying initiation of a response and controlling the orientation of an organism to an odor source (Vickers, 2000; Willis, 2008). Irrespectively of whether bilateral or sequential comparison of odor concentrations is used for orientation, a cockroach following a background concentration gradient should balance between the responses of the ON and OFF ORNs. Clearly, strong responses of an ON ORN indicate the direction toward the odor source. Weak responses will also do so, provided that a change in the insect's course produces a stronger response in the OFF ORN. Strong responses of the OFF ORN indicate that concentration is falling. From a perceptual perspective, falling-concentration bias results in an overestimation of drops relative to jumps. In terms of accuracy, drops are not only perceived by the cockroach as being stronger than they actually are, they also specify the location of plume edges to be closer than they are. In this view, the cockroach uses the responses of the ON ORNs for distance information and the responses of the ON ORNs as alert or warning information. From the cockroach's perspective, tendencies in concentration changes rather than exact values of concentration change suffice for responding appropriately to odor pulses and odor gaps and provide timely arrival at the odor source (**Figure 4**).

The discharge of ORNs to concentration jumps superimposed on different background levels have recently been described in the fruit fly. In the experiments with OR59b ORNs (Kim et al., 2011), odor stimulation consisted of a step-like sequence of 3 different concentrations of acetone. Each concentration was presented for 2 s and created the background for the next step. After an initial phasic increase to the concentration step, the ORNs displayed relatively constant rates of discharge over the 2-s stimulation period. The peak discharge to equal-amplitude acetone steps gradually decreased with increasing background level. Therefore, ORNs are unable to measure accurately the concentration change. In a study of ab3A ORNs it was shown that the peak discharge rates to 500 ms puffs of methyl butyrate, ethyl acetate and ethyl butyrate decreased with increasing background concentration (Martelli et al., 2013). However, when the discharge rates to different concentration puffs were normalized by the peak responses to the same odorant, the diminishing effect of the increasing background concentration disappeared. Moreover, the dynamics of the normalized responses did not depend on the dynamics of the brief concentration puff, even if the concentration of the odor puff was varied. This independence of the normalized dynamic responses on the dynamics of the odor puff was interpreted as being a prerequisite for ab3A ORNs to use the dynamics of their responses for mediating characteristics of the odor stimulus such as the presence of different compound in the mixture.

The inability of ORNs in insects and crustaceans to accurately measure the magnitude of concentration change is not a matter of variance of the discharge rates. It is rather the concession of their additional dependence on the background concentration. Since the ON and OFF ORNs adapt relatively slowly and only partially to the background level, the discharge rates signal relative concentration changes. ORNs adapting minimally or not at all may be capable of signaling the actual level of odor concentration. Tonic systems are well suited to convey information about unchanging concentrations, but would fail to signal concentration changes because their ORNs remain excited after the change has ceased. Such maintained discharge would distort temporal information.

AUTHOR CONTRIBUTIONS

MH and HT conceived and designed experiments, MH performed experiments and analyzed data; MH and HT interpreted results and wrote the paper; MH prepared figures; HT edited and revised manuscript.

ACKNOWLEDGMENTS

This work was supported by Austrian Science Fund Grant P 21777-B17.

REFERENCES

Bogacz, R., Wagenmakers, E.-J., Forstmann, B. U., and Nieuwenhuis, S. (2009). The neural basis of the speed-accuracy tradeoff. *Trends Neurosci.* 33, 10–16. doi: 10.1016/j.tins.2009.09.002

Borroni, P. F., and Atema, J. (1988). Adaptation in chemoreceptor cells. I. Self-adapting backgrounds determine threshold and cause parallel shift of response function. *J. Comp. Physiol. A.* 164, 64–74.

Burgstaller, M., and Tichy, H. (2011). Functional asymmetries in cockroach ON and OFF olfactory receptor neurons. *Eur. J. Neurophysiol.* 105, 834–845. doi: 10.1152/jn.00785.2010

Burgstaller, M., and Tichy, H. (2012). Adaptation as a mechanism for gain control in cockroach ON and OFF olfactory receptor neurons. *Eur. J. Neurosci.* 35, 519–526. doi: 10.1111/j.1460-9568.2012.07989.x

Drugowitsch, J., and Pouget, A. (2012). Probabilistic vs. non-probabilistic approaches to the neurobiology of perceptual decision-making. *Curr. Opin. Neurosci.* 22, 963–969. doi: 10.1016/j.conb.2012.07.007

Heitz, R. P. (2014). The speed-accuracy tradeoff: history, physiology, methodology, and behavior. *Front. Neurosci.* 8:150. doi: 10.3389/fnins.2014.00150

Heitz, R. P., and Schall, J. D. (2012). Neural mechanisms of speed-accuracy trade-off. *Neuron* 76, 616–628. doi: 10.1016/j.neuron.2012.08.030

Hinterwirth, A., Zeiner, R., and Tichy, H. (2004). Olfactory receptor cells on the cockroach antennae: responses to the directions and rate of change in food odour concentration. *Eur. J. Neurosci.* 19, 3389–3392. doi: 10.1111/j.0953-816X.2004.03386.x

Kelling, F. J., Ialenti, F., and Den Otter, C. J. (2002). Background odour induces adaptation and sensitization of olfactory receptors in the antennae of houseflies. *Med. Vet. Entomol.* 16, 161–169. doi: 10.1046/j.1365-2915.2002.00359.x

Kim, A. J., Lazar, A. A., and Slutskiy, Y. B. (2011). System identification of Drosophila olfactory sensory neurons. *J. Comput. Neurosci.* 30, 143–161. doi: 10.1007/s10827-010-0265-0

Martelli, C., Carlson, J. R., and Emonet, T. (2013). Intensity invariant dynamics and odor-specific latencies in olfactory receptor neuron response. *J. Neurosci.* 33, 6285–6297. doi: 10.1523/JNEUROSCI.0426-12.2013

Moore, P. A., and Atema, J. (1991). Spatial information in the three-dimensional fine structure of an aquatic odor plume. *Biol. Bull.* 181, 408–418. doi: 10.2307/1542361

Roitman, J. D., and Shadlen, M. N. (2002). Responses of neurons in the lateral intraprietal area during a combined visual discrimination reaction time task. *J. Neurosci.* 2, 33–42. doi: 10.3410/f.1002839.152957

Tichy, H., Hinterwirth, A., and Gingl, E. (2005). Olfactory receptors on the cockroach antenna signal odour ON and odour OFF by excitation. *Eur. J. Neurosci.* 22, 3147–3160. doi: 10.1111/j.1460-9568.2005.04501.x

Vickers, N. J. (2000). Mechanisms of animal navigation in odor plumes. *Biol. Bull.* 198, 203–212. doi: 10.2307/1542524

Willis, M. A. (2008). Chemical plume tracking behavior in animals and mobile robots. *Navigation* 55, 127–135. doi: 10.1002/j.2161-4296.2008.tb00423.x

Zimmer-Faust, R. K., Finelli, C. M., Pentcheff, N. D., and Wethey, D. S. (1995). Odor plumes and animal navigation in turbulent water flow: a field study. *Biol. Bull.* 188, 111–116. doi: 10.2307/1542075

Conflict of Interest Statement: The authors declare that the research was conducted in the absence of any commercial or financial relationships that could be construed as a potential conflict of interest.

frontiers in Physiology

ORIGINAL RESEARCH
published: 28 July 2015
doi: 10.3389/fphys.2015.00208

It takes two—coincidence coding within the dual olfactory pathway of the honeybee

Martin F. Brill[*†‡], *Anneke Meyer*[‡] *and Wolfgang Rössler*[*]

Behavioral Physiology and Sociobiology, Biozentrum, University of Würzburg, Würzburg, Germany

OPEN ACCESS

Edited by:
Sylvia Anton, Institut National de la Recherche Agronomique, France

Reviewed by:
Dominique Martinez, LORIA, France
Hong Lei, University of Arizona, USA

***Correspondence:**
Martin F. Brill, Cold Spring Harbor Laboratory, 1 Bungtown Road, Cold Spring Harbor, New York, NY 11724, USA
mbrill@cshl.edu;
Wolfgang Rössler, Behavioral Physiology and Sociobiology, Biozentrum, University of Würzburg, Am Hubland, 97074 Würzburg, Germany
roessler@biozentrum.uni-wuerzburg.de

†Present Address:
Martin F. Brill, Cold Spring Harbor Laboratory, Cold Spring Harbor, New York, USA

‡These authors have contributed equally to this work.

Specialty section:
This article was submitted to Invertebrate Physiology, a section of the journal Frontiers in Physiology

Received: *05 May 2015*
Accepted: *10 July 2015*
Published: *28 July 2015*

Citation:
Brill MF, Meyer A and Rössler W (2015) It takes two—coincidence coding within the dual olfactory pathway of the honeybee. Front. Physiol. 6:208. doi: 10.3389/fphys.2015.00208

To rapidly process biologically relevant stimuli, sensory systems have developed a broad variety of coding mechanisms like parallel processing and coincidence detection. Parallel processing (e.g., in the visual system), increases both computational capacity and processing speed by simultaneously coding different aspects of the same stimulus. Coincidence detection is an efficient way to integrate information from different sources. Coincidence has been shown to promote associative learning and memory or stimulus feature detection (e.g., in auditory delay lines). Within the dual olfactory pathway of the honeybee both of these mechanisms might be implemented by uniglomerular projection neurons (PNs) that transfer information from the primary olfactory centers, the antennal lobe (AL), to a multimodal integration center, the mushroom body (MB). PNs from anatomically distinct tracts respond to the same stimulus space, but have different physiological properties, characteristics that are prerequisites for parallel processing of different stimulus aspects. However, the PN pathways also display mirror-imaged like anatomical trajectories that resemble neuronal coincidence detectors as known from auditory delay lines. To investigate temporal processing of olfactory information, we recorded PN odor responses simultaneously from both tracts and measured coincident activity of PNs within and between tracts. Our results show that coincidence levels are different within each of the two tracts. Coincidence also occurs between tracts, but to a minor extent compared to coincidence within tracts. Taken together our findings support the relevance of spike timing in coding of olfactory information (temporal code).

Keywords: olfaction, insect, coincidence, multi-electrode-recording, antennal lobe, mushroom body

Introduction

Animals process sensory input rapidly in order to behave adequately in their natural environment. In order to manage this challenging task, neural systems have developed a broad variety of mechanisms. Among these, parallel processing and coincidence detection appear to be almost universally useful throughout modalities and animal taxa. Parallel processing codes different aspects of the same stimulus along separate pathways. This way it increases both computational capacity and overall processing speed (Nassi and Callaway, 2009). In contrast, coincidence detection is an efficient way to integrate information from different sources and form association between these, to eventually promote learning (Hebb, 1949; Bliss and Lømo, 1973; Heisenberg, 2003) or stimulus feature detection (Jeffress, 1948; Hassenstein and Reichardt, 1951). In the honeybee olfactory system either one of these mechanisms could potentially be realized by

projection neurons (PNs) that transfer information from the primary olfactory neuropile, the antennal lobe (AL) to the multimodal integration center, the mushroom body (MB).

Parallel processing is most prominently known from the vertebrate visual system (Livingstone and Hubel, 1988), where color and shape of a stimulus are analyzed in parallel with a possible motion of the stimulus. Similar distribution of stimulus features on different pathways has been described in the auditory (Rauschecker and Scott, 2009) and the somatosensory systems (Gasser and Erlanger, 1929; Reed et al., 2005). In insects, parallel pathways were described both in vision (Ribi and Scheel, 1981; Fischbach and Dittrich, 1989; Strausfeld et al., 2006; Paulk et al., 2008, 2009) and audition (Helversen and Helversen, 1995). More recently, advances have been made to investigate the role of parallel processing in vertebrate olfaction. These works indicate a division of olfactory bulb output into parallel channels of olfactory information mediated by mitral and tufted cells (Fukunaga et al., 2012; Igarashi et al., 2012; Payton et al., 2012). The two output tract responses differ in their phase to the respiratory oscillation cycle and in detail, tufted cell phase is unperturbed in response to purely excitatory odorants, whereas mitral cell phase is advanced in a graded, stimulus-dependent manner (Fukunaga et al., 2012). However, the existence of a similar spike timing mechanism in insects remains uncertain (Galizia and Rössler, 2010; Sandoz, 2011).

In favor of potential roles of parallel processing and spike timing, recent anatomical work in the honeybee (Kirschner et al., 2006) and other Hymenoptera (Rössler and Zube, 2011) has shown a dual tract system that pervades from the sensory input stage at the antenna to higher level processing in the MB (**Figure 1**). Olfactory receptor neurons (ORNs) provide mainly redundant input (Carcaud et al., 2012; Galizia et al., 2012) to the two prominent subsystems of the AL: the ventral and dorsal hemilobe (Kirschner et al., 2006). The ventral hemilobe comprises about 88 spheroidal neuropiles called glomeruli, and gives rise to the lateral antennal lobe tract (l-ALT, new tract nomenclature after Ito et al., 2014) containing about 510 PNs. The dorsal hemilobe consists of about 77 glomeruli which send out about 410 PNs via the medial ALT (m-ALT) (Abel et al., 2001; Kirschner et al., 2006; Rybak, 2012) PNs from the two separate tracts respond to a similar stimulus space. For instance there is no apparent specialization for either floral odors or pheromones. Nevertheless, PNs of l-and m-ALT differ in physiological properties, like response latency, odor specificity and response dynamics (Müller et al., 2002; Krofczik et al., 2008; Nawrot, 2012; Brill et al., 2013; Carcaud et al., 2015), implying different functions. Both the anatomical layout and the physiological distinction make l-ALT and m-ALT candidates well suited for parallel processing of different stimulus aspects.

Having said that, the dual olfactory pathway also displays mirror-imaged like trajectories which could likewise implement coincidence detection. The m-ALT first innervates the MB and finalizes in the lateral horn (LH), known for innate odor responses (Gupta and Stopfer, 2012; Roussel et al., 2014; Strutz et al., 2014). The l-ALT runs exactly opposite, projects first to the LH and ends in the MB. This counter-rotating neuronal architecture thus produces a substantial temporal delay between

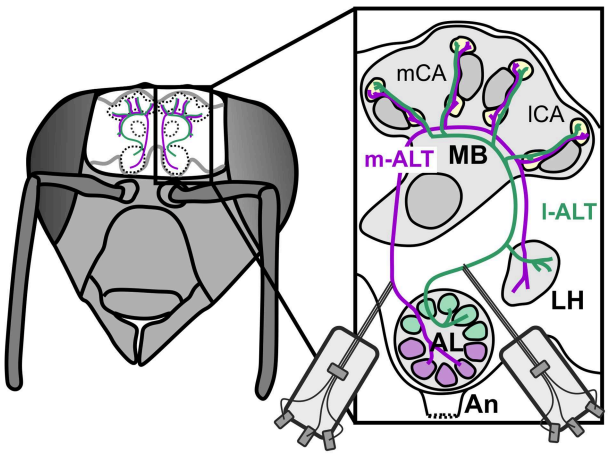

FIGURE 1 | Schematic overview of the dual olfactory pathway and its connectivity with upstream neurons into the mushroom body of the honeybee brain. Drawing of a bee's head with the brain exposed and arrangement of the dual olfactory pathway in both brain hemispheres (purple: m-ALT, green l-ALT). Magnification of one hemisphere illustrating the innervation pattern of the m-ALT (purple) and l-ALT (green). Uniglomerular PNs of the dorsal AL hemilobe first innervate the MB lip and basal ring (Br) and finalize their innervation in the lateral horn (LH), giving rise to the m-ALT. The l-ALT emerges from ventral AL glomeruli runs to the LH and later innervates the olfactory MB input sites. An, Antennal nerve; AL, Antennal Lobe; vL, vertical Lobe; mCa and lCa, medial and lateral Calyx; Co, collar.

the two tracts depending on which downstream neuron is activated in the MB. For instance, is a medial KC activated the l-ALT PNs will need a comparably longer time to reach that cell in contrast to the m-ALT. In comparison, is a more distal lateral KC activated the l-ALT will have reached the neuron earlier than the m-ALT (see Figure 4 in Rössler and Brill, 2013). This counter-rotating layout resembles detectors of coincidence for stimulus features such as delay lines known from the vertebrate auditory system, where sound localization is achieved by coincident input from neurons of both ears (Jeffress, 1948; Joris et al., 1998). A structural similarity that naturally has inspired speculations about a similar function in odor processing (Galizia and Rössler, 2010; Rössler and Brill, 2013).

Principle neurons of the MB, the Kenyon cells (KCs) receive highly convergent PN input (Caron et al., 2013; Gruntman and Turner, 2013). Moreover, PNs sent diverging output onto several KCs (Yasuyama et al., 2002; Leiss et al., 2009; Groh et al., 2012). Combined, both connectivity patterns lead to a temporally and spatially sparse KC population code (locust, e.g., Perez-Orive et al., 2002; honeybee, e.g., Szyszka et al., 2005; moth, e.g., Ito et al., 2008; fly, e.g., Turner et al., 2008). This code includes that individual KCs are activated only by highly coincident input from many PNs (Gruntman and Turner, 2013). Accordingly, synchronous activation of PNs has repeatedly been shown to be an important strategy for detection and learning of odors (e.g., Christensen et al., 2003; Martin et al., 2013; Riffell et al., 2013). Moreover, about 25% of PNs show odor specific latencies, which are shorter for l-ALT PNs than for m-ALT PNs (Krofczik et al., 2008; Brill et al., 2013). This latency code, in combination with the counter-rotating inputs, may lead to odor

specific activation of different KC ensembles due to step-by-step coincidence between l-ALT and m-ALT PNs (Rössler and Brill, 2013).

While our knowledge about PN-tracts supports both, parallel processing and coincident delay lines, the two mechanisms put different constraints on the system. A prerequisite for an olfactory delay line would be that the information carried by the different tracts is combined. Accordingly, activity of individual neurons responding at the same time to the same stimulus should be highly coincident between the different tracts (see **Figure 4**, Rössler and Brill, 2013). And might also incorporate coincidental activity within tracts, which has been shown in other insects (Stopfer et al., 1997). Instead, parallel processing does not require the combination of inputs from different tracts, but might rather integrate information carried by neurons within the same tract.

To investigate how olfactory information is combined along the two tracts, we recorded odor responses of simultaneously active PNs and measured coincident activity within and between different PN subpopulations. Our results illustrate that coincidence is differently pronounced within each of the two tracts. Coincidence between tracts is present but does not outplay coincidence within the individual tracts. Taken together the findings strengthen the idea of parallel processing and the relevance of spike timing in coding of olfactory information in the olfactory system of the honeybee.

Material and Methods

Animal Preparation

Foragers of the European honeybee *Apis mellifera carnica* (Pollmann) were caught from a feeder filled with saccharose solution (Apiinvert, 50%) and harnessed and movement restrained according to standard routines. The brain was exposed by opening the head capsule. Glands, trachea and neurolemma were removed carefully. A reference electrode (chloride Ag-wire, 150 μm, AGT05100 WPI, Germany) was placed between the ocelli, a second electrode monitored proboscis movements by recording muscle activity. Tetrodes to record from the olfactory tracts were inserted outside the AL where l- and m-tract run in separate loops to the MB. Following electrode placement the brain was either covered with two component low viscosity silicone (Kwik-Sil, WPI, USA) or left untreated (Brill et al., 2014).

Odor Stimulation

Odor and control stimuli were delivered by a custom build olfactometer under constant stream of humidified and charcoal filtered clean air. Stimulation airstream was removed by an exhaust. The mean delay between stimulus expulsion from the olfactometer and the arrival at the animals antenna was 99 ms as estimated from Electro Antennogram (EAG, c.p below). Each animal was stimulated with the full set of 12 different odors in randomized order. The set comprised key elements of general plant odors (limonene, hexanal, 1-pentanol, 1-octanol, 2-octanone), natural plant odors (clove oil, orange oil, citral), and pheromones (geranylic acid, isoamylacetate, 1-hexanol, 2-heptanone) (**Table 1**). All stimuli were diluted 1:100 in mineral oil, applied in pulses of 500 ms and response measured repeatedly in 20 trials each. Mineral oil and pure air were applied as control stimuli.

For further details of stimulus application and data acquisition refer to Brill et al. (2013).

Electrophysiology

Multi-unit Recordings

Electrodes consisted of three micro-wires made of copper (polyurethane-coated, 15 μm diameter, Elektrisola, Germany) and glued together with melted dental wax (Brill et al., 2014). One of these electrode shanks was placed to record from the l-, a second from the m-ALT, both of which were connected to a switchable headstage (SH16, Tucker-Davis-Technologies, USA). A silver-wire reference electrode was placed between the ocelli. Signals were fed into a custom designed connection module (INT-03M, NPI, Germany) and transferred to a custom-made amplifier system consisting of 16 custom designed low noise differential amplifier modules (DPA-2FL, NPI, Germany). To control for a potential influence of muscle activity on multi-unit recordings, the activity of the proboscis muscle, M17 was monitored. Recordings from all channels were 5 k differentially amplified to the reference electrode, band-pass filtered (300–8000 Hz), and shank-wise differentiated, that is: potentials recorded from each micro-wire within one shank were pairwise subtracted from each other to eliminate interfering signals (e.g., muscle activity, electrical hum). Subsequently data was stored for offline analysis. Sampling rate was 31,250 Hz at 16 bit resolution on each channel.

Electro-Antennogram (EAG) Recordings

EAGs were measured from the antenna ipsilateral to multi-unit recordings in five bees tested with the complete odor panel. Low-resistance (<0.5 M Ohm) borosilicate electrodes (1B100F-3,WPI,USA) were pulled with a horizontal filament puller (DMZ Universal Puller, Germany) and filled with 0.5 M KCL-solution. A tungsten electrode below the scapus of the same antenna served as reference. Signals were amplified first by an intracellular headstage (Gain 10, Model 1600, A-M-Systems, USA) and subsequently by the same custom build amplifier as the multi-unit recordings (Gain 100) and band-pass filtered (0.1–100 Hz). Prior to analysis recordings were smoothed offline with an algorithm provided by Spike2 (time constant 32 μs). Smoothed EAGs were averaged over repeated trials. Response onset was defined as the relative maximum preceding the steepest negative slope of the potential drop which demarcated an odor response (Meyer and Galizia, 2012).

Spike Sorting

Spikes were sorted using established routines implemented in commercial software (Spike2, v7.4, Cambridge Electronic Design, England). Each channel was preprocessed by smoothing with a FIR-filter (time constant 80 μs) and DC removal (time constant 3.2 ms). Signals recorded from all three channels were used for spike- sorting, unless one of the channels had to be excluded due to insufficient signal-to-noise (SNR) ratio, in which case the remaining two channels were used. We performed semi-automated template-matched spike sorting with an amplitude

TABLE 1 | Odor stimuli used in the experiments.

Odor	Abbreviation	CAS number	Odor type	Biological significance
Spontaneous	spont			
Control air	ctr			
Citral	Cit	5392-40-5	terpen	floral and pheromone
Geranyl acid	Ger	459-80-3	terpen	floral and pheromone
Isoamylacetate	IAA	123-92-2	esther	pheromone
(+) Limonene	Lim	5989-27-5	terpen	floral
Clove oil	Clv	8000-34-8	natural blends	floral
Orange oil	Orng	8008-57-9	natural blends	floral
Hexanal	6-al	66-25-1	aldehyde	floral
1-Pentanol	1-5-ol	71-41-0	alcohol	floral
1-Hexanol	1-6-ol	111-27-3	alcohol	pheromone
1-Octanol	1-8-ol	111-87-5	alcohol	pheromone
2-Heptanone	2-7-ne	110-43-0	ketone	pheromone
2-Octanone	2-8-ne	111-13-7	ketone	floral

Odor abbreviations, the chemical abstract service number (CAS), chemical group of odorants and their biological significance for the honeybee are given. The used trials per odor are 20, number of recorded bees is 12, and the number of single PNs from the l-ALT is 54 and m-ALT 65, respectively.

threshold set to the mean spontaneous activity ±3 standard deviations. Spontaneous activity was recorded over at least 1 min of activity prior to odor-test trials. Templates were formatted in semi-automated fashion in time windows from −0.4 to 0.8 ms around each spike's peak. Units were clustered and sorted by applying the Spike2 built-in dialogs based on PCA and additional feature extraction. For more detailed description refer to previous publications based on the same dataset (Brill et al., 2013).

Data Analyses

After spike sorting individual units were judged with respect to responsiveness and reliability (see paragraph "identification of odor-response profiles in PNs" in Materials and Methods in Brill et al., 2013). We wanted to know if coincident activity is a mechanism that is potentially used by honey bee PNs to combine the odor information that is carried in their spike trains. To isolate odor related activity, we excluded trials without odor-responses as well as those that were corrupted by artifacts (e.g., hum from the mains, muscular activity etc.) We analyzed coincidence within each animal between simultaneously active PN units using cross correlation. From each of the 12 animals we extracted eight units on average. Altogether 102 units were included in the analyses. Based on electrode placement these units could be identified as either l-ALT (49 units, on average 4 per animal, minimum 2, maximum 6) or m-ALT PNs (53 units, on average 4 per animal, minimum 3, maximum 6) such that coincidence within and between tracts could be identified. Analysis routines were custom written in Matlab (2010a; The MathWorks, Inc.).

Detection of Simultaneous Odor Responses Across Units

Our objective was to analyze simultaneous odor evoked activity in small ensembles of PNs. For this purpose we compared the activity between units within one animal and selected pairs that were responsive to the same stimulus. In brief, we detected for each individual unit which odors were effective in evoking responses. Subsequently we matched each unit's response spectrum to those of the other units in the same recording. This way we ended up with pairs of l-ALT, m-ALT (within tract) and l-m-ALT (between tracts) units that were simultaneously active.

In order to achieve the response detection for each unit, we employed a fully automated routine of five successive steps: (1) To detect responses from averaged trials we re-sampled to bins of 1 ms and averaged trials of repeated presentation of the same stimulus. (2) We estimated the rate function of this averaged trial by convolution with a symmetric smoothing filter (Savitzky and Golay, 1964, polynomial order 0, 301 ms width, Welch-windowed). (3) Baseline firing rate was estimated over an interval of 600 ms before stimulus onset. (4) A response was defined as a deviation from baseline ±2 standard deviations with duration of at least 50 ms in a time window from 0 to 600 ms post stimulus. Deviations above threshold correspond to excitations–deviations below baseline correspond to inhibitions. (5) If a response was indicated in the average trial, we repeated the procedure on the level of the underlying single trial spike trains. (6) If a response occurred in at least half of all single trials, we accepted the odor as a potent stimulus for the given unit. Setting the threshold for responsiveness to 25 or 75% did not significantly change the quantitative results (Brill et al., 2013). Trials without a response as well as inhibited responses (<1%) were excluded from further analysis.

Control stimuli are expected to evoke no (air) or only weak (mineral oil) responses. In order to monitor baseline coincident activity we included all control trials into the analysis irrespective of whether or not a response was detected.

Cross Correlation

We detected coinciding spikes between different units by estimating the cross-correlation function for simultaneously recorded spike trains carrying odor information.

After selecting those trials in which a given pair of neurons was active simultaneously, we estimated cross-correlation using the observed elapsed times from one spike in the first unit's train to all spikes in the second unit's train in time window υ. In repeating this procedure for every spike, we obtained for each unit pair the set of all possible differences between spike times for all simultaneous trains in the cross-correlation window $-\upsilon$ to $+\upsilon$.

Next we estimated the density function of this cross-correlogram using a Gaussian kernel with a fixed bandwidth of 25 ms ($\sigma = 5$ ms). This procedure is equivalent to classical cross-correlation but avoids *a-priori* determination of fixed bin sizes with equal weight. The density function reflects the probability of simultaneous occurring events at a given time. It is normalized to the total number of events within the underlying data.

At our chosen bandwidth of 25 ms, 68% of all integrated events fall within the central 10 ms of the kernel. A timing that resemble the integration time at a possible post synapse of a KC receiving input from both of the correlated units (PNs) as was shown by modeling approaches in honeybee, locust, and moth (Perez-Orive et al., 2004; Cassenaer and Laurent, 2007; Finelli et al., 2008; Martin et al., 2013).

To account for stimulus induced and random coincidence of spiking events, we subtracted a shuffle predictor from the density function of the raw cross-correlogram. The shuffle predictor was obtained by the same routine as explained above but from non-simultaneous trains of the same neuron pair. Bootstrap resampling from this non-simultaneous cross-correlation yielded a 95% confidence interval. Coincident activity was accepted as significant when the density function of the raw cross-correlogram exceeded the upper bound of the 95% confidence interval of the shuffle predictor.

To quantify coincident activity within a pair of units, we calculated the *Coincidence Index (CI)*. *CI* is the summed Area from periods of significant coincident activity [$t(D_{95\%})$] under the density function of the shuffle corrected cross correlogram ($D_{cross} - D_{shuffle}$).

$$\boldsymbol{CI} = ((\boldsymbol{D_{cross}} > \boldsymbol{D}_{95\%}) - \boldsymbol{D_{shuffle}})$$

CI reflects the significant coincident activity exceeding the expected coincidence.

Statistical Testing

We hypothesized that coincident activity is differently distributed between tracts. To test this assumption we needed a non-parametric procedure suitable for samples of unequal size but dependent data. In using a bootstrap hypothesis test all these requirements were met. We proceeded as follows: Each time we tested two out of the three possible datasets (coincidence strength of l-tract, m-tract and lm-tract, respectively) against each other. From each set, we drew 500 bootstrap resamples, the same size as the smaller of the two underlying dataset. A bootstrap resample is defined as a random sample drawn with replacement from the empirical distribution. We calculated the population median for each of these resamples, which left us with two equal sized samples. Given that these two samples distribute around equal medians, subtracting one sample from the other should yield a distribution around zero. A hypothesis (H0) that can easily be tested by calculating the probability of the observed median and comparing it to a predefined level of significance (alpha). We set our alpha to 0.05 but corrected for multiple testing using the Bonferroni procedure, yielding a final alpha of 0.016, if all three possible combinations (l-tract:m-tract; l-tract:lm-tracst; m-tract:lm-tracts) were tested.

Correlation Matrix

We wanted to test if strong odor responses go hand in hand with high coincident activity. For this purpose, we correlated the tuning to an odor with coincident activity. We extracted odor tuning as follows: We measured response magnitude of each of our 102 units to every of the 12 odors used for stimulation. Response strength was given by the peak rate of the evoked firing rate change. Next, we ranked response strength within each unit. We thus obtained for every odor 102 position ranks between 1 and 12. We extracted the matching coincidence activity as follows: For each unit we summed its strength of coincident activity with all other simultaneously recorded units that responded to a given odor. Like for the odor tuning, we ranked coincidence strength to each of the 12 stimuli within every unit. This left us with another vector of 102 position ranks for each odor. The relationship between these two population vectors describing odor response strength and coincident activity was assessed by correlation. High correlation is associated with similar ranks in both tuning vectors, low correlation with very different ranks.

Results

When different neurons fire action potentials in close succession their activity is detected as coincident by a shared postsynaptic target. Coincident activity can be used by the neural system to combine information carried by individual neurons. We wanted to know whether this mechanism may be utilized by the medial and lateral AL tracts of the honeybees' dual olfactory pathway.

For this purpose we analyzed extracellularly recorded spike trains from a whole of 102 units (49 l-ALT, 53 m-ALT, 12 animals). Units from both tract of each animal were recorded simultaneously and stimulated repeatedly (20 trials each) with 12 different odors (Brill et al., 2013). Each unit responded simultaneously with at least one other unit of the same recording to at least one odor, resulting in a total of 397 combinations. Simultaneous odor responses occurred within one tract (85 unit pairs in l-ALT, 96 unit pairs in m-ALT) and between the two tracts (216 unit pairs l-ALT:m-ALT). Whenever a unit pair responded simultaneously to a set of stimuli it also displayed coincidental activity to at least one of these stimuli (100% congruence in l:l, 99,5% in l:m, 96% in m:m), however, not necessarily to every single of the effective stimuli. On average a given unit pair displayed coincident activity for 84% of the odors that were effective in driving simultaneous responses.

In order to remove spurious coincidence, we corrected for stimulus modulation of firing rates, by subtracting a shuffle predictor from the original cross correlogram (see methods). Further, we only considered coincident activity that exceeded a 95% confidence interval.

Coincidence Increases with Odor Stimulation

A prerequisite for every mechanism potentially encoding environmental information is that it should be more pronounced in the presence of a stimulus than in its absence. We compared recordings of spontaneous activity (**Figure 2A**) with odor stimulation trials (**Figure 2B**) to test whether this applies to coincidental activity of PNs within and between tracts. For this purpose we calculated a *Coincidence Index (CI)*. *CI* reflects the significant coincident activity exceeding the expected coincidence.

Coincidence was present in both cases, but significantly higher under conditions of odor stimulation, than under spontaneous activity (**Figure 2C**; Wilcoxon signed rank test, $p < 0.001$). The amount of units expressing coincidental activity varied between recordings (animals). While coincidence was generally high in some ensembles (**Figures 2A,B** bottom row) it was rather low in others (**Figures 2A,B** middle row). Likewise, coincidence was not equally distributed between units of the same recording. While some units did not coincide with any other unit, others fired in close succession with many of the simultaneously recorded units, giving the impression of a "coincidence hub". As a general rule, units with high spontaneous coincidence showed even stronger odor related coincidence. Considering our careful correction for spurious coincidence, this odor related effect cannot be attributed to the pure increase in firing rate that naturally follows excitatory responses.

m-ALT Units Show More Coincidence Activity than l-ALT Units

PNs from the l- and m-ALT differ both in morphology and their functional properties. In how far do they produce different degrees of coincidental activity?

As can be seen from visual inspection of ensemble plots alone, m-ALT units (**Figure 2B** right column) are more likely to produce coinciding spikes than l-ALT units (**Figure 2B** left column). Coincidence between tracts seems to appear more often than within the l-ALT but less pronounced as compared to activity within the m-ALT. This qualitative observation is confirmed by a quantitative bootstrap hypothesis test (Bonferroni correction, $p < 0.002$, **Figure 2D**): With a median *CI* of 44%, pairs of m-ALT units were significantly more prone to engage in synchronous firing than pairs of l-ALT units ($CI = 32\%$) or mixed pairs of units from both tracts ($CI = 36\%$). Strongest coincidence of unit-odor pairs occurred at relative times of 11 ms

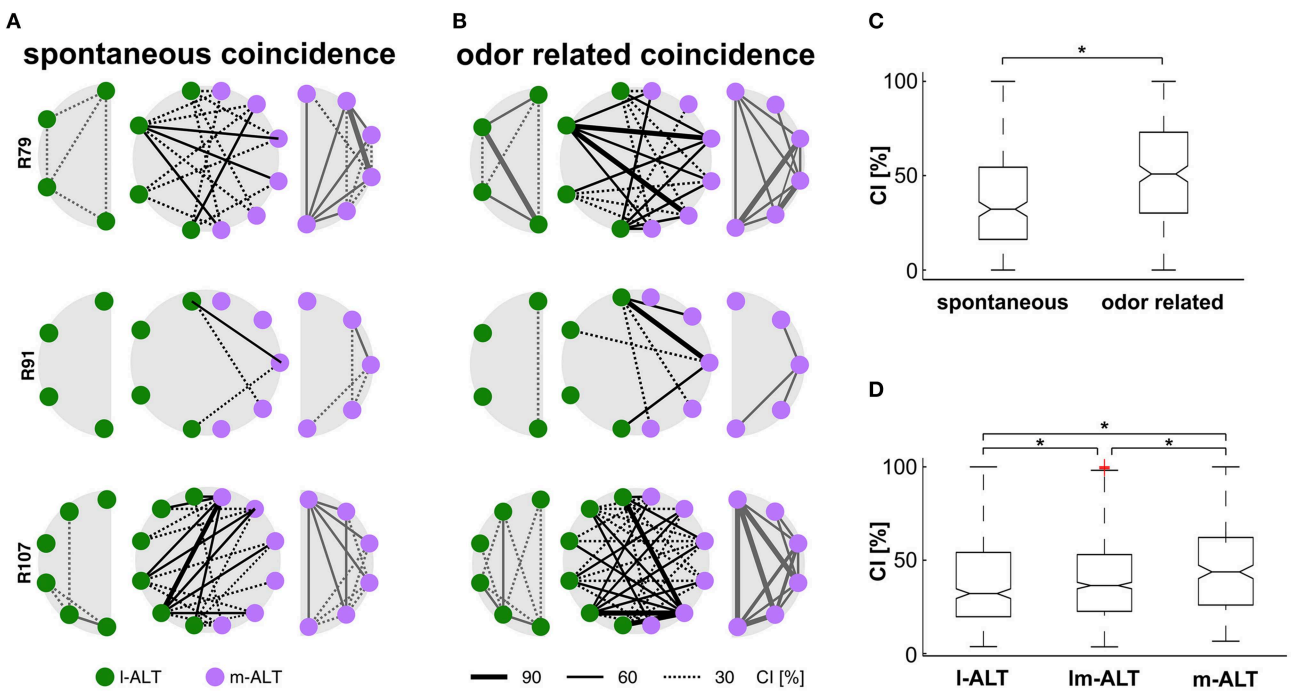

FIGURE 2 | Coincidental activity of single PNs within and between tracts. (A) Significant coincident activity during recordings of spontaneous activity within l-ALT PNs (green, left row), m-ALT PNs (purple, right row) and between PNs of both tracts (middle row) from simultaneously multi-unit recordings in three honeybees as example. Lines indicate coincidence strength across PN pairs estimated by the coincidence index CI. **(B)** Significant coincident activity during odor stimulation trials. Colors and Indices as in **(A)**. **(C)** Quantitative measurement of coincident activity across all 392 combinations of recorded PN pairs, indicates significant increase of coincidence during odor stimulation (*Wilcoxon signed rank test, $p < 0.001$). **(D)** Coincident activity is highest within the m-ALT, followed by significant coincidence across PNs from both tracts. This qualitative observation is confirmed by a quantitative bootstrap hypothesis test (*Bonferroni correction, $p < 0.002$).

in the l-ALT, 10 ms in m-ALT and 9 ms between unit pairs of both tracts. A delay that is within the integration time of a postsynaptic KC as estimated by modeling approaches (Perez-Orive et al., 2004; Cassenaer and Laurent, 2007; Finelli et al., 2008; Martin et al., 2013). The unintended variability of electrode placement in the range of about 100 µm at the output of the AL is of minor relevance since a presumed neuronal conduction velocity of about 20 cm/s (Oleskevich et al., 1997) would add a temporal variance of less than 1 ms.

Unit-pairs with Similar Odor-tuning do not Synchronize Stronger than Controls

Neural codes typically involve the identity of individual neurons. Extracellular measurements sample randomly from groups of neurons with various identities, i.e., different odor specific characteristics. To access the possibility of an odor-specific code of coincidence that depends on unit identity, we investigated coincident activity of unit pairs with similar tuning properties. To assess similarity we ranked odor responses within each unit according to strength. We compared these tuning profiles of ranked odor responses by correlation. Positive correlation was indicative for similar tuning. Non-significant correlation around zero was indicative for dissimilar tuning. Altogether 50 unit pairs (l:l 8 pairs, m:m 20 pairs, l:m 22 pairs) showed significantly positive correlated tuning (**Figures 3A,B**). Compared to unit pairs with non-correlated tuning (344 pairs, random examples **Figures 3C,D**) similarly tuned units did not differ significantly in coincidence strength (bootstrap hypothesis test, $p < 0.05$). However, there was a tendency for similar tuned units being rather less well synchronized than others.

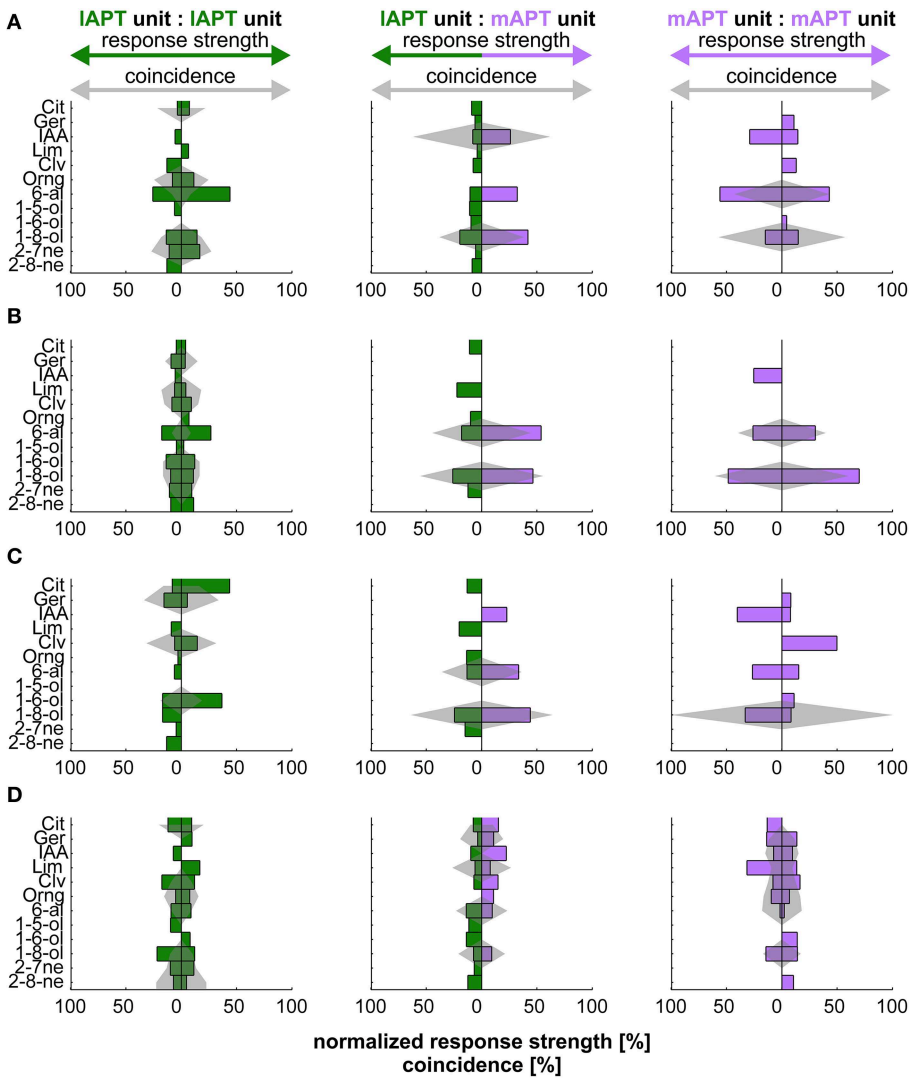

FIGURE 3 | Relationship between tuning and coincidence of exemplary unit pairs. Odor tuning of individual units and coincidence of unit pairs within and between tracts. Barplots show tuning in percent response rate of the individual unit. Gray shaded areas indicate the strength of coincidence in percent of overall coincidence of a given pair. Rows **(A,B)** give examples of units with similar tuning (significantly positive correlated). Rows **(C,D)** show examples of unit pairs with dissimilar tuning (no correlation). Green: l-ALT; purple: m-ALT.

Qualitative assessment of this relation shows that this trend was particularly visible for unit-pairs within the l-ALT. Odors that evoked low response rates could produce strong coincidence (**Figures 3A,C:** left column, row **A,** orange Oil or row **C**, clove oil). Pairs, in which both l-ALT units showed a strong tuning to one particular odor, usually did not synchronize to that same odor (**Figures 3A,C:** left column, row A, hexanal or row **C**, hexanol). On the contrary, for unit pairs within the m-ALT at least one unit, less often both, showed prominent tuning to an odor if the pair produced notable coincidence (cp.: **Figures 3A,B**: right column, row **A**, hexanal, row **B**, octanol). For mixed pairs between the l-ALT and the m-ALT an odor that evoked strong rate responses in both units likewise exhibited strong coincidence (cp.: **Figures 3A,C**: middle column, row **A**, octanol, row **C**, octanol). Octanol and hexanal appeared to be particularly potent in driving both response rates and coincidence of m-ALT units.

Odor Identity is not Reflected in a Simple Code of Coincidence Strength

Identification of biologically relevant odors is a key function of the olfactory system in behaving animals. Recent approaches have repeatedly described temporal relationships between neurons to be involved in this task (Stopfer et al., 1997; Perez-Orive et al., 2002; Riffell et al., 2013). We observed particularly strong coincidence amongst m-ALT units evoked by octanol and hexanal. Accordingly, we were curious whether odor identity was reflected by coincidental activity between units of the same or different tracts.

In a first step, we broke down the overall coincidence to the individual odor stimuli. For this purpose, we plotted the median *CI* distribution for each odor in the stimulus set, within and between tracts (**Figure 4**). Under the assumption that odor identity could be coded simply by the magnitude of coincidence, one would expect to see a systematic variation across animals in this distribution. Such a simple relationship however was not apparent. The median *CI* overlapped broadly between 0 and 80% for unit pairs within both tracts (**Figures 4A,C**). Between tracts, coincident activity was less dispersed but likewise overlapping (**Figure 4B**). None of the odors evoked a systematically high or low coincident activity. To the contrary, an odor that produced high *CI* scores in one recording could show low scores for another recording.

We conclude that a relationship between odor identity and coincident activity within an ensemble of units is not captured by a simple but inflexible code of coincidence strength.

Odor Tuning Correlates with Coincidence Strength in m- but not in l-ALT Units

We suspected a more flexible and thus more useful way of odor coding might get apparent when properties of individual units were taken into account. Based on the observations we made on single unit pairs within the m-ALT and between l- and m-ALT, we hypothesized that highly coincident activity

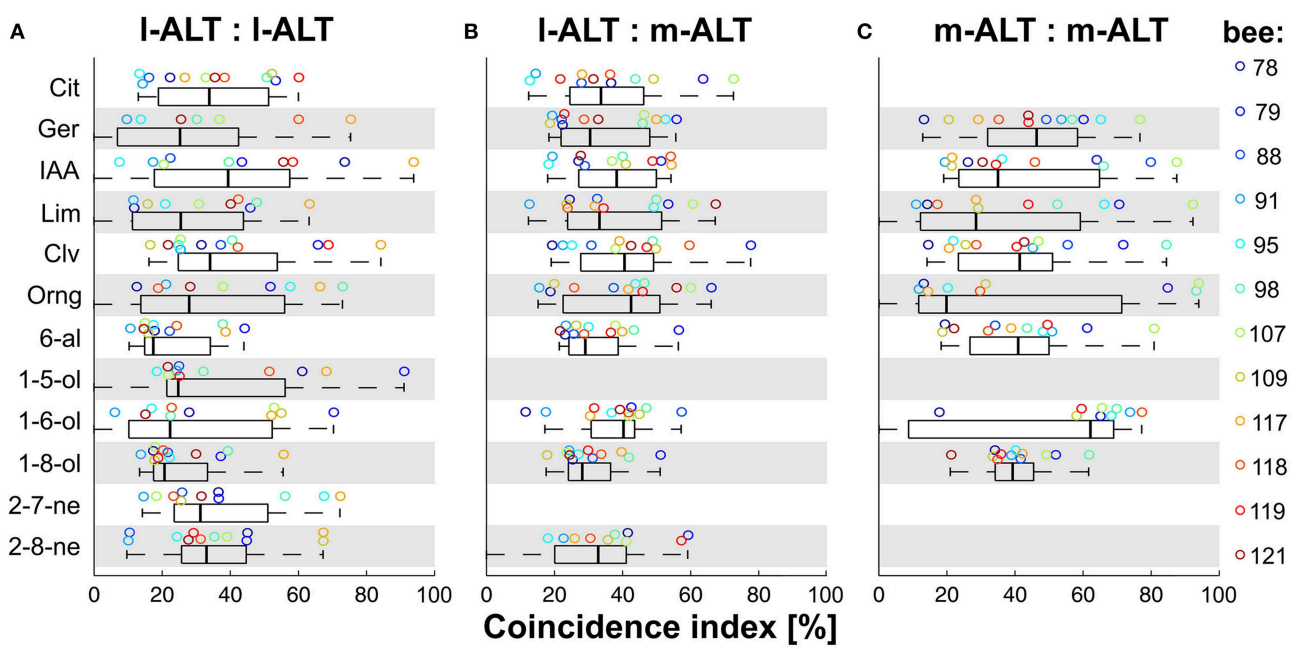

FIGURE 4 | Odor-specificity of coincident activity of PN pairs within and between tracts. **(A)** Odor-wise analysis of coincidental activity of l-ALT PN pairs. **(B)** Odor-wise analysis of coincidental activity of mixed l-ALT to m-ALT PN pairs. **(C)** Odor-wise analysis of coincidental activity of m-ALT PN pairs. Note: since the m-ALT was shown to respond to odors sparsely with high odor specificity (lifetime sparseness), in 2 out of 12 odors not more than one PN fired in coincidence with l-ALT PNs, whereas in 2 out of 12 odors no m-ALT PN fired in significant coincidence with neither l- or m-ALT PNs. Box-plots of all analyzed PN pairs in response to the given odors with box-line as median, Box: first and third quartile, whiskers: first and ninth centile. Circles indicate the bee-wise median.

would be more likely to appear for an odor that a given unit was better tuned to. To investigate the possibility of such a relationship we determined the response strength for every odor in each individual unit together with the strength of the corresponding coincidence. Next we correlated odor tuning with its corresponding coincident activity (**Figure 5**). The resulting correlation matrixes illustrate a marked difference between tracts: while the relationship appeared negligible within the l-ALT (**Figure 5A**), a strong pattern of significant correlation was apparent within the m-ALT (**Figure 5B**).

The emerging correlation matrix of the m-ALT met our expectations, since a positive correlation between odor tuning (e.g., to citral) and coincidence for the same odor (citral) was clearly visible. In practice: a unit that was strongly tuned to a given odor likewise showed strong coincidence, another unit with low tuning to the same odor would instead produce little coincidence. Surprisingly, positive correlation was not exclusively describing the relationship between tuning and coincidence to the same odor, but occurred similarly, even though generally less pronounced, to different odors belonging to similar chemical groups; e.g., citral and limonene (terpene); clove oil and orange oil (natural blends); pentanol and hexanol (alcohol). In contrast, negative correlations dominated the relationship between tuning and coincidence to odors from more distinct chemical classes; e.g., citral (terpene) and hexanol (alcohol). In fact, the characteristic pattern of positive and negative correlations might help the receiving mushroom-body circuits to discriminate and by this identify odors.

The marked lack of a similar relationship in the l-ALT is in congruence with both its previously documented rather stimulus unspecific responses (Brill et al., 2013) and its less pronounced coincident activity (c.f.: above). Our findings thus strengthen the notion of l-ALT and m-ALT being responsible for processing different stimulus properties and imply the utilization of different mechanisms for this purpose.

Discussion

In the present work, we set out to investigate in what fashion olfactory information is combined along the separate tracts of the honeybee dual olfactory pathway. Does coincident activity between the tracts foster a detection of stimulus features comparable to the delay line system of the vertebrate auditory system? That is: do l-ALT and m-ALT PN show prominent coincident activity? Or is coincidence a potential mechanism to integrate information within the same tract, facilitating parallel processing of stimulus properties comparable to the prominently known parallel visual pathways? That is: do neurons within the same tract show prominent coincident activity? To answer these questions, we recorded odor responses of simultaneously active PNs and measured coincident activity within and between the different subpopulations. Our results illustrate that coincidence is differently pronounced within each of the two tracts. Coincidence between tracts is present but does not outplay coincidence within the individual tracts. Taken together the findings presented in this work support the notion of

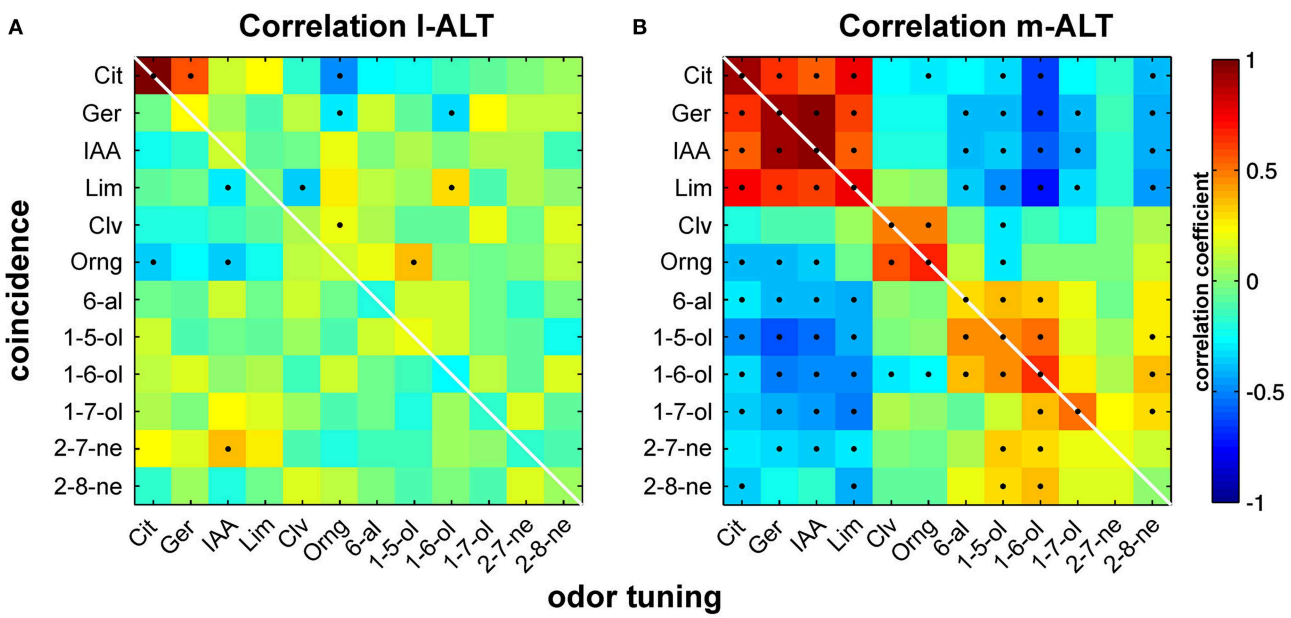

FIGURE 5 | Correlation of odor tuning with temporal coincidence of activity. Correlation of odor tuning and spike time coincidences is high in PNs of the m-ALT and supports a potential relevance of spike timing in odor identity coding. Virtually no correlation between both parameters was found in the l-ALT. **(A)** Correlation of coincidence and odor tuning for l-ALT PNs. Odor tuning is given by ranked response strengths of individual PNs to a given odor. Coincidence is depicted by the ranked summed activity to a given odor, estimated by the coincidence index *CI*. Correlation for each odor is calculated across the entire PN population. Color heat map indicates the correlation coefficient. Significant correlations ($p < 0.05$) are indicated as black dots. **(B)** Correlation of odor tuning with coincidence strength in the medial antennal lobe tract (m-ALT).

coincidence as an important mechanism in olfactory processing and, at the same time, strengthen the idea of parallel processing and delay-line coding in the dual olfactory system of the honeybee.

Synchrony within the AL has been shown to correlate with odor identity and intensity (Christensen et al., 2000; Lei et al., 2004; Riffell et al., 2009a,b) and has been suggested to represent a common encoding dimension for food odors and pheromones (Martin and Hildebrand, 2010). In agreement with these works, we find that PNs produce significant amounts of coincident spikes. More importantly however, this activity is specifically related to the presence of an odor stimulus. This relationship does not seem to be realized by the magnitude of coincidence alone. Accordingly, we could not find indications for a systematic relationship between coincidence strength and odor identity *per se*. Coincidence is the product of coordinated activity between at least two neurons. As such it represents the smallest unit of a processing network. Information processing in neuronal networks is believed to underlie higher order computations rather than an easy mathematical relationship (Laurent, 2002; Friedrich, 2013). Within the framework of network, our results and those of related works (Riffell et al., 2009a; Martin et al., 2013) suggest coincident activity to be a highly flexible mechanism that crucially depends on factors like the individual neurons' odor tuning and is as such suited to integrate biologically relevant information in upstream neurons.

In the same line of thinking, many studies have stressed the importance of coincidence detection by mushroom body KCs in the context of odor learning (Riemensperger et al., 2005; Cassenaer and Laurent, 2007; Gervasi et al., 2010) and odor discrimination (Perez-Orive et al., 2004; Jortner et al., 2007; Riffell et al., 2009a,b; Martin et al., 2013). Based on studies like these, the MB has been assumed as a coincidence detector for synchronous activity provided by the AL (Heisenberg, 2003; Rybak and Menzel, 2010; Davis, 2011). So far however, it has been difficult to disentangle what contribution is made by which type of neuron. Closing this knowledge gap is an important step in order to understand the function of different AL-neuron subpopulations (Galizia and Rössler, 2010). Moreover, it will help to develop refined models describing how upstream neurons in the MB make use of the information provided by the AL.

Using simultaneous dual-tract recordings we show for the first time coincidental activity that can directly be attributed to different morphological subclasses of AL PNs, which give rise to the lateral and medial tract projecting from the AL to the MB. The amount to which coincident activity is provided differs significantly within and between tracts. A finding that inspires to speculate about underlying mechanisms.

How is the striking difference in coincidence within l-ALT and m-ALT to be explained? What makes m-ALT PNs more likely to unite in synchronous firing than l-ALT PNs? And what impact might these differences have on upstream neurons? On the one hand, quantitative analysis of odor-evoked spike trains have attested higher overall firing rates in l-ALT units (Brill et al., 2013). On the other hand, qualitative observations of spiking patterns from both tracts have repeatedly led to descriptions of irregular and burst-like, phasic activity in m-ALT PNs contrasted by tonic activity in l-ALT PNs (Abel et al., 2001; Müller et al., 2002). When coding for comparable signals, bursts, in comparison with single spikes, have been shown to improve the SNR ratio (Sherman, 2001) and are suggested to improve information transfer between neurons (Lisman, 1997). Accordingly, the tendency of m-ALT PNs to display more burst-like activity might in fact outplay higher firing frequencies of l-ALT PNs when it comes to producing coincidence.

However, from the generally lower expression of synchronous firing in l-ALT PNs, it does not necessarily follow that coincidence within this tract is negligible. Even tough to a lesser degree than within the m-ALT, l-ALT units do produce significant amounts of coincident firing which upstream KCs could make use of. Input from PNs of the dual tracts might be processed differently: pyramidal neurons of the weakly electric fish have been shown to extract different aspects of stimulus information from coinciding burst-like and coinciding tonic spike trains (Oswald et al., 2004). If similar mechanisms exist in insect KCs has not yet been investigated.

Moreover, we should consider that KCs—just like vertebrate pyramidal neurons—might possess more than one type of coincidence detection (for reviews of coincidence detection in pyramidal neurons see Spruston, 2008). In our analysis of simultaneously recorded extracellular unit activity, we mimicked temporal summation by means of density estimation with a kernel about the length of possible postsynaptic integration. Our experimental approach did not allow to likewise consider coincidence detection as a result of spatial summation. Spatial summation crucially depends on large numbers of synaptic contacts. As a matter of fact, mature l-ALT PNs make more contacts with KCs than m-ALT PNs (Groh et al., 2012). Based on these morphological findings l-ALT PNs might thus be better suited to provide spatially coincident input, while m-ALT PNs give more temporally coinciding input, as indicated by our results.

In summary, the apparent differences of coincident activity as detected by our analysis illustrate that different mechanisms govern odor processing in each of the two tracts establishing the dual pathway. However, the final interpretation of these differences remains a matter of upstream KCs. In order to understand the interplay between PN output and KC response simultaneous recordings from all three types of neurons would be highly desirable.

Magnitude is not the only aspect in which coincident activity differs between l-ALT and m-ALT. We found a strong relationship of odor tuning vs. coincidence activity within the m-ALT, but not within the l-ALT. Based on these observations it is tempting to conclude that coincident activity of m-ALT PNs allows upstream KCs to specifically process odor identity; an assumption that is further supported by studies of stimulus specificity within the two tracts. Multi-unit recordings as well as calcium imaging from m-ALT PNs show significantly higher odor specificity than those of units from the l-ALT (Brill et al., 2013; Carcaud et al., 2015). A finding that could not be seen in a previous attempt using calcium imaging (Yamagata et al., 2009), most likely as a result of GABAergic mechanisms that impact PN activity in imaging approaches (Grünewald, 1999; Ganeshina

and Menzel, 2001; Froese et al., 2014). Interestingly, recent imaging results from m-ALT glomeruli do show coding related to chemical groups of odors (Carcaud et al., 2012). A finding, that complements nicely with our tuning-coincidence correlation, where we likewise found similar relationships between odors of the same chemical group. In agreement with the higher odor specificity, m-ALT PNs seem to keep track of the single odorants if challenged by odor mixtures (Krofczik et al., 2008)—a strategy termed elementary odor coding. Joint activity of odor specific m-ALT PNs could allow for a combinatorial code of mixture embedded odor identity by the receiving KCs.

The picture that emerges from our results for l-ALT PNs is very different, particularly regarding odor identity coding. The striking lack of correlation between odor tuning and coincidence implies that joint activity of l-ALT PNs conveys poor information about odor identity. This however appears little surprising considering that l-ALT PNs are rather broadly tuned and express little odor specificity (Brill et al., 2013; Carcaud et al., 2015). In contrast to the m-ALT, l-ALT PNs are characterized by shorter latencies (Krofczik et al., 2008; Brill et al., 2013) and start to respond to odors already at very low concentrations (Yamagata et al., 2009; Schmuker et al., 2011; Carcaud et al., 2012). If challenged by odor mixtures they tend to respond to the mixture as a whole, rather than the single odorant (Krofczik et al., 2008). It might well be that any of these characteristics could produce significant correlation with coincident activity for l-ALT PNs but not m-ALT neurons - an assumption that due to the lack of suitable experimental data has to remain speculative for the time being.

Taken together, our results imply that coincidence within the tracts of the dual olfactory pathway serves different functions. These functions probably rely on the characteristics of the PN subgroups that allow for dedicated processing of different stimulus aspects. These findings support the suggestion that the dual olfactory pathway is ideally suited to implement parallel processing.

Parallel processing keeps information from different sources separated. An olfactory delay line, in contrast, would combine information from different sources. As detailed above, the coincident activity we found within each tract gives strong support to the implementation of parallel processing by the dual olfactory pathway. However, we also found significant coincident activity across tracts. Even though joint activity between l-ALT and m-ALT PNs did not outplay activity within individual tracts, it produced significant amounts of coincidence which might just as likely be used by upstream KCs. Hence our finding complies likewise with the existence of olfactory delay lines. Could both of these mechanisms coexist? In fact, morphological evidence supports a possible implementation of both mechanisms in parallel (**Figure 6**). Mass-fill studies in different Hymenoptera have shown that PNs project to different sub-regions of the MB (Kirschner et al., 2006; Nishikawa et al., 2012). These separated inputs are received by various types of KCs. Some KCs make synaptic contacts only in one of the two PN input regions and likewise provide output to different regions (Strausfeld et al., 2000). That is, these types of KC maintain the possible separation of parallel pathways until its convergent input to extrinsic MB

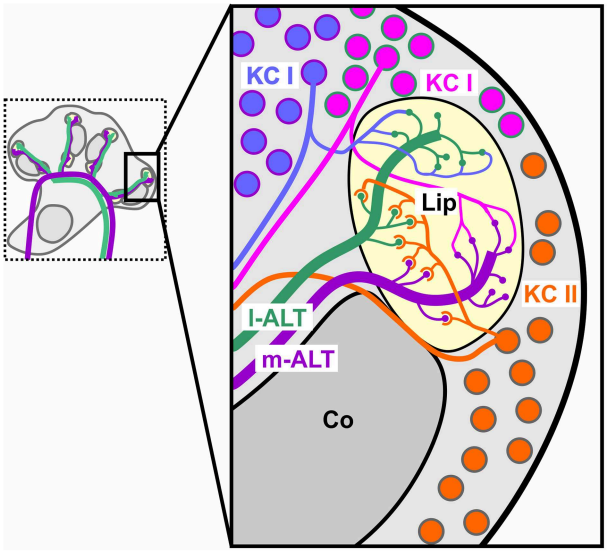

FIGURE 6 | Putative connectivity scheme of different KC subtypes and PNs. Connections are partly inferred from morphological studies in other insect species. Non-compact KC (KC I, blue, magenta) most likely contact exclusively target regions of the m-ALT (purple) or l-ALT (green). Clawed KCs (KC II, orange) are likely to span over both the l- and m-ALT innervation areas within the olfactory lip.

neurons (Rybak and Menzel, 1993). Another population of KCs, the so called clawed KCs (KC II; Mobbs, 1982), span their postsynapses across the innervation fields of both l- and m-ALT PNs (Strausfeld, 2002). Patch clamp recordings in the fly could show that these clawed KCs, on average, require coinciding input from about 4–6 PNs in order to be driven above threshold (Gruntman and Turner, 2013). Patch clamp experiments in cockroaches likewise support coincident activation of KCs, as indicated by their high action potential threshold (Demmer and Kloppenburg, 2009). Similarly, indications emanate from studies showing that input of PNs conveying information about different odors in changing temporal relationships evoke activity in KCs specifically tuned to certain asynchronous inputs (Saha et al., 2013). An observation that recently was also found in the vertebrate's olfactory cortex (Haddad et al., 2013). This subtype of KCs is hence predestinated to function as a coincidence detector for information coming from both tracts (Rössler and Brill, 2013).

In this perspective, subclasses of olfactory PNs of the honeybee first of all establish parallel pathways. Subclasses of KCs again could realize an implementation of both maintained parallel processing and delay-line like coincidence detection. Although our experimental paradigm favors the idea of parallel processing, further experiments which take KC activity directly into account need to prove, if delay line coding in the olfactory system does exist. Along this line further experiments also should test which of the mentioned coding strategies, either parallel processing or coincidence coding, benefit the animal in detecting complex odors.

As proposed earlier (Rössler and Brill, 2013) the dual olfactory pathway reminds of a delay-line system. Taking the proposed

neuronal conduction velocity of about 20 cm/s in honeybees into account (Oleskevich et al., 1997), we assumed that indeed different delays between the PN tracts activate different KCs within the MB calyx at different places. In favor of a delay-line coding the measured maximal coincidence of about 10 ms within and 9 ms across tracts could add up on already measured latency differences between tracts and between individual PNs (Krofczik et al., 2008; Brill et al., 2013). The measured maximal coincidence as well as response latency would thus enable the system to implement an even more fine-scaled temporal and spatial KC activation pattern, a prerequisite for sparse coding.

While parallel processing is most probable important for tasks like odor identification and learning, an olfactory delay line and temporal coding could help e.g., to navigate along a concentration gradient to a food source or a mate. These abilities are obviously not only vitally important for honeybees and other Hymenoptera but likewise for behaviorally less complex insects like flies or moths. In recent years several attempts have been made to understand the possible functional relevance of the dual olfactory pathway of Hymenoptera (Abel et al., 2001; Müller et al., 2002; Krofczik et al., 2008; Yamagata et al., 2009; Brandstaetter and Kleineidam, 2011; Dacks and Nighorn, 2011; Rössler and Zube, 2011; Nishikawa et al., 2012; Brill et al., 2013; Carcaud et al., 2015). In the long run the knowledge gained from these studies might be transferred to insects with different tract layouts (Galizia and Rössler, 2010; Martin et al., 2011) and thus promote a more fundamental understanding of olfactory guided behavior.

Acknowledgments

The authors would like to thank Martin P. Nawrot for valuable discussions. This work was supported by the Deutsche Forschungsgemeinschaft (DFG, SPP 1392, Ro1177/5-2) to WR. This publication was funded by the German Research Foundation (DFG) and the University of Würzburg in the funding program Open Access Publishing.

References

Abel, R., Rybak, J., and Menzel, R. (2001). Structure and response patterns of olfactory interneurons in the honeybee, *Apis mellifera*. *J. Comp. Neurol.* 437, 363–383. doi: 10.1002/cne.1289

Bliss, T., and Lømo, T. (1973). Long-lasting potentiation of synaptic transmission in the dentate area of the anaesthetized rabbit following stimulation of the perforant path. *J. Physiol.* 232, 331–356. doi: 10.1113/jphysiol.1973.sp010273

Brandstaetter, A. S., and Kleineidam, C. J. (2011). Distributed representation of social odors indicates parallel processing in the antennal lobe of ants. *J. Neurophysiol.* 106, 2437–2449. doi: 10.1152/jn.01106.2010

Brill, M. F., Reuter, M., Rössler, W., and Strube-Bloss, M. F. (2014). Simultaneous long-term recordings at two neuronal processing stages in behaving honeybees. *J. Vis. Exp.* e51750. doi: 10.3791/51750

Brill, M. F., Rosenbaum, T., Reus, I., Kleineidam, C. J., Nawrot, M. P., and Rössler, W. (2013). Parallel processing via a dual olfactory pathway in the honeybee. *J. Neurosci.* 33, 2443–2456. doi: 10.1523/JNEUROSCI.4268-12.2013

Carcaud, J., Giurfa, M., and Sandoz, J.-C. (2015). Differential combinatorial coding of pheromones in two olfactory subsystems of the honey bee brain. *J. Neurosci.* 35, 4157–4167. doi: 10.1523/JNEUROSCI.0734-14.2015

Carcaud, J., Hill, T., Giurfa, M., and Sandoz, J.-C. (2012). Differential coding by two olfactory subsystems in the honeybee brain. *J. Neurophysiol.* 108, 1106–1121. doi: 10.1152/jn.01034.2011

Caron, S. J. C., Ruta, V., Abbott, L. F., and Axel, R. (2013). Random convergence of olfactory inputs in the Drosophila mushroom body. *Nature* 497, 113–117. doi: 10.1038/nature12063

Cassenaer, S., and Laurent, G. (2007). Hebbian STDP in mushroom bodies facilitates the synchronous flow of olfactory information in locusts. *Nature* 448, 709–714. doi: 10.1038/nature05973

Christensen, T. A., Lei, H., and Hildebrand, J. G. (2003). Coordination of central odor representations through transient, non-oscillatory synchronization of glomerular output neurons. *Proc. Natl. Acad. Sci. U.S.A.* 100, 11076–11081. doi: 10.1073/pnas.1934001100

Christensen, T. A., Pawlowski, V. M., Lei, H., and Hildebrand, J. G. (2000). Multi-unit recordings reveal context-dependent modulation of synchrony in odor-specific neural ensembles. *Nat. Neurosci.* 3, 927–931. doi: 10.1038/78840

Dacks, A. M., and Nighorn, A. J. (2011). The organization of the antennal lobe correlates not only with phylogenetic relationship, but also life history: a Basal hymenopteran as exemplar. *Chem. Senses* 36, 209–220. doi: 10.1093/chemse/bjq121

Davis, R. L. (2011). Traces of Drosophila memory. *Neuron* 70, 8–19. doi: 10.1016/j.neuron.2011.03.012

Demmer, H., and Kloppenburg, P. (2009). Intrinsic membrane properties and inhibitory synaptic input of kenyon cells as mechanisms for sparse coding? *J. Neurophysiol.* 102, 1538–1550. doi: 10.1152/jn.00183.2009

Finelli, L. A., Haney, S., Bazhenov, M., Stopfer, M., and Sejnowski, T. J. (2008). Synaptic learning rules and sparse coding in a model sensory system. *PLoS Comput. Biol.* 4:e1000062. doi: 10.1371/journal.pcbi.1000062

Fischbach, K. F., and Dittrich, A. P. M. (1989). The optic lobe of *Drosophila melanogaster*. I. A Golgi analysis of wild-type structure. *Cell Tissue Res.* 258, 441–475. doi: 10.1007/bf00218858

Friedrich, R. W. (2013). Neuronal computations in the olfactory system of zebrafish. *Annu. Rev. Neurosci.* 36, 383–402. doi: 10.1146/annurev-neuro-062111-150504

Froese, A., Szyszka, P., and Menzel, R. (2014). Effect of GABAergic inhibition on odorant concentration coding in mushroom body intrinsic neurons of the honeybee. *J. Comp. Physiol. A Neuroethol. Sens. Neural. Behav. Physiol.* 200, 183–195. doi: 10.1007/s00359-013-0877-8

Fukunaga, I., Berning, M., Kollo, M., Schmaltz, A., and Schaefer, A. T. T. (2012). Two distinct channels of olfactory bulb output. *Neuron* 75, 320–329. doi: 10.1016/j.neuron.2012.05.017

Galizia, C. G., Franke, T., Menzel, R., and Sandoz, J.-C. (2012). Optical imaging of concealed brain activity using a gold mirror in honeybees. *J. Insect Physiol.* 58, 743–749. doi: 10.1016/j.jinsphys.2012.02.010

Galizia, C. G., and Rössler, W. (2010). Parallel olfactory systems in insects: anatomy and function. *Annu. Rev. Entomol.* 55, 399–420. doi: 10.1146/annurev-ento-112408-085442

Ganeshina, O., and Menzel, R. (2001). GABA-immunoreactive neurons in the mushroom bodies of the honeybee: an electron microscopic study. *J. Comp. Neurol.* 437, 335–349. doi: 10.1002/cne.1287

Gasser, H., and Erlanger, J. (1929). The role of fiber size in the establishment of a nerve block by pressure or cocaine. *Am. J. Physiol.* 88, 581–591.

Gervasi, N., Tchénio, P., and Preat, T. (2010). PKA dynamics in a Drosophila learning center: coincidence detection by rutabaga adenylyl cyclase and spatial regulation by dunce phosphodiesterase. *Neuron* 65, 516–529. doi: 10.1016/j.neuron.2010.01.014

Groh, C., Lu, Z., Meinertzhagen, I. A., and Rössler, W. (2012). Age-related plasticity in the synaptic ultrastructure of neurons in the mushroom body calyx of the adult honeybee *Apis mellifera*. *J. Comp. Neurol.* 520, 3509–3527. doi: 10.1002/cne.23102

Grünewald, B. (1999). Morphology of feedback neurons in the mushroom body of the honeybee, *Apis mellifera*. *J. Comp. Neurol.* 404, 114–126.

Gruntman, E., and Turner, G. C. (2013). Integration of the olfactory code across dendritic claws of single mushroom body neurons. *Nat. Neurosci.* 16, 1821–1829. doi: 10.1038/nn.3547

Gupta, N., and Stopfer, M. (2012). Functional analysis of a higher olfactory center, the lateral horn. *J. Neurosci.* 32, 8138–8148. doi: 10.1523/JNEUROSCI.1066-12.2012

Haddad, R., Lanjuin, A., Madisen, L., Zeng, H., Murthy, V. N., and Uchida, N. (2013). Olfactory cortical neurons read out a relative time code in the olfactory bulb. *Nat. Neurosci.* 16, 949–957. doi: 10.1038/nn.3407

Hassenstein, B., and Reichardt, W. (1951). Funktionsanalyse der Bewegungsperzeption eines Käfers. *Naturwissenschaften* 38, 507–507. doi: 10.1007/BF00628864

Hebb, D. (1949). *The Organization of Behavior*. New York, NY: John Wiley & Sons.

Heisenberg, M. (2003). Mushroom body memoir: from maps to models. *Nat. Rev. Neurosci.* 4, 266–275. doi: 10.1038/nrn1074

Helversen, D., and Helversen, O. (1995). Acoustic pattern recognition and orientation in orthopteran insects: parallel or serial processing? *J. Comp. Physiol. A* 177, 767–774. doi: 10.1007/BF00187635

Igarashi, K. M., Ieki, N., An, M., Yamaguchi, Y., Nagayama, S., Kobayakawa, K., et al. (2012). Parallel mitral and tufted cell pathways route distinct odor information to different targets in the olfactory cortex. *J. Neurosci.* 32, 7970–7985. doi: 10.1523/JNEUROSCI.0154-12.2012

Ito, I., Ong, R. C., Raman, B., and Stopfer, M. (2008). Sparse odor representation and olfactory learning. *Nat. Neurosci.* 11, 1177–1184. doi: 10.1038/nn.2192

Ito, K., Shinomiya, K., Ito, M., Armstrong, J. D., Boyan, G., Hartenstein, V., et al. (2014). A systematic nomenclature for the insect brain. *Neuron* 81, 755–765. doi: 10.1016/j.neuron.2013.12.017

Jeffress, L. A. (1948). A place theory of sound localization. *J. Comp. Physiol. Psychol.* 41, 35–39. doi: 10.1037/h0061495

Joris, P. X. P., Smith, P. H., and Yin, T. T. C. T. (1998). Coincidence detection minireview in the auditory system: 50 years after Jeffress. *Neuron* 21, 1235–1238. doi: 10.1016/S0896-6273(00)80643-1

Jortner, R. A., Farivar, S. S., and Laurent, G. (2007). A simple connectivity scheme for sparse coding in an olfactory system. *J. Neurosci.* 27, 1659–1669. doi: 10.1523/JNEUROSCI.4171-06.2007

Kirschner, S., Kleineidam, C. J., Zube, C., Rybak, J., Grünewald, B., and Rössler, W. (2006). Dual olfactory pathway in the honeybee, *Apis mellifera*. *J. Comp. Neurol.* 499, 933–952. doi: 10.1002/cne.21158

Krofczik, S., Menzel, R., and Nawrot, M. P. (2008). Rapid odor processing in the honeybee antennal lobe network. *Front. Comput. Neurosci.* 2:9. doi: 10.3389/neuro.10.009.2008

Laurent, G. (2002). Olfactory network dynamics and the coding of multidimensional signals. *Nat. Rev. Neurosci.* 3, 884–895. doi: 10.1038/nrn964

Lei, H., Christensen, T. A., and Hildebrand, J. G. (2004). Spatial and temporal organization of ensemble representations for different odor classes in the moth antennal lobe. *J. Neurosci.* 24, 11108. doi: 10.1523/JNEUROSCI.3677-04.2004

Leiss, F., Groh, C., Butcher, N. J., Meinertzhagen, I. A., and Tavosanis, G. (2009). Synaptic organization in the adult Drosophila mushroom body calyx. *J. Comp. Neurol.* 517, 808–824. doi: 10.1002/cne.22184

Livingstone, M., and Hubel, D. (1988). Segregation of form, color, movement, and depth: anatomy, physiology, and perception. *Science* 240, 740–749. doi: 10.1126/science.3283936

Lisman, J. E. (1997). Bursts as a unit of neural information: making unreliable synapses reliable. *Trends Neurosci.* 20, 38–43. doi: 10.1016/S0166-2236(96)10070-9

Martin, J. P., Beyerlein, A., Dacks, A. M., Reisenman, C. E., Riffell, J. A., Lei, H., et al. (2011). The neurobiology of insect olfaction: sensory processing in a comparative context. *Prog. Neurobiol.* 95, 427–447. doi: 10.1016/j.pneurobio.2011.09.007

Martin, J. P., and Hildebrand, J. G. (2010). Innate recognition of pheromone and food odors in moths: a common mechanism in the antennal lobe? *Front. Behav. Neurosci.* 4:159. doi: 10.3389/fnbeh.2010.00159

Martin, J. P., Lei, H., Riffell, J. A., and Hildebrand, J. G. (2013). Synchronous firing of antennal-lobe projection neurons encodes the behaviorally effective ratio of sex-pheromone components in male *Manduca sexta*. *J. Comp. Physiol. A Neuroethol. Sens. Neural. Behav. Physiol.* 199, 963–979. doi: 10.1007/s00359-013-0849-z

Meyer, A., and Galizia, C. G. (2012). Elemental and configural olfactory coding by antennal lobe neurons of the honeybee (*Apis mellifera*). *J. Comp. Physiol. A Neuroethol. Sens. Neural. Behav. Physiol.* 198, 159–171. doi: 10.1007/s00359-011-0696-8

Mobbs, P. (1982). The brain of the honeybee *Apis Mellifera*. I. The connections and spatial organization of the mushroom bodies. *Philos. Trans. R. Soc. Lond. B Biol. Sci.* 298, 309–354. doi: 10.1098/rstb.1982.0086

Müller, D., Abel, R., Brandt, R., Zöckler, M., and Menzel, R. (2002). Differential parallel processing of olfactory information in the honeybee, *Apis mellifera* L. *J. Comp. Physiol. A Neuroethol. Sens. Neural. Behav. Physiol.* 188, 359–370. doi: 10.1007/s00359-002-0310-1

Nassi, J. J., and Callaway, E. M. (2009). Parallel processing strategies of the primate visual system. *Nat. Rev. Neurosci.* 10, 360–372. doi: 10.1038/nrn2619

Nawrot, M. P. (2012). Dynamics of sensory processing in the dual olfactory pathway of the honeybee. *Apidologie* 43, 269–291. doi: 10.1007/s13592-012-0131-3

Nishikawa, M., Watanabe, H., and Yokohari, F. (2012). Higher brain centers for social tasks in worker ants, *Camponotus japonicus*. *J. Comp. Neurol.* 520, 1584–1598. doi: 10.1002/cne.23001

Oleskevich, S., Clements, J. D., and Srinivasan, M. V. (1997). Long-term synaptic plasticity in the honeybee. *J. Neurophysiol.* 78, 528–32.

Oswald, A.-M. M., Chacron, M. J., Doiron, B., Bastian, J., and Maler, L. (2004). Parallel processing of sensory input by bursts and isolated spikes. *J. Neurosci.* 24, 4351–4362. doi: 10.1523/JNEUROSCI.0459-04.2004

Paulk, A. C., Dacks, A. M., and Gronenberg, W. (2009). Color processing in the medulla of the bumblebee (*Apidae: Bombus* impatiens). *J. Comp. Neurol.* 513, 441–456. doi: 10.1002/cne.21993

Paulk, A. C., Phillips-Portillo, J., Dacks, A. M., Fellous, J.-M., and Gronenberg, W. (2008). The processing of color, motion, and stimulus timing are anatomically segregated in the bumblebee brain. *J. Neurosci.* 28, 6319–6332. doi: 10.1523/JNEUROSCI.1196-08.2008

Payton, C. A., Wilson, D. A., and Wesson, D. W. (2012). Parallel odor processing by two anatomically distinct olfactory bulb target structures. *PLoS ONE* 7:e34926. doi: 10.1371/annotation/eb15723f-2df7-4cd6-8113-c565652d0628

Perez-Orive, J., Bazhenov, M., and Laurent, G. (2004). Intrinsic and circuit properties favor coincidence detection for decoding oscillatory input. *J. Neurosci.* 24, 6037–6047. doi: 10.1523/JNEUROSCI.1084-04.2004

Perez-Orive, J., Mazor, O., Turner, G. C., Cassenaer, S., Wilson, R. I., and Laurent, G. (2002). Oscillations and sparsening of odor representations in the mushroom body. *Science* 297, 359–365. doi: 10.1126/science.1070502

Rauschecker, J. P., and Scott, S. K. (2009). Maps and streams in the auditory cortex: nonhuman primates illuminate human speech processing. *Nat. Neurosci.* 12, 718–724. doi: 10.1038/nn.2331

Reed, C. L., Klatzky, R. L., and Halgren, E. (2005). What vs. where in touch: an fMRI study. *Neuroimage* 25, 718–726. doi: 10.1016/j.neuroimage.2004.11.044

Ribi, W. A., and Scheel, M. (1981). The second and third optic ganglia of the worker bee. *Cell Tissue Res.* 221, 17–43. doi: 10.1007/BF00216567

Riemensperger, T., Völler, T., Stock, P., Buchner, E., and Fiala, A. (2005). Punishment prediction by dopaminergic neurons in Drosophila. *Curr. Biol.* 15, 1953–1960. doi: 10.1016/j.cub.2005.09.042

Riffell, J. A., Lei, H., Christensen, T. A., and Hildebrand, J. G. (2009a). Characterization and coding of behaviorally significant odor mixtures. *Curr. Biol.* 19, 335–340. doi: 10.1016/j.cub.2009.01.041

Riffell, J. A., Lei, H., and Hildebrand, J. G. (2009b). Neural correlates of behavior in the moth *Manduca sexta* in response to complex odors. *Proc. Natl. Acad. Sci. U.S.A.* 106, 19219–19226. doi: 10.1073/pnas.0910592106

Riffell, J. A., Lei, H., Abrell, L., and Hildebrand, J. G. (2013). Neural basis of a pollinator's buffet: olfactory specialization and learning in *Manduca sexta*. *Science* 339, 200–204. doi: 10.1126/science.1225483

Rössler, W., and Brill, M. F. (2013). Parallel processing in the honeybee olfactory pathway: structure, function, and evolution. *J. Comp. Physiol. A Neuroethol. Sens. Neural. Behav. Physiol.* 199, 981–996. doi: 10.1007/s00359-013-0821-y

Rössler, W., and Zube, C. (2011). Dual olfactory pathway in Hymenoptera: evolutionary insights from comparative studies. *Arthropod Struct. Dev.* 40, 349–357. doi: 10.1016/j.asd.2010.12.001

Roussel, E., Carcaud, J., Combe, M., Giurfa, M., and Sandoz, J.-C. (2014). Olfactory coding in the honeybee lateral horn. *Curr. Biol.* 24, 561–567. doi: 10.1016/j.cub.2014.01.063

Rybak, J. (2012). "The digital honey bee brain Atlas," in *Honeybee Neurobiology and Behavior*, eds C. G. Galizia, D. Eisenhardt, and M. Giurfa (Dordrecht: Springer), 125–140.

Rybak, J., and Menzel, R. (1993). Anatomy of the mushroom bodies in the honey bee brain: the neuronal connections of the alpha-lobe. *J. Comp. Neurol.* 465, 444–465. doi: 10.1002/cne.903340309

Rybak, J., and Menzel, R. (2010). "Mushroom body of the honeybee," in *Handbook of Brain Microcircuits*, eds G. M. Shepherd and S. Grillner (New York, NY: Oxford University Press), 433–438. doi: 10.1093/med/9780195389883.003.0044

Saha, D., Leong, K., Li, C., Peterson, S., Siegel, G., and Raman, B. (2013). A spatiotemporal coding mechanism for background-invariant odor recognition. *Nat. Neurosci.* 16, 1830–1839. doi: 10.1038/nn.3570

Sandoz, J. (2011). Behavioral and neurophysiological study of olfactory perception and learning in honeybees. *Front. Syst. Neurosci.* 5:98. doi: 10.3389/fnsys.2011.00098

Savitzky, A., and Golay, M. (1964). Smoothing and differentiation of data by simplified least squares procedures. *Anal. Chem.* 36, 1627–1639. doi: 10.1021/ac60214a047

Schmuker, M., Yamagata, N., Nawrot, M. P., and Menzel, R. (2011). Parallel representation of stimulus identity and intensity in a dual pathway model inspired by the olfactory system of the honeybee. *Front. Neuroeng.* 4:17. doi: 10.3389/fneng.2011.00017

Sherman, S. M. (2001). Tonic and burst firing: dual modes of thalamocortical relay. *Trends Neurosci.* 24, 122–126. doi: 10.1016/S0166-2236(00)01714-8

Spruston, N. (2008). Pyramidal neurons: dendritic structure and synaptic integration. *Nat. Rev. Neurosci.* 9, 206–221. doi: 10.1038/nrn2286

Stopfer, M., Bhagavan, S., Smith, B. H., and Laurent, G. (1997). Impaired odour discrimination on desynchronization of odour-encoding neural assemblies. *Nature* 390, 70–74. doi: 10.1038/36335

Strausfeld, N. J. (2002). Organization of the honey bee mushroom body: representation of the calyx within the vertical and gamma lobes. *J. Comp. Neurol.* 450, 4–33. doi: 10.1002/cne.10285

Strausfeld, N. J., Douglass, J. K., Campbell, H., and Higgins, C. (2006). "Parallel processing in the optic lobes of flies and the occurrence of motion computing circuits," in *Invertebrate Vision*, eds E. Warrant and D.-E. Nilsson (Cambridge: Cambridge University Press), 349–398.

Strausfeld, N. J., Homberg, U., and Kloppenburg, P. (2000). Parallel organization in honey bee mushroom bodies by peptidergic Kenyon cells. *J. Comp. Neurol.* 424, 179–195. doi: 10.1002/1096-9861(20000814)424:13.3.CO;2-B

Strutz, A., Soelter, J., Baschwitz, A., Farhan, A., Grabe, V., Rybak, J., et al. (2014). Decoding odor quality and intensity in the Drosophila brain. *Elife* 3, 1–21. doi: 10.7554/eLife.04147

Szyszka, P., Ditzen, M., Galkin, A., Galizia, C. G., and Menzel, R. (2005). Sparsening and temporal sharpening of olfactory representations in the honeybee mushroom bodies. *J. Neurophysiol.* 94, 3303–3313. doi: 10.1152/jn.00397.2005

Turner, G. C., Bazhenov, M., and Laurent, G. (2008). Olfactory representations by Drosophila mushroom body neurons. *J. Neurophysiol.* 99, 734–746. doi: 10.1152/jn.01283.2007

Yamagata, N., Schmuker, M., Szyszka, P., Mizunami, M., and Menzel, R. (2009). Differential odor processing in two olfactory pathways in the honeybee. *Front. Syst. Neurosci.* 3:16. doi: 10.3389/neuro.06.016.2009

Yasuyama, K., and Meinertzhagen, I. A., and Schürmann, F. W. (2002). Synaptic organization of the mushroom body calyx in *Drosophila melanogaster*. *J. Comp. Neurol.* 445, 211–226. doi: 10.1002/cne.10155

Conflict of Interest Statement: The authors declare that the research was conducted in the absence of any commercial or financial relationships that could be construed as a potential conflict of interest.

frontiers in Physiology

ORIGINAL RESEARCH
published: 08 March 2016
doi: 10.3389/fphys.2016.00080

Intrinsic and Network Mechanisms Constrain Neural Synchrony in the Moth Antennal Lobe

Hong Lei[1], *Yanxue Yu*[2], *Shuifang Zhu*[2] *and Aaditya V. Rangan*[3]*

[1] Department of Neuroscience, The University of Arizona, Tucson, AZ, USA, [2] Institute of Plant Quarantine, Chinese Academy of Inspection and Quarantine, Beijing, China, [3] Department of Mathematics, Courant Institute of Mathematical Sciences, New York University, New York, NY, USA

Projection-neurons (PNs) within the antennal lobe (AL) of the hawkmoth respond vigorously to odor stimulation, with each vigorous response followed by a ∼1 s period of suppression—dubbed the "afterhyperpolarization-phase," or AHP-phase. Prior evidence indicates that this AHP-phase is important for the processing of odors, but the mechanisms underlying this phase and its function remain unknown. We investigate this issue. Beginning with several physiological experiments, we find that pharmacological manipulation of the AL yields surprising results. Specifically, (a) the application of picrotoxin (PTX) lengthens the AHP-phase and reduces PN activity, whereas (b) the application of Bicuculline-methiodide (BIC) reduces the AHP-phase and increases PN activity. These results are curious, as both PTX and BIC are inhibitory-receptor antagonists. To resolve this conundrum, we speculate that perhaps (a) PTX reduces PN activity through a disinhibitory circuit involving a heterogeneous population of local-neurons, and (b) BIC acts to hamper certain intrinsic currents within the PNs that contribute to the AHP-phase. To probe these hypotheses further we build a computational model of the AL and benchmark our model against our experimental observations. We find that, for parameters which satisfy these benchmarks, our model exhibits a particular kind of synchronous activity: namely, "multiple-firing-events" (MFEs). These MFEs are causally-linked sequences of spikes which emerge stochastically, and turn out to have important dynamical consequences for all the experimentally observed phenomena we used as benchmarks. Taking a step back, we extract a few predictions from our computational model pertaining to the real AL: Some predictions deal with the MFEs we expect to see in the real AL, whereas other predictions involve the runaway synchronization that we expect when BIC-application hampers the AHP-phase. By examining the literature we see support for the former, and we perform some additional experiments to confirm the latter. The confirmation of these predictions validates, at least partially, our initial speculation above. We conclude that the AL is poised in a state of high-gain; ready to respond vigorously to even faint stimuli. After each response the AHP-phase functions to prevent runaway synchronization and to "reset" the AL for another odor-specific response.

Keywords: antennal lobe, afterhyperpolarization (AHP), projection neuron, local neuron, disinhibition, computational model, synchrony, multiple-firing-event (MFE)

OPEN ACCESS

Edited by:
Sylvia Anton,
Institut National de la Recherche Agronomique, France

Reviewed by:
Thomas Nowotny,
University of Sussex, UK
Matthieu Dacher,
Université Pierre et Marie Curie, France

***Correspondence:**
Aaditya V. Rangan
adirangan@gmail.com

Specialty section:
This article was submitted to Invertebrate Physiology, a section of the journal Frontiers in Physiology

Received: *03 October 2015*
Accepted: *18 February 2016*
Published: *08 March 2016*

Citation:
Lei H, Yu Y, Zhu S and Rangan AV (2016) Intrinsic and Network Mechanisms Constrain Neural Synchrony in the Moth Antennal Lobe. Front. Physiol. 7:80. doi: 10.3389/fphys.2016.00080

INTRODUCTION

It has long been understood that recurrent connectivity as well as intrinsic cellular properties both play a role in the dynamics of the insect Antennal Lobe (AL) (Hansson and Anton, 2000; Vosshall et al., 2000; Assisi et al., 2007; Galizia and Rössler, 2010). Nevertheless, it is still unclear how these features interact, and to what extent they influence the functional properties of the AL. In this paper we investigate this question within the hawkmoth (*Manduca sexta*) AL.

The *Manduca* AL itself houses many interneurons, including both Local Neurons (LNs) as well as Projection Neurons (PNs) which send information further downstream (Homberg et al., 1989; Lei et al., 2010). These neurons are organized into functional and morphological modules—a.k.a. glomeruli—which are each stimulated by different classes of odorants. In this paper we largely concentrate on two such glomeruli—named the "cumulus" and "toroid" in male moth—which form the so-called Macroglomerular Complex (MGC) (Matsumoto and Hildebrand, 1981; Christensen and Hildebrand, 1987). This MGC serves as the first central stage of detection and processing of conspecific female sex-pheromones, and plays a crucial role in many of the *Manduca*'s mating behaviors (Schneiderman et al., 1986; Hansson et al., 1991).

Our previous work, along with the work of others, has shown that PNs and LNs within the *Manduca*'s MGC respond—with a vigorous depolarization—to brief puffs of odor containing the appropriate chemical components found in the animal's sex-pheromones (Warren and Kloppenburg, 2014; Kim et al., 2015; Lavialle-Defaix et al., 2015). Intriguingly, the response of the PNs also drops precipitously after each brief odor pulse—a phenomenon we refer to as the "After HyperPolarization" (AHP) phase of each response (Lei et al., 2002; Reisenman et al., 2005). Our previous work has shown that this AHP-phase is somehow implicated in odor-processing: pharmacological manipulation which interferes with the AHP-phase also prohibits *Manduca* from reliably detecting and responding to pheromone pulses (see e.g., Lei et al., 2009). Moreover, similar AHP-like phases have been widely reported as important for the sensory systems of many other animals (Wilson and Goldberg, 2006; Saito et al., 2008). Thus, rather than being a mere curiosity, the AHP-phase seems to be a rather general dynamical feature which plays a necessary functional role in sensory processing.

Our goal in this paper is to probe the dynamical mechanisms responsible for the AHP-phase and its associated currents within the *Manduca* AL. As mentioned above, we expect these mechanisms to include both intrinsic cellular properties (see e.g., Pedarzani et al., 2005), as well as recurrent connectivity (see e.g., the role played by GABA-B receptors discussed in Otmakhova and Lisman, 2004; Wilson and Laurent, 2005). Some intrinsic and recurrent mechanisms have also been studied in the modeling work done by Belmabrouk et al. (2011a,b). By clarifying how these mechanisms either compete or assist one another, we hope to reveal some of the computational principles at work in the olfactory system.

The main conclusions of this paper are that the dynamics of the hawkmoth antennal-lobe are consistent with: (a) strong heterogeneous inter- and intra-glomerular synaptic connectivity, and (b) slow inhibitory intrinsic currents acting on the PNs. Feature (a) grants the AL a kind of automatic-gain-control—i.e., allowing the AL to respond very sensitively to faint odor puffs with the robust activation of multiple PNs—involving a kind of synchrony we refer to as "multiple-firing-events." Feature (b) protects such a sensitive AL from "runaway synchronization," allowing the AL to respond effectively to sequences of odor-stimuli separated by a few hundred milliseconds.

The Results section of our paper is organized as follows. First, in Section R1 we describe some of our experimental results. These experiments involve the application of various pharmacological agents to the AL, and motivate our computational model, which we discuss in Section R2. We use our computational model to try and understand the kinds of dynamics which underlie the phenomena we observe in experiment. This computational model then informs several predictions (Section R3), some of which we test in Section R4. Finally, we close with a discussion; touching on possible consequences of our investigation, as well as related work.

MATERIALS AND METHODS

In this section we give an overview of our experimental and computational methods. This section is reinforced by material in the online Supplementary Information.

Insect Preparation

Manduca sexta (L.) (Lepidoptera: Sphingidae) were reared in the laboratory on artificial diet under a long-day photoperiod, and adult male moths, 4 days post-emergence, were prepared for experiments as described previously (Hansson et al., 1991). For electrophysiological recordings, the moth was restrained in a plastic tube with its head fully exposed. The labial palps, proboscis and cibarial musculature were then removed to allow access to the brain. To eliminate movement, the head was isolated and pinned to a wax-coated glass Petri dish with the ALs facing upward. Tracheae and a small part of the sheath overlying one AL were then removed with fine forceps. The preparation was continuously superfused with physiological saline solution containing 150 mM NaCl, 3 mM CaCl2, 3 mM KCl, 10 mM TES buffer (pH 6.9), and 25 mM sucrose.

Electrophysiological Recording

To allow long-term recording from single neurons, which is needed for the pharmacological experiments in this study, we used a juxtacellular recording technique modified from Pinault (1996) and tested in Lei et al. (2009). In short, electrodes resembling those used for patch recording were pulled from thin-wall borosilicate glass capillaries using Sutter P-2000 laser puller and filled with physiological saline, resulting in <10 mΩ electrode resistance. An Axoprobe-1A amplifier connected to a 10x DC amplifier (Model FC-23B, WPI, Sarasota, FL) was used to amplify the signal up to 1000x. Calibration pulses from the Axoprobe-1A amplifier were added to the output channels. A Leica micromanipulator was used to advance the electrode into the MGC region of an AL until a contact similar to that used for

perforated-patch recording was achieved. A key technique in this configuration is to bring the electrode tip close to a neurite, nearly touching but not impaling it. We found that the amplitude of the recording was affected by the closeness of the electrode tip with the neurite. During the course of an entire experiment the relative position between the juxtacellular-electrode and neurite may drift, causing visible changes in the amplitude of the recorded spikes, but not their frequency or timing.

Sensory Stimulation and Characterization of Neurons

Olfactory stimuli were delivered to the preparation by injecting odor-laden air puffs onto a constant air flow that was controlled at 1 liter per minute. The flow was directed at the middle of the antenna ipsilateral to the AL from which recordings were made. Trains of 5 air puffs (50 ms) with 2 s inter-pulse intervals were generated by means of a solenoid-activated valve controlled by an electronic stimulator (WPI, Sarasota, FL). Shorter or longer intervals were used in particular experiments to test the effect of intervals on response consistency (**Figure 2**). These air puffs were directed through a glass syringe containing a piece of filter paper, bearing various amounts of a single pheromone component (0.1–100 ng in decadal steps). Not every concentration was used in all experiments. The stimulus compounds used were: (i) E10,Z12-hexadecadiennal (EZ, the primary component of the conspecific female's sex pheromone); (ii) E11,E12,Z14-hexadecatriennal (EEZ, a second essential component of the sex pheromone). MGC-PNs were characterized using 3 physiological criteria: (1) randomly bursting spontaneous firing pattern; (2) response specificity to pheromone components; and (3) multiphasic pattern of responses. In *M. sexta*, uniglomerular MGC-PNs have been shown repeatedly to give predictable responses to the pheromone components according to the MGC glomerulus in which their dendrites arborize (Christensen and Hildebrand, 1987; Heinbockel et al., 1999, 2004; Lei et al., 2002): Cumulus PNs are excited by antennal stimulation with EEZ but inhibited (or not affected) by stimulation with EZ, whereas the Toroid PNs are excited by stimulation with EZ but inhibited (or not affected) by stimulation with EEZ. These types of PNs typically exhibit a biphysic response pattern in juxtacellular recordings, i.e., a depolarization phase followed by a period of afterhyperpolarization (Lei et al., 2009). Finally, the spontaneous activity of MGC-PNs typically is more randomly bursting, while that of LNs is more tonic (Lei et al., 2011).

Pharmacological Manipulation

Picrotoxin, bicuculline methiodide, L-2-4-diaminobutyric acid and nipecotic acid (Sigma-Aldrich, >95%) were diluted in physiological saline solution to 200 μM and then bath-applied to moth preparations as described previously (Lei et al., 2009). In short, pharmacological agents were applied to moth preparations through a syringe drip system. The time when the drugs took effect was determined by observing the change of spontaneous activity of the recorded neuron. Spontaneous activity and odor-evoked responses were first recorded under the normal physiological saline solution and then repeated under the drug treatment, and finally the normal saline wash. Note that the final saline wash was typically applied many minutes after the initial recordings, during which the juxtacellular electrode may drift slightly, reducing the amplitude of the recorded spikes (see e.g., **Figure 4A**).

Data Acquisition and Analysis

Spike traces were digitized at 25 kHz sampling rate using Datapack 2k2 software (Run Technologies, Mission Viejo, CA), and the time stamp of each spike was extracted off-line with the event-extraction function within the software package. The spike train data (columns of time stamps) were imported into a custom-written Matlab (The Mathworks Inc, Natick, MA) script, which calculates interspike-interval derived parameters such as mean instantaneous firing-rate and duration of the afterhyperpolarization. To determine the width of the response window, the spike train data were exported into Neuroexplorer (Nex Technologies, Littleton, MA) for plotting the peri-stimulus time histograms (PSTH), which allowed approximate estimation of response duration. Then the average of instantaneous spiking frequency (i.e., inverse of inter-spike interval) within the response window was calculated. We chose a 500 ms period starting from 120 ms after the onset of solenoid opening as response window. We also examined different window size such as 400, 600, and 750 ms and found no significant changes on our quantification of responses. This robustness may be due to the fact that the measurement is derived from averaging individual interspike intervals (ISI). In order to measure the duration of the afterhyperpolarization, we compared the ISI in a sequential manner after the stimulus onset. If an interval is at least 5 times longer than its previous interval, this later interval is considered as the afterhyperpolarization. All statistical comparisons were performed using the Statistics Toolbox of Matlab. To statistically compare the pharmacological effects in a balanced data set (i.e., across the same group of neurons at different stages, such as control vs. drug vs. wash), we selected the non-parametric Friedman's test (**Figures 4**, **8**). Where there were only two groups in comparison (**Figures 6**, **9**), we selected the non-parametric Mann-Whitney *U*-test. In both tests, the cut-off for type-I error were set at the 5% level (i.e., alpha = 5%). Following the Friedman's test, the Tukey-Kramer multi-comparison method was applied to determine the pairwise significance level.

Computational Model

We constructed a spiking network model of the AL with a modest number of architectural features—allowing it to simulate certain kinds of AL phenomena—while at the same time having few enough parameters to allow for serious benchmarking and subsequent investigation. While we sketch out our model in this section, the full details of our model are contained within the Supplementary Information.

The network model discussed in this paper contains PNs, as well as two subclasses of local neurons: LN1s and LN2s. These neurons (totaling several dozen altogether) are organized into clusters that represent distinct glomeruli. The neurons are interconnected, both within each glomerulus and across glomeruli. This connectivity is illustrated in **Figure 1**.

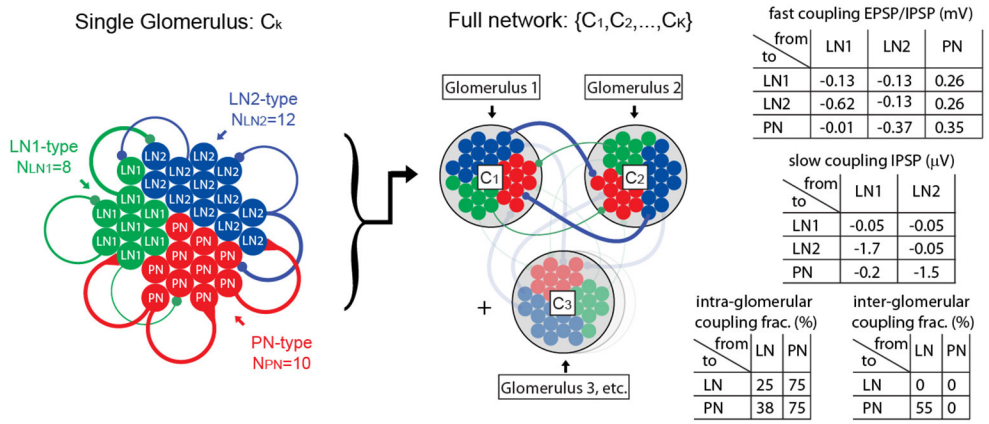

FIGURE 1 | Illustration of computational network architecture. On the left we illustrate the anatomy of a single glomerulus, comprising 10 PNs, 8 LN1s, 12 LN2s, each modeled using single-compartment integrate-and-fire equations. These neuronal populations are connected together sparsely via local intra-glomerular connections. Representative connections are illustrated in this diagram with colored lines, the thickness of which roughly corresponds to the coupling strength. In the middle we illustrate our full network, comprising K glomeruli (e.g., K = 2–6). The neuronal populations within each of these glomeruli are connected together sparsely via long-range inter-glomerular connections; these long-range connections have the same synaptic strength as the intra-glomerular connections, but are randomly connected using different sparsity coefficients. On the right we list a few tables for the synaptic coupling strengths (given in terms of approximate EPSP and IPSP amplitudes), and sparsity coefficients. A full description of the network, as well as the parameters involved, is given in the Supplementary Information.

Within our network model, each neuron is modeled by a single-compartment integrate-and-fire equation, driven by a combination of intrinsic, feedforward and synaptic currents:

$$\tau_V \frac{d}{dt} V(t) = -\left(V - V^L\right) + I^{SK} + I^{input}_{fast} + I^{syn,LN1}_{fast} + I^{syn,LN1}_{slow} + I^{syn,LN2}_{fast} + I^{syn,LN2}_{slow} + I^{syn,PN}_{fast},$$

The intrinsic currents determine how each neuron responds to stimuli, and are different for the different neuron types (e.g., *PN*s are equipped with *SK*-channels). The feedforward-input currents are independent (uncorrelated) between neurons, and are given by a feedforward Poisson input with time-varying rate. This feedforward Poisson input rate—which again depends on neuron type—comprises both a background (low rate) plus the time-varying stimulus-induced input (which can be high rate).

The synaptic currents involve recurrent nicotinic-type excitation (2 ms timescale), as well as GABA-A-type inhibition (2 ms timescale), as well as a slower synaptic inhibition (e.g., GABA-B-type with a ∼750 ms timescale). The coupling strengths depend on the pre- and post-synaptic neuron types (e.g., the LN1 population inhibits the LN2s differently than the PNs). In our model we assume that local neurons (LN1s and LN2s) are inhibitory, whereas PNs are excitatory. We do not explicitly model any excitatory local neurons (see Olsen et al., 2007, as well as Shang et al., 2007), although the effective inter- and intra-glomerular excitation associated with such neurons might be similar to the excitatory effects of our PNs (see Huang et al., 2010).

The recurrent connectivity matrix for our network is chosen to be an Erdos-Renyi random graph (i.e., each edge chosen independently with some given coupling probability) with coupling probabilities that are functions of the pre- and post-synaptic neuron type and are slightly different for inter-glomerular connections vs. intra-glomerular connections.

As we will discuss below, we use our model to conduct numerical simulations: we subject our model to various stimuli while attempting to mimic a variety of experimental conditions. One important detail within this methodology is how we translate PTX and BIC application from the real world to our model. For our purposes, we will simulate PTX application as though PTX reduces the efficacy of GABA-A type receptors. When our model is operating under the influence of PTX (i.e., "PTX-on" condition), the postsynaptic currents associated with GABA-A synapses will be reduced by 75%. We similarly reduce by 75% the postsynaptic GABA-A currents under BIC application. In addition, we drastically reduce the SK-currents under this "BIC-on" condition (as motivated by the discussion in Section R1). Going forward, we will compare and contrast the behavior of our model in the PTX-on and BIC-on conditions with the "control" or CTRL-condition (i.e., CTRL = fully functional GABA-A and SK currents).

We emphasize two important features of our network are:

(1) We ensure that the inhibitory synaptic connections made by our LNs are "heterogeneous"; i.e., the distribution of post-synaptic connection strengths varies widely across the LN population. As mentioned above, we enforce this heterogeneity by dividing our LNs into two "subclasses" labeled LN1 and LN2. While both subclasses of LNs are connected sparsely and randomly to the other neurons in our model, the distribution of connection strengths is different for the LN1 and LN2 subclasses. This heterogeneity implies that some LNs will mostly inhibit PNs, without inhibiting too many other LNs, whereas some other LNs will do

the opposite. This heterogeneity is crucial for allowing our model to facilitate PTX-on disinhibition of the PNs (see Section R1 for discussion).

(2) We ensure that the PNs are equipped with intrinsic SK-currents. These inhibitory currents are driven by each PN's own firing, serving to prevent that PN from firing multiple times in a row. Once elevated, this current persists for quite some time, decaying after ∼400 ms. The presence of such a persistent intrinsic inhibitory current is crucial for allowing our model to facilitate the BIC-on shortening of the AHP-phase (see Section R1 for discussion).

Benchmarking the Model

The model described above has several parameters which influence its dynamics. These parameters include both the strength and sparsity of the synaptic connections, as well as the strength of the intrinsic SK-currents and feedforward currents. Many of these parameters are constrained somewhat by physiology (e.g., the synaptic coupling strengths must be compatible with the observed sizes of EPSPs and IPSPs). Nevertheless, even as these parameters are varied within physiological bounds, the network can still produce a wide variety of dynamical regimes, ranging from the physiologically realistic to the unrealistic.

In order to further constrain these network parameters we "benchmark" our model. That is, we choose a variety of experimentally observed phenomena associated with the real AL (i.e., benchmarks) and demand that our network satisfy these benchmarks. Given any particular set of parameters—thought of as a point in parameter space—our network will operate within a particular dynamical regime and, generally speaking, few-to-none of these benchmarks will be satisfied. Our goal is to find a region in parameter space that corresponds to dynamical regimes that satisfy *all* of our benchmarks; we hope that these dynamical regimes will be "realistic" to some extent.

Our benchmarks are listed below:

(1) Firing-rates, EPSPs and IPSPs: In the real AL, PN and LN firing-rates are between 5 and 15 Hz in background (i.e., when unstimulated), and usually between 40 and 80 Hz when stimulated. EPSPs and IPSPs are usually smaller than 1 mV. We require that corresponding values for our network lie within these acceptable ranges.

(2) Pulse-response attenuation: In the real AL, the PNs will respond less vigorously to an odor puff if that puff was immediately preceded by a previous puff. This phenomenon gives rise to attenuation of the PN response to a rapid sequence of odor pulses. We require that our network exhibit a similar attenuation when stimulated with simulated odor pulses. Compare **Figure 2** and **Figure 3**.

(3) PTX response when unstimulated: This benchmark is intended to capture the phenomena discussed in Section R1. As mentioned above, the pharmacological application of PTX to the real AL is translated in our network to the reduction of GABA-A presynaptic currents by ∼75%. We require that, when compared against CTRL, the PTX-on condition exhibit both (i) a reduction in spontaneous PN firing-rates, as well as (ii) an increase in the typical spontaneous PN ISIs. Compare **Figure 4** and **Figure 5**.

(4) PTX response when stimulated: This benchmark is intended to capture the effects of PTX on the PN response to a train of odor pulses. As per experiment, we require that (i) the mean PN response per pulse for the PTX-on condition should

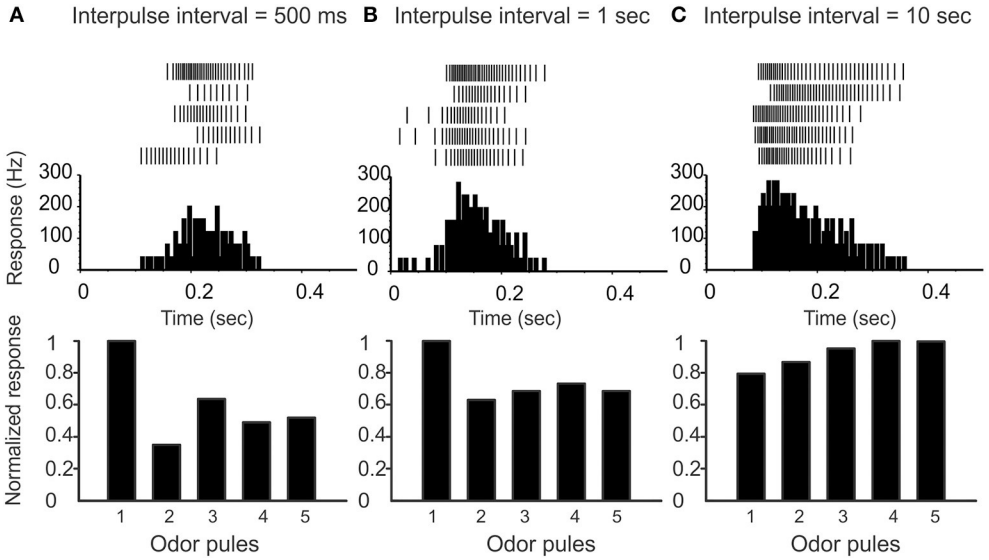

FIGURE 2 | Varying the inter-pulse-interval (IPI) affects the attenuation of PN responses. (A) On top we show raster-plots of a PN response to five pulses in sequence (IPI 500 ms). The peristimulus-time-histogram is shown in the middle, and the normalized response per pulse is shown on the bottom. Note that there is a marked attenuation of PN response following the first pulse. **(B)** IPI = 1 s, and the attenuation is less marked. **(C)** IPI = 10 s, which is significantly greater than the AHP-phase; there is no attenuation of PN response.

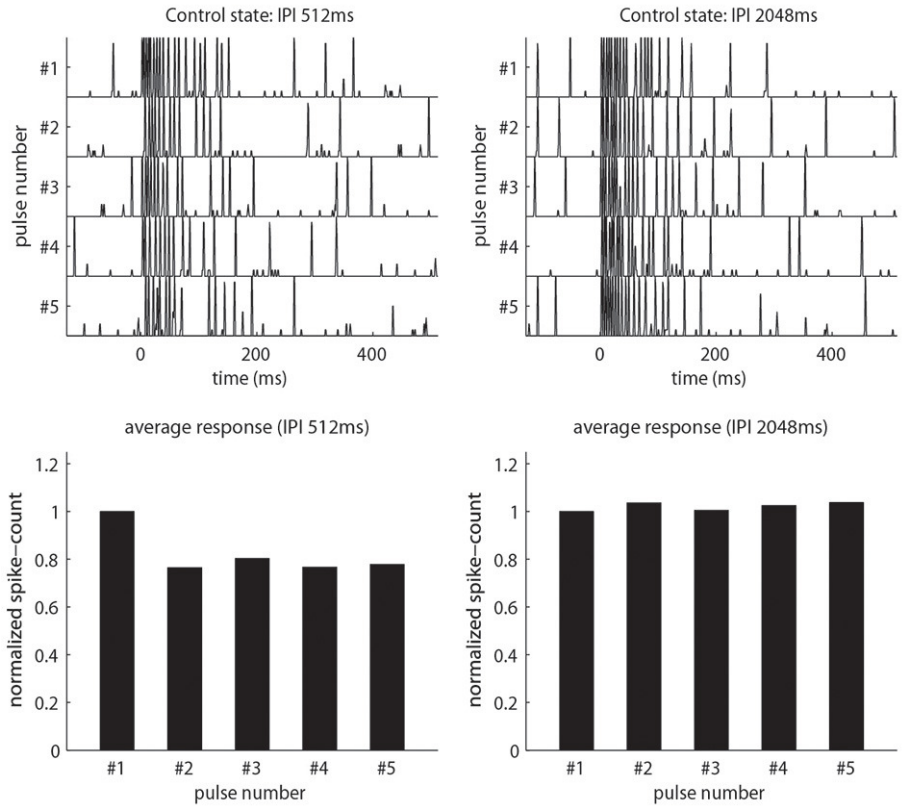

FIGURE 3 | Our model qualitatively reproduces the pulse-response attenuation seen in Figure 2. On top we show traces of PN-activity for a model glomerulus responding to a sequence of five pulses. On the bottom we show the normalized spike-count per-pulse. On the left we use an IPI of 512 ms. On the right we use an IPI of 2048 ms, which is significantly longer than the AHP-phase.

be comparable to that of the CTRL-condition, whereas (ii) the standard-deviation in PN response per pulse should be significantly higher when PTX is on. Compare **Figure 10** and **Figure 11**.

(5) BIC response when stimulated: This benchmark is intended to capture the phenomena discussed in Section R1. As mentioned above, the pharmacological application of BIC to the real AL is translated in our network to the combination of (i) a reduction of GABA-A presynaptic currents by ∼75%, as well as (ii) a reduction in the strength of the intrinsic SK-currents that follow hyperpolarization of the PNs. We require that, when BIC is on, our model PNs exhibit prolonged responses to odor stimuli; responses that show a much diminished AHP-phase. Consequently, the BIC-on state should reduce PN pulse-response attenuation and prevent PNs from faithfully tracking rapid sequences of odor pulses. Compare (Lei et al., 2009) with Supplementary Figure S7.

(6) BIC response when unstimulated: This benchmark is intended to capture the effects of BIC on the spontaneous state. We require that, when BIC is on, the PNs exhibit slow modulation in their background dynamics, switching between long epochs of periodic firing and long epochs of relative silence (typical epoch length should be several seconds to tens of seconds). Compare **Figure 12** and **Figure 13**.

To actually perform our benchmarking we repeatedly scanned sections of parameter-space by varying one or two parameters at a time, covarying the most influential parameters whenever possible. For each scan we chose the "best" set of parameters (i.e., those which came closest to satisfying our benchmarks) and scanned again; varying different parameters the next time. This repeated parameter-scanning was done by hand (and not automated) so that (i) we could gain some intuition for the vastly different kinds of dynamic-regimes our network was capable of producing, and (ii) we could be sure that our results were not too sensitive to any single parameter. We continued searching until we found a large open region in parameter-space, each point of which gave rise to a rather similar dynamical regime that exhibits all of our benchmarks. **Figure 1** lists sample values for many of these coupling and connectivity parameters for one point within such a region.

After benchmarking our network, we investigated the mechanisms at work within the resulting dynamical regime. We found that the dynamical regime that supported the above phenomena was one of "high-gain," with strong recurrent connectivity that gives rise to multiple-firing-events (MFEs). This regime is discussed at length below in Section R2.

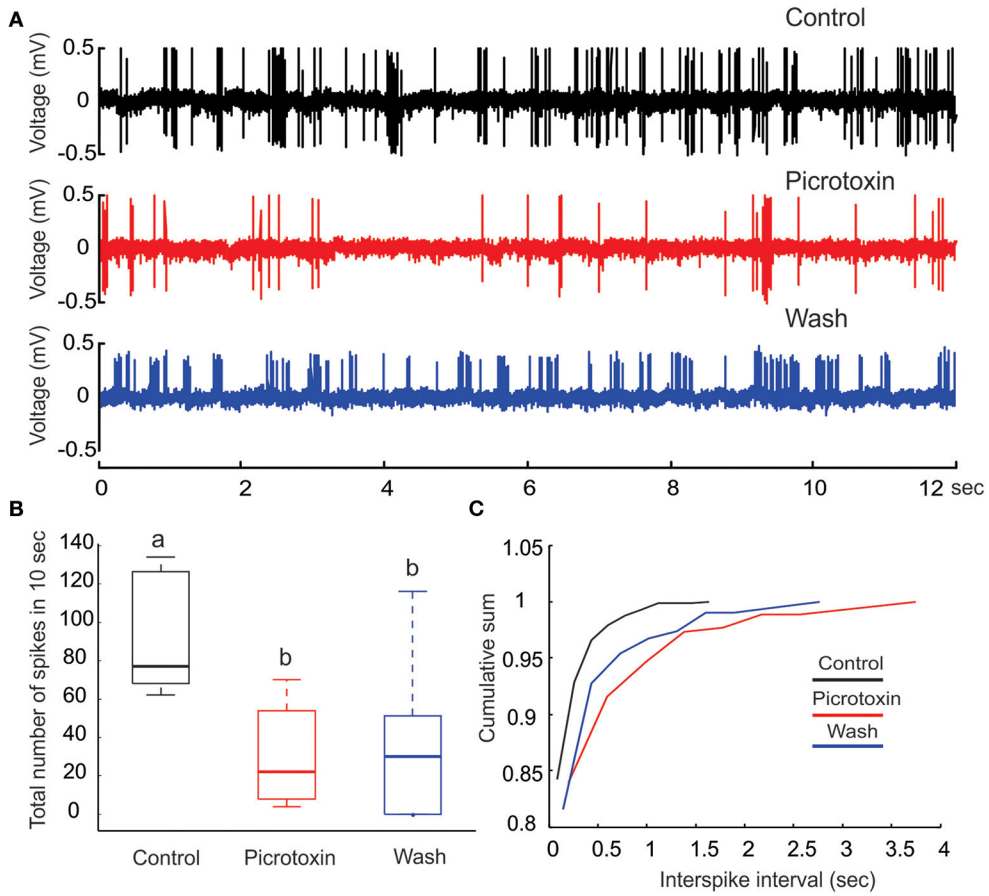

FIGURE 4 | Picrotoxin reduces PN's spontaneous activities. (A) Juxtacellular recording traces (12 s long) show a marked reduction in the number spikes due to the application of picrotoxin. **(B)** The reduction of number of spikes due to picrotoxin is statistically significant (*Friedman* test, $p < 0.01$, $n = 8$) but the effect is not fully reversible. Different letters on top of the box plots indicate statistical significance. **(C)** Cumulative sum of interspike intervals (ISI) shows that the picrotoxin treatment prolongs the maximal ISI to about 4 s (red line) while the maximal ISI under saline control is only about 1.5 s (black line). Moreover, nearly all (about 98%) ISIs under saline control are less than 0.5 s but about 87% of ISIs under picrotoxin are within this range. Saline wash produces a pattern that is between the drug treatment and control (blue line).

RESULTS

Section R1: Initial Experiments

In this section we present some of our experiments which hint at the nature of the after-hyperpolarization (AHP) phase in projection neuron (PN) response. These experiments will strongly suggest that the AHP-phase comprises both inhibitory synaptic currents as well as hyperpolarizing intrinsic currents.

To preface, recall that the "control-condition" (i.e., saline wash, rather than any active pharmacological agent) produces spontaneous PN activity in the range of 6–12 Hz (see, e.g., **Figure 4A**). When stimulated by a pheromone pulse, the PN activity increases vigorously, and is usually followed by an AHP-phase, expressed as a nearly silent period in the raster plots and PSTH following each pulse (see e.g., **Figure 6A**). This AHP-phase not only truncates the excitatory response evoked by each odor pulse but also lasts for about a second or so. As a result, the AHP-phase caused by any given odor pulse can interfere with—and reduce—the magnitude of excitatory response to any subsequent odor pulse occurring shortly after the first. To quantify this attenuation, we stimulate the MGC with a rapid sequence of five successive odor pulses (see methods) characterized by an "inter-pulse-interval" (IPI) ranging from IPI = 0.5–10 s. As expected, the PN response shows a marked attenuation when the IPI is less than or equal to the observed duration of the AHP (see **Figure 2**). On the other hand, when the IPI = 2 s or longer, the AHP from each pulse dies away before the next pulse arrives, and so the AHP does not significantly affect the PN response across pulses (i.e., there is little to no attenuation when IPI $\geq$ 2 s).

Our first set of experiments perturbs the scenario above through the pharmacological application of picrotoxin (PTX) to the MGC. PTX has been shown to be an effective GABA-A receptor antagonist in both vertebrate and invertebrate preparations (Newland and Cull-Candy, 1992; Anthony et al., 1993; Laurent et al., 1999; Lee et al., 2003; Choudhary et al., 2012; Warren and Kloppenburg, 2014). Consequently, we expect PTX application to increase the PN response. However, to the contrary:

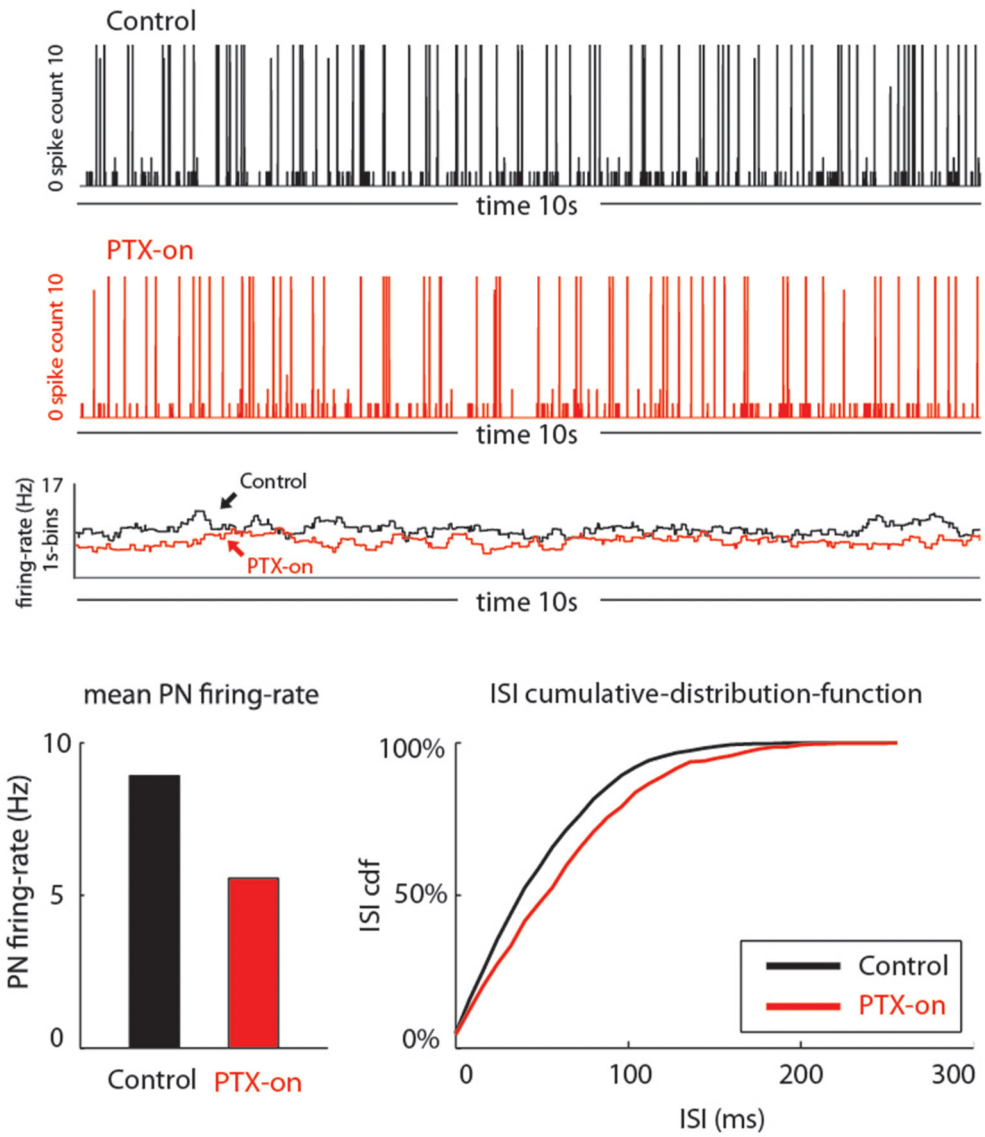

FIGURE 5 | Our model qualitatively reproduces the PTX-induced phenomena seen in Figure 4. On top we show traces of PN-activity for a model glomerulus in background, both in the control state (black) and PTX-on state (red). Below these traces we plot the time-averaged PN firing-rate (averaged over 1 s bins). On the bottom we show the average PN firing rates (left) and cumulative-distribution-function for the ISI-intervals (right).

PTX Decreases PN's Spontaneous Activity

Under our experimental conditions, perfusing the moth AL with PTX (200 μM) significantly reduced the level of spontaneous activities on PNs (**Figures 4A,B**; *Friedman* test, $p < 0.01$, $n = 8$). Despite a reduction of the number of spikes (from 70 to 120 with median of 79 in a 10-s window to 10–50 with median of 20, **Figure 4B**), the bursting pattern was not altered (**Figure 4A**, middle panel). Apparently, the reduction of number of spikes was primarily caused by the increase of ISI, especially those intervals between the bursts. This inference was further confirmed by plotting the cumulative probability sum of ISI across saline control (812 ISIs pooled from eight neurons), PTX treatment (261 ISIs) and saline wash (309 ISIs; **Figure 4C**). Without PTX (i.e., saline control), the maximal ISI was 1.72 s (**Figure 4C**, black line), but this number went up to 3.95 s with PTX, an increase of 129% (**Figure 4C**, red line). Moreover, the distribution of ISIs associated with the saline control group was shifted (toward shorter ISI times) relative to the distribution of ISIs associated with the PTX treatment. For example, 95% of the control-ISIs were shorter than 0.2 s, whereas this range only comprised about 85% of the ISIs under PTX-treatment. Saline wash did not reverse the ISI distribution to the control pattern completely, but rather to a pattern between the saline control and drug treatment (**Figure 4C**, blue line).

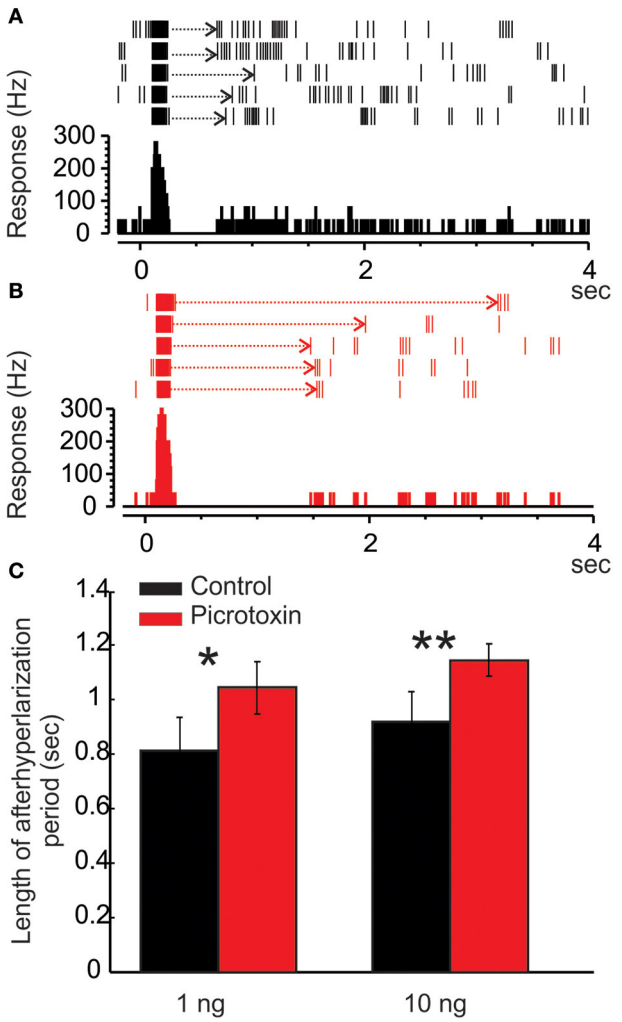

FIGURE 6 | Picrotoxin increases the duration of afterhyperpolarization (AHP). (A) Raster plot and peristimulus histogram show a typical excitatory response of a Toroid PN to five pulses of EZ stimulation. The stimulus onset is at time zero and lasts for 50 ms. Note the AHP (dotted arrows) following the bursts of excitatory responses. **(B)** Under the picrotoxin treatment, the duration of AHP is significantly increased, along with a reduced spontaneous activity. **(C)** Group data showing that the picrotoxin-induced increase of AHP duration is statistically significant either under 1 or 10 ng stimulation (*Mann Whitney U*-test, $p < 0.05$ or 0.01, $n = 8$; asterisks indicate the significance level).

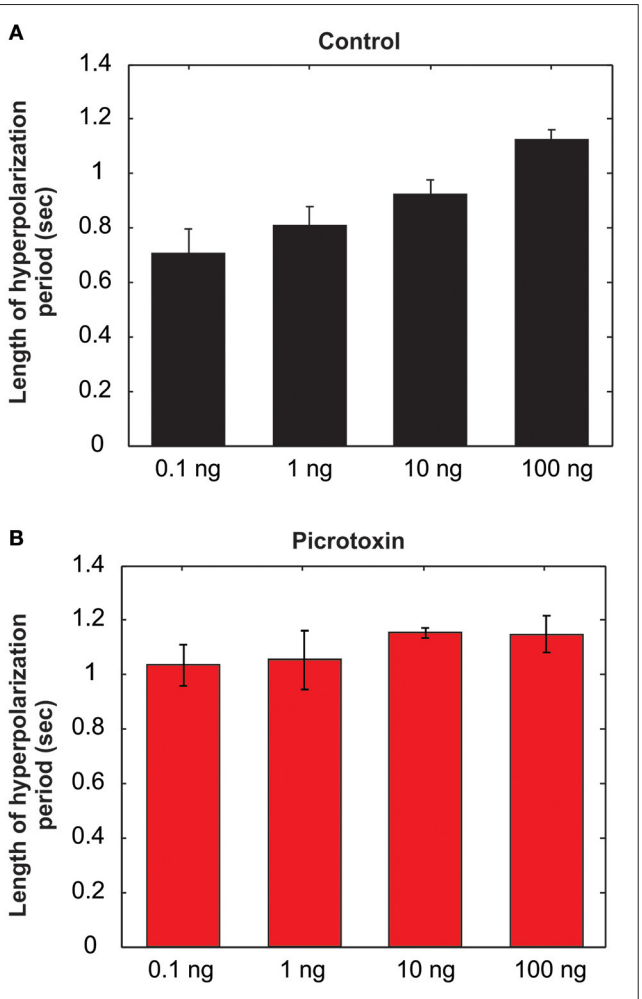

FIGURE 7 | The length of the afterhyperpolarization (AHP) period is positively related to the odor concentrations under saline control (A), but the linear relationship is lost after picrotoxin treatment (B) ($N = 8$).

In addition to measuring the effects of PTX on spontaneous activity, we also measured the effects of PTX on the AHP-phase. We observed that:

PTX Increases the Duration of PN's AHP Phase

As mentioned above, the MGC PNs' excitatory response to pheromones is usually followed by an AHP-phase, expressed as a gap in the raster plots and PSTH (**Figure 6A**, dotted arrows). The length of the AHP period was significantly increased by PTX application (**Figure 6B**, dotted arrows). Because the AHP is positively correlated with odor concentrations (**Figure 7A**), we also compared the PTX effect on low (1 ng) and high (10 ng) dose evoked responses. In both cases, PTX significantly increased the length of AHP (*Mann Whitney U*-test, $p < 0.05$ or 0.01, $n = 8$; **Figure 6C**). Interestingly, PTX application disrupted the linear correlation between odor concentrations and the duration of AHP (**Figure 7B**).

Thus, despite the fact that PTX is a GABA-A receptor antagonist, perfusion of PTX actually enhances the inhibitory modulation of the PNs. Moreover, because PTX increases the duration of the AHP-phase, these effects likely stem from an increase in the inhibitory currents responsible for the AHP-phase, and not to secondary-effects of PTX which might block nicotinic-excitation (as seen, e.g., in honeybee, see Barbara et al., 2005). Based on these considerations, we will explore the hypothesis that the PNs may be involved in a disinhibitory network operating within the MGC or even spanning the AL (for motivation, see Christensen et al., 1998a or Buckley and Nowotny, 2011).

As a very simple example of such disinhibition, one may consider a 3-neuron circuit consisting of a single local neuron (LN1) inhibiting a second local neuron (LN2) which inhibits

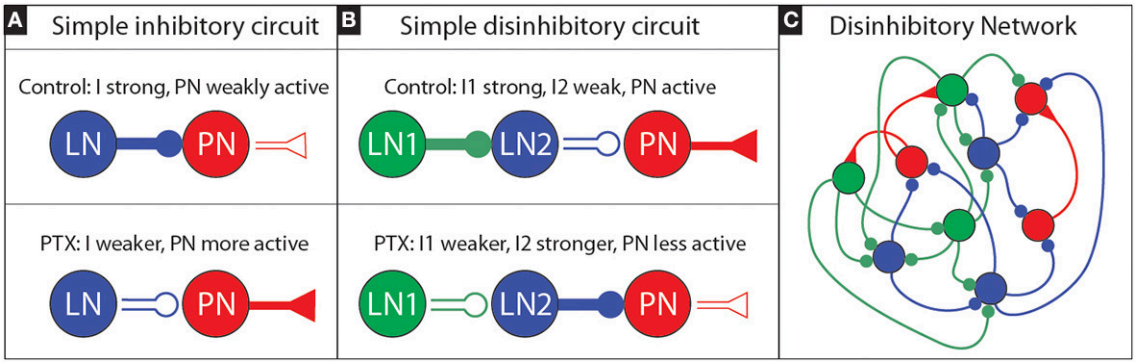

FIGURE 8 | Sketch of an inhibitory and disinhibitory circuit, as well as a more realistic disinhibitory network: (A) We illustrate a simple inhibitory circuit, involving a single LN which produces presynaptic inhibitory current I that inhibits a single PN. Under PTX we expect the efficacy of inhibitory synapses to decrease; thus I should get smaller, implying that the PN activity will increase. **(B)** We illustrate a simple disinhibitory circuit, involving an LN1 which produces a presynaptic inhibitory current I1 that inhibits another LN2. This LN2, in turn, produces a presynaptic inhibitory current I2 that inhibits a single PN. If the activity level of the first LN1 is high, we may expect LN2 to be only weakly active, and for the PN to be active. Under PTX we expect that the efficacy of inhibitory synapses will decrease: as a result I1 will decrease, and so the activity level of LN2 will increase. This increased activity level—combined with the now decreased efficacy of inhibitory synapses—will alter I2. If the activity level increase of LN2 is sufficiently large, it is possible for I2 to actually increase overall (even though PTX has been applied). As a consequence, it is possible for the PN activity level to actually decrease overall—even though PTX has been applied. **(C)** A more realistic disinhibitory network would involve not just three neurons, but rather a collection of LNs and PNs, with the former heterogeneously coupled. In the heterogeneous network shown we have colored the various LNs according to the role they might play with regards to disinhibition: those LNs that predominantly inhibit PNs are classified as "LN2s" and colored blue, while the LNs that predominantly inhibit the LN2s are classified as "LN1s" and colored green. In reality the roles are not so clear cut; some LNs will both inhibit PNs as well as inhibit other LNs, and it may not always be possible to clearly classify each and every LN into a specific role.

a projection neuron (PN). The layout for this simple circuit is illustrated in **Figure 8**. We'll also assume—for exposition—that this simple circuit is operating in a mean-driven regime (see, e.g., Destexhe and Sejnowski, 2009; Buckley and Nowotny, 2011). In such a regime, each neuron receives independent feedforward input currents that—alone—would be sufficient to cause them to fire at high rates. As we'll discuss next, this mean-driven regime can be understood by analyzing its firing-rates.

The "control" situation for this simple circuit involves LN1 being very active with high firing-rate m_1. In this condition, since LN1 is very active, the inhibitory presynaptic currents to LN2—denoted by "I_1" will be proportional to the LN1 activity. That is to say, I_1 will be roughly $S \times m_1$ for some "synaptic strength" S. The large presynaptic current I_1 will ensure that LN2 is only weakly active, with a firing-rate m_2 which will be a function [i.e., f(·)] of the total input current to LN2. In this case we expect $m_2 = f(E - I_1) = f(E - Sm_1)$, where f depends on both I_1, as well as some background excitatory current E; m_2 should be lower as I_1 increases. The presynaptic inhibition to the PN—denoted by I_2—will be proportional to $f(E - I_1)$, roughly determined by something like $I_2 = S \times f(E - I_1) = Sf(E - Sm_1)$. Because m_1 and S are high, I_1 will be high, so $m_2 = f(E - I_1)$ will be low, so I_2 will be low, and the PN activity will be high.

When PTX is applied to this simple circuit, the situation will change. The LN1 will remain active, but no longer inhibit LN2 as much. If the application of PTX blocks, say, three-quarters of the GABA-A receptors, we might imagine the synaptic-strength S reduced to ¼S. With this reduction the presynaptic inhibition to LN2 is only $I_1 = ¼Sm_1$, and so the new (higher) firing rate of LN2 will be $m_2 = f(E - ¼Sm_1)$. This new firing-rate m_2 might be much higher than before (i.e., the firing-rate may be a nonlinear function of the presynaptic currents), implying that the presynaptic inhibitory current to the PN will change to $I_2 = ¼Sm_2 = ¼Sf(E - ¼Sm_1)$. If f has the appropriate structure, it is certainly possible that I_2 might actually be higher under PTX than under the control condition. In such a situation, we would observe the PN activity drop under PTX.

To be clear, we are not suggesting that each PN in the MGC is the target of an idealized disinhibitory circuit such as in **Figure 8B**, nor that the MGC operates in a mean-driven regime where such a firing-rate analysis is valid. Rather, we are suggesting that perhaps the collection of LNs in the MGC may be interconnected in such a way as to give rise to a similar disinhibitory phenomena– even without any single simple mean-driven disinhibitory circuit existing in isolation (see e.g., **Figure 8C**). Put another way: we suggest that an appropriately *heterogeneous* LN population (i.e., a population of LNs that have varying degrees of connectivity and coupling strength, both to each other and to the PNs) might—as a gestalt—give rise to the PTX-induced phenomena we observed above.

If, indeed, the MGC PNs are targets of such emergent disinhibition, we would expect many of the results we see under PTX to also manifest under other pharmacological agents which increase the overall level of inhibition in the MGC. One way to test this intuition is to use GABA transporter blockers—specifically L-2-4-diaminobutyric acid (L-DABA) and nipecotic acid. These blockers should increase the GABA concentration in the tissue (Mbungu et al., 1995; Oland et al., 2010). As confirmed below, this increase in GABA concentration has similar effects to PTX:

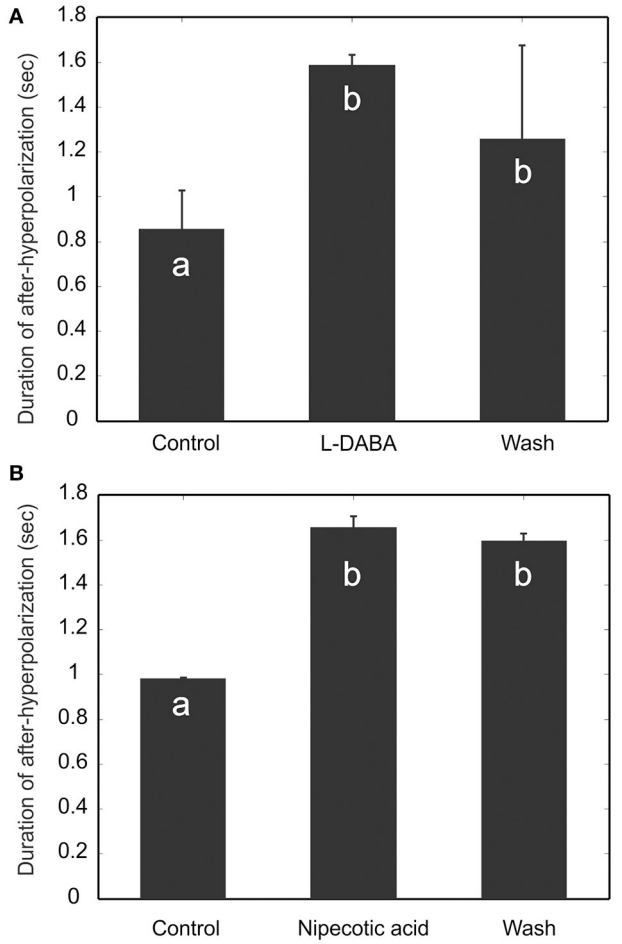

FIGURE 9 | Blocking GABA transporters increases the duration of afterhyperpolarization (AHP). Two GABA transporter blockers, L-DABA **(A)** and Nipecotic acid **(B)**, were used to treat the experimental preparations, and both blockers increase significantly the duration of AHP. The saline wash, however, does not fully reverse the drug effect. Different letters on the bar graphs indicate statistical significance (*Friedman* test, $p < 0.01$, $n = 5$).

GABA Transporter Blockers Enhance AHP

We perfused the AL with GABA transporter blockers, L-2-4-diaminobutyric acid (L-DABA) and nipecotic acid. As expected, both blockers increased the AHP duration significantly (**Figure 9**) (*Friedman* test, $p < 0.01$, $n = 5$). The saline wash, however, did not have significant effects. This could be due to insufficient amount of washing time limited by recording sessions.

Based on the PTX, L-DABA and nipecotic acid experiments above, we concluded that (i) the PNs in the MGC participate in some kind of disinhibitory circuit, and (ii) that disinhibitory circuit gives rise to an inhibitory presynaptic current within the PNs that contributes to the AHP-phase.

While sensible given the experiments we've discussed so far, this conclusion is not obviously consistent with some of our previous experiments involving bicuculline methiodide (BIC; see Lei et al., 2009). To elaborate, BIC is similar to PTX, in that both agents are putative GABA-A receptor antagonists within the *Manduca* AL (Christensen et al., 1998b). Because there may be differences in the affinity of each agent for GABA-A, we don't expect BIC to act in exactly the same way as PTX. Nevertheless, at first blush we expected the effects of BIC to be qualitatively similar to PTX: i.e., to also lengthen the AHP within PN MGCs. To the contrary, however:

BIC Eliminates the PN's AHP-Phase

BIC application substantially reduces the length of the AHP-phase well below ∼200 ms, and sometimes eliminates the AHP-phase altogether. Consequently, under BIC the PN response exhibits a much prolonged excitatory phase, persisting several hundred milliseconds after the pheromone stimulus is removed. In addition, due to the lack of an AHP-phase, the PN response exhibits little to no attenuation from one odor pulse to the next—even when those odor pulses are within 1 s of one another (e.g., an IPI of 512 ms). Thus, this BIC-induced lack of attenuation prevents PNs from faithfully tracking the dynamics of a pulsatile odor stimulus (Lei et al., 2009).

These results are surprising; the BIC induced phenomena within the MGC seem diametrically opposite to the PTX induced phenomena. Thus, even though they are both GABA-A receptor antagonists (Waldrop et al., 1987)[1], PTX and BIC cannot be doing the same thing to the MGC.

One potential explanation for this paradox is that BIC is actually more than just a GABA-A receptor antagonist. Specifically, BIC could also block certain channels within the PNs – channels that give rise to intrinsic currents which, in the absence of BIC, ordinarily contribute to the AHP-phase (for precedent see Villalobos et al., 2004; Pedarzani et al., 2005; Belmabrouk et al., 2011a). While this leap of logic may seem farfetched at first, we believe that there is a natural candidate for such channels: namely, calcium-dependent small-conductance potassium channels (SK-channels). Indeed, in a functional study of cloned SK-channels using *Xenopus* oocytes, BIC was found to block two types of SK-channels (Khawaled et al., 1999).

Although there is no direct molecular evidence that proves that *Manduca* PNs possess SK-channels, there are several pieces of evidence that point toward this possibility:

(1) In the fruit fly, *Drosophila melanogaster*, one type of SK channel was reported. Moreover, this channel is likely important for sensory processing, since the photoreceptors of the mutant flies lacking the gene of this channel produce oscillatory currents that hinder their responses under dim conditions (Abou Tayoun et al., 2011).
(2) In mammals, SK-channels are believed to mediate the AHP-currents following action potentials, both inhibiting cell firing and limiting the firing frequency of repeatable action potentials (Bond et al., 1999; Adelman et al., 2012).

[1]Even though we used different methods to introduce PTX and BIC into the AL—bath perfusion vs. multibarrel pressure injection—we do not believe that this difference in procedure could be wholly responsible for the extreme discrepancies we observed in the PN dynamics.

(3) An SK channel homolog, KCNL-2, has also been characterized in the nervous system of *C. elegans* and is believed to regulate egg laying behavior (Chotoo et al., 2013).

Is it possible that *Manduca* PNs are indeed equipped with SK-channels, and that these channels are both partially responsible for the AHP and blocked by BIC? On the surface, this scenario might be consistent with the experiments described above. Recall that PTX and BIC gave rise to, respectively, a lengthening and shortening of the AHP-phase. Perhaps, as previously discussed, PTX reduces the effectiveness of GABA-A receptors, thus lengthening the AHP-phase of the PNs through a disinhibitory network of LNs. Now BIC should also reduce the effectiveness of GABA-A receptors somewhat, but could also block putative SK-channels within the PNs. While the former alone would reduce the PN activity, just like PTX, the latter could remove a substantial component of the AHP-currents, increasing PN activity. Perhaps a combination of these two effects could somehow result in both the PTX-induced phenomena we see above, as well as the BIC-induced phenomena observed in Lei et al. (2009).

Going forward, we will explore this possibility: We will use computational modeling to investigate the scenario sketched out in the previous paragraph. More specifically, we will create a spiking neuronal network that has (a) strong heterogeneous recurrent connectivity across the LN population, and (b) SK-channels within the PNs. We will determine whether or not it is even possible to benchmark such a network against the PTX- and BIC-induced phenomena described above. In doing so, we'll expose mechanisms that may be at work within the MGC or, more generally, across many glomeruli within the AL.

Before we embark on such a project, we comment on two somewhat more subtle phenomena we have observed; the first relating to PTX application, the second to BIC:

PTX Disrupts PN's Response Consistency across Repeated Isolated Stimuli

Recall that, in response to isolated pulses of pheromonal stimuli, the MGC PNs typically generate bursts of action potentials tracking each stimulus pulse (**Figures 10A,B**). Because the inter-pulse-interval (IPI = 2 s) in this case was sufficiently greater than the typical AHP-length (compare, e.g., **Figure 6C** with **Figures 10A,B**), the response from one pulse did not "interact" with the following pulse; consequently, there was little to no attenuation of the PN response across pulses. The same holds under PTX application, which did not significantly change the PNs' response magnitude, measured as the mean instantaneous firing rate during the response window across odor pulses

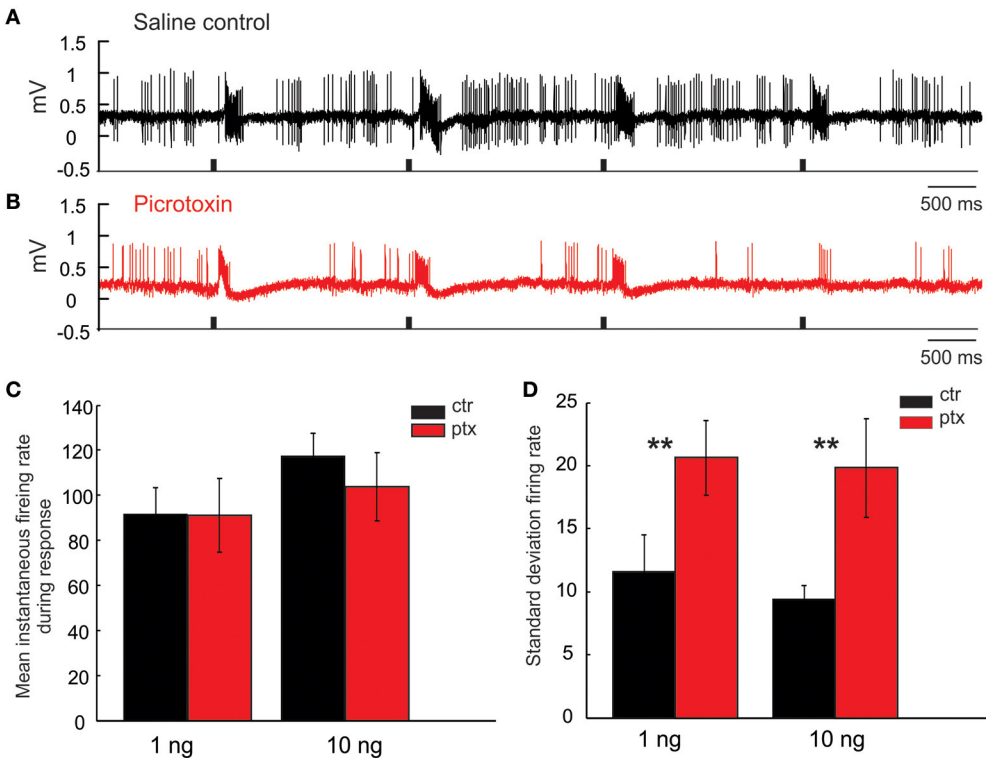

FIGURE 10 | Picrotoxin increases response variations. (A,B) Juxtacellular recording traces show the responses of a Toroid PN to four pulses of EZ stimulation under saline control (black trace) and picrotoxin treatment (red trace). **(C,D)** Picrotoxin does not significantly change the mean instantaneous firing rate during the response window either to 1 or 10 ng stimulation; however, the treatment significantly increases the response variation measured by the standard deviation of firing rate across odor pulses (*Mann Whitney U*-test, $p < 0.01$, $n = 8$; asterisks indicate the significance level).

(**Figure 10C**, *Mann Whitney U*-test, $p > 0.05$, $n = 8$). However, under PTX, the excitatory responses from pulse to pulse were not as consistent as those under the saline control, shown by a significant increase of the standard deviation of the mean instantaneous firing rate across all 5 odor-evoked responses (**Figure 10D**, *Mann Whitney U*-test, $p < 0.01$, $n = 8$). These drug effects were similarly observed when using low (1 ng) or high (10 ng) concentration of odors (**Figures 10C,D**). See **Figure 11** for comparison with our model.

BIC Introduces Structure into the PN Spontaneous Activity

When unstimulated, the MGC PNs usually produce sporadic spontaneous activity with no obvious structure. Under BIC application, the spontaneous PN activity can change into a long-lasting structured pattern, which alternates between epochs of fast-periodic-spiking and epochs of near total quiescence. The epochs of fast-spiking are characterized by ISI-intervals of ~50 ms, whereas the quiescent epochs have firing-rates near 0 Hz. The epochs can each last for several tens of seconds, and alternation between the spiking and silent epochs continues for as long as BIC is supplied. The transition between any given spiking epoch and the subsequent silent epoch can be very abrupt—often much less than 100 ms—and sometimes even instantaneous. While we had originally observed this phenomenon in our previous work (Lei et al., 2009), we confirmed it once again with a new set of experiments. In these recent experiments we again observed BIC-induced spontaneous activity patterns, this time with even more variation than what we had originally seen in 2009. Although the spiking activity was generally increased by BIC application, only one MGC PN exhibited extreme rhythmicity when alternating between quiescent and spiking epochs (asterisk in **Figure 12A**). The other MGC PNs also exhibited long-lasting epochs of spiking as well as quiescent epochs, but were less rhythmic (Rows 1–3 of raster plots in **Figure 12A**).

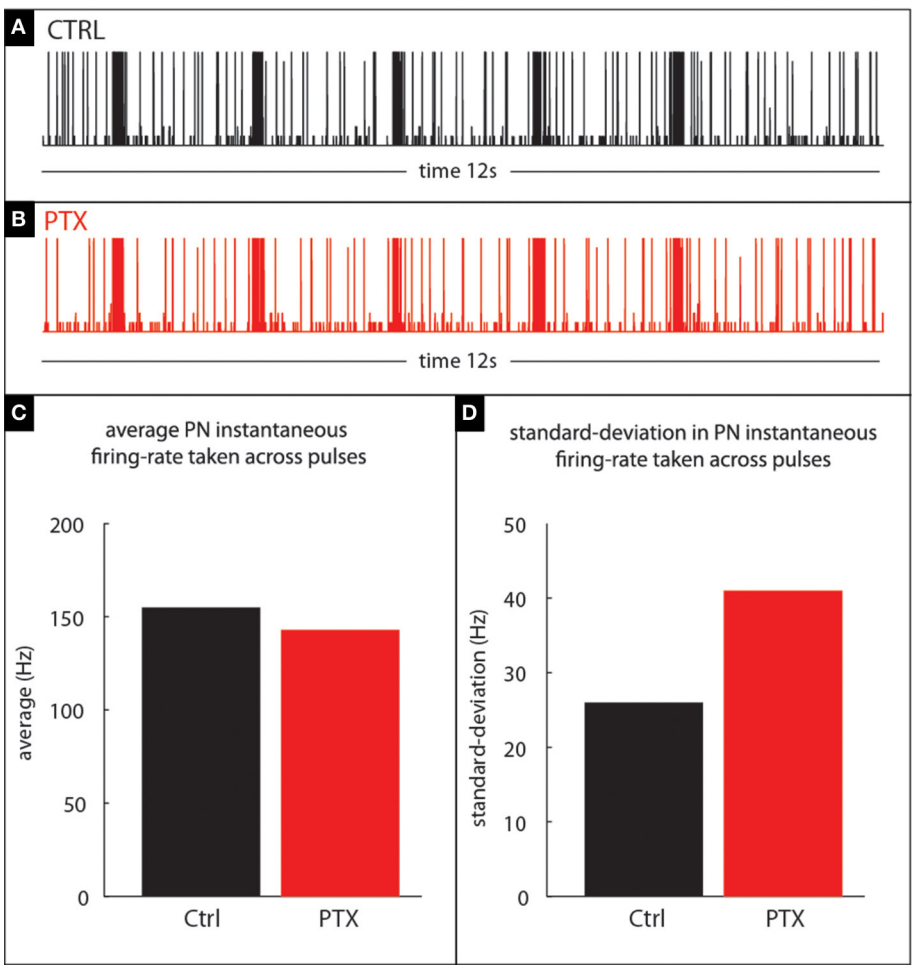

FIGURE 11 | Our model qualitatively reproduces the PTX-induced phenomena illustrated in Figure 10. (A,B) PN-activity for a model glomerulus subject to a train of stimulus pulses separated by an IPI of 2 s. **(C)** The PTX-on state induces small changes in the mean PN-response—i.e., instantaneous firing-rate—averaged across pulses. **(D)** The PTX-on state induces larger changes in the standard-deviation (across pulses) of PN-response.

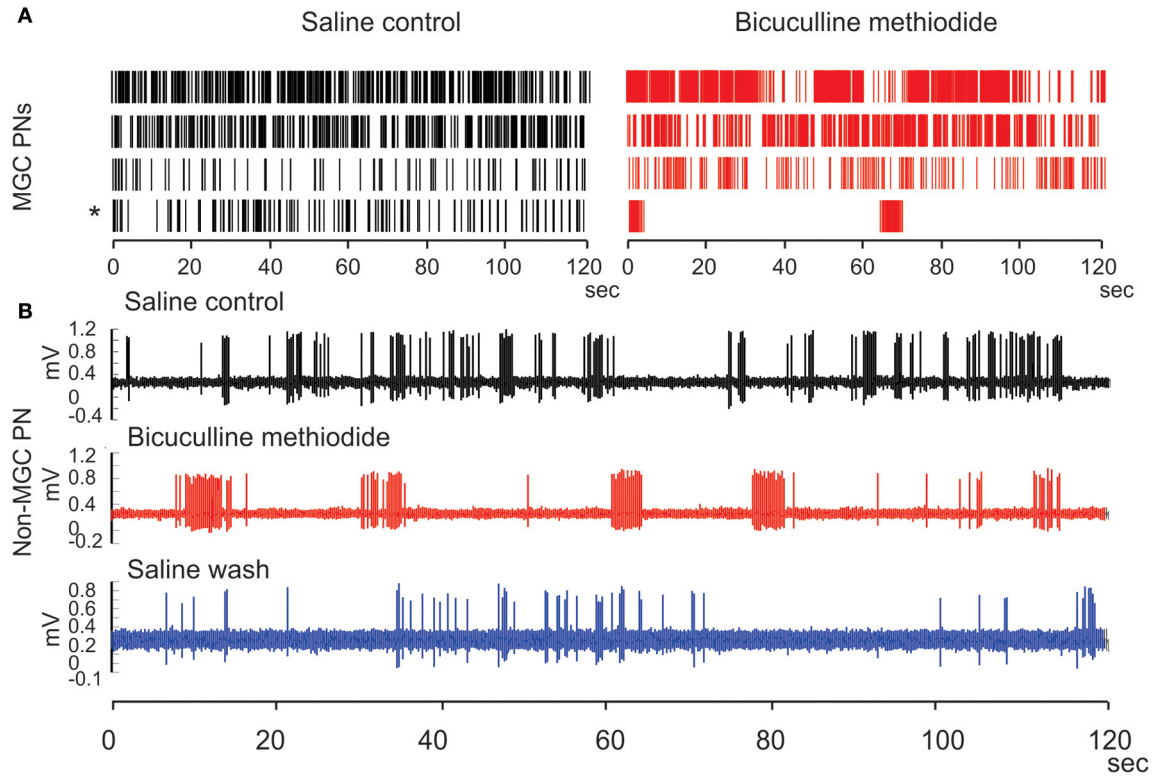

FIGURE 12 | Bicuculline methiodide (BIC) alters the spiking patterns of the spontaneous activity of PNs both in the MGC and in the ordinary glomeruli. **(A)** Raster plots show that BIC treatment generally increases the spontaneous activity level of MGC PNs, opposite to the picrotoxin treatment, and produces the run-away pattern (asterisk) in some PNs. **(B)** Such run-away patterns are also present outside the MGC when BIC is used, verifying the predictions from the network model.

These two phenomena both expose rather specific dynamic features of the MGC and neither is an obvious epiphenomenon of the mechanisms we have proposed so far. To elaborate, even if PTX does disrupt a disinhibitory network involving the PNs, why would such a disruption necessarily reduce the consistency of PN response across isolated pulses? Furthermore, even if BIC does block SK-channels—which have dynamics in the 100–500 ms range—why would blocking these channels give rise to structured spontaneous activity on a 10 s time-scale?

Thus, to further constrain and validate our computational modeling, we will use the above two phenomena as additional benchmarks. That is to say, we will determine if our computational model, possessing both (a) heterogeneous connectivity across the LNs and (b) SK-channels within the PNs, can reproduce all the phenomena discussed so far.

Section R2: Computational Modeling

In this section we briefly describe our computational model, and use it to probe the potential consequences of disinhibition and SK-channels within the moth MGC.

Note that ours is certainly not the first model to investigate these mechanisms within the *Manduca* AL. For example, a mean-field model by Buckley and Nowotny (2011) analyzes the role of disinhibition within an idealized inhibitory network without fast synapses. As another example, a spiking network-model by Belmabrouk et al. (2011a) includes SK-type channels in order to replicate some of the pharmacological results seen in Lei et al. (2009)—specifically the elimination of the AHP-phase and diminished pulse-tracking properties observed under BIC-application.

We view both these works as encouraging, and take them as additional support for the disinhibition and SK-channel hypotheses. That being said, our model—which combines disinhibition and SK-channels—is the only model we are aware of that attempts to capture the broad range of PTX- and BIC-induced phenomena we observed in Section R1. Moreover, as we will eventually discuss later, our modeling study illuminates the importance of multiple-firing-events, which depend critically on fast synapses and cannot be well understood via a mean-field framework.

Our model is a spiking network model of a few interconnected glomeruli within the *Manduca* AL. This network is built out of several dozen spiking single-compartment integrate-and-fire neurons, using the voltages and conductances of the individual neurons as microscopic variables. Each glomerulus in our model corresponds to a relatively tightly knit cluster of a few dozen neurons, including inhibitory LNs and excitatory PNs. In terms of connectivity, we have abstracted the complex topology of

the real AL as follows: we assume that different populations of neurons are interconnected sparsely and randomly, both within each glomerulus as well as across glomeruli. We remark that we do not explicitly model excitatory LNs, instead assuming that their effects are similar to the effects of the excitatory PNs (to which they may be strongly connected—see e.g., Huang et al., 2010).

With regards to the network's dynamics, we equip our neurons with fast synaptic currents, corresponding to nicotinic-type excitation and GABA-A-type inhibition, as well as slower inhibitory synaptic currents with a decay time ∼750 ms. Both our LNs and PNs exhibit fast sodium-like spikes (modeled via the integrate-and-fire equations), but our PNs are also equipped with a slow intrinsic inhibitory current mimicking the putative SK-currents discussed above (decay time-scale ∼400 ms). Each neuron in our network is also driven by independent feedforward Poisson input comprising (i) a background drive and (ii) a stimulus-specific drive targeting specific glomeruli at specific times.

These are the main ingredients of our model. Note that, as described in the Methods Section and in the Supplementary Material, our model has (a) heterogeneous recurrent inhibition provided by the LNs, as well as (b) slow intrinsic SK-currents within the PNs; while the latter is considered in Belmabrouk et al. (2011b), the former is not. The parameters for our model include excitatory and inhibitory couplings strengths (both within and across glomeruli), the strength of the SK-currents within the PNs, and the strengths of the feedforward input currents. As mentioned in the methods section and discussed in more detail in the Supplementary Material, we proceeded to tune this model by varying the parameters. Our goal when tuning was to search for parameters for which our model was "biologically plausible." That is, for which our model satisfied all the benchmarks associated with our observations of the AL. We found that, indeed:

Our model allows for "biologically plausible" behavior

There exists a region in parameter space for which our model can simultaneously exhibit the following phenomena discussed in Section R1: (1) Firing-rates, EPSPs and IPSPs similar to those observed in the real AL; (2) Pulse-response attenuation for IPIs < 1 s, (3) PTX-induced reduction in PN spontaneous firing rates, (4) PTX-induced loss of consistency across isolated stimulus pulses, (5) BIC-induced reduction in PN pulse-response attenuation and pulse-tracking, and (6) BIC-induced slow patterns when unstimulated. These phenomena are illustrated in **Figures 3**, **5**, **11**, **13**, as well as in Supplementary Figure S7.

Even this modicum of success points toward the plausibility of our previous hypothesis. Namely, that the phenomena we observed might be due to (a) heterogeneous recurrent connectivity involving the LNs and (b) intrinsic SK-currents within the PNs. More importantly, however, our computational model gives a hint as to how these architectural mechanisms give rise to the phenomena at hand, and how those phenomena might coexist within a single dynamical regime.

After analyzing our model, we discovered that all the biologically plausible regimes we found shared a few things in common:

(1) *Strong recurrent inhibition:* Unsurprisingly, all our biologically plausible regimes had large inhibitory coupling strengths. This is to be expected, as we engineered our model to possess a heterogeneous collection of LNs capable of disinhibition. In order for our network to exhibit the desired PTX-induced reduction in PN firing rates, the effects of such disinhibition should be significant. Strong recurrent inhibition seemed to be a necessary prerequisite for this.

(2) *Strong intrinsic SK-currents:* Also unsurprisingly, all our biologically plausible regimes had large amplitude SK-currents within the PNs, corroborating previous modeling work by Belmabrouk et al. (2011a). This again is expected, as we required PNs in our model network to exhibit a BIC-induced reduction in the AHP-phase. Recall that, in our network, BIC-on corresponds to a reduction in both GABA-A-currents and SK-currents. Given that the former alone would lengthen the AHP-phase (through disinhibition), it is crucial that the AHP-phase also comprise a strong intrinsic inhibitory component—in our case this was an SK-current. In order for the BIC-on state to shorten the AHP-phase, this SK-current must be strong enough that its removal (under BIC) "outweighs" the additional presynaptic inhibition received by the PNs due to the disinhibitory network.

(3) *High gain:* Our model functioned well when the feedforward, intrinsic and synaptic currents combined to ensure that, most of the time, at least some neurons in the network had membrane potentials that were not too far from the firing-threshold. This requirement is tantamount to the statement that—barring obvious exceptions such as PNs in the AHP-phase—the currents driving each neuron were neither overwhelmingly excitatory nor overwhelmingly inhibitory. This "high gain" regime allowed neurons to be responsive to fluctuations in their input currents; this responsivity played an important role in all the phenomena we sought.

(4) *Strong recurrent excitation:* Finally, all our biologically plausible regimes had large excitatory coupling strengths. In this case "large coupling strengths" specifically means that the typical EPSP was of the same order as—or not too much smaller than—the typical IPSP coming from the heterogeneous network of LNs. This requirement can be thought of as a special case of the "high-gain" requirement from the previous paragraph, restricted to presynaptic currents. These large coupling strengths were instrumental in producing the somewhat more subtle dynamic phenomena discussed toward the end of Section R1.

These last two requirements—a high-gain state with strong recurrent excitation—were crucial for our model, and gave rise to a very important dynamic feature:

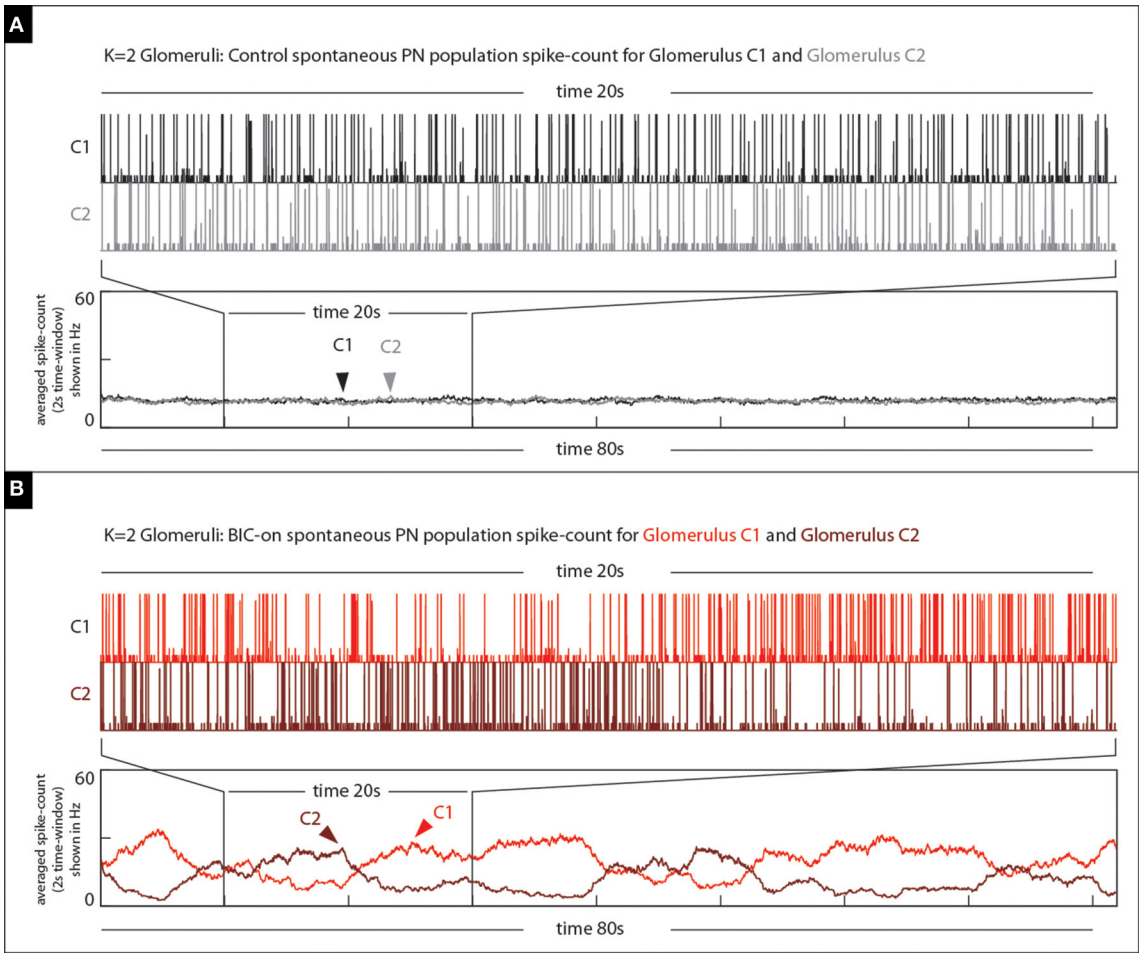

FIGURE 13 | Our model qualitatively reproduces the BIC-induced phenomena illustrated in Figure 12. (A) On top we show the spontaneous PN-activity for both glomeruli (two shades of gray) in a $K = 2$ glomeruli model. The time-averaged spike-count (2 s bins) is shown on the bottom. **(B)** On top we show the spontaneous PN-activity for both glomeruli (two shades of red) in the same $K = 2$ glomeruli model under the BIC-on state. Note that not only are there long periods of elevated activity observed within each of the glomeruli, but also that these periods of activity are anti-correlated with one another.

Our Model Exhibits Emergent "Multiple-Firing-Events" —or MFEs

These MFEs are a special kind of causally-linked synchronization across subsets of PNs. This brief synchronization occurs because the PNs are in a high-gain state; there are often a few PNs which are not too far from the firing-threshold. Because of the strong recurrent excitation, one or two typical EPSPs can close this gap, causing one spike to lead to the next. That is to say, it will not be uncommon for any given PN spike to drive at least one other postsynaptic PN over the spiking-threshold, causing a second PN spike almost immediately (i.e., within 1–2 ms). This second spike may cause a third, and so forth, resulting in a chain reaction including several PNs over a comparatively short period of time (say, <5 ms).

That these chain-reactions *can* occur depends on the high-gain and strong recurrent excitation; whether or not a chain-reaction *will* occur at any given time is due primarily to luck—which PNs have high subthreshold voltages and which do not. While it is certainly possible for MFEs to occur spontaneously (i.e., when the model is unstimulated), most MFEs occur during the initial response to stimulation. This initial response period corresponds to the "highest-gain" of the PNs, before they will be suppressed by the inhibitory currents from the forthcoming AHP-phase.

An example of an MFE within an idealized 3-neuron network is shown in **Figure 14A**. This network comprises 3 PNs which are stimulated with feedforward Poisson input similar to our full network; the synaptic time constants are also similar to our full network (i.e., 2 ms), but the synaptic coupling strengths are about a factor of 10 higher so that MFEs clearly manifest. On the top left we show a short 5 ms sample trajectory from this network with the subthreshold voltage of each PN color-coded in accordance with the network to the right. Because each neuron is modeled using the integrate-and-fire equations, each subthreshold-voltage will fluctuate (based on its combination of input currents) until it reaches the firing-threshold (VT), at which point the neuron will

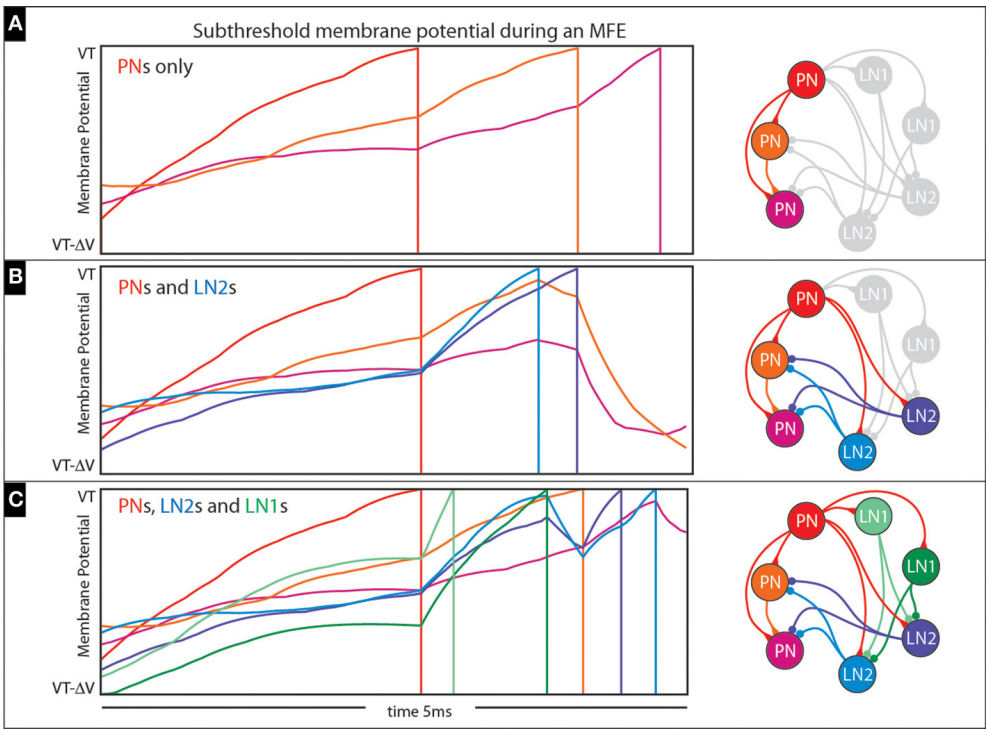

FIGURE 14 | Illustration of multiple-firing-events (MFEs): (A–C) Here we use a collection of small networks to illustrate the kinds of chain-reactions we see in our simulations. See text for details.

fire and reset to VR (firing denoted by vertical line), no longer participating in this short stretch of dynamics. Note that the first PN to fire adds an excitatory input current to the second PN and encourages it to fire as well; the combined effects of these first two PNs adds a substantial excitatory presynaptic current to the third PN, causing it to fire less than a millisecond later. This entire cascade takes place over <3 ms, and is similar to the MFEs in our larger network.

Of course, the chain-reactions we've been describing don't just include PNs; the first few PNs to initiate a chain-reaction will also cause firing amongst the LNs, many of which also benefit from the high-gain state. How such a chain-reaction unfolds can be very complicated and situation-dependent; recall that the LN population is heterogeneous. LN1s inhibit LN2s; LN2s inhibit PNs. The short-time-scale dynamics within each MFE can be rather complicated, with PNs, LN1s and LN2s competing over the fate of the cascade.

This complexity is illustrated in **Figures 14B,C**. In **Figure 14B** we expand the 3-neuron network of **Figure 14A** to include two LN2s (see addition blue neurons on the right, as well as bluish trajectories on the left), which affect how the cascade unfolds. This time, the first PN again adds excitatory presynaptic current to the other two PNs, but also to the two LN2s; these LN2s manage to fire before the other PNs would fire, giving rise to inhibitory presynaptic currents which actually prevent these other PNs from firing altogether. Another example is shown in **Figure 14C**, where the simple network is further expanded to include two LN1s (see additional green neurons on the right, as well as greenish trajectories on the left). This time the first PN to fire causes one of the LN1s to fire second, which actually inhibits and delays the spikes coming from the LN2s. As a result, the LN2s are not capable of completely curtailing the cascade, and one of the remaining PNs manages to fire (compare **Figure 14B** with **Figure 14C**).

Thus, the specifics of any given MFE are rather variable: it is possible for a chain-reaction of PN spikes to trigger LN2 spikes which halt the cascade or to trigger LN1 spikes which help the cascade continue via disinhibition. When each MFE concludes—usually due to a barrage of inhibition—the PNs involved experience an abundance of persistent inhibitory currents: both presynaptic and intrinsic. If the system is stimulated, a sufficiently strong feedforward input can override these inhibitory currents and cause further firing. On the other hand, when the network is unstimulated, these inhibitory currents are usually sufficient to prevent further firing.

MFEs Strongly Affect the Dynamics of Our Model

As one can see from the description above, MFEs represent a particular kind of synchrony; they are most decidedly *causal* in nature, stemming from strong and fast competition between synaptic excitation and inhibition. In this regard, MFEs can be viewed as a more complicated version of the "sandpile" cascades discussed in Bak et al. (1987) and later considered in the context of neuroscience by Mirollo and Strogatz (1990), Gerstner and van Hemmen (1993), DeVille and Zheng (2014)

and others. We also believe MFEs to be related to the "neuronal avalanches" studied by Plenz et al. (2011) and Beggs and Plenz (2003).

By contrast, MFEs are quite distinct from many other forms of synchrony that have been studied, such as synchrony borne from (i) correlated feedforward inputs, (ii) global fluctuations in firing-rate, (iii) strong sources of synaptic depression, or (iv) synaptic delays. The MFEs we see in our model are not easily characterized analytically as an additional feedforward Poisson spiking process (see Brunel, 2000), or as fluctuations of a balanced state (see van Vreeswijk and Sompolinsky, 1998).

While we don't yet have a full characterization of MFEs ourselves, we have studied them in a less complex network (Rangan and Young, 2013b). Even this simpler case required serious effort to analyze mathematically (Rangan and Young, 2013a; Zhang et al., 2014a,b; Zhang and Rangan, 2015). Thus, at present we eschew any sort of detailed analysis, instead describing in words the dynamic picture we see in our model:

MFEs Manifest Within the Control State

In terms of the model's spontaneous activity, many of the PN firing-events are isolated (i.e., not part of any MFE), but some PN spikes occur synchronously (see **Figure 15A**). When the model is driven by an odor pulse the activity levels of both the PNs and LNs rise; again the PN activity comprises both MFEs and isolated spikes, although with both occurring at a much higher frequency than in the spontaneous state. Shortly after any odor pulse the PN activity dies down, and the PNs are driven predominantly by persistent inhibitory currents. These inhibitory currents combine slow synaptic inhibition with intrinsic SK-currents, giving rise to an AHP-phase. During this AHP-phase, our model PNs are no longer in a high-gain state, and exhibit very little firing at all (i.e., very few isolated spikes or MFEs).

MFEs Underlie the PTX-on Phenomena

When PTX is applied, the GABA-A coupling strengths are reduced; the LN2 presynaptic inhibitory current drops; the LN2 population moves closer to the spiking threshold; the LN2 firing rate increases significantly; and the net inhibitory presynaptic currents to the PNs increases somewhat. The net effect of all this on spontaneous activity is rather simple: the spontaneous PN firing-rate is somewhat lower in the PTX-on state than in the control state. The excess inhibitory currents lower both the probability of isolated spikes and MFEs.

With regard to stimulated activity, however, the story is more intricate. As we discussed in **Figure 14**, predominantly excitatory networks (i.e., networks without strong disinhibition, similar to **Figure 14A**) tend to have more stereotyped MFEs than networks that are capable of strong disinhibition (i.e., networks with strongly competing LN1s and LN2s, similar to **Figure 14C**). A corollary to this claim is: networks with stronger disinhibition tend to be more variable than networks without. We believe that this mechanism underlies the PTX-on reduction in PN consistency.

To elaborate: recall that the PTX-on state causes the LN2 population to fire more vigorously (i.e., to be "higher gain") than in background. As a consequence, the competition between the LN1s, LN2s and PNs is more acutely felt when PTX is on. This increased competition means that—for certain choices of parameters—the cascades that occur within any given MFE are even more variable than in the control state. This extra variability gives rise to the PTX-induced reduction in PN consistency across isolated stimulus pulses. As corroborated by numerical experiments, this reduction in PN consistency is accentuated as the overall level of disinhibition rises (see Supplementary Figure S6F). Note that this phenomenon is not captured via a mean field reduction, and thus will not manifest in most standard firing-rate models.

MFEs Underlie the BIC-on Phenomena

Recall that the BIC-on state in our network involves both a reduction of GABA-A coupling strengths as well as a reduction in the intrinsic SK-currents within the PNs. The effect of the former alone would be identical to the PTX-on state. However, the removal of the SK-currents changes the story quite significantly. When the PNs no longer have SK-currents, the conclusion of each MFE no longer heralds the onset of intrinsically generated AHP-currents. As a result, the PNs participating in any one MFE are free to participate in another shortly afterwards, as long as they are not suppressed by inter-glomerular inhibition coming from elsewhere in the AL.

Thus, under BIC it is possible for the network to generate "runaway synchronization," where any one glomerulus produces a stochastic sequence of MFEs with a characteristic period determined by the feedforward input currents (typically in the 50 ms range). An example of such behavior is illustrated in **Figure 15B**. During such an MFE-sequence many of the other glomeruli will be suppressed by this active glomerulus (due to strong inter-glomerular inhibition, enhanced by the disinhibitory effects of BIC). This runaway synchronization typically continues until the active glomerulus "falters," and by chance fails to generate an MFE. At this point another glomerulus—one that was initially suppressed—has a chance to grab the reins and begin its own runaway sequence of MFEs. Such a coup—if it occurs—typically takes place rather abruptly, as the successor only needs a short window of opportunity to nucleate an MFE and take over.

In this manner the spontaneous activity in the BIC-on state can produce—for any given glomerulus—epochs of periodic firing (i.e., when the glomerulus is active) alternating with epochs of quiescence (i.e., when another glomerulus is active). The time-scale of these epochs is determined by the probability that a bout of runaway synchronization "falters." Depending on the choice of parameters, this falter-probability can be quite small—corresponding to long epoch timescales in the tens of seconds. Our intuition underlying this argument is essentially the same as the discussion in Section 10.6 of Zhang and Rangan (2015), which also presents an analysis of this phenomenon. As before, this BIC-induced phenomenon is not captured by a mean-field reduction.

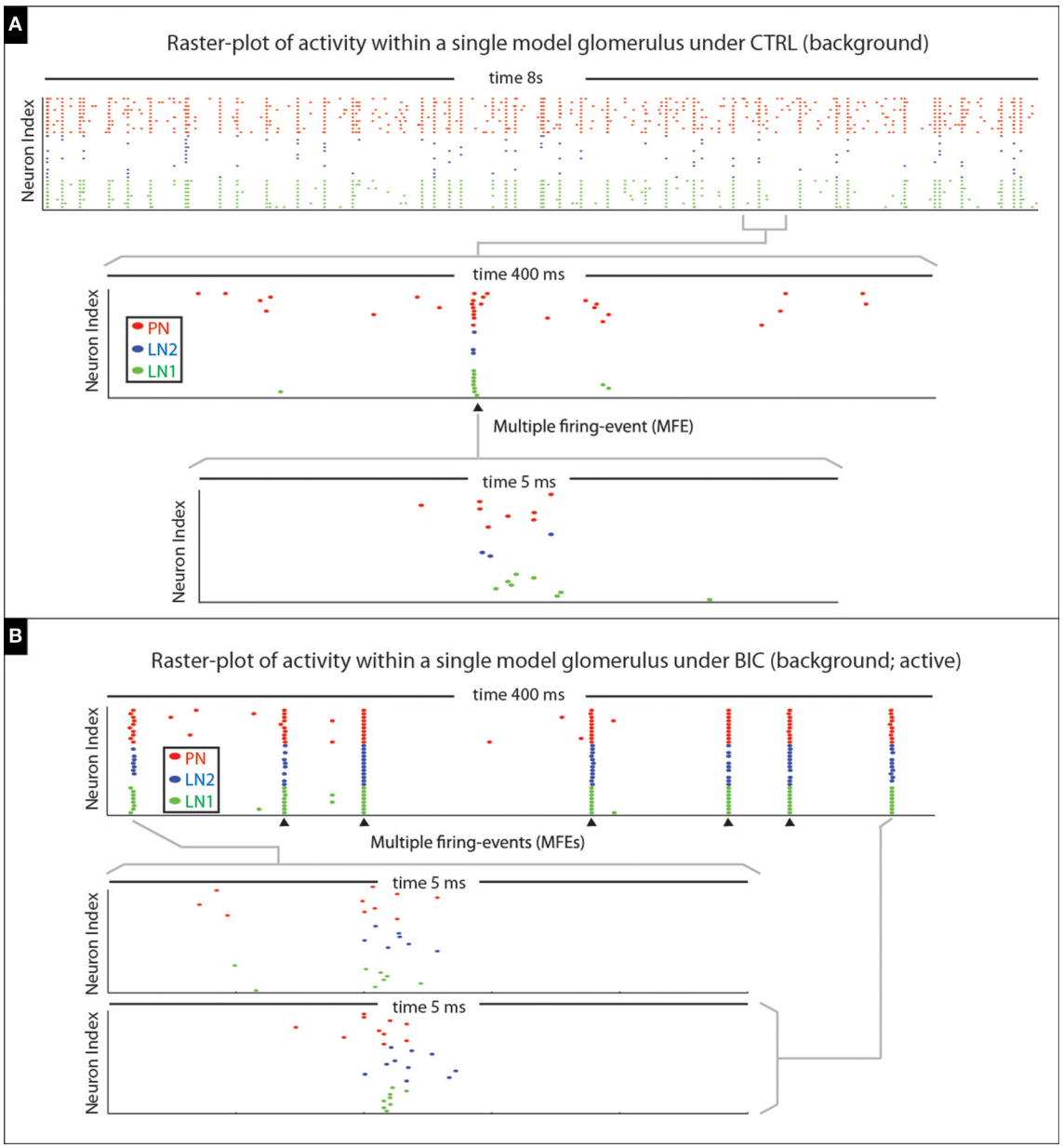

FIGURE 15 | Illustration of multiple-firing-events (MFEs) within our model network. (A) Here we show a raster-plot of spontaneous activity within a single model glomerulus from our network. The spikes associated with the different kinds of neurons are indicated via different colored dots. By zooming-in we can see an example of a MFE transpiring over ∼5 ms. **(B)** Here we show a raster-plot of spontaneous activity spontaneous activity from the same model-glomerulus under the BIC-on condition, with two MFEs displayed in more detail underneath. This raster-plot is taken during an active-epoch, where this glomerulus is firing at roughly 20 Hz. Two MFEs are shown in detail; the rest indicated with arrowheads. Note that the firing-events within each MFE are far from independent, instead occurring in brief synchronous bursts. In each case the MFE is precipitated by the firing of one or more PNs; these first few spikes trigger a cascade which includes more PNs, as well as LN1s and LN2s.

Summary

The narration we have provided above captures—as best we can—the essential dynamical features of our computational model. As described, the architectural features of our network give rise to a dynamical regime with many interdependent mechanisms that interact in a complicated way. Whether or not any of these mechanisms applies to the real AL is an important question, which we turn to now.

Section R3: Model Predictions

It is expected that many of the specific dynamical details of our model will vary depending on our exact choice of parameters. In the previous section we attempted to gloss over these minutiae

and focus only on the salient features of our model: features that persisted across all the parameters which satisfied our benchmarks. Some of these salient features take the form of emergent dynamical mechanisms; mechanisms that we did not explicitly build into our model, but which arose naturally from the interactions of the network. Such emergent mechanisms give rise to predictions regarding the real AL.

Below are two such predictions; both involve emergent dynamical mechanisms which are integral to the function of our model and robust to our choice of parameters.

1. Our model predicts that PNs in the AL participate in MFEs. While many PN spikes are isolated, many also occur as a result of other spikes. This latter phenomenon can involve just 2 PNs, or (more rarely) all the PNs in a glomerulus, and often includes LN spikes as well. These MFEs are most common during the initial response to a stimulus; but can also occur during spontaneous activity.

We feel quite comfortable with this prediction for two reasons. Firstly, MFEs emerged ubiquitously across a very wide swath of parameters that was much larger than—and included—the region in parameter-space that was biologically plausible. Put another way, our model never did anything even remotely reasonable without MFEs occurring. Secondly, we believe that MFEs are a key ingredient in the dynamical interactions responsible for both the PTX- and BIC-induced phenomena.

2. Furthermore, our model predicts that the BIC-induced structured activity encompasses not just the MGC, but many other glomeruli as well. Any glomerulus with a foreshortened AHP-phase—as induced by BIC—can begin producing MFE sequences. Moreover, different glomeruli compete to produce these MFE-sequences: such activity within any one glomerulus ensures—through interglomerular inhibition—that other glomeruli are suppressed. Conversely, a quiescent epoch observed in any one glomerulus necessarily implies an active epoch occurring someplace else.

We are also comfortable with this second prediction for two reasons. Firstly, despite all of our parameter-scanning, we were never able to produce BIC-induced structured activity without the underlying mechanism of competing MFE-sequences. This held true even when we searched across parameters that didn't even satisfy our other benchmarks. In other words, our model seemed incapable of producing structured activity on a 10 s timescale in any other way. Secondly, we have observed a similar mechanism at work in a model of the primate visual cortex (Rangan and Young, 2013b). In this previous work, competing MFE-sequences of much the same nature give rise to the slowly shifting patterns of activity observed in the anesthetized cortex—a state which, like our BIC-on state, does not exhibit a prolonged AHP and thus also allows for runaway synchronization.

Section R4: Validating the Model with Further Experiments

We now depart from our computational model and return to physiology to try and find evidence confirming our two predictions.

Our first prediction above—i.e., the existence of MFEs—has been observed indirectly under a variety of experimental conditions. For example, Christensen et al. (2000) found that PN activity within *Manduca* was not independent, but rather correlated to varying degrees depending on the stimulus. Later work by Lei et al. (2002) found that PNs in the MGC often fired synchronously (i.e., within 5 ms of one another), with the preponderance of synchronous spikes dependent on the recurrent presynaptic inhibition. The nature of this synchrony was further clarified by Christensen et al. (2003), which confirmed that—like the MFEs we see in our model—the synchronous PN firings observed in experiment could not be attributed to coordinated firing-rate fluctuations coming from the LFP. Finally, recent work by Martin et al. (2013) found that, when stimulated, at least 15% of the PN spikes produced within the *Manduca* MGC were participants in a synchronous event spanning <2 ms and involving at least one other PN.

While these experiments have yet to directly confirm (i) the chain of causality linking one spike to the next and (ii) the participation of LNs, taken altogether they strongly suggest that the MFEs we see in our model might be occurring in the AL. Because we did not use these experiments as benchmarks to constrain the dynamics of our model, we can consider them as a kind of validation of the dynamical picture we discovered. Conversely, we could also view the emergent MFEs from our model as further support for many of the conclusions that have been drawn from this experimental work (see e.g., Martin et al., 2011).

Our second prediction above—i.e., that BIC-induced spontaneous patterns involve many glomeruli—has not yet been confirmed. While structured spontaneous activity has been observed within the MGC (see, e.g., our benchmark Lei et al., 2009), such activity outside the MGC has not yet been reported. We take this step here, measuring from glomeruli outside the *Manduca* MGC under BIC application. These new experiments were able to verify aspects of our second prediction:

BIC Induces Structured Spontaneous Activity Encompassing Glomeruli Outside the MGC

We moved our recording electrode to the medial portion of AL, and recorded from a plant-odorants (hibiscus oil) responsive neuron. This neuron displayed spontaneous bursting patterns, implying that it was a PN (Lei et al., 2011). We found that, under BIC application, this neuron displayed epochs of fast-periodic-spiking lasting 5–10 s long interspersed with quiescent epochs lasting about 20 s long. As exhibited in **Figure 12**, the time-scale, distribution of, and transitions between these epochs seem commensurate with those reported within the MGC. These drug-induced changes could be reversed by saline wash.

We view this experimental result as an indication that our reasoning is on the right track. Nevertheless, we have yet to directly confirm that (i) the fast-spiking epochs are due to MFE-sequences, and (ii) that the glomeruli compete antagonistically with one another, with only one glomerulus active at a time. Naturally, we hope to carry out such experiments in the future, further illuminating the mechanisms at work within the AL. For

now, however, we take a step back and try and interpret the results we have so far.

DISCUSSION

This paper describes somewhat of a journey; a trajectory beginning with physiological experiments, passing through the realm of modeling and simulation, and ending back again with more experiments. We started out by measuring the PN dynamics and AHP-phase within the MGC under a variety of pharmacological agents. The drastic differences between PTX- and BIC-application lead us to conjecture that the AHP-phase involved both (a) disinhibition mediated by heterogeneous LN connectivity, as well as (b) intrinsic SK-currents produced by the PNs themselves. To determine whether or not these two mechanisms could, simultaneously, give rise to all the phenomena we observed, we built and benchmarked a computational model. This model highlighted the occurrence of MFEs—a dynamical mechanism that we did not directly observe in experiment, but which emerged naturally from the high-gain state of our biologically plausible model. Using our model as a stepping-stone, we then returned to experiment; confirming at least partially some of the predictions we had regarding the existence of MFEs and their dynamical consequences.

It is certainly possible that our hypotheses are not correct, or that we have omitted an important feature; PTX and BIC could affect a variety of specific targets in different ways. For example, rather than involving SK-channels, BIC could primarily affect the synapses of the LN2s while PTX primarily affected the synapses of the LN1s. Nevertheless, we found that our hypotheses were sufficient to explain the phenomena under study, and we feel comfortable concluding that:

(a) There exists strong fast recurrent excitatory and inhibitory connectivity throughout the *Manduca* AL—both between and within glomeruli. Moreover, this connectivity is heterogeneous—i.e., different neurons can have very different distributions of pre- and post-synaptic connections. Such heterogeneous connectivity implies that the network is capable of disinhibiting the PNs under the right circumstances.
(b) While the strong recurrent inhibition described in (a) definitely contributes to the strong AHP-phase of the PNs, the AHP-phase also depends on intrinsic inhibitory currents produced by the PNs themselves.
(c) The strong fast excitation mentioned above facilitates MFEs—causally linked spikes spanning subsets of neurons within the AL. Rapid sequences of MFEs are typically held in check by the presence of the AHP-phase, which prevents PNs from participating in many successive MFEs.

These conclusions are bolstered, to one degree or another, by various lines of experimental evidence, much of which we have referenced along the way. For example, regarding Conclusion-A, Christensen et al. (1998a) found that PN activity in the *Manduca* AL was modulated by disinhibitory microcircuits involving two GABAergic LNs. Regarding Conclusion-B, we have the results of Lei et al. (2009), which clearly show that BIC-application shortens the AHP-phase. Finally, regarding Conclusion-C, we have an abundance of circumstantial evidence (Christensen et al., 2000, 2003; Lei et al., 2002; Martin et al., 2013), as well as our own BIC-induced results of **Figure 12**, all of which point toward synchrony within the *Manduca* AL.

Nevertheless, not all experimental observations line up with our conclusions. For completeness we briefly discuss some conflicting evidence.

Is There Disinhibition in the Silkworm Moth?

A recent study (Fujiwara et al., 2014) probed the inhibitory circuits in the AL of another moth species—the silkworm moth *Bombyx mori*—and concluded that odor stimulation produced both recurrent excitatory and inhibitory currents, with the latter emerging after some time delay and supressing the excitatory phase of subsequent odor-evoked responses. This point itself is not inconsistent with our conclusion-A but is based on a different measurement. They then further examined how PTX-application affected the PN dynamics. Unlike our experiments discussed in Section R1, Fujiwara et al. measured the odor-evoked PN spike counts, instead of measuring the AHP. They reported that PTX-application did increase spike counts, in contrast to our observation that PTX-application lengthened the AHP-phase (**Figure 6**). From their observations they concluded that PTX-application elevates excitatory currents to the PNs; a conclusion that seems diametrically opposite to our work in Section R1, where we concluded that PTX-application actually enhances the inhibitory currents impinging on the PNs. This discrepancy may be due to the species difference or experimental conditions, but is also likely related to the specifics of the measurement used. We remark that, while our conclusions regarding the role of PTX may differ, both we and Fujiwara et al. agree that PTX does not affect the mean odor-evoked firing-frequency (**Figure 10**). While we don't yet have resolution to this conundrum, earlier work by Waldrop et al., (1987; Christensen et al., 1998a) points out that direct excitatory, inhibitory and disinhibitory connections may all affect the PNs. Antagonizing GABA-A receptors (i.e., PTX) may produce a syndrome of effects that requires us to consider the entire network.

Does the AHP-Phase Combine Recurrent and Intrinsic Currents in the Swordgrass Moth?

Based on our Conclusion-B, we would predict that the duration of the AHP phase should be positively correlated with increased odor concentration; an increased concentration causes higher LN and PN firing, the former giving rise to more recurrent inhibition, the latter to a stronger intrinsic SK-current. This is indeed the case (**Figure 7**), and moreover this dose-response relation is disrupted by PTX-application. It's unclear how the duration of the AHP phase could encode odor concentrations, but our data at least suggest that the GABA-A receptor-mediated inhibition is related to the dynamic range of PN's responsiveness. However, in another moth species—the black swordgrass moth

Agrotis ipsilon—the duration of the AHP (termed Inhibitory Phase) is not correlated with odor concentrations (Jarriault et al., 2009). While we cannot yet explain this discrepancy, we noticed that their data do reveal that the magnitude—rather than the duration—of the AHP is concentration-dependent (Figure 7 in Jarriault et al., 2009). Thus, in summary, while we are reasonably confident of the dynamic picture we have painted for the *Manduca*, the mechanisms may reveal themselves differently in other insect species.

SUMMARY

If indeed our picture is accurate and the *Manduca* AL does exhibit the mechanisms we propose, we are lead naturally to the grander question: what purpose could they serve? We hypothesize that perhaps the *Manduca* has evolved to excel at certain difficult sensory tasks, such as finding a mate on the wing through a highly dynamic scent plume. One necessary computation for such behavior would be to reliably detect and respond to a faint odor-filament spun across a turbulent breeze.

As a moth flies, it encounters such filaments intermittently, with each brief exposure to pheromone lasting no more than a few 10 s of millisecond, and with subsequent glimpses of the odor separated by several 100 s of millisecond. In this kind of scenario it makes some amount of sense for the AL to be in a very high-gain state; with even the slightest hint of pheromone eliciting a vigorous response. Of course, given the brevity of the stimulus, a firing-rate code seems inefficient, and a temporal code (such as the temporal-binding of odor-specific synchronous subsets) might be much more elegant and efficient (Martin et al., 2011). The high-gain state we predict in this paper is consistent with both of these requirements; producing vigorous synchronous bursts of PN activity in response to brief stimulus pulses.

Carrying this narrative forwards, one can imagine the moth having just encountered one such odor-filament, its MGC responding furiously. At this point the moth's AL is blind to the world; after all, a typical consequence of maintaining such a high-gain state is that—after the initial response—it is very easy for recurrent excitatory connectivity to perpetuate that response, regardless of any new stimulus. It is at this point that the AHP-phase steps in; the recurrent inhibition and intrinsic currents curtailing such a runaway response, and allowing the MGC to "reset" after 100–500 ms. This characteristic AHP-time is not too different from the typical time it might take before the moth bumps into the next odor-filament. At that point the moth's AL will be in a high-gain state once more; fresh and ready to respond vigorously a second time.

In conclusion, our integrated theoretical and empirical approach supports the notion that both recurrent network interactions and intrinsic currents contribute to the dynamical properties of the projection neurons in the antennal lobe. These properties render a high-gain state, which may be an adaptive feature for the animal's olfactory behaviors.

AUTHOR CONTRIBUTIONS

HL, designed and performed experiments, analyzed data, drafted manuscript; YY, performed experiments and analyzed data; SZ, provided overall support for YY and guided the project partially; AR, built the mathematical model and analyzed its performance, revised manuscript.

FUNDING

This work is supported by the National Science Foundation (DMS-2100009 to HL and AR), as well as the National Institute of Health (R01-DC-02751 to John G. Hildebrand), and the National Science and Technology Support Program of China (2015BAD08B01 to YY).

ACKNOWLEDGMENTS

The authors wish to thank Dr. Hildebrand for his generous support; Mrs. Teresa Gregory for lab maintenance.

SUPPLEMENTARY MATERIAL

The Supplementary Material for this article can be found online at: http://journal.frontiersin.org/article/10.3389/fphys.2016.00080

REFERENCES

Abou Tayoun, A. N., Li, X., Chu, B., Hardie, R. C., Juusola, M., and Dolph, P. J. (2011). The *Drosophila* SK channel (dSK) contributes to photoreceptor performance by mediating sensitivity control at the first visual network. *J. Neurosci.* 31, 13897–13910. doi: 10.1523/JNEUROSCI.3134-11.2011

Adelman, J. P., Maylie, J., and Sah, P. (2012). Small-conductance Ca^{2+}-activated K^{+} channels: form and function. *Annu. Rev. Physiol.* 74, 245–269. doi: 10.1146/annurev-physiol-020911-153336

Anthony, N. M., Harrison, J. B., and Sattelle, D. B. (1993). GABA receptor molecules of insects. *EXS* 63, 172–209. doi: 10.1007/978-3-0348-7265-2_8

Assisi, C., Stopfer, M., Laurent, G., and Bazhenov, M. (2007). Adaptive regulation of sparseness by feedforward inhibition. *Nat. Neurosci.* 10, 1176–1184. doi: 10.1038/nn1947

Bak, P., Tang, C., and Wiesenfeld, K. (1987). Self-organized criticality: an explanation of 1/f noise. *Phys. Rev. Lett.* 59, 381–384. doi: 10.1103/PhysRevLett.59.381

Barbara, G., Zube, C., Ryback, J., Gauthier, M., and Grunewald, B. (2005). Acetylcholine, GABA and glutamate induce ionic currents in cultured antennal lobe neurons of the honeybee, *Apis mellifera*. *J. Comp. Physiol. A Neuroethol. Sens. Neural Behav. Physiol.* 191, 823–836. doi: 10.1007/s00359-005-0007-3

Beggs, J. M., and Plenz, D. (2003). Neuronal avalanches in neocortical circuits. *J. Neurosci.* 23, 11167–11177.

Belmabrouk, H., Nowotny, T., Rospars, J. P., and Martinez, D. (2011a). Interaction of cellular and network mechanisms for efficient pheromone coding in moths. *Proc. Natl. Acad. Sci. U.S.A.* 108, 19790–19795. doi: 10.1073/pnas.1112367108

Belmabrouk, H., Rospars, J. P., and Martinez, D. (2011b). A computational model of the moth macroglomerular complex. *BMC Neurosci.* 12(Suppl. 1):P212. doi: 10.1186/1471-2202-12-S1-P212

Bond, C. T., Maylie, J., and Adelman, J. P. (1999). Small-conductance calcium-activated potassium channels. *Ann. N.Y. Acad. Sci.* 868, 370–378. doi: 10.1111/j.1749-6632.1999.tb11298.x

Brunel, N. (2000). Dynamics of sparsely connected networks of excitatory and inhibitory spiking neurons. *J. Comp. Neurosci.* 8, 183–208. doi: 10.1023/A:1008925309027

Buckley, C. L., and Nowotny, T. (2011). Multiscale model of an inhibitory network shows optimal properties near bifurcation. *Phys. Rev. Lett.* 106, 238109. doi: 10.1103/PhysRevLett.106.238109

Chotoo, C. K., Silverman, G. A., Devor, D. C., and Luke, C. J. (2013). A small conductance calcium-activated K^+ channel in *C. elegans*, KCNL-2, plays a role in the regulation of the rate of egg-laying. *PLoS ONE* 8:e75869. doi: 10.1371/journal.pone.0075869

Choudhary, A. F., Laycock, I., and Wright, G. A. (2012). γ-Aminobutyric acid receptor A-mediated inhibition in the honeybee's antennal lobe is necessary for the formation of configural olfactory percepts. *Eur. J. Neurosci.* 35, 1718–1724. doi: 10.1111/j.1460-9568.2012.08090.x

Christensen, T. A., and Hildebrand, J. G. (1987). Male-specific, sex pheromone-selective projection neurons in the antennal lobes of the moth *Manduca sexta*. *J. Comp. Physiol. A* 160, 553–569. doi: 10.1007/BF00611929

Christensen, T. A., Lei, H., and Hildebrand, J. G. (2003). Coordination of central odor representations through transient, non-oscillatory synchronization of glomerular output neurons. *Proc. Natl. Acad. Sci. U.S.A.* 100, 11076–11081. doi: 10.1073/pnas.1934001100

Christensen, T. A., Pawlowski, V. M., Lei, H., and Hildebrand, J. G. (2000). Multi-unit recordings reveal context-dependent modulation of synchrony in odor-specific neural ensembles. *Nat. Neurosci.* 3, 927–931. doi: 10.1038/78840

Christensen, T. A., Waldrop, B. R., and Hildebrand, J. G. (1998a). GABAergic mechanisms that shape the temporal response to odors in moth olfactory projection neurons. *Ann. N.Y. Acad. Sci.* 855, 475–481. doi: 10.1111/j.1749-6632.1998.tb10608.x

Christensen, T. A., Waldrop, B. R., and Hildebrand, J. G. (1998b). Multitasking in the olfactory system: context-dependent responses to odors reveal dual GABA-regulated coding mechanisms in single olfactory projection neurons. *J. Neurosci.* 18, 5999–6008.

Destexhe, A., and Sejnowski, T. J. (2009). The Wilson-Cowan model, 36 years later. *Biol Cybern*. 101, 1–2. doi: 10.1007/s00422-009-0328-3

DeVille, L., and Zheng, Y. (2014). Synchrony and periodicity in excitable neural networks with multiple subpopulations. *SIAM J. Appl. Dynam. Syst*. 13, 1060–1081. doi: 10.1137/130943261

Fujiwara, T., Kazawa, T., Sakurai, T., Fukushima, R., Uchino, K., Yamagata, T., et al. (2014). Odorant concentration differentiator for intermittent olfactory signals. *J. Neurosci.* 34, 16581–16593. doi: 10.1523/JNEUROSCI.2319-14.2014

Galizia, C. G., and Rössler, W. (2010). Parallel olfactory systems in insects: anatomy and function. *Annu. Rev. Entomol.* 55, 399–420. doi: 10.1146/annurev-ento-112408-085442

Gerstner, W., and van Hemmen, J. L. (1993). Coherence and incoherence in a globally coupled ensemble of pulse-emitting units. *Phys. Rev. Lett.* 71, 312. doi: 10.1103/physrevlett.71.312

Hansson, B. S., and Anton, S. (2000). Function and morphology of the antennal lobe: new developments. *Annu. Rev. Entomol.* 45, 203–231. doi: 10.1146/annurev.ento.45.1.203

Hansson, B. S., Christensen, T. A., and Hildebrand, J. G. (1991). Functrionally distinct subdivisions of the macroglomerular complex in the antennal lobe of the male sphinx moth *Manduca sexta*. *J. Comp. Neurol.* 312, 264–278. doi: 10.1002/cne.903120209

Heinbockel, T., Christensen, T. A., and Hildebrand, J. G. (1999). Temporal tuning of odor responses in pheromone-responsive projection neurons in the brain of the sphinx moth Manduca sexta. *J. Comp. Neurol.* 409, 1–12.

Heinbockel, T., Christensen, T. A., and Hildebrand, J. G. (2004). Representation of binary pheromone blends by glomerulus-specific olfactory projection neurons. *J. Comp. Physiol.* A 190, 1023–1037. doi: 10.1007/s00359-004-0559-7

Homberg, U., Christensen, T. A., and Hildebrand, J. G. (1989). Structure and function of the deutocerebrum in insects. *Annu. Rev. Entomol.* 34, 477–501. doi: 10.1146/annurev.en.34.010189.002401

Huang, J., Zhang, W., Qiao, W., Hu, A., and Wang, Z. (2010). Functional connectivity and selective odor responses of excitatory local interneurons in *Drosophila* antennal lobe. *Neuron* 67, 1021–1033. doi: 10.1016/j.neuron.2010.08.025

Jarriault, D., Gadenne, C., Rospars, J. P., and Anton, S. (2009). Quantitative analysis of sex-pheromone coding in the antennal lobe of the moth *Agrotis ipsilon*: a tool to study network plasticity. *J. Exp. Biol.* 212, 1191–1201. doi: 10.1242/jeb.024166

Khawaled, R., Bruening-Wright, A., Adelman, J. P., and Maylie, J. (1999). Bicuculline block of small-conductance calcium-activated potassium channels. *Pflügers Arch.* 438, 314–321. doi: 10.1007/s004240050915

Kim, A. J., Lazar, A. A., and Slutskiy, Y. B. (2015). Projection neurons in *Drosophila* antennal lobes signal the acceleration of odor concentrations. *Elife* 4:e06651. doi: 10.7554/eLife.06651

Laurent, G., MacLeod, K., Stopfer, M., and Wehr, M. (1999). Dynamic representation of odours by oscillating neural assemblies. *Entomol. Exp. Appl.* 91, 7–18. doi: 10.1046/j.1570-7458.1999.00460.x

Lavialle-Defaix, C., Jacob, V., Monsempés, C., Anton, S., Rospars, J. P., Martinez, D., et al. (2015). Firing and intrinsic properties of antennal lobe neurons in the noctuid moth *Agrotis ipsilon*. *Biosystems* 136, 46–58. doi: 10.1016/j.biosystems.2015.06.005

Lee, D., Su, H., and O'Dowd, D. K. (2003). GABA receptors containing Rdl subunits mediate fast inhibitory synaptic transmission in *Drosophila* neurons. *J. Neurosci.* 23, 4625–4634. Available online at: http://www.jneurosci.org/content/23/11/4625.full

Lei, H., Christensen, T. A., and Hildebrand, J. G. (2002). Local inhibition modulates odor-evoked synchronization of glomerulus-specific output neurons. *Nat. Neurosci.* 5, 557–565. doi: 10.1038/nn0602-859

Lei, H., Oland, L. A., Riffell, J. A., Beyerlein, A., and Hildebrand, J. G. (2010). "Microcircuits for olfactory information processing in the antennal lobe of *Manduca sexta*," in *Handbook of Brain Microcircuits*, eds M. S. Gordon and S. Grillner (Oxford University Press), 417–426.

Lei, H., Reisenman, C. E., Wilson, C. H., Gabbur, P., and Hildebrand, J. G. (2011). Spiking patterns and their functional implications in the antennal lobe of the tobacco hornworm *Manduca sexta*. *PLoS ONE* 6:e23382. doi: 10.1371/journal.pone.0023382

Lei, H., Riffell, J. A., Gage, S. L., and Hildebrand, J. G. (2009). Contrast enhancement of stimulus intermittency in a primary olfactory network and its behavioral significance. *J. Biol.* 8, 21. doi: 10.1186/jbiol120

Martin, J. P., Beyerlein, A., Dacks, A. M., Reisenman, C. E., Riffell, J. A., Lei, H., et al. (2011). The neurobiology of insect olfaction: sensory processing in a comparative context. *Prog. Neurobiol.* 95, 427–447. doi: 10.1016/j.pneurobio.2011.09.007

Martin, J. P., Lei, H., Riffell, J. A., and Hildebrand, J. G. (2013). Synchronous firing of antennal-lobe projection neurons encodes the behaviorally effective ratio of sex-pheromone components in male *Manduca sexta*. *J. Comp. Physiol. A Neuroethol. Sens. Neural Behav. Physiol.* 199, 963–979. doi: 10.1007/s00359-013-0849-z

Matsumoto, S. G., and Hildebrand, J. G. (1981). Olfactory mechanisms in the moth *Manduca sexta*: response characteristics and morphology of central neurons in the antennal lobes. *Proc. Roy. Soc. Lond. B* 213, 249–277. doi: 10.1098/rspb.1981.0066

Mbungu, D., Ross, L. S., and Gill, S. S. (1995). Cloning, functional expression, and pharmacology of a GABA transporter from *Manduca sexta*. *Arch. Biochem. Biophys.* 318, 489–497. doi: 10.1006/abbi.1995.1258

Mirollo, R. E., and Strogatz, S. H. (1990). Synchronization of pulse-coupled biological oscillators. *SIAM J. Appl. Math.* 50, 1645–1662. doi: 10.1137/0150098

Newland, C. F., and Cull-Candy, S. G. (1992). On the mechanism of action of picrotoxin on GABA receptor channels in dissociated sympathetic neurones of the rat. *J. Physiol.* 447, 191–213. doi: 10.1113/jphysiol.1992.sp018998

Oland, L. A., Gibson, N. J., and Tolbert, L. P. (2010). Localization of a GABA transporter to glial cells in the developing and adult olfactory pathway of the moth *Manduca sexta*. *J. Comp. Neurol.* 518, 815–838. doi: 10.1002/cne.22244

Olsen, S. R., Bhandawat, V., and Wilson, R. I. (2007). Excitatory interactions between olfactory processing channels in the drosophila antennal lobe. *Neuron* 54, 89–103. doi: 10.1016/j.neuron.2007.03.010

Otmakhova, N. A., and Lisman, J. E. (2004). Contribution of I_h and $GABA_B$ to synaptically induced afterhyperpolarizations in CA_1: a brake on the NMDA response. *J. Neurophysiol.* 92, 2027–2039. doi: 10.1152/jn.00427.2004

Pedarzani, P., McCutcheon, J. E., Rogge, G., Skaaning Jensen, B., Christophersen, P., Hougaard, C., et al. (2005). Specific enhancement of SK channel activity

selectively potentiates the afterhyperpolarizing current IAHP and modulates the firing properties of hippocampal pyramidal neurons. *J. Biol. Chem.* 280, 41404–41411. doi: 10.1074/jbc.M509610200

Pinault, D. (1996). A novel single-cell staining procedure performed *in vivo* under electrophysiological control: morpho-functional features of juxtacellularly labeled thalamic cells and other central neurons with biocytin or Neurobiotin. *J. Neurosci. Methods* 65, 113–136.

Plenz, D., Stewart, C. V., Shew, W., Yang, H., Klaus, A., and Bellay, T. (2011). Multi-electrode array recordings of neuronal avalanches in organotypic cultures. *J. Vis. Exp.* 54:2949. doi: 10.3791/2949

Rangan, A., and Young, L. S. (2013a). Dynamics of spiking neurons: between homogeneity and synchrony. *J. Comp. Neurosci.* 34, 433–460. doi: 10.1007/s10827-012-0429-1

Rangan, A., and Young, L. S. (2013b). Emergent dynamics in a model of visual cortex. *J. Comp. Neurosci.* 35, 155–167. doi: 10.1007/s10827-013-0445-9

Reisenman, C. E., Christensen, T. A., and Hildebrand, J. G. (2005). Chemosensory selectivity of output neurons innervating an identified, sexually isomorphic olfactory glomerulus. *J. Neurosci.* 25, 8017–8026. doi: 10.1523/JNEUROSCI.1314-05.2005

Saito, Y., Takazawa, T., and Ozawa, S. (2008). Relationship between afterhyperpolarization profiles and the regularity of spontaneous firings in rat medial vestibular nucleus neurons. *Eur. J. Neurosci.* 28, 288–298. doi: 10.1111/j.1460-9568.2008.06338.x

Schneiderman, A. M., Hildebrand, J. G., Brennan, M. M., and Tumlinson, J. H. (1986). Trans-sexually grafted antennae alter pheromone-directed behaviour in a moth. *Nature* 323, 801–803. doi: 10.1038/323801a0

Shang, Y., Claridge-Chang, A., Sjulson, L., Pypaert, M., and Miesenbock, G. (2007). Excitatory local circuits and their implications for olfactory processing in the fly antennal lobe. *Cell* 128, 601–612. doi: 10.1016/j.cell.2006.12.034

van Vreeswijk, C., and Sompolinsky, H. (1998). Chaotic balanced state in a model of cortical circuits. *Neural. Comput.* 10, 1321–1371. doi: 10.1162/089976698300017214

Villalobos, C., Shakkotai, V. G., Chandy, G. K., Michelhaugh, S. K., and Andrade, R. (2004). SKCa channels mediate the medium but not the slow calcium-activated afterhyperpolarization in cortical neurons. *J. Neurosci.* 24, 3537–3524. doi: 10.1523/JNEUROSCI.0380-04.2004

Vosshall, L. B., Wong, A. M., and Axel, R. (2000). An olfactory sensory map in the fly brain. *Cell* 102, 147–159. doi: 10.1016/S0092-8674(00)00021-0

Waldrop, B., Christensen, T. A., and Hildebrand, J. G. (1987). GABA-mediated synaptic inhibition of projection neurons in the antennal lobes of the sphinx moth, *Manduca sexta*. *J. Comp. Physiol. A* 161, 23–32. doi: 10.1007/BF00609452

Warren, B., and Kloppenburg, P. (2014). Rapid and slow chemical synaptic interactions of cholinergic projection neurons and GABAergic local interneurons in the insect antennal lobe. *J. Neurosci.* 34, 13039–13046. doi: 10.1523/JNEUROSCI.0765-14.2014

Wilson, C. J., and Goldberg, J. A. (2006). Origin of the slow afterhyperpolarization and slow rhythmic bursting in striatal cholinergic interneurons. *J. Neurophysiol.* 95, 196–204. doi: 10.1152/jn.00630.2005

Wilson, R. I., and Laurent, G. (2005). Role of GABAergic inhibition in shaping odor-evoked spatiotemporal patterns in the Drosophila antennal lobe. *J. Neurosci.* 25, 9069–9079. doi: 10.1523/JNEUROSCI.2070-05.2005

Zhang, J., Newhall, K., Zhou, D., and Rangan, A. (2014a). Distribution of correlated spiking events in a population-based approach for Integrate-and-Fire networks. *J. Comp. Neurosci.* 36, 279–295. doi: 10.1007/s10827-013-0472-6

Zhang, J., Zhou, D., Cai, D., and Rangan, A. (2014b). A coarse-grained framework for spiking neuronal networks: between homogeneity and synchrony. *J. Comp. Neurosci.* 37, 81–104. doi: 10.1007/s10827-013-0488-y

Zhang, J. W., and Rangan, A. V. (2015). A reduction for spiking integrate-and-fire network dynamics ranging from homogeneity to synchrony. *J. Comp. Neurosci.* 38, 355–404. doi: 10.1007/s10827-014-0543-3

Conflict of Interest Statement: The authors declare that the research was conducted in the absence of any commercial or financial relationships that could be construed as a potential conflict of interest.

frontiers in Physiology

ORIGINAL RESEARCH
published: 12 May 2015
doi: 10.3389/fphys.2015.00148

Unexpected plant odor responses in a moth pheromone system

Angéla Rouyar[1], *Nina Deisig*[1], *Fabienne Dupuy*[2], *Denis Limousin*[1†], *Marie-Anne Wycke*[1], *Michel Renou*[1] *and Sylvia Anton*[2*]

[1] *Institut d'Ecologie et des Sciences de l'Environnement de Paris, INRA, Université Pierre et Marie Curie, Versailles, France,*
[2] *Neuroéthologie-RCIM, INRA-Université d'Angers, Beaucouzé, France*

OPEN ACCESS

Edited by:
Anders Garm,
University of Copenhagen, Denmark

Reviewed by:
Paul Szyszka,
Universität Konstanz, Germany
Neil Kirk Hillier,
Acadia University, Canada

***Correspondence:**
Sylvia Anton,
Neuroéthologie-RCIM,
INRA-Université d'Angers, UPRES EA 2647 USC INRA 1330, 42, rue Georges Morel, 49071 Beaucouzé cedex, France
sylvia.anton@angers.inra.fr

†Present Address:
Denis Limousin,
Faculté des Sciences et Techniques, Institut de Recherche sur la Biologie de l'Insecte (Centre National de la Recherche Scientifique UMR 7261), Université François Rabelais, Tours, France

Specialty section:
This article was submitted to Invertebrate Physiology, a section of the journal Frontiers in Physiology

Received: *26 February 2015*
Paper pending published: *25 March 2015*
Accepted: *26 April 2015*
Published: *12 May 2015*

Citation:
Rouyar A, Deisig N, Dupuy F, Limousin D, Wycke M-A, Renou M and Anton S (2015) Unexpected plant odor responses in a moth pheromone system. Front. Physiol. 6:148. doi: 10.3389/fphys.2015.00148

Male moths rely on olfactory cues to find females for reproduction. Males also use volatile plant compounds (VPCs) to find food sources and might use host-plant odor cues to identify the habitat of calling females. Both the sex pheromone released by conspecific females and VPCs trigger well-described oriented flight behavior toward the odor source. Whereas detection and central processing of pheromones and VPCs have been thought for a long time to be highly separated from each other, recent studies have shown that interactions of both types of odors occur already early at the periphery of the olfactory pathway. Here we show that detection and early processing of VPCs and pheromone can overlap between the two sub-systems. Using complementary approaches, i.e., single-sensillum recording of olfactory receptor neurons, *in vivo* calcium imaging in the antennal lobe, intracellular recordings of neurons in the macroglomerular complex (MGC) and flight tracking in a wind tunnel, we show that some plant odorants alone, such as heptanal, activate the pheromone-specific pathway in male *Agrotis ipsilon* at peripheral and central levels. To our knowledge, this is the first report of a plant odorant with no chemical similarity to the molecular structure of the pheromone, acting as a partial agonist of a moth sex pheromone.

Keywords: insect olfaction, sex pheromone, volatile plant compounds, interaction, olfactory receptor neuron, antennal lobe, central neuron

Introduction

Most insects use olfactory cues to communicate and find resources necessary for survival and reproduction. Olfactory-guided behavior, as well as the detection and central processing of sex pheromone and general odor cues have been particularly well studied in moths, in which the olfactory system shows a prominent sexual dimorphism related to sex pheromone communication. Female moths release a species-specific sex pheromone blend, which triggers a well-described oriented flight behavior along the pheromone plume in males, leading them toward the pheromone source (Cardé and Willis, 2008). Both sexes use also flower odors to find nectar sources, and females use plant volatiles in their search for oviposition sites on host plants. Male moths might also use host-plant volatiles to approach the habitat from which females are likely to be calling (Light et al., 1993; Coracini et al., 2004).

Insects detect odorants with olfactory receptor neurons (ORNs), housed within cuticular sensilla on their antennae. In male moths, species-specific pheromones and volatile plant compounds (VPCs) are usually detected and processed by two distinct olfactory pathways (Masson and Mustaparta, 1990) and separation between pheromone and plant signals occurs already at the

peripheral level. Information about the pheromone blend is transferred from the antennae via the axons of pheromone-specific olfactory receptor neurons (Phe-ORNs) to the primary olfactory center, the antennal lobe (AL) where it is processed in a male-specific area, the macroglomerular complex (MGC). Information about plant odors is transferred via a different class of olfactory receptor neurons (VPC-ORNs) and processed in sexually isomorphic areas of the AL, the ordinary glomeruli (OG) (Hansson and Anton, 2000). Because natural insect behavior results generally from the integration of multiple information sources, determining to which extent the two sub-systems are completely separated has recently become a very important case study in sensory ecology. More and more information is accumulating, indicating that simultaneous stimulation with pheromone and plant odors leads to interactions at all levels from detection up to behavioral output. The most frequently observed effect of mixture interaction in Phe-ORNs is suppression of pheromone responses when a VPC is added (Den Otter et al., 1978; Kaissling et al., 1989; Pophof and Van Der Goes Van Naters, 2002; Party et al., 2009; Rouyar et al., 2011). In the antennal lobe, plant volatiles either enhance pheromone responses (Namiki et al., 2008; Trona et al., 2010), or have a suppressive effect (Chaffiol et al., 2012; Deisig et al., 2012). Behavioral tests in the wind tunnel or in the field show often synergistic effects of plant odors added to the pheromone, more males being attracted to the mixture. In *Spodoptera exigua*, for example, phenyl-acetaldehyde, (Z)-3-hexenyl acetate or linalool increased captures of males in pheromone traps (Deng et al., 2004), and in wind tunnel experiments (Z)-3-hexen-1-ol, (+)-terpinen-4-ol, (E)-β-caryophyllene and methyl salicylate released with sub-optimal pheromone doses caused a synergistic effect in *Eupoecilia ambiguella* (Schmidt-Büsser et al., 2009). However, in spite of the observed interactions, so far the pheromone and plant odor inputs to the nervous system have been postulated to be highly separated up to their integration in the moth ALs. This consensual view of a high specificity of the pheromone sub-system arises from the repeated observation of a narrow chemical tuning of the pheromone receptor neurons to pheromone-like structures (Masson and Mustaparta, 1990). This high pheromone selectivity has been confirmed by heterologous expression of sex-pheromone receptors from several moth species, confirming they selectively bind the pheromone components over their close structural isomers (Nakagawa et al., 2005; Wanner et al., 2010; Liu et al., 2013). It is thus generally admitted that these olfactory receptors, narrowly tuned to pheromone components, act as molecular filters, preventing the activation of the pheromone pathway by general odorants. However, most studies have focused on pheromone-related compounds, so the capacity of general odorants to be bound to pheromone receptors should be more specifically addressed. As a matter of fact, if in *Helicoverpa zea* or *Spodoptera littoralis*, plant volatiles alone did not elicit responses from the Phe-ORNs (Ochieng et al., 2002; Party et al., 2009), high doses of plant compounds have been observed to activate Phe-ORNs in *Agrotis segetum* (Hansson et al., 1989). We revisit here the question of the sensitivity of the moth pheromone sub-system to plant odorants.

In the present study, using electrophysiological recordings and *in vivo* calcium imaging we show how plant volatiles in the noctuid moth *Agrotis ipsilon* activate not only the plant odor-specific pathway but also Phe-ORNs and the sex pheromone-specific MGC. The VPC heptanal used primarily in our study, with its seven-carbon chain length and an aldehyde function is emitted by various flowers such as linden flowers (*Tilia* sp.) that are attractive to *A. ipsilon* when searching for food (Wynne et al., 1991; Zhu et al., 1993), and is structurally different from the three acetates that constitute the sex pheromone blend of *A. ipsilon*. In the wind tunnel, male *A. ipsilon* were previously shown to be attracted by a linden flower extract (Deisig et al., 2012). We compare here in detail the upwind flight behavior toward heptanal and the pheromone blend. To determine if effects found for heptanal are specific, we also tested Phe-ORN responses to different other plant volatiles.

Materials and Methods

Insects

Larvae of *A. ipsilon* were reared in the laboratory on an artificial diet in individual plastic containers at 23°C and 60% relative humidity until pupation. Sexes were separated at pupal stage, and females and males were kept in separate rooms under a reversed 16 h:8 h light:dark photoperiod under similar temperature and humidity conditions. Newly emerged adults were collected every day and provided *ad libitum* with a 20% sucrose solution. The day of emergence was considered day zero of adult life. Four or five day old sexually mature virgin males were used for electrophysiological, optical imaging and wind tunnel experiments. All experiments were performed during the scotophase, when male moths are sexually active. Some complementary experiments were run on males of *S. littoralis,* which were reared under the same conditions as *A. ipsilon*.

Chemicals

Sex Pheromones

We used a highly attractive synthetic sex pheromone blend of *A. ipsilon* based on the three components identified previously in natural extracts of the female gland (Picimbon et al., 1997; Gemeno and Haynes, 1998): (Z)-7-dodecen-1-yl acetate (Z7-12:OAc), (Z)-9-tetradecen-1-yl acetate (Z9-14:OAc) and (Z)-11-hexadecen-1-yl acetate (Z11-16:OAc), mixed at a ratio of 4:1:4. This blend was further proven to be the most attractive to males in field tests (Causse et al., 1988) and it has been shown to elicit the same behavior as natural extracts in a wind tunnel (Barrozo et al., 2010b; Vitecek et al., 2013). We preferred in this paper to use the pheromone as a whole to investigate heptanal interactions with the complete stimulus at all integration levels. The three compounds were purchased from Sigma Aldrich (Saint-Quentin Fallavier, France) and diluted in hexane (>98% purity, CAS 110-54-3, Carlo-Erba, Val-de-Reuil, France). Amounts of 10 ng and/or 100 ng of the sex pheromone blend were used in the electrophysiological and calcium imaging experiments; these doses had previously been described as behaviorally and electrophysiologically active (Gadenne et al., 2001; Barrozo et al., 2010a; Chaffiol et al., 2012; Deisig et al., 2012). For ORN

recordings from pheromone sensilla in *S. littoralis*, the major sex pheromone component, (Z)-9 (E)-11 tetradecadienyl acetate (Z9,E11-14:Ac) was used (Ljungberg et al., 1993).

Volatile Plant Compounds

Heptanal (98% purity, CAS 66-25-1, confirmed by GC analysis, revealing no traces of pheromone compounds) and VPCs belonging to different chemical families (aldehydes, acetates, terpenes as well as one aromatic compound) were used for some experiments: (Z)-3-hexenyl acetate (Z3-6Ac) (98% purity, CAS 3681-71-8), hexanal (>99% purity, CAS 66-25-1), octanal (98% purity, CAS 124-30-0), linalool (97% purity, CAS 78-70-6), 2-phenylethanol (99% purity, CAS 60-12-8), and α-pinene (97% purity, CAS 7758-70-8). Mineral oil (CAS 8042-47-5) was used to prepare volume-to-volume dilutions at 0.1 and 1%. All compounds were purchased from Sigma Aldrich (Sigma Aldrich, Saint-Quentin Fallavier, France).

Olfactory Stimulation

Odorants were delivered as described previously (Rouyar et al., 2011). Briefly, charcoal-filtered air was re-humidified and divided in eight equal flows (220 ml/min) directed each to a three-way miniature valve. From there the flow could be directed to one 4 ml glass vial containing the stimulus source by activating the appropriate valve. The connections to the vials were made using PTFE tubing (1.32 mm ID) and hypodermic needles (18 G size). For practical reasons, due to their differences in volatility and polarity it was not possible to use the same type of stimulus sources for pheromone and heptanal or other volatile compounds. For VPCs, the vial contained 1 ml of solution in mineral oil at the appropriate concentration vol/vol. For the pheromone, the vial contained a section of PTFE tubing (1.6 mm ID; L = 20 mm) directly connected to a hypodermic needle and containing 10 or 100 ng of the sex pheromone. Stimulus- and clean air-carrying tubes were maintained together in a 10 cm long metal tubing constituting the stimulation pencil. A plastic cone of a P1000 pipette was placed at the output of the stimulation pencil to serve as a mixing chamber. It was placed approximately 5 mm in front of one of the moths' antennae and focused on antennal sensilla, when we recorded ORNs. In order to stimulate the whole antenna, the cone was placed 20 mm in front of the head in optical imaging experiments, or 5 mm in front of the antenna when we recorded MGC neurons intracellularly. Programming of the electric valves was performed using a Valve Bank (AutoMate Scientific, Berkeley, USA) synchronized with the PC acquisition software.

Measures of Aerial Concentrations of VPCs

To trace the olfactory stimulus at the output of the delivery system we used a fast response miniature photo ionization detector (Justus et al., 2002) (PID, from Aurora Scientific Inc, Aurora, Canada). Pheromone components could not be traced by this technique due to the high ionization potential of the pheromone molecules, which is above the energy of the PID lamp (10.6 eV). In turn, as all VPCs except phenyl ethanol and octanal produced measurable PID signals in the relevant concentration range we could estimate their concentrations in ppm_V at the output of the stimulator used in electrophysiological experiments.

In a first step, we calibrated the response of the PID to a source of known increasing concentrations of the VPCs. To generate these concentrations, we used an automatic syringe driver (Harvard Apparatus, model 55-2222) equipped with a 250 µl gastight microsyringe (Hamilton) to inject the pure compound at known rate into a controlled flow of charcoal filtered air (60 l/h, controlled by a flowmeter Meterate tube). The probe of the PID was inserted into the flow and the PID gain was settled at x10. The amplitude of the PID signal was measured after each increase of the delivery rate. Knowing the air flow rate and the chemical injection rate, it is possible to calculate the theoretical concentration in the final air (Chaffiol, personal communication) according to Equation 1:

$$C = (F_{chem} * (\mu/M) * Vmolar)/F_{air}$$

Where:

C = final concentration of the compound in ppb_V
F_{chem} = flow rate of the chemical (µl/h)
F_{air} = (m^3/h)
µ = density of the compound (g/cm^3)
M = molecular weight of the compound (g/mol)
Vmolar = molar volume for ideal gasses at 25°C (25.10^3 ml).

The speed of the syringe driver was adjusted to the suitable rate, and the concentration was allowed to stabilize for 1 min after which the output signal of the PID was measured three times. Subsequently the speed of the syringe pump was increased to reach the next rate step. Measures were done for at least 10 different rates, presented in increasing orders, until the saturation response of the PID (10 mV) was reached. The rates were converted (Equation 1) into ppm_V and the experimental data were fitted to a polynomial regression according to the procedure recommended by the PID constructor for calibration (Equation 2):

$$(S_{PID} = aC^2 + bC)$$

where S_{PID} is the amplitude of the PID response in volts, and C the concentration in ppm_V.

For measurements, the probe of the PID was introduced into the olfactory stimulator to quantify the concentrations of the compounds in the odorized air flows. Compounds were delivered at three dilution levels (0.5, 1, and 10% vol/vol in mineral oil) in the same conditions used for our electrophysiological experiments, and measures were repeated five times. The data in mV were converted into ppm_V using equation and values for 0.1% extrapolated from the resulting curve. The concentration measures are summarized in **Table 1** where data for 0.1% were extrapolated.

Electrophysiology

Single Sensillum Recording of ORNs

Males were briefly anesthetized with CO_2 and restrained in a Styrofoam holder. One antenna was immobilized with adhesive tape. Single sensillum recordings were performed with electrolytically sharpened tungsten wires. The reference electrode was inserted into the antenna, 1-3 segments from the segment carrying recorded sensilla, and the recording electrode was

TABLE 1 | Estimation of the concentrations in ppm_V at the output of the stimulator used in the electrophysiological experiments for five different volatile plant compounds released from sources containing 1 ml of mineral oil with 0.1, 1, and 10% of the respective compound as calculated from measurements with a photo ionization detector.

Compound	0.1% v/v	1% v/v	10% v/v
Heptanal	3.9	14.4	119.1
α-pinene	0.6	0.7	8.0
Linalool	0.7	3.1	14.4
Hexanal	16.5	19.4	95.6
Z3-6Ac	0.7	0.9	17.2

inserted into the base of a sensillum. We recorded two types of sensilla: long trichoid hairs based on antennal branches known to house Phe-ORNs and short trichoid hairs situated on the antennal stem known to house VPC-ORNs in a closely related species, *A. segetum* (Hansson et al., 1989). Recording and reference electrodes were connected to a Neurolog preamplifier (Digitimer, Hertfordshire, UK). The signal was filtered (0.2–10 kHz) and amplified 1000 times. The electrophysiological activity was sampled at 10 kHz and 12 bit resolution with a Data Translation DT3001 analog to digital card. Signals were monitored on the computer screen using Awave software (Marion-Poll, 1995). For analysis, spike sorting and extraction of spike occurrence times from the recordings were also done using Awave software. In some recordings from long trichoid hairs housing Phe-ORNs, the activities of two neurons with different spike amplitudes were analyzed, but only one neuron showed changes in firing rate in response to the sex pheromone. Also earlier recordings from Phe-ORNs showed that several neurons could be present in a given sensillum in *A. ipsilon*, but in all cases only one of them responded to a pheromone compound (Renou et al., 1996; Jarriault et al., 2010).

Intracellular Recordings of MGC Neurons

Males were slipped inside a 1 ml plastic pipette cone cut at the top. Only the head exceeded the plastic cone and was fixed with dental wax to prevent any movement. As described earlier (Gadenne and Anton, 2000), the head capsule was opened and tracheal sacs and muscles were removed from the front of the head to expose the brain. The neurolemma was removed from the surface of the antennal lobe to facilitate microelectrode penetration. Standard intracellular recording techniques were used (Christensen and Hildebrand, 1987). The preparation was superfused with Tucson Ringer (Christensen and Hildebrand, 1987). The microelectrode was randomly placed into the MGC. Electrode resistances were about 20–100 MΩ. The reference electrode was placed in contact with the brain. Signals were amplified with an AxoClamp-2B amplifier (Molecular Devices, Sunnyvale, California, USA). Neural activity was recorded, digitized, and spike occurrence times extracted using P-clamp software (Molecular Devices, Sunnyvale, California, USA).

Experimental Protocol

Phe-ORN and MGC Neuron Responses to Heptanal

We tested the response of Phe-ORNs and MGC neurons to heptanal by stimulating the antenna with a 200 ms heptanal puff at a dose of 0.1 and 1%. Phe-ORNs were recorded during 1 min and the odorant stimulation started at 30 s, lasting for 200 ms. For MGC neurons, odorant stimulation started 5 s after recording onset and inter-stimulus-intervals lasted for 10 s. Ten second interstimulus intervals are sufficient to allow AL neurons to reach the pre-stimulus spontaneous activity level and have been used in earlier studies of AL neurons in *A. ipsilon* (e.g., Barrozo et al., 2010a). We tested the pheromone at 100 ng and as controls, pure mineral oil and hexane, each for 200 ms.

Phe-ORN Responses to other VPCs

As we obtained unexpected responses of Phe-ORNs to heptanal, we also tested the effects of other VPCs on these ORNs: Z3-6Ac, hexanal, octanal, linalool, 2-phenylethanol and α-pinene. To check if we were recording from Phe-ORNs, we first stimulated the antenna with a 100 ng pheromone puff. Then puffs of the other compounds at 1% were randomly presented. As controls, the solvents hexane and mineral oil were tested.

VPC-ORN Responses to Pheromone

To check if VPC-ORNs also respond to the pheromone, we stimulated short trichoid sensilla situated on the stem of the antenna with 100 ng pheromone during 200 ms. To test if we had indeed contact with VPC-ORNs, we presented puffs of 0.1% of the VPCs heptanal, Z3-6Ac, hexanal, octanal, linalool, 2-phenylethanol, and α-pinene. As controls, we tested the solvents hexane and mineral oil.

Species Specificity of Phe-ORN Responses to VPCs

To test if the effect induced in Phe-ORNs by VPCs is specific to *A. ipsilon*, we recorded long trichoid sensilla in male *S. littoralis,* which have been shown to house one Phe-ORN tuned to the major sex pheromone compound Z9,E11-14:Ac. We stimulated sensilla with heptanal and linalool at 1% during 200 ms. To test if we were recording from Phe-ORNs, we first stimulated the antenna with 100 ng pheromone during 200 ms. As controls we presented the two solvents hexane and mineral oil.

Calcium Imaging

Insect Preparation

Males were mounted individually in Plexiglas chambers and the head was fixed to prevent movements. The head capsule was opened and glands and trachea were removed. Ten microliter of dye solution (50 mg Calcium Green 2-AM dissolved in 50 ml Pluronic F-127, 20% in dimethylsulfoxide, Molecular Probes, Eugene, OR, USA) were bath-applied on the brain for a minimum of 1 h. The brain was then washed with saline solution (Tucson Ringer) containing 150 mmol/l NaCl, 3 mmol/l $CaCl_2$, 3 mmol/l KCl, 10 mmol/l N-Tris-methyl-2-aminoethanesulfonic acid buffer, and 25 mmol/l sucrose (pH 6.9).

Data Acquisition

Recordings were done using a T.I.L.L. Photonics imaging system (Martinsried, Germany) coupled to an epifluorescent microscope (Olympus BX-51WI, Olympus, Hamburg, Germany) equipped with a 10x water immersion objective. Images were taken using a 1004 × 1002 pixel 14-bit monochrome CCD camera (Andor iXON) cooled to −70°C. Each measurement consisted of 80

frames at a rate of 5 frames/s (integration time for each frame: 10–15 ms). The excitation light was applied using a monochromator (T.I.L.L. Polychrom V). The microscope was equipped with a GFP-BP filter set composed of a 490 nm dichroic beamsplitter and a 525/550 nm emission filter.

Data Analyses

Because identification of individual glomeruli by anatomical staining of the AL after calcium imaging experiments is not possible in *A. ipsilon,* we defined regions of interests (ROI), possibly referring to individual glomeruli for OGs. Homologous ROIs could be identified by superposing activity maps using Adobe Photoshop (CS3). Raw data were analyzed using custom-made software written in IDL (Research Systems Inc., Colorado, USA) and Visual Basic (Microsoft Excel). Each recording corresponded to a three-dimensional matrix with two spatial dimensions (x and y size in pixels of the ROI) and a temporal dimension (length of the recording, 80 frames). Signals were subjected to three treatments: (i) For reduction of photon (shot) noise, raw data were filtered in both the spatial and temporal dimensions using a median filter with a size of 3 pixels. (ii) Relative fluorescence changes ($\Delta F/F$) were calculated as $(F\text{-}F_0)/F_0$, taking as reference background F_0 the average of five frames (frames 5 to 10) before odor stimulation. (iii) To correct for bleaching and for possible irregularities of lamp illumination in the temporal dimension, we subtracted from each pixel in each frame the median value of all the pixels of that frame. The maximum signal was obtained about 3 s after odor onset (around frame 30) and the minimum about 12 s after odor onset (around frame 60). We present activity maps with the best possible spatial definition of odor-induced signals from frames 30 to 60 where each pixel represents the mean of its values at frames 29–31 minus the mean of its values at frames 59–61.

For quantitative analysis of the data, we focused on the fast (positive) signal component evoked by odor stimulations, which is related to an intracellular calcium increase from the extracellular medium, thought to reflect mostly pre-synaptic neuronal activity from ORNs (Galizia et al., 1998; Sachse and Galizia, 2003). For each identified activity spot, the time course of relative fluorescence changes was calculated by averaging 25 pixels (5×5) at the center of each activity spot and well within its borders. The amplitude of odor-induced responses was calculated as the mean of three frames at the signal's maximum (frames 29–31) minus the mean of three frames before the stimulus (frames 7–9). This value was then used in all computations.

Experimental Protocol

Each animal was subjected to three series of olfactory stimulations with interstimulus intervals (ISIs) of 100 s. Odor stimulation started 3 s after recording onset and lasted for 200 ms. One AL was recorded in each insect. All animals were tested with a dose of 1% heptanal, 1% linalool as well as 100 ng of the pheromone. As control, we tested pure mineral oil and hexane.

Wind Tunnel Experiments

The behavior of male moths responding to pheromone or heptanal was observed in a wind tunnel made of 19 mm thick Plexiglas, with a flight section of 190 cm length × 75 cm width × 75 cm height (VT Plastics, Genevilliers, France). Plexiglas doors on the front side of the tunnel allowed access to the test section. The down- and upwind ends were enclosed with screen made of white synthetic fabric to prevent the insects from escaping but let the air pass through. An exhaust fan at the downwind end of the tunnel sucked the air into the tunnel at a speed of $0.3\ ms^{-1}$ and evacuated contaminated air to the outside of the building. The room housing the tunnel was maintained in darkness with a single red bulb to provide low intensity light for visual observations. Side infrared illumination for video tracking was provided by an array of eight 5 W IR lamps, of 54 LEDs each, emitting at 850 nm. A vertical screen bearing a randomly arranged pattern of 10 cm diameter black circles was positioned 30 cm behind the rear wall of the tunnel to provide visual cues to the moths outside the camera field.

Moth flight tracks were recorded and analyzed using Trackit 3D 2.0 (SciTracks, Pfaffhausen, Switzerland). Two cameras (Basler Pilot, piA640-210 m with Tamron ½" 4-12F/1.2 lenses) were positioned above the tunnel at 60 cm from each other to cover the whole flight section with overlapping fields. The images from the two cameras were analyzed in real time and the x, y, and z coordinates of each moth's position were extracted every 10 ms. Tracks were saved on the computer in form of ".csv" files that were further processed using scripts developed in R Core Team (2013).

Experiments were performed at 23°C, 40 ± 10% relative humidity, during the second half of the scotophase (i.e., 4–7 h after lights turned off) which corresponds to the peak activity of male *A. ipsilon*. Five-day old virgin males were tested. A single male was introduced inside a cage on a 36 cm high holder in the middle of the tunnel width and 160 cm downwind from the odor source. After allowing the moth to adapt to the airflow, we applied the odor stimulation and monitored the male's behavior for 3 min. We compared the responses of males to either the pheromone at 100 ng or heptanal at 0.1 or 1% dilutions. Control experiments (no odor) were performed with a clean filter paper as source. Each individual was tested only once. Olfactory stimuli were delivered using the same model of stimulator as in our electrophysiological experiments enabling to deliver odorants by switching solenoid-driven Lee micro valves via a Valve-Bank controller, with separate channels for each odorant. Hypodermic 18 G needles fixed in the middle of the upwind side of the tunnel were used as odor nozzles delivering odorized air flows at the upwind end of the tunnel. The solution of sex pheromone in hexane was deposited on a filter paper introduced in a 4 ml glass vial after solvent evaporation. Heptanal was diluted in 1 ml of mineral oil.

Four behavioral items were scored: activation (walking activity and/or wing fanning on the take-off platform), take off (taking off from the platform) partial flight during the test (flight half way between the release site and the odor source) and source flight (flight ending within 20 cm of the source) before the end of the test (180 s). All males stimulated with the pheromone blend showed activation and performed a take-off in less than 90 s after the beginning of the test, so 90 s was taken as the time limit for scoring these two items for all subsequent experiments.

To compare the orientation of males toward the wind direction in presence of the different odor sources the .csv files produced by Trackit were used to calculate distribution plots of the positions of the male along the tunnel width. The tracks were first smoothed using a local polynomial regression fitting [function "loess()" from R package "stats," (R Core Team, 2013)]. We then extracted the section of the smoothed tracks from the departing point (platform), up to the point where the moth reached its maximum value on the length axis. Finally we calculated the cumulated distribution along the width axis of the males, within the whole length after take off (the first 10 cm from the platform were excluded) and plotted it for each treatment (pheromone, 1% heptanal, 0.1% heptanal, and control).

Statistical Analyses

For electrophysiological experiments, spike occurrence times were analyzed using custom-written R scripts (R Core Team, 2013). Firing rates were calculated using the local slope of the cumulative function of spike times (Blejec, 2005). The slope was calculated over a moving spike window between the n−2 and n+2 spikes (5 spikes). Thus, each spike was attributed a firing rate and its occurrence time. The maximum firing rate during the 1st second from stimulus start was measured for each recording. The mean ± standard error of the maximum firing rates was calculated for each stimulation. Data were compared using a Student *t*-test for paired data followed by tests to check for data set normality (Shapiro test) and variance homogeneity (Fisher-Snedecor test), concerning data from ORN recordings, or were compared using a Wilcoxon test for paired data for data from MGC neuron recordings.

The experimental decline of the averaged responses was fitted with an exponential asymptotic decay function by determining the non-linear least-squares estimates of parameter of an exponential model (function nls of R). Curves of firing rates were standardized relatively to the maximum firing rate. The asymptotic decay functions were estimated from the time of the maximum firing rate to 1 s after the stimulation times (Equation 3):

$$FR = a + b * e^{(-c * time)}$$

where *FR* is the maximum firing rate, a is the offset, b the initial firing rate, and c the rate coefficient of the curve. The time values for 90% decay (td90) were calculated from Equation 3.

We estimated the response latency for each recording using custom-written R scripts. First, we calculated a threshold for excitation response as the 95th percentile of spike firing rates before stimulation onset (spontaneous activity). Second, we looked for the first spike crossing this threshold within the expected response time window corresponding to 1 s after stimulation start. We defined this spike occurrence time as response latency. We compared median latencies between two treatments using a chi-square test.

Calcium responses induced by different odors in different glomeruli were compared using Statistica (Version'99, www.statsoft.com). We performed One- or Two-Way ANOVAs for repeated measures with the two factors odor and glomerulus. When interactions among factors were significant, simple effects were analyzed by means of a One-Way ANOVA with or without the RM factor, and then followed by a Tukey's test for *post-hoc* comparisons if necessary.

For wind tunnel experiments, a Fisher's exact test was used to compare scores of response of male moths to heptanal and the pheromone.

Results

Heptanal Activates VPC-ORNs but also Phe-ORNs

The antennae of *A. ipsilon* are bipectinate with ORNs tuned to pheromone (Phe-ORNs) mainly housed in the trichoid sensilla situated on the branches while ORNs tuned to volatile plant compounds (VPC-ORNs) are predominantly housed within sensilla localized on the antenna stem (Renou et al., 1996). We thus recorded from olfactory sensilla sampled either from the antennal branches or antennal stem and attributed functional types to ORNs according to the most active stimulus. An extensive screening of noctuid pheromone components has evidenced a majority (32 out 52) of Phe-ORNs responding exclusively to Z7-12:Ac, some neurons responding mainly to Z5-10:Ac but also to Z8 and Z9-12:Ac, and only one neuron responding to Z9-14:Ac, but no neuron responding to Z11-16:Ac (Renou et al., 1996). These functional types of Phe-ORNs were never encountered in a same sensillum. On the antennal branches, 92% of all Phe-ORNs encountered responded to Z7-12:Ac (Renou et al., 1996). Thus, we expected the latter neuron type to largely dominate our results. Our single-sensillum recordings showed that Phe-ORNs on the branches responded to the pheromone in a phasic-tonic mode (**Figure 1A**) and already at a dose of 1 ng (**Figure 1B**, red curve). Interestingly, these Phe-ORNs responded also to 1% heptanal (**Figure 1B**, solid green curve). This dilution corresponds to a total amount of 8.1 mg heptanal at the source and an aerial concentration of 14 ppm. The response amplitude to heptanal increased with increasing doses at the source but did not reach saturation at the highest dose tested (**Figure 1B**, solid green curve). The heptanal dose-response curve was clearly shifted toward higher concentrations, compared to the dose-response curve for the pheromone, indicating a lower potency for heptanal to activate Phe-ORNs.

On the other hand, the ORNs housed in olfactory hairs located on the antennal stem did not respond to the pheromone as expected from VPC-ORNs, but responded to heptanal with higher firing rates and a lower threshold compared to Phe-ORNs. These VPC-ORNs started to respond already at a dose of 0.1% corresponding to 0.81 mg (3.9 ppm_v) heptanal at the source (**Figure 1B**, dashed green curve). In the following experiments, 10 and 100 ng or 0.1 and 1% will designate low and medium stimulus strengths for pheromone and heptanal, respectively.

We then compared the response dynamics of Phe-ORNs to the pheromone and 1% heptanal (**Figure 2**). All 51 Phe-ORNs examined responded to the pheromone by a simple phasic-tonic excitatory response (**Figures 2A,B**, left) with 0.331 s median latency (**Figure 2C** left). Among these 51 Phe-ORNS,

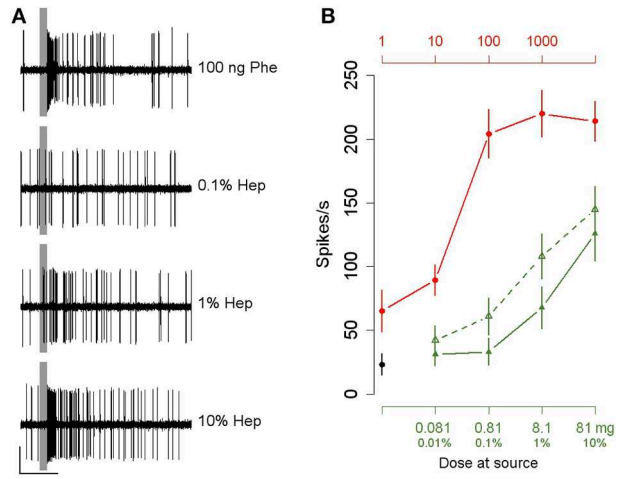

FIGURE 1 | *Agrotis ipsilon* Phe-ORNs respond to heptanal. (A) Typical examples of the responses of Phe-ORNs to the pheromone (Phe) and three doses of heptanal (Hep). Scale: vertical bar = 1 mV; horizontal bar = 1 s. The vertical gray bars indicate the stimulus (200 ms). **(B)** Dose-response curves of Phe-ORNs to a 200 ms puff of the pheromone or of Phe-ORNs and VPC-ORNs to heptanal. Mean of the maximum firing rates during the 1st second from stimulus start (± SEM). Doses of heptanal are in v/V % of dilution in mineral oil with their equivalance in mg (lower horizontal axis); doses of pheromone are in ng deposited on filter paper (upper horizontal axis). Phe-ORNs responded already to the lowest pheromone dose tested and the maximum firing rate increased with increasing doses (solid red line, $n = 16$). Phe-ORNs started to respond to heptanal at a dose of 1% (solid green curve, $n = 12$) while VPC-ORNs responded already at a dose of 0.1% (dashed green curve, $n = 14$). Controls (black dot) refer to pooled data of stimulation with pure hexane and pure mineral oil.

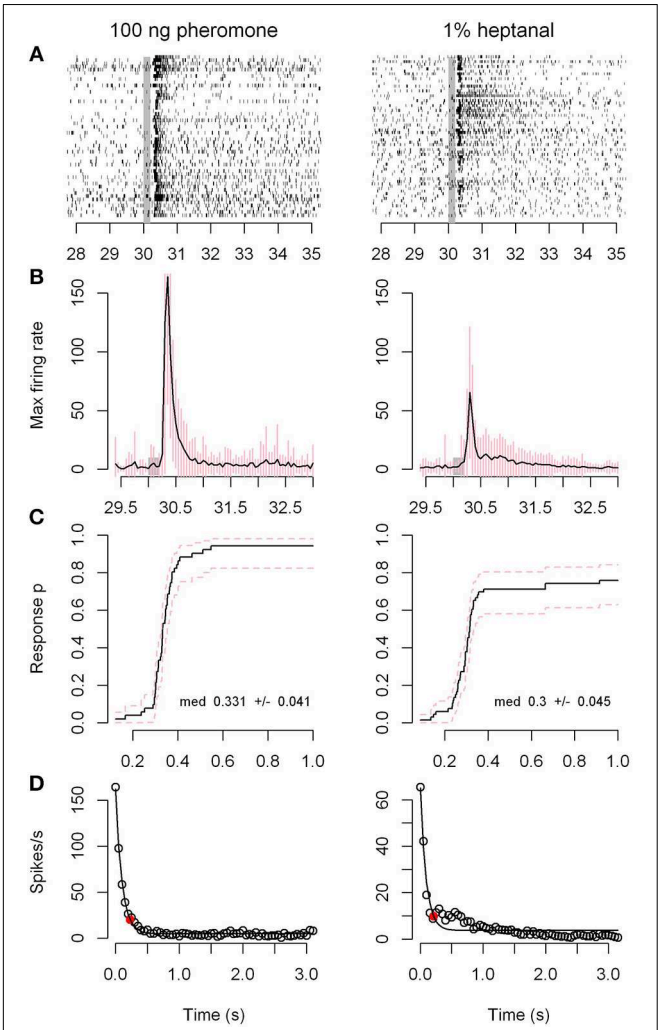

FIGURE 2 | Response dynamics of Phe-ORNs to the pheromone or heptanal are very similar. The dynamics of the response of ORNs sampled on antennal branches to a 200 ms pulse of 100 ng pheromone (left column) or 1% heptanal (right column) are compared. **(A)** Raster plots of the firing activity of 51 individual neurons. The vertical gray bars show the stimulus time. **(B)** Frequency plots of the maximum firing rates for the same sample of neurons (time bin = 50 ms). Means of the 51 recordings. Error bars in pink represent standard deviation. **(C)** Kaplan-Meier curves of the response latencies; p is the proportion of neurons that responded to the olfactory stimulus at a given time. **(D)** Exponential decrease model for response end. The red dots represent the estimated values for 90% decrease.

40 responded also to 0.1% heptanal, even though with lower firing frequencies (**Figures 2A,B**, right). The latency of the response to heptanal (median = 0.3 s **Figure 2C** right) was not significantly different from the response to pheromone (Student's t-test, $p = 0.22$). The firing responses to heptanal were generally phasic-tonic. However, the response patterns were more variable compared to those to pheromone (**Figure 2A**). In seven Phe-ORNs the responses to heptanal showed prolonged after-response firing activity, while in several others, responses presented a post-stimulus period of silence. Nevertheless, the decay of the response to pheromone or heptanal showed globally equivalent kinetics (**Figure 2D**), the firing rate decreased by 90% after 0.250 s with pheromone vs. 0.229 s in response to heptanal. However, the experimental data for heptanal were less well fitted to the theoretical exponential decay function than with the pheromone (**Figure 2D**), due to the post stimulus firing activity above the level expected from the simple exponential decay model in some neurons.

Different Other Volatile Plant Compounds Activate Phe-ORNs

Most of the ORNs housed in the sensilla sampled on the branches also increased their firing in response to some of the VPCs tested at 1%, although the maximum firing rate in response to VPCs was generally lower compared to pheromone. Heptanal and the six additional VPCs elicited generally a single excitatory phase in Phe-ORNs (**Figure 3A**). Hexanal, however, triggered also an excitatory-inhibitory response in some Phe-ORNs (**Figure 3A**). Out of 46 tested ORNs situated on the branches of the antennae and showing clear responses to the pheromone, 40 responded also to Z3-6Ac, 27 to hexanal, 30 to linalool, 26 to octanal, 11 to 2-phenylethanol and only 2 to α-pinene (**Figure 3B**). However, the Phe-ORNs could not be sorted into functional subtypes according to their response profiles to the seven VPCs (**Figure 3B**). The intensity or frequency of the firing response of Phe-ORNs to VPCs was apparently not correlated to their

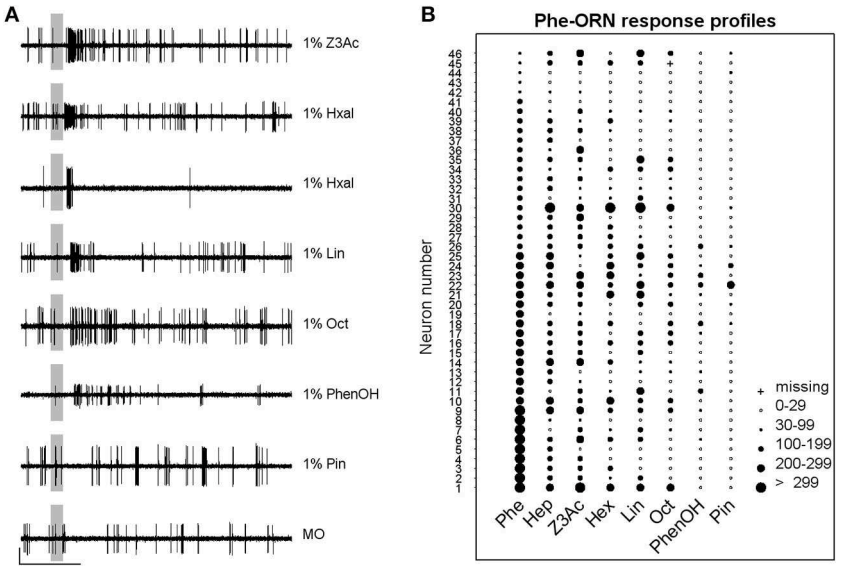

FIGURE 3 | Phe-ORNs respond to different volatile plant compounds. (A) Typical examples of responses of Phe-ORNs to different volatile plant compounds. Single sensillum recordings from different sensilla show that Phe-ORN responses are similar between odors except for hexanal which induced two different response patterns. Scale: vertical bar = 1 mV; horizontal bar = 1 s. The vertical gray bar indicates the stimulus (200 ms). **(B)** Response-profiles of individual Phe-ORNs to seven VPCs. Each line presents the responses of a single ORN; each column shows the responses of different neurons to one odorant. The diameter of circles is proportional to the intensity of the response measured as the absolute maximum firing rate reached within 1 s after stimulus onset. Phe, pheromone; Hep, heptanal; Z3Ac, (Z)-3-Hexenyl acetate; Hxal, hexanal; Lin, linalool; Oct, octanal; PhenOH, 2-phenylethanol; Pin, α-pinene.

chemical structure, nor to their volatility. For instance, aldehydes were not globally more active than the other VPCs; α-pinene was practically inactive although its vapor pressure is quite close to that of heptanal (500 and 300 Pa, respectively). For five Phe-ORNs, maximum firing rates were slightly higher for certain VPCs than for the pheromone itself.

The Pheromone Does not Activate ORNs on the Antennal Stem

Another set of single sensillum recordings was performed from the short sensilla trichodea localized on the antennal stem. The results revealed that only one of the sampled presumed VPC-ORNs ($n = 26$), which responded to at least one of the VPCs (examples of recordings in **Figure 4A**), responded also strongly to 100 ng of the pheromone (**Figure 4B**). This confirms a clear, but not exclusive spatial segregation of general odorant and pheromone detection in the antennae, most of the ORNs contained in the stem area being tuned to general odorants, while Phe-ORNs are mostly housed in branch hairs. The level of firing activity during responses was generally lower and stem-ORNs showed more specificity in their responses to the different VPCs compared to Phe-ORNs which each responded to several VPCs (**Figures 3B, 4B**).

Heptanal Does not Activate Phe-ORNs of *S. littoralis*

To verify if VPC responses in Phe-ORNs are species-, or pheromone structure-dependent, we also recorded from 10 sensilla housing Phe-ORNs in another noctuid moth species, *S. littoralis*. Phe-ORNs responded to 100 ng of the major sex pheromone compound Z9,E11-14:Ac with a maximum firing rate of 228.1 spikes/s ± 30.6 (mean of 10 replicates ± SEM) while the firing activity in response to 1% heptanal (31.8 ± 16.3) was not significantly different from that to the control (11.3 ± 5.04; paired Student'*t*-test $p = 0.148$) (**Figure 5**).

Heptanal Evokes Calcium Responses in the MGC

In vivo calcium imaging was performed to obtain a global pattern of the odor-evoked input to the antennal lobe. Global brain staining with a calcium-sensitive dye reveals odor-induced activity of all neuronal populations, however, due to their quantitative predominance, activity recorded originates mainly from ORN responses. Thus, such global responses are complementary to individual neuronal responses obtained with SSR or intracellular recordings. Stimulating the antennae of male *A. ipsilon* revealed calcium responses induced by the plant odors heptanal and linalool in the area of ordinary glomeruli. The pheromone elicited responses in the MGC. The solvents hexane and mineral oil did not elicit any response (**Figure 6A**). Odor-evoked signals were typical stereotyped biphasic signals usually obtained with bath application of the dye Calcium Green 2-AM, with first a fast fluorescence increase followed by a slow fluorescence decrease below baseline (**Figure 6B**; Galizia et al., 1997; Stetter et al., 2001; Sandoz et al., 2003). The two VPCs (heptanal and linalool) induced calcium responses in ROIs within the area of OGs (**Figures 6B,D**). Response intensity to 1% heptanal in ROIs 6, 7, and 8 was significantly stronger compared to response intensities induced by 1% linalool (**Figure 6D**, *Post-hoc* Tukey's test, ROI 6: $p = 0.05$; ROI 7: $p = 0.02$; ROI 8: $p = 0.005$), while

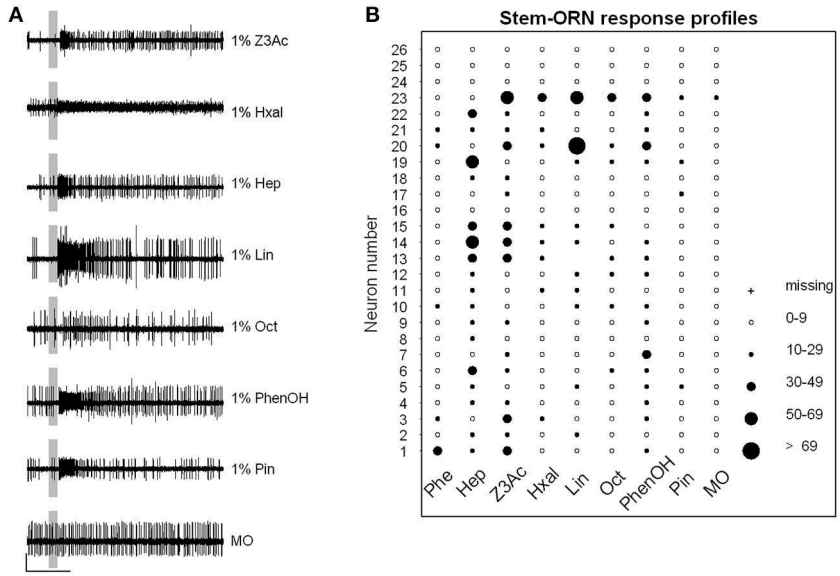

FIGURE 4 | VPCs activate general odorant ORNs. (A) Typical examples of responses of Stem-ORNs from different sensilla to the set of VPCs. Single sensillum recordings show the presence of several spike sizes in most sensilla and generally excitatory responses in one of the ORNs of each sensillum. Scale: vertical bar = 1 mV; horizontal bar = 1 s. The vertical gray bar indicates the stimulus (200 ms). **(B)** Response-profiles of ORNs sampled on the antennal stem to seven VPCs and the pheromone. Only one of the ORNs responded to the sex pheromone. Each line presents the responses of a single ORN ($n = 26$); each column shows the responses of the different neurons to one odorant. The diameter of circles is proportional to the intensity of the response quantified as the absolute maximum firing rate reached during 1 s following stimulus onset. Phe, pheromone; Hep, heptanal; Z3Ac, (Z)-3-Hexenyl acetate; Hxal, hexanal; Lin, linalool; Oct, octanal; PhenOH, 2-phenylethanol; Pin, α-pinene; MO, mineral oil control.

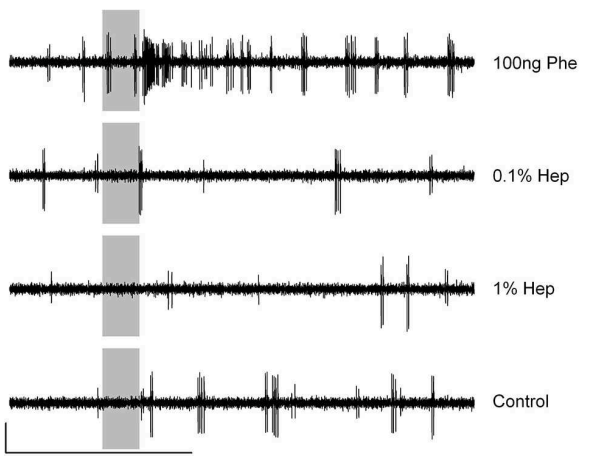

FIGURE 5 | Typical recordings of the firing activity of *Spodoptera littoralis* Phe-ORNs stimulated with pheromone or VPCs. ORNs identified as pheromone receptor neurons from their position within long trichoid sensilla of the male antenna and their strong response to 100 ng Z9,E11-14:Ac (upper recording) did neither respond to 0.1% heptanal (middle trace) nor to 1% heptanal (lower trace). Scale: vertical bar = 1 mV; horizontal bar = 1 s. The vertical gray bar indicates the stimulus (200 ms).

linalool did not induce significantly stronger responses in any of the observed ROIs compared to heptanal (**Figures 6B,D**). The pheromone did not induce significant responses in the area of ordinary glomeruli (**Figure 6D**). In agreement with data obtained from our single sensillum recordings, not only stimulations with 100 ng sex pheromone, but also with 1% heptanal and 1% linalool evoked calcium responses in the pheromone-specific MGC of the AL (**Figures 6B,C**). Statistical analysis of the activity of 3 ROIs within the MGC area revealed that overall response intensity was not different between the 3 ROIs. Pooled data of the 3 ROIs within the MGC were not significantly different between heptanal-, linalool-, and pheromone-induced calcium signals [One-Way ANOVA, $F_{(2,\ 15)} = 2.53$, $p = 0.11$, **Figure 6C**, $n = 6$].

Heptanal Activates MGC Neurons in the Antennal Lobe

We recorded intracellularly from 35 MGC neurons with clear responses to the pheromone. Twenty-five of the recorded neurons showed an excitatory response followed by an inhibitory phase to 100 ng pheromone (type A neurons, **Figure 7A**) and 10 neurons showed a purely excitatory response (type B neurons, **Figure 7B**). Although more than half of the neurons responded to 1% heptanal with the same pattern as to the pheromone (**Figure 7**, and neurons 1 to 5 in **Figure 8**), responses to heptanal were more variable than to the pheromone (**Figure 8**). For both concentrations of heptanal, purely inhibitory responses or an initial inhibitory phase before an excitatory response appeared in addition to the excitatory responses to the pheromone (**Figure 8**). When stimulated with 0.1% heptanal, more than half of the neurons responded with pure inhibition (e.g., neurons 3, 5, 6, 7 in **Figure 8**) or not at all (e.g., neurons 2, 8, 9 in **Figure 8**). Also the evolution of response patterns from 0.1 to 1% heptanal was highly variable (**Figure 8**).

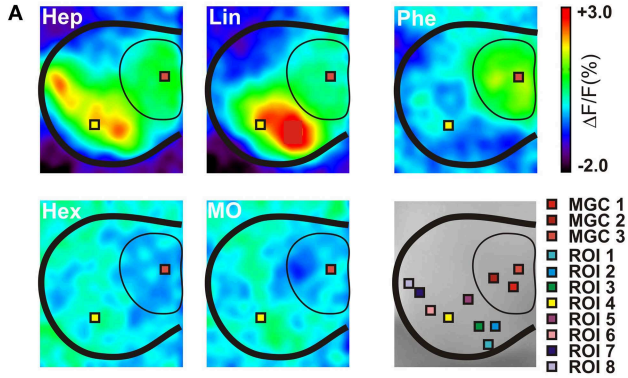

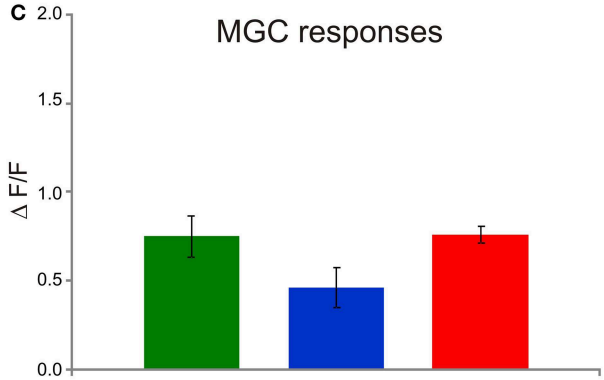

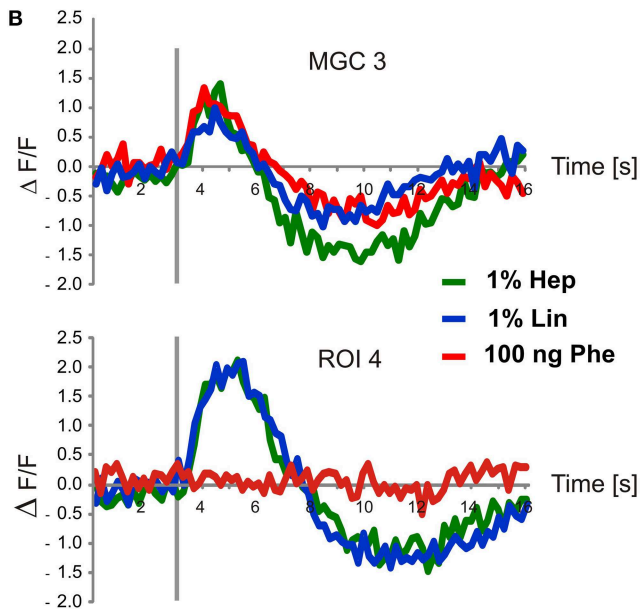

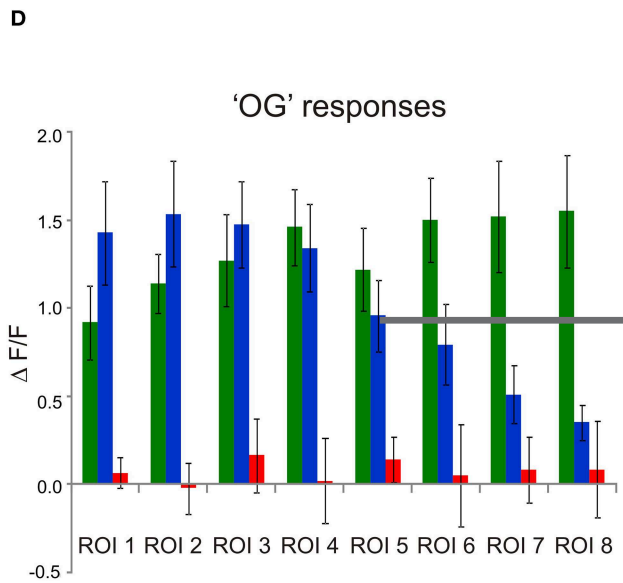

FIGURE 6 | Heptanal and pheromone evoke calcium responses in the AL. (A) Odor induced *in vivo*-calcium imaging signals obtained in a male stimulated with heptanal, linalool, pheromone, pure hexane, and pure mineral oil. All maps are scaled to the same minimum/maximum. Eight ROIs were defined to cover the areas of OG (ROI1 to ROI8). Due to the large size of the MGC, three ROIs were defined within the MGC (MGC1 to MGC3). **(B)** Time course of odor-evoked calcium activity in the MGC and OG4 in the isomorphic glomeruli indicated in **(A)**. **(C)** Mean (± SEM) calcium response intensity in the MGC and **(D)** in OG1 to OG8 induced by heptanal ($n = 6$), linalool ($n = 6$), and the pheromone ($n = 6$), hexane ($n = 4$) and mineral oil ($n = 4$). The gray bar in **(B)** indicates the stimulus (200 ms). Hep, Heptanal; Lin, linalool; Phe, pheromone; MO, mineral oil; Hex, hexane; OG, ordinary glomeruli.

To compare responses between the three stimuli quantitatively, we pooled all neurons displaying an excitatory phase and compared maximum firing rates and latencies statistically (**Figure 9**). Maximum firing rates in MGC neurons were significantly higher in response to the pheromone than to 0.1% heptanal (Wilcoxon signed rank test for paired data, $V = 625$, $p = 5.821^{-10}$) and to 1% heptanal ($V = 535$, $p = 1.51^{-5}$). Maximum firing rates in response to 1% heptanal were significantly higher than responses to control ($V = 561$, $P = 1.454^{-5}$) but not to 0.1% heptanal ($V = 295$, $p = 0.972$). Response latencies were also statistically different between the three stimuli ($\chi^2 = 65.2$ on 2 degrees of freedom, $p = 7.11^{-15}$). But latencies in response to the pheromone were not only shorter, but also less variable than in response to heptanal (**Figure 9**). The Kaplan-Meier estimator curves for latency illustrate the larger spreading of response latencies to heptanal, especially to the lower concentration and the large proportion of non-responding neurons (**Figure 9**).

Heptanal Does not Trigger Complete Upwind Flight

Male moths were generally very active in the wind tunnel, even in the absence of an olfactory stimulus as shown by the high percentage of activation (78%) and take off (56%) in control tests (**Table 2**). However, none of these active moths reached the upwind end of the tunnel in control experiments. A significantly higher percentage of males were taking off (96.0%, $\chi^2 = 19.73$ $p < 0.001$) and performed a sustained flight (92.0%, $\chi^2 = 19.42$

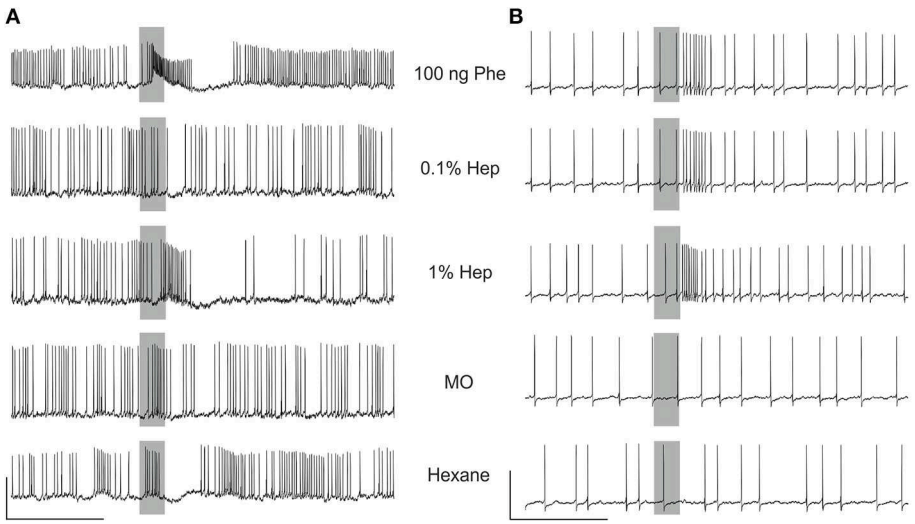

FIGURE 7 | MGC neurons respond to the pheromone and heptanal. Examples of recordings of a biphasic **(A)** and a monophasic **(B)** neuron, responding similarly to the pheromone and heptanal. Note the responses in A to solvent controls, probably of mechanosensory origin (Jarriault et al., 2009). The gray bars indicate the stimulus (200 ms). Vertical scale A: 10 mV, B: 20 mV; horizontal scale 1 s.

TABLE 2 | Flight responses of virgin male *A. ipsilon* to heptanal and the pheromone in a wind tunnel.

Stimulus	Number of males	Activation	Taking off	Partial flight	Source flight
Pheromone	50	100	96.0	92.0	34.0
0.1% heptanal	26	84.6	76.9	61.5	0.0
1% heptanal	24	91.7	79.2	75.0	0.0
Control	50	78.0	56.0	50.0	0.0

Data are the percentages of four behavioral items carried out within 90 s.

$p < 0.001$), reaching the half-length of the tunnel before the end of the test (34%, $\chi^2 = 48.52$ $p < 0.001$) in presence of the pheromone compared to the control stimulation. Males took off significantly earlier in response to the pheromone (median time for take off = 21.5 s), compared to heptanal 0.1 and 1% or control (59.0, 53.0, and 56.0 s, respectively; $\chi^2 = 48.7$ on three degrees of freedom, $p = 1.51^{-10}$). Male *A. ipsilon* arrived close to the source only in presence of the pheromone. There was no statistical difference between heptanal at 0.1% and control stimulation for all items. In turn significantly more males took off (79.2%; $\chi^2 = 19.73$, $p < 0.001$) and performed a partial flight (75.0%; $\chi^2 = 19.42$, $p < 0.001$) when stimulated with heptanal at 1%, compared to controls (**Table 2**).

In presence of the pheromone, the distribution map of moths in the wind tunnel revealed a strong density of male presence in the longitudinal axis downwind to the pheromone source (**Figure 10**). In turn, in presence of both concentrations of heptanal, males did not fly upwind. Control tracks showed a preference of male moths for the front side revealing a possible un-controlled heterogeneity in the room environment but no preference for the longitudinal median axis.

Discussion

Phe-ORNs are Sensitive to Volatile Plant Compounds

Using complementary approaches, we show that heptanal and other plant odorants activate the pheromone-specific pathway in male *A. ipsilon*. Still, heptanal was less efficient than the sex pheromone—dose response curves were shifted toward higher concentrations—thus behaving as a partial agonist at the detection level. Although we used a three-component pheromone blend for stimulation, we suppose that we primarily investigated the detection of plant odorants within Phe-ORNs tuned to the major pheromone component Z7-12:Ac, because these ORNs represent more than 90% of all pheromone-detecting neurons on the antennal branches, which we recorded from Renou et al. (1996). Insect olfactory receptors (ORs) involved in the detection of compounds having high biological relevance to the insect's biology show generally narrow tuning ranges (Wang et al., 2010) confering high selectivity to ORNs that express them. Among ORNs, Phe-ORNs are thus considered as specialists, narrowly tuned to individual pheromone constituents and not responding to general odorants (Masson and Mustaparta, 1990). However, some exceptions to this rule are known: receptor neurons tuned to the main pheromone component, codlemone, in the antennae of male *Cydia pomonella* respond also to pear ester, ethyl (E,Z)-2,4-decadienoate (De Cristofaro et al., 2004). In this particular example, the structural resemblance between codlemone and pear ester, could account for the capacity of this compound to excite Phe-ORNs. The OR for codlemone has not yet been found but curiously, CpomOR3, later identified as a specific receptor for pear ester (Bengtsson et al., 2014) and having a close relationship with moth pheromone receptors, did not bind components of the codling moth pheromone blend. In turn, responses of Phe-ORNs to short chain alcohols or

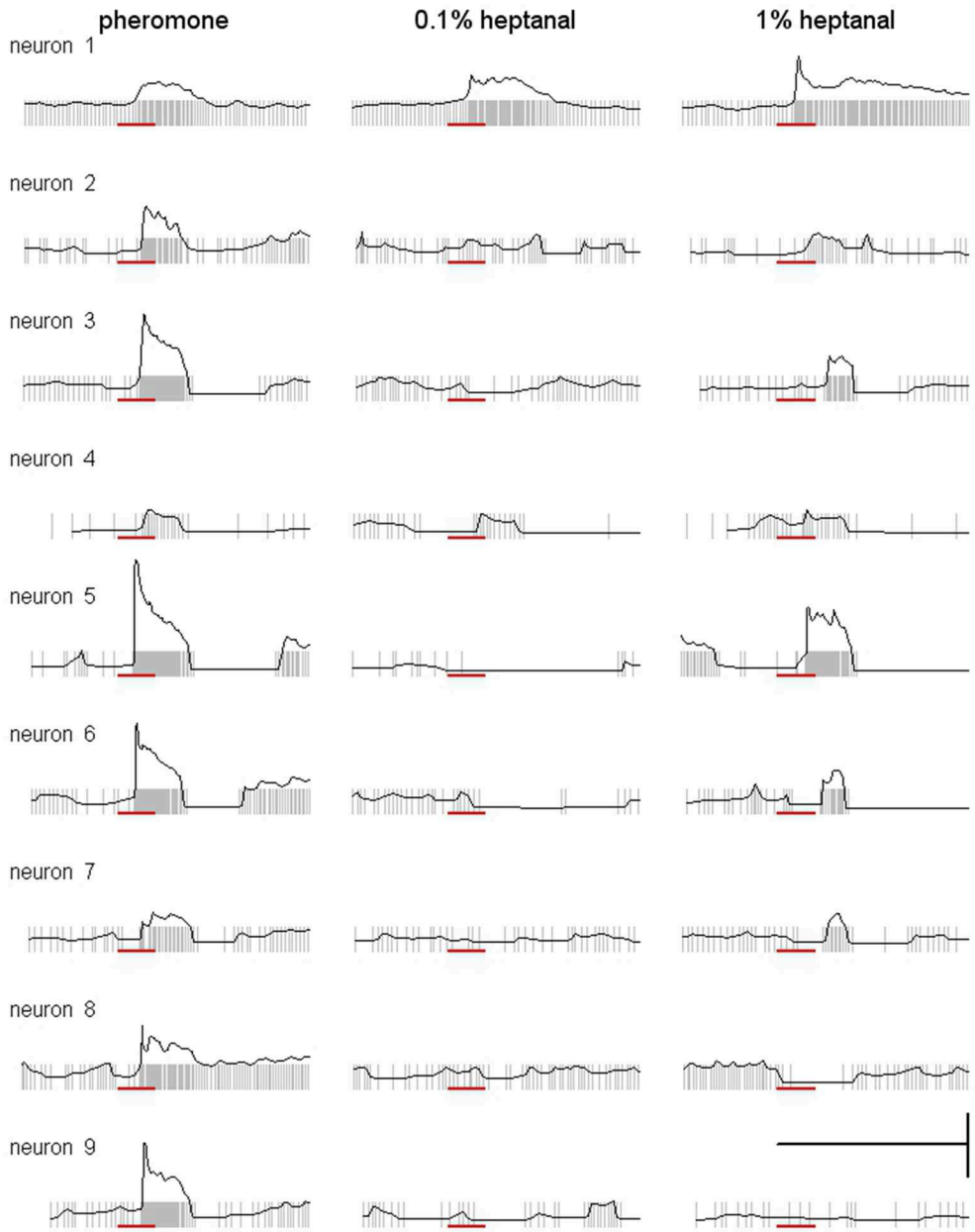

FIGURE 8 | Heptanal evokes more variable responses in MGC neurons than the pheromone. Superimposed raster and frequency plots of responses of MGC neurons illustrating the variability of responses to heptanal between neurons and between pheromone and the two concentrations of heptanal within neurons. Scale: vertical bar = 100 spikes, horizontal bar = 1 s. Red bar indicates the stimulus (200 ms).

monoterpenes have been mentioned in *A. segetum* and *S. exigua* whose pheromones are long-chain acetates (Hansson et al., 1989; Dickens et al., 1993). Besides these few examples of their direct activation by VPCs, Phe-ORNs' specificity can also be challenged by mixture interactions with pheromone as reported in various moth species (Rouyar et al., 2011 and references therein). However, to our knowledge, the present work is the first detailed report of a plant odorant with no chemical similarity to the molecular structure of the pheromone acting on its own as a partial agonist of a moth pheromone. Besides heptanal several other plant volatile compounds were found to activate the firing of Phe-ORNs in *A. ipsilon*. In turn, most Phe-ORNs did not respond to α-pinene. To determine whether the aldehyde function was important for activity, we tested two other short chain aldehydes, hexanal and octanal. Both compounds did not elicit higher responses compared to the other VPCs, showing that there is no simple correlation between chemical structure and the capacity to excite Phe-ORNs. The finding that Phe-ORNs respond to higher concentrations of VPCs compared to pheromone is well in agreement with the observation that

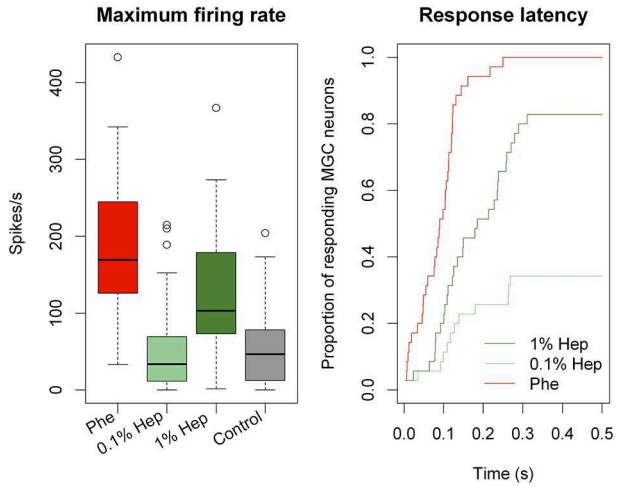

FIGURE 9 | Quantitative analysis of MGC neuron responses to the pheromone and heptanal. Boxplot of mean maximum firing rates (Box = median with first and third quartiles, whiskers = second and fourth quartiles, circles = outliers) and Kaplan-Meier estimator curves for the latencies of MGC neuron ($n = 35$) responses. MGC neurons respond with lower maximum firing rates and longer latencies to 0.1 and 1% heptanal compared to the pheromone. Control refers to pooled data of stimulation with pure hexane and pure mineral oil. Hep, heptanal; Phe, pheromone.

OR specificity is generally dose dependent, an increase in the concentration of the odorants broadening the response spectra (Hallem and Carlson, 2006). Although we cannot exclude that *A. ipsilon* Phe-ORNs might express multiple OR types, we hypothesize that pheromone-binding ORs are activated by high doses of heptanal in this species in analogy to what has been found for interactions between pheromones and plant odors at the molecular level: Modifications of pheromone responses by certain plant volatiles have been shown to be dependent on a pheromone-specific OR in *Heliothis virescens* (Pregitzer et al., 2012). It should be noted that in the field VPC concentrations needed to activate Phe-ORN might be reached only very close to their plant sources.

Contrasting with this ability of heptanal, and to lesser extent linalool, to activate pheromone receptors in *A. ipsilon*, both compounds did not activate the Phe-ORNs tuned to the main pheromone component in *S. littoralis*. On the contrary, linalool has been shown to be an antagonist of pheromone detection in the latter species (Party et al., 2009). Such differences between moth species support the hypothesis that activation of heptanal might not be an unspecific pharmacological effect. Differences between the two moth species might result from binding affinity in the pheromone ORs for heptanal, correlated to the different chemical structure of their pheromone ligands. Alternatively, this cross-sensitivity of *A. ipsilon* Phe-ORNs, but not those of *S. littoralis*, to pheromone and heptanal could reflect a specific adaptation of male *A. ipsilon* due to the ecological advantage for them to detect plant odorants attractive to sexually mature females (Landolt and Phillips, 1997).

MGC Neurons are Sensitive to Volatile Plant Compounds

Calcium imaging at the AL level showed strong calcium responses to heptanal, and to a lesser degree to linalool in the MGC, showing that the activation of Phe-ORNs by VPCs produces a strong input in the pheromone-specialized areas of the olfactory centers. Interestingly, the size of the activated area in the MGC and the number of activated OGs was larger at the high concentration (1%), compared to the low concentration (0.1%) suggesting a broadening of responses at high stimulus concentration, probably due to additional responses from ORNs which are less tuned to the ligand.

Almost all MGC neurons responding to 100 ng of the pheromone were also activated by 1% heptanal. However, maximum firing rates were significantly lower with 1% heptanal and the response patterns were much more variable than those to the pheromone and in many cases included an initial inhibition before the excitatory response. These results are in accordance with earlier studies in *A. ipsilon,* where both stimuli elicited responses, although tested only at lower doses (Jarriault et al., 2009; Barrozo et al., 2011; Chaffiol et al., 2012). Activation of MGC neurons by VPCs at behaviorally active doses has been also reported in several other moth species: *S. littoralis* (Anton and Hansson, 1995), *Manduca sexta* (Reisenman et al., 2008), *C. pomonella* (Trona et al., 2010), and *Cydia molesta* (Varela et al., 2011). This across-pathway stimulation has so far essentially been explained to originate from the AL network linking ordinary glomeruli to the MGC by local interneurons (LNs) and thus allowing indirect input of VPC information to the MGC via interglomerular excitation and/or inhibition and allowing interactions between different odorants at the central nervous level (Lei and Vickers, 2008). Our new data in *A. ipsilon* show now that VPC activation within the MGC is probably a combination of direct activation of Phe-ORNs by VPCs directly transmitted to the MGC and indirect activation through the network activity of local interneurons, themselves receiving VPC-ORN input within OGs. In those MGC neurons, which respond in the same way to the pheromone and heptanal, it is likely that a direct activation of Phe-ORNs by VPCs is dominant. The more variable response patterns to heptanal and specifically the initial inhibition in the heptanal responses in the remaining MGC neurons not occurring for the pheromone, indicates that input from VPC neurons might activate the inhibitory LN network of the AL. In the future we will need to test the contribution of the AL network to global MGC input and individual MGC neuron responses to volatile plant components by different experimental approaches, using for example blockers of GABA or histamine, the main local interneuron transmitters (Galizia and Szyszka, 2008).

Behavioral Significance of Responses to VPCs in the Pheromone Subsystem

Since heptanal activated Phe-ORNs and central neurons in the MGC it was interesting to investigate the behavioral consequences. Moths' upwind flight responses to floral volatiles that signal for nectar sources are well established (Riffell et al., 2013). Male *A. ipsilon* were found to perform upwind flights not only to a linden flower extract in a wind tunnel (Barrozo et al.,

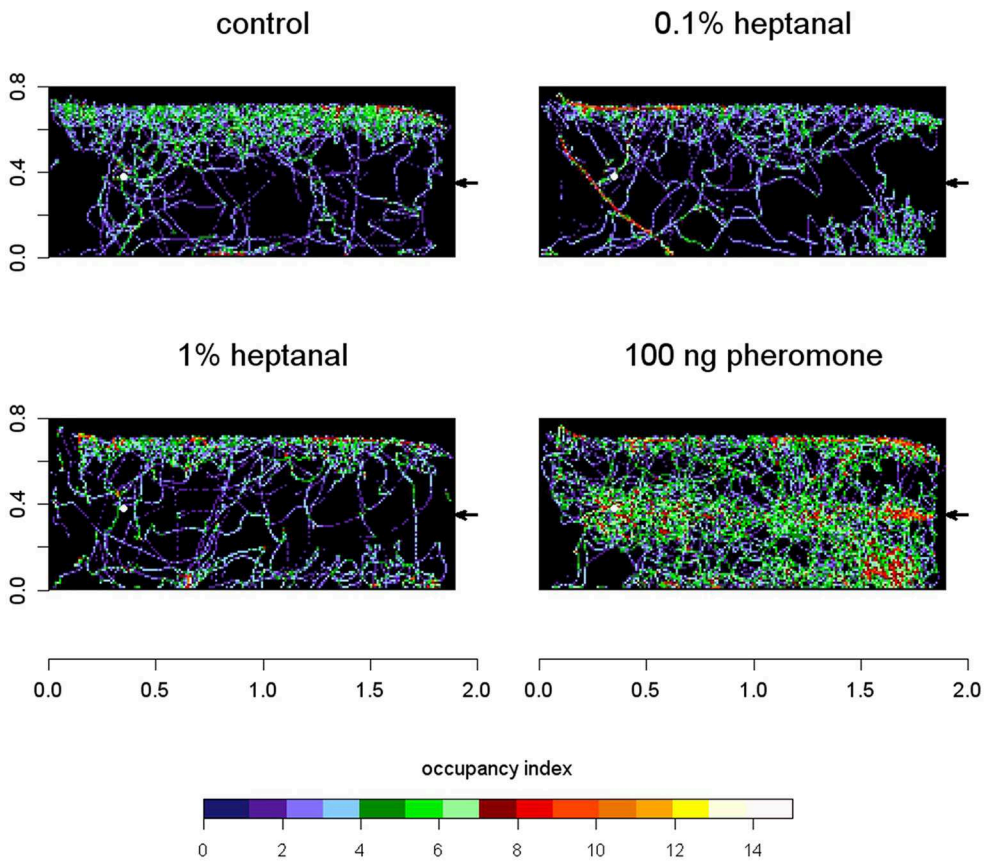

FIGURE 10 | Males perform upwind flight to pheromone but not to heptanal in a wind tunnel. Occupancy maps present side views of the summated tracks of male *A. ipsilon* in the wind tunnel. $n = 37$ tracks (100 ng pheromone); $n = 21$ (0.1% heptanal), $n = 18$ (1% heptanal), $n = 25$ (control). The arrow at the right of each diagram indicates the position of the stimulus source and the direction of the wind. The white dot indicates the point of male departure. Scales are given in meters. To draw the map, the summated numbers of recordings of a male presence within a 1 cm square were calculated from the coordinates of 3D tracks and color-coded.

2010a), but also in response to 100 μg of heptanal disposed on a filter paper (Deisig et al., 2012). Looking only at male flight scores in the wind tunnel does not reveal if an odor is perceived as a sexual or a feeding signal. We undertook here a more precise comparison of male flight behavior in the wind tunnel in presence of pheromone or heptanal with the same stimulation device as in physiological experiments. Male moths did take off in presence of heptanal and performed sustained flight at the high heptanal dose but they did not orient to the source. This absence of oriented flight toward heptanal in virgin males that responded readily to the pheromone strongly suggests that in spite of the activation of the pheromone pathway male moths did not perceive heptanal as a sexual signal. Since heptanal triggered intense activity in the MGC, the question is to determine which part of the olfactory system is responsible to operate discrimination of the pheromone from general odorants when the chemical specificity of Phe-ORNs is challenged. The convergence of a great number of ORNs on a few projection neurons and reciprocal interconnections between projection neurons through LNs do probably not facilitate the discrimination of heptanal from pheromone within the AL. However, a high degree of divergence occurs again between AL output and mushroom bodies, where a couple of hundred projection neurons make synaptic contact with high numbers of Kenyon cells (2500 in *D. melanogaster;* up to 170 000 in the honey bee; numbers provided in Galizia and Szyszka, 2008). Both intrinsic properties of Kenyon cells, such as active dendritic conductance, high action potential thresholds (Perez-Orive et al., 2002; Demmer and Kloppenburg, 2009) and postsynaptic inhibition (Papadopoulou et al., 2011) contribute to sparse coding within the mushroom bodies. This particular circuitry described in the upper levels of the olfactory system might allow better extraction of pheromone information from the contextual odorants (essentially a background of plant odors), especially when those contextual odorants trigger some activity in the pheromone sub-system. In addition, a spatially much broader representation of heptanal within the antennal lobe compared to the pheromone might contribute to the discrimination between the two signals.

Ecological Relevance of Heptanal Cross-Activity

Although heptanal is not rare among the volatile organic compounds emitted by plants, its role in insect chemical ecology

is relatively poorly documented. References in the literature indicate that this aldehyde is present in odor blends that have proven to be either attractive or repellent according to the species considered. Its production and release are induced for instance in maize following its infestation by leafhoppers, but the semiochemical activity on the insects has not been assessed (Oluwafemi et al., 2012). Heptanal has been reported to attract ovipositing females of the potato tuber moth, *Phtorimaea operculella* (Ma and Xiao, 2013). In turn, it is a component of synthetic blends designed as repellent for conifer infecting bark beetles (Huber et al., 2001). Blossoms of linden (*Tilia americana*) are intensively visited by adult *A. ipsilon* as a source of nectar (Wynne et al., 1991; Zhu et al., 1993). Blooming linden liberate huge amounts of volatiles among which heptanal is a major constituent so that it might be an environmental cue to *A. ipsilon* males indicating food sources and indirectly also the presence of females. This could explain that developing sensitivity to high concentrations of heptanal might be advantageous in the context of pheromone communication for males, largely compensating the drawback associated to reduced specificity of the pheromone sub-system. *S. littoralis*, on the other hand, is mainly distributed in Africa and the middle east. Adults feed on a large variety of flowering plants, including e.g., Solanaceae, citrus, and clover. Even though heptanal is emitted in small amounts from a variety of flowering plants visited by *S. littoralis*, such as strawberry (Klatt et al., 2013), it is not known to specifically attract this species. In turn, linden trees, emitting considerable amounts of heptantal and attracting *A. ipsilon* are native throughout the temperate northern hemisphere and not present in the natural habitat of *S. littoralis*. Such ecological differences might explain the differences in sensory physiology between the two moth species.

Acknowledgments

The authors thank Christophe Hanot for technical assistance, Corinne Chauvet and Cyril Le Corre for insect rearing, and the two referees for very helpful comments on an earlier version of the manuscript. The research was funded by grants from the French national research funding agency (ANR-11-BSV7-0026) and the Plant Health and Environment Department (SPE) of the French National Agricultural Research Institute (INRA). AR was supported by a PhD fellowship from the French Ministry of Science and Education.

References

Anton, S., and Hansson, B. S. (1995). Sex pheromone and plant-associated odour processing in antennal lobe interneurons of male *Spodoptera littoralis* (Lepidoptera:Noctuidae). *J. Comp. Physiol.* 176, 773–789. doi: 10.1007/BF00192625

Barrozo, R. B., Gadenne, C., and Anton, S. (2010a). Switching attraction to inhibition: mating-induced reversed role of sex pheromone in an insect. *J. Exp. Biol.* 213, 2933–2939. doi: 10.1242/jeb.043430

Barrozo, R. B., Jarriault, D., Deisig, N., Gemeno, C., Monsempes, C., Lucas, P., et al. (2011). Mating-induced differential coding of plant odour and sex pheromone in a male moth. *Eur. J. Neurosci.* 33:1841–1850. doi: 10.1111/j.1460-9568.2011.07678.x

Barrozo, R. B., Jarriault, D., Simeone, X., Gaertner, C., Gadenne, C., and Anton, S. (2010b). Mating-induced transient inhibition of responses to sex pheromone in a male moth is not mediated by octopamine or serotonin. *J. Exp. Biol.* 213:1100–1106. doi: 10.1242/jeb.040139

Bengtsson, J. M., Gonzalez, F., Cattaneo, A. M., Montagné, N., Walker, W. B., Bengtsson, M., et al. (2014). A predicted sex pheromone receptor of codling moth *Cydia pomonella* detects the plant volatile pear ester. *Front. Ecol. Evol.* 2:33. doi: 10.3389/fevo.2014.00033

Blejec, A. (2005). Statistical method for detection of firing rate changes in spontaneously active neurons. *Neurocomputing* 65, 557–563. doi: 10.1016/j.neucom.2004.10.103

Cardé, R. T., and Willis, M. A. (2008). Navigational strategies used by insects to find distant, wind-borne sources of odor. *J. Chem. Ecol.* 34, 854–866. doi: 10.1007/s10886-008-9484-5

Causse, R., Buès, R., Barthes, J., and Toubon, J. (1988). Mise en évidence expérimentale de nouveaux constituants des phéromones sexuelles de *Scotia ipsilon* et *Mamestra suasa*. Médiateurs chimiques: comportement et systématique des lépidoptères. *Coll. INRA* 46, 75–82.

Chaffiol, A., Kropf, J., Barrozo, R. B., Gadenne, C., Rospars, J., and Anton, S. (2012). Plant odour stimuli reshape pheromonal representation in neurons of the antennal lobe macroglomerular complex of a male moth. *J. Exp. Biol.* 215, 1670–1680. doi: 10.1242/jeb.066662

Christensen, T. A., and Hildebrand, J. G. (1987). Male-specific, sex pheromone-selective projection neurons in the antennal lobes of the moth, *Manduca sexta*. *J. Comp. Physiol. A* 160, 553–569. doi: 10.1007/BF00611929

Coracini, M., Bengtsson, M., Liblikas, I., and Witzgall, P. (2004). Attraction of codling moth males to apple volatiles. *Entomol. Exp. Appl.* 110, 1–10. doi: 10.1111/j.0013-8703.2004.00124.x

De Cristofaro, A., Ioriatti, C., Pasqualini, E., Anfora, G., Germinara, G. S., Villa, M., et al. (2004). Electrophysiological responses of *Cydia pomonella* to codlemone and pear ester ethyl (*E,Z*)-2,4-decadienoate: peripheral interactions in their perception and evidences for cells responding to both compounds. *Bull. Insectol.* 57, 137–144.

Deisig, N., Kropf, J., Vitecek, S., Pevergne, D., Rouyar, A., Sandoz, J. C., et al. (2012). Differential interactions of sex pheromone and plant odour in the olfactory pathway of a male moth. *PLoS ONE* 7:e33159. doi: 10.1371/journal.pone.0033159

Demmer, H., and Kloppenburg, P. (2009). Intrinsic membrane properties and inhibitory synaptic input of kenyon cells as mechanisms for sparse coding? *J. Neurophysiol.* 102, 1538–1550. doi: 10.1152/jn.00183.2009

Deng, J., Wei, H., Huang, Y., and Du, J. (2004). Enhancement of attraction to sex pheromones of *Spodoptera exigua* by volatile compounds produced by host plants. *J. Chem. Ecol.* 30, 2037–2045. doi: 10.1023/B:JOEC.0000045593.62422.73

Den Otter, C. J., Schuil, H. A., and Oosten, A. S.-V. (1978). Reception of host-plant odours and female sex pheromone in *Adoxophyes orana* (Lepidoptera: Tortricidae): electrophysiology and morphology *Entomol. Exp. Appl.* 24, 570–578. doi: 10.1111/j.1570-7458.1978.tb02818.x

Dickens, J. C., Visser, J. H., and Van Der Pers, J. N. C. (1993). Detection and deactivation of pheromone and plant odor components by the beet armyworm, *Spodoptera exigua* (Hubner) (Lepidoptera: Noctuidae). *J. Insect Physiol.* 39, 503–516.

Gadenne, C., and Anton, S. (2000). Central processing of sex pheromone stimuli is differentially regulated by juvenile hormone in a male moth. *J. Insect Physiol.* 46, 1195–1206. doi: 10.1016/S0022-1910(00)00040-8

Gadenne, C., Dufour, M. C., and Anton, S. (2001). Transient post-mating inhibition of behavioural and central nervous responses to sex pheromone in an insect. *Proc. Biol.* Sci. 268, 1631–1635. doi: 10.1098/rspb.2001.1710

Galizia, C. G., Joerges, J., Küttner, A., Faber, T., and Menzel, R. (1997). A semi-*in-vivo* preparation for optical recording of the insect brain. *J. Neurosci. Methods* 76, 61–69. doi: 10.1016/S0165-0270(97)00080-0

Galizia, C. G., Nägler, K., Hölldobler, B., and Menzel, R. (1998). Odour coding is bilaterally symmetrical in the antennal lobes of honeybees (*Apis*

mellifera). *Eur. J. Neurosci.* 10, 2964–2974. doi: 10.1111/j.1460-9568.1998.00303.x

Galizia, C. G., and Szyszka, P. (2008). Olfactory coding in the insect brain: molecular receptive ranges, spatial and temporal coding. *Entomol. Exp. Appl.* 128, 81–92. doi: 10.1111/j.1570-7458.2007.00661.x

Gemeno, C., and Haynes, K. F. (1998). Chemical and behavioral evidence for a third pheromone component in a north american population of the black cutworm moth, *Agrotis ipsilon*. *J. Chem. Ecol.* 24, 999–1011. doi: 10.1023/A:1022398318465

Hallem, E. A., and Carlson, J. R. (2006). Coding of odors by a receptor repertoire. *Cell* 125, 143–160. doi: 10.1016/j.cell.2006.01.050

Hansson, B. S., and Anton, S. (2000). Function and morphology of the antennal lobe: new developments. *Annu. Rev. Entomol.* 45, 203–231. doi: 10.1146/annurev.ento.45.1.203

Hansson, B. S., Van der Pers, J. N. C., and Löfqvist, J. (1989). Comparison of male and female olfactory cell response to pheromone compounds and plant volatiles in the turnip moth, *Agrotis segetum*. *Physiol. Entomol.* 14, 147–155. doi: 10.1111/j.1365-3032.1989.tb00946.x

Huber, D. P. W., Borden, J. H., and Stastny, M. (2001). Response of the pine engraver, *Ips pini* (Say) (Coleoptera: Scolytidae), to conophtorin and other angiosperm bark volatiles in the avoidance of non-hosts. *Agric. Forest Entomol.* 3, 225–232. doi: 10.1046/j.1461-9555.2001.00111.x

Jarriault, D., Gadenne, C., Lucas, P., Rospars, J. P., and Anton, S. (2010). Transformation of the sex pheromone signal in the noctuid moth *Agrotis ipsilon*: from peripheral input to antennal lobe output. *Chem. Senses* 35, 705–715. doi: 10.1093/chemse/bjq069

Jarriault, D., Gadenne, C., Rospars, J. P., and Anton, S. (2009). Quantitative analysis of sex-pheromone coding in the antennal lobe of the moth *Agrotis ipsilon*: a tool to study network plasticity. *J. Exp. Biol.* 212, 1191–1201. doi: 10.1242/jeb.024166

Justus, K. A., Murlis, J., Jones, C., and Carde, R. T. (2002). Measurement of Odor-plume structure in a wind tunnel using a photoionization detector and a Tracer Gas. *Environ. Fluid Mech.* 2, 115–142. doi: 10.1023/A:1016227601019

Kaissling, K. E., Meng, L. Z., and Bestmann, H.-J. (1989). Responses of bombykol receptor cells to *(Z,E)*-4,6-hexadecadiene and linalool. *J. Comp. Physiol. A* 165, 147–154. doi: 10.1007/BF00619189

Klatt, B. K., Burmeister, C., Westphal, C., Tscharntke, T., and Fragstein, M. (2013). Flower volatiles, crop varieties and bee responses. *PLoS ONE* 8:e72724. doi: 10.1371/journal.pone.0072724

Landolt, P. J., and Phillips, T. W. (1997). Host plant influences on sex pheromone behavior of phytophagous insects. *Annu. Rev. Entomol.* 42, 371–391. doi: 10.1146/annurev.ento.42.1.371

Lei, H., and Vickers, N. J. (2008). Central processing of natural odor mixtures in insects. *J. Chem. Ecol.* 34, 915–927. doi: 10.1007/s10886-008-9487-2

Light, D., Flath, R., Buttery, R., Zalom, F., and Rice, R. (1993). Host-plant green-leaf volatiles synergize the synthetic sex pheromones of the corn earworm and codling moth (Lepidoptera). *Chemoecology* 4, 145–152.

Liu, Y., Liu, C., Lin, K., and Wang, G. (2013). Functional specificity of sex pheromone receptors in the cotton bollworm *Helicoverpa armigera*. *PLoS One* 8:e62094. doi: 10.1371/journal.pone.0062094

Ljungberg, H., Anderson, P., and Hansson, B. S. (1993). Physiology and morphology of pheromone-specific sensilla on the antennae of male and female *Spodoptera littoralis* (Lepidoptera: Noctuidae). *J. Insect Physiol.* 39, 253–260. doi: 10.1016/0022-1910(93)90096-A

Ma, Y. F., and Xiao, C. (2013). Push-pull effects of three plant secondary metabolites on oviposition of the potato tuber moth, *Phtorimaea operculella*. *J. Insect Sci.* 13, 128. doi: 10.1673/031.013.12801

Marion-Poll, F. (1995). Object-oriented approach to fast display of electrophysiological data under MS-windows. *J. Neurosci. Methods* 63, 197–204. doi: 10.1016/0165-0270(95)00110-7

Masson, C., and Mustaparta, H. (1990). Chemical information processing in the olfactory system of insects. *Physiol. Rev.* 70, 199–245.

Nakagawa, T., Sakurai, T., Nishioka, T., and Touhara, K. (2005). Insect sex-pheromone signals mediated by specific combinations of olfactory receptors. *Science* 307, 1638–1642. doi: 10.1126/science.1106267

Namiki, S., Iwabuchi, S., and Kanzaki, R. (2008). Representation of a mixture of pheromone and host plant odor by antennal lobe projection neurons of the silkmoth *Bombyx mori*. *J. Comp. Physiol. A* 194, 501–515. doi: 10.1007/s00359-008-0325-3

Ochieng, S. A., Park, K. C., and Baker, T. C. (2002). Host plant volatiles synergize responses of sex pheromone-specific olfactory receptor neurons in male *Helivoverpa zea*. *J. Comp. Physiol A* 188, 325–333. doi: 10.1007/s00359-002-0308-8

Oluwafemi, S., Birkett, M. A., Caulfield, J., and Pickett, J. A. (2012). Variability of volatile organic compounds emitted by seedlings of seven African maize varieties when infested by adult *Cicadulina storeyi* China leafhopper vectors of maize streak virus. *Afr. Crop Sci. J.* 20, 117–124.

Papadopoulou, M., Cassenaer, S., Nowotny, T., and Laurent, G. (2011). Normalization for sparse encoding of odors by a wide-field interneuron. *Science* 332, 721–725. doi: 10.1126/science.1201835

Party, V., Hanot, C., Said, I., Rochat, D., and Renou, M. (2009). Plant terpenes affect intensity and temporal parameters of pheromone detection in a moth. *Chem. Senses* 34, 763–774. doi: 10.1093/chemse/bjp060

Perez-Orive, J., Mazor, O., Turner, G. C., Cassenaer, S., Wilson, R. I., and Laurent, G. (2002). Oscillations and sparsening of odor representations in the mushroom body. *Science* 297, 359–365. doi: 10.1126/science.1070502

Picimbon, J. F., Gadenne, C., Becard, J. M., Clement, J. L., and Sreng, L. (1997). Sex pheromone of the French black cutworm moth, *Agrotis ipsilon* (Lepidoptera: Noctuidae): identification and regulation of a multicomponent blend. *J. Chem. Ecol.* 23, 211–230. doi: 10.1023/B:JOEC.0000006355.13207.91

Pophof, B., and Van Der Goes Van Naters, W. (2002). Activation and inhibition of the transduction process in silkmoth olfactory receptor neurons. *Chem. Senses* 27, 435–443. doi: 10.1093/chemse/27.5.435

Pregitzer, P., Schubert, M., Breer, H., Hansson, B. S., Sachse, S., and Krieger, J. (2012). Plant odorants interfere with detection of sex pheromone signals by male *Heliothis virescens*. *Front. Cell. Neurosci.* 6:42. doi: 10.3389/fncel.2012.00042

R Core Team. (ed.). (2013). *R: A language and Environment for Statistical Computing Vienna, Austria: Foundation for Statistical Computing*. Available online at: http://www.R-project.org/

Reisenman, C. E., Heinbockel, T., and Hildebrand, J. G. (2008). Inhibitory interactions among olfactory glomeruli do not necessarily reflect spatial proximity. *J. Neurophysiol.* 100, 554–564. doi: 10.1152/jn.90231.2008

Renou, M., Gadenne, C., and Tauban, D. (1996). Electrophysiological investigations of pheromone-sensitive sensilla in the hybrids between two moth species. *J. Insect Physiol.* 42, 267–277. doi: 10.1016/0022-1910(95)00108-5

Riffell, J. A., Lei, H., Abrell, L., and Hildebrand, J. G. (2013). Neural basis of a pollinator's buffet: olfactory specialization and learning in *Manduca sexta*. *Science* 339, 200–204. doi: 10.1126/science.1225483

Rouyar, A., Party, V., Prešern, J., Blejec, A., and Renou, M. (2011). A general odorant background affects the coding of pheromone stimulus intermittency in specialist olfactory receptor neurones *PLoS ONE* 6:e26443. doi: 10.1371/journal.pone.0026443

Sachse, S., and Galizia, C. G. (2003). The coding of odour-intensity on the honeybee antennal lobe: local computation optimizes odour representation. *Eur. J. Neurosci.* 18, 2119–2132. doi: 10.1046/j.1460-9568.2003.02931.x

Sandoz, J. C., Galizia, C. G., and Menzel, R. (2003). Side-specific olfactory conditioning leads to more specific odor representation between sides but not within sides in the honeybee antennal lobes. *Neuroscience* 120, 1137–1148. doi: 10.1016/S0306-4522(03)00384-1

Schmidt-Büsser, D., Von Arx, M., and Guerin, P. M. (2009). Host plant volatiles serve to increase the response of male European grape berry moths, *Eupoecilia ambiguella*, to their sex pheromone. *J. Comp. Physiol. A* 195, 853–864. doi: 10.1007/s00359-009-0464-1

Stetter, M., Greve, H., Galizia, C. G., and Obermayer, K. (2001). Analysis of calcium imaging signals from the honeybee brain by nonlinear models. *Neuroimage* 13, 119–128. doi: 10.1006/nimg.2000.0679

Trona, F., Anfora, G., Bengtsson, M., Witzgall, P., and Ignell, R. (2010). Coding and interaction of sex pheromone and plant volatile signals in the antennal lobe of the codling moth *Cydia pomonella*. *J. Exp. Biol.* 213, 4291–4303. doi: 10.1242/jeb.047365

Varela, N., Avilla, J., Gemeno, C., and Anton, S. (2011). Ordinary glomeruli in the antennal lobe of male and female tortricid moth *Grapholita molesta* (Busck) (Lepidoptera: Tortricidae) process sex pheromone and host-plant volatiles. *J. Exp. Biol.* 214, 637–645. doi: 10.1242/jeb.047316

Vitecek, S., Maria, A., Blais, C., Duportets, L., Gaertner, C., Dufour, M. C., et al. (2013). Is the rapid post-mating inhibition of pheromone response triggered by ecdysteroids or other factors form the sex accessory glands in the male moth *Agrotis ipsilon*? *Horm. Behav.* 63, 700–708. doi: 10.1016/j.yhbeh.2013.03.010

Wang, G., Carey, A. F., Carlson, J. R., and Zwiebel, L. J. (2010). Molecular basis of odor coding in the malaria vector mosquito Anopheles gambiae. *Proc. Natl. Acad. Sci. U.S.A.* 107, 4418–4423. doi: 10.1073/pnas.0913392107

Wanner, K. W., Nichols, A. S., Allen, J. E., Bunger, P. L., Garczynski, S. F., Linn, C. E., et al. (2010). Sex pheromone receptor specificity in the European corn borer moth, *Ostrinia nubilalis*. *PLoS ONE* 5:e8685. doi: 10.1371/journal.pone.0008685

Wynne, J. W., Keaster, A. J., Gerhardt, K. O., and Krause, G. F. (1991). Plant species identified as food sources for adult black cutworm (Lepidoptera:Noctuidae) in Northern Missouri. *J. Kansas Enomol. Soc.* 64, 381–387.

Zhu, Y., Keaster, A. J., and Gerhard, K. O. (1993). Field observations on attractiveness of selected blooming plants to noctuid moths and electroantennogram responses of black cutworm (Lepidoptera: Noctuidae) moths to flower volatiles. *Environ. Entomol.* 22, 162–166. doi: 10.1093/ee/22.1.162

Conflict of Interest Statement: The authors declare that the research was conducted in the absence of any commercial or financial relationships that could be construed as a potential conflict of interest.

frontiers in Physiology

ORIGINAL RESEARCH
published: 25 April 2016
doi: 10.3389/fphys.2016.00143

A Challenge for a Male Noctuid Moth? Discerning the Female Sex Pheromone against the Background of Plant Volatiles

*Elisa Badeke, Alexander Haverkamp, Bill S. Hansson and Silke Sachse **

Department of Evolutionary Neuroethology, Max Planck Institute for Chemical Ecology, Jena, Germany

OPEN ACCESS

Edited by:
Sylvia Anton,
Institut National de la Recherche Agronomique, France

Reviewed by:
Michel Renou,
Institut National de la Recherche Agronomique, France
Bente Gunnveig Berg,
Norwegian University of Science and Technology, Norway

***Correspondence:**
Silke Sachse
ssachse@ice.mpg.de

Specialty section:
This article was submitted to Invertebrate Physiology, a section of the journal Frontiers in Physiology

Received: *31 January 2016*
Accepted: *04 April 2016*
Published: *25 April 2016*

Citation:
Badeke E, Haverkamp A, Hansson BS and Sachse S (2016) A Challenge for a Male Noctuid Moth? Discerning the Female Sex Pheromone against the Background of Plant Volatiles. Front. Physiol. 7:143. doi: 10.3389/fphys.2016.00143

Finding a partner is an essential task for members of all species. Like many insects, females of the noctuid moth *Heliothis virescens* release chemical cues consisting of a species-specific pheromone blend to attract conspecific males. While tracking these blends, male moths are also continuously confronted with a wide range of other odor molecules, many of which are plant volatiles. Therefore, we analyzed how background plant odors influence the degree of male moth attraction to pheromones. In order to mimic a natural situation, we tracked pheromone-guided behavior when males were presented with the headspaces of each of two host plants in addition to the female pheromone blend. Since volatile emissions are also dependent on the physiological state of the plant, we compared pheromone attraction in the background of both damaged and intact plants. Surprisingly, our results show that a natural odor bouquet does not influence flight behavior at all, although previous studies had shown a suppressive effect at the sensory level. We also chose different concentrations of single plant-emitted volatiles, which have previously been shown to be neurophysiologically relevant, and compared their influence on pheromone attraction. We observed that pheromone attraction in male moths was significantly impaired in a concentration-dependent manner when single plant volatiles were added. Finally, we quantified the amounts of volatile emission in our experiments using gas chromatography. Notably, when the natural emissions of host plants were compared with those of the tested single plant compounds, we found that host plants do not release volatiles at concentrations that impact pheromone-guided flight behavior of the moth. Hence, our results lead to the conclusion that pheromone-plant interactions in *Heliothis virescens* might be an effect of stimulation with supra-natural plant odor concentrations, whereas under more natural conditions the olfactory system of the male moth appears to be well adapted to follow the female pheromone plume without interference from plant-emitted odors.

Keywords: *Heliothis virescens*, pheromone-guided flight behavior, plant volatiles, wind tunnel, GC-MS

INTRODUCTION

Odors present in the environment provide information that is crucial for insect survival and reproduction. Most insects use these olfactory cues for finding food, identifying suitable oviposition sites and communicating with their mates. Volatiles that are emitted by plants represent major cues with which an insect detects suitable host plants (Visser, 1986; Bruce et al., 2005), while pheromones are used for intraspecific identification and communication. Lepidoptera males, for example, are able to detect conspecific females releasing a species-specific pheromone blend. In the heliothine moth *Heliothis virescens* (Lepidoptera, Noctuidae), it has been shown that females produce a complex blend of up to seven components in their pheromone glands (Roelofs et al., 1974; Tumlinson et al., 1975; Klun et al., 1979; Pope et al., 1982). Wind tunnel and field experiments have shown that the behavioral activity of this pheromone blend depends highly on the ratio of its individual components (Vetter and Baker, 1983; Ramaswamy and Roush, 1986; Vickers et al., 1991). The pheromone blend is detected by specialized olfactory sensory neurons (OSNs) housed in sensilla trichoidea on the male antenna (Almaas and Mustaparta, 1990, 1991; Berg et al., 1995; Vickers et al., 2001). These OSNs send their axons to the antennal lobe (AL), which represents the primary olfactory processing neuropil, consisting of an array of olfactory glomeruli. Sex pheromone information is processed in a male-specific part of the AL (Hansson and Anton, 2000), the macroglomerular complex (MGC), which in male *Heliothis virescens* comprises four glomeruli (Christensen and Hildebrand, 1987; Hansson et al., 1992, 1995; Vickers and Baker, 1996; Berg et al., 1998; Vickers et al., 1998). The remaining, so-called ordinary, glomeruli process the information of all other odorants including plant and fruit volatiles (Galizia et al., 2000; Hillier and Vickers, 2007). This segregation of the olfactory pathway is partially maintained in the higher brain centers, such as the lateral horn (Zhao et al., 2014).

Heliothis virescens is a pest species, and feeds on many plants and crops such as cotton, tomato, soybean, tobacco and chickpea (Fitt, 1989; Cunningham and Zalucki, 2014). Several studies have shown that the olfactory system of both males and females is able to detect and process many volatiles emitted by these host plants (Loughrin et al., 1990; Tingle and Mitchell, 1992; Stranden et al., 2003; Rostelien et al., 2005; Hillier et al., 2006; Hillier and Vickers, 2007). Notably, the chemical diversity of volatile compounds found in all the floral scents investigated so far has been estimated to more than 1700 chemicals (Knudsen et al., 2006). Furthermore, the volatile composition of plants can change depending on environment and stress (reviewed by Dicke and Van Loon, 2000; Beyaert and Hilker, 2014). Damaged plants often emit different volatiles as well as different ratios of the volatile composition compared to undamaged plants. Considering this enormous diversity of chemical compounds, finding a sexual partner in such a complex environment is a big challenge for male moths. They have to detect minute amounts of the conspecific female pheromone blend against a constant background of many other odors. Although pheromone compounds are processed in a separate part of the olfactory system, it has been shown in several moth species that plant volatiles can influence pheromone detection and *vice versa* (Chaffiol et al., 2014; Deisig et al., 2014). Interestingly, plant compounds can even enhance the detection of pheromone components. For example, in the corn earworm *Helicoverpa zea*, simultaneous application of plant odorants with the major sex pheromone component of the moth increases the firing rate of pheromone-responsive OSNs in males, although those neurons do not respond to stimulation with plant odorants separately (Ochieng et al., 2002). Moreover, in beetles (Nakamuta et al., 1997) and many lepidopteran species (Dickens et al., 1993; Light et al., 1993; Reddy and Guerrero, 2000; Deng et al., 2004; Namiki et al., 2008; Schmidt-Büsser et al., 2009; Gurba and Guerin, 2015) the behavioral response is also increased when plant compounds are combined with the corresponding pheromone components. In contrast, a variety of studies demonstrated that pheromone detection can also be inhibited by interactions with plant odorants (Den Otter et al., 1978; Kaissling and Bestmann, 1989; Pophof and Van Der Goes Van Naters, 2002; Party et al., 2009, 2013; Hillier and Vickers, 2011; Chaffiol et al., 2012; Deisig et al., 2012; Pregitzer et al., 2012; Hatano et al., 2015). Hatano et al. (2015) showed this inhibitory effect even at the behavioral level. These contradictory findings give raise to the question whether the olfactory background is modulating the intraspecific communication of insects. Indeed, in *Heliothis virescens,* certain plant-emitted volatiles reduce the detection of *Z*11-16:Ald, the major sex pheromone component, at the level of the pheromone receptor HR13 (Pregitzer et al., 2012). Single sensillum recordings of *Z*11-16:Ald-tuned OSNs concur with this inhibitory effect (Hillier and Vickers, 2011). Moreover, in the same study, a suppressive effect for OSNs being tuned to the minor component *Z*9-14:Ald could be demonstrated. However, whether these effects at the sensory level are maintained throughout the olfactory system and thus may affect male moth behavior is unknown. We therefore analyzed whether a background of plant volatiles influences pheromone-guided behavior in *Heliothis virescens* using wind tunnel experiments. We analyzed the impact of complete and naturally occurring odor blends as well as of individual plant volatiles at different concentrations. Furthermore, we quantified the volatile emissions of all stimuli using gas chromatography analysis. Surprisingly, we observed pheromone-plant interactions only at high and supra-natural odor concentrations. We therefore conclude that pheromone-plant interactions in *Heliothis virescens* might not occur under natural conditions and that male moths are able to detect their conspecific female against a complex background of plant volatiles.

MATERIALS AND METHODS

Insect Rearing

We obtained *Heliothis virescens* from the Department of Entomology in the Max Planck Institute of Chemical Ecology in Jena. Moths originated from Clemson University in Clemson, South Carolina. These were maintained at the institute for several generations, where they were reared as follows: Eggs of *H. virescens* were gained from single pair matings in 0.5 l cups. In order to minimize inbreeding depression, females and

males of different families were chosen. A mesh on top of the mating cups allowed the females to oviposit their eggs. Larvae were subsequently maintained in 10-cm Petri dishes containing artificial pinto bean diet (Burton, 1979). They were separated at second instar. After eclosion, about 15–20 males of the same age were segregated into 30 × 30 × 30 cm rearing cages. A 10% sucrose solution was provided *ad libitum*. Animals were kept at 60% rel. humidity and at 23–25°C under a 16:8 h light-dark cycle. The light level during scotophase was 0.4 lux. 2- to 6-day-old virgin male moths were used for behavioral experiments.

Plant Material

In order to use the headspaces of whole plants for volatile collection and behavioral experiments, cotton (*Gossypium hirsutum*) and tomato plants (*Solanum lycopersicum*) were grown individually in 1-liter pots in the greenhouse at 23–25°C and 50–70% rel. humidity under a 16:8 h light-dark cycle. After the beginning of their elongation stage and until the experiments were performed, plants were transferred to a climate chamber providing 22–25°C and 60–70% relative humidity. They were watered daily with 100 ml tap water supplemented with 0.12 g*ml-1 fertilizer. For the experimental approach undamaged or damaged plants were taken. In order to damage plants, four to five third- and fourth-instar larvae of *H. virescens* were allowed to feed on the plant before the behavioral assay was conducted. Larvae were removed from the plants after 24 h.

Behavioral Approach

Wind Tunnel

Insects were tested in a 220 × 90 × 90 cm Plexiglas wind tunnel (**Figure 1A**) under infrared and red light conditions with a white light supply of 0.4 lux. A purified, humidified and tempered airflow of 0.27 m/s was blown through the wind tunnel, providing 23°C and 60–70% relative humidity.

Stimulus Device

For synthetic odorants the odor plume was created by connecting separately two 50 ml glass bottles via *Teflon* tubing to the stimulus outlet on a stick 55 cm long (**Figure 1**). The distance to the upwind end of the wind tunnel was 23 cm. Pumps, which sucked the ambient air through a charcoal filter for cleaning, generated a stimulus flow of 0.48–0.50 l/min through the tubing leaving

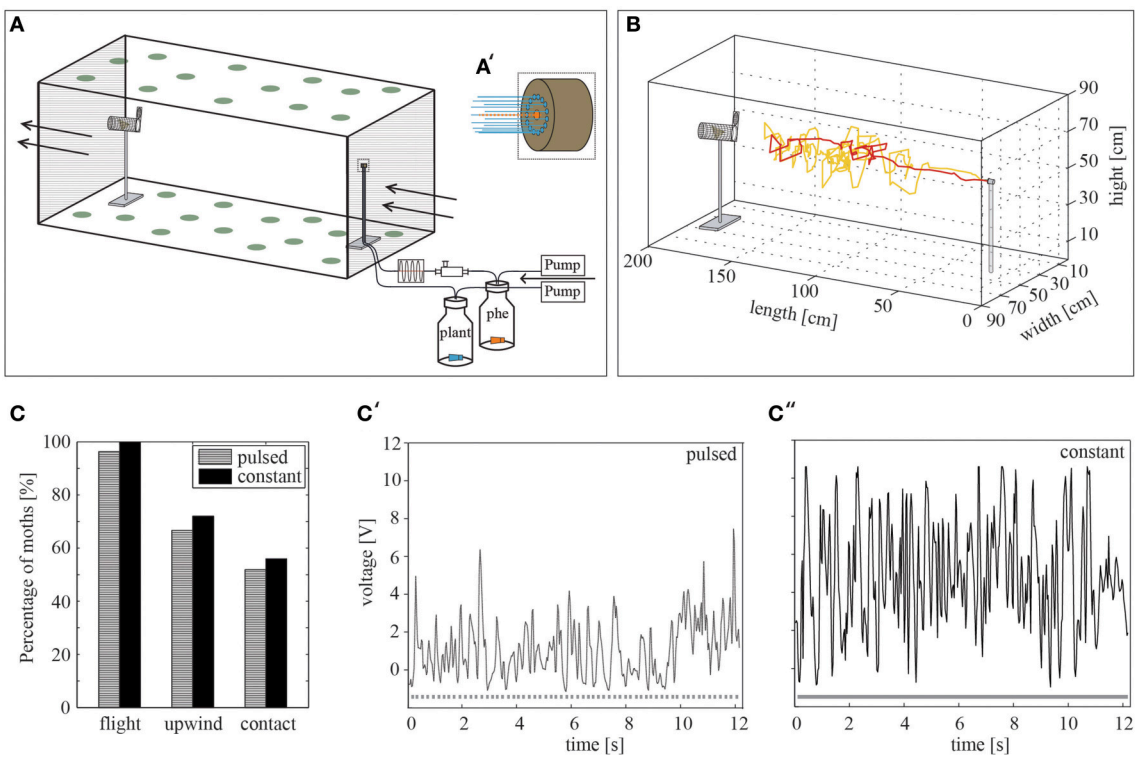

FIGURE 1 | The wind tunnel system. (A) Schematic representation of the wind tunnel system including the stimulus device. The ceiling and the floor were covered by green dots in order to provide a pattern for the insects to orient on. Arrows indicate the air stream. An air flow is transported via pumps through the stimulus bottles and released by the stimulus outlet. The pheromone-loaded air is pulsed beforehand at 10 Hz by using a cross-valve. phe = pheromone **(A')** Magnification of the stimulus outlet (dashed square). The dotted orange line represents the middle nozzle, which emits a pulsed pheromone stimulus, while the blue lines highlight the constant plant odor flow released by the surrounding nozzles. **(B)** Two representative flights of different males (yellow, red) toward the pheromone blend. **(C)** The percentage of male *H. virescens* attempting flight behavior, achieving upwind flight and making source contact is similar for constant ($N = 25$) and pulsed ($N = 27$) pheromone stimulation ($p > 0.05$, Fisher's exact test). **(C',C'')** Visualization of the constant and pulsed odor plume using a photoionization detector (PID) at 110 cm distance from the stimulus outlet. Dotted and continuous lines below the curves represent the odor stimulation. Fewer volatiles can be detected in the pulsed **(C')** odor plume than in the constant plume **(C'')**. PID measurements: $U_{pulsed} = 1.81$ V, $U_{constant} = 4.77$ V.

the bottles. In each of the bottles, a rubber septum loaded with the test odorants was inserted. The bottle, which contained the pheromone blend, was additionally connected to an *Arduino* microprocessor-controlled cross-valve before being released by the middle nozzle (ID 1 mm) of the stimulus outlet (**Figure 1A′**). Thus, pulsed stimulations of 10 Hz could be achieved. It has been shown that pulsed stimulation affects the flight behavior of male moths in the wind tunnel (Vickers and Baker, 1994). We therefore compared pheromone attraction to either a constant pheromone plume or a pulsed pheromone plume using an optimal pulse frequency of 10 Hz (**Figure 1C**). The second stimulus bottle was connected to the circular arranged nozzles (ID 0.5 mm each). For experiments using the headspaces of different plants, a glass cylinder (10 l) containing a plant was connected to the system instead of to the second stimulus bottle. A Teflon disc on the bottom with a central opening separated green plant material from soil and roots. Compressed, charcoal-filtered air with a flow of 1 l/min was inserted into the cylinder. Only 0.48–0.54 l/min of the cylinder headspace was sucked via a pump into to the wind tunnel.

Animal Handling

All experiments were performed 2–7 h during scotophase, when pheromone responsiveness is highest (Shorey and Gaston, 1965). At least 1 h before testing, male moths were transferred individually into Ø 7 × 10 cm mesh tubes and placed in a small room near the wind tunnel that had the same conditions. Active moths were chosen for testing. At the beginning of each experiment, a mesh tube containing a moth was inserted into a releasing device in the odor plume at the downwind end of the wind tunnel. The releasing device was controlled via the microprocessor in order to open the cage automatically 2 min after placing the moth in the mesh tube. Flight behavior was subsequently recorded for 5 min. After the first source contact within this time interval, males' behavior was tracked for 2 min.

3-D Video Tracking

During the experiment the releasing device, all wind tunnel conditions and the flight paths were computer-controlled from a separate room. In order to observe odor-guided flight behavior, we used a custom-built video tracking system. Four cameras (C615, Logitech, Newark, NJ, USA, 800 × 600 pixels, 0.3 cm^2 pixel size), which were located at the side and on the top of the wind tunnel, recorded the flight path of each moth. By using a background subtraction algorithm, the position of each moth was calculated at a rate of 10 Hz. A fifth camera, which was attached to the upwind end of the wind tunnel, allowed the recording of males' behavior close to the odor source.

Determining Optimal Conditions for the Wind Tunnel

In order to monitor pheromone attraction and to study whether it is influenced by background volatiles, we started to find the best conditions for the bioassay. A stimulus device was used to create a point source emitting either a pulsed or a constantly emitted pheromone blend of *Heliothis virescens* together with a surrounding odor plume of a constant solvent release (**Figure 1A′**). When stimulating with the conspecific pheromone blend, male moths showed clear pheromone-guided upwind flight behavior. This behavior can be characterized by locking on to the pheromone plume followed by upwind flight, zigzagging, casting behavior and, finally, contact with the source (**Figure 1B**). When placed in a constant or a pulsed pheromone plume, all moths started their flight within 5 min. (**Figure 1C**). Hence, the type of stimulation influenced neither the percentage of moths attempting upwind flight nor the number of source contacts. In order to compare the pulsed and constant odor plume structure, we measured the presence of volatiles using a photoionization detector (PID). The results showed that the probability that a moth hits a volatile in a pulsed odor plume is less than the probability that a moth hits one in a constant plume (**Figures 1C′,C″**). However, although the odor plume structure was different, pheromone attraction was similar for both odor applications. We chose pulsed pheromone stimulation for all subsequent experiments in our study.

Odorants

All synthetic odorants tested were commercially available and acquired from Sigma (http://www.sigma-aldrich.com), Bedoukian (http://www.bedoukian.com) or pherobank (http://www.pherobank.com). They were obtained in the highest available purity. β-caryophyllene (CAS 87-44-5, purity > 98.5%), racemic linalool (CAS 78-70-6, purity > 97%) and (*Z*)3-hexen-1-ol (CAS 928-96-1, purity > 98%) are well-described plant compounds. They are detectable by male and female *Heliothis virescens* (Paré, 1997; De Moraes et al., 2001; Skiri et al., 2004; Rostelien et al., 2005; Hillier and Vickers, 2007), and they have been used previously in studies investigating plant-pheromone interaction on *H. virescens* (Dickens et al., 1993; Hillier and Vickers, 2011; Pregitzer et al., 2012).

A synthetic pheromone blend, which contained the seven components, (*Z*)-11-hexadecenal (*Z*11-16:Ald, CAS 53939-28-9, purity 97-98%), (*Z*)-9-tetradecenal (*Z*9-14:Ald, CAS 53939-27-8, purity > 93%), tetradecenal (14:Ald, purity > 98%), hexadecanal (16:Ald, CAS 629-80-1, purity > 93%), (*Z*)-7-hexadecenal (*Z*7-16:Ald, CAS 56797-40-1, > 95%), (*Z*)-9-hexadecenal (*Z*9-16:Ald, CAS 56219-04-6, purity > 90%) and (*Z*)-11-hexadecenol (*Z*11-16:OH, CAS 56683-54-6, purity > 98%), was used (Roelofs et al., 1974; Tumlinson et al., 1975; Klun et al., 1979). We prepared the blend relative to *Z*11-16:Ald (100%) and added 5% *Z*9-14:Ald, 5% 14:Ald, 10% 16:Ald, 2% *Z*7-16:Ald, 2% *Z*9-16:Ald and 1% *Z*11-16:OH of the compounds (Pope et al., 1982), in order to test the sexual attraction of *H. virescens* males toward their conspecific pheromone blend. Tetradecenal was synthesized from commercially available tetradecanol (Sigma) by the Research Group Mass Spectrometry/Proteomics in the Max Planck Institute of Chemical Ecology in Jena.

Both synthetic plant compounds and the pheromone blend consisted additionally of 1.25% of the antioxidant 3.5-Di-tert-butyl-4-hydroxytoluene (BHT, CAS 128-37-0, purity ≥ 99%, Sigma). They were subsequently pipetted on individual rubber septa (Thomas Scientific, http://www.thomassci.com/). Before being used, rubber septa were cleaned with hexane (CAS 110-54-3, Sigma), which was furthermore used as a solvent for all odorants. For plant components, concentrations between 30 and

300 μg/μl were used. The pheromone blend was adjusted to *Z*11-16:Ald with a concentration of 300 μg/μl. We always indicate the final concentration for each rubber septum.

Volatile Collection, Analysis, and Quantification

In order to quantify the actual amount of volatiles being released by the rubber septum and pumped through the tubing into the wind tunnel, we used polydimethylsiloxane (PDMS) tubes (OD 2.3 mm, Reichelt Chemietechnik, http://www.rct-online.de). By introducing the PDMS tubes for 2 h into the odor flow close to the stimulus outlet, we could collect volatiles during testing. Volatiles being released by plants were collected with the same approach. Samples were stored at -20°C until use. All samples were examined on an Agilent 7890A gas chromatograph (Agilent Technologies, CA) running in splitless mode and being connected to an Agilent 5975C mass spectrometer (electron impact mode, 70 eV, ion source: 230°C, quadrupole: 150°C, mass scan range: 33–350 u). We used a nonpolar column (HP-5 MS UI, 30 m length, 0.25 mm ID, 0.25 μm film thickness, J and W Scientific) under constant helium flow of 1.1 ml/min. The GC oven was programmed to hold 40°C for 3 min, to increase the temperature at 5C°/min to 200°C, then to increase temperature at 20°C/min to 260°C. The maximum temperature was held for 10 min. For identification, mass spectra were compared with Kovats retention time indices to reference compounds or to those published by the National Institute of Standards and Technologies (NIST, version 2.0). Retention times for all compounds were determined by using standards. Quantifications of emission rates were subsequently calculated based on the comparison of the internal standard of 10 ng/μl 1-Bromohexane (CAS 111-25-1, purity 98 %, Sigma) and peak area of single compounds.

Data Analysis and Statistics

Microsoft Excel, Gnu R, custom-written Matlab scripts (MATLAB version- Mathworks, USA) and Adobe Illustrator were used in order to analyze and plot all data. Statistics were performed with the software Gnu R and GraphPad Instat. We calculated the emission rate of volatiles being released within 1 h for each compound based on the internal standard by using the commercial software GC ChemStation (Agilent Technologies) and Microsoft Excel.

In order to investigate the attractiveness of volatiles in the wind tunnel, we calculated the percentage of moths (1) starting to fly, (2) achieving upwind flight, and (3) contacting the source for each group of odor stimulation. An odor plume was called attractive if moths reached and contacted the odor source. In order to investigate pheromone-plant interaction, we further examined the average number of source contacts per male out of all individual moths within a group for the test period. We quantified the number of contacts for another 2 min after the first contact. Males without contacts were counted as zeros. For statistical analysis, the group tested with the pheromone blend alone was always taken as a control group. The percentage of moth within a test group was compared to the pheromone group by means of Fisher's exact test, with a Bonferroni-Holm correction. The number of source contacts was evaluated using the Kruskal-Wallis test with Dunn's multiple comparisons test. The pheromone-guided flight behavior of each attracted male was analyzed in more detail by calculating the percentage of relative abundance of flight angles in y- and z-direction and the average upwind speed within an 80 cm distance from the stimulus outlet. Both angles and upwind speed were measured with an interval of 10 Hz. The last 10 cm of the track were excluded due to the fact that it could not be tracked reliably in all moths. Animals which performed zigzagging and casting movements possessed flight angles greater than zero degrees. Angles around zero degrees exhibit straight upwind movement. Upwind speed (cm/s) is the speed of an animal relative to the odor source. Positive values indicate upwind movement, negative values downwind movement, while values around zero indicate cross-wind movement. The Kruskal-Wallis test and Dunn's multiple comparisons test were used for statistics.

RESULTS

Host Plant Headspaces Did Not Affect Pheromone Attraction

Since it has been shown that different plant-emitted volatiles affect detection of the major sex pheromone component *Z*11-16:Ald in male *Heliothis virescens* at the physiological level (Hillier and Vickers, 2011; Pregitzer et al., 2012), we tested whether behavioral performance is similarly affected. In order to provide a naturally occurring odor source, we used the headspaces of two host plants, tomato and cotton, to examine their influence on pheromone-guided flight behavior (**Figure 2A**, left panel). First, we tested the headspaces of the two host plants alone. We observed that both the tomato headspace as well as the cotton headspace induced only very low degrees of upwind flight and source contact ($N = 17$–20, upwind 1–3 moths, contact 0–1 moth; data not shown). We next applied the conspecific pheromone blend to each plant headspace simultaneously. The results reveal that a pheromone plume with a background of either tomato (**Figure 2A**, middle panel) or cotton headspace (**Figure 2A**, right panel) showed similar attractiveness as compared to a pheromone blend with no plant odor background. The number of source contacts was also not affected (**Figure 2C**, **Table 1**). Hence the pheromone-guided flight was not influenced by the presence of a naturally occurring plant odor blend.

It has been shown that larval damage influences the composition and/or the emission rate of plant volatiles (De Moraes et al., 1998). The attraction of female moths to a damaged plant headspace depends on the amount of herbivore-induced plant volatiles (Späthe et al., 2013). In order to examine whether herbivore damage significantly influences pheromone detection, we let four to five larvae feed on both host plants and tested the attractiveness of the induced headspace in our wind tunnel. Only three moths at most moved upwind when placed in a damaged tomato or cotton odor plume, but none of them contacted the source ($N = 15$–17; data not shown). When a damaged tomato plant headspace was

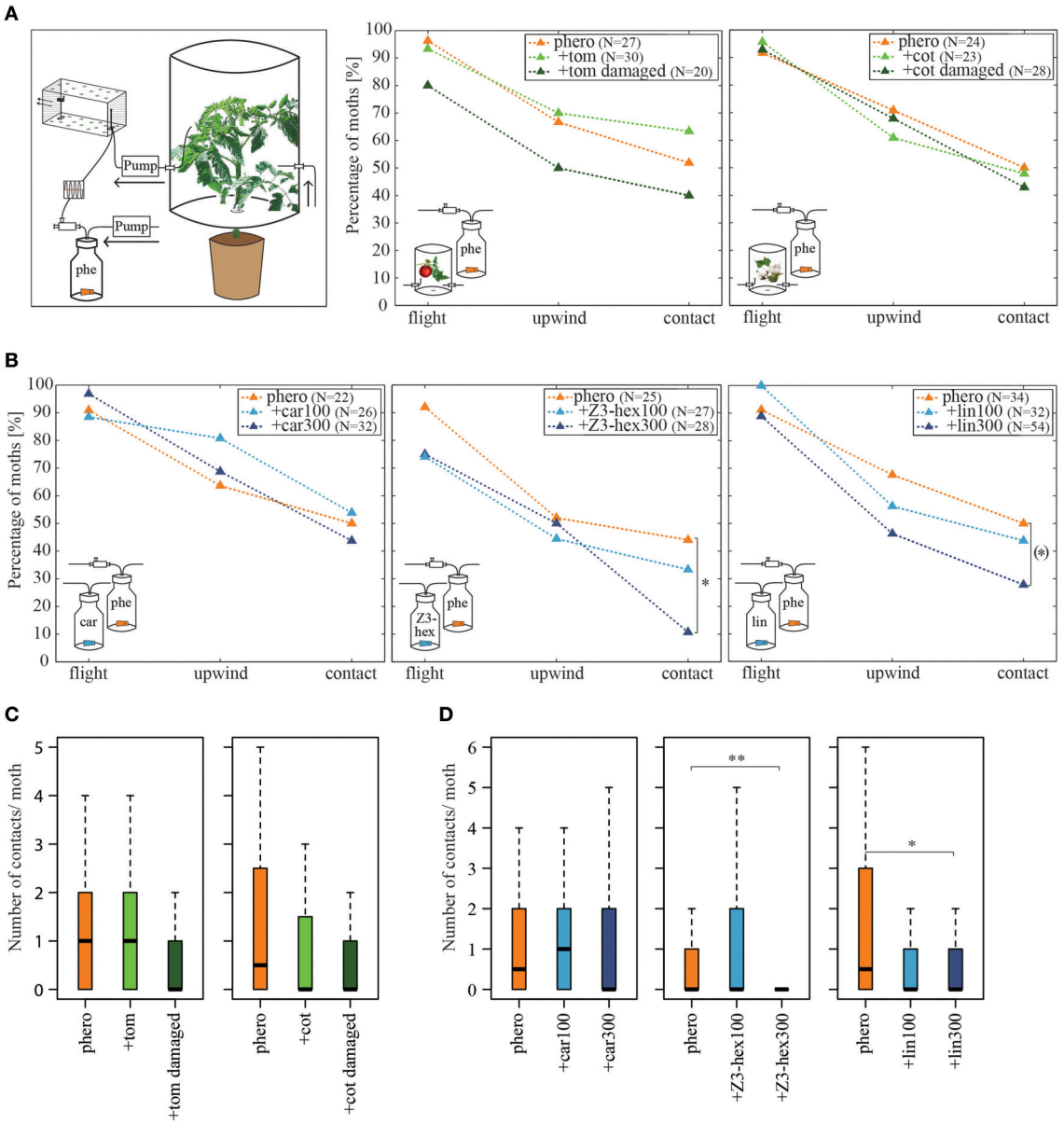

FIGURE 2 | Influence of host plant headspaces on pheromone-guided flight behavior. (A) Percentage of moths attempting flight behavior, achieving upwind flight and making source contact, when simultaneously stimulated with the pheromone blend and a tomato (middle panel) or cotton (right panel) plant headspace. Plants were intact or damaged by larvae. The left panel highlights the changes in the odor stimulation device. The headspace of the plants was sucked via a pump through the wind tunnel. The pulsed pheromone stimulation was implemented as described in **Figure 1**. There was no significant difference in pheromone attraction when insects were stimulated simultaneously with undamaged or damaged tomato or cotton headspaces compared to pheromone stimulation alone ($p > 0.05$, Fisher's exact test, Bonferroni-Holm correction). **(B)** Percentage of moths attempting flight behavior, achieving upwind flight and making source contact, when simultaneously stimulated with the pheromone blend and the synthetic odorants β-caryophyllene (left panel), (*Z*)3-hexenol (middle panel) or linalool (right panel) each in two different concentrations (100 and 300 μg/μl). While β-caryophyllene did not affect pheromone-guided flight behavior, high concentrations of (*Z*)3-hexenol decreased the amount of moths contacting the source. A similar tendency was observed for linalool. Asterisks represent significant differences ($p < 0.05$, Fisher's exact test with Bonferroni-Holm correction). The bracket indicates significant differences without Bonferroni-Holm correction ($p = 0.0426$). **(C)** Number of contacts per individual moth for all tested males from **(A)**. No differences in the number of contacts when different plant headspaces were used ($p > 0.05$, the Kruskal-Wallis test, Dunn's multiple comparisons test). **(D)** Number of contacts per individual moth for all tested males from **(B)**. Moths had significantly fewer contacts when high dosages of (*Z*)3-hexenol or linalool were applied to the septa than when they were not ($p < 0.05$, the Kruskal-Wallis test, Dunn's multiple comparisons test). car, β-caryophyllene; cot, cotton; lin, linalool; phe/phero, pheromone; tom, tomato; *Z*3-hex, (*Z*)3-hexenol.

TABLE 1 | Effect of intact and damaged tomato and cotton plants on pheromone-guided flight behavior.

Stim. 1	Stim. 2	Sample size	Flight [%]	Upwind [%]	Source contact [%]	Upwind speed [cm/s] ± SD	Number of contacts ± SD
–	Phero	27	96.3	66.7	51.9	25.8 ± 29.6	1.19 ± 1.71
Tom	Phero	30	93.3	70	63.3	22.7 ± 27.3	1.37 ± 1.56
Tom damaged	Phero	20	80	50	40	24 ± 22.7	0.6 ± 0.99
–	Phero	24	91.7	70.8	50	24 ± 22.7	1.75 ± 2.67
Cot	Phero	23	95.7	60.9	47.8	30.5 ± 23	1 ± 1.38
Cot damaged	Phero	28	92.9	67.9	42.9	25.1 ± 33.6	0.75 ± 1.17

*Number of tested individuals and the percentages of male moths, for the experiments shown in **Figures 2A,C**, which started their flight, showed upwind movement and had source contact; also their upwind speed. The last column represents the number of contacts for all tested males. Stimulus (stim.) 1 and 2 together form the odor plume. Odorants of stimulus 1 were emitted continuously, while stimulus 2 (pheromone) was pulsed. A (–) in stimulus 1 represents the use of a solvent instead of an odorant. SD, standard deviation.*
no significant differences within a column to the solvent-pheromone stimulation ($p > 0.05$, Fisher's exact test with Bonferroni-Holm correction; Number of contacts and upwind speed: Kruskal-Wallis with Dunn's multiple comparisons test).
cot, cotton; phero, pheromone; tom, tomato.

presented together with the pheromone blend, we observed that 12% fewer individuals reached the source as compared to the pure pheromone blend (**Figure 2A**, middle panel, **Table 1**). However, this decrease was not significantly different from the response to the pheromone blend without background. Likewise, moths flying in a pheromone plume did not contact the source significantly more often (**Figure 2C**, **Table 1**). The same applies for the cotton headspace: larval damage in cotton plants affected neither pheromone-guided flight behavior nor the number of odor source contacts (**Figure 2A**, right panel, **Figure 2C**, **Table 1**).

In order to analyze pheromone-guided flight behavior in more detail, we dissected the flight mechanism. We asked how males manoeuver in response to an odor source and if their flight patterns are influenced by different odor plumes. We therefore examined the flight angles of attracted individuals as well as individual's upwind speed (**Figure 3**). In **Figure 3A** the relative abundance of flight angles for male moths in a pure pheromone plume and a tomato-pheromone plume are representative examples. Independent of odor stimulation, the most abundant flight angles of male *Heliothis virescens* were around zero degrees, indicating a relatively straight upwind flight. Angles up to $\pm 180^{\circ}$ represented additional zigzagging and casting behavior. Analysis of the upwind speed of the attracted insects resulted in values around 27 cm/s regardless of the odors present in the plume (**Figure 3B**, **Table 1**). In summary, we observed that neither the number of source contacts nor the flight pattern was affected when a complete plant headspace was applied simultaneously with the pheromone blend.

Certain Plant-Emitted Volatiles Reduced Pheromone Attraction

Interestingly, we did not observe the significant reduction in pheromone-elicited flight behavior suggested in previous studies. These however reported plant-pheromone interactions in moths using single plant-related compounds instead of complete headspaces. In order to analyze whether single plant volatiles could affect the pheromone response, we tested the three plant-emitted volatiles, β-caryophyllene, (*Z*)3-hexenol and linalool, each in two different concentrations based on the study by Pregitzer et al. (2012). As a side note, all of these compounds are up-regulated in larval-damaged plants (Paré, 1997; De Moraes et al., 1998, 2001; Stranden et al., 2003; Morawo and Fadamiro, 2014).

In comparison to pure pheromone stimulation, both concentrations of β-caryophyllene in combination with the pheromone did not reduce the attractiveness of the pheromone (**Figures 2B,D**, left panels, **Table 2**); moreover, β-caryophyllene alone did not attract any male moths, independent of its concentration (tested concentrations: 60, 100, 200, 300 μg/μl; $N = 16$–19; data not shown). Likewise, male moths did not respond to (*Z*)3-hexenol alone (100, 300 μg/μl; $N = 16$; data not shown). However, adding 300 μg/μl of (*Z*)3-hexenol to the pheromone plume significantly reduced the number of individuals (by 33%) and their frequency contacting the source, although equal percentages displayed upwind flight (**Figures 2B,D,** middle panels, **Table 2**). Interestingly, lowering the concentration of (*Z*)3-hexenol (i.e., 100 μg/μl) did not significantly decrease the moths' response to pheromones. We observed a similar dose-dependent effect when insects were stimulated simultaneously with the pheromone blend and the odor linalool. Linalool alone at concentrations of 30, 60, 100, 200, or 300 μg did not attract males at all and resulted in no upwind flights ($N = 15$–30; data not shown). However, adding the highest concentration of linalool to the pheromone plume resulted in 22% fewer individuals contacting the source compared to the number contacting the source when only the pheromone was used (**Figures 2B,D**, right panels, **Table 2**). This effect was also concentration-dependent, since we did not observe any reduction in pheromone-guided flight behavior when we reduced the concentration of linalool.

We observed similar flight angles in a pheromone plume compared to those in a plume consisting of the pheromone blend and β-caryophyllene, (*Z*)3-hexenol or linalool, as shown for β-caryophyllene and (*Z*)3-hexenol (**Figure 3A**, **Table 2**). The distribution histograms represent the cumulated azimuth and zenith angles of all male moths contacting the stimulus outlet. Since we measured less animals for (*Z*)3-hexenol, the histogram shows less cumulated angles. However, the distribution of the angles is similar to those of the other stimuli. Most angles were around zero degrees. Furthermore, males moved upwind to the

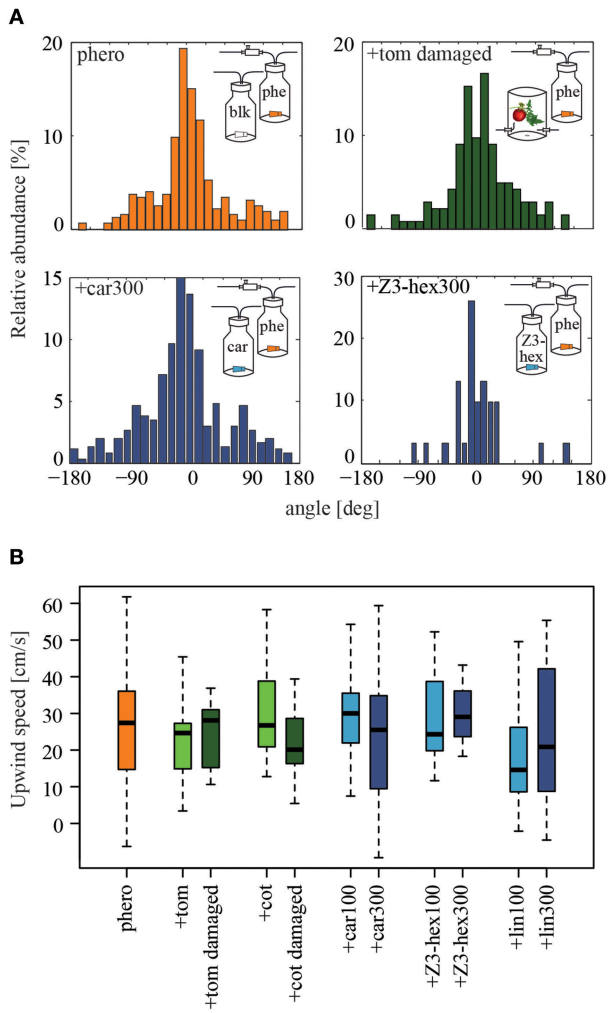

FIGURE 3 | Influence of individual plant volatiles on pheromone-guided flight behavior. (A) Relative abundance of flight angles being performed by male moths within the upwind section of the wind tunnel close to the source, when pheromones alone (orange), a pheromone and the headspace of a damaged tomato plant (dark green), pheromone and β-caryophyllene or (*Z*)3-hexenol (dark blue, both with 300 µg), were used for stimulation. The distribution histograms cumulate all tracks of moths contacting the stimulus outlet. Flight angles are shown as cumulated azimuth and zenith angles. Most of the time insects facing upwind in the odor plume they perceived performed zigzagging and casting activities. **(B)** Males moths showed similar upwind speeds ($p > 0.05$, the Kruskal-Wallis test, Dunn's multiple comparisons test), when stimulated with the pheromone alone (orange, $N = 41$), or the pheromone in combination with 100 µg (N_{car}= 12, $N_{Z3-hex} = 8$, $N_{lin} = 9$) or 300 µg ($N_{car} = 13$, $N_{Z3-hex} = 3$, $N_{lin} = 14$) of artificial odorants (blue), or with the headspaces of cotton ($N_{intact} = 8$, $N_{dam} = 13$), or tomato plants ($N_{intact} = 10$, $N_{dam} = 7$) (green). blk, blank; car, β-caryophyllene; cot, cotton; lin, linalool; phe/phero, pheromone; tom, tomato; *Z*3-hex, (*Z*)3-hexenol.

source with on average 25 cm/s (**Figure 3B**). In summary, adding certain plant-related compounds at high concentration to the pheromone plume reduced the pheromone-guided response in male *Heliothis virescens* but did not lead to a different flight pattern: neither the flight direction in order to approach the odor source nor the upwind speed was influenced by plant volatiles.

Concentration Quantification of Synthetic Odorants vs. Plant-Released Volatiles

Our experiments show that only the application of linalool and (*Z*)3-hexenol at high concentration reduced the attractiveness of male *Heliothis virescens* to the pheromone, while the headspace of host plants did not show any influence. In order to analyze whether the difference is just a matter of odor concentration, we quantified the actual amount of the synthetic odorants released by the rubber septa (**Figures 4A,B**). While 3 ng of the major sex pheromone component *Z*11-16:Ald could be quantified via PDMS tubes, the plant components, β-caryophyllene, (*Z*)3-hexenol and linalool, were measured in much higher amounts. The amount of β-caryophyllene was 3.5-fold higher than the amount of (*Z*)3-hexenol, while the linalool release was 5-fold higher than the amount of (*Z*)3-hexenol. When pipetting three times the concentration on a rubber septum, both plant volatiles resulted in doubled emission rates, while only 1.5-fold of linalool was detected.

Are the synthetic single odor quantities that reduced the attractiveness of pheromones in our wind tunnel studies similar to those released by intact and damaged tomato and cotton plants? To find out, we quantified the release rate of β-caryophyllene, (*Z*)3-hexenol and linalool in damaged and undamaged host plants (**Figure 4C**). Larval damage in tomato and cotton plants led to an increase of β-caryophyllene (**Figure 4C**, left panel), and β-caryophyllene was released in quantities comparable to those of the synthetic odorant. However, β-caryophyllene had no effect on pheromone-guided flight behavior in male moths (**Figure 2A**). In contrast, (*Z*)3-hexenol and linalool could not be detected in undamaged plants or were found in only low quantities in damaged plants (**Figure 4C**, middle and right panels). This discrepancy shows that the concentrations of (*Z*)3-hexenol and linalool that reduced pheromone attraction (**Figure 2A**) were much higher than the natural emission of an entire plant. Hence, odorants that influence pheromone-guided behavior in male moths are not emitted in comparable quantities by plants. We therefore conclude that plant-pheromone interactions in *Heliothis virescens* most likely occur only under laboratory conditions, where very high odor concentrations are used.

DISCUSSION

We show that pheromone-plant odor interactions occur at the behavioral level of male *Heliothis virescens*, similar to those previously observed at the sensory level (Hillier and Vickers, 2011; Pregitzer et al., 2012). However, we also show that these interactions occur only at supra-natural concentrations of certain plant-emitted volatiles. Our findings therefore suggest that, in a natural environment, male moths are able to detect their conspecific female against a complex background of plant volatiles without negative effects on their pheromone-directed flight behavior.

Certain plant-related volatiles interfere with the detection of the major sex pheromone component of *Heliothis virescens* at the pheromone receptor HR13 and thereby reduce the

TABLE 2 | Effect of β-caryophyllene, (*Z*)3-hexenol and linalool on pheromone-guided flight behavior.

Stim. 1	Stim. 2	Sample size	Flight [%]	Upwind [%]	Source contact [%]	Upwind speed [cm/s] ± SD	Number of contacts ± SD
–	Phero	22	90.1	63.6	50	22.6 ± 25.5	1 ± 1.23
car100	Phero	26	88.5	80.8	53.8	28.9 ± 28	1.04 ± 1.22
car300	Phero	32	96.9	68.8	43.8	24.7 ± 33.4	1.09 ± 1.53
–	Phero	25	92	52	44	29.1 ± 21.8	1.16 ± 1.84
Z3-hex100	Phero	27	74.1	44.4	33.3	31.1 ± 28.2	1 ± 1.71
Z3-hex300	Phero	28	75	50	10.7*	30.2 ± 28	0.27 ± 0.93**
–	Phero	34	91.2	67.6	50	15.8 ± 30.2	1.32 ± 1.66
lin100	Phero	32	100	56.3	43.8	16.1 ± 40.4	0.94 ± 1.9
lin300	Phero	54	88.9	46.3	27.8 (*)	23.7 ± 34.5	0.63 ± 1.51*

*Number of tested individuals and the percentages of male moths, for the experiments shown in **Figures 2B,D**, which started their flight, showed upwind movement, and had source contact; also, their upwind speed. The last column includes the number of contacts for all tested males. The stimuli were applied as described in **Table 1**. SD, standard deviation.*
**Within a column indicate significant differences to the solvent-pheromone stimulation (*$p < 0.05$, **$p < 0.01$, Fisher's exact test with Bonferroni-Holm correction, (*) $p < 0.05$, Fisher's exact test, $p > 0.025$ with Bonferroni-Holm correction; Number of contacts and upwind speed: Kruskal-Wallis with Dunn's multiple comparisons test).*
car, β-caryophyllene; lin, linalool; phero, pheromone; Z3-hex, (Z)3-hexenol.

response of pheromone-detecting OSNs in the MGC (Pregitzer et al., 2012). Interestingly, this interference varies for different plant compounds: linalool and (Z)3-hexanol strongly suppress the pheromone response, while other compounds, such as β-caryophyllene, do not lead to any reduction. These findings correlate well with our behavioral results from experiments using the wind tunnel: while β-caryophyllene did not influence pheromone-guided flight behavior, high concentrations of (*Z*)3-hexenol and linalool reduced the attractiveness of the pheromone by at least 22%. Hence our results show that the coding of pheromone-plant interactions at the sensory level corresponds to the altered behavioral responsiveness of male moths. The representation of odor-induced activity in the AL therefore allows a prediction of the behavioral outcome. Notably, a correlation between the representation of odors in the AL and the behavioral performance has already been demonstrated in several species, such as honeybees (Guerrieri et al., 2005), flies (Knaden et al., 2012) and moths (Kuebler et al., 2012).

The behavioral performance of the moth ultimately results from the odor representation in higher brain centers and is determined by the integration of different processing channels within the neuronal network. Interestingly, when the antenna of the male *Heliothis virescens* moth was stimulated with β-caryophyllene and the major sex pheromone component *Z*11-16:Ald, single sensillum recordings showed an enhanced spiking activity compared to the response evoked by *Z*11-16:Ald alone (Hillier and Vickers, 2011). In contrast, when the major pheromone component was exchanged for the minor pheromone component, *Z*9-14:Ald, the pheromone response was suppressed (Hillier and Vickers, 2011). Although β-caryophyllene is influencing the neuronal activity of pheromone-responsive OSNs in the periphery, we did not observe any effect of this plant volatile onto the pheromone-guided flight behavior in our windtunnel experiments. Since β-caryophyllene modulates the major and minor pheromone pathways in opposing directions (Hillier and Vickers, 2011), the detection of the whole pheromone blend, including the two compounds, *Z*11-16:Ald and *Z*9-14:Ald, might not be modulated in the end.

Moreover, in the same physiological study (Hillier and Vickers, 2011), both major and minor sex pheromone components, when blended with the plant volatile linalool or (*Z*)3-hexenol, elicited reduced spiking activity in the corresponding pheromone-responsive OSNs. Likewise, in our wind tunnel assay, when high concentrations of the two plant compounds were added, the attractiveness of the complete pheromone blend was decreased, which resulted in reduced pheromone-guided flight behavior.

The three compounds that we used in our study are not the only volatiles being detected in plant headspaces. It would therefore be interesting to know if and how other plant volatiles, when added to the pheromone blend, influence the pheromone-guided behavior of a moth. This is of particular interest, since it has been observed that some of these green leaf volatiles increase the number of males caught in pheromone traps (Dickens et al., 1993). However, when we tested the whole headspaces of cotton and tomato plants, independently of their physiological condition, we did not find any influence on pheromone-guided flight behavior.

Host plants of *Heliothis virescens* that are damaged by larval feeding release volatiles such as β-caryophyllene, (*Z*)3-hexenol and linalool (e.g., Paré, 1997; De Moraes et al., 1998; Morawo and Fadamiro, 2014). All of these were used in our study. When we quantified the natural emission of these compounds, we realized that, except for β-caryophyllene, these odorants occur in only very low concentrations in the headspace of intact or damaged cotton and tomato plants. Although volatiles are usually emitted in higher amounts during daytime than in the dark (De Moraes et al., 2001), male moths are active in the scotophase. Therefore, they will encounter low concentrations of plant volatiles. When the results from the wind tunnel and GC-MS experiments were combined, we observed that unnaturally high concentrations of (*Z*)3-hexenol and linalool reduced the heliothine moths' attraction to pheromones, while a lower dose, which represents the more natural situation, did not affect the attraction.

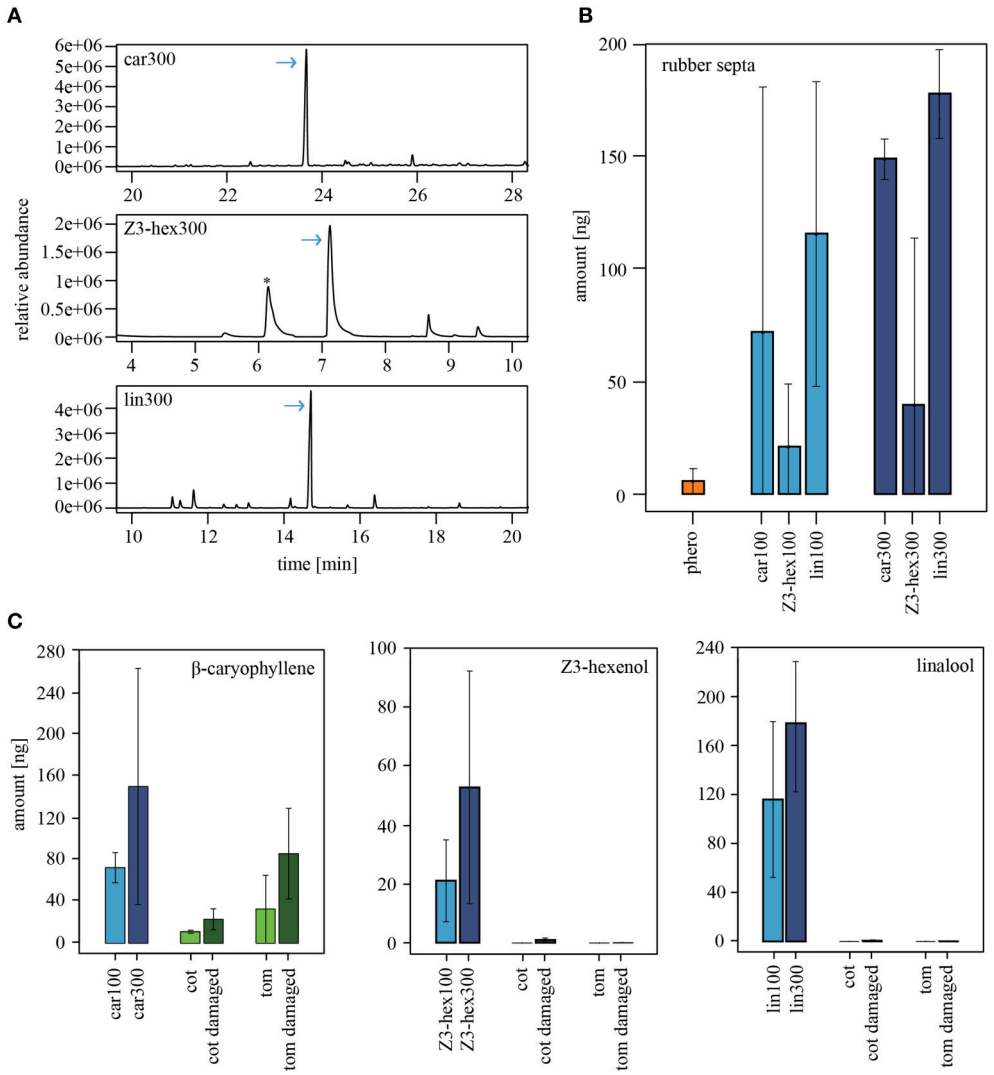

FIGURE 4 | Emission rates of volatiles from rubber septa and entire plants. (A) GC-MS example traces showing the relative abundance of the synthetic odorants β-caryophyllene (upper panel), (*Z*)3-hexenol (middle panel) or linalool (lower panel). 300 μg/μl of the odorant were loaded on a rubber septum, and the headspace was collected for 2 h with PDMS tubes. Arrows indicate the corresponding odor peak in the headspace. The asterisk represents the peak of a siloxane, which is a constituents of PDMS tubes. **(B)** Amounts of volatiles, which were released by rubber septa loaded with the pheromone blend ($N_{300\mu g} = 2$), β-caryophyllene ($N_{100\mu g} = 3$, $N_{300\mu g} = 3$), (*Z*)3-hexenol ($N_{100\mu g} = 2$, $N_{300\mu g} = 2$), or linalool ($N_{100\mu g} = 3$, $N_{300\mu g} = 3$). The averaged emission rates are shown as bar plots (±SEM). Bars represent odorants used in a concentration of 100 μg/μl (light blue) or 300 μg/μl (dark blue). **(C)** Comparison of the odor amount emitted from the rubber septa shown in **(B)** and the corresponding compounds in the plant headspace of intact (light green) and damaged (dark green) tomato ($N_{intact} = 2$, $N_{dam} = 4$) and cotton plants ($N_{intact} = 2$, $N_{dam} = 4$). Bars represent the averaged emission rates. Similar amounts of β-caryophyllene (left panel) were found in the odor emitted from the rubber septa and in odors released by the plants. (*Z*)3-hexenol (middle panel) and linalool (right panel) released from the plants were either not detected or occurred in low amounts that were not comparable to the amounts being released by the rubber septa. car, β-caryophyllene; cot, cotton; lin, linalool; phero, pheromone; tom, tomato; *Z*3-hex, (*Z*)3-hexenol.

Taken together, our study underlines the importance of using natural concentrations in order to investigate the ecological relevance of odorants and their influence on animals' behavior.

AUTHOR CONTRIBUTIONS

EB and SS together conceived and designed the study. EB planned and carried out all experiments. EB and SS analyzed and interpreted the results, prepared the figures and wrote the paper. AH helped to analyze the windtunnel data. BSH provided intellectual and financial support. All authors critically revised the article.

ACKNOWLEDGMENTS

We are grateful to Daniel Veit for technical support and Pedro Gouveia for his help with the 3D tracking. The authors would like to thank Gabriel Walther and Regina Seibt for their

contribution to the insect rearing as well as Jerrit Weißflog for the synthesis of tetradecenal. Furthermore we would like to thank Sonja Bisch-Knaden, Jürgen Krieger, David Heckel, and Sinéad O'Keeffe for comments and Emily Wheeler for editorial assistance. This study was supported by a grant of the Deutsche Forschungsgemeinschaft (SPP 1392, SA909/3-2) to EB and SS, the Max Planck Society (BSH and SS) and the Federal Ministry of Education and Research (BMBF research grant to SS).

REFERENCES

Almaas, T. J., and Mustaparta, H. (1990). Pheromone reception in tobacco budworm, *Heliothis virescens*. *J. Chem. Ecol.* 16, 1331–1347. doi: 10.1007/bf01021030

Almaas, T., and Mustaparta, H. (1991). *Heliothis virescens*: Response characteristics of receptor neurons in sensilla trichoidea type 1 and type 2. *J. Chem. Ecol.* 17, 453–472. doi: 10.1007/bf01395602

Berg, B. G., Almaas, T. J., Bjaalie, J. G., and Mustaparta, H. (1998). The macroglomerular complex of the antennal lobe in the tobacco budworm moth *Heliothis virescens*: specified subdivision in four compartments according to information about biologically significant compounds. *J. Comp. Physiol. A* 183, 669–682. doi: 10.1007/s003590050290

Berg, B. G., Tumlinson, J. H., and Mustaparta, H. (1995). Chemical communication in heliothine moths: IV. Receptor neuron responses to pheromone compounds and formate analogues. *J. Comp. Physiol. A* 177, 527–534. doi: 10.1007/BF00207182

Beyaert, I., and Hilker, M. (2014). Plant odour plumes as mediators of plant–insect interactions. *Biol. Rev.* 89, 68–81. doi: 10.1111/brv.12043

Bruce, T. J. A., Wadhams, L. J., and Woodcock, C. M. (2005). Insect host location: a volatile situation. *Trends Plant Sci.* 10, 269–274. doi: 10.1016/j.tplants.2005.04.003

Burton, R. L. (1979). A low-cost artificial diet for the corn earworm. *J. Econ. Entomol.* 63, 1969–1970. doi: 10.1093/jee/63.6.1969

Chaffiol, A., Dupuy, F., Barrozo, R. B., Kropf, J., Renou, M., Rospars, J.-P., et al. (2014). Pheromone modulates plant odor responses in the antennal lobe of a moth. *Chem. Senses* 39, 1–13. doi: 10.1093/chemse/bju017

Chaffiol, A., Kropf, J., Barrozo, R. B., Gadenne, C., Rospars, J.-P., and Anton, S. (2012). Plant odour stimuli reshape pheromonal representation in neurons of the antennal lobe macroglomerular complex of a male moth. *J. Exp. Biol.* 215, 1670–1680. doi: 10.1242/jeb.066662

Christensen, T. A., and Hildebrand, J. G. (1987). Male-specific, sex pheromone-selective projection neurons in the antennal lobes of the moth *Manduca sexta*. *J. Comp. Physiol. A* 160, 553–569.

Cunningham, J. P., and Zalucki, M. P. (2014). Understanding Heliothine (Lepidoptera: Heliothinae) pests: What is a host plant? *J. Econ. Entomol.* 107, 880–896. doi: 10.1603/ec14036

De Moraes, C. M., Mescher, M. C., and Tumlinson, J. H. (2001). Caterpillar-induced nocturnal plant volatiles repel conspeci®c females. *Nature* 410, 577–580. doi: 10.1038/35069058

De Moraes, C. M., Pare, P. W., Alborn, H. T., and Tumlinson, J. H. (1998). Herbivore-infested plants selectively attract parasitoids. *Nature* 393, 570–573. doi: 10.1038/31219

Deisig, N., Dupuy, F., Anton, S., and Renou, M. (2014). Responses to pheromones in a complex odor world: sensory processing and behavior. *Insects* 5, 399–422. doi: 10.3390/insects5020399

Deisig, N., Kropf, J., Vitecek, S., Pevergne, D., Rouyar, A., Sandoz, J.-C., et al. (2012). Differential interactions of sex pheromone and plant odour in the olfactory pathway of a male moth. *PLoS ONE* 7:e33159. doi: 10.1371/journal.pone.0033159

Den Otter, C. J., Schuil, H. A., and Sander-Van Oosten, A. (1978). Reception of host-plant odours and female sex pheromone in *Adoxophyes orana* (Lepidoptera: Tortricidae): Electrophysiology and morphology. *Proc. 4th Insect/Host Plant Symp.* 24, 370–378. doi: 10.1111/j.1570-7458.1978.tb02818.x

Deng, J.-Y., Wei, H.-Y., Huang, Y.-P., and Du, J.-W. (2004). Enhancement of attraction to sex pheromones of *Spodoptera exigua* by volatiles compounds produced by host plants. *J. Chem. Ecol.* 30, 2037–2045. doi: 10.1023/B:JOEC.0000045593.62422.73

Dicke, M., and Van Loon, J. J. (2000). Multitrophic effects of herbivore−induced plant volatiles in an evolutionary context. *Entomol. Exp. Appl.* 97, 237–249. doi: 10.1046/j.1570-7458.2000.00736.x

Dickens, J. C., Smith, J. W., and Light, D. M. (1993). Green leaf volatiles enhance sex attractant pheromone of the tobacco budworm, *Heliothis virescens* (Lep.: Noctuidae). *Chemoecology* 4, 175–177. doi: 10.1007/BF01256553

Fitt, G. P. (1989). The ecology of *Heliothis* species in relation to agroecosystems. *Ann. Rev. Entomol.* 34, 17–52. doi: 10.1146/annurev.en.34.010189.000313

Galizia, C. G., Sachse, S., and Mustaparta, H. (2000). Calcium responses to pheromones and plant odours in the antennal lobe of the male and female moth *Heliothis virescens*. *J. Comp. Physiol. A* 186, 1049–1063. doi: 10.1007/s003590000156

Guerrieri, F., Schubert, M., Sandoz, J. C., and Giurfa, M. (2005). Perceptual and neural olfactory similarity in honeybees. *PLoS Biol.* 3:e60. doi: 10.1371/journal.pbio.0030060

Gurba, A., and Guerin, P. M. (2015). Short-chain alkanes synergise responses of moth pests to their sex pheromones. *Soc. Chem. Industry*. 72, 870–876. doi: 10.1002/ps.4061

Hansson, B. S., Almaas, T. J., and Anton, S. (1995). Chemical communication in heliothine moths: V. Antennal lobe projection patterns of pheromone-detecting olfactory receptor neurons in the male *Heliothis virescens* (Lepidoptera: Noctuidae). *J. Comp. Physiol. A* 177, 535–543. doi: 10.1007/BF00207183

Hansson, B. S., and Anton, S. (2000). Function and morphology of the antennal lobe: New Developments. *Annu. Rev. Entomol.* 45, 203–231.

Hansson, B. S., Ljungberg, H., Hallberg, E., and Lofstedt, C. (1992). Functional specialization of olfactory glomeruli in a moth. Science 256, 1313–1315.

Hatano, E., Saveer, A. M., Borrero-Echeverry, F., Strauch, M., Zakir, A., Bengtsson, M., et al. (2015). A herbivore-induced plant volatile interferes with host plant and mate location in moths through suppression of olfactory signalling pathways. *BMC Biol.* 13:75. doi: 10.1186/s12915-015-0188-3

Hillier, N. K., Kleineidam, C., and Vickers, N. J. (2006). Physiology and glomerular projections of olfactory receptor neurons on the antenna of female *Heliothis virescens* (Lepidoptera: Noctuidae) responsive to behaviorally relevant odors. *J. Comp. Physiol. A* 192, 199–219. doi: 10.1007/s00359-005-0061-x

Hillier, N. K., and Vickers, N. J. (2007). Physiology and antennal lobe projections of olfactory receptor neurons from sexually isomorphic sensilla on male *Heliothis virescens*. *J. Comp. Physiol. A* 193, 649–663. doi: 10.1007/s00359-007-0220-3

Hillier, N. K., and Vickers, N. J. (2011). Mixture interactions in moth olfactory physiology: examining the effects of odorant mixture, concentration, distal stimulation, and antennal nerve transection on sensillar responses. *Chem. Senses* 36, 93–108. doi: 10.1093/chemse/bjq102

Kaissling, K.-E. M., and Bestmann, H.-J. (1989). Responses of bombykol receptor cells to (Z,E)-4,6-hexadecadiene and linalool. *J. Comp. Physiol. A* 165, 14–154. doi: 10.1007/BF00619189

Klun, J. A., Plimmer, J. R., Bierl-Leonhardt, B. A., Sparks, A. N., and Chapman, O. L. (1979). Trace chemicals: the essence of sexual communication. *Science* 204, 1328–1330. doi: 10.1126/science.204.4399.1328

Knaden, M., Strutz, A., Ahsan, J., Sachse, S., and Hansson, B. S. (2012). Spatial representation of odorant valence in an insect brain. *Cell Report* 1, 392–399. doi: 10.1016/j.celrep.2012.03.002

Knudsen, J. T., Erikson, R., Gershenzon, J., and Stahl, B. (2006). Diversity and distribution of floral scent. *Bot. Rev.* 72, 1–120. doi: 10.1663/0006-8101(2006)72[1:DADOFS]2.0.CO;2

Kuebler, L. S., Schubert, M., Kárpáti, Z., Hansson, B. S., and Olsson, S. B. (2012). Antennal lobe processing correlates to moth olfactory behaviour. *J. Neurosci.* 32, 5772–5782. doi: 10.1523/JNEUROSCI.6225-11.2012

Light, D. M., Flath, R. A., Buttery, R. G., Zalom, F. G., Rise, R. E., Dickens, J. C., et al. (1993). Host-plant green-leaf volatiles synergize the synthetic

sex pheromones of the corn earworm and codling moth (Lepidoptera). *Chemoecology* 4, 145–152. doi: 10.1007/BF01256549

Loughrin, J. H., Hamilton-Kemp, T. R., Andemen, A. R., and Hildebrand, D. F. (1990). Headspace compounds from flowers of *Nicotiana tabacum* and related species. *J. Agric. Food Chem.* 38, 455–460. doi: 10.1021/jf00092a027

Morawo, T., and Fadamiro, H. (2014). Duration of plant damage by host larvae affects attraction of two parasitoid species (Microplitis croceipes and Cotesia marginiventris) to cotton: implications for interspecific competition. *J. Chem. Ecol.* 40, 1176–1185. doi: 10.1007/s10886-014-0525-y

Nakamuta, K., Leal, W. S., Nakashima, T., Tokoro, M., Ono, M., and Nakanishi, M. (1997). Increase of trap catches by a combination of male sex pheromones and floral attractant in longhorn beetle, *Anaglyptus subfasciatus*. *J. Chem. Ecol.* 23, 1635–1640. doi: 10.1023/B:JOEC.0000006427.56337.6c

Namiki, S., Iwabuchi, S., and Kanzaki, R. (2008). Representation of a mixture of pheromone and host plant odor by antennal lobe projection neurons of the silkmoth *Bombyx mori*. *J. Comp. Physiol. A* 194, 501–515. doi: 10.1007/s00359-008-0325-3

Ochieng, S. A., Park, K. C., and Baker, T. C. (2002). Host plant volatiles synergize responses of sex pheromone-specific olfactory receptor neurons in male *Helicoverpa zea*. *J. Comp. Physiol. A* 188, 325–333. doi: 10.1007/s00359-002-0308-8

Paré, P. W. (1997). *De novo* biosynthesis of volatiles induced by insect herbivory in cotton plants. *Plant Physiol.* 114, 1161–1167.

Party, V., Hanot, C., Said, I., Rochat, D., and Renou, M. (2009). Plant terpenes affect intensity and temporal parameters of pheromone detection in a moth. *Chem. Senses* 34, 763–774. doi: 10.1093/chemse/bjp060

Party, V., Hanot, C., Schmidt-Büsser, D., Rochat, D., and Renou, M. (2013). Changes in odor background affect the locomotory response to pheromone in moths. *PLoS ONE* 8:e52897. doi: 10.1371/journal.pone.0052897

Pope, M. M., Gaston, L. K., and Baker, T. C. (1982). Composition, quantification and periodicity of sex pheromone gland volatiles from individual *Heliothis virescens* females. *J. Chem. Ecol.* 8, 1043–1055. doi: 10.1007/BF00987885

Pophof, B., and Van Der Goes Van Naters, W. (2002). Activation and inhibition of the transduction process in silkmoth olfactory receptor neurons. *Chem. Senses* 27, 435–443. doi: 10.1093/chemse/27.5.435

Pregitzer P., Schubert M., Breer H., Hansson B. S., Sachse S., and Krieger J. (2012). Plant odorants interfere with the detection of sex pheromone signals by male *Heliothis virescens*. *Front. Cell. Neurosci.* 6:42. doi: 10.3389/fncel.2012.00042

Reddy, G. V., and Guerrero, A. (2000). Behavioral responses of the diamondback moth, *Plutella xylostella*, to green leaf volatiles of *Brassica oleracea* Subsp. capitata. *J Agric. Food Chem.* 48, 6025–6029. doi: 10.1021/jf0008689

Roelofs, W. L., Hill, A. S., and Carde, R. T. (1974). Two sex pheromone components of the tobacco budworm moth, *Heliothis virescens*. *Life Sci.* 14, 1555–1562. doi: 10.1016/0024-3205(74)90166-0

Rostelien, T., Stranden, M., Borg-Karlson, A.-K., and Mustaparta, H. (2005). Olfactory receptor neurons in two heliothine moth species responding selectively to aliphatic green leaf volatiles, aromatic compounds, monoterpenes and sesquiterpenes of plant origin. *Chem. Senses* 30, 443–461. doi: 10.1093/chemse/bji039

Ramaswamy, S. B., and Roush, R. T. (1986). Sex pheromone titers in females of *Heliothis virescens* from three geographical locations (Lepidoptera: Noctuidae). *Entomol. Gener.* 12, 19–23.

Schmidt-Büsser, D., von Arx, M., and Guerin, P. M. (2009). Host plant volatiles serve to increase the response of male European grape berry moths, *Eupoecilia ambiguella*, to their sex pheromone. *J. Comp. Physiol. A* 195, 853–864. doi: 10.1007/s00359-009-0464-1

Shorey, H. H., and Gaston, L. K. (1965). Sex pheromones of noctuid moths. *V. Circadian* rhythm of pheromone-responsiveness in males of *Autographa californica*, *Heliothis virescens*, *Spodoptera exigua*, and *Trichoplusia ni* (Lepidoptera: Noctuidae). *Ann. Entomol. Soc. Am.* 58, 597–600. doi: 10.1093/aesa/58.5.597

Skiri, H. T., Galizia, C. G., and Mustaparta, H. (2004). Representation of primary plant odorants in the antennal lobe of the moth *Heliothis virescens* using calcium imaging. *Chem. Senses* 29, 253–267. doi: 10.1093/chemse/bjh026

Späthe, A., Reinecke, A., Haverkamp, A., Hansson, B. S., and Knaden, M. (2013). Host plant odors represent immiscible information entities - blend composition and concentration matter in hawkmoths. *PLoS ONE* 8:e77135. doi: 10.1371/journal.pone.0077135

Stranden, M., Rostelien, T., Liblikas, I., Almaas, T. J., Borg-Karlson, A.-K., and Mustaparta, H. (2003). Receptor neurons in three heliothine moths responding to floral and inducible plant volatiles. *Chemoecology* 13, 143–154. doi: 10.1007/s00049-003-0242-4

Tingle, F. C., and Mitchell, E. R. (1992). Attraction of *Heliothis virescens* (F.) (Lepidoptera: Noctuidae) to volatiles from extracts of cotton flowers. *J. Chem. Ecol.* 18, 907–914. doi: 10.1007/BF00988331

Tumlinson, J. H., Hendricks, P. E., Mitchel, E. R., Doolittle, R. E., and Brennan, M. M. (1975). Isolation, identification and synthesis of the sex pheromone of the tobacco budworm. *J. Chem. Ecol.* 1, 203–214. doi: 10.1007/BF00987869

Vetter, R. S., and Baker, T. C. (1983). Behavioral response of male *Heliothis virescens* in a sustained-flight tunnel to combinations of seven compounds identified from female sex pheromone glands. *J. Chem. Ecol.* 9, 747–759. doi: 10.1007/BF00988780

Vickers, N. J., and Baker, T. C. (1994). Reiterative responses to single strands of odor promote sustained upwind flight and odor source location by moths. *Proc. Natl. Acad. Sci.* 91, 5756–5760.

Vickers, N. J., and Baker, T. C. (1996). Latencies of behavioral response to interception of filaments of sex pheromone and clean air influence flight track shape in *Heliothis virescens* (F.) males. *J. Comp. Physiol. A* 178, 831–847. doi: 10.1007/BF00225831

Vickers, N. J., Christensen, T. A., and Hildebrand, J. G. (1998). Combinatorial odor discrimination in the arain: attractive and antagonist odor blends are represented in distinct combinations of uniquely identifiable glomeruli. *J. Comp. Neurol.* 400, 35–56.

Vickers, N. J., Christensen, T. A., Baker, T. C., and Hildebrand, J. G. (1991). Chemical communication in heliothine moths: III. Flight behavior of male Helicoverpa zea and *Heliothis virescens* in response to varying ratios of intra- and interspecific sex pheromone components. *J. Comp. Physiol. A* 169, 275–280. doi: 10.1007/BF00206991

Vickers, N. J., Christensen, T. A., Baker, T. C., and Hildebrand, J. G. (2001). Odour-plume dynamics influence the brain's olfactory code. *Nature* 410, 466–470. doi: 10.1038/35068559

Visser, J. H. (1986). Host odor perception in phytophagous insects. *Ann. Rev. Entomol.* 31, 121–144. doi: 10.1146/annurev.en.31.010186.001005

Zhao, X.-C., Kvello, P., Lofaldi, B. B., Lillevoll, S. C., Mustaparta, H., and Berg, B. C. (2014). Representation of pheromones, interspecific signals, and plant odors in higher olfactory centers; mapping physiologically identified antennal-lobe projection neurons in the male heliothine moth. *Front. Syst. Neurosci.* 8:186. doi: 10.3389/fnsys.2014.00186

Conflict of Interest Statement: The authors declare that the research was conducted in the absence of any commercial or financial relationships that could be construed as a potential conflict of interest.

frontiers in Physiology

REVIEW
published: 23 June 2016
doi: 10.3389/fphys.2016.00244

Comparative Neuroanatomy of the Lateral Accessory Lobe in the Insect Brain

Shigehiro Namiki and Ryohei Kanzaki*

Research Center for Advanced Science and Technology, The University of Tokyo, Tokyo, Japan

The lateral accessory lobe (LAL) mediates signals from the central complex to the thoracic motor centers. The results obtained from different insects suggest that the LAL is highly relevant to the locomotion. Perhaps due to its deep location and lack of clear anatomical boundaries, few studies have focused on this brain region. Systematic data of LAL interneurons are available in the silkmoth. We here review individual neurons constituting the LAL by comparing the silkmoth and other insects. The survey through the connectivity and intrinsic organization suggests potential homology in the organization of the LAL among insects.

Keywords: command neuron, premotor center, ventral body, lateral lobe, descending neuron

OPEN ACCESS

Edited by:
Sylvia Anton,
Institut National de la Recherche Agronomique, France

Reviewed by:
Uwe Homberg,
Philipps-Universität Marburg, Germany
Steffen Harzsch,
University of Greifswald, Germany

****Correspondence:***
Shigehiro Namiki
namiki@rcast.u-tokyo.ac.jp

Specialty section:
This article was submitted to Invertebrate Physiology, a section of the journal Frontiers in Physiology

Received: *20 February 2016*
Accepted: *03 June 2016*
Published: *23 June 2016*

Citation:
Namiki S and Kanzaki R (2016) Comparative Neuroanatomy of the Lateral Accessory Lobe in the Insect Brain. Front. Physiol. 7:244. doi: 10.3389/fphys.2016.00244

The lateral accessory lobe (LAL) is a neuropil that is highly associated with the central complex (CX). The LAL is thought to facilitate communication between the CX and the motor centers. For example, it is proposed that the LAL receives input from the CX and selects the activity of descending output (Wolff and Strausfeld, 2015). Perhaps due to the deep location and lack of the clear anatomical boundaries, few studies have focused on the LAL. A variety of response properties have been reported in the neurons innervating the LAL in different species: flight-correlated activity in locusts (Homberg, 1994), walking-correlated activity in crickets and moths (Kanzaki et al., 1994; Zorović and Hedwig, 2013), driving backwards walking in flies (Bidaye et al., 2014). The LAL is present in all insect species reported thus far and they seem to have a common set of subdomains, suggesting the ground pattern of the LAL organization. It is not clear whether the neuronal homology is present at individual neuron level.

This paper examines the comparability of individual neurons among different species by summarizing the experimental data available for the LAL. Systematic analysis of neuronal morphology has been performed heretofore only in the silkmoth *Bombyx mori* (Mishima and Kanzaki, 1999; Iwano et al., 2010; Namiki et al., 2014). The large-scale data of neuronal morphology is available in *Drosophila* (Chiang et al., 2011; Jenett et al., 2012; Milyaev et al., 2012; Costa et al., 2013), which cover the entire brain. We compare the organization of the LAL in the silkmoth with *Drosophila* and other insects.

ANATOMY

The CX is defined as a group of four midline neuropils: the protocerebral bridge, the fan-shaped body, the ellipsoid body, and the paired noduli (Ito et al., 2014). We essentially follow the terminology proposed by Insect Brain Nomenclature Working Group, though some other studies describe the LAL also as a part of the CX (Boyan and Reichert, 2011; Shih et al., 2015). To improve comparability among arthropod, another definition is also used: the CX as a group

of interconnected neuropils, including the central body, the protocerebral bridge, and the LAL (Richter et al., 2010). Heinze et al. (2013) introduced the term "sun compass neuropils" for the LAL, anterior optic tubercle and the members of the CX because these neuropils are highly interconnected and process compass-related stimuli, such as polarized light (Heinze et al., 2013).

The LAL is located on the lateral side of the CX in insects (**Figure 1**; Williams, 1975; Ito et al., 2014). The term "ventral body" is also used in the studies of Diptera. The area surrounding the CX, including the LAL, is called the lateral complex (Ito et al., 2014) or the CX accessory regions (Lin et al., 2013). Comparative neuroanatomy for the organization of the lateral complex is in progress. The LAL and the bulb, a small satellite neuropil, are classified as members of the lateral complex in *Drosophila* (Ito et al., 2014). **Figure 2** shows the GABA-like immunoreactivity in the LAL and surrounding region in *Bombyx*. There is a small satellite neuropil located dorsal to the LAL, termed the median olive (Iwano et al., 2010), which shows dense immunoreactivity (**Figure 2**, termed bulb). This area is rarely connected with the LAL. Based on its position and its immunoreactivity, this region might correspond to the lateral triangle in the monarch butterfly (Heinze and Reppert, 2012), the bulb in *Drosophila* (Ito et al., 2014), the median olive (medial bulb) and the lateral triangle (lateral bulb) in the locust (Heinze and Homberg, 2008; Träger et al., 2008; el Jundi et al., 2014), and the lateral complex in the ant (Schmitt et al., 2015). We denote this neuropil as the bulb, according to the brain nomenclature (Ito et al., 2014; **Figure 2**). The structure similar to the microglomerular complex (Träger et al., 2008; Seelig and Jayaraman, 2013) is present in the bulb (**Figure 2**).

A small protruding region in the superior-lateral tip of the LAL is present in the fly, called the gall, and is defined as a part of the LAL (Ito et al., 2014). Similarly, a small sub-region called the anterior loblet, is present in the LAL of the monarch butterfly brain (Heinze and Reppert, 2012). The homologous region exists in *Bombyx* because of the presence of a small region with GABA-like immunoreactivity in the LAL (referred to as gall in **Figure 2**), and neurons with similar morphology to that of the columnar neurons of the ellipsoid body that project to a similar location as the anterior loblet.

The anterior side of the LAL is relatively well-defined, whereas no clear anatomical boundary for the posterior side in most cases (el Jundi et al., 2009; Iwano et al., 2010; Heinze and Reppert, 2012; Ito et al., 2014; Montgomery and Ott, 2015). Practically, the posterior boundary is often defined by the antennal lobe tracts (Iwano et al., 2010; Heinze and Reppert, 2012), which are well-conserved across species (Galizia and Rössler, 2010; Ito et al., 2014). Immunoreactivity often helps to define the anatomical boundary. **Figure 3** shows the serotonin-like immunoreactivity of the LAL and surrounding area (Iwano et al., 2010). The antibody-staining covers the entire LAL in *Bombyx* (**Figure 3**) and might be useful in demarcating the anatomical border of the LAL (Heinze and Reppert, 2012).

Whereas brain regions are usually defined by their anatomy, Chiang et al. (2011) determined brain regions based on the statistical criterion for the clustering of individual neurons, called "local processing units" (Chiang et al., 2011). Using a large-scale data set of single neuron morphology in *Drosophila,* they have identified 41 local processing units. In most cases, the structured neuropils satisfy the criteria for local processing units. The definition is based on individual neuronal morphology, and hence is more functional than the traditional definition based on anatomical landmarks. Through this process, the authors refined the anatomical boundary of the LAL, and defined the inferior dorsofrontal procerebra (IDFP; Chiang et al., 2011), which is composed of four subdomains, including the hammer body, which occupies the largest volume in the LAL, the round body, and the ventral/dorsal spindle bodies.

FUNCTION

The function of the LAL is still incompletely understood. We introduce several examples of the experimental data in different insects, which are helpful to consider the function. Especially we focus on a population of descending neurons (DNs) that originate in the brain and project to the thoracic motor centers.

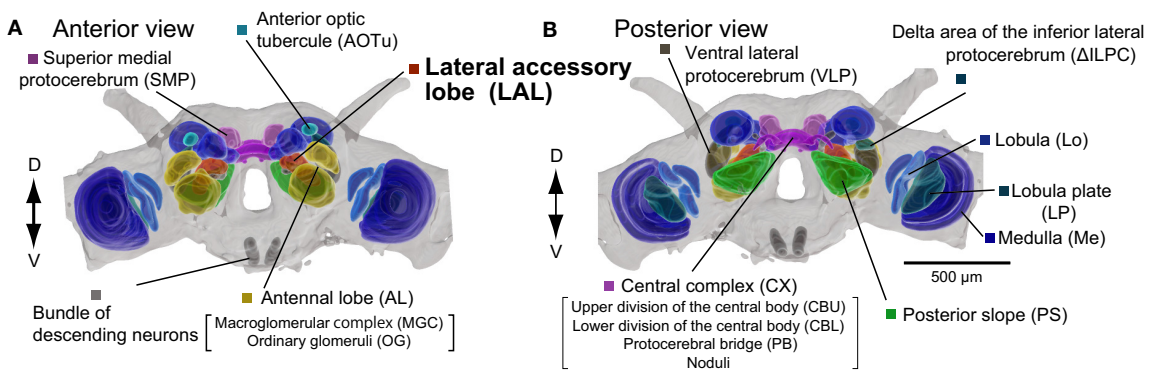

FIGURE 1 | Organization of the silkmoth brain. Anterior and posterior views of the silkmoth brain are shown **(A,B)**. Neuropils were segmented based on immunoreactivity of anti-synatotagmin antibody staining in whole-mount sample. Segmentation of unstructured neuropils are not precise because of the lack of clear anatomical boundaries. Images are modified from Namiki et al. (2014). D, dorsal; V, ventral.

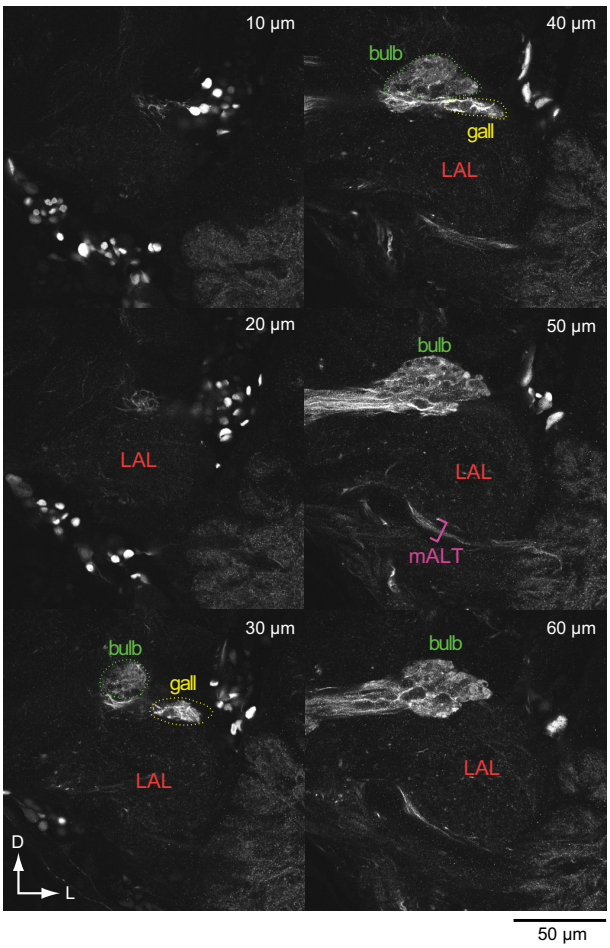

FIGURE 2 | GABA-like immunoreactivity in the lateral accessory lobe and surrounding area in the silkmoth. Confocal stacks at the different depth are shown. Anti-GABA antibody was used for the immunoreactivity (wholemount brains; Namiki et al., 2013). D, dorsal; mALT, medial antennal lobe tract; L, lateral.

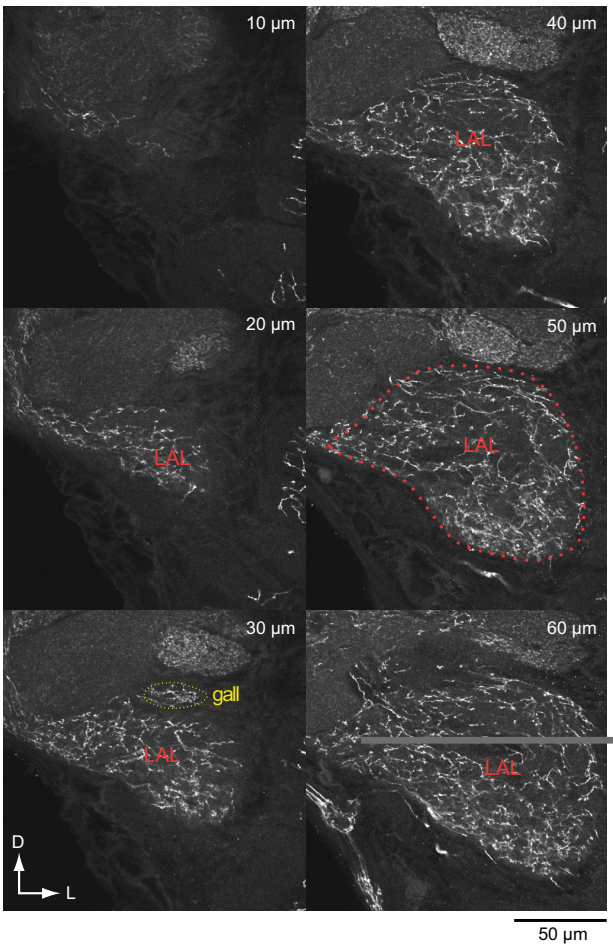

FIGURE 3 | Serotonin-like immunoreactivity of the lateral accessory lobe and surrounding area in the silkmoth. Confocal stacks for different depth are shown. Anti-serotonin antibody was used for the immunoreactivity (vibratome sections; Iwano et al., 2010).

Pheromone Orientation

Male moths orient to conspecific females by the use of sex pheromones. The circuit within the LAL generates pheromone-evoked persistent firing in the silkmoth (Kanzaki et al., 1994; Namiki et al., 2014). The identical pheromone input can cease persistent activity. The neuronal activity is termed flip-flop, which is a neural signal named after the toggle property. Extracellular recording studies show (1) the correlation between flip-flop neural signals from descending axons and antennal positions and (2) the correlation between antennal positions and turning direction (Olberg, 1983). From these observations, the flip-flop signal is thought to mediate walking commands for pheromone orientation.

Three types of DNs that show flip-flop neural signals have been identified so far (Mishima and Kanzaki, 1999; Wada and Kanzaki, 2005; **Figure 4**). All DNs innervate the LAL. Group-IA DN has smooth processes in the ipsilateral LAL and the varicose processes in the contralateral LAL (Mishima and Kanzaki, 1999), which are the indicators for the postsynaptic and presynaptic terminals (Cardona et al., 2010). Group-IIA and group-IID DNs have smooth processes in the ipsilateral LAL and descend ipsilateral neck connective (Wada and Kanzaki, 2005). The axonal projection in the ventral nervous system is unknown in the silkmoth.

Pheromone information is processed by multiple neural circuits in the silkmoth brain and the pheromone-evoked persistent firing activity is only observed in the neurons innervating the LAL (Namiki et al., 2014), suggesting that the LAL is the site where the flip-flop neural signal is produced.

Flight-Correlated Activity

Although the behavioral consequence is not known, the sensory response of LAL DNs are examined in the locust under the tethered flight condition (Homberg, 1994). The flight status is monitored by myographic recordings from the first basaler muscle of the hind wing. The VG3, DN innervating the ipsilateral LAL and descending the contralateral neck connective, shows

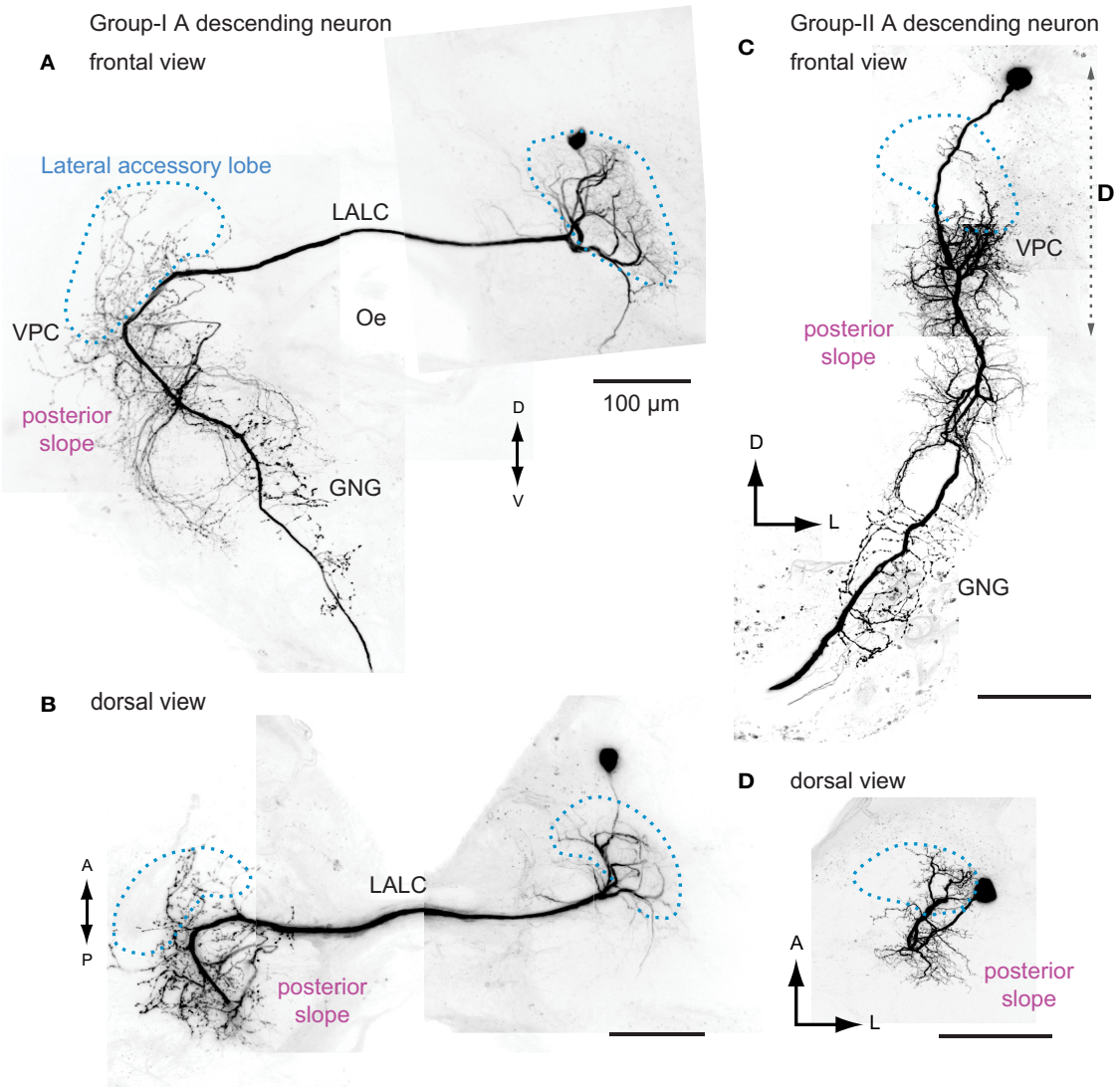

FIGURE 4 | The morphology of flip-flop descending neurons innervating the lateral accessory lobe in the silkmoth. Frontal and dorsal views of the group-IA DN **(A,B)** and the group-IIA DN **(C,D)** are shown. Group-IA DN has smooth processes mainly within the ipsilateral LAL and varicose processes in the contralateral LAL, ventral protocerebrum, posterior slope, and the gnathal ganglia **(A,B)**. Group-IIA DN has smooth processes in the ipsilateral LAL, ventral protocerebrum and posterior slope, and varicose processes in the ipsilateral posterior slope, gnathal ganglia **(C,D)**. Outline of the LAL is shown with broken line (*blue*). The range of maximum intensity projection for **(D)** is shown by broken line in **(C)**. GNG, gnathal ganglion; Oe, esophagus; VPC, ventral protocerebram. Images are prepared based on the data used in Mishima and Kanzaki (1999). A, anterior; LALC, lateral accessory lobe commissure; GNG, gnathal ganglia; Oe, esophagus; P, posterior; VPC, ventral lateral protocerebrum.

wind-elicited excitation, which precedes the onset of flight motor activity. The dendritic branch is concentrated in the ventral shell of the LAL. The other ipsilateral LAL DNs also show the flight-preceding activity and innervation mostly to the ventral region of the LAL. Further ascending neurons projecting to the LAL show tonic excitation during flight, and these receive the input from wing proprioreceptors. Based on single cell recording and staining data, the LAL appears to link ascending and descending pathways.

Phonotactic Steering

Female crickets orient toward conspecific males by the use of a calling song. Intracellular recording and staining from brain interneurons reveal the information flow from the ascending neurons via local interneurons toward DNs and indicate the relevance of the LAL for the phonotaxis of the cricket *Gryllus bimaculatus* (Zorović and Hedwig, 2011). Ascending interneurons transmit sound information into the brain. A local interneuron that projects from the axonal area of the ascending

interneuron toward the LAL has been reported (Zorović and Hedwig, 2011).

A bilateral LAL DN termed the B-DC1(5) is thought to mediate sensory-motor pathways for phonotaxis (Zorović and Hedwig, 2013). This neuron has smooth, dendrite-like processes in the ipsilateral LAL and the blebby, axon-like processes in the contralateral LAL, and descends on the contralateral side. The morphology is quite similar to the group-IA DN in silkmoths. The depolarization of the B-DC1(5) elicits walking and steering on the contralateral side, and hyperpolarization causes the cessation of walking. The B-DC1(5) response can follow the temporal structure of the male song both in standing and walking conditions, whereas most of the DNs show state-dependent responses, such as gating (Böhm and Schildberger, 1992; Staudacher, 2001). Additionally, unilateral LAL DN termed the B-DI1(1) innervates the ipsilateral LAL and is able to trigger walking, though the effect is less reliable than the B-DC1(5) (Zorović and Hedwig, 2013).

Obstacle Negotiating Behavior

Harley and Ritzmann (2010) examined the transition behavior for negotiating obstacles in the cockroach *Blaberus discoidalis*. The authors developed an electrolytic lesioning technique that enabled ablation in a small region, and they examined the effect of the lesion on the behavioral task, including climbing over a block, climbing over/tunneling under a shelf, walking up a wall, and walking in U-shaped track (Harley and Ritzmann, 2010). The authors systematically performed electrolytic lesions within the central complex neuropils and the LAL and evaluated the behavioral abnormality. The lesion within the LAL caused a strong phenotype in most, if not all, obstacle negotiation behaviors, supporting the anatomical observation that the LAL is a major output site of the CX. Additionally, the lesion of the LAL on one side exhibited turning abnormalities in both directions, suggesting the possibility that the turning behavior is not caused by the operation of a single LAL, but rather the coordination of the LAL on both sides is required.

Backwards Walking

Using genetic engineering in *Drosophila melanogaster*, a recent study identified two pairs of neurons for controlling backwards walking, named the moonwalker DN (MDN; Bidaye et al., 2014). When the MDN is activated using thermogenetics, the probability of backwards walking becomes significantly higher, and the silencing of the DNs nearly abolished the movement. These DNs have putative dendritic innervations mainly to the LAL, which is suggested by a synaptic marker. In contrast to the LAL DNs reported in the other insects, MDN innervates the LAL on both sides. The MDN sends projections to leg neuropils in the ventral nervous system on one side. This pattern of innervation is similar to the other ipsilateral LAL DN, aSP3 (Yu et al., 2010), which shows a striking similarity in the morphology in the brain to the group-II DNs of the silkmoth.

Polarized Light Processing

Locusts are known for its long-distance migration. They use the polarized light as a sky-compass information for navigation. The neuronal pathway of the polarized light processing has been investigated in detail (Heinze, 2014). Columnar neurons of the CX respond to sky compass signal in locusts (Vitzthum et al., 2002; Heinze and Homberg, 2007), butterflies (Heinze and Reppert, 2011), and beetles (el Jundi et al., 2015). Because the columnar neurons project to the LAL, the area might be relevant for polarized light processing. Polarized sensitive neurons that can be postsynaptic to the CX neurons have been described (Heinze and Homberg, 2009). One of these neurons connects the ipsilateral LAL to the contralateral triangle and show the polarization opponency, suggesting the polarized light processing in the LAL. The LAL-pPC neuron, projects to the posterior protocerebrum, which may correspond to the posterior slope in the silkmoth and the posterior slope/inferior bridge in *Drosophila*. This neuron might supply a polarization-sensitive descending neurons in the locust (Träger and Homberg, 2011).

Overall, these examples suggest the LAL function on locomotion, such as steering toward left or right, and moving forward or backward. Steering-related functions appear to be rare in the other types of DNs, which do not innervate to the LAL, including middle leg contractions for fast escape in the giant fiber (von Reyn et al., 2014), triggering courtship behavior in the pIP10 (von Philipsborn et al., 2011) and the P2b (Kohatsu et al., 2011), grooming in antennal DNs (Hampel et al., 2015), leg motion in a dopaminergic DN in *Drosophila* (Tschida and Bhandawat, 2015), flight initiation in TCG in locusts (Bicker and Pearson, 1983), and song generation in the B-DC-3 of crickets (Hedwig and Heinrich, 1997). In this respect, it would be interesting to identify whether the deviation sensitive DNs, such as the DCI and the PI(2)5 in locusts (Hensler, 1988; Hensler and Rowell, 1990) that are assumed to generate steering responses, have dendritic innervation into the LAL.

NEURONAL MORPHOLOGY

The LAL is connected to various regions of the protocerebrum (Strausfeld et al., 1998; Namiki et al., 2014). In this section we introduce the morphology of LAL interneurons according to the connectivity. We also examine the comparability in their morphology, which suggests homology of the LAL among insects.

Central Complex

There are dense connections between the fan-shaped body/protocerebral bridge and the LAL (Shih et al., 2015). Detailed morphology of individual neurons has been reported in *Drosophila*, the desert locust, and the monarch butterfly (Heinze and Homberg, 2008; Heinze et al., 2013; Lin et al., 2013; Wolff et al., 2015). The cytoarchitecture and the morphology of individual neurons seem to be conserved. The LAL receives input from populations of columnar neurons connected to the ellipsoid body via eb-pb-vbo (EIP)/CL1a neurons, protocerebral bridge via the pb-eb-idfp (PEI)/CL1b,d neurons, and the fan-shaped body and protocerebral bridge via the pb-fb-idfp (PFI)/CPU1,2 neurons (Heinze and Homberg, 2008; Heinze et al., 2013; Lin et al., 2013). The basic neuronal components are similar in other

insects, including the cricket (Schildberger, 1983), honeybee (Homberg, 1985), beetle (Wegerhoff et al., 1996), and silkmoth (Namiki et al., 2014) (Supplementary Figure 1). There are connections between the LAL and circuit components of the CX that travel in opposite directions and form functional loops (Lin et al., 2013; Shih et al., 2015).

Anterior Optic Tubercle

The anterior optic tubercle is the most prominent anterior optic focus in the protocerebrum. There are parallel processing pathways for processing polarized light in the locust. The upper unit of the anterior optic tubercle supplies the LAL, whereas the lower unit supplies the bulb (median olive and lateral triangle; Homberg et al., 2003). Connections between the anterior optic tubercle and the LAL have been reported in *Drosophila* (Yang et al., 2013; e.g., Cha-F-600143, Cha-F-000252, fru-M-800104, Gad1-F-300056), honeybee (Mota et al., 2011), bumblebee (Pfeiffer and Kinoshita, 2012), and silkmoth (Namiki et al., 2014). This pathway underlies sky-compass navigation that uses polarized light in insects (Homberg et al., 2011).

Superior Medial Protocerebrum

The superior medial protocerebrum is an unstructured neuropil located in the dorsal medial part of the protocerebrum. The brain region is identified as the relay station between the lateral protocereberum and the LAL through a pheromone processing pathway in the silkmoth (Namiki et al., 2014). Dye injection into the LAL labels this region. The neurons projecting from superior medial protocerebrum to the contralateral LAL have been identified (Supplementary Figure 2) (Namiki et al., 2014). A connectome study suggested the presence of this connectivity in *Drosophila*. The superior dorsofrontal protocerebrum, which roughly corresponds to the superior medial protocerebrum, is highly connected with the IDFP (mostly overlap to the LAL; Shih et al., 2015), and interneurons that connect these regions are present (e.g., Cha-F-000105, TH-F-200089, TH-F-200092, VGlut-F-000104; Chiang et al., 2011). The connection between the superior medial protocerebrum and the LAL are also indicated by studies based on clonal units (Ito et al., 2013; Yang et al., 2013). The dorsal-anterior-lateral neurons, which are relevant to memory retention, connect the superior dorsofrontal protocerebrum and IDFP (Chen et al., 2012). The F1 neurons, which are a neuronal population involved in visual pattern memory for contour orientation (Liu et al., 2006; Li et al., 2009), innervate LAL, fan-shaped body and the superior medial protocerebrum. The neurons connecting the LAL and the superior medial protocerebrum have also been reported in the flesh fly (Phillips-Portillo and Strausfeld, 2012) the desert locust (Homberg et al., 2003) and the monarch butterfly (Heinze et al., 2013).

The brain region is characterized by several unique features. The interneurons innervating this region respond to multimodal sensory stimulation and often show spontaneous burst activity in the silkmoth (Supplementary Figure 3). Connectomics studies identify the superior medial protocerebrum as a hub in the whole brain network in *Drosophila* (Ito et al., 2013; Shih et al., 2015). The entire population of output neurons from the mushroom body lobes has been described in *Drosophila*, and the majority of them supply the superior medial protocerebrum (Aso et al., 2014). These anatomical data suggest the importance of this brain region. Neuronal activity preceding walking is reported in the crayfish (Kagaya and Takahata, 2011). The neuron has the dendritic branch in the area close to the central body, which locates potentially similar to the superior medial protocerebrum in insects.

Lobula Complex

Namiki et al. (2014) identified a pathway from the lobula complex (**Figure 5**) directly innervating the LAL. The wide-filed dendritic branches in the lobula plate is reminiscent of the lobula-plate tangential cells in Diptera (Hengstenberg et al., 1982). Optic lobe projection neurons from both the medulla and the lobula complex project to the posterior slope in *Bombyx*. However, only the neurons from the lobula complex have additional processes onto the LAL. The direct inputs from the lobula complex to the LAL are also present in *Drosophila* (e.g., VGlut-F-800153 for ipsilateral, VGlut-F-300218 for contralateral LAL; data available from FlyCircuit Database; Chiang et al., 2011). The leukokinin-immunoreactive neurons connecting the anterior lobe of the lobula and the LAL have been reported in locusts (Homberg et al., 2003).

The direct input from the lobula plate to the LAL might enable integration of olfactory and visual information. Walking activity evoked by sex pheromones is modulated by the presence of the optic flow, especially in the surge phase, in the silkmoth (Pansopha et al., 2014). Silkmoths utilize visual information to modify locomotor commands to adapt to perturbations in the sensory-motor feedback gain (Ando et al., 2013). Although there is no experimental evidence, the identified direct pathway to the LAL might underlie this behavior.

Thoracic Motor Centers

There is similarity in the morphology of DNs innervating LALs among insect species (**Figure 6**). For example, the characteristic morphological features of group-II DNs in *Bombyx* are: (1) cell bodies belong to the cluster located on the anterior surface beside the anterior optic tubercle, (2) they descend the ipsilateral side of the neck connective, and (3) they have smooth processes in the LAL. The neurons that meet these morphological features have been reported in other species, including the sphinx moth *Manduca sexta* (Kanzaki et al., 1991a), the cricket *Gryllus bimaculatus* (Zorović and Hedwig, 2013), the locust *Schistocerca gregaria* (Homberg, 1994), and the fruit fly *Drosophila melanogaster* (Yu et al., 2010). This observation suggests the homology of neuronal morphology for at least some types of DNs. In this respect, testing the axonal projections into the ventral nervous system would be interesting, but has not been studied thus far. Similarly, some bilateral LAL DNs also share their morphological features: group-IA DNs in moths (**Figure 6D**), VGlut-F-500726 in *Drosophila* (**Figure 6E**), VG3 in locusts (**Figure 6F**), and B-DC1(5) in crickets (Homberg, 1994; Mishima and Kanzaki, 1999; Zorović and Hedwig, 2011).

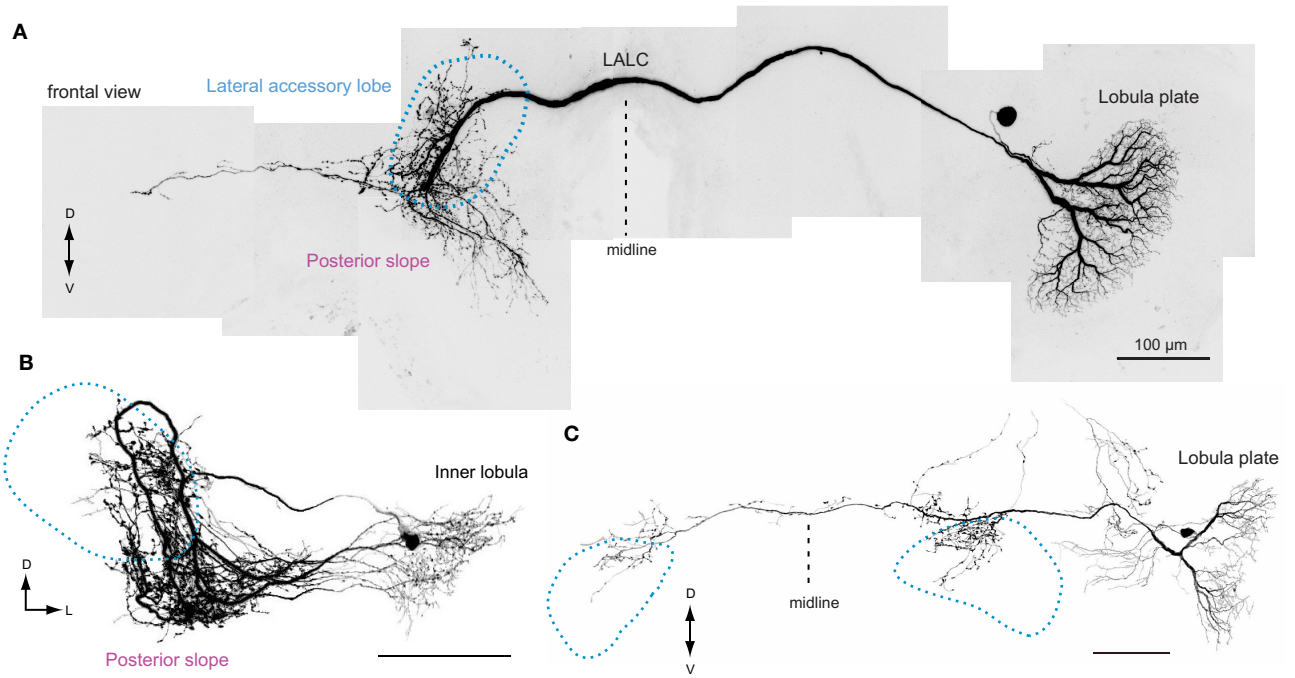

FIGURE 5 | The morphology of lobula complex widefield cells supplying the lateral accessory lobe in the silkmoth. (A) This neuron has smooth process in the ipsilateral lobula plate and varicose processes onto the contralateral LAL and posterior slope. The varicose processes are mainly concentrated onto the upper division of the LAL. **(B)** A neuron with smooth branches in the inner lobula and has varicose processes in the ipsilateral LAL and the posterior slope. **(C)** A neuron with smooth branches in the lobula plate and varicose processes to the bilateral LALs. In each case, the projection within the LAL are biased to the upper division. Images are modified from Namiki et al. (2014). LALC, lateral accessory lobe commissure.

Potentially similar neurons are present in ants (Yamagata et al., 2007) and dragonflies (Olberg, 1986).

The bilateral LAL DNs have smooth processes and putative dendritic regions in one side of the LAL in most cases. An exception is the MDN that has dendritic innervations in bilateral LALs (Bidaye et al., 2014). MDN-like cells might be implemented in other insect species that show backwards walking, such as the stick insect (Graham and Epstein, 1985). The silkmoth does not show backwards walking at least in normal condition. Even though intracellular recording on a continuous basis has been performed, which targets the LAL over the past two decades, we have never observed this neuron type in the silkmoth.

Posterior Slope

Although several lines of evidence indicate function of the CX on behavioral control such as place learning (Ofstad et al., 2011), spatial navigation (Neuser et al., 2008; Seelig and Jayaraman, 2015; el Jundi et al., 2015), locomotor control (Martin et al., 2015), the information flow from the CX and thoracic motor centers is still unclear. Because the CX might have very few or no direct descending outputs (Staudacher, 1998; Okada et al., 2003; Cardona et al., 2009; Hsu and Bhandawat, 2016), some other parts of the brain must be involved in relaying the command information. The LAL is the primary candidate because of its dense connections with the CX and the several examples of DNs that control locomotion (Zorović and Hedwig, 2013; Bidaye et al., 2014). The number of DNs innervating the LAL, however, is much smaller than that in other parts of the brain, such as the posterior slope, lateral protocerebrum, and gnathal ganglion (Strausfeld et al., 1984; Ito et al., 1998; Okada et al., 2003). In the silkmoth, we estimate that approximately 10 DNs innervate the LAL on each side. One possibility is that such a small number of neurons enable a versatile behavioral repertoire. Another possibility is that another brain region, that is downstream to either the CX and/or the LAL, might relay information to the thoracic motor centers.

We postulate that the posterior slope connects the LAL with the major population of DNs and then transmits the information to the thoracic motor centers. The posterior slope is the inferior part of the posterior brain, where extensive arborizations of descending and ascending neurons are observed (Strausfeld, 1976; Ito et al., 2014). Lobula plate neurons supplies this region, and hence is thought to be involved in the processing of motion cues (Strausfeld and Bassemir, 1985; Paulk et al., 2009; Borst, 2014). The posterior slope contains the largest number of DNs in the cerebral ganglia. In all of the species studied thus far, the posterior-ventral part of the brain is densely labeled by backfilling from the neck connective (Kanzaki et al., 1994; Staudacher, 1998; Okada et al., 2003; Cardona et al., 2009; Hsu and Bhandawat, 2016). Additionally, the posterior slope has connections with the LAL, which might be bidirectional. Namiki et al. (2014) reported the connection with the LAL by injecting the fluorescent dye into the posterior slope. From the neuronal morphology

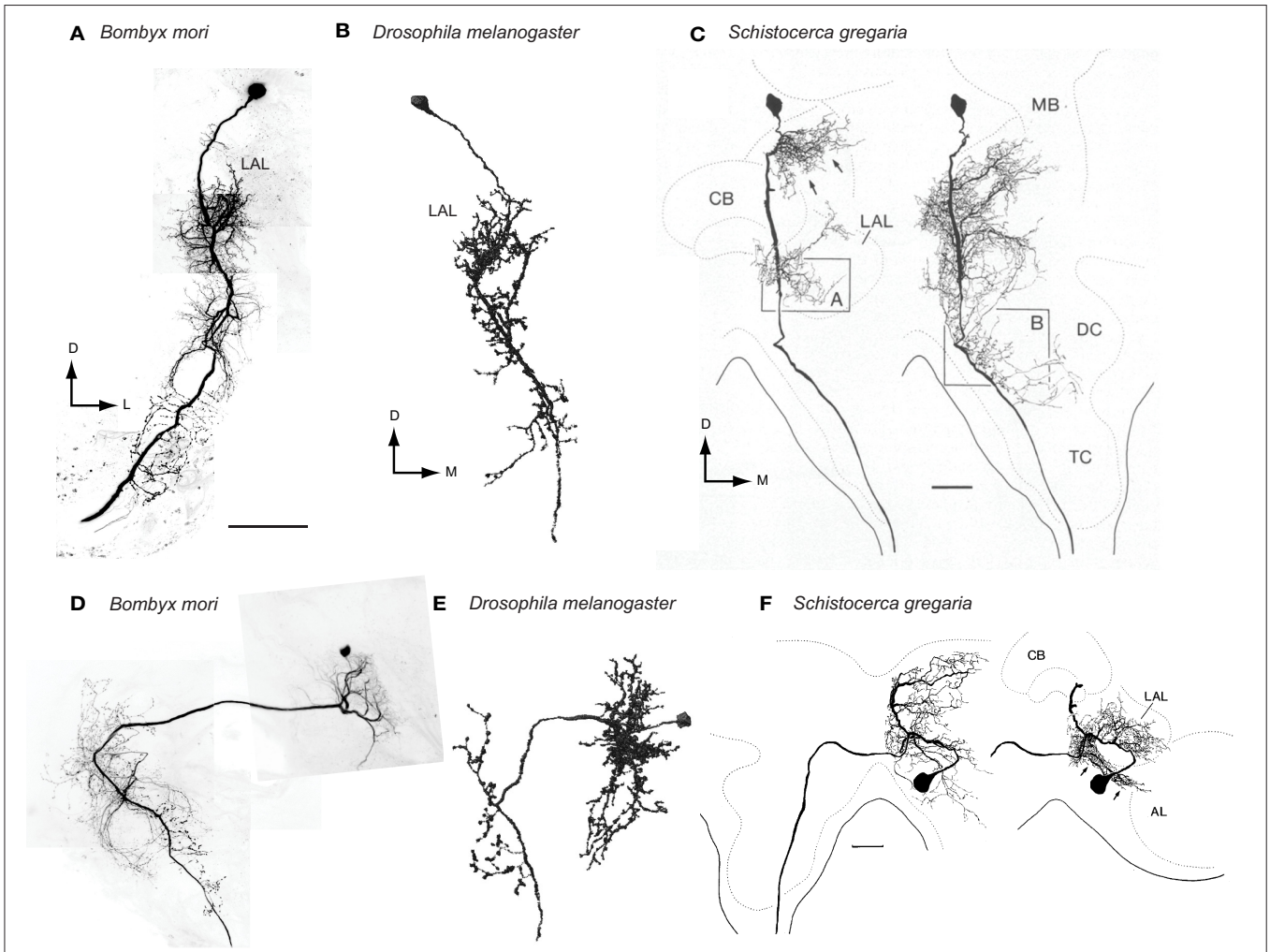

FIGURE 6 | Comparison of neuronal morphology of the LAL bilateral neurons across species. (A) Ipsilateral LAL DN of the silkmoth, *Bombyx mori* (Mishima and Kanzaki, 1999). **(B)** Ipsilateral LAL DN of the fruit fly *Drosophila melanogaster* (VGlut-F-200356, FlyCircuit Database; Chiang et al., 2011). The neuron has smooth processes in the ipsilateral LAL, vest, wedge and superior posterior slope and descend the ipsilateral neck connective. **(C)** Ipsilateral LAL DN of the desert locust, *Schistocerca gregaria* (Homberg, 1994). **(D)** Bilateral LAL DN of the silkmoth, *Bombyx mori* (Mishima and Kanzaki, 1999). **(E)** Bilateral LAL DN of the fruit fly *Drosophila melanogaster* (VGlut-F-500726, FlyCircuit Database; Chiang et al., 2011). This neuron has smooth processes in the ipsilateral LAL, epaulete, vest, inferior posterior slope and superior posterior slope and varicose processes in the contral lateral vest, inferior posterior slope and superior posterior slope. **(F)** Bilateral LAL DN of the desert locust, *Schistocerca gregaria* (Homberg, 1994). Scale bars = 100 μm. AL, antennal lobe; CB, central body; DC, deep deutocerebrum; LAL, lateral accessory lobe; M, medial; MB, mushroom body; TC, tritocerebrum.

obtained by intracellular staining, there are candidate neurons for these connections. For example, a subpopulation of the LAL interneurons identified so far in *Bombyx* actually have innervations to the posterior slope (**Figure 7**). About half of the LAL interneurons have varicose processes in the posterior slope (40%, $n = 20$ for bilateral neurons; 55%, $n = 9$ for unilateral neurons; Namiki et al., 2014). A group of unilateral interneurons connects the LAL and the posterior slope (Iwano et al., 2010). Neurons connecting the LAL and the posterior protocerebrum have been reported in the locust (Heinze and Homberg, 2009) and butterfly (Heinze and Reppert, 2012).

Next, we considered the possibility that the DNs themselves transmit information from the LAL to the posterior slope. A subpopulation of bilateral DNs have smooth processes in the LAL in the ipsilateral side and varicose processes in the contralateral side that might mediate the information flow from the posterior slope to the LAL (**Figure 4**). Group-I DNs, all of which show bilateral innervations, have varicose terminal processes in the contralateral posterior slope, and all of the ipsilateral LAL DNs studied so far have varicose terminals in the ipsilateral posterior slope (Mishima and Kanzaki, 1999; Namiki et al., 2014). The putative homologous neurons of the *Bombyx* group-I DNs in *Drosophila* show similar morphological feature. They also have additional innervations in the posterior slope (e.g., VGlut-F-500726; **Figure 6E**, VGlut-F-000150, and fru-F-100073; FlyCircuit Database; Chiang et al., 2011). These anatomical

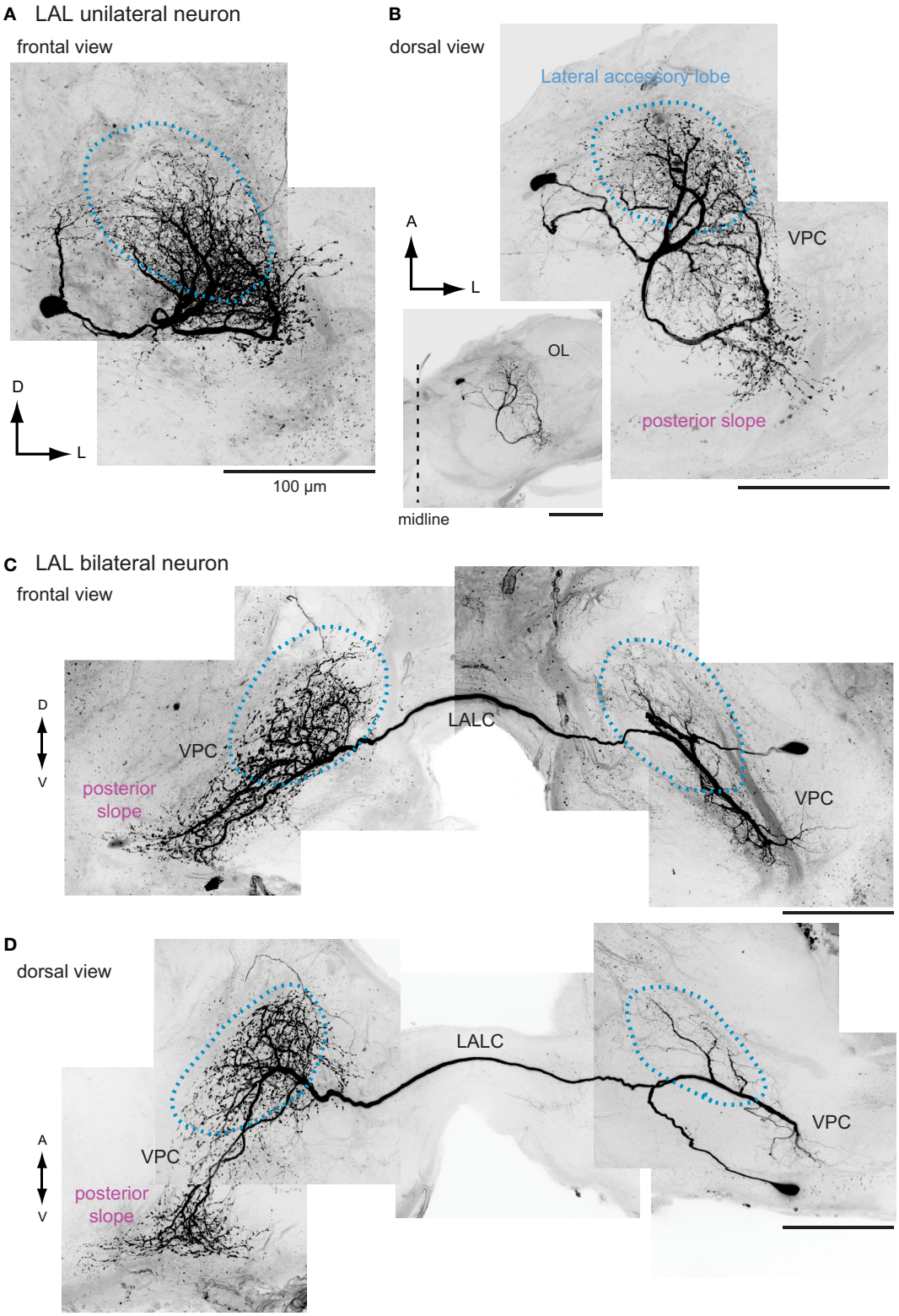

FIGURE 7 | The morphology of interneurons innervating the lateral accessory lobe in the silkmoth. Frontal and dorsal views of unilateral LAL interneurons **(A,B)** and bilateral LAL interneurons **(C,D)** are shown. Images are prepared based on the data used in Iwano et al. (2010). LALC, lateral accessory lobe commissure; VPC, ventral protocerebrum.

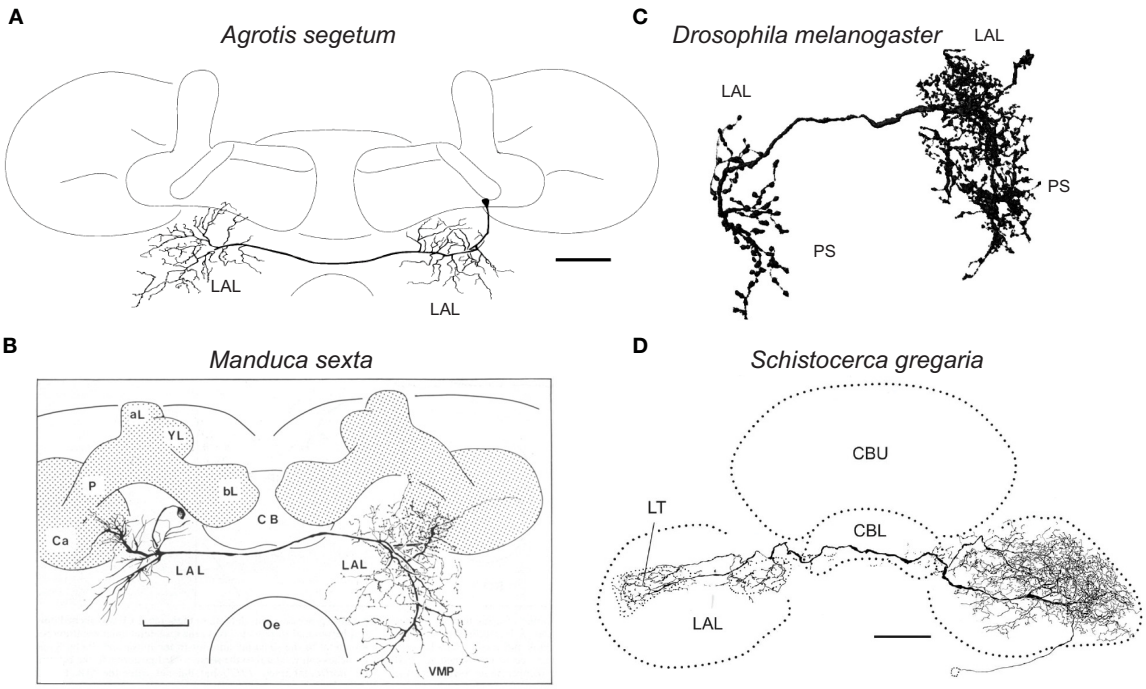

FIGURE 8 | Comparison of neuronal morphology of the LAL bilateral neurons across species. (A) LAL bilateral neuron of the turnip moth *Agrotis segetum* (Lei et al., 2001). **(B)** LAL bilateral neuron of the sphinx moth *Manduca sexta* (Kanzaki et al., 1991b). **(C)** LAL bilateral neuron of the fruit fly *Drosophila melanogaster* (Fru-M-200330, FlyCircuit Database; Chiang et al., 2011). The neuron has smooth processes in the ipsilateral LAL, epaulete, wedge, vest and superior posterior slope and varicose processes in the contralateral LAL, inferior posterior slope and superior posterior slope. **(D)** LAL bilateral neuron of the desert locust, *Schistocerca gregaria* (Heinze and Homberg, 2009). Scale bars, 50 μm for **(A)**, 100 μm for **(B,D)**. aL, alpha-lobe of the mushroom body; bL, beta-lobe of the mushroom body; Ca, calyx of the mushroom body; CB, central body; CBL, lower division of the central body; CBU, upper division of the central body; LAL, lateral accessory lobe; LT, lateral triangle; Oe, esophagus; P, pedunculus of the mushroom body; PS, posterior slope; VMP, ventral-medial protocerebrum.

connections suggest a large degree of interplay between these two circuits.

Other Regions

The LAL is also connected with other neuropils in the protocerebrum, such as the ventrolateral protocerebrum in the moth (Pfuhl et al., 2013), locust (Homberg, 1994), and *Drosophila* (e.g., Gad1-F-000101, fru-M-300049; Chiang et al., 2011). This region contains descending output (Milde and Strausfeld, 1990; Okada et al., 2003). Although the number of neurons involved in this connection might be small, this pathway might also underlie the transmission of command from the CX (Strausfeld and Hirth, 2013).

Although the number of neurons is small, connections with the mushroom body are present in *Drosophila* (Ito et al., 1998). The connection between the LAL and the medial lobe of the mushroom body has been described in the blowfly *Calliphora erythrocephala* (Strausfeld, 1976). A neuron connecting the LAL and the mushroom body pedunculus has been reported in the cockroach, which are sensitive to mechanosensory stimuli (Strausfeld and Li, 1999).

INTRINSIC ORGANIZATION

The LAL appears to have modular organization in the silkmoth (Namiki et al., 2014). We here review the intrinsic organization in the silkmoth by comparing the neuronal morphology with other insects.

The interneurons of the LAL are classified into two groups: unilateral neurons innervating one side of the LAL and bilateral neurons innervating both sides of the LAL (**Figure 7**). One prominent feature in circuit organization is the dense connection between both hemispheres, which contains bilateral neurons (Homberg et al., 1987; Homberg and Hildebrand, 1989, 1991; Breidbach, 1990; Müller et al., 1997; Dacks et al., 2006). In the silkmoth, about 60 fibers run through the LAL commissure, a bundle of bilateral neurons connecting the LALs on both sides. This neuronal population is thought to have a crucial role on generating walking command (Kanzaki, 1997). Among these, many neurons show GABA-like immunoreactivity (Iwano et al., 2010). Additionally, there are two pairs of bilateral neurons in the LAL with serotonin-like immunoreactivity, which are present also in other species including Lepidoptera, Coleoptera, and Diptera (Dacks et al., 2006). A population of LAL bilateral neurons has been identified by clustering analysis of FlyCircuit Database (Cluster 31 in supercluster XII; Chiang et al., 2011; Costa et al., 2014). The anatomy of single neuron morphology of the LAL bilateral interneurons has been reported in moths including *Heliothis virescens* (Pfuhl and Berg, 2007), *Agrotis segetum* (**Figure 8A**; Lei et al., 2001), and *Manduca sexta* (**Figure 8B**; Kanzaki et al., 1991b), fruit flies (**Figure 8C**; Hanesch

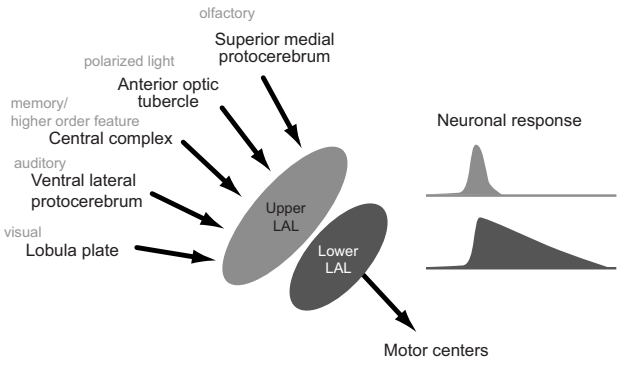

FIGURE 9 | Schematics of the hypothesized organization of the lateral accessory lobe. Inputs from the protocerebram converge onto the upper division and the descending output originates the lower division. Neuronal response to the sex pheromone, which trigger the locomotion, is longer for neurons innervating the lower division.

et al., 1989; Chiang et al., 2011), crickets (Zorović and Hedwig, 2011), and locusts (**Figure 8D**; Müller et al., 1997; Heinze and Homberg, 2009). A similar neuron is present in the malaria mosquito *Anopheles gambiae* (Ignell et al., 2005).

The LAL is classified into two subdivisions that are delineated by the LAL commissure that is the prominent bundle connecting the bilateral LALs: upper division and lower division (Iwano et al., 2010). The LAL bilateral neurons can be classified into two morphological classes based on the degree of neurite innervation into the upper and lower divisions (Supplementary Figure 4). The same morphological feature is observed in *Drosophila* (VGlut-F-800201 for the lateral side, VGlut-F-700549 and VGlut-F-800001 for the medial side of the IDFP) and locust (Homberg, 1994). The interneurons with biased innervations to the lower division of the LAL exhibit activity with a longer duration in response to sex pheromones (Supplementary Figure 5) (Namiki et al., 2014). This suggests the functional difference between the upper and lower divisions.

The inputs from the CX terminate in specific sub-regions within the LAL (Heinze et al., 2013; Lin et al., 2013; Namiki et al., 2014), suggesting the presence of a functional module within the LAL. Most of the input from the CX converges onto the upper division of the LAL in *Bombyx* (Supplementary Figure 6) (Namiki et al., 2014), the ventral LAL in monarch butterfly (Heinze et al., 2013), and the dorsal shell of the LAL in locust (Heinze and Homberg, 2008). The columnar neurons project to the lateral side of the IDFP or LAL in the *Drosophila* (Lin et al., 2013; Wolff et al., 2015). In terms of connectivity, the ventral shell might be homologous to the monarch butterfly's dorsal LAL and the upper division of the LAL in *Bombyx* and *Drosophila*. The lobula complex also supplies biased inputs to the LAL (Supplementary Figure 6) and the same morphological feature is observed in *Drosophila* (Namiki et al., 2014). The projection of a population of dopaminergic PPM3 neurons in *Drosophila* seems to be biased toward the lateral side of the LAL (Nässel and Elekes, 1992; Ueno et al., 2012; Alekseyenko et al., 2013).

The dendritic innervation of LAL DNs is biased to the lower division (Supplementary Figure 7, right). For example, group-IA DN has small dendritic field in the upper division and much more innervation in the lower division, and Group-IID DN shows almost no innervation to the upper division (Supplementary Figure 7, left). Overall, the relative volume of innervations in the lower division is significantly more than those in the upper division (Namiki et al., 2014).

Putative homologous neurons of *Bombyx* group-I DNs in *Drosophila* show similar features (VGlut-F-500726, VGlut-F-000150; FlyCircuit Database; Chiang et al., 2011). Their neurite innervations within the LAL are more toward the medial side of the IDFP. This morphological feature seems to be obvious in other LAL DNs such as the MDN, which controls walking direction (Bidaye et al., 2014).

From these anatomical observations, we propose the modular organization of the LAL is common across insects. The upper division integrates the information from multiple protocerebral regions in addition to the CX, while the lower division produces the premotor signal output via DNs (**Figure 9**).

CONCLUSION

We reviewed the neuronal components of the LAL in the silkmoth and described the neurons with similar morphology in *Drosophila* and other insects. There are plentiful examples for their potential homology at the level of individual neurons, suggesting the presence of a ground pattern organization. Insects adapt to various environments in different ways, but the same basic design of the nervous system may underlie diverse behavioral repertoire. Expanding the application of a comparative neurobiological approach provides a powerful clue to explore these mechanisms.

AUTHOR CONTRIBUTIONS

All authors listed, have made substantial, direct, and intellectual contribution to the work, and approved it for publication.

ACKNOWLEDGMENTS

We are grateful to Chika Iwatsuki, Ryota Fukushima, Satoshi Iwabuchi, Poonsup Pansopha Kono, Masaaki Iwano, Evan Hill for their technical assistance, the reviewers for their comments which improved the manuscript. We are grateful to the FlyCircuit database from the NCHC (National Center for High-performance Computing) and NTHU (National Tsing Hua University). This work is supported by JSPS KAKENHI Grant Number 15H04399 to RK.

SUPPLEMENTARY MATERIAL

The Supplementary Material for this article can be found online at: http://journal.frontiersin.org/article/10.3389/fphys.2016.00244

REFERENCES

Alekseyenko, O. V., Chan, Y. B., Li, R., and Kravitz, E. A. (2013). Single dopaminergic neurons that modulate aggression in *Drosophila*. *Proc. Natl. Acad. Sci. U.S.A.* 110, 6151–6156. doi: 10.1073/pnas.1303446110

Ando, N., Emoto, S., and Kanzaki, R. (2013). Odour-tracking capability of a silkmoth driving a mobile robot with turning bias and time delay. *Bioinspir. Biomim.* 8:016008. doi: 10.1088/1748-3182/8/1/016008

Aso, Y., Hattori, D., Yu, Y., Johnston, R. M., Iyer, N. A., Ngo, T.-T. B., et al. (2014). The neuronal architecture of the mushroom body provides a logic for associative learning. *Elife* 3:e04577. doi: 10.7554/eLife.04577

Bicker, G., and Pearson, K. G. (1983). Initiation of flight by an identified wind sensitive neurone (TCG) in the locust. *J. Exp. Biol.* 104, 289–293.

Bidaye, S. S., Machacek, C., Wu, Y., and Dickson, B. J. (2014). Neuronal control of *Drosophila* walking direction. *Science* 344, 97–101. doi: 10.1126/science.1249964

Böhm, H., and Schildberger, K. (1992). Brain neurones involved in the control of walking in the cricket *Gryllus bimaculatus*. *J. Exp. Biol.* 166, 113–130.

Borst, A. (2014). Fly visual course control: behaviour, algorithms and circuits. *Nat. Rev. Neurosci.* 15, 590–599. doi: 10.1038/nrn3799

Boyan, G. S., and Reichert, H. (2011). Mechanisms for complexity in the brain: generating the insect central complex. *Trends Neurosci.* 34, 247–257. doi: 10.1016/j.tins.2011.02.002

Breidbach, O. (1990). Serotonin-immunoreactive brain interneurons persist during metamorphosis of an insect: a developmental study of the brain of *Tenebrio molitor* L. *(Coleoptera). Cell Tissue Res.* 259, 345–360. doi: 10.1007/BF00318458

Cardona, A., Larsen, C., and Hartenstein, V. (2009). Neuronal fiber tracts connecting the brain and ventral nerve cord of the early *Drosophila* larva. *J. Comp. Neurol.* 515, 427–440. doi: 10.1002/cne.22086

Cardona, A., Saalfeld, S., Preibisch, S., Schmid, B., Cheng, A., Pulokas, J., et al. (2010). An integrated micro- and macroarchitectural analysis of the *Drosophila* brain by computer-assisted serial section electron microscopy. *PLoS Biol.* 8:e1000502. doi: 10.1371/journal.pbio.1000502

Chen, C. C., Wu, J. K., Lin, H. W., Pai, T. P., Fu, T. F., Wu, C. L., et al. (2012). Visualizing long-term memory formation in two neurons of the *Drosophila* brain. *Science* 335, 678–685. doi: 10.1126/science.1212735

Chiang, A. S., Lin, C. Y., Chuang, C. C., Chang, H. M., Hsieh, C. H., Yeh, C. W., et al. (2011). Three-dimensional reconstruction of brain-wide wiring networks in *Drosophila* at single-cell resolution. *Curr. Biol.* 21, 1–11. doi: 10.1016/j.cub.2010.11.056

Costa, M., Ostrovsky, A. D., Manton, J. D., Prohaska, S., and Jefferis, G. S. X. E. (2014). NBLAST: Rapid, sensitive comparison of neuronal structure and construction of neuron family databases. *bioRxiv* 006346. doi: 10.1101/006346. Available online at: http://www.biorxiv.org/content/early/2014/08/09/006346

Costa, M., Reeve, S., Grumbling, G., and Osumi-Sutherland, D. (2013). The *Drosophila* anatomy ontology. *J. Biomed. Semantics* 4:32. doi: 10.1186/2041-1480-4-32

Dacks, A. M., Christensen, T. A., and Hildebrand, J. G. (2006). Phylogeny of a serotonin-immunoreactive neuron in the primary olfactory center of the insect brain. *J. Comp. Neurol.* 498, 727–746. doi: 10.1002/cne.21076

el Jundi, B., Huetteroth, W., Kurylas, A. E., and Schachtner, J. (2009). Anisometric brain dimorphism revisited: implementation of a volumetric 3D standard brain in *Manduca sexta*. *J. Comp. Neurol.* 517, 210–225. doi: 10.1002/cne.22150

el Jundi, B., Pfeiffer, K., Heinze, S., and Homberg, U. (2014). Integration of polarization and chromatic cues in the insect sky compass. *J. Comp. Physiol. A Neuroethol. Sens. Neural Behav. Physiol.* 200, 575–589. doi: 10.1007/s00359-014-0890-6

el Jundi, B., Warrant, E. J., Byrne, M. J., Khaldy, L., Baird, E., Smolka, J., et al. (2015). Neural coding underlying the cue preference for celestial orientation. *Proc. Natl. Acad. Sci. U.S.A.* 112, 11395–11400. doi: 10.1073/pnas.1501272112

Galizia, C. G., and Rössler, W. (2010). Parallel olfactory systems in insects: anatomy and function. *Annu. Rev. Entomol.* 55, 399–420. doi: 10.1146/annurev-ento-112408-085442

Graham, D., and Epstein, S. (1985). Behaviour and motor output for an insect walking on a slippery surface: II. backward walking. *J. Exp. Biol.* 118, 287–296.

Hampel, S., Franconville, R., Simpson, J. H., and Seeds, A. M. (2015). A neural command circuit for grooming movement control. *Elife* 4:e08758. doi: 10.7554/eLife.08758

Hanesch, U., Fischbach, K. F., and Heisenberg, M. (1989). Neuronal architecture of the central complex in *Drosophila melanogaster*. *Cell Tissue Res.* 257, 343–366. doi: 10.1007/BF00261838

Harley, C. M., and Ritzmann, R. E. (2010). Electrolytic lesions within central complex neuropils of the cockroach brain affect negotiation of barriers. *J. Exp. Biol.* 213, 2851–2864. doi: 10.1242/jeb.042499

Hedwig, B., and Heinrich, R. (1997). Identified descending brain neurons control different stridulatory motor patterns in an acridid grasshopper. *J. Comp. Physiol. A Sens. Neural Behav. Physiol.* 180, 285–294. doi: 10.1007/s003590050048

Heinze, S. (2014). "Polarized-light processing in insect brains: recent insights from the desert locust, the monarch butterfly, the cricket, and the fruit fly," in *Polarized Light and Polarization Vision in Animal Sciences*, ed G. Horváth (Berlin; Heidelberg: Springer), 61–111.

Heinze, S., Florman, J., Asokaraj, S., el Jundi, B., and Reppert, S. M. (2013). Anatomical basis of sun compass navigation II: the neuronal composition of the central complex of the monarch butterfly. *J. Comp. Neurol.* 521, 267–298. doi: 10.1002/cne.23214

Heinze, S., and Homberg, U. (2007). Maplike representation of celestial E-vector orientations in the brain of an insect. *Science* 315, 995–997. doi: 10.1126/science.1135531

Heinze, S., and Homberg, U. (2008). Neuroarchitecture of the central complex of the desert locust: intrinsic and columnar neurons. *J. Comp. Neurol.* 511, 454–478. doi: 10.1002/cne.21842

Heinze, S., and Homberg, U. (2009). Linking the input to the output: new sets of neurons complement the polarization vision network in the locust central complex. *J. Neurosci.* 29, 4911–4921. doi: 10.1523/JNEUROSCI.0332-09.2009

Heinze, S., and Reppert, S. M. (2011). Sun compass integration of skylight cues in migratory monarch butterflies. *Neuron* 69, 345–358. doi: 10.1016/j.neuron.2010.12.025

Heinze, S., and Reppert, S. M. (2012). Anatomical basis of sun compass navigation I: the general layout of the monarch butterfly brain. *J. Comp. Neurol.* 520, 1599–1628. doi: 10.1002/cne.23054

Hengstenberg, R., Hausen, K., and Hengstenberg, B. (1982). The number and structure of giant vertical cells (VS) in the lobula plate of the blowfly *Calliphora erythrocephala*. *J. Comp. Physiol. A* 149, 163–177. doi: 10.1007/BF00619211

Hensler, K. (1988). The pars intercerebralis neurone PI(2)5 of locusts: convergent processing of inputs reporting head movements and deviations from straight flight. *J. Exp. Biol.* 140, 511–533.

Hensler, K., and Rowell, H. F. (1990). Control of optomotor responses by descending deviation detector neurones in intact flying locusts. *J. Exp. Biol.* 149, 191–205.

Homberg, U. (1985). Interneurones of the central complex in the bee brain (*Apis mellifera*, L.). *J. Insect Physiol.* 31, 251–264. doi: 10.1016/0022-1910(85)90127-1

Homberg, U. (1994). Flight-correlated activity changes in neurons of the lateral accessory lobes in the brain of the locust *Schistocerca gregaria*. *J. Comp. Physiol. A* 175, 597–610. doi: 10.1007/BF00199481

Homberg, U., Heinze, S., Pfeiffer, K., Kinoshita, M., and el Jundi, B. (2011). Central neural coding of sky polarization in insects. *Philos. Trans. R. Soc. Lond. B Biol. Sci.* 366, 680–687. doi: 10.1098/rstb.2010.0199

Homberg, U., and Hildebrand, J. G. (1989). Serotonin-immunoreactive neurons in the median protocerebrum and suboesophageal ganglion of the sphinx moth *Manduca sexta*. *Cell Tissue Res.* 258, 1–24. doi: 10.1007/BF00223139

Homberg, U., and Hildebrand, J. G. (1991). Histamine-immunoreactive neurons in the midbrain and suboesophageal ganglion of the sphinx moth *Manduca sexta*. *J. Comp. Neurol.* 307, 647–657. doi: 10.1002/cne.903070410

Homberg, U., Hofer, S., Pfeiffer, K., and Gebhardt, S. (2003). Organization and neural connections of the anterior optic tubercle in the brain of the locust, *Schistocerca gregaria*. *J. Comp. Neurol.* 462, 415–430. doi: 10.1002/cne.10771

Homberg, U., Kingan, T. G., and Hildebrand, J. G. (1987). Immunocytochemistry of GABA in the brain and suboesophageal ganglion of *Manduca sexta*. *Cell Tissue Res.* 248, 1–24. doi: 10.1007/BF01239957

Hsu, C. T., and Bhandawat, V. (2016). Organization of descending neurons in *Drosophila melanogaster*. *Sci. Rep.* 6:20259. doi: 10.1038/srep20259

Ignell, R., Dekker, T., Ghaninia, M., and Hansson, B. S. (2005). Neuronal architecture of the mosquito deutocerebrum. *J. Comp. Neurol.* 493, 207–240. doi: 10.1002/cne.20800

Ito, K., Shinomiya, K., Ito, M., Armstrong, J. D., Boyan, G., Hartenstein, V., et al. (2014). A systematic nomenclature for the insect brain. *Neuron* 81, 755–765. doi: 10.1016/j.neuron.2013.12.017

Ito, K., Suzuki, K., Estes, P., Ramaswami, M., Yamamoto, D., and Strausfeld, N. J. (1998). The organization of extrinsic neurons and their implications in the functional roles of the mushroom bodies in *Drosophila melanogaster* Meigen. *Learn. Mem.* 5, 52–77.

Ito, M., Masuda, N., Shinomiya, K., Endo, K., and Ito, K. (2013). Systematic analysis of neural projections reveals clonal composition of the *Drosophila* brain. *Curr. Biol.* 23, 644–655. doi: 10.1016/j.cub.2013.03.015

Iwano, M., Hill, E. S., Mori, A., Mishima, T., Mishima, T., Ito, K., et al. (2010). Neurons associated with the flip-flop activity in the lateral accessory lobe and ventral protocerebrum of the silkworm moth brain. *J. Comp. Neurol.* 518, 366–388. doi: 10.1002/cne.22224

Jenett, A., Rubin, G. M., Ngo, T. T., Shepherd, D., Murphy, C., Dionne, H., et al. (2012). A GAL4-driver line resource for *Drosophila* neurobiology. *Cell Rep.* 2, 991–1001. doi: 10.1016/j.celrep.2012.09.011

Kagaya, K., and Takahata, M. (2011). Sequential synaptic excitation and inhibition shape readiness discharge for voluntary behavior. *Science* 332, 365–368. doi: 10.1126/science.1202244

Kanzaki, R. (1997). "Pheromone processing in the lateral accessory lobes of the moth brain: flip-flopping signals related to zigzagging upwind walking," in *Insect Pheromone Research, New Directions*, eds R. T. Cardé and A. K. Minks (New York, NY: Chapman & Hall), 291–303. Available online at: http://www.springer.com/us/book/9780412996115

Kanzaki, R., Arbas, E. A., and Hildebrand, J. G. (1991a). Physiology and morphology of descending neurons in pheromone-processing olfactory pathways in the male moth *Manduca sexta*. *J. Comp. Physiol. A* 169, 1–14. doi: 10.1007/BF00198168

Kanzaki, R., Arbas, E. A., and Hildebrand, J. G. (1991b). Physiology and morphology of protocerebral olfactory neurons in the male moth *Manduca sexta*. *J. Comp. Physiol. A* 168, 281–298. doi: 10.1007/BF00198348

Kanzaki, R., Ikeda, A., and Shibuya, T. (1994). Morphological and physiological properties of pheromone-triggered flipflopping descending interneurons of the male silkworm moth, *Bombyx mori*. *J. Comp. Physiol. A Sens. Neural Behav. Physiol.* 175, 1–14. doi: 10.1007/BF00217431

Kohatsu, S., Koganezawa, M., and Yamamoto, D. (2011). Female contact activates male-specific interneurons that trigger stereotypic courtship behavior in *Drosophila*. *Neuron* 69, 498–508. doi: 10.1016/j.neuron.2010.12.017

Lei, H., Anton, S., and Hansson, B. S. (2001). Olfactory protocerebral pathways processing sex pheromone and plant odor information in the male moth *Agrotis segetum*. *J. Comp. Neurol.* 432, 356–370. doi: 10.1002/cne.1108

Li, W., Pan, Y., Wang, Z., Gong, H., Gong, Z., and Liu, L. (2009). Morphological characterization of single fan-shaped body neurons in *Drosophila melanogaster*. *Cell Tissue Res.* 336, 509–519. doi: 10.1007/s00441-009-0781-2

Lin, C. Y., Chuang, C. C., Hua, T. E., Chen, C. C., Dickson, B. J., Greenspan, R. J., et al. (2013). A comprehensive wiring diagram of the protocerebral bridge for visual information processing in the *Drosophila* brain. *Cell Rep.* 3, 1739–1753. doi: 10.1016/j.celrep.2013.04.022

Liu, G., Seiler, H., Wen, A., Zars, T., Ito, K., Wolf, R., et al. (2006). Distinct memory traces for two visual features in the *Drosophila* brain. *Nature* 439, 551–556. doi: 10.1038/nature04381

Martin, J. P., Guo, P., Mu, L., Harley, C. M., and Ritzmann, R. E. (2015). Central-complex control of movement in the freely walking cockroach. *Curr. Biol.* 25, 2795–2803. doi: 10.1016/j.cub.2015.09.044

Milde, J. J., and Strausfeld, N. J. (1990). Cluster organization and response characteristics of the giant fiber pathway of the blowfly *Calliphora erythrocephala*. *J. Comp. Neurol.* 294, 59–75. doi: 10.1002/cne.902940106

Milyaev, N., Osumi-Sutherland, D., Reeve, S., Burton, N., Baldock, R. A., and Armstrong, J. D. (2012). The virtual fly brain browser and query interface. *Bioinformatics* 28, 411–415. doi: 10.1093/bioinformatics/btr677

Mishima, T., and Kanzaki, R. (1999). Physiological and morphological characterization of olfactory descending interneurons of the male silkworm moth, *Bombyx mori*. *J. Comp. Physiol. A Sens. Neural Behav. Physiol.* 184, 143–160. doi: 10.1007/s003590050314

Montgomery, S. H., and Ott, S. R. (2015). Brain composition in *Godyris zavaleta*, a diurnal butterfly, reflects an increased reliance on olfactory information. *J. Comp. Neurol.* 523, 869–891. doi: 10.1002/cne.23711

Mota, T., Yamagata, N., Giurfa, M., Gronenberg, W., and Sandoz, J. C. (2011). Neural organization and visual processing in the anterior optic tubercle of the honeybee brain. *J. Neurosci.* 31, 11443–11456. doi: 10.1523/JNEUROSCI.0995-11.2011

Müller, M., Homberg, U., and Kühn, A. (1997). Neuroarchitecture of the lower division of the central body in the brain of the locust (*Schistocerca gregaria*). *Cell Tissue Res.* 288, 159–176. doi: 10.1007/s004410050803

Namiki, S., Iwabuchi, S., Pansopha Kono, P., and Kanzaki, R. (2014). Information flow through neural circuits for pheromone orientation. *Nat. Commun.* 5:5919. doi: 10.1038/ncomms6919

Namiki, S., Takaguchi, M., Seki, Y., Kazawa, T., Fukushima, R., Iwatsuki, C., et al. (2013). Concentric zones for pheromone components in the mushroom body calyx of the moth brain. *J. Comp. Neurol.* 521, 1073–1092. doi: 10.1002/cne.23219

Nässel, D. R., and Elekes, K. (1992). Aminergic neurons in the brain of blowflies and *Drosophila*: dopamine-and tyrosine hydroxylase-immunoreactive neurons and their relationship with putative histaminergic neurons. *Cell Tissue Res.* 267, 147–167. doi: 10.1007/BF00318701

Neuser, K., Triphan, T., Mronz, M., Poeck, B., and Strauss, R. (2008). Analysis of a spatial orientation memory in *Drosophila*. *Nature* 453, 1244–1247. doi: 10.1038/nature07003

Ofstad, T. A., Zuker, C. S., and Reiser, M. B. (2011). Visual place learning in *Drosophila melanogaster*. *Nature* 474, 204–207. doi: 10.1038/nature10131

Okada, R., Sakura, M., and Mizunami, M. (2003). Distribution of dendrites of descending neurons and its implications for the basic organization of the cockroach brain. *J. Comp. Neurol.* 458, 158–174. doi: 10.1002/cne.10580

Olberg, R. (1983). Pheromone-triggered flip-flopping interneurons in the ventral nerve cord of the silkworm moth, *Bombyx mori*. *J. Comp. Physiol. A* 152, 297–307. doi: 10.1007/BF00606236

Olberg, R. M. (1986). Identified target-selective visual interneurons descending from the dragonfly brain. *J. Comp. Physiol. A* 159, 827–840. doi: 10.1007/BF00603736

Pansopha, P., Ando, N., and Kanzaki, R. (2014). Dynamic use of optic flow during pheromone tracking by the male silkmoth, *Bombyx mori*. *J. Exp. Biol.* 217, 1811–1820. doi: 10.1242/jeb.090266

Paulk, A. C., Dacks, A. M., Phillips-Portillo, J., Fellous, J. M., and Gronenberg, W. (2009). Visual processing in the central bee brain. *J. Neurosci.* 29, 9987–9999. doi: 10.1523/JNEUROSCI.1325-09.2009

Pfeiffer, K., and Kinoshita, M. (2012). Segregation of visual inputs from different regions of the compound eye in two parallel pathways through the anterior optic tubercle of the bumblebee (*Bombus ignitus*). *J. Comp. Neurol.* 520, 212–229. doi: 10.1002/cne.22776

Pfuhl, G., and Berg, G. (2007). "Morphological and functional characterisation of the lateral accessory lobe in moth," in *The 8th Congress of the International Society for Neuroethology* (Vancouver, BC).

Pfuhl, G., Zhao, X.-C., Ian, E., Surlykke, A., and Berg, B. G. (2013). Sound-sensitive neurons innervate the ventro-lateral protocerebrum of the heliothine moth brain. *Cell Tissue Res.* 355, 289–302. doi: 10.1007/s00441-013-1749-9

Phillips-Portillo, J., and Strausfeld, N. J. (2012). Representation of the brain's superior protocerebrum of the flesh fly, *Neobellieria bullata*, in the central body. *J. Comp. Neurol.* 520, 3070–3087. doi: 10.1002/cne.23094

Richter, S., Loesel, R., Purschke, G., Schmidt-Rhaesa, A., Scholtz, G., Stach, T., et al. (2010). Invertebrate neurophylogeny: suggested terms and definitions for a neuroanatomical glossary. *Front. Zool.* 7:29. doi: 10.1186/1742-9994-7-29

Schildberger, K. (1983). Local interneurons associated with the mushroom bodies and the central body in the brain of *Acheta domesticus*. *Cell Tissue Res.* 230, 573–586. doi: 10.1007/BF00216202

Schmitt, F., Stieb, S. M., Wehner, R., and Rössler, W. (2015). Experience-related reorganization of giant synapses in the lateral complex: potential role in plasticity of the sky-compass pathway in the desert ant *Cataglyphis fortis*. *Dev. Neurobiol.* 76, 390–404. doi: 10.1002/dneu.22322

Seelig, J. D., and Jayaraman, V. (2013). Feature detection and orientation tuning in the *Drosophila* central complex. *Nature* 503, 262–266. doi: 10.1038/nature12601

Seelig, J. D., and Jayaraman, V. (2015). Neural dynamics for landmark orientation and angular path integration. *Nature* 521, 186–191. doi: 10.1038/nature 14446

Shih, C. T., Sporns, O., Yuan, S. L., Su, T. S., Lin, Y. J., Chuang, C. C., et al. (2015). Connectomics-based analysis of information flow in the *Drosophila* brain. *Curr. Biol.* 25, 1249–1258. doi: 10.1016/j.cub.2015.03.021

Staudacher, E. (1998). Distribution and morphology of descending brain neurons in the cricket *Gryllus bimaculatus*. *Cell Tissue Res.* 294, 187–202. doi: 10.1007/s004410051169

Staudacher, E. M. (2001). Sensory responses of descending brain neurons in the walking cricket, *Gryllus bimaculatus*. *J. Comp. Physiol. A* 187, 1–17. doi: 10.1007/s003590000171

Strausfeld, N. J. (1976). *Atlas of an Insect Brain*. Berlin: Springer.

Strausfeld, N. J., and Bassemir, U. K. (1985). Lobula plate and ocellar interneurons converge onto a cluster of descending neurons leading to neck and leg motor neuropil in *Calliphora erythrocephala*. *Cell Tissue Res.* 240, 617–640. doi: 10.1007/BF00216351

Strausfeld, N. J., Bassemir, U., Singh, R. N., and Bacon, J. P. (1984). Organizational principles of outputs from Dipteran brains. *J. Insect Physiol.* 30, 73–93. doi: 10.1016/0022-1910(84)90109-4

Strausfeld, N. J., Hansen, L., Li, Y., Gomez, R. S., and Ito, K. (1998). Evolution, discovery, and interpretations of arthropod mushroom bodies. *Learn. Mem.* 5, 11–37.

Strausfeld, N. J., and Hirth, F. (2013). Deep homology of arthropod central complex and vertebrate basal ganglia. *Science* 340, 157–161. doi: 10.1126/science.1231828

Strausfeld, N. J., and Li, Y. (1999). Organization of olfactory and multimodal afferent neurons supplying the calyx and pedunculus of the cockroach mushroom bodies. *J. Comp. Neurol.* 409, 603–625.

Träger, U., and Homberg, U. (2011). Polarization-sensitive descending neurons in the locust: connecting the brain to thoracic ganglia. *J. Neurosci.* 31, 2238–2247. doi: 10.1523/JNEUROSCI.3624-10.2011

Träger, U., Wagner, R., Bausenwein, B., and Homberg, U. (2008). A novel type of microglomerular synaptic complex in the polarization vision pathway of the locust brain. *J. Comp. Neurol.* 506, 288–300. doi: 10.1002/cne.21512

Tschida, K., and Bhandawat, V. (2015). Activity in descending dopaminergic neurons represents but is not required for leg movements in the fruit fly *Drosophila*. *Physiol. Rep.* 3:e12322. doi: 10.14814/phy2.12322

Ueno, T., Tomita, J., Tanimoto, H., Endo, K., Ito, K., Kume, S., et al. (2012). Identification of a dopamine pathway that regulates sleep and arousal in *Drosophila*. *Nat. Neurosci.* 15, 1516–1523. doi: 10.1038/nn.3238

Vitzthum, H., Muller, M., and Homberg, U. (2002). Neurons of the central complex of the locust *Schistocerca gregaria* are sensitive to polarized light. *J. Neurosci.* 22, 1114–1125. Available online at: http://www.jneurosci.org/cgi/pmidlookup?view=long&pmid=11826140

von Philipsborn, A. C., Liu, T., Yu, J. Y., Masser, C., Bidaye, S. S., and Dickson, B. J. (2011). Neuronal control of *Drosophila* courtship song. *Neuron* 69, 509–522. doi: 10.1016/j.neuron.2011.01.011

von Reyn, C. R., Breads, P., Peek, M. Y., Zheng, G. Z., Williamson, W. R., Yee, A. L., et al. (2014). A spike-timing mechanism for action selection. *Nat. Neurosci.* 17, 962–970. doi: 10.1038/nn.3741

Wada, S., and Kanzaki, R. (2005). Neural control mechanisms of the pheromone-triggered programmed behavior in male silkmoths revealed by double-labeling of descending interneurons and a motor neuron. *J. Comp. Neurol.* 484, 168–182. doi: 10.1002/cne.20452

Wegerhoff, R., Breidbach, O., and Lobemeier, M. (1996). Development of locustatachykinin immunopositive neurons in the central complex of the beetle *Tenebrio molitor*. *J. Comp. Neurol.* 375, 157–166.

Williams, J. L. D. (1975). Anatomical studies of the insect central nervous system: A ground-plan of the midbrain and an introduction to the central complex in the locust, *Schistocerca gregaria* (Orthoptera). *J. Zool.* 176, 67–86. doi: 10.1111/j.1469-7998.1975.tb03188.x

Wolff, G. H., and Strausfeld, N. J. (2015). "The insect brain: a commentated primer," in *Structure and Evolution of Invertebrate Nervous Systems*, eds A. Schmidt-Rhaesa, S. Harzsch, and G. Purschke (Oxford: Oxford University Press), 597–639. doi: 10.1093/acprof:oso/9780199682201.001.0001

Wolff, T., Iyer, N. A., and Rubin, G. M. (2015). Neuroarchitecture and neuroanatomy of the *Drosophila* central complex: a GAL4-based dissection of protocerebral bridge neurons and circuits. *J. Comp. Neurol.* 523, 997–1037. doi: 10.1002/cne.23705

Yamagata, N., Nishino, H., and Mizunami, M. (2007). Neural pathways for the processing of alarm pheromone in the ant brain. *J. Comp. Neurol.* 505, 424–442. doi: 10.1002/cne.21500

Yang, J. S., Awasaki, T., Yu, H. H., He, Y., Ding, P., Kao, J. C., et al. (2013). Diverse neuronal lineages make stereotyped contributions to the *Drosophila* locomotor control center, the central complex. *J. Comp. Neurol.* 521, 2645–2662. doi: 10.1002/cne.23339

Yu, J. Y., Kanai, M. I., Demir, E., Jefferis, G. S. X. E., and Dickson, B. J. (2010). Cellular organization of the neural circuit that drives *Drosophila* courtship behavior. *Curr. Biol.* 20, 1602–1614. doi: 10.1016/j.cub.2010.08.025

Zorović, M., and Hedwig, B. (2011). Processing of species-specific auditory patterns in the cricket brain by ascending, local, and descending neurons during standing and walking. *J. Neurophysiol.* 105, 2181–2194. doi: 10.1152/jn.00416.2010

Zorović, M., and Hedwig, B. (2013). Descending brain neurons in the cricket *Gryllus bimaculatus* (de Geer): auditory responses and impact on walking. *J. Comp. Physiol. A Neuroethol. Sens. Neural Behav. Physiol.* 199, 25–34. doi: 10.1007/s00359-012-0765-7

Conflict of Interest Statement: The authors declare that the research was conducted in the absence of any commercial or financial relationships that could be construed as a potential conflict of interest.

frontiers in Physiology

REVIEW
published: 12 August 2015
doi: 10.3389/fphys.2015.00229

The neural bases of host plant selection in a Neuroecology framework

Carolina E. Reisenman[1]* *and Jeffrey A. Riffell*[2]

[1] Department of Molecular and Cell Biology, University of California, Berkeley, CA, USA, [2] Department of Biology, University of Washington, Seattle, WA, USA

Understanding how animals make use of environmental information to guide behavior is a fundamental problem in the field of neuroscience. Similarly, the field of ecology seeks to understand the role of behavior in shaping interactions between organisms at various levels of organization, including population-, community- and even ecosystem-level scales. Together, the newly emerged field of "Neuroecology" seeks to unravel this fundamental question by studying both the function of neurons at many levels of the sensory pathway and the interactions between organisms and their natural environment. The interactions between herbivorous insects and their host plants are ideal examples of Neuroecology given the strong ecological and evolutionary forces and the underlying physiological and behavioral mechanisms that shaped these interactions. In this review we focus on an exemplary herbivorous insect within the Lepidoptera, the giant sphinx moth *Manduca sexta*, as much is known about the natural behaviors related to host plant selection and the involved neurons at several level of the sensory pathway. We also discuss how herbivore-induced plant odorants and secondary metabolites in floral nectar in turn can affect moth behavior, and the underlying neural mechanisms.

Keywords: Neuroecology, insect olfaction, oviposition, moths, neurons

OPEN ACCESS

Edited by:
Sylvia Anton, Institut National de la Recherche Agronomique, France

Reviewed by:
Zainulabeuddin Syed, University of Notre Dame, USA
Marcus Carl Stensmyr, Lund University, Sweden

***Correspondence:**
Carolina E. Reisenman, Department of Molecular and Cell Biology, University of California, Berkeley, 16 Barker Hall # 3204, Berkeley, CA 94720-3204, USA
creisenman@berkeley.edu

Specialty section:
This article was submitted to Invertebrate Physiology, a section of the journal Frontiers in Physiology

Received: *10 June 2015*
Accepted: *28 July 2015*
Published: *12 August 2015*

Citation:
Reisenman CE and Riffell JA (2015) The neural bases of host plant selection in a Neuroecology framework. Front. Physiol. 6:229. doi: 10.3389/fphys.2015.00229

Herbivory and Host Specialization

Herbivory is a major evolutionary achievement in eukaryotic animals and in particular in insects, with nearly half of all existing species feeding on living plants (Gilbert, 1979). Lepidoptera (moths and butterflies) are the largest lineage of plant-feeding organisms, and their evolution is intimately related to the radiation of angiosperms in the Cretaceous (Grimaldi and Engel, 2005). The other large groups of phytophagous insects are found among the Coleoptera and include weevils, leaf beetles, and the long-horned beetles (Grimaldi and Engel, 2005).

The evolutionary processes that cause the diversification of herbivorous insects are not completely understood but host–plant interactions, and in particular plant chemistry, are thought to be a critical factor (Ehrlich and Raven, 1964; Jaenike, 1990; Whiteman and Jander, 2010). Plant volatiles contribute to sympatric speciation and reproductive isolation involving host plant shifts, such as those observed in races of the larch bud moth *Zyraphera diniana* having different host preferences (Emelianov et al., 2003; Syed et al., 2003), and in the apple maggot *Rhagoletis pomonella* (Linn et al., 2003; Olsson et al., 2006). Changes in host plant preferences can occur very fast, particularly in cases in which few genes participate in mediating host plant selections (Linn et al., 2003; Schoonhoven et al., 2005). However, for divergent plants that have converged on a similar

chemical profile, the similarity can facilitate exploitation by related herbivores—an example of this occurs in checkerspot butterfly larvae *Euphydryas chalcedona*, which are stimulated by host plants that have iridoid glycosylates (Bowers, 1983).

While many herbivorous insects feed in many plant species, most herbivorous are specialists, with larvae feeding and adults ovipositing on a small number of closely related plant species, usually within the same family (Jaenike, 1990). Transitions from a generalist lifestyle to specialization are common, and it has been suggested that they resulted from genetically based trade-offs in offspring performance (Jaenike, 1990). Many morphological and physiological adaptations accompany host plant specialization, including detoxification mechanisms against plant defenses and sensory specializations for the detection of host-derived chemical (olfactory and taste) cues (Schoonhoven et al., 2005). In particular, the importance of the chemosensory system in host plant choice, along with the fact that specialists outnumber generalists, suggests that the evolution of insect–plant interactions is based on changes within the insect nervous system (Olsson et al., 2006), with such changes occurring before host plant shifts (e.g., Dekker et al., 2006; Lavista-Llanos et al., 2014).

In this review we focus on the neural mechanisms underlying host plant selection by moths in a "Neuroecological" context, that is, the function of neurons in an adaptive biologically relevant framework. Almost all of what we review here draws from studies in the exemplary giant sphinx moth *Manduca sexta* (Spinghidae, Lepidoptera), as we know much about both the anatomical and functional organization of its chemosensory system and about the olfactory cues that guide host finding in this crepuscular/nocturnal insect.

Host Plants Chemical Signals

Olfactory signals play decisive roles in the lives of adult moths, including *M. sexta*. Both sexes of this nocturnally active insect must find flowers on which to feed, males must find females, and gravid females must find the proper host plants on which to lay their eggs. A particularly well characterized olfactory-guided behavior of adult *M. sexta* (as well as of many other moth species) is the oriented flight response of males to the sex-pheromone blend released by conspecific females (Baker, 1990; Willis and Arbas, 1991). Corresponding neurophysiological studies have shown that specialized male-specific neurons at several levels of the olfactory pathway faithfully encode the pheromone signal and control male behavior (Schneiderman et al., 1986; Christensen et al., 1996; Heinbockel et al., 1999, 2004; Lei et al., 2002; Dacks et al., 2007; Riffell et al., 2008a).

How the olfactory system process information about feeding and oviposition resources, in contrast, only recently begun to be understood. Both sexes feed on nectar from flowers, but gravid females require host plants also as oviposition sites (Madden and Chamberlin, 1945; Reisenman et al., 2010; **Figures 1A,B**). Thus, females need specialized receptors and neurons for detecting appropriate host plants for oviposition. Like many other hawkmoths, *M. sexta* adults pollinate large, tubular, night-blooming white or pale flowers (Sparks, 1969, 1973; Alarcón et al., 2008) which produce large quantities of volatile organic compounds (VOCs) (Raguso and Willis, 2002; Raguso et al., 2003). In the Southwestern USA, the sacred daturas or jimsonweeds, *D. wrightii* and *D. discolor*, attract *M. sexta* as pollinators and also function as host plants for their larvae (Mira and Bernays, 2002; **Figures 1A,B**). Their flowers provide rich nectar sources to foraging adults (Raguso and Willis, 2002) and bloom once over a single night, but a plant can produce >200 flowers in one season. Floral odors and visual signals, alone or in combination, are innately attractive to adults of both sexes (Raguso and Willis, 2002; Goyret, 2010; Kaczorowski et al., 2012; Riffell and Alarcón, 2013), but only the simultaneous presence of both signals elicits nectar feeding (Ramaswamy, 1988; Raguso et al., 2003).

The selection of appropriate host plants for oviposition by gravid moths is undoubtedly crucial for the success of her larval offspring. In contrast to feeding, female *M. sexta* rely primarily on olfactory cues to locate and identify host plants for oviposition (Sparks, 1973; Ramaswamy, 1988; Reisenman et al., 2010; Späthe et al., 2013). As other Lepidoptera (Renwick and Chew, 1994), female *M. sexta* may contact host plants with their tarsi prior to oviposition (Yamamoto et al., 1969; Sparks, 1973), but this behavior is not a requirement (Mechaber et al., 2002). In general, the contribution of taste to host plant selection is not completely understood, although highly specialized taste receptors are present in specialist herbivores. Once the host plant is located, taste receptors mediate a sequence of behavioral events leading to egg lying (Schoonhoven et al., 2005).

As many herbivores, *M. sexta* moths are highly specialized. Larvae feed almost exclusively (but see Mira and Bernays, 2002; Mechaber et al., 2002) on plants of the family Solanaceae [e.g., native jimsonweeds (*Datura* sp.), native and cultivated species of tobacco (*Nicotiana* sp.), tomato, eggplant, pepper, etc., (Madden and Chamberlin, 1945; Yamamoto and Fraenkel, 1960; Tichenor and Seigler, 1980; el Campo et al., 2001)]. Although both nectar and leaves of some of these plants contain alkaloids which are toxic for many other insect species, moths have detoxification mechanisms that allow them to deal with these secondary compounds (Glendinning, 2002; Adler et al., 2006; Hare and Walling, 2006). Though plant defensive compounds can be toxic to specialist herbivores at high (unnatural) concentrations, on average, specialist herbivores are less negatively impacted than generalists (Berenbaum et al., 1989; Cornell and Hawkins, 2003). Thus, both chemosensory specialization and tolerance to toxic components are both crucial components for insect host plant specialization and coevolution.

Herbivory and Host Plants: a Dynamically Changing Olfactory Environment

While specific olfactory cues from host plants are necessary for acceptance and egg laying by gravid females (Yamamoto and Fraenkel, 1960), the VOCs released by plants are not static, but are rather affected by the time of the day and other physiological and environmental factors (De Moraes et al., 2001). For instance, plants respond to herbivory with changes in plant chemistry and physiology that make them more resistant to further attack, such as the induction of toxic metabolites that

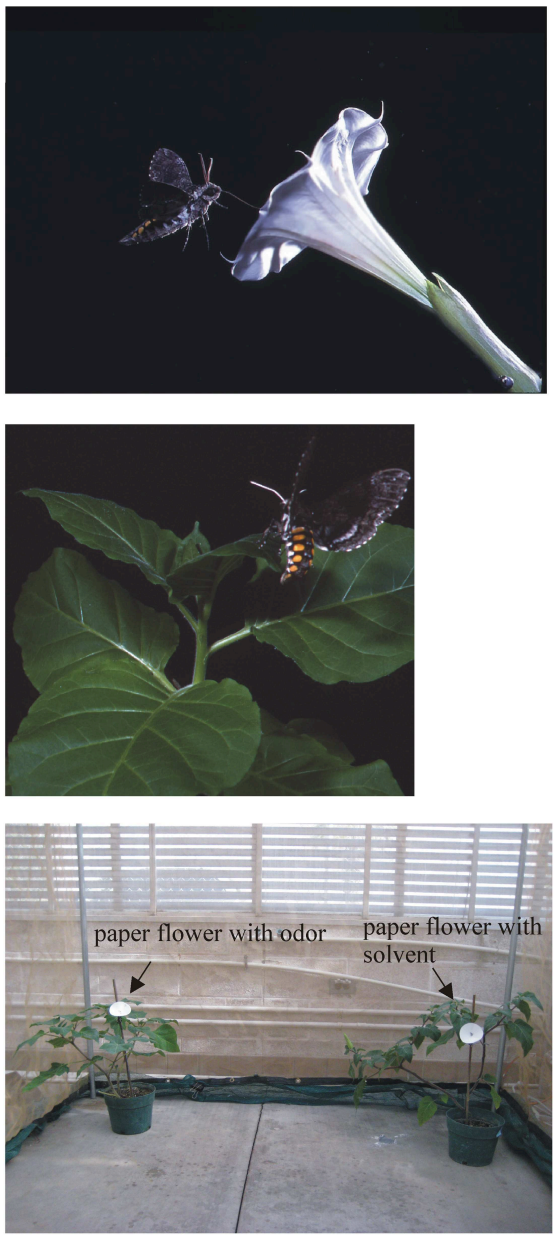

FIGURE 1 | (A) Adult *M. sexta* feeding on nectar from a flower from one of its favorite host plants, the jimsonweed *Datura wrightii*. **(B)** Females also use this plant as an oviposition resource (Picture by C. Hedgcock). **(C)** Experimental set-up used to study the oviposition behavior of females in the laboratory. Singly mated female are released in a flight cage in a dual-choice experiment. In this case, the insect is offered two plants, one with an artificial paper flower loaded with a synthetic odor (experimental) and the other loaded with the solvent (control).

can poison attacking herbivores or slow their growth (Karban and Baldwin, 1997; Baldwin and Preston, 1999). Plants also use indirect defenses, i.e., synthesize and release complex blends of VOCs that attract the natural enemies of the herbivores (De Moraes et al., 1998; Turlings et al., 1998; Baldwin and Preston, 1999; Paré and Tumlinson, 1999; Dicke and van Loop, 2000; Halitschke et al., 2000; Schnee et al., 2006). These VOCs, which include monoterpenes, sesquiterpenes, and aromatics (Paré and Tumlinson, 1999) are produced *de novo* (Paré and Tumlinson, 1997), systemically (De Moraes et al., 1998) and slowly (>24-h post-attack; Kessler and Baldwin, 2001), and are qualitatively different from the VOCs released by mechanically damaged plants (Paré and Tumlinson, 1999; Halitschke et al., 2000; De Moraes et al., 2001; Kessler and Baldwin, 2001; Reisenman et al., 2013). For instance, feeding by *M. sexta* larvae on *Nicotiana* sp. (tobacco) induces both direct and indirect defenses (Halitschke et al., 2000; De Moraes et al., 2001; Adler et al., 2006; McCall and Karban, 2006). In principle, a gravid female should avoid ovipositing in such induced plants, as they are likely to host insects that will compete with her offspring and also natural enemies attracted by the induced VOCs. Indeed, both *M. sexta* and *M. quinquemaculata* moths avoid ovipositing on larva-damaged plants (Kessler and Baldwin, 2001) in a plant-species specific manner (Reisenman et al., 2013; Späthe et al., 2013). Alternatively, as observed in other insect species, egg-lying by multiple females in nearby sites could reduce predation risk for each female's offspring (Jaenike, 1978). Also, in certain moth species, oviposition is deterred by VOCs emitted by larval frass (Anderson et al., 1992; Xu et al., 2006) and in *M. sexta* is affected by the presence of con-specific larvae (Reisenman et al., 2013).

Insect herbivores are agents of selection on plant defense traits because plant populations excluded from herbivory evolve lower resistance and higher competitive ability, but these populations can quickly regain increased resistance when re-exposed to the herbivore (Agrawal et al., 2012; Uesugi and Kessler, 2013; Sakata et al., 2014). Thus, moths will be experiencing a spatiotemporally changing landscape of suitable host plants, many of whom will vary in their induced chemical defenses, resources, and growth potential. For instance, induction of plant defense pathways in tomato or *Arabidopsis sp.* results in significant reduction in growth, physiological performance, and fitness (Cipollini, 2010; Corrado et al., 2011), all of which can indirectly affect the growth of the developing larvae. Moreover, this spatiotemporal complexity in the plant community—*via* induction of plant defenses—provide different kinds of information to the herbivore and the plant community: (1) for plants, it can reduce the probability of secondary attacks and provide host cues for the natural enemies of the herbivores, while providing information to and from neighboring plants; and (2) for the herbivore, it provides information about the suitability of the host plant with regards to its chemical defenses and its metabolic and physiological health.

The detection and decision-making ability of adult moths in response to the dynamic host plant chemical information is additionally affected when the host plants serve also as floral nectar resources. For instance, leaf herbivory can result in smaller flowers and fewer open flowers (Mothershead and Marquis, 2000; Adler et al., 2001), leading to lower amounts of floral VOC emissions and less pollinator visitation. Additionally, the biosynthetic pathways of inducible plant defenses can be constitutively expressed throughout the plant tissue. Thus, when damaged, there lies the potential that floral scent is modified (Heil and Ton, 2010). However, results from this hypothesis are mixed: in one study larvae damaged by *M. sexta* of sweet tobacco

(*Nicotiana suaveolens*) did not significantly increase floral volatile production (Effmert et al., 2008), while in wild tomato plants (*S. peruvianum*) damaged by the same herbivore the floral blend significantly differed from that of non-damaged plants (Kessler and Halitschke, 2009). For other plant families, induction of plant defenses appears to be systemic and flowers can either produce VOCs *de novo* in response to herbivory (Loughrin et al., 1994; Röse and Tumlinson, 2004) or decrease emissions altogether (Pareja et al., 2012). Thus, the interplay between pollinator attraction and host plant defense provides a unique system to identify the cues and associated sensory mechanisms by which plants manipulate their interaction with insects.

A Naturalistic Insect–plant Interaction

In contrast with older studies which use artificially selected crops grown in simple agro-ecosystems (Harvey et al., 2015), much work in the last decade focused on more naturalistic insect–plant interactions. For instance, a particularly interesting mutually beneficial association exists in the Sonoran Desert in Southwest USA between *M. sexta* and the jimsonweed *D. wrightii*: while flowers are pollinated by adults (Alarcón et al., 2008; Riffell et al., 2008b), the plants serve as food resources for the larvae (Mechaber and Hildebrand, 2000; **Figures 1A,B**). Detoxification mechanisms (Glendinning, 2002) enable larvae to cope with herbivory-induced toxic secondary compounds (Adler et al., 2006; Hare and Walling, 2006), and plants cope with the negative effects of herbivory by quickly recovering after larval damage (Reisenman et al., 2013). Importantly, plants benefit from this association because jimsonweeds set more fruit by cross-pollination (Nunez-Farfan et al., 1996; Raguso et al., 2003) and plants are not completely defoliated, as eggs and larvae suffer high levels of parasitism in the field (Strauss and Agrawal, 1999; Kester et al., 2002; Mira and Bernays, 2002). Furthermore, feeding of larva in vegetative tissues, while causing changes in the vegetative VOC profile, does not affect the quantitative and qualitative composition of the floral VOCs that are necessary to mediate feeding attraction (Riffell et al., 2009b; Reisenman et al., 2013). Thus, this insect–plant interaction has been described as a non-obligatory mutualistic pollinator-herbivore association (Bronstein et al., 2009). In the next section we describe the neural pathway/s and substrates used by the moths to detect and locate suitable host plants. We argue that this exemplar insect–plant interaction illustrates an undeniable perspective: that neurobiological experimentation in a "Neuroecology" context has the most chances of helping discovering how neural circuits function to ultimately produce behavior.

The Moth Olfactory Pathway

The anatomy and physiology of the olfactory system is remarkably similar across insects, including moths. Here we describe that of our exemplar herbivorous insect, the moth *M. sexta*. Antennae are the main olfactory organs of moths: the flagellum of each antenna carries thousands of cuticular hair- or peg-like olfactory organules (sensilla), each of which contains one or a few olfactory sensory neurons (OSNs) (Lee and Strausfeld, 1990). The axons of OSNs in each antennae project centrally via the antennal nerve and terminate in one of the paired primary olfactory centers in the insect brain (Tolbert and Hildebrand, 1981), the ipsilateral antennal lobe (AL) (**Figure 2A**). As in all insects, the ALs have numerous glomeruli, the functional modules of the AL and the first synaptic sites in the olfactory pathway (Boeckh and Tolbert, 1993; Sun et al., 1997; **Figure 2B**). In the fruitfly *Drosophila melanogaster* and likely in all insects, most types of OSNs expresses only one type of olfactory receptor protein (OR), and the axons of OSNs expressing the same OR converge on the same glomerulus (Gao et al., 2000; Vosshall et al., 2000). Males have OSNs which respond to the individual components of the con-specific female sex pheromone (Kaissling et al., 1989), but in some moth species certain plant odorants chemically unrelated to the sex pheromone can activate the male-detecting sex pheromone pathway at both the peripheral and the central level (Rouyar et al., 2015). The antennae of *M. sexta* also have OSNs which respond to volatiles emitted by host plant foliage, including aliphatic, aromatic, and terpenoid compounds bearing a variety of functional groups (Shields and Hildebrand, 2001; Späthe et al., 2013; **Figure 7**). The labial palps of moths of both sexes also have OSNs that respond to changes in ambient CO_2(including floral CO_2), a cue that is important in moth behavior, and converge in a single glomerulus in each AL (Guerenstein et al., 2004; Thom et al., 2004; Goyret et al., 2008).

Initial three-dimensional reconstructions based on anatomical analysis indicated that the ALs of *M. sexta* have 63 $\pm$ 1 identifiable glomeruli (Rospars and Hildebrand, 1992, 2000) (**Figure 2B**), some of which were characterized physiologically (Christensen and Hildebrand, 1987; Roche King et al., 2000; Guerenstein et al., 2004; Reisenman et al., 2004, 2005). More recent studies conducted using a non-histochemical approach based on confocal laser scanning microscopy followed by computer-assisted 3D reconstruction indicate that there are actually 70 $\pm$ 1 glomeruli in females and 68 in males (Grosse-Wilde et al., 2011). As in other moths (e.g., Berg et al., 2002), the majority of glomeruli (ca. 60) are sexually isomorphic (**Figure 2B**) and are involved in the processing of olfactory information about plant VOCs and perhaps other odors (e.g., **Figure 4C**; Guerenstein et al., 2004; Lei et al., 2004; Reisenman et al., 2005; Hillier and Vickers, 2007; Riffell et al., 2009a,b; Varela et al., 2011). A second AL subsystem comprises three male-specific glomeruli (the so-called macroglomerular complex) which process information about the conspecific female's sex pheromone (**Figure 2B**; Christensen and Hildebrand, 1987; Heinbockel et al., 1999, 2004). Females have a pair of large female-specific glomeruli (LFGs, **Figures 2B,C**, **4A,B**) which respond to particular host plant VOCs (Roche King et al., 2000; Reisenman et al., 2004) and are involved in mediating oviposition behavior (Kalberer et al., 2010), and three smaller female-specific glomeruli (Grosse-Wilde et al., 2011). Correspondingly, three male-specific and five female-specific OR genes have been described in *M. sexta* (Grosse-Wilde et al., 2011). Moreover, sequence data indicates that homologous female-specific OR genes exist in different moth families (Grosse-Wilde et al., 2011), indicating that certain VOCs are important for mediating oviposition behavior across distant species.

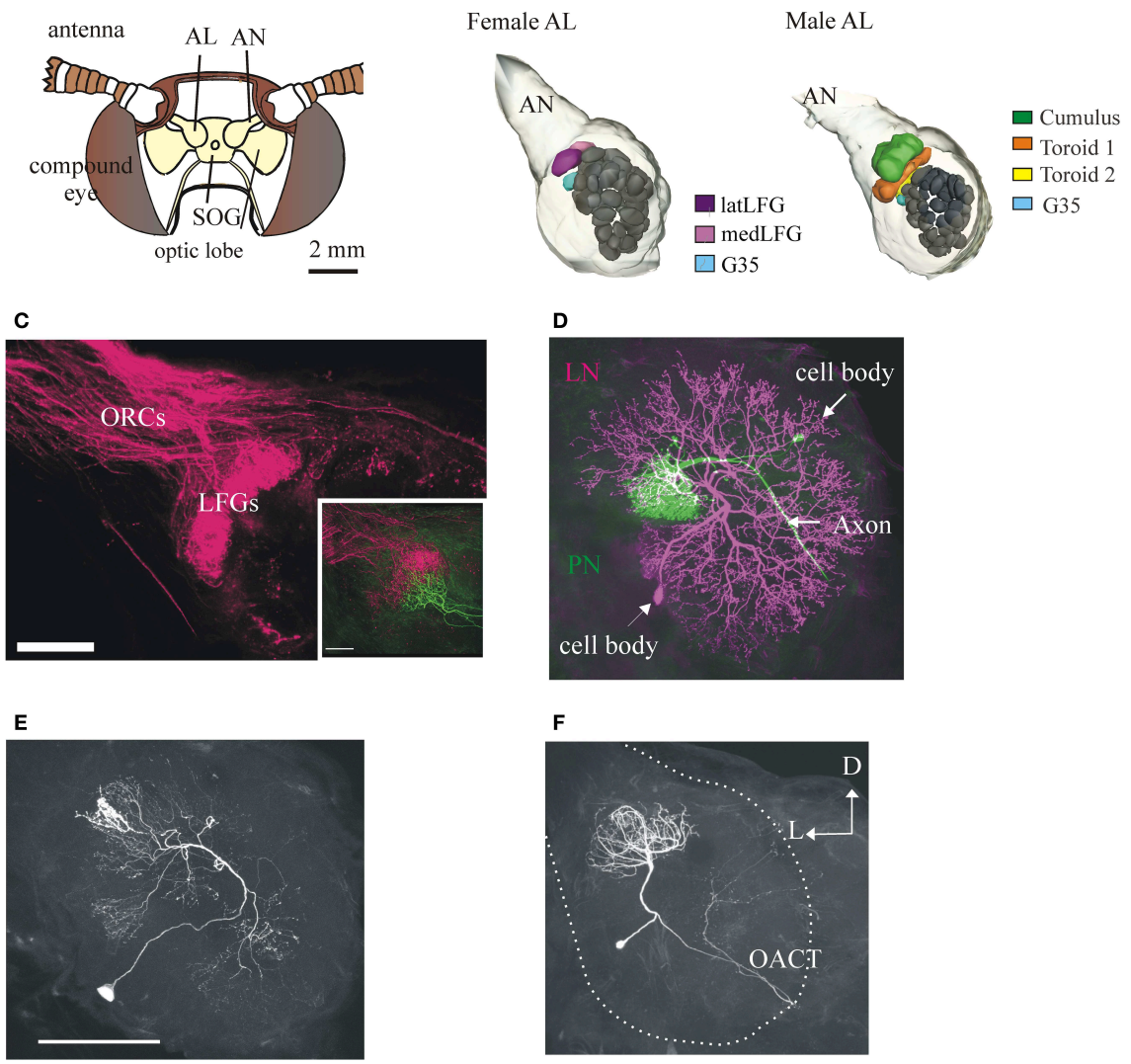

FIGURE 2 | Anatomy of the primary olfactory center of the moth *M. sexta* and its neuronal components. (A) Schematic frontal view of the moth's head. Each antennal lobe (AL) receives input from antennal olfactory sensory neurons (OSNs) through the antennal nerve (AN) (one glomerulus receives input from the labial palps, not shown). SOG, suboesophageal ganglion. **(B)** 3-D reconstructions of the *M. sexta* ALs from a female (left) and a male (right), showing the sexually dimorphic glomeruli (LFGs in females, the Cumulus and the two Toroids in males) and a sexually isomorphic glomerulus (G35, in light blue) of known odor input. Scale bar: 50 μm. **(C)** Confocal image showing OSN afferent input to the LFGs. Inset: mass-labeled OSNs with a single-labeled LFG projection neuron (in green). Scale bar: 100 μm. Figure with permission from Dr. J. Hildebrand. **(D)** A female AL showing the two main types of neurons, a uniglomerular projection neuron (PN, in magenta) and a local interneuron (LN, in green). PNs have an axon that projects from the AL to higher brain centers in the protocerebrum; LNs are intrinsic to the AL and connect many glomeruli. Scale bar: 100 μm. **(E)** LNs are heterogeneous. A LN with arborizations restricted to relatively low number of glomeruli (compare with the LN in **D**). Scale bar: 100 μm. **(F)** The ALs also contain a sizable number of multiglomerular PNs (Homberg et al., 1988), whose functions have not been systematically studied. This PN (from a female) has arborizations in 6–8 glomeruli (including the LFGs) and projects to the protocerebrum via the outer antenno-cerebral tract (OACT) to areas clearly distinct from those where most uniglomerular terminate (compare with **Figure 3A**; Homberg et al., 1989). Same orientation in all panels; D, dorsal, L, lateral.

As in many other insects, two classes of AL neurons have been identified in *M. sexta*: local interneurons (LNs; $n \approx 360$) and projection neurons (PNs; $n \approx 800$) (**Figures 2D–F**, **4**). Many studies indicate that the architecture and function of AL neurons is remarkably similar among moths (e.g., Hartlieb et al., 1997; Lei and Hansson, 1999; Kanzaki et al., 2003; Seki and Kanzaki, 2008; Namiki and Kanzaki, 2011). Most PNs have dendritic arborizations restricted to a single glomerulus and an axon projecting to higher brain centers (Homberg et al., 1988). Some PNs arborize in multiple glomeruli (**Figure 2F**), and it is likely that they process information about particular odor blends (Heinbockel et al., 1999). The LNs receive input from OSNs, have dendritic arborizations restricted to the AL, interconnect few or many glomeruli (**Figures 2D,E**; Matsumoto and Hildebrand,

1981; Reisenman et al., 2011), and interact synaptically (mainly through inhibition, but see Olsen et al., 2007) with other AL neurons (Christensen et al., 1993; Reisenman et al., 2008). The major targets of PN axons are the lateral horn of the protocerebrum (PC), the inferior lateral PC, and the calyces of the ipsilateral mushroom body (**Figures 3A–C**, **4A**; Homberg et al., 1988, 1989). Neurons in these higher-order brain centers integrate information about different odor compounds (Kanzaki et al., 1991; Lei et al., 2013; an example is shown in **Figure 3C**) and are involved in learning and memory (Davis, 2004; Fahrbach, 2006). Although better characterized in males, downstream neurons in the lateral accessory lobe and ventral protocerebrum (an example is shown in **Figure 3D**), which are thought to be main target of olfactory-responding protocebral neurons, mediate the moth characteristic olfactory-evoked sequential zigzag turns (Kanzaki and Shibuya, 1992).

Centrifugal neurons perform several important functions in the moth brain by linking different neural networks and modulating neural circuits that together lead to important physiological and behavioral responses. In particular, a small number of large aminergic centrifugal neurons have important behavioral effects. For instance, fibers from octopamine-immunoreactive neurons are found in the AL, mushroom bodies, and the lateral protocerebrum (Dacks et al., 2005); similarly, fibers from dopaminergic and serotoninergic neurons are also found in the AL and other higher brain areas, including the lateral horn. These neuromodulators increase odor-evoked responses in the majority of antennal lobe PNs and LNs, but can also decrease responses in a smaller subset (Dacks et al., 2008, 2012). Thus these neuromodulators can serve to increase the gain and sensitivity of the neural ensemble in the AL—an important feature for the moths when flower and host plants are temporally and spatially dynamic.

Butterflies and Moths: More Similar than Different

Among herbivorous insects, searching for a suitable host plant may involve input from different sensory modalities (Schoonhoven et al., 2005). However, the importance of olfactory cues in host finding maybe a more generalized phenomenon among the Lepidoptera than previously thought. It has long been assumed that butterflies, which are adapted to a diurnal lifestyle, use mostly visual cues to find host plants. Recent studies in the comma butterfly *Polygonia c-album*, however, showed that the anatomical and physiological characteristics of their olfactory system are remarkably similar to that of moths, despite more than 100 million years of divergence (Carlsson et al., 2011). For instance, the numerical glomeruli composition of AL of this butterfly species is comparable to that of moths, AL neurons faithfully respond to host plant extracts and plant-derived compounds, and odor-evoked AL responses match well described features such as unique and overlapping patterns of activated glomeruli (Carlsson et al., 2011). Also, studies in the butterfly *Pieris rapae*, which has an extremely well developed visual system, showed that insects can distinguish a host from a non-host plant based solely on olfactory cues (Ikeura et al., 2010).

Another interesting study compared the neural representation of plant-derived odorants in five moth species belonging to two phylogenetically distant families (Sphingidae and Noctuidae). While moths in these two families shared some (but not all) foraging and oviposition characteristics, the basic AL mapping of host plant odorants was comparable across species. Thus, these results demonstrate that similar coding strategies are used even by families separated more than 65 million years ago (Bisch-Knaden et al., 2012).

Putting It All Together: Plant Chemical Signals, Neurons, and Behavior

Using *M. sexta* as an exemplary, in this section we present our current knowledge on the neural processing of relevant, naturally occurring host plant signals at several levels of the olfactory pathway, and its consequences for natural behavior. As we mentioned before, the sacred *D. wrightii* and the nocturnal moth *M. sexta* form a pollinator-plant and herbivore-plant association (Bronstein et al., 2009), with females using the plant both as a nectar (Alarcón et al., 2008; Riffell et al., 2008b) and as an oviposition resource (Mechaber and Hildebrand, 2000). Correspondingly, feeding and oviposition behaviors often co-occur in gravid females (Bronstein et al., 2009; Reisenman et al., 2010). What are the floral and vegetative VOCs that guide these behaviors, and how are they processed in the moth brain? Although *D. wrightii* flowers produce a bouquet composed of more than 60 odorants (Raguso et al., 2003) a blend of just three floral components [(±)-linalool, benzaldehyde, and benzyl alcohol], presented in appropriates ratios and concentrations, is an effective mimic of the floral scent, eliciting feeding behavior in naïve moths of both sexes (Riffell et al., 2009b). Although adult moths are innately attracted to the *D. wrightii* floral scent, they readily learn to feed on other nectar sources through olfactory conditioning (Riffell et al., 2008b).

While OSNs in the female antenna of *M. sexta*, as in other moths (e.g., Hillier et al., 2006; Ulland et al., 2008), respond to a chemical variety of host plant VOCs (**Figure 7**; Shields and Hildebrand, 2001; Späthe et al., 2013), we found that (±)-linalool, a floral volatile characteristic of many moth-pollinated night-blooming flowers including *D. wrightii*, has important roles mediating behavior (Riffell et al., 2008b, 2009a; Reisenman et al., 2010, 2013). Behavioral and electrophysiological recordings from AL-PNs showed that the two naturally occurring enantiomers of linalool present in flowers mediate feeding and oviposition through two neural pathways, one that is sexually isomorphic and non-enantioselective, and another that is female-specific and enantioselective (**Figures 4B**, **5**; Reisenman et al., 2004, 2010). In one hand, the (+) and (−) enantiomers of linalool respectively contribute to oviposition attraction and repellence and are discriminated by female-specific PNs (**Figures 1C**, **4**, **5**). Linalool-responsive sexually isomorphic PNs do not discriminate between linalool enantiomers (Reisenman et al., 2004) and

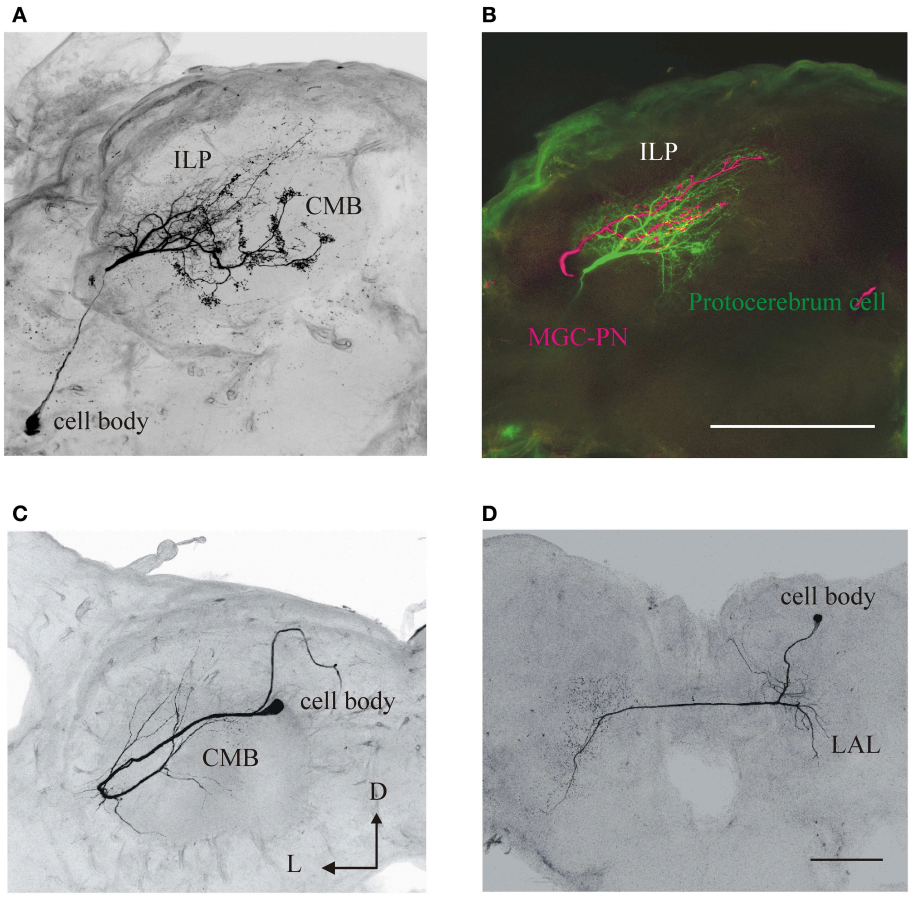

FIGURE 3 | Anatomy and morphology of olfactory neurons arborizing in second and third-order brain centers in *M. sexta*. These neurons might respond to other sensory modalities. **(A)** A protocerebral neuron with dendritic arborizations in the inferior lateral protocerbrum (ILP) and the calyx of the mushroom bodies (CMB). **(B)** In the same preparation a male-specific (MGC) neuron was differentially stained (in magenta) showing that both neurons have arborizations in overlapping areas (yellow). Scale bar: 100 μm. D, dorsal; L, lateral. **(C)** An olfactory-responsive neuron with arborizations in the CMB. **(D)** A neuron in the lateral accessory lobe (LAL), an area which receives input from olfactory protocerebral neurons. Scale: 200 μm. Same orientation in all panels; D, dorsal; L, lateral.

correspondingly, the enantiomers are not discriminated in the feeding context (Reisenman et al., 2010). Interestingly, two homologous receptors to the *Bombyx mori* linalool-ORs, MsexOR-5 and 6, have been described in *M. sexta* (Grosse-Wilde et al., 2010, 2011), and are likely candidates to mediate (at least in part) these behaviors. This, together with the fact that these moth species belong to evolutionary distant families, suggest that these receptors and the corresponding neurons play an important role in moth, and probably Lepidoptera, olfaction (Grosse-Wilde et al., 2011).

While *M. sexta* uses a variety of host plants for oviposition, choice experiments showed that females prefer to oviposit on *D. wrightti* plants, and that this preference is mostly mediated by olfactory cues (Späthe et al., 2013). Although females avoid ovipositing in larva-damaged plants (**Figure 5E**), this avoidance is plant- specific: females strongly avoid larva-damaged tomato and tobacco plants, but they do not avoid ovipositing in larva-damaged *D. wrightti* plants, despite that these plants can be clearly distinguished from non-damaged plants by their VOC profile and by the peripheral OSNs (**Figures 6**, **7**; Reisenman et al., 2013; Späthe et al., 2013). An important consideration is that moths use these plant species differently: while the annuals tomato and tobacco are only used by moths for oviposition, the jimsonweeds are also pollinated by the adults. Thus, we propose that the differences in oviposition preference toward larvae-damaged plants of different species are due to the different relationships between *M. sexta* and these host plants. The beneficial association is emphasized further by the finding that at least some of the *D. wrightii* floral VOCs that are important to mediate feeding– and hence pollination–remained unchanged in herbivore-induced plants (Reisenman et al., 2013).

As we mentioned before, (+)-linalool has an important role in mediating oviposition attraction. In contrast, we found that plants with (−)-linalool added are avoided by ovipositing females (**Figure 5D**; Reisenman et al., 2010),

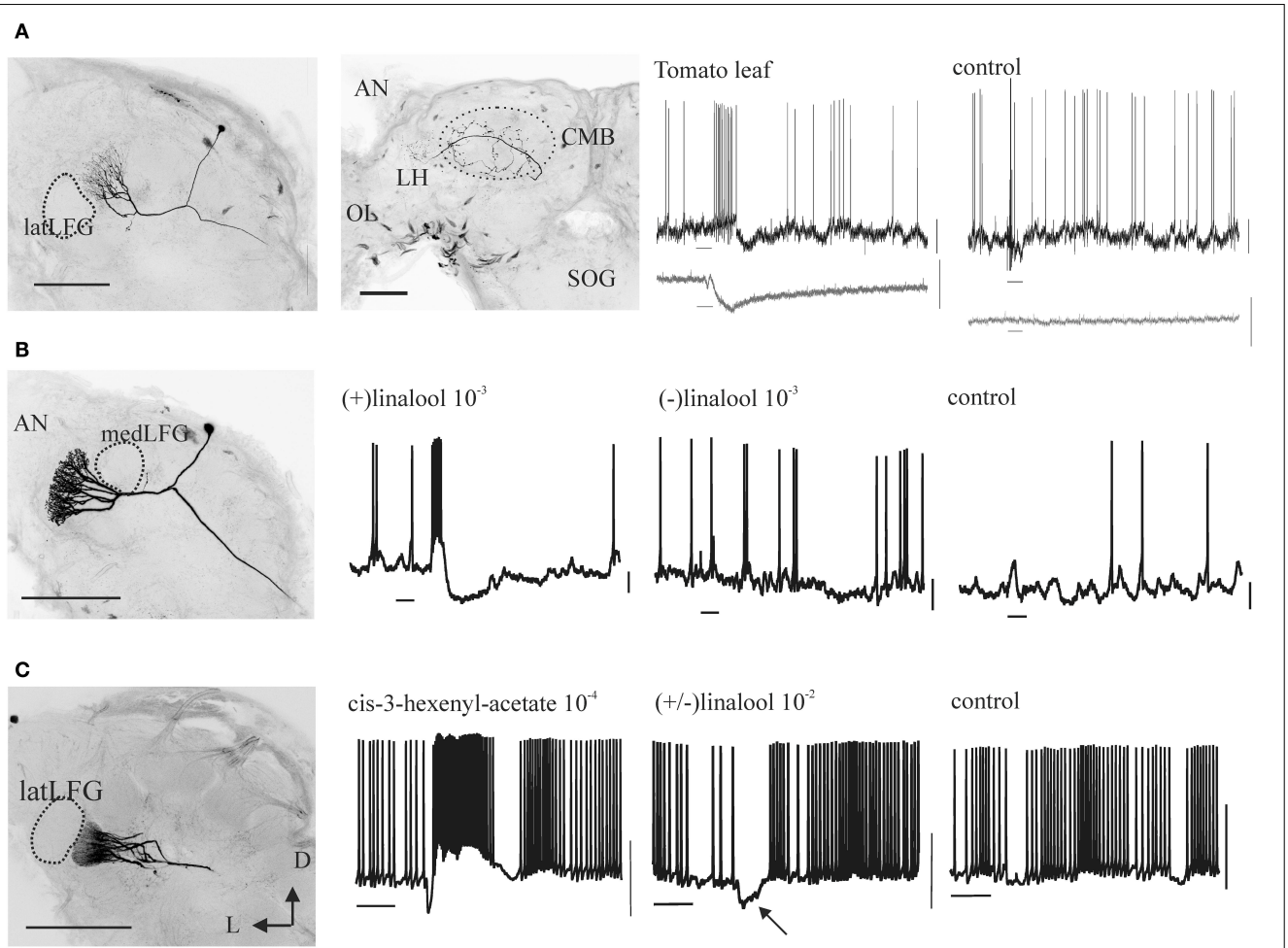

FIGURE 4 | Morphology and odor responses of female-specific antennal lobe PNs (A: medLFG-PN, B: latLFG-PN) and of a sexually isomorphic PN in the adjacent glomerulus G35 (C). Scale bars: 200 m. D, dorsal; L, lateral. The second panel in **(A)** shows the projection sites of LFG-PNs in the protocerebrum, the lateral horn (LH) and the calyx of the mushroom body (CMB); the optic lobe (OL) and the suboesophageal ganglion (SOG) are shown for reference. Most uniglomerular PNs also project to these sites. Shown are intracellular recordings obtained from these neurons to stimulation (duration = 200 ms, bars below records) with vegetative material **(A)** or odors **(B,C)** at the concentrations (% vol/vol) indicated. In **(A)** the bottom traces (in gray) show the simultaneously recorded electroantennograms (EAGs). Control stimuli are air from an empty cartridge **(A)** or the mineral-oil solvent **(B,C)**. Calibration bars: 10 mV (intracellular trace), 1 mV (EAG). Note that medLFG-PNs are excited by tomato leaf volatiles, latLFG-PNs respond differentially to the two linalool enantiomers, and G35-PNs are excited by *cis*-3-hexenyl acetate and hyperpolarized by (±)-linalool (arrow), i.e., by input to the adjacent latLFG.

and that this compound is significantly increased in larva-damaged tomato plants (Reisenman et al., 2013). The antenna of the cabbage moth *Mamestra brassicae* is, as that of *M. sexta* (Reisenman, not shown), more sensitive to (−)-linalool than to (+)-linalool (Ulland et al., 2006). Collectively, these results suggest that (−)-linalool (alone or together with other with other induced VOCs; Reisenman et al., 2013), might act as an oviposition repellent and also as a plant defense, attracting the natural enemies of herbivores (Baldwin et al., 2002). The finding that this unique odorant is similarly processed and discriminated by moths in different families also suggests that common components and neural mechanisms are involved in the selection of suitable host plants.

Although linalool has important roles in mediating oviposition, it is very likely that the choice of suitable host plant sites is mediated by a suite of VOCs. A powerful technique to address this issue, which has been already used to investigate the VOCs involved in mediating feeding (Riffell et al., 2009a,b), is to couple the use of gas chromatography for chemical detection and multi-unit recordings from AL neurons (GC-MR; **Figure 8A**). This technique allows to simultaneously visualize the activity of many neurons in response to components from behaviorally active plant extracts as they elute from the GC column. For instance, **Figure 8B** shows an example of a neuron that responds specifically to a single larva-damaged component. The use of the multi-unit recording technique allows stimulating many neurons with different bioactive plant

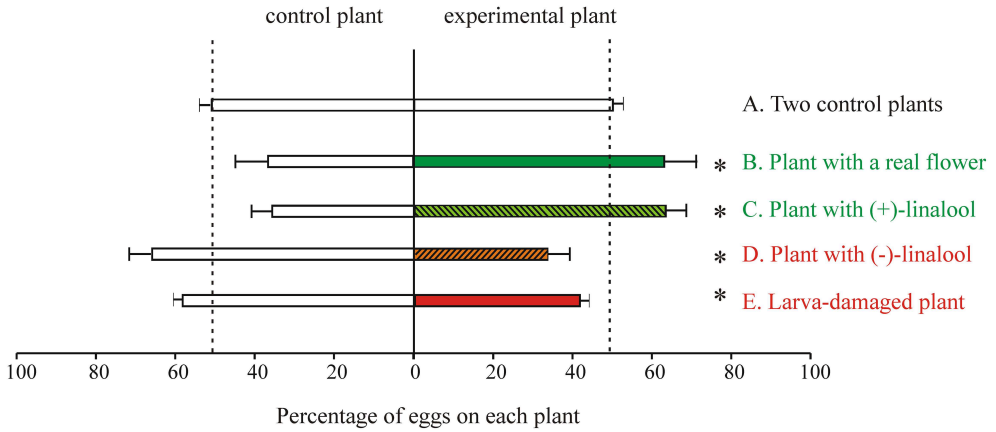

FIGURE 5 | Oviposition behavior of *M. sexta* in the laboratory. In all cases single mated females were offered a choice between a control and a test plant in a flight tent (as shown in **Figure 1C**) and allowed to oviposit during 10 min after take-off. Plant pairs of the jimsonweed *D. wrighttii* **(A–D)** or tomato (*Solanum lycopersicum*) **(E)** were used. In **(A)** two control plants were offered to control for spatial asymmetries ($n = 25$). The following experimental series were conducted: **(B)** a plant with a newly opened flower vs. a plant with a paper flower ($n = 12$); **(C,D)** a plant with a paper flower loaded with (+)-linalool (**(C)**, $n = 16$) or (–)-linalool (**(D)**, $n = 16$) vs. a plant with a paper flower loaded with solvent (linalool was loaded in the paper flowers at the naturally-occurring concentrations); **(E)** a larva-damaged plant vs. an intact plant ($n = 38$). Data represent the percentage (average ± SE) of eggs oviposited in each plant. Moths and plant pairs were used only once. Asterisks indicate significant differences ($p < 0.05$; Sign tests). Green-hue and red-hue colors, respectively indicate oviposition attraction or repellence for the experimental plant (Data modified from Reisenman et al., 2010, 2013).

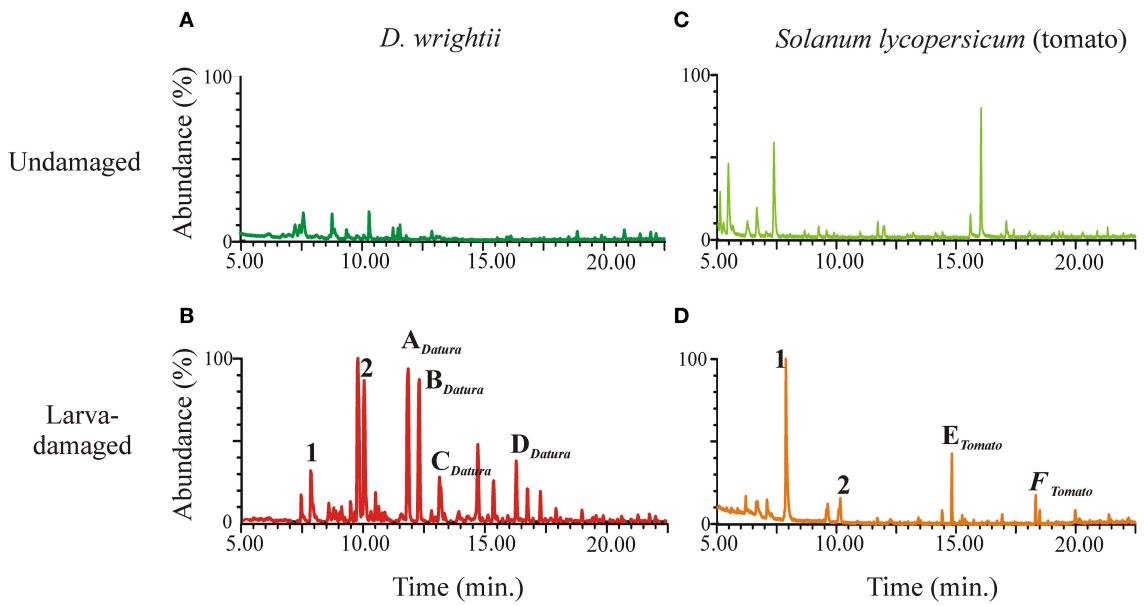

FIGURE 6 | Plant VOC response to herbivory. *M. sexta* larvae were allowed to feed on plants during 2–3 days, after which larvae and frass were removed and vegetative VOCs collected and analyzed via GC-MS as described in Reisenman et al. (2013). Representative ion chromatograms of the headspace from undamaged *D. wrightii* **(A)**, larva-damaged *D. wrightii* **(B)**, undamaged tomato **(C)**, and larva-damaged tomato **(D)**. In **(C,D)** same numbers or letters, respectively indicate common and different compounds emitted by larva-damaged vegetation.

extracts (**Figure 8C**). Quantification of individual neuron responses to repetitive stimulation evinced plant- and status- (intact or damaged) specific responses, either excitatory or inhibitory (**Figures 8C,D**). To evaluate the population response, we calculated a dissimilarity index, which indeed demonstrate that the AL discriminates between larva-damaged and intact plants (**Figure 8E**). Knowledge of the compounds that are discriminated at this level of olfactory processing readily informs about the suite of VOCs that could potentially mediate the behavioral selection of appropriate host plants.

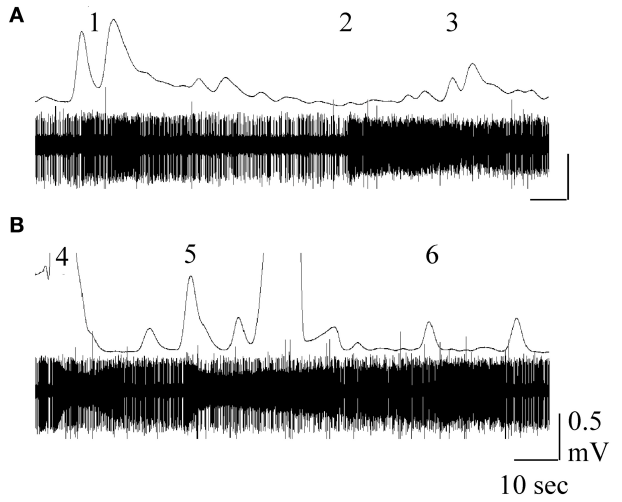

FIGURE 7 | Simultaneous GC trace (top) and single sensillum recording (bottom trace) obtained in response to stimulation with *M. sexta* larva-damaged tobacco (*Nicotiana attenuata*, A) or *D. wrightti* (B). Numbers indicate neuron responses to phenol (1), 4-methyl pentanol (2), *cis*-3-hexanol (3), cis-3-hexenyl acetate (4), benzyl alcohol (5) and methyl-benzoate (6). For methods, see Späthe et al. (2013). Figure courtesy of Drs. S. Kesevan and S. Olsson.

Olfactory Responses in Sexually Isomorphic Pathways and Interconnected Glomeruli

As described above, female specific neurons are involved in mediating female-specific behaviors such as oviposition (Roche King et al., 2000; Reisenman et al., 2004) and in some moth species, detection of male pheromones (Hillier et al., 2006). As in many insects, the orientation of males toward the female-specific sex pheromone is crucial for the species survival, and the role of male-specific neurons in mediating this behavior is well-established in many moth species (e.g., Anton et al., 1997; Berg et al., 1998; Lei and Hansson, 1999; Vickers and Christensen, 2003). Although it might be tempting to argue that sexually dimorphic pathways are particularly selective as they mediate fundamental behaviors related to reproduction, we found that PNs in sexually isomorphic glomeruli can also be highly specific. For instance, PNs in an identified glomerulus (glomerulus 35, which neighbors the sexually dimorphic glomeruli in both sexes, **Figure 2B**) are extremely selective and sensitive to another host plant volatile, cis-3-hexenyl acetate (**Figure 4C**), responding to concentrations <1 ppm (Reisenman et al., 2005). While the specific role of this VOC for behavior is not yet elucidated (although its production is augmented in larva-damaged plants; Hare, 2007), knowledge of the specific VOCs that activate specific sets of glomeruli has provided a tool to study interactions between glomeruli involved in mediating different behaviors. Previously, Lei and coworkers elegantly demonstrated that the temporal output of each male-specific glomerulus is enhanced by reciprocal inhibitory interglomerular interactions, and that this serves to synchronize the activity of neurons processing the components of the sex pheromone blend (Lei et al., 2002). Using known odor inputs to activate specific glomeruli beyond the sex-specific system, we found that the two AL subsystems interact synaptically in a distant-independent, non-reciprocal fashion (**Figure 4C**, middle panel; Reisenman et al., 2008), and that these interactions are mediated by a functionally and morphologically heterogeneous population of local interneurons (**Figures 2D,E**; Reisenman et al., 2011). Interactions between odors with different behavioral significance have been also described in other moth species, both at a behavioral and at a neural level (e.g., Chaffiol et al., 2012, 2014; Deisig et al., 2012; Trona et al., 2013).

Experiments conducted in many insect species, including *M. sexta*, indicate not only that glomeruli interact synaptically, but that sets of interconnected glomeruli are likely involved in the processing of behaviorally relevant odor blends. At the AL level, this idea is supported by the fact that a sizeable proportion of LNs interconnect a restricted subset of glomeruli (**Figure 2E**; Reisenman et al., 2011). The existence of PNs that arborize in multiple -but restricted- glomeruli, also supports this hypothesis (**Figure 2F**). At the level of the chemical signals, it is known that some of the active compounds identified in the host plant headspace are ubiquitous floral and vegetative VOCs. Thus, it is possible that a suite of compounds presented in particular proportions (Thiery and Visser, 1986; Zhang et al., 1999; Riffell et al., 2008b, 2009a), rather than a single compound, activates a subset of glomeruli to mediate host plant selection. For instance, a blend of just three floral *D. wrightii* VOCs (but not any of the single VOCs) can elicit feeding (Riffell et al., 2009b). Similarly, the sole presence of linalool is not sufficient to mediate oviposition, although the presence of this component in plants has profound behavioral effects (**Figure 5**; Reisenman et al., 2010). Because different host plants are readily accepted for oviposition by females, it is possible that that individual VOCs shared across plant species activate a functionally connected glomerular subset (which necessarily involves at least some of the female-specific glomeruli), the output of which ultimately control oviposition behavior. The chemical composition of that bouquet, however, remains to be identified.

Moths Find Plants, but How Do the Plants Impact the Moths?

While in the previous section we discussed the neural processing of naturally occurring signals and its consequences for behavior, in this section we highlight some plant cues and signals that in turn, can influence moth behavior. From the plant prospective, what matters is to attract efficient pollinators. In the case of *D. wrightti*, as we mentioned, this has the un-intended consequence of also attracting gravid females. This plant species can effectively cope with this, as plants can tolerate high levels of defoliation, quickly regrow after herbivory, reduce photosynthetic rates, and redirect resources to storage in the roots upon herbivory (cited in Reisenman et al., 2010). However, once moths probe flowers, other gustatory sensory cues present in nectar appear to have profound effects in guiding behavioral decisions.

As mentioned before, plants often produce secondary compounds (e.g., alkaloids, glycosides, and phenolic compounds) to deter herbivores and pathogens (Karban and Baldwin, 1997). Interestingly, these secondary compounds are also present in floral nectar (Adler, 2000) and can be induced by herbivory in a plant-species specific manner (Adler et al., 2006; Hare and Walling, 2006; Kessler and Halitschke, 2009). It has been suggested that the presence of these components in nectar increases pollinator fidelity, repel nectar robbers, and improve pollen transfer by intoxicating pollinators (Adler, 2000).

In the case of *D. wrightii*, an obvious advantage for female *M. sexta* is that visits to flowering plants provide both nectar and oviposition resources. However, because of the limited availability of the flowers (which bloom for only one evening) and the effects of herbivory (which limits the number of healthy host plants), female moths encounter resources that are spatio-temporally patchy. The moth nervous system has the ability to adjust its activity so that behavioral output is maximally beneficial for survival within an often harsh and patchy environment. This plasticity is accomplished by the release of specific neuromodulators—including serotonin, octopamine and dopamine—within restricted brain regions like the AL, the lateral horn and the mushroom bodies. For example, herbivory-induced damage to *D. wrightii* plants elicits high concentrations of certain alkaloids in the flower nectar which *M. sexta* finds aversive. Tropane alkaloids (including scopolamine) in the nectar of damaged *D. wrightii* increase more than 20-fold in damaged plants (Dacks et al., 2012). Over time, moths learn the association between the alkaloid content and the floral and vegetative scent so that these damaged plants become avoided. Dopamine release in the moth brain—including the ALs and the mushroom bodies—has shown to be a critical signal mediating aversive learning and signaling the presence of an aversive stimulus. For instance, when the ALs of female moths were injected with a dopamine receptor antagonist, moths could no longer learn the association of the aversive nectar and the flower scent. Furthermore, when dopamine was superfused on to the AL, the neural ensemble showed enhanced responses to the flower odor stimulus. Dopaminergic modulation of AL circuits thus plays an important role in the memory formation of repellent flower scents and the discrimination of larva-damaged plants. Interestingly, the effects of alkaloids in moth preference are shaped by both the plant species and the behavioral context. For instance, females prefer to oviposit in tobacco plants which have higher concentrations of nicotine in nectar (Adler et al., 2006), but they remove less nectar from these plants (Kessler and Baldwin, 2006). Thus, the nervous system can differentially evaluate the same plant sensory cue (in this case, nicotine) according to the behavioral context.

What are the effects of nectar secondary compounds on insect behavior? In general, naturally-occurring concentrations of secondary compounds do not deter nectar-feeding insects, whether specialists or generalists. In generalist insects such as bees, low concentrations of certain secondary compounds such as nicotine and caffeine elicit feeding preference (Singaravelan et al., 2005). This preference is not mediated by peripheral taste receptors, but is probably due to the effect of these substances in reward brain centers (Singaravelan et al., 2005; Kessler et al., 2015). In contrast, prolonged exposure to high concentrations of these compounds (e.g., such as those found in flowering crops sprayed with neonicotinoid pesticides) can impair olfactory learning and memory (Williamson and Wright, 2013). The effects of these substances in learning and memory in herbivorous insects which are exposed to natural concentrations of plant secondary defenses have not been yet studied, but tobacco plants which have been engineered to completely lack nicotine in nectar have more nectar removed per night (Kessler and Baldwin, 2006). Unlike bees, taste receptors in the mouthparts of moths can readily detect bitter compounds such as caffeine (Bernays et al., 2002; Glendinning et al., 2006), which are commonly present in their host plants. The effects of these substances on behavior, however, remain to be investigated in the appropriate ecological and behavioral context.

Summary and Conclusions

In the last couple of decades, research in the neuroscience field has focused on a small number of "model" species offering various advantages, at the expense of potentially creating a bottleneck which limits or compromises our understanding of how nervous systems operate (Brenowitz and Zakon, 2015). Today, several genome project efforts, and increasingly available tools that allow DNA editing, are bridging this gap. However, an integrative approach that includes ecological and community relationships, natural signals, neurons and behavior, has always been and it will always remain key to understand the function of nervous systems.

Here we used an exemplary specialized herbivorous insect, the moth *M. sexta*, to review the function of the moth's olfactory system in a naturalistic context. While floral odors attract moths for feeding and oviposition, volatiles released from larva-damaged plants mediate oviposition repellence. Specific plant volatiles are involved in mediating these behaviors, and are processed in both sexually isomorphic and dimorphic neural pathways according to the behavioral context (feeding and oviposition). Furthermore, some of these volatiles also mediate behavior in distant moth species, suggesting important roles for certain plant volatiles and commonalities in their neural processing. In addition, for the plant benefit, plant secondary compounds can affect host-plant finding and behavior through processes such as learning and memory.

While today we have a deeper understanding of how the nervous system process information about behaviorally relevant VOCs in *M. sexta* and other insect species, many issues, at several levels of interactions, need to be addressed. For instance, do different populations of host plants differ in their VOC profile, and what are the behavioral consequences? Given that *M. sexta* is found throughout a wide range in the American continent, is there a common set of VOCs that guide oviposition choice, despite that moths across the distribution range use different host plant species? Is there a minimum VOC blend that produces acceptance and egg lying? Would this blend suffice to guide oviposition choice in different moth populations? Are

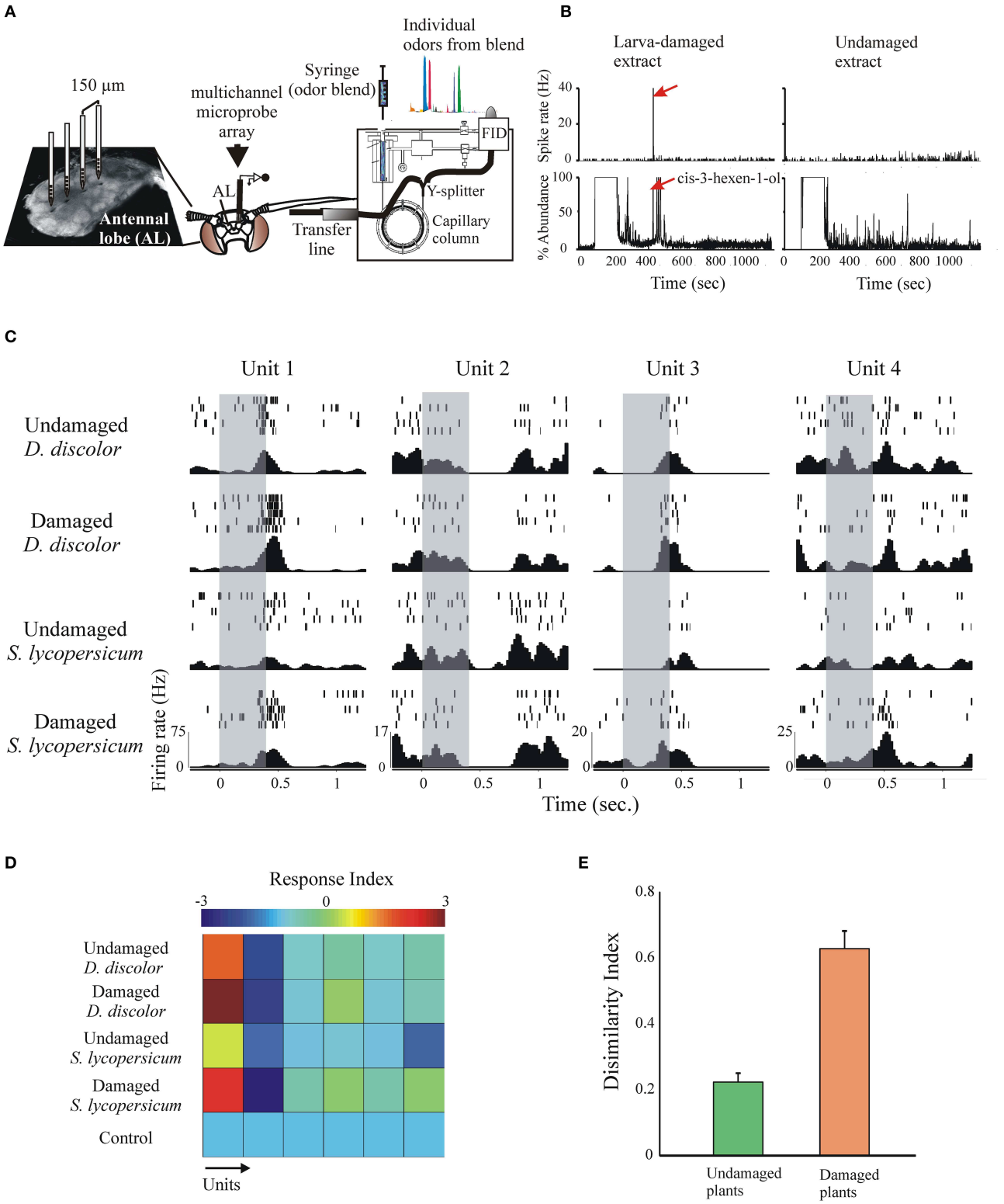

FIGURE 8 | The response of many simultaneously recorded AL neurons to VOC extracts and single components can be studied using a multi-unit recording electrode coupled to gas-chromatographic analysis (GC-MRA). **(A)** Plant extracts are injected on the GC inlet; after leaving the GC column a Y-splitter divides the effluent for simultaneous antenna stimulation and chemical identification of individual components. **(B)** GC-MRA analysis showing a neuron with robust responses to the larva-damaged VOCs responding selectively to only one peak in the GC effluent (arrow, cis-3-hexen-1-ol). **(C)** Simultaneously recorded

(Continued)

FIGURE 8 | Continued
responses of 4 units to stimulation (duration = 200 ms, gray bars) with the plant extracts indicated to the left. Shown are individual spikes (tick marks) during repetitive stimulation (rows), and the peri-event histograms calculated across trials (bottom). Note that different units respond differently to different stimuli, and that the same unit responds differentially to intact and larva-damaged extracts. **(D)** Response indexes (or z-scores, color-coded, calculated as spiking rate during stimulation—spiking rate pre-stimulation/SD) for six simultaneously recorded neurons in response to stimulation with the extracts indicated. The first two units showed stronger responses to stimulation with larva-damaged plants. **(E)** The dissimilarity index (Riffell et al., 2009a) indicates stronger AL neuronal ensemble responses to larva-damaged plants.

populations in other regions as specialized in certain host plants as the Southwest USA population? Do background odors affect olfactory-guided oviposition choices? Do other other factors such as temperature and humidity affect host plant choice? In nature, do females actually avoid ovipositing on plants where other larvae are already present, and if so, how do they achieve this? An interesting possibility, given that *M. sexta* host plants naturally produce alkaloids which can be readily detected by moths (Bernays et al., 2002; Glendinning et al., 2006), is that plants manipulate nicotine concentrations in nectar to their benefit, as these substances could act as postingestive stimulants and even have addictive properties, improving flower finding and efficiency (Singaravelan et al., 2005; Kessler et al., 2015). We know much about the "Neuroecology" of oviposition and feeding behavior in adult insects, but do larvae make choices within a plant, and how are these choices guided? Do larvae prefer younger or older leaves, small or big? Importantly, a comparative strategy has the power of help unraveling general neural mechanisms and strategies that guide host plant choice. We propose that all these issues by necessity need to be investigated in an appropriate Neuroecology framework.

Finally, along with a deep understanding of the relationships of organisms with their natural environment, we believe that in the near future genomic tools now available to many insect species will permit a deeper and more complete understanding of how the insect nervous system produces adaptive behavior.

Acknowledgments

We thank Drs. John Hildebrand and Kristin Scott for their support and encouragement, and to the two reviewers for their comments and suggestions that greatly improved this manuscript. CR and JR were initially supported by an award from NSF (IOS-0822709). JR was supported by awards from NSF (IOS-1354159 and DMS-1361145) and the Human Frontiers in Science Program (RGP0022). We thank Drs. S. Olsson and S. Kesevan for generously providing **Figure 7**, and Dr. J. Hildebrand for allowing the use of **Figure 2C**.

References

Adler, L. S. (2000). The ecological significance of toxic nectar. *Oikos* 91, 409–420. doi: 10.1034/j.1600-0706.2000.910301.x

Adler, L. S., Karban, R., and Strauss, S. Y. (2001). Direct and indirect effects of alkaloids on plant fitness via herbivory and pollination. *Ecology* 82, 2032–2044. doi: 10.1890/0012-9658(2001)082[2032:DAIEOA]2.0.CO;2

Adler, L. S., Wink, M. D., Distl, M., and Lentz, A. J. (2006). Leaf herbivory and nutrients increase nectar alkaloids. *Ecol. Lett.* 9, 960–967. doi: 10.1111/j.1461-0248.2006.00944.x

Agrawal, A. A., Hastings, A. P., Johnson, M. T. J., Maron, J. L., and Salminen, J.-P. (2012). Insect herbivores drive real-time ecological and evolutionary change in plant populations. *Science* 338, 113–116. doi: 10.1126/science.1225977

Alarcón, R., Davidowitz, G., and Bronstein, J. (2008). Nectar usage in a southern Arizona hawkmoth community. *Ecol. Entomol.* 33, 503–509. doi: 10.1111/j.1365-2311.2008.00996.x

Anderson, P., Hilker, M., Hansson, B. S., Bombosch, S., Klein, B., and Schildknecht, H. (1992). Oviposition deterring components in larval frass of *Spodoptera littoralis* (Boisd.) (Lepidoptera: Noctuidae): a behavioral and electrophysiological evaluation. *J. Insect Physiol.* 39, 129–137. doi: 10.1016/0022-1910(93)90104-Y

Anton, S., Löfstedt, C., and Hansson, B. S. (1997). Central nervous processing of sex pheromones in two strains of the european corn borer *Ostrinia nubilalis* (Lepidoptera: Pyralidae). *J. Exp. Biol.* 200, 1073–1087.

Baker, T. C. (1990). "Upwind flight and casting flight: complimentary phasic and tonic systems used for location of sex pheromone sources by male moths," in *ISOT X. Proceedings of Tenth International Symposium on Olfaction and Taste*, ed K. B. Doving (Oslo: University of Oslo), 18–25.

Baldwin, I. T., Kessler, A., and Halitschke, R. (2002). Volatile signaling in plant-plant-herbivore interactions: what is real? *Curr. Opin. Plant Biol.* 5, 351–354. doi: 10.1016/S1369-5266(02)00263-7

Baldwin, I. T., and Preston, C. A. (1999). The eco-physiological complexity of plant responses to insect herbivores. *Planta* 208, 137–145. doi: 10.1007/s004250050543

Berenbaum, M. R., Zangerl, A. R., and Lee, K. (1989). Chemical barriers to adaptation by a specialist herbivore. *Oecologia* 80, 501–506. doi: 10.1007/BF00380073

Berg, B. G., Almaas, T. J., Bjaalie, J. G., and Mustaparta, H. (1998). The macroglomerular complex of the antennal lobe in the tobacco budworm moth *Heliothis virescens*: specified subdivision in four compartments according to information about biologically significant compounds. *J. Comp. Physiol. A* 183, 669–682. doi: 10.1007/s003590050290

Berg, B. G., Galizia, C. G., Brandt, R., and Mustaparta, H. (2002). Digital atlases of the antennal lobe in two species of tobacco budworm moths, the oriental *Helicoverpa assulta* (male) and the american *Heliothis virescens* (male and female). *J. Comp. Neurol.* 446, 123–134. doi: 10.1002/cne.10180

Bernays, E. A., Chapman, R. F., and Hartmann, T. (2002). A taste receptor neurone dedicated to the perception of pyrrolizidine alkaloids in the medial galeal sensillum of two polyphagous arctiid caterpillars. *Physiol. Entomol.* 27, 312–321. doi: 10.1046/j.1365-3032.2002.00304.x

Bisch-Knaden, S., Carlsson, M. A., Sugimoto, Y., Schubert, M., Mißbach, C., Sachse, S., et al. (2012). Olfactory coding in five moth species from two families. *J. Exp. Biol.* 215, 1542–1551. doi: 10.1242/jeb.068064

Boeckh, J., and Tolbert, L. P. (1993). Synaptic organization and development of the antennal lobe in insects. *Microsc. Res. Tech.* 24, 260–280. doi: 10.1002/jemt.1070240305

Bowers, M. D. (1983). The role of iridoid glycosides in host-plant specificity of checkerspot butterflies. *J. Chem. Ecol.* 9, 475–493. doi: 10.1007/BF00990220

Brenowitz, E. A., and Zakon, H. H. (2015). Emerging from the bottleneck: benefits of the comparative approach to modern neuroscience. *Trends Neurosci.* 38, 273–278. doi: 10.1016/j.tins.2015.02.008

Bronstein, J. L., Huxman, T., Horvath, B., Farabee, M., and Davidowitz, G. (2009). Reproductive biology of *Datura wrightii*: the benefits of a herbivorous pollinator. *Ann. Bot.* 103, 1435–1443. doi: 10.1093/aob/mcp053

Carlsson, M. A., Bisch-Knaden, S., Schäpers, A., Mozuraitis, R., Hansson, B. S., and Janz, N. (2011). Odour maps in the brain of butterflies with divergent host-plant preferences. *PLoS ONE* 6:e24025. doi: 10.1371/journal.pone.0024025

Chaffiol, A., Dupuy, F., Barrozo, R. B., Kropf, J., Renou, M., Rospars, J.-P., et al. (2014). Pheromone modulates plant odor responses in the antennal lobe of a moth. *Chem. Senses* 39, 451–463. doi: 10.1093/chemse/bju017

Chaffiol, A., Kropf, J., Barrozo, R. B., Gadenne, C., Rospars, J.-P., and Anton, S. (2012). Plant odour stimuli reshape pheromonal representation in neurons of the antennal lobe macroglomerular complex of a male moth. *J. Exp. Biol.* 215, 1670–1680. doi: 10.1242/jeb.066662

Christensen, T. A., Heinbockel, T., and Hildebrand, J. G. (1996). Olfactory information processing in the brain: encoding chemical and temporal features of odors. *J. Neurobiol.* 30, 82–91.

Christensen, T. A., and Hildebrand, J. G. (1987). Male-specific, sex pheromone-selective projection neurons in the antennal lobes of the moth *Manduca sexta*. *J. Comp. Physiol. A* 160, 553–569. doi: 10.1007/BF00611929

Christensen, T. A., Waldrop, B. R., Harrow, I. D., and Hildebrand, J. G. (1993). Local interneurons and information processing in the olfactory glomeruli of the moth *Manduca sexta*. *J. Comp. Physiol. A* 173, 385–399. doi: 10.1007/BF00193512

Cipollini, D. (2010). Constitutive expression of methyl jasmonate-inducible responses delays reproduction and constrains fitness responses to nutrients in *Arabidopsis thaliana*. *Evol. Ecol.* 24, 59–68. doi: 10.1007/s10682-008-9290-0

Cornell, H. V., and Hawkins, B. A. (2003). Herbivore responses to plant secondary compounds: a test of phytochemical coevolution theory. *Am. Nat.* 161, 507–522. doi: 10.1086/368346

Corrado, G., Agrelli, D., Rocco, M., Basile, B., Marra, M., and Rao, R. (2011). Systemin-inducible defence against pests is costly in tomato. *Biol. Plant.* 55, 305–311. doi: 10.1007/s10535-011-0043-5

Dacks, A. M., Christensen, T. A., Agricola, H.-J., Wollweber, L., and Hildebrand, J. G. (2005). Octopamine-immunoreactive neurons in the brain and subesophageal ganglion of the hawkmoth *Manduca sexta*. *J. Comp. Neurol.* 488, 255–268. doi: 10.1002/cne.20556

Dacks, A. M., Christensen, T. A., and Hildebrand, J. G. (2008). Modulation of olfactory information processing in the antennal lobe of *Manduca sexta* by serotonin. *J. Neurophysiol.* 99, 2077–2085. doi: 10.1152/jn.01372.2007

Dacks, A. M., Guerenstein, P. G., Reisenman, C. E., Martin, J. P., Lei, H., and Hildebrand, J. G. (2007). "Olfaction: invertebrates – Manduca," in *New Encyclopedia of Neuroscience*, ed R. S. Larry (Oxford: Academic Press), 49–57.

Dacks, A. M., Riffell, J. A., Martin, J. P., Gage, S. L., and Nighorn, A. J. (2012). Olfactory modulation by dopamine in the context of aversive learning. *J. Neurophysiol.* 108, 539–550. doi: 10.1152/jn.00159.2012

Davis, R. L. (2004). Olfactory learning. *Neuron* 44, 31–48. doi: 10.1016/j.neuron.2004.09.008

Deisig, N., Kropf, J., Vitecek, S., Pevergne, D., Rouyar, A., Sandoz, J.-C., et al. (2012). Differential interactions of sex pheromone and plant odour in the olfactory pathway of a male moth. *PLoS ONE* 7:e33159. doi: 10.1371/journal.pone.0033159

Dekker, T., Ibba, I., Siju, K. P., Stensmyr, M. C., and Hansson, B. S. (2006). Olfactory shifts parallel superspecialism for toxic fruit in *Drosophila melanogaster* sibling, *D. sechellia*. *Curr. Biol.* 16, 101–109. doi: 10.1016/j.cub.2005.11.075

del Campo, M. L., Miles, C. I., Schroeder, F. C., Mueller, C., Booker, R., and Renwick, J. A. (2001). Host recognition by the tobacco hornworm is mediated by a host plant compound. *Nature* 411, 186–189. doi: 10.1038/35075559

De Moraes, C. M., Lewis, W. J., Pare, P. W., Alborn, H. T., and Tumlinson, J. H. (1998). Hervibore-infested plants selectively attract parasitoids. *Nature* 393, 570–573. doi: 10.1038/31219

De Moraes, C. M., Mescher, M. C., and Tumlinson, J. H. (2001). Caterpillar-induced nocturnal plant volatiles repel conspecific females. *Nature* 410, 577–580. doi: 10.1038/35069058

Dicke, M., and van Loop, J. J. A. (2000). Multitrophic effects of herbiovre-induced plant volatiles in an evolutionary context. *Entomol. Exp. App.* 97, 237–249. doi: 10.1046/j.1570-7458.2000.00736.x

Effmert, U., Dinse, C., and Piechulla, B. (2008). Influence of green leaf herbivory by *Manduca sexta* on floral volatile emission by *Nicotiana suaveolens*. *Plant Physiol.* 146, 1996–2007. doi: 10.1104/pp.107.112326

Ehrlich, P. R., and Raven, P. H. (1964). Butterflies and plants: a study in coevolution. *Evolution* 18, 586–608. doi: 10.2307/2406212

Emelianov, I., Simpson, F., Narang, P., and Mallet, J. (2003). Host choice promotes reproductive isolation between host races of the larch budmoth *Zeiraphera diniana*. *J. Evol. Biol.* 16, 208–218. doi: 10.1046/j.1420-9101.2003.00524.x

Fahrbach, S. E. (2006). Structure of the mushroom bodies of the insect brain. *Ann. Rev. Entomol.* 51, 209–232. doi: 10.1146/annurev.ento.51.110104.150954

Gao, Q., Yuan, B., and Chess, A. (2000). Convergent projections of *Drosophila* olfactory neurons to specific glomeruli in the antennal lobe. *Nat. Neurosci.* 3, 780–785. doi: 10.1038/75753

Gilbert, L. E. (1979). Development of theory in the analysis of insect–plant interactions. *Anal. Ecol. Syst.* 3, 117.

Glendinning, J. I. (2002). How do herbivorous insects cope with noxious secondary plant compounds in their diet? *Entomol. Exp. App.* 104, 15–25. doi: 10.1046/j.1570-7458.2002.00986.x

Glendinning, J. I., Davis, A., and Rai, M. (2006). Temporal coding mediates discrimination of "bitter" taste stimuli by an insect. *J. Neurosci.* 26, 8900–8908. doi: 10.1523/JNEUROSCI.2351-06.2006

Goyret, J. (2010). Look and touch: multimodal sensory control of flower inspection movements in the nocturnal hawkmoth *Manduca sexta*. *J. Exp. Biol.* 213, 3676–3682. doi: 10.1242/jeb.045831

Goyret, J., Markwell, P. M., and Raguso, R. A. (2008). Context- and scale-dependent effects of floral CO_2 on nectar foraging by *Manduca sexta*. *Proc. Natl. Acad. Sci. U.S.A.* 105, 4565–4570. doi: 10.1073/pnas.0708629105

Grimaldi, D., and Engel, M. S. (2005). Evolution of the Insects. New York, NY: Cambridge University Press.

Grosse-Wilde, E., Kuebler, L. S., Bucks, S., Vogel, H., Wicher, D., and Hansson, B. S. (2011). Antennal transcriptome of *Manduca sexta*. *Proc. Natl. Acad. Sci. U.S.A.* 108, 7449–7454. doi: 10.1073/pnas.1017963108

Große-Wilde, E., Stieber, R., Forstner, M., Krieger, J., Wicher, D., and Hansson, B. S. (2010). Sex-Specific odorant receptors of the tobacco hornworm *Manduca sexta*. *Front. Cell. Neurosci.* 4:22. doi: 10.3389/fncel.2010.00022

Guerenstein, P., Christensen, T. A., and Hildebrand, J. G. (2004). Sensory processing of ambient-CO_2 information in the brain of the moth *Manduca sexta*. *J. Comp. Physiol. A* 190, 707–725. doi: 10.1007/s00359-004-0529-0

Halitschke, R., Keßler, A., Kahl, J., Lorenz, A., and Baldwin, I. T. (2000). Ecophysiological comparison of direct and indirect defenses in *Nicotiana attenuata*. *Oecologia* 124, 408–417. doi: 10.1007/s004420000389

Hare, J. (2007). Variation in herbivore and methyl jasmonate-induced volatiles among genetic lines of *Datura wrightii*. *J. Chem. Ecol.* 33, 2028–2043. doi: 10.1007/s10886-007-9375-1

Hare, J. D., and Walling, L. L. (2006). Constitutive and jasmonate-inducible traits of *Datura wrightii*. *J. Chem. Ecol.* 32, 29–47. doi: 10.1007/s10886-006-9349-8

Hartlieb, E., Anton, S., and Hansson, B. S. (1997). Dose-dependent response characteristics of antennal lobe neurons in the male *Agrotis segetum* (Lepidoptera: Noctuidae). *J. Comp. Physiol. A* 181, 469–476. doi: 10.1007/s003590050130

Harvey, J. A., Malcicka, M., and Ellers, J. (2015). Integrating more biological and ecological realism into studies of multitrophic interactions. *Ecol. Entomol.* 40, 349–352. doi: 10.1111/een.12204

Heinbockel, T., Christensen, T. A., and Hildebrand, J. G. (1999). Temporal tuning of odor responses in pheromone-responsive projection neurons in the brain of the sphinx moth *Manduca sexta*. *J. Comp. Neurol.* 409, 1–12.

Heinbockel, T., Christensen, T. A., and Hildebrand, J. G. (2004). Representation of binary pheromone blends by glomerulus-specific olfactory projection neurons. *J. Comp. Physiol. A* 190, 1023–1037. doi: 10.1007/s00359-004-0559-7

Heil, M., and Ton, J. (2010). "Systemic resistance induction by vascular and airborne signaling," in *Progress in Botany 71*, eds U. Lüttge, W. Beyschlag, B. Burkhard, and D. Francis (Berlin; Heidelberg: Springer), 279–306.

Hillier, N., Kleineidam, C., and Vickers, N. J. (2006). Physiology and glomerular projections of olfactory receptor neurons on the antenna of female *Heliothis virescens* (Lepidoptera:Noctuidae) responsive to behaviorally relevant odors. *J. Comp. Physiol. A* 192, 199–219. doi: 10.1007/s00359-005-0061-x

Hillier, N. K., and Vickers, N. J. (2007). Physiology and antennal lobe projections of olfactory receptor neurons from sexually isomorphic sensilla on male

Heliothis virescens. *J. Comp. Physiol. A* 193, 649–663. doi: 10.1007/s00359-007-0220-3

Homberg, U., Christensen, T. A., and Hildebrand, J. G. (1989). Structure and function of the deutocerebrum in insects. *Ann. Rev. Entomol.* 34, 477–501. doi: 10.1146/annurev.en.34.010189.002401

Homberg, U., Montague, R. A., and Hildebrand, J. G. (1988). Anatomy of antennocerebral pathways in the brain of the sphinx moth *Manduca sexta*. *Cell Tissue Res.* 254, 255–281. doi: 10.1007/BF00225800

Ikeura, H., Kobayashi, F., and Hayata, Y. (2010). How do *Pieris rapae* search for Brassicaceae host plants? *Biochem. Syst. Ecol.* 38, 1199–1203. doi: 10.1016/j.bse.2010.12.007

Jaenike, J. (1978). On optimal oviposition behaviour in phytophagous insects. *Theor. Popul. Biol.* 14, 350–356. doi: 10.1016/0040-5809(78)90012-6

Jaenike, J. (1990). Host specialization in phytophagous insects. *Ann. Rev. Ecol. Syst.* 21, 243–273. doi: 10.1146/annurev.es.21.110190.001331

Kaczorowski, R. L., Seliger, A. R., Gaskett, A. C., Wigsten, S. K., and Raguso, R. A. (2012). Corolla shape vs. size in flower choice by a nocturnal hawkmoth pollinator. *Func. Ecol.* 26, 577–587. doi: 10.1111/j.1365-2435.2012.01982.x

Kaissling, K. E., Hildebrand, J. G., and Tumlinson, J. H. (1989). Pheromone receptor cells in the male moth *Manduca sexta*. *Arch. Insect Biochem. Physiol.* 10, 273–279. doi: 10.1002/arch.940100403

Kalberer, N. M., Reisenman, C. E., and Hildebrand, J. G. (2010). Male moths bearing transplanted female antennae express characteristically female behaviour and central neural activity. *J. Exp. Biol.* 213, 1272–1280. doi: 10.1242/jeb.033167

Kanzaki, R., and Shibuya, T. (1992). Long-lasting excitation of protocerebral bilateral neurons in the pheromone-processing pathways of the male moth *Bombyx mori*. *Brain Res.* 587, 211–215. doi: 10.1016/0006-8993(92)90999-P

Kanzaki, R., Arbas, A. E., and Hildebrand, J. G. (1991). Physiology and morphology of protocerebral olfactory neurons in the male moth *Manduca sexta*. *J. Comp. Physiol. A* 168, 281–298. doi: 10.1007/BF00198348

Kanzaki, R., Soo, K., Seki, Y., and Wada, S. (2003). Projections to higher olfactory centers from subdivisions of the antennal lobe macroglomerular complex of the male silkmoth. *Chem. Senses* 28, 113–130. doi: 10.1093/chemse/28.2.113

Karban, R., and Baldwin, I. T. (1997). Induced *Responses* to *Herbivory*. Chicago, IL: Chicago University Press. doi: 10.7208/chicago/9780226424972.001.0001

Kessler, A., and Baldwin, I. T. (2001). Defensive function of herbivore-induced plant volatile emissions in nature. *Science* 291, 2141–2144. doi: 10.1126/science.291.5511.2141

Kessler, A., and Halitschke, R. (2009). Testing the potential for conflicting selection on floral chemical traits by pollinators and herbivores: predictions and case study. *Func. Ecol.* 23, 901–912. doi: 10.1111/j.1365-2435.2009.01639.x

Kessler, D., and Baldwin, I. T. (2006). Making sense of nectar scents: the effects of nectar secondary metabolites on floral visitors of *Nicotiana attenuata*. *Plant J.* 49, 840–854. doi: 10.1111/j.1365-313X.2006.02995.x

Kessler, S. C., Tiedeken, E. J., Simcock, K. L., Derveau, S., Mitchell, J., Softley, S., et al. (2015). Bees prefer foods containing neonicotinoid pesticides. *Nature* 521, 74–76. doi: 10.1038/nature14414

Kester, K. M., Peterson, S. C., Hanson, F., Jackson, D. M., and Severson, R. F. (2002). The roles of nicotine and natural enemies in determining larval feeding site distributions of *Manduca sexta* L. and *Manduca quinquemaculata* (Haworth) on tobacco. *Chemoecology* 12, 1–10. doi: 10.1007/s00049-002-8320-6

Lavista-Llanos, S., Svatoš, A., Kai, M., Riemensperger, T., Birman, S., Stensmyr, M. C., et al. (2014). Dopamine drives *Drosophila sechellia* adaptation to its toxic host. *eLife* 3:e03785. doi: 10.7554/eLife.03785

Lee, J. K., and Strausfeld, N. J. (1990). Structure, distribution and number of surface sensilla and their receptor cells on the olfactory appendage of the male moth *Manduca sexta*. *J. Neurocytol.* 19, 519–538. doi: 10.1007/BF01257241

Lei, H., Chiu, H.-Y., and Hildebrand, J. G. (2013). Responses of protocerebral neurons in *Manduca sexta* to sex-pheromone mixtures. *J. Comp. Physiol. A*. 11, 997–1014. doi: 10.1007/s00359-013-0844-4

Lei, H., Christensen, T. A., and Hildebrand, J. G. (2002). Local inhibition modulates odor-evoked synchronization of glomerulus-specific output neurons. *Nat. Neurosci.* 5, 557–565. doi: 10.1038/nn0602-859

Lei, H., Christensen, T. A., and Hildebrand, J. G. (2004). Spatial and temporal organization of ensemble representations for different odor classes in the moth antennal lobe. *J. Neurosci.* 24, 11108–11119. doi: 10.1523/JNEUROSCI.3677-04.2004

Lei, H., and Hansson, B. S. (1999). Central processing of pulsed pheromone signals by antennal lobe neurons in the male moth *Agrotis segetum*. *J. Neurophysiol.* 81, 1113–1122.

Linn, C. Jr., Feder, J. L., Nojima, S., Dambroski, H. R., Berlocher, S. H., and Roelofs, W. L. (2003). Fruit odor discrimination and sympatric host race formation in *Rhagoletis*. *Proc. Natl. Acad. Sci. U.S.A.* 100, 11490–11493. doi: 10.1073/pnas.1635049100

Loughrin, J. H., Manukian, A., Heath, R. R., Turlings, T. C. J., and Tumlinson, J. H. (1994). Diurnal cycle of emission of induced volatile terpenoids by hervibore-injured cotton plants. *Proc. Natl. Acad. Sci. U.S.A.* 91, 11836–11840. doi: 10.1073/pnas.91.25.11836

Madden, A. H., and Chamberlin, F. S. (1945). *Biology of the Tobacco Hornworm in the Southern Cigar Tobacco District,* US Department of Agriculture Technical Bulletin.

Matsumoto, S. G., and Hildebrand, J. G. (1981). Olfactory mechanisms in the moth *Manduca sexta*: response characteristics and morphology of central neurons in the antennal lobes. *Proc. R. Soc. B Biol. Sci* 213, 249–277. doi: 10.1098/rspb.1981.0066

McCall, A. C., and Karban, R. (2006). Induced defense in *Nicotiana attenuata* (Solanaceae) fruit and flowers. *Oecologia* 146, 566–571. doi: 10.1007/s00442-005-0284-0

Mechaber, W. L., Capaldo, C. T., and Hildebrand, J. G. (2002). Behavioral responses of adult female tobacco hornworms, *Manduca sexta*, to hostplant volatiles change with age and mating status. *J. Insect Sci.* 2:5. doi: 10.1673/031.002.0501

Mechaber, W., and Hildebrand, J. G. (2000). Novel, non-solanaceous host-plant record for *Manduca sexta* (Lepidoptera: Sphingidae) in the southwestern United States. *Ann. Entomol. Soc. Am.* 93, 447–451. doi: 10.1603/0013-8746(2000)093[0447:NNSHRF]2.0.CO;2

Mira, A., and Bernays, E. A. (2002). Trade-offs in host use by *Manduca sexta*: plant characters vs natural enemies. *Oikos* 97, 387–397. doi: 10.1034/j.1600-0706.2002.970309.x

Mothershead, K., and Marquis, R. J. (2000). Fitness impacts of herbivory through indirect effects on plant-pollinator interactions in *Oenothera macrocarpa*. *Ecology* 81, 30–40. doi: 10.2307/177131

Namiki, S., and Kanzaki, R. (2011). Heterogeneity in dendritic morphology of moth antennal lobe projection neurons. *J. Comp. Neurol.* 519, 3367–3386. doi: 10.1002/cne.22754

Nunez-Farfan, J., Cabrales-Vargas, R. A., and Dirzo, R. (1996). Mating system consequences on resistance to herbivory and life history traits in *Datura stramonium*. *Am. J. Bot.* 83, 1041–1049. doi: 10.2307/2445993

Olsen, S. R., Bhandawat, V., and Wilson, R. I. (2007). Excitatory interactions between olfactory processing channels in the drosophila antennal lobe. *Neuron* 54, 89–103. doi: 10.1016/j.neuron.2007.03.010

Olsson, S. B., Linn, C. E. Jr., and Roelofs, W. L. (2006). The chemosensory basis for behavioral divergence involved in sympatric host shifts II: olfactory receptor neuron sensitivity and temporal firing pattern to individual key host volatiles. *J. Comp. Physiol. A* 192, 289–300. doi: 10.1007/s00359-005-0066-5

Paré, P. W., and Tumlinson, J. H. (1997). Induced synthesis of plant volatiles. *Nature* 385, 30–31. doi: 10.1038/385030a0

Paré, P. W., and Tumlinson, J. H. (1999). Plant volatiles as a defefnse against insect herbivores. *Plant Physiol.* 121, 325–331. doi: 10.1104/pp.121.2.325

Pareja, M., Qvarfordt, E., Webster, B., Mayon, P., Pickett, J., Birkett, M., et al. (2012). Herbivory by a phloem-feeding insect inhibits floral volatile production. *PLoS ONE* 7:e31971. doi: 10.1371/journal.pone.0031971

Raguso, R. R., Henzel, C., Buchmann, S. L., and Nabhan, G. P. (2003). Trumpet flowers of the sonoran desert: floral biology of *Peniocereus cacti* and sacred *Datura*. *Int. J. Plant Sci.* 164, 877–892. doi: 10.1086/378539

Raguso, R. R., and Willis, M. A. (2002). Synergy between visual and olfactory cues in nectar feeding by naive hawkmoths, *Manduca sexta*. *Anim. Behav.* 64, 685–695. doi: 10.1006/anbe.2002.4010

Ramaswamy, S. B. (1988). Host finding by moths: sensory modalities and behavior. *J. Insect Physiol.* 34, 235–249. doi: 10.1016/0022-1910(88)90054-6

Reisenman, C., Dacks, A., and Hildebrand, J. G. (2011). Local interneuron diversity in the primary olfactory center of the moth *Manduca sexta*. *J. Comp. Physiol. A* 197, 653–665. doi: 10.1007/s00359-011-0625-x

Reisenman, C. E., Christensen, T. A., Francke, W., and Hildebrand, J. G. (2004). Enantioselectivity of projection neurons innervating identified olfactory glomeruli. *J. Neurosci.* 24, 2602–2611. doi: 10.1523/JNEUROSCI.5192-03.2004

Reisenman, C. E., Christensen, T. A., and Hildebrand, J. G. (2005). Chemosensory selectivity of output neurons innervating an identified, sexually isomorphic olfactory glomerulus. *J. Neurosci.* 25, 8017–8026. doi: 10.1523/JNEUROSCI.1314-05.2005

Reisenman, C. E., Heinbockel, T., and Hildebrand, J. G. (2008). Inhibitory interactions among olfactory glomeruli do not necessarily reflect spatial proximity. *J. Neurophys.* 100, 554–564. doi: 10.1152/jn.90231.2008

Reisenman, C. E., Riffell, J. A., Bernays, E. A., and Hildebrand, J. G. (2010). Antagonistic effects of floral scent in an insect-plant interaction. *Proc. R. Soc. Lond. B Biol.* 277, 2371. doi: 10.1098/rspb.2010.0163

Reisenman, C. E., Riffell, J. A., Duffy, K., Pesque, A., Mikles, D., and Goodwin, B. (2013). Species-specific effects of herbivory on the oviposition behavior of the moth *Manduca sexta*. *J. Chem. Ecol.* 39, 76–89. doi: 10.1007/s10886-012-0228-1

Renwick, J. A. A., and Chew, F. S. (1994). Oviposition behavior in Lepidoptera. *Ann. Rev. Entomol.* 39, 377–400. doi: 10.1146/annurev.en.39.010194.002113

Riffell, J. A., Abrell, L., and Hildebrand, J. G. (2008a). Physical processes and real-time chemical measurement of the insect olfactory environment. *J. Chem. Ecol.* 34, 837–853. doi: 10.1007/s10886-008-9490-7

Riffell, J. A., and Alarcón, R. (2013). Multimodal floral signals and moth foraging decisions. *PLoS ONE* 8:e72809. doi: 10.1371/journal.pone.0072809

Riffell, J. A., Alarcón, R., Abrell, L., Bronstein, J., Davidowitz, G., and Hildebrand, J. G. (2008b). Behavioral consequences of innate preferences and olfactory learning in hawkmoth-flower interactions. *Proc. Natl. Acad. Sci. U.S.A.* 105, 3404–3409. doi: 10.1073/pnas.0709811105

Riffell, J. A., Lei, H., Christensen, T. A., and Hildebrand, J. G. (2009a). Characterization and coding of behaviorally significant odor mixtures. *Curr. Biol.* 19, 335–340. doi: 10.1016/j.cub.2009.01.041

Riffell, J. A., Lei, H., and Hildebrand, J. G. (2009b). Neural correlates of behavior in the moth *Manduca sexta* in response to complex odors. *Proc. Natl. Acad. Sci. U.S.A.* 106, 19219–19226. doi: 10.1073/pnas.0910592106

Roche King, J., Christensen, T. A., and Hildebrand, J. G. (2000). Response characteristics of an identified, sexually dimorphic olfactory glomerulus. *J. Neurosci.* 20, 2391–2399.

Röse, U. S. , and Tumlinson, J. H. (2004). Volatiles released from cotton plants in response to *Helicoverpa zea* feeding damage on cotton flower buds. *Planta* 218, 824–832. doi: 10.1007/s00425-003-1162-9

Rospars, J. P., and Hildebrand, J. G. (1992). Anatomical identification of glomeruli in the antennal lobes of the male sphinx moth *Manduca sexta*. *Cell Tissue Res.* 270, 205–227. doi: 10.1007/BF00328007

Rospars, J. P., and Hildebrand, J. G. (2000). Sexually dimorphic and isomorphic glomeruli in the antennal lobes of the sphinx moth *Manduca sexta*. *Chem. Senses* 25, 119–129. doi: 10.1093/chemse/25.2.119

Rouyar, A., Deisig, N., Dupuy, F., Limousin, D., Wycke, M.-A., Renou, M., et al. (2015). Unexpected plant odor responses in a moth pheromone system. *Front. Physiol.* 6:148. doi: 10.3389/fphys.2015.00148

Sakata, Y., Yamasaki, M., Isagi, Y., and Ohgushi, T. (2014). An exotic herbivorous insect drives the evolution of resistance in the exotic perennial herb *Solidago altissima*. *Ecology* 95, 2569–2578. doi: 10.1890/13-1455.1

Schnee, C., Köllner, T. G., Held, M., Turlings, T. C. J., Gershenzon, J., and Degenhardt, J. (2006). The products of a single maize sesquiterpene synthase form a volatile defense signal that attracts natural enemies of maize herbivores. *Proc. Natl. Acad. Sci. U.S.A.* 103, 1129–1134. doi: 10.1073/pnas.0508027103

Schneiderman, A. M., Hildebrand, J. G., Brennan, M. M., and Tumlinson, J. H. (1986). Trans-sexually grafted antennae alter pheromone-directed behaviour in a moth. *Nature* 323, 801–803. doi: 10.1038/323801a0

Schoonhoven, L. M., van Loon, J. J. A., and Dicke, M. (2005). *Insect-plant Biology*. Oxford: Oxford University Press.

Seki, Y., and Kanzaki, R. (2008). Comprehensive morphological identification and GABA immunocytochemistry of antennal lobe local interneurons in *Bombyx mori*. *J. Comp. Neurol.* 506, 93–107. doi: 10.1002/cne.21528

Shields, V. D., and Hildebrand, J. G. (2001). Responses of a population of antennal olfactory receptor cells in the female moth *Manduca sexta* to plant-associated volatile organic compounds. *J. Comp. Physiol. A* 186, 1135–1151. doi: 10.1007/s003590000165

Singaravelan, N., Nee'man, G., Inbar, M., and Izhaki, I. (2005). Feeding responses of free-flying honeybees to secondary compounds mimicking floral nectars. *J. Chem. Ecol.* 31, 2791–2804. doi: 10.1007/s10886-005-8394-z

Sparks, M. R. (1969). A surrogate leaf for oviposition by the tobacco hornworm. *J. Econ. Entomol.* 63, 537–540. doi: 10.1093/jee/63.2.537

Sparks, M. R. (1973). Physical and chemical stimuli affecting oviposition preference of *Manduca sexta* (Lepidoptera: Sphingidae). *Ann. Entomol. Soc. Am.* 66, 571–573. doi: 10.1093/aesa/66.3.571

Späthe, A., Reinecke, A., Olsson, S. B., Kesavan, S., Knaden, M., and Hansson, B. S. (2013). Plant species- and status-specific odorant blends guide oviposition choice in the moth *Manduca sexta*. *Chem. Senses* 38, 147–159. doi: 10.1093/chemse/bjs089

Strauss, S. Y., and Agrawal, A. A. (1999). The ecology and evolution of plant tolerance to herbivory. *Trends Ecol. Evol.* 14, 179–185. doi: 10.1016/S0169-5347(98)01576-6

Sun, X. J., Tolbert, L. P., and Hildebrand, J. G. (1997). Synaptic organization of the uniglomerular projection neurons of the antennal lobe of the moth *Manduca sexta*: a laser scanning confocal and electron microscopy study. *J. Comp. Neurol.* 379, 2–20.

Syed, Z., Guerin, P. M., and Baltensweiler, W. (2003). Antennal responses of the two host races of the larch bud moth, *Zeiraphera diniana*, to larch and cembran pine volatiles. *J. Chem. Ecol.* 29, 1691–1708. doi: 10.1023/A:1024287117128

Thiery, D., and Visser, J. H. (1986). Masking of host plant odour in the olfactory orientation of the colorado potato beetle. *Entomol. Exp. App.* 41, 165–172. doi: 10.1111/j.1570-7458.1986.tb00524.x

Thom, C., Guerenstein, P. G., Mechaber, W. L., and Hildebrand, J. G. (2004). Floral CO_2 reveals flower profitability to moths. *J. Chem. Ecol.* 30, 1285–1288. doi: 10.1023/B:JOEC.0000030298.77377.7d

Tichenor, L. H., and Seigler, D. S. (1980). Electroantennogram and oviposition responses of *Manduca sexta* to volatile components of tobacco and tomato. *J. Insect Physiol.* 26, 309–314. doi: 10.1016/0022-1910(80)90139-0

Tolbert, L. P., and Hildebrand, J. G. (1981). Organization and synaptic ultrastructure of glomeruli in the antennal lobes of the moth *Manduca sexta*: a study using thin sections and freeze-fracture. *Proc. R. Soc. Lond. B. Biol.* 213, 279–301. doi: 10.1098/rspb.1981.0067

Trona, F., Anfora, G., Balkenius, A., Bengtsson, M., Tasin, M., Knight, A., et al. (2013). Neural coding merges sex and habitat chemosensory signals in an insect herbivore. *Proc. R. Soc. Lond. B. Biol.* 280:20130267. doi: 10.1098/rspb.2013.0267

Turlings, T. C. J., Bernasconi, M. L., Bertossa, R., Bigler, F., Caloz, G., and Dorn, S. (1998). The induction of volatile emissions in maize by three herbivore species with different feeding habits: possible consequences for their natural enemies. *Biol. Control* 11, 122–129. doi: 10.1006/bcon.1997.0591

Uesugi, A., and Kessler, A. (2013). Herbivore exclusion drives the evolution of plant competitiveness via increased allelopathy. *New Phytol.* 198, 916–924. doi: 10.1111/nph.12172

Ulland, S., Ian, E., Borg-Karlson, A. K., and Mustaparta, H. (2006). Discrimination between enantiomers of linalool by olfactory receptor neurons in the cabbage moth *Mamestra brassicae*. *Chem. Senses* 31, 325–334. doi: 10.1093/chemse/bjj036

Ulland, S., Ian, E., Stranden, M., Borg-Karlson, A.-K., and Mustaparta, H. (2008). Plant volatiles activating specific olfactory receptor neurons of the cabbage moth *Mamestra brassicae* L. (Lepidoptera, Noctuidae). *Chem. Senses* 33, 509–522. doi: 10.1093/chemse/bjn018

Varela, N., Avilla, J., Gemeno, C., and Anton, S. (2011). Ordinary glomeruli in the antennal lobe of male and female tortricid moth *Grapholita molesta* (Busck) (Lepidoptera: Tortricidae) process sex pheromone and host-plant volatiles. *J. Exp. Biol.* 214, 637–645. doi: 10.1242/jeb.047316

Vickers, N. J., and Christensen, T. A. (2003). Functional divergence of spatially conserved olfactory glomeruli in two related moth species. *Chem. Senses* 28, 325–338. doi: 10.1093/chemse/28.4.325

Vosshall, L. B., Wong, A. M., and Axel, R. (2000). An olfactory sensory map in the fly brain. *Cell* 102, 147–159. doi: 10.1016/S0092-8674(00)00021-0

Whiteman, N. K., and Jander, G. (2010). Genome-enabled research on the ecology of plant-insect interactions. *Plant Physiol.* 154, 475–478. doi: 10.1104/pp.110.161117

Williamson, S. M., and Wright, G. A. (2013). Exposure to multiple cholinergic pesticides impairs olfactory learning and memory in honeybees. *J. Exp. Biol.* 216, 1799–1807. doi: 10.1242/jeb.083931

Willis, M. A., and Arbas, E. A. (1991). Odor-modulated upwind flight of the sphinx moth, *Manduca sexta* L. *J. Comp. Physiol. A* 169, 427–440. doi: 10.1007/BF00197655

Xu, H., Li, G., Liu, M., and Xing, G. (2006). Oviposition deterrents in larval frass of the cotton boll worm, *Helicoverpa armigera* (Lepidoptera: Noctuidae): chemical identification and electroantennography analysis. *J. Insect Physiol.* 52, 320–326. doi: 10.1016/j.jinsphys.2005.11.011

Yamamoto, R. T., and Fraenkel, G. S. (1960). The specificity of the tobacco hornworm, *Protoparce sexta*, to solanaceous plants. *Ann. Entomol. Soc. Am.* 53, 503–507. doi: 10.1093/aesa/53.4.503

Yamamoto, R. T., Jenkins, R. Y., and McClusky, R. K. (1969). Factors determining the selection of plants for oviposition by the tobacco hornworm *Manduca sexta*. *Entomol. Exp. App.* 12, 504–508. doi: 10.1111/j.1570-7458.1969.tb02548.x

Zhang, A. J., Linn, C., Wright, S., Propoky, R., Reissig, W., and Roelofs, W. (1999). Identification of a new blend of apple volatiles attractive to apple maggot, *Rhagoletis pomonella*. *J. Chem. Ecol.* 25, 1221–1232. doi: 10.1023/A:1020910305873

Conflict of Interest Statement: The authors declare that the research was conducted in the absence of any commercial or financial relationships that could be construed as a potential conflict of interest.

frontiers in Physiology

REVIEW
published: 30 June 2016
doi: 10.3389/fphys.2016.00271

Neuroethology of Olfactory-Guided Behavior and Its Potential Application in the Control of Harmful Insects

Carolina E. Reisenman[1], *Hong Lei*[2†] *and Pablo G. Guerenstein*[3,4*]

[1] Department of Molecular and Cell Biology and Essig Museum of Entomology, University of California, Berkeley, Berkeley, CA, USA, [2] Department of Neuroscience, University of Arizona, Tucson, AZ, USA, [3] Lab. de Estudio de la Biología de Insectos, CICyTTP-CONICET, Diamante, Argentina, [4] Facultad de Ingeniería, Universidad Nacional de Entre Ríos, Oro Verde, Argentina

Harmful insects include pests of crops and storage goods, and vectors of human and animal diseases. Throughout their history, humans have been fighting them using diverse methods. The fairly recent development of synthetic chemical insecticides promised efficient crop and health protection at a relatively low cost. However, the negative effects of those insecticides on human health and the environment, as well as the development of insect resistance, have been fueling the search for alternative control tools. New and promising alternative methods to fight harmful insects include the manipulation of their behavior using synthetic versions of "semiochemicals", which are natural volatile and non-volatile substances involved in the intra- and/or inter-specific communication between organisms. Synthetic semiochemicals can be used as trap baits to monitor the presence of insects, so that insecticide spraying can be planned rationally (i.e., only when and where insects are actually present). Other methods that use semiochemicals include insect annihilation by mass trapping, attract-and- kill techniques, behavioral disruption, and the use of repellents. In the last decades many investigations focused on the neural bases of insect's responses to semiochemicals. Those studies help understand how the olfactory system detects and processes information about odors, which could lead to the design of efficient control tools, including odor baits, repellents or ways to confound insects. Here we review our current knowledge about the neural mechanisms controlling olfactory responses to semiochemicals in harmful insects. We also discuss how this neuroethology approach can be used to design or improve pest/vector management strategies.

Keywords: crop pest, disease vector, integrated pest management, odor attractant, disruption of behavior, odor repelllent, insect neuroethology

OPEN ACCESS

Edited by:
Sylvia Anton,
Institut National de la Recherche Agronomique, France

Reviewed by:
Rickard Ignell,
Swedish University of Agricultural Sciences, Sweden
Andrey Nikolaevich Frolov,
All-Russian Research Institute of Plant Protection, Russia

****Correspondence:***
Pablo G. Guerenstein
pguerenstein@bioingenieria.edu.ar

†Present Address:
Hong Lei,
School of Life Sciences, Arizona State University, Tempe, AZ, USA

Specialty section:
This article was submitted to Invertebrate Physiology, a section of the journal Frontiers in Physiology

Received: *02 February 2016*
Accepted: *16 June 2016*
Published: *30 June 2016*

Citation:
Reisenman CE, Lei H and Guerenstein PG (2016) Neuroethology of Olfactory-Guided Behavior and Its Potential Application in the Control of Harmful Insects. Front. Physiol. 7:271. doi: 10.3389/fphys.2016.00271

INTRODUCTION

Humans benefit from insects, mainly as pollinators of crops, but an important number of other insects are pests of crops or damage storage goods, are vectors of serious human and animal diseases, or are simply a nuisance. For centuries, humans have been fighting harmful insects, and the use of synthetic or genetically modified plant-produced chemical insecticides has made this fight much more efficient. However, the use and overuse of those chemicals has led to a number of undesirable consequences, such as contamination of our environment, food and water,

and insecticide resistance. In addition, the rising of the organic agriculture movement demands insecticide-free food (van der Goes van Naters and Carlson, 2006).

Chemicals other than insecticides can be used to fight insects through the manipulation of specific olfactory behaviors, profiting from the existence of natural compounds used for communication between organisms, the semiochemicals (Pickett et al., 1997). Pheromones are perhaps the most well-known class of semiochemicals. Pheromones mediate interactions between organisms of the same species, and include, sex, aggregation, and alarm substances, while allelochemicals are semiochemicals that mediate inter-specific interactions (see Dusenbery, 1992; Wyatt, 2003 for further details).

The potential use of semiochemicals to monitor, disrupt, lure, repel, confuse, or mass-trap insect pests was rapidly acknowledged and has fueled much research (Wyatt, 2003; Witzgall et al., 2010) with the promise of clean, safe, and highly specific pest and vector control tools. For instance, mating disruption, in which large amounts of a synthetic sex pheromone are released in a crop, has been used to eradicate insect pests that became resistant to pesticides (Wyatt, 2003; Witzgall et al., 2010). Semiochemicals can also be used for trapping insects in integrated pest and vector control management strategies. Thus, when trapping devices include insecticides, insects attracted to a semiochemical also pick up lethal substances or pathogens (a strategy known as "lure and kill"; Pickett et al., 1997; Wyatt, 2003).

In the last decades, many studies focused on the neural mechanisms underlying behavioral responses to semiochemicals. These investigations aid the design of odor-based strategies for insect control, as they help understanding how the olfactory system processes information about odors and also allow generating predictions about the insect's olfactory behavior (e.g., Hildebrand, 1996; Guerenstein and Hildebrand, 2008). Unfortunately, research in the fields of neuroethology and insect control has been often segregated, which may hamper the development of novel and efficient control tools and strategies. In light of this, here we review our current knowledge about the neural mechanisms controlling olfactory responses to semiochemicals in harmful insects, and also discuss how this neuroethology approach can be used to manipulate insect behavior and therefore improve pest/vector management strategies. We start by briefly summarizing the structure and function of the insect olfactory system.

THE INSECT OLFACTORY SYSTEM

Olfactory receptor cells (ORCs) are the first neural elements in the olfactory pathway and are housed in variable numbers in hair-like, multi-porous structures known as olfactory sensilla. Olfactory sensilla are located mainly on the antennae and in some insects also in the mouthparts. After entering the sensillum through its wall pores, odors diffuse in the aqueous sensillum lymph (sometimes transported by odorant binding proteins, Vogt and Riddiford, 1981; Tsuchihara et al., 2005; Leal, 2013) and reach the dendrites of the ORCs. There, odors interact with different classes of chemoreceptor proteins: odorant receptors (ORs), ionotropic receptors (IRs), or gustatory receptors (GRs; Vosshall et al., 1999; Larsson et al., 2004; Vosshall and Stocker, 2007; Vosshall and Hansson, 2011; Suh et al., 2014). Many ORCs respond to only one or a few related odor compounds, particularly when tested at behaviorally relevant and naturally-occurring concentrations, but others are more broadly tuned (e.g., de Bruyne et al., 1999; Hansson et al., 1999; Stranden et al., 2003; Yao et al., 2005; Hallem and Carlson, 2006; Martelli et al., 2013). In all cases their response spectra depends on the odor tuning of the chemoreceptor protein/s expressed (e.g., Hallem and Carlson, 2006; Andersson et al., 2015). Each type of ORC usually expresses only one type of OR, IR, or GR (e.g., Vosshall et al., 1999; Galizia and Sachse, 2010). However, in some ORCs more than one OR, IR, or GR types, and even different chemoreceptor protein types (most commonly ORs and IRs), are co-expressed, and in those cases odors interact with more than one chemoreceptor protein type (e.g., Fishilevich and Vosshall, 2005; Abuin et al., 2011; Rytz et al., 2013; Hussain et al., 2016; see below).

Odorant receptors are usually expressed in ORCs within single-walled (basiconic or trichoid) sensilla. They are part of a heteromeric complex consisting of an OR-subunit which binds the odor ligand (thus conferring odor specificity) and the highly conserved OR co-receptor (ORCO). Experimental evidence suggests alternative mechanisms of odor activation, one in which OR-ORCO forms a non-selective ligand-activated cation channel, and the other in which ORCO itself functions as a cation channel (Sato et al., 2008; Wicher et al., 2008). Although ORCO orthologs exist in many insect species, to date there is no agreement on how ORCO functions during olfactory transduction *in vivo* (Stengl and Funk, 2013).

ORCs that respond to compounds such as ammonia, short chain carboxylic acids and amines are housed in double-walled (grooved peg and coeloconic) sensilla (Pappenberger et al., 1996; Diehl et al., 2003; Benton et al., 2009; Hussain et al., 2016) and do not express ORs but instead IRs. The IRs form ionic channels activated by ligands (Benton et al., 2009) and are expressed with one or two broadly expressed co-receptors different from ORCO (Abuin et al., 2011; Ai et al., 2013; Rytz et al., 2013). In addition, the very volatile molecule CO_2, which is of primordial importance for the olfactory orientation of blood-sucking insects and some herbivores (Guerenstein and Hildebrand, 2008), is detected by two to three members of the GR family co-expressed in a single ORC type (Suh et al., 2004; Jones et al., 2007; Kwon et al., 2007; Lu et al., 2007; Kent et al., 2008; Wang et al., 2013).

The axons of the ORCs project to the first processing center of olfactory information in the insect brain, the antennal lobe (AL; e.g., Anton and Homberg, 1999). The AL, analogous to the vertebrate olfactory bulb, is composed of distinct spheroid structures called glomeruli (Anton and Homberg, 1999; Fishilevich and Vosshall, 2005). Usually, the terminals of ORCs expressing the same chemoreceptor protein converge onto a single glomerulus (Vosshall et al., 2000; Guerenstein et al., 2004a; Rytz et al., 2013; Suh et al., 2014; Hussain et al., 2016). Each glomerulus also houses neurites of local interneurons (LNs) and

of projection neurons (PNs). LNs are restricted to the AL and have dendritic arborizations in several glomeruli; PNs usually arborize in one glomerulus and have an axon that projects to higher brain areas in the protocerebrum such as the lateral horn, the inferior lateral PC, and the calyces of the ipsilateral mushroom body (Homberg et al., 1988, 1989; Jefferis et al., 2007; Galizia and Rössler, 2010; Tanaka et al., 2012; Roussel et al., 2014). Neurons in these higher-order brain centers show diverse responses and integrate information about different odor compounds (e.g., Jefferis et al., 2007; Turner et al., 2008; Gupta and Stopfer, 2012; Lei et al., 2013); neurons receiving input from the mushroom body calyces are involved in mediating learning and memory processes (e.g., Davis, 2004; Fahrbach, 2006; Liu et al., 2012). Further downstream, circuits in the lateral accessory lobe and the ventral protocerebrum have been linked, particularly in moths, to important aspects of olfactory behaviors (e.g., Olberg, 1983; Iwano et al., 2010).

In the next sections we review current knowledge about the neural and behavioral mechanisms underlying responses to diverse classes of pheromones, host odors, and plant volatiles, mechanisms of olfactory repellence, disruption of olfactory behavior, and the effects of experience and learning in olfactory-driven behaviors.

OLFACTORY ATTRACTION FOR MONITORING AND TRAPPING

Use of Sex Pheromones

Pheromones are usually mixtures of several compounds. Thus, the development of synthetic pheromone-blend attractants as trap lures involves knowledge of the compound identities, their concentrations, and their relative proportions. In several sympatric moth species, females release sex pheromones of overlapping chemical composition but with species-specific compound ratios, suggesting that males use this information to find conspecific females. For instance, different strains of the European corn borer (*Ostrinia nubilalis*) are attracted to precise pheromone blend ratios (Klun et al., 1973). Similarly, different species of *Yponomeuta* moths, which feed on the same host and share the same three pheromone constituents, are reproductively isolated due to differential attraction to species-specific blend ratios (Löfstedt et al., 1991). Similar findings were also reported on aphids (Dewhirst et al., 2010) and plant bugs (Byers et al., 2013). While the importance of ratios is crucial for the design of trap lures, the neural mechanisms underlying this phenomenon just began to be understood (e.g., Martin et al., 2013).

Sex pheromones can be used for monitoring and trapping many insect species. While we review and discuss what is known across different insect species, much is known about the neurobiological bases of mate seeking and finding in the moth *Manduca sexta*. Knowledge gained through studies in this insect could be applied to other insect-pest species, particularly other moths, as it is likely that similar neural mechanisms underlie mate odor-guided seeking behavior.

In moths and cockroaches, information about the female sex pheromone is processed by a small number of male-specific AL glomeruli forming a distinct structure, the macroglomerular complex (MGC; e.g., Boeckh and Boeckh, 1979; Hildebrand et al., 1980). Although the MGC sub-system of moths is distinctive and particularly large, the synaptic organization and structure of its constituent glomeruli is akin to that of the rest of the AL glomeruli. In some moth species, each MGC glomerulus processes a cognate pheromone component (e.g., *Heliothis virescens*; Berg et al., 1998), but in other species multiple components are encoded in the same MGC subcompartment (e.g., *Spodoptera littoralis*; Anton and Hansson, 1995). In other cases, pheromones and plant odorants are processed by the same MGC neurons (e.g., *Agrotis ipsilon*; Rouyar et al., 2015). Given this complexity, the use of simpler model systems (e.g., see next) can be experimentally advantageous and help the discovery of common, basic principles underlying the processing of complex odor blends.

The MGC of *M. sexta* has two main glomeruli, the Cumulus and the Toroid, each processing information about one of the two major female sex pheromone blend components (Hansson et al., 1991, 1992; Heinbockel et al., 1999). Because only these two components (out of eight total) are required to elicit odor-induced orientation behaviors in males (Tumlinson et al., 1989), this provides a simple binary system to investigate the neural mechanisms mediating pheromone processing, including blend ratio processing. When males are stimulated with the pheromone blend, two distinct populations of ORCs are specifically activated by those two essential components, one evoking excitatory responses in Cumulus projection neurons (cPNs) and the other in Toroid projection neurons (tPNs; Kaissling et al., 1989; Hansson et al., 1992; Hildebrand, 1996; Heinbockel et al., 1999; Lei et al., 2002). Additionally, recent findings suggest that cPNs and tPNs correlate their synaptic output to signal the presence of the pheromone blend (Lei et al., 2013; Martin et al., 2013). In principle, the odor-evoked spiking activity of cPNs and tPNs could serve to report the chemical identity and concentration of each blend component. However, since their outputs converge in the same regions in the protocerebrum (the delta region of the lateral horn and the mushroom body calyces), the relative timing of input spikes from cPNs and tPNs in postsynaptic neurons may have a physiological effect, that is, coincident spikes would evoke a stronger response in postsynaptic neurons than sequential spikes, allowing the representation of an odor mixture as a single odor object (see also Section Effects of Background Odor).

Indeed, using simultaneous dual-electrode intracellular recordings, Lei et al. (2002) showed inter- and intra-glomerular spike synchrony among PNs in response to pheromone blend stimulation. Odor-induced interglomerular synchrony in the AL was also reported in cockroaches using voltage-sensitive-dye imaging methods, suggesting that the synchrony code operates at a broad spatial scale (Watanabe, 2012). Moreover, experiments that simultaneously recorded neuronal activity across the glomerular array in *M. sexta* showed that neurons with the most similar odor response profiles produced the highest degree of coincident spikes (Lei et al., 2004). These results support the notion that PNs may use a correlative neural code. In addition, local field potential oscillations in the mushroom bodies, which

are thought to reflect evolving ensemble synchrony of PNs across the entire array of AL glomeruli, were reported in many insect species, including locusts, fruit flies, and moths (MacLeod and Laurent, 1996; Ito et al., 2009; Tanaka et al., 2009). Further, it has been shown that spike coincidence in *M. sexta* AL neurons is modulated by the pheromone blend ratio. Behaviorally, the moths respond best to the mixture of the two essential pheromone components at the naturally occurring 1:2 ratio, and deviations from this ratio deteriorate blend attractiveness (Martin et al., 2013). By stimulating AL neurons with varying blend ratios while simultaneously recording the activity of PN pairs, it was shown that MGC-PNs produce peak correlations at the natural 1:2 blend ratio, and those correlations significantly deteriorate in response to stimulation with behaviorally sub-optimal blend proportions (Martin et al., 2013). Such stimulus-quality-affected correlations in the PN spikes were also reported for glomeruli other than those of the MGC, in experiments that manipulated the ratios of naturally-occurring hostplant blends (Riffell et al., 2009a).

The mechanisms determining spike correlations are unknown, but balanced inhibition may be involved. Upon pheromonal stimulation, both PNs and LNs are activated, with cPNs and tPNs excited by their cognate pheromone constituents and reciprocally inhibited through GABAergic LNs (Lei et al., 2002). LNs likely respond in a dose-dependent manner, allowing the inhibitory effect exerted onto PNs to be modulated by the relative proportion of the blend constituents. Moreover, the degree of spike coincidence between PNs is positively correlated with the strength of the inhibitory input onto those PNs (Lei et al., 2002). Similarly, in the AL of cockroaches, GABAergic LNs also mediate synchronization of PN outputs (Watanabe, 2012). Thus, balanced lateral inhibition is a plausible mechanism by which stimulation with a pheromone blend of optimal ratio can produce the highest degree of correlated spikes in PNs. These ideas are yet to be experimentally confirmed, but have already been explored to some extent in a modeling study (Zavada et al., 2011). Given the diversity of LNs in the AL (Wilson and Laurent, 2005; Seki and Kanzaki, 2008; Reisenman et al., 2011), lateral inhibition may involve particular LN types. Indeed, a recent study on the silkmoth *B. mori* revealed the existence of both spiking and non-spiking LNs, and showed that non-spiking LNs can inhibit PNs (Tabuchi et al., 2015). Some of these effects may be species-specific, as spiking LNs in the AL of the cockroach *Periplaneta americana* can inhibit PNs (Warren and Kloppenburg, 2014), while non-spiking LNs (at least those surveyed) do not (Husch et al., 2009).

If the observed spike correlations are meaningful, then the correlated code should be read by postsynaptic neurons. Indeed, although rare, some lateral horn protocerebral neurons, which are known to receive direct input from AL neurons and thought to mostly mediate innate behaviors (e.g., Homberg et al., 1989; Anton and Homberg, 1999; Jefferis et al., 2007; Galizia and Rössler, 2010; Roussel et al., 2014; Kohl et al., 2015), produce the strongest response to the two-component pheromone blend presented at the naturally occurring ratio (Lei et al., 2013). Such correlation hypothesis is also supported by a recent study in *Drosophila melanogaster*. The odor-evoked spikes of PNs innervating a particular glomerulus (DA1) are highly correlated and provide converging input to their target neurons in the lateral horn (Jeanne and Wilson, 2015). Although the ligand of DA1-PNs is a single pheromone compound (cis-vaccenyl acetate), these experiments demonstrate that synchrony between PNs (arborizing in the same glomerulus in this case) occur, and could be related to coincident detection in post-synaptic neurons (Jeanne and Wilson, 2015). The identity of other *Drosophila* volatile pheromone compounds, and their processing circuits, were recently reported, although it is not yet known which mixtures are behaviorally significant in this species (Dweck et al., 2015).

In summary, both behavioral and neurobiological data indicate that not just the identity of the sex pheromone constituents, but also the constituents' ratios, are of paramount importance in mediating natural behavior. The neural mechanisms underlying the coding of ratios, particularly at the higher brain level, are still not fully understood. Because responses to sex pheromone mixtures are often species-specific, those mixtures represent an effective way to control specific species, which is much preferable to the use of insecticides as these often affect non-target species.

Use of Other Pheromones

In this section we focus on aggregation and alarm pheromones, since those are the only non-sex pheromone types that have been used to manipulate olfactory behavior. We will briefly review what is known for the major groups of harmful insects.

Aggregation pheromones promote conglomerates of individuals and are ubiquitous among arthropods, including many harmful species of beetles, moths, thrips, triatomines, locusts, mosquitoes, sand flies, and ticks (Wertheim et al., 2005; Sonenshine, 2006; Cook et al., 2007; Lorenzo Figueiras et al., 2009). Often, the decay, fermentation and pathogenesis associated with insect aggregations are the cause of important economic damage to crops and goods (Wertheim et al., 2005; van der Goes van Naters and Carlson, 2006). For instance, all throughout North America pine forests have been succumbing to massive bark beetle infestations that destroyed expanse forests and increase the risks of mudslides and forest fires (Chapman et al., 2012; Raffa et al., 2013). Beetle aggregation pheromones have been used for monitoring and mass-trapping, and also to recruit large number of insects on trap trees that are then destroyed (see Cook et al., 2007 for a review). A recent study used single-sensillum recordings to investigate the odor response profiles of ORCs in both sexes of the brown spruce longhorn beetle *Tetropium fuscum*. Interestingly, it was found that the responses to aggregation pheromones and plant volatiles are not completely segregated and can be synergized by the presence of volatiles indicative of host stress (MacKay et al., 2015).

While in general aggregation pheromones attract both sexes (Wertheim et al., 2005), in some species gravid females are attracted to a pheromone that induces aggregated oviposition. For instance, females of the sandfly *Lutzomia longipalpis*, which transmit leshmaniasis, use an oviposition aggregation pheromone which benefits the offspring of unrelated individuals by preventing fungal contamination of larval food (Wertheim

et al., 2005). *Culex quinquefasciatus* gravid females, which are vectors of filariasis and West Nile Virus (among others), are attracted to a pheromone released from maturing eggs in conjunction with an indole compound derived from grass infusions (Mboera et al., 2000; Logan and Birkett, 2007), and these components evoke electrophysiological activity from antennal ORCs (Mordue et al., 1992; Blackwell et al., 1993). In other non-insect arthropods such as ticks, which transmit Lyme disease, fecal components promote arrestment and aggregation, and tarsi contact chemoreceptors respond to some of these components (e.g., guanine) with extremely high sensitivity (Grenacher et al., 2001; Sonenshine, 2006). Such information about the most effective bioactive components can have practical applications for tick control. For instance, aggregation pheromones can be used together with an acaricide that when applied to vegetation or livestock kills ticks upon contact (Sonenshine, 2006).

Alarm pheromones inform or alert a conspecific about impending danger; they are highly volatile, disperse quickly, and do not persist long (see Napper and Pickett, 2008 for a review). They are released by a variety of glands and include compounds belonging to different chemical classes (e.g., terpenes, hydrocarbons, nitrogen compounds). In blood-sucking insects, alarm pheromones could be used as repellents. Bed bugs release alarm pheromones in response to injury and ant attacks, causing conspecifics to disperse (Levinson et al., 1974a). This alarm pheromone is species-specific to a certain extent, and consists of two major components detected by antennal sensilla (Levinson et al., 1974b; Reinhardt and Siva-Jothy, 2007; Olson et al., 2009). When disturbed, adult triatomines release an alarm pheromone mainly composed of isobutyric acid that repels conspecifics (Guerenstein and Guerin, 2004; Manrique et al., 2006; May-Concha et al., 2013; Minoli et al., 2013a,b), which could be used as a triatomine monitoring tool (Minoli et al., 2013b). Isobutyric acid is detected by ORCs in grooved peg sensilla on the triatomine antenna (Guerenstein and Guerin, 2001), likely through the action of an IR (Guidobaldi et al., 2014).

Alarm signals are also conspicuously present in other hemipterans of economic importance such as stink bugs. Heteropteran alarm semiochemicals often have a six-carbon skeleton (e.g., trans-2-hexenal) and have little species specificity (Napper and Pickett, 2008). Insects of economic importance in other orders that produce an alarm pheromone include thrips and aphids. The alarm pheromone of thrips reduces oviposition and causes larvae to fall from plants, and thus could be used to pull insects away from crops (Pickett et al., 1997). When aphids are attacked, they release an alarm pheromone (trans-ß-farnesene; Bowers et al., 1972; Dewhirst et al., 2010; Vandermoten et al., 2012) that causes dispersion of other nearby aphids, including inter-specific responses across subfamilies (Napper and Pickett, 2008). This and other alarm aphid compounds have been used for controlling aphids in both greenhouse and field settings (Pickett et al., 1997; Dewhirst et al., 2010; Vandermoten et al., 2012).

Interestingly, sometimes a semiochemical can function as an alarm or an aggregation pheromone, depending on its concentration. This has been shown for trans-2-hexenal in cockroaches (Napper and Pickett, 2008), and for isobutyric acid in the blood-sucking triatomine bug *Rhodnius prolixus* (Guerenstein and Guerin, 2004; Manrique et al., 2006; Minoli et al., 2013a). Thus, not only the compound identity needs to be considered in tools for insect control, but also its concentration and behavioral context. While aggregation and alarm pheromones could be used to manipulate the olfactory behavior of harmful insects, we just started to understand how these signals are processed, particularly at the peripheral level. Control strategies can certainly benefit from a deeper understanding of the neural mechanisms controlling these olfactory-driven behaviors.

Use of Host Odors

Many insects that feed or oviposit on a host such as a plant or a vertebrate are pests of crops or transmit human and/or animal diseases. It is well-established that host odors, including CO_2, are a key cue for host detection and orientation (van der Goes van Naters and Carlson, 2006; Guerenstein and Hildebrand, 2008; McMeniman et al., 2014; van Breugel and Dickinson, 2014; Reisenman and Riffell, 2015). Much work has been done on the attraction of harmful insects toward natural and synthetic host odors and its neurobiological bases (Guidobaldi et al., 2014 and references therein), information that sometimes has been used to develop odor baits for traps (e.g., Krockel et al., 2006; Ryelandt et al., 2011; Mukabana et al., 2012; Guidobaldi and Guerenstein, 2013). Importantly, manipulation of host-seeking behavior offers many opportunities to disrupt harmful insects. Insects usually respond to specific mixtures of host odorants, even when they include ubiquitous (including non-host) odorants (Bruce and Pickett, 2011). Even when some constituents of those odor mixtures are essential to evoke a behavioral response (e.g., Geier et al., 1996; Guidobaldi and Guerenstein, 2013), in some cases certain components could have redundant roles and therefore, could be removed without decreasing attraction (e.g., Cha et al., 2008). Moreover, key components could be replaced without affecting attractiveness (Tasin et al., 2007). The neurophysiological bases of this phenomenon are not clear, but it is possible that in certain cases key odorants are detected by broadly tuned ORCs (that is, the same ORC could be involved in the detection of several behaviorally redundant key odorants). Thus, studies on the physiological responses of ORCs can have important implications for the design of attractive odor baits. Indeed, ORCs detecting different constituents of a natural odor mixture are sometimes co-localized in the same sensilla (Stensmyr et al., 2003). This, along with the finding that sometimes ORCs within a single sensillum interact (Nikonov and Leal, 2002; Ochieng et al., 2002, Su et al., 2012), makes possible the simultaneous detection and processing of mixture components already at the peripheral level.

As a general rule, odorant identities in the AL are encoded in spatial patterns of glomerular activation (Carlsson et al., 2002; Hansson et al., 2003; Wang et al., 2003; Lei et al., 2004), with some glomeruli narrowly tuned to certain odorants, including hostplant volatiles. For instance, PNs in a specific glomerulus of the *M. sexta* AL are extremely sensitive and narrowly tuned to the plant volatile cis-3-hexenyl acetate (Reisenman et al.,

2005). Moreover, other PNs in a female-specific glomerulus can discriminate, with high sensitivity, the (+) and (−) enantiomers of linalool (Reisenman et al., 2004). PNs in sexually isomorphic glomeruli, in contrast, are equally responsive to both enantiomers of linalool (Reisenman et al., 2004). Interestingly, these neurophysiological findings served to predict behavioral responses that were readily tested. Thus, later studies found that the two enantiomers of linalool respectively mediate oviposition attraction and repellence (Reisenman et al., 2010, 2013), and that these two compounds are equally effective in mediating feeding (Reisenman et al., 2010).

Different features of host odor blends are encoded in glomerular activity patterns. For instance, the encoding of odor mixture identity involves synchronous firing of PNs throughout the activated glomeruli, which may serve to "bind" the components of the odor mixture (Riffell et al., 2009a,b). In addition, stimulation with an odor mixture can evoke a glomerular activation pattern which is different from that evoked by the summation of the activity patterns evoked by each component (see below). The importance of ratios in the detection of host odor mixtures has been shown in different insects (e.g., Najar-Rodriguez et al., 2010; Guidobaldi and Guerenstein, 2016). In oriental fruit moths, for instance, particular ratios within a synthetic plant odor mixture affected oviposition attraction negatively. Corresponding neurophysiological studies found that information about component ratios occurs non-uniformly across AL glomeruli, and that further processing takes place in higher-order brain centers (Najar-Rodriguez et al., 2010).

As mentioned above, insects usually respond to specific host odor mixtures (e.g., Geier et al., 1999a; Barrozo and Lazzari, 2004a; Krockel et al., 2006). For example, triatomines are sensitive to various human compounds (e.g., CO_2, lactic acid, ammonia, carboxylic acids; Guerenstein and Lazzari, 2009), and a mixture of ammonia, lactic acid, and pentanoic acid evokes attraction, whereas there is low or no attraction to the single constituents (Guidobaldi and Guerenstein, 2013). Furthermore, in aphids, individual constituents of an otherwise attractive blend can have repellent effects (Webster et al., 2010). Some constituents of host odor mixtures can act synergistically to evoke attraction (e.g., Bosch et al., 2000; Barrozo and Lazzari, 2004a; Smallegange et al., 2005; Piñero et al., 2008; Guidobaldi and Guerenstein, 2013). In females of the oriental fruit moth *Cydia molesta*, minute amounts of benzonitrile added to an unattractive mixture resulted in a mixture that is as attractive as a natural blend. At the AL level, this bioactive mixture evoked strong activation and synergistic effects in an additional glomerulus not activated by the unattractive mixture (Piñero et al., 2008). Besides synergistic phenomena, additive effects in response to odor mixtures are also found at the central level (e.g., Lei and Vickers, 2008). Therefore, multi-component odor baits will likely be more attractive than single odorants, as they may form specific and reliable "odor objects" (e.g., Späthe et al., 2013, see Section Effects of Background Odor). Interestingly, it has been proposed that just a few (sometimes just three) key components of an odor blend are sufficient for reliable host recognition, even when the insects can detect a higher number of host odorants (Qiu et al., 2007; Riffell et al., 2009a; Guerenstein and Lazzari, 2010; Bruce and Pickett, 2011; Guidobaldi and Guerenstein, 2013).

CO_2 is a food and/or oviposition host cue used by some herbivorous and hematophagous insects (Guerenstein and Hildebrand, 2008). Glomerulus-specific CO_2 PNs in the AL of *M. sexta* can follow high frequency CO_2 pulses, suggesting that these PNs report information about long-distance CO_2 cues (Guerenstein et al., 2004a). This idea is also supported by the finding that nectar-rich flowers emit relatively high levels of CO_2 (Guerenstein et al., 2004b). In fact, foraging moths use floral CO_2 as a long-distance cue to find those flowers (Thom et al., 2004; Goyret et al., 2008). This and other examples (e.g., van Breugel et al., 2015) again show that neurobiological studies can predict behavior, and ultimately can inspire odor-based control strategies (van der Goes van Naters and Carlson, 2006). The fact that blood-sucking insects are proving difficult to control (Logan and Birkett, 2007), and that they transmit an ever increasing number of diseases to humans and animals, emphasizes that further studies are needed to develop effective tools for insect behavioral manipulation. It should be noted that any odor-based control strategy should consider that different types of natural odor stimuli (including background odors) often interact (e.g., Chaffiol et al., 2012, 2014, see also Section Effects of Background Odor). In addition, it should be considered that the physiological state of the insects (e.g., mating, feeding) as well as learning affects their responses to odors (e.g., Barrozo et al., 2010; Saveer et al., 2012; Reisenman, 2014; Matthews et al., 2016; Section Plasticity in the Responses to Semiochemicals).

Combined Use of Pheromones and Plant Volatiles

When insects detect a mate, their olfactory system is confronted with not only sex pheromones, but also background odors such as plant volatiles. In principle, sex pheromones admixed with green leaf volatiles should be very attractive to phytophagous insects because such mixture may indicate the presence of a calling mate in a proper context. Therefore, at least in certain cases, it would be important to include hostplant volatiles in sex pheromone traps. For instance, in the case of the codling moth *Cydia pomonella*, addition of plant volatiles [e.g., (*E*)-β-farnesene] to the sex pheromone (codlemone) significantly increased the proportion of males flying to the pheromone in wind tunnel experiments (Schmera and Guerin, 2012; Trona et al., 2013). In addition, it has been shown that females of the Egyptian cotton leafworm *S. littoralis* exposed to cotton volatiles start calling earlier than females exposed to non-host volatiles, and that mating pairs exposed to these volatiles start mating earlier. Also, more males reach (or arrive nearby) the pheromone source when hostplants, rather than non-hosts, are present (Binyameen et al., 2013).

Integration of sex pheromone and plant volatile information may occur at the peripheral level. For example, in the noctuid moth *Agrotis ipsilon* pheromone ORCs can be directly excited by plant volatiles (Rouyar et al., 2015). Moreover, in pheromone-specific ORCs of *Helicoverpa zea,* stimulations with binary mixtures of sex pheromone and single hostplant odorants [either linalool or (*Z*)-3-hexenol] produce stronger responses than

stimulation with the sex pheromone alone due to interactions between ORCs (Ochieng et al., 2002). Mixtures containing pheromone and plant odorants can also have a suppressive effect. For instance, in *S. littoralis*, herbivore-induced plant odorants can directly suppress the response of pheromone-specific ORCs (Hatano et al., 2015). Direct suppression has also been observed in *Heliothis virescences* males upon stimulation of pheromone-specific ORCs with a sex pheromone component and a number of plant volatiles (Pregitzer et al., 2012). Suppressive effects can also be due to interactions between ORCs (Andersson et al., 2010). Interestingly, in woodboring beetles (*T. fuscum*), some ORCs respond specifically to their aggregation pheromone, although other ORCs specifically respond to the aggregation pheromone combined with at least one plant compound (MacKay et al., 2015).

The olfactory sub-system dealing with the processing of sex pheromone signals has traditionally been considered as a specialized system different from the "main" olfactory sub-system dealing with the processing of host/food odors. This notion was strongly supported by the identification of pheromone-specific ORCs (Bray and Amrein, 2003; Mitsuno et al., 2008; Krieger et al., 2009; Grosse-Wilde et al., 2010; Montagné et al., 2012; Zhang et al., 2015) which in some insect species (particularly within Lepidoptera) project to a small but distinct number of male-specific glomeruli (the aforementioned MGC; Kanzaki and Shibuya, 1983; Christensen and Hildebrand, 1987; Hansson et al., 1992, 1995, 2003; Berg et al., 1998; Rospars and Hildebrand, 2000; Masante-Roca et al., 2002; Sadek et al., 2002; Lei et al., 2004). In spite of this anatomical and often functional separation, it is clear that the two olfactory sub-systems also interact at the AL level. Both suppressive and additive interactions between pheromone and plant odorants have been reported in the MGC of different Lepidoptera species. In some cases, suppressive effects were observed (Chaffiol et al., 2012; Deisig et al., 2012), while in others responses were enhanced (Namiki et al., 2008). The responses of neurons in sexually isomorphic glomeruli can also be affected by the presence of female pheromones in several species, but showed more interspecific variations (Namiki et al., 2008; Chaffiol et al., 2014). Moreover, in *C. pomonella,* both response enhancement and suppression in response to mixtures of pheromones and plant odors has been observed in sexually dimorphic and isomorphic glomeruli, respectively (Trona et al., 2013). Interactions between the two sub-systems are not necessarily reciprocal or determined by spatial proximity (Namiki et al., 2008; Reisenman et al., 2008; Trona et al., 2013). Furthermore, additive effects for single and pulsed stimulations with mixtures of pheromone and plant odors have been reported (Chaffiol et al., 2014). Because in most cases ORCs that respond to plant odorants do not respond to sex pheromones (and are located in different sensilla), the responses of AL neurons to sex pheromones in sexually isomorphic glomeruli likely result from AL network interactions (Reisenman et al., 2008; Deisig et al., 2012; Chaffiol et al., 2014). The processing of combined signals (i.e., pheromone and non-pheromonal) in higher brain centers is less understood, but it is likely that neurons in these centers further contribute to this interaction.

All these results, both at the peripheral (ORC) and AL level challenge the traditional idea that pheromone and hostplant odor reception and processing are segregated. Thus, these results indicate that olfactory neural circuits are perhaps far more functionally diverse than previously thought. At the same time, these findings highlight the idea that in order to develop efficient tools to manipulate mate-finding behavior it is important to consider the odor context of that signal (e.g., if appropriate for the species, pheromonal baits could also include a host odor).

Visual cues play important roles in modulating the olfactory behavior of insects (e.g., Green, 1986, 1993; Cardé and Gibson, 2010; Willis et al., 2011; Gaudry et al., 2012; McQuate, 2014; van Breugel et al., 2015), and thus, visual cues are often added to odor baits in traps (e.g., Green, 1994). As integration of visual and olfactory stimuli at the CNS has already been documented (e.g., Balkenius et al., 2009), further studies in higher brain centers could help improve the development of multimodal baits. Even when this integration of information is relevant for the manipulation of olfactory behavior, it exceeds the aim of this review, and will not be discussed here.

Effects of Background Odor

Odor mixtures are thought to be represented in the insect brain as single "odor objects," so that the unique mixture identity prevails over the information about its constituents (Lei and Vickers, 2008; Wilson and Sullivan, 2011; Stierle et al., 2013). When odor baits (usually odor mixtures) are used in the field for insect monitoring and control, they are necessarily presented against an odorous dynamic background (another odor mixture/s). Background odors can either be irrelevant, "mask" the target odor (making it unrecognizable), or can enhance the response to a target odor (Schroeder and Hilker, 2008). In principle, it is conceivable that the bait (target) plus the background odor are perceived as a single mixture, creating a new and emergent "odor object" that can interfere with the identification of the target odor. If that were the case, how do insects orient toward natural odor sources such as hosts, mates, and oviposition sites? In this section we review the importance of background odors in shaping the responses to a target odor bait.

Detecting and discriminating a target odor mixture requires binding its different components (e.g., Deisig et al., 2006; Riffell et al., 2009b), and this "odor object" should be salient even in the presence of background odors. How do nervous systems accomplish this task? In rats, prolonged odor stimulation leads to fast habituation of neurons in the olfactory cortex, so that new odors evoke clear, distinct, responses. As a result, when the two odors are present, the constant odor (background) is filtered while the target odor evokes a neural response, suggesting that animals can separate the target stimulus from its background (Kadohisa and Wilson, 2006; Linster et al., 2007). This idea is also supported by experiments in honeybees, in which odorants presented simultaneously (simulating components of a single odor source) were represented as a single object, while odorants presented with an inter-stimulus delay were represented separately (Szyszka et al., 2012; Stierle et al., 2013). Although interglomerular inhibitory interactions contribute to bind components into a single odor object (e.g., Deisig et al.,

2006; Riffell et al., 2009b; Stierle et al., 2013), it has been shown that asynchronous mixtures activate more inhibitory interactions than synchronous mixtures (Stierle et al., 2013). How could this target-background object separation happen in natural odor plumes? Since insect ORCs can have short (<2 ms) response latencies, the thin filaments of target odors that intermingle with those of background odors could be resolved temporally, thus allowing target-background odor segregation (Szyszka et al., 2014).

Convincing and exciting experiments in moths showed that constant odor backgrounds that are chemically different from the target odor do not affect the representation of the target odor, whereas backgrounds that contain a constituent in common with the target odor do (Riffell et al., 2014), a phenomenon akin to the masking effect reported in mosquitoes and other insects (Logan et al., 2008; Schroeder and Hilker, 2008, see Section Odor Masking). Background odors with a constituent in common with the target evoke a change in the balance of excitation and inhibition in AL neurons with respect to the response to the target odor alone, thus altering the representation of the target odor (Riffell et al., 2014). Pre-exposure to this type of background odors produces an exacerbated change in the response to the target odor, resulting from neurons being adapted to the common constituent (Riffell et al., 2014). Stierle et al. (2013, see above) used a different insect species and different experimental conditions, although also tested dissimilar target- background odors presented simultaneously, and arrived to different conclusions (Stierle et al., 2013). These authors found that this mixture is represented as a single distinctive odor object, while Riffell et al. (2014) reported efficient target-background discrimination.

Still, there is an experimental situation that has not been tested yet: similar target- background odors (or target and background with a common blend constituent) presented asynchronously. Because in nature background odor plumes can have a different temporal structure than target odor plumes, insects could exploit these temporal differences to segregate a target odor from its background, even when these have common constituents (Stierle et al., 2013; Szyszka, 2014; Rusch et al., 2016). Experience may also help this segregation, as learning increases the distinction between different scents (Fernandez et al., 2009; Riffell et al., 2013). While in the work described synthetic blends were used, it would be most informative to use complete natural blends as targets since in principle, it should be easier to alter the neural representation of a synthetic mixture consisting of just a few constituents than that of a multi-component natural odor. Somewhat related to this idea, it has been suggested that redundant odor blends reduce uncertainty as they convey more robust information (Wilson et al., 2015).

As mentioned above (Section Combined Use of Pheromones and Plant Volatiles), plant odors could influence the response to pheromones both at the peripheral and the AL levels. Moreover, supression of attraction to the sex pheromone by hervivore-induced plant volatiles has been reported in *S. littoralis* (Hatano et al., 2015). However, *H. virescens* males can be effectively attracted to the conspecific female sex pheromone in a constant background of naturally-occurring hostplant odors, including hervivore-induced plant volatiles (Badeke et al., 2016). While these results parallel those reported by Riffell et al. (2014), the attraction of *H. virescens* to the female pheromone is impaired in a background of high and supra-natural plant odor concentrations (Badeke et al., 2016). These results not only further underlie the importance of using natural, realistic stimuli, but also that additional studies are necessary to fully understand the mechanisms underlying target/background discrimination, as the chemical identity of the odors used, as well as the species under study, could certainly influence the results.

A particular constituent of the volatile background, CO_2, also affects the behavior of at least some insects (Guerenstein and Hildebrand, 2008). Information about this odor cue is processed as information about other odors, while the background level of CO_2 is simultaneously encoded (Guerenstein et al., 2004a). In hematophagous insects this cue is used to detect and find vertebrate hosts (e.g., Geier et al., 1999b; Barrozo and Lazzari, 2004b), while in moths it is used to detect and find oviposition sites and nectar resources (Stange, 1997; Thom et al., 2004; Goyret et al., 2008). While those CO_2 sources evoke clear responses from the CO_2 ORCs at natural CO_2 background levels, higher CO_2 background levels interfere with those responses (Guerenstein and Hildebrand, 2008). In mosquitoes, an elevated CO_2 background impedes take-off and source contact by masking the stimulus signal (Majeed et al., 2014). Moreover, the oviposition behavior of *Cactoblastis cactorum,* a moth particularly sensitive to CO_2, is also affected by elevated CO_2 backgrounds (Stange, 1997) because ORCs stop firing at such high CO_2 levels (Stange et al., 1995). However, the behavior and ORC responses of *M. sexta* moths are not affected by moderate increases in CO_2 background levels, but instead by high-amplitude CO_2 oscillations (Abrell et al., 2005). In addition, certain background odorants can modulate the activity of CO_2 ORCs (e.g., Guerenstein et al., 2004a) or even evoke a response *per se* in those receptors (Turner et al., 2011), thus interfering with CO_2-mediated behaviors.

In conclusion, the odor background can affect responses to target odors (e.g., Büchel et al., 2014). Thus, for example, efficient odor baits developed in the laboratory could fail to attract insects under field conditions, where different background odors are present. Although more research is needed to understand its role in insect behavior, the odor background should be taken into account when planning an odor-based pest/vector management strategy. In addition, it would be important to investigate the feasibility of techniques to disrupt natural olfactory behavior using masking (see Section Odor Masking) and/or background odorants, as this could improve the methods currently used to disrupt behavior using natural odorants (see Section Disruption of Natural Olfactory Behavior).

OLFACTORY REPELLENCE

According to Barton-Browne (1977) a repellent is "a chemical that acting in the vapor phase prevents an insect from reaching a target to which it would otherwise be attracted." A repellent

has also been defined as a product causing the insect "to leave the prospective host, with true behavioral repellency involving avoidance of the source of the repellent material, whether placed on the prospective host or near it" (Pickett et al., 2008). While these definitions are based on behavioral effects, the mechanisms of action of repellents are not considered. Repellents are used to stop a pest from finding a valued resource; topical repellents are usually applied onto the skin offering individual protection, while spatial repellents volatilize into the air, creating a vector-free space which provides protection for multiple individuals (Achee et al., 2012). Typically, volatile repellents are used to protect humans from insect (and other arthropod) bites, particularly from arthropods which are vectors of diseases (Foster and Harris, 1997). Repellents have also been used to protect crops: for example, the alarm pheromone of a number of aphids has been used against these pests (Foster and Harris, 1997; Pickett et al., 1997).

For centuries humans have used diverse parts of plants to repel biting insects (Moore and Lenglet, 2004). Among these so-called "botanical repellents," various species of basil (*Ocimum* spp.) have been historically used to repel mosquitoes. In addition, oil extract from the leaves of neem (*Azadirachta indica*) has also been used as a personal mosquito and sandfly repellent (Yarnell and Abascal, 2004). Other botanical insect repellents include the oil from leaves of citronella (*Cymbopogon nardus*), palmarosa (*C. martinii martinii)*, lemongrass (*C. citratus*), and Eucaliptus (*Eucalyptus* spp.). The active components of these botanical repellents are often unknown although citral, a major ingredient in volatiles from lemongrass oil, and p-menthane-3,8-diol, from lemon eucalyptus, have repellent effects on a variety of mosquitoes (Yarnell and Abascal, 2004). Repellents can also be derived from other natural sources such as insects (as in the case of alarm pheromones or defense secretions), or may be purely artificial (Foster and Harris, 1997).

The world's most widely used synthetic topical insect repellent, with broad effectiveness against many insects, is *N,N*-diethyl-3-methylbenzamide, also known as N,N-diethyl-m-toluamide (DEET; White, 2007; Syed et al., 2011). Other synthetic repellents include Picaridin and IR3535 (or EBAAP, Ethyl Butyl-acetyl-aminopropionate). A full understanding of the mechanism of action of insect repellents and in particular, the identification of their molecular targets, can help design safer and more effective compounds. DEET appears to act both as a contact chemo-repellent that stimulates insect gustatory receptor cells that respond to aversive compounds (Lee et al., 2010), and as a volatile chemo-repellent acting on the olfactory system.

The mode of action of volatile repellents is still under debate and has been comprehensively reviewed recently (Leal, 2014); therefore, here we briefly summarize the most relevant investigations. In *D. melanogaster* and in the mosquitoes *Aedes aegypti* and *Anopheles gambiae* DEET appears to modulate the responses of ORCs to attractive odors (Davis and Sokolove, 1976; Ditzen et al., 2008). This effect depends both on ORCO (Ditzen et al., 2008) and on the molecular identity of the OR in the OR-ORCO complex (Pellegrino et al., 2011). However, for other repellents, it was proposed that DEET acts by just blocking ORCO (Tsitoura et al., 2015). On the other hand, Syed and Leal (2008) suggested that the mosquito *C. quinquefasciatus* can smell DEET directly and that that stimulation results in avoidance even in the absence of other odor cues. Similar results were reported in triatomines, suggesting a common mode of action for the repellent action of DEET (Zermoglio et al., 2015). Moreover, other additional findings further support the hypothesis that insects can smell DEET: (1) the existence of an ORC in *D. melanogaster* which is sensitive to DEET, picaridin and IR3535 (Syed et al., 2011) and, (2) electroantennogram (EAG) and single sensillum responses to DEET in *A. aegypti* (Stanczyk et al., 2010, 2013).

In an attempt to clarify some of these apparently contradictory results, Bohbot and Dickens (2010) characterized the effects of a number of repellents [DEET, 2-undecanone (2-U), IR3535 and Picaridin] on two OR-ORCO heteromers of *A. aegypti* individually expressed in *Xenopus* oocytes. Their results suggest that different mechanisms mediate the action of different repellents. That is, repellents could be smelled directly (acting as receptor agonists) or could inhibit the responses to odors (acting as receptor antagonists; Bohbot and Dickens, 2010).

It is now well established that insects can smell DEET (Leal, 2014). Studies in mosquitos suggest that ORCO and the OR pathway are necessary for the repellent effects of DEET as: (1) wild-type *A. aegypti* avoid DEET whereas ORCO mutants do not (DeGennaro et al., 2013) and, (2) in *C. quinquefasciatus,* different repellents activate a particular OR (*Cqui*OR136) in a dose-dependent manner, whereas knockdown of this OR resulted in loss of EAG and behavioral responses to DEET (Xu et al., 2014). These results suggest that an OR is involved in the direct detection of DEET (Xu et al., 2014). As the natural plant repellent methyl jasmonate elicits responses in ORCs expressing *Cqui*OR136, it has been proposed that this OR is tuned to natural repellents with long insect–plant evolutionary histories (Xu et al., 2014).

In summary, different hypotheses have been suggested to explain the mechanisms involved in the olfactory repellency of DEET in blood-sucking insects. They include: (1) DEET may silence ORs responsive to attractive odors, a hypothesis that has now little support; (2) DEET is detected by one or a few ORs; (3) DEET may act as a "confusant" by modulating the activity of many ORs. Although it is possible that more than one of these mechanisms act simultaneously, it is likely that they are species-specific. Because all these proposed mechanisms involve ORs, these are relevant candidate molecular targets for the development of new repellents (Leal, 2014). Thus, based on knowledge on the molecular receptors, more efficient and safer volatile mosquito repellents could be developed. The need to develop new repellents is emphasized by the finding that some populations of *A. aegypti* are insensitive to DEET (Stanczyk et al., 2010). Besides the repellent effects of DEET discussed above, application of DEET on human skin results in an altered host odor chemical profile due to a fixative effect of DEET, and that effect could also contribute to repellency (Syed and Leal, 2008; Section Odor Masking). Finally, certain constituents of non-host odors can act as arthropod repellents (e.g., interaction between cattle flies and heifers: Birkett et al., 2004; interaction between fruit flies and fruit: Linn et al., 2005; interaction between

ticks and dogs: Borges et al., 2015), providing opportunities for the development of natural, safer repellents. It should be noted that the response to an attractive host odor blend can be manipulated by adding non-host odorants (e.g., Linn et al., 2005), and also by altering the proportions of one or more host odorants (Section Odor Masking), causing either repellency (avoidance), or masking (loss of attraction; Section Odor Masking).

DISRUPTION OF NATURAL OLFACTORY BEHAVIOR

Mating Disruption

The most common behavior that has been disrupted using semiochemicals is mating. This strategy has been used to eradicate insects that became resistant to pesticides, including pests of apples, peaches, cotton, and grapes (see Wyatt, 2003; Witzgall et al., 2010). The basic idea of mating disruption involves the broadcasting of a chemical signal similar to the sex pheromones of the target species. The first registration of a mating disruption product in the USA was for the pink bollworm (Brooks et al., 1979); currently there are more than 120 disruption products registered in the US. Mating disruption usually involves the release of large amounts of species-specific synthetic sex pheromones (e.g., Witzgall et al., 2010); these high concentrations often "overload" the insects' sensory system, interfering with the detection of the usually lower amounts of pheromone released by mating partners (Cardé, 1990, see below). Besides this traditional approach (see below), new techniques and approaches are being developed to improve efficacy. A new design, which is literally an auto-confusion disruption method, involves the application of electrostatically charged wax powder (dubbed Entostat) onto the cuticle of male moths. Because the powder can be loaded with large quantities of female sex pheromone, male moths function as mobile dispensers. Indeed, Entostat-exposed codling moth males remained as attractive as a 0.1-mg pheromone lure for up to 24 h in laboratory experiments (Huang et al., 2010). The behavior of male moths that are normally attracted to natural sources of pheromone was completely disrupted after treatment with Entostat powder. Moreover, the males' ability to orientate to the pheromone lure remained significantly impaired 6 days post-application, arguing that Entostat augments the effect of sensory (peripheral) adaptation and CNS habituation (Huang et al., 2010).

According to Miller and Gut (2015), mating disruption methods can be broadly divided into two categories, i.e., non-competitive and competitive. Non-competitive methods involve interference with the sensory capabilities of males or females, or hampering pheromone emission, and examples include mating/calling suppression, camouflage, sensory imbalance, and desensitization. Competitive methods do not involve changes on the insects' sensory capabilities or on pheromone emission and, therefore, insects can respond equally well to other insects and trap lures. Thus, several mechanisms can mediate pheromonal mating disruption, including loss of sensitivity in ORCs (sensory adaptation), loss of sensitivity at the CNS level (habituation), camouflaging of the female's odor trail, competition between dispensers and natural pheromone, and unbalanced components in the synthetic pheromone (Cardé, 1990). We next discuss sensory adaptation and habituation.

Stimulation with high concentrations of pheromones generally reduce the response sensitivity of pheromone ORCs (i.e., ORCs adapt to the stimulus), a phenomenon which can be quantified using EAG. For instance, in male oriental fruit moths, the EAG amplitude decreased as animals approached high emission-rate sources, and this reduction was correlated with upwind flight cessation (Baker and Haynes, 1989). In another moth species, long-lasting EAG adaptation after pheromone pre-exposure occurred over a range of pheromone dosages and lasted more than 10 min (Stelinski et al., 2005). There appear to be significant species-specific variations in the capability of the olfactory system to adapt to pheromones. For instance, *Grapholita molesta* moths have a three-fold greater level of sensory adaptation after pre-exposure than *Choristoneura rosaceana* (Trimble and Marshall, 2010), a finding which may explain why *G. molesta* is readily more controllable using mating disruption than *C. rosaceana*. The mechanisms underlying sensory adaptation were investigated in the moth *M. sexta.* After presentation of an adapting pheromone stimuli, and in response to the pheromone test stimulus, type I trichoid sensilla produced sensillar potentials of lower amplitude than those from non-adapted sensilla, while the pheromone ORC spike frequency of adapted sensilla was concomitantly lower (Dolzer et al., 2003). Furthermore, pheromone stimuli lasting several seconds strongly activated protein kinase C in pheromone ORCs, while minute-long stimuli elevated cGMP concentrations. These results indicate the existence of distinct intracellular signaling mechanisms mediating short-term and long-term adaptation (Dolzer et al., 2008).

In order to produce habituation in AL neurons and, therefore, disrupt behavior, unnaturally high stimulus concentrations and/or frequencies can be used. In AL PNs, pheromone stimulation typically produces a burst of action potentials followed by an after-hyperpolarization (AHP) inhibitory phase (Christensen and Hildebrand, 1988; Lei et al., 2009). The AHP is critical to enable PNs to resolve intermittent stimuli, which is a universal feature of natural odor plumes (Murlis et al., 1992; Lei et al., 2009). Within a certain range of stimulus frequencies, PNs respond with a burst of action potentials (followed by a short AHP) to each odor pulse, faithfully reporting the temporal structure of the stimulus train. However, when the pulsing rate exceeds the response range of PNs (>10 Hz), neurons can only respond with a single burst of action potentials followed by a prolonged AHP (Christensen and Hildebrand, 1988; Lei and Hansson, 1999; Heinbockel et al., 2004). In addition, the excitatory and inhibitory phases can be both habituated by high stimulus concentrations. Increasing stimulus concentrations decreases the delay to the onset of the excitatory phase and increases firing rate eventually reaching saturation (Heinbockel et al., 2004; Fujiwara et al., 2009), while also decreases the delay to the onset of the inhibitory phase and increases its duration. In the upper range of concentrations, PNs only produce a brief (high-rate) burst that is followed by a lengthy AHP, which is similar to the habituating pattern evoked

by high frequency stimuli. Thus, under sustained stimulation and high concentrations, PNs show responses which are not likely linked to natural behaviors. Because PNs also receive input from LNs, these may also contribute to PN habituation, as observed in *D. melanogaster* (Seki et al., 2010). Because many LNs are GABAergic and can therefore inhibit PNs (Hoskins et al., 1986; Christensen et al., 1993; Wilson and Laurent, 2005; Seki and Kanzaki, 2008), LN habituation would produce sustained PN disinhibition, potentially interfering with triggering natural behavior. Although the roles of LNs are still being investigated, it is thought that they may render the response of some PNs concentration-independent (e.g., Asahina et al., 2009; Olsen et al., 2010). In summary, investigations on sensory adaptation and habituation can be helpful to find the most effective chemicals that can be used to disrupt mating.

Odor Masking

As mentioned above (Sections Use of Sex Pheromones and Use of Host Odors), not just the identity of the constituents of an odor mixture but also their proportions (ratios) are important for attraction. For instance, humans are differentially attractive to mosquitoes and this could be due to individual host odor mixture variability (Logan et al., 2008 and references therein). In some cases low attractiveness has been linked to low levels of some odors. For example, in *A. aegypti*, addition of lactic acid to the skin of formerly unattractive humans can increase their attractiveness (Steib et al., 2001). Low or no-attractiveness to a natural host odor blend could also result from higher-than-normal concentrations of a natural constituent of the attractive blend (e.g., Birkett et al., 2004; Logan et al., 2008, 2009), a phenomenon attributed to blend repellency or masking (see also Section Effects of Background Odor).

Comparisons of the odor profiles of individuals with different attractiveness revealed that a few compounds are present in higher relative amounts in less-attractive individuals, including 6-methyl-5-hepten-2-one (Logan et al., 2008, 2009). When low and naturally occurring doses of this odor were added to naturally attractive human odor, upwind flight and probing were reduced. Although a repellent-blend effect can occur (Logan et al., 2009), a small increase in the amount (ratio) of a particular compound within the natural host odor mixture could also produce masking of the target odor so that the host is no longer recognized as such (Logan et al., 2008; see also Bruce and Pickett, 2011 for examples in phytophagous insects).

Many semiochemicals can be used in conjunction with other chemical tools in "push-pull" strategies. These strategies divert insects away from a valuable resource (the "push" away from, for example, a host) into an attractant (the "pull" component; Pickett et al., 1997; Cook et al., 2007). Masking odors could be used in push-pull control strategies to prevent host location ("pushing" insects away from the hosts) while at the same time, attractive odors could be used as baits in traps to "pull" the insects away from hosts (Cook et al., 2007; Logan et al., 2008). Neuroethology approaches could readily speed up the discovery of effective masking odors for use in control strategies. For instance, one strategy could be to test the degree of odor-object transformation in the AL (i.e., the change in the spatio-temporal response pattern of an ensemble of AL neurons) that is evoked by altered ratios of different compounds within the natural host odor mixture.

Carbon dioxide is an important odor that mediates the behavior of many harmful insects (Guerenstein and Hildebrand, 2008). Therefore, manipulation of the odors that modulate the response of the CO_2 receptors (Section Effects of Background Odor; Turner et al., 2011), including inhibitory odorants that can mask human scent (Tauxe et al., 2013), can profoundly impact CO_2-mediated behaviors. Moreover, large CO_2 fluctuations can "confuse" the insect's detection of natural CO_2 sources (Abrell et al., 2005 and references therein), which may be used for interfering with the behavior of CO_2-sensing insects.

Odor Antagonism

As in many lepidopterans, *Heliothine* females release a sex pheromone that attracts conspecific males. However, certain compounds of the somewhat similar sex pheromone of a sympatric *Heliothine* species make the former blend unattractive. Indeed, the addition of such interspecific compounds to a species' sex pheromone blend can eliminate attraction in conspecific males, thus acting as antagonists (Vickers and Baker, 1997). In the AL of both *H. virescens* and *H. zea* the two essential components of their species-specific pheromone blends are represented in two separate MGC glomeruli. Odorants that antagonize attraction, when added to the respective pheromonal blends, evoked excitatory activity in PNs restricted to a third MGC glomerulus in both species (Vickers et al., 1998). Therefore, attractive and antagonist odor blends are represented in distinct combinations of MGC glomeruli, thus providing a combinatorial code for sex pheromone discrimination in sympatric species.

While approaching a female, male moths also emit volatile chemicals through specialized male structures such as the hairpencils (Birch et al., 1990). It has been shown that *H. virescens* hairpencil volatiles have both aphrodisiac and repellent effects on conspecific females and males, respectively. Interestingly, the male ORCs that respond to a conspecific hairpencil compound also respond to an interspecific sex pheromone antagonist (Hillier et al., 2006). Antagonist compounds (including both interspecific sex pheromone and conspecific hairpencil volatiles) are certainly amongst the important chemicals that can be used to manipulate harmful-insect behavior.

PLASTICITY IN THE RESPONSES TO SEMIOCHEMICALS

Behavioral plasticity (including associative and non-associative learning) affects chemosensory-guided behaviors in all insects. For simplicity, we define learning as a permanent change in behavior resulting from experience (Papaj, 2009). Associative learning involves pairing of two stimuli in a way that the response to one of the stimulus is altered as a consequence of the pairing, which is typically evaluated in classical/Pavlovian or operant/instrumental paradigms. For instance, a well-studied case of classical learning involves the pairing of an appetitive stimulus (e.g., sugar) that elicits a reflexive response (e.g., extension of the proboscis) with an odor; when an association

between the two stimuli is formed, the sole presentation of the odor stimulus elicits proboscis extension (Bitterman et al., 1983). Behavioral habituation, a form of non-associative learning, reduces responsiveness to stable and repetitive stimuli, which can be important for detecting predators, food, and/or mate odors in an irrelevant and/or even complex olfactory background (Kadohisa and Wilson, 2006; Linster et al., 2007; Riffell et al., 2014; see also Section Effects of Background Odor). Behavioral sensitization is also a form of non-associative learning in which repeated presentation of a stimulus can result in amplification of responses to that and/or a related stimulus (Papaj, 2009).

Learning has profound effects on the chemosensory behavior of insects, including harmful ones. This is true even in the case of innate signals of prime biological relevance, such as sex pheromones. In moths, the action of sex pheromones depends on factors such as the presence of host-odors, sexual maturity, and mating status (Barrozo et al., 2011; Chaffiol et al., 2012, 2014; Guerrieri et al., 2012). Furthermore, moths can be trained to associate food with a sex pheromone (Hartlieb et al., 1999; Hartlieb and Hansson, 1999). In other cases, recognition of pheromones necessarily involves learning. In social insects, kin and nest-mate pheromones are learned by young larvae inside the nest, and maggot flies need to experience their own host-marking pheromone before they can discriminate between an occupied and an unoccupied fruit in which to lay eggs (Roitberg and Prokopy, 1981). Furthermore, in phytophagous insects, this kind of olfactory learning can promote the transition to new hosts of agricultural importance (Prokopy and Papaj, 1988; Papaj and Prokopy, 1989).

The way in which plasticity affects many different behaviors in herbivorous insects has been recently reviewed (see Anderson and Anton, 2014). In herbivorous insects, both larval feeding and adult experience can affect olfactory-guided oviposition, mate choice, and feeding (Riffell et al., 2008; Thöming et al., 2013; Anderson and Anton, 2014; Carrasco et al., 2015). In moths, plant volatiles can enhance male orientation toward the conspecific female sex pheromone (Chaffiol et al., 2012, 2014; Guerrieri et al., 2012). The learning abilities of pest insects should be particularly considered in control strategies. For instance, a "trap crop" (which always represents a small proportion of the cropping area) might be completely inefficient if insects first find the profitable crop and prefer this over the trap crop (Cook et al., 2007). Thus, the selection of the most effective crop border plants is crucial, and this can be achieved by screening plant cultivars coupled with identification of behaviorally and electrophysiological bioactive volatiles (Schröder et al., 2015). Other cognitive processes, such as habituation, have important implications in the management of pest insects (Section Mating Disruption). In diamondback moths, exposure to non-hosts can increase oviposition preference toward these plants, perhaps leading to host range expansion (Zhang and Liu, 2006).

In the case of insects vectors of human and animal diseases, learning and previous experience can have important epidemiological implications for disease transmission (McCall and Kelly, 2002). For instance, mosquito host choice is influenced by prior foraging experience, which causes them to return to less-defensive hosts and to hosts where feeding was more successful (McCall and Kelly, 2002; Lyimo and Ferguson, 2009). Not only that, but variation in the physical and chemical properties of blood can influence fitness and cause host feeding preferences (see Lyimo and Ferguson, 2009 for details). Thus, it has been suggested that pathogen transmission can be reduced by altering host choice (Lyimo and Ferguson, 2009). Also, mosquitoes tend to return to the same villages, houses, host species, and oviposition sites (McCall and Kelly, 2002). Then, it is not surprising that research in this area has expanded in the last couple of years, and it is now clear that blood-sucking insects can indeed learn and form new memories (Kaur et al., 2003; Jhumur et al., 2006; Tomberlin et al., 2006; Bouyer et al., 2007; Sanford and Tomberlin, 2011; Vinauger et al., 2011a,b, 2013, 2014; Chilaka et al., 2012; Sanford et al., 2013). Classical and operant paradigms showed that blood-sucking insects can associate stimuli of different modality (thermal, odor, gustatory, visual) while searching for a host and selecting oviposition sites. In *A. aegypti*, the association between odorants and a thermal appetitive stimulus is odor-dependent (e.g., certain odors can be readily learned, others are untrainable, etc). Furthermore, associative learning can modify the aversive deterrent effect of DEET in both kissing bugs and mosquitoes (Stanczyk et al., 2013; Vinauger et al., 2014). Learning processes also affect the responses to odors which are crucial for survival (e.g., pheromones). In triatomine bugs, a brief exposure to the alarm pheromone produces sensitization and increases the tendency to respond, while long-term pre-exposure elicits behavioral habituation (Minoli et al., 2013a). In blood sucking insects, however, our knowledge on the neural mechanisms underlying the effects of experience on chemosensory responses is mostly restricted to the periphery, as we discuss below.

In both blood-sucking and herbivorous insects the activity of ORCs can be affected by experience (e.g., long-term odor exposure and sensory adaptation to deterrents; see Section Mating Disruption). Experience can also cause downregulation of olfactory responses according to the feeding/mating status, and the time of the day (e.g., Almaas et al., 1991; Fox et al., 2001; Takken et al., 2001; Glendinning et al., 2009; Saveer et al., 2012; Stanczyk et al., 2013; Anderson and Anton, 2014; Claudianos et al., 2014; Reisenman, 2014). In general, associative learning is not usually represented at this level, although recent work in honeybees revealed that olfactory memories downregulate the expression of specific ORs. Furthermore, these changes occurred after conditioning and concomitantly, the population activity of antennal ORCs (measured as changes in EAG responses) decreased after learning (Claudianos et al., 2014). In mosquitoes, a reduction in the EAG responses to DEET correlates well with a post-exposure reduction in behavioral sensitivity to this repellent (Stanczyk et al., 2013).

The mushroom bodies mediate behaviors affected by learning and experience (e.g., Fahrbach et al., 1998; Zars et al., 2000; Huetteroth et al., 2015). However, in fruit flies and honeybees, learning already produces changes in glomerular volume and in synaptic distribution and density (e.g., Winnington et al., 1996; Devaud et al., 2001; Brown et al., 2002; Sachse et al.,

2007; Arenas et al., 2012), and can modify neural representations at the AL level (e.g., Faber et al., 1999; Chen et al., 2015), including glomerulus-specific neural plasticity (Rath et al., 2011). In moths, pre-exposure to the conspecific female sex pheromone increases the response of male PNs (Anderson et al., 2007), and associative learning with an appetitive cue causes recruitment of additional responsive neurons (Daly et al., 2001, 2004). Furthermore, learning of the scent of flowers which are profitable but are not innately preferred increases activity in AL neurons (Riffell, 2012; Riffell et al., 2013), and serotonin and octopamine are both involved in this process (Dacks et al., 2008, 2012). Experience might also have important effects facilitating segregation between a target odor and its odor background (see Section Effects of Background Odor), by modifying the balance of excitation and inhibition in AL neurons (Riffell et al., 2014; Szyszka, 2014; Chen et al., 2015). Noctuid moths switch their olfactory preference from food odors to egg-laying (e.g., cotton) odors following mating, and calcium imaging experiments demonstrated that this switch is due to changes in the representation of these odors across the AL glomerular array (Saveer et al., 2012). The mechanisms involving AL plasticity include modulation of the activity of ORCs by inhibitory interneurons (Ignell et al., 2009; Chou et al., 2010; Root et al., 2011), and neuromodulation by biogenic amines, neuropeptides and hormones (Nässel and Homberg, 2006; Dacks et al., 2008; Saveer et al., 2012).

In summary, experience and learning readily affect the odor oriented behavior of harmful insects through many neurophysiological mechanisms, which need to be considered in control strategies that include baits, repellents, use of trap crops, etc. Neurophysiological studies could help discover the most effective control methods; e.g., through high through-output screening of potential repellents that do not cause adaptation in ORCs.

CONCLUSIONS

Odor sources are widely used to manipulate the behavior of harmful insects. In recent decades, the neurobiological bases underlying insect olfactory behavior started to be unraveled. The insect olfactory system is able to encode the quality, quantity, and temporal features of the odor stimuli. Information about odor mixtures is also encoded, including the ratio between their components and discrimination in complex backgrounds. Moreover, responses to odors are modulated by the animal's internal and external state, and by experience and learning. Natural odors are usually odor mixtures (against a "noisy" background), and are represented as particular odor objects in the AL. Those odor objects signify relevant odor sources such as a host or a conspecific that, at least in some cases, could be "mimicked" in a simplified way using synthetic compounds, e.g., a male moth can be lured into a trap using synthetic versions containing few sex pheromone constituents. This facilitates the development of relatively simple and long-lasting odor baits to manipulate insect behavior. The simplified and optimal imitation of a natural odor mixture is challenging because it requires using only key mixture constituents, and this sometimes includes minor components within the natural mixture. Insect behavior can also be manipulated using repellents or "confusants." The studies mentioned in this work and others are helping us to understand how the olfactory system processes information about odors, making possible to design very efficient odor baits, repellents, or ways to confound the insects. Moreover, those studies also generate predictions about natural olfactory behavior that are useful to devise odor-based strategies for insect control. Clearly, the fields of neuroethology and insect control could certainly benefit from reciprocal interactions, which need to be fostered by all partners involved, including funding agencies. Encouraging new steps are being taken in this direction such as a recent initiative between different agencies on the beneficial and antagonistic interactions between plants (including agricultural plants) and their pathogens (including insects). We hope that the information provided in this review will help find gaps in the knowledge about the neural bases of olfactory behavior that are worth filling, encourage related studies, and promote the application of existing information in the development of better methods to manipulate insect behavior for control purposes.

AUTHOR CONTRIBUTIONS

PG contributed the general idea, wrote several sections, corrected the whole manuscript, and prepared the final version. CR wrote several sections, made several general suggestions, corrected the whole manuscript, and prepared the final version. HL wrote several sections, made general suggestions, and corrected the whole manuscript.

ACKNOWLEDGMENTS

HL was supported by an award from NSF (DMS 2100004). PG thanks Agencia Nacional de Promoción Científica y Tecnológica (ANPCyT), Argentina, for funding during part of this project through grant PICT-PRH-2009-43. We thank Dr. John Hildebrand (University of Arizona) for continuous inspiration, support, advice and encouragement throughout the years. CR also thanks Dr. Kristin Scott (UC Berkeley) for support and encouragement. We sincerely thank the reviewers for their many insightful comments and suggestions that substantially improved this manuscript.

REFERENCES

Abrell, L., Guerenstein, P. G., Mechaber, W. L., Stange, G., Christensen, T. A., and Nakanishi, K. (2005). Effect of elevated atmospheric CO_2 on oviposition behavior in *Manduca sexta* moths. *Global Change Biol.* 11, 1272–1282. doi: 10.1111/j.1365-2486.2005.00989.x

Abuin, L., Bargeton, B., Ulbrich, M. H., Isacoff, E. Y., Kellenberger, S., and Benton, R. (2011). Functional architecture of olfactory ionotropic

glutamate receptors. *Neuron* 69, 44–60. doi: 10.1016/j.neuron.2010.11.042

Achee, N. L., Bangs, M. J., Farlow, R., Killeen, G. F., Lindsay, S., Logan, J. G., et al. (2012). Spatial repellents: from discovery and development to evidence-based validation. *Malaria J.* 11:164. doi: 10.1186/1475-2875-11-164

Ai, M., Blais, S., Park, J.-Y., Min, S., Neubert, T. A., and Suh, G. S. B. (2013). Ionotropic glutamate receptors IR64a and IR8a form a functional odorant receptor complex *in vivo* in *Drosophila*. *J. Neurosci.* 33, 10741–10749. doi: 10.1523/JNEUROSCI.5419-12.2013

Almaas, T. J., Christensen, T. A., and Mustaparta, H. (1991). Chemical communication in heliothine moths. I. Antennal receptor neurons encode several features of intra-and interspecific odorants in the male corn earworm moth *Helicoverpa zea*. *J. Comp. Physiol. A* 169, 249–258.

Anderson, P., and Anton, S. (2014). Experience-based modulation of behavioural responses to plant volatiles and other sensory cues in insect herbivores. *Plant Cell Environ.* 37, 1826–1835. doi: 10.1111/pce.12342

Anderson, P., Hansson, B. S., Nilsson, U., Han, Q., Sjöholm, M., Skals, N., et al. (2007). Increased behavioral and neuronal sensitivity to sex pheromone after brief odor experience in a moth. *Chem. Senses* 32, 483–491. doi: 10.1093/chemse/bjm017

Andersson, M. N., Larsson, M. C., Blazenec, M., Jakus, R., Zhang, Q.-H., and Schlyter, F. (2010). Peripheral modulation of pheromone response by inhibitory host compound in a beetle. *J. Exp. Biol.* 213, 3332–3339. doi: 10.1242/jeb.044396

Andersson, M. N., Löfstedt, C., and Newcomb, R. D. (2015). Insect olfaction and the evolution of receptor tuning. *Front. Ecol. Evol.* 3:53. doi: 10.3389/fevo.2015.00053

Anton, S., and Hansson, B. S. (1995). Sex-pheromone and plant-associated odor processing in antennal lobe interneurons of male *Spodoptera littoralis* (Lepidoptera, Noctuidae). *J. Comp. Physiol. A* 176, 773–789. doi: 10.1007/BF00192625

Anton, S., and Homberg, U. (1999). "Antennal lobe strucure," in *Insect Olfaction,* ed B. S. Hansson (Berlin: Springer), 97–124.

Arenas, A., Giurfa, M., Sandoz, J. C., Hourcade, B., Devaud, J. M., and Farina, W. M. (2012). Early olfactory experience induces structural changes in the primary olfactory center of an insect brain. *Eur. J. Neurosci.* 35, 682–690. doi: 10.1111/j.1460-9568.2012.07999.x

Asahina, K., Louis, M., Piccinotti, S., and Vosshall, L. (2009). A circuit supporting concentration-invariant odor perception in *Drosophila*. *J. Biol.* 8, 19. doi: 10.1186/jbiol108

Badeke, E., Haverkamp, A., Hansson, B. S., and Sachse, S. (2016). A challenge for a male noctuid moth? Discerning the female sex pheromone against the background of plant volatiles. *Front. Physiol.* 7:143. doi: 10.3389/fphys.2016.00143

Baker, T. C., and Haynes, K. F. (1989). Field and laboratory electroantennographic measurements of pheromone plume structure correlated with oriental fruit moth behaviour. *Physiol. Entomol.* 14, 1–12. doi: 10.1111/j.1365-3032.1989.tb00931.x

Balkenius, A., Bisch-Knaden, S., and Hansson, B. (2009). Interaction of visual and odour cues in the mushroom body of the hawkmoth *Manduca sexta*. *J. Exp. Biol.* 212, 535–541. doi: 10.1242/jeb.021220

Barrozo, R. B., Gadenne, C., and Anton, S. (2010). Switching attraction to inhibition: mating-induced reversed role of sex pheromone in an insect. *J. Exp. Biol.* 213, 2933–2939. doi: 10.1242/jeb.043430

Barrozo, R. B., Jarriault, D., Deisig, N., Gemeno, C., Monsempes, C., Lucas, P., et al. (2011). Mating-induced differential coding of plant odour and sex pheromone in a male moth. *Eur. J. Neurosci.* 33, 1841–1850. doi: 10.1111/j.1460-9568.2011.07678.x

Barrozo, R. B., and Lazzari, C. R. (2004a). Orientation behaviour of the blood-sucking bug Triatoma infestans to short-chain fatty acids: synergistic effect of L-lactic acid and carbon dioxide. *Chem. Senses* 29, 833–841. doi: 10.1093/chemse/bjh249

Barrozo, R. B., and Lazzari, C. R. (2004b). The response of the blood-sucking bug *Triatoma infestans* to carbon dioxide and other host odours. *Chem. Senses* 29, 319–329. doi: 10.1093/chemse/bjh035

Barton-Browne, L. (1977). "Host-related responses and their suppression: some behavioral considerations," in *Chemical Control of Insect Behavior: Theory and Application*, eds H. H. Shorey and J. J. McKelvey (New York, NY: Wiley), 117–127.

Benton, R., Vannice, K. S., Gomez-Diaz, C., and Vosshall, L. B. (2009). Variant ionotropic glutamate receptors as chemosensory receptors in *Drosophila*. *Cell* 136, 149–162. doi: 10.1016/j.cell.2008.12.001

Berg, B., Almaas, T., Bjaalie, J. G., and Mustaparta, H. (1998). The macroglomerular complex of the antennal lobe in the tobacco budworm moth *Heliothis virescens*: specified subdivision in four compartments according to information about biologically significant compounds. *J. Comp. Physiol. A* 183, 669–682. doi: 10.1007/s003590050290

Binyameen, M., Hussain, A., Yousefi, F., Birgersson, G., and Schlyter, F. (2013). Modulation of reproductive behaviors by non-host volatiles in the polyphagous Egyptian cotton leafworm, *Spodoptera littoralis*. *J. Chem. Ecol.* 39, 1273–1283. doi: 10.1007/s10886-013-0354-4

Birch, M. C., Poppy, G. M., and Baker, T. C. (1990). Scents and eversible scent structures of male moths. *Annu. Rev. Entomol.* 35, 25–58. doi: 10.1146/annurev.en.35.010190.000325

Birkett, M. A., Agelopoulus, N., Jensen, V., Jesperen, M. B., Pickett, J. A., Prijs, J., et al. (2004). The role of volatile semiochemicals in mediating host location and selection by nuisance and disease-transmitting cattle flies. *Med. Vet. Entomol.* 18, 313–322. doi: 10.1111/j.0269-283X.2004.00528.x

Bitterman, M. E., Menzel, R., Fietz, A., and Schäfer, S. (1983). Classical conditioning of proboscis extension in honeybees (*Apis mellifera*). *J. Comp. Psychol.* 97, 107–119. doi: 10.1037/0735-7036.97.2.107

Blackwell, A., Mordue, A. J., Hansson, B. S., Wadhams, L. J., and Pickett, J. A. (1993). A behavioral and electrophysiological study of oviposition cues for *Culex quinquefasciatus*. *Physiol. Entomol.* 18, 343–348. doi: 10.1111/j.1365-3032.1993.tb00607.x

Boeckh, J., and Boeckh, V. (1979). Threshold and odor specificity of pheromone-sensitive neurons in the deutocerebrum of *Antheraea pernyi* and *A. polyphemus* (Saturniidae). *J. Comp. Physiol. A* 132, 235–242. doi: 10.1007/BF00614495

Bohbot, J. D., and Dickens, J. C. (2010). Insect repellents: modulators of mosquito odorant receptor activity. *PLoS ONE* 5:e12138. doi: 10.1371/journal.pone.0012138

Borges, L. M. F., Gomes de Oliveira Filho, J., Ferreira, L. L., Braz Louly, C. C., Pickett, J. A., and Birkett, M. A. (2015). Identification of non-host semiochemicals for the brown dog tick, *Rhipicephalus sanguineus sensu lato* (Acari: Ixodidae), from tick-resistant beagles, *Canis lupus* familiaris. *Ticks Tick-Borne Dis.* 6, 676–682. doi: 10.1016/j.ttbdis.2015.05.014

Bosch, O. J., Geier, M., and Boeckh, J. (2000). Contribution of fatty acids to olfactory host finding of female *Aedes aegypti*. *Chem. Senses* 25, 323–330. doi: 10.1093/oxfordjournals.chemse.a014042

Bouyer, J., Pruvot, M., Bengaly, Z., Guerin, P. M., and Lancelot, R. (2007). Learning influences host choice in tsetse. *Biol. Lett.* 3, 113–117. doi: 10.1098/rsbl.2006.0578

Bowers, W. S., Nault, L. R., Webb, R. E., and Dutky, S. R. (1972). Aphid alarm pheromone: isolation, identification, synthesis. *Science* 177, 1121–1122. doi: 10.1126/science.177.4054.1121

Bray, S., and Amrein, H. (2003). A putative *Drosophila* pheromone receptor expressed in male-specific taste neurons is required for efficient courtship. *Neuron* 39, 1019–1029. doi: 10.1016/S0896-6273(03)00542-7

Brooks, T. W., Doane, C. C., and Staten, R. T. (1979). "Experience with the first commercial pheromone communication disruptive for suppression of an agricultural pest," in *Chemical Ecology: Odour Communication in Animals*, ed F. J. Ritter (Amsterdam: Elsevier), 375–388.

Brown, S. M., Napper, R. M. T. C. M., and Mercer, A. (2002). Stereological analysis reveals striking differences in the structural plasticity of two readily identifiable glomeruli in the antennal lobes of the adult worker honeybee. *J. Neurosci.* 22, 8514–8522.

Bruce, T. J. A., and Pickett, J. A. (2011). Perception of plant volatile blends by herbivorous insects – finding the right mix. *Phytochemistry* 72, 1605–1611. doi: 10.1016/j.phytochem.2011.04.011

Büchel, K., Austel, N., Mayer, M., Gershenzon, J., Fenning, T. M., and Meiners, T. (2014). Smelling the tree and the forest: elm background odours affect egg parasitoid orientation to herbivore induced terpenoids. *Biocontrol* 59, 29–43. doi: 10.1007/s10526-013-9544-9

Byers, J. A., Fefer, D., and Levi-Zada, A. (2013). Sex pheromone component ratios and mating isolation among three *Lygus* plant bug species of North America. *Naturwiss* 100, 1115–1123. doi: 10.1007/s00114-013-1113-7

Cardé, R. T. (1990). "Principles of mating disruption," in *Behavior-Modifying Chemicals for Insect Management, Applications of Pheromones and Other Attractants*, eds R. L. Ridgway, R. M. Silverstein, and M. N. Inscoe (New York, NY: Dekker), 47–72.

Cardé, R. T., and Gibson, G. (2010). "Host finding by female mosquitoes: mechanisms of orientation to host odours and other cues" in *Olfaction in Vector-Host Interactions,* eds W. Takken and B. Knols (Wageningen: Wageningen Academic Publishers), 115–141.

Carlsson, M. A., Galizia, C. G., and Hansson, B. S. (2002). Spatial representation of odours in the antennal lobe of the moth *Spodoptera littoralis* (Lepidoptera: Noctuidae). *Chem. Senses* 27, 231–244. doi: 10.1093/chemse/27.3.231

Carrasco, D., Larsson, M. C., and Anderson, P. (2015). Insect host plant selection in complex environments. *Curr. Opin. Insect Sci.* 8, 1–7. doi: 10.1016/j.cois.2015.01.014

Cha, D. H., Nojima, S., Hesler, S. P., Zhang, A., Linn, C. E., Roelofs, W. L., et al. (2008). Identification and field evaluation of grape shoot volatiles attractive to female grape berry moth (*Paralobesia viteana*). *J. Chem. Ecol.* 34, 1180–1189. doi: 10.1007/s10886-008-9517-0

Chaffiol, A., Dupuy, F., Barrozo, R. B., Kropf, J., Renou, M., Rospars, J.-P., et al. (2014). Pheromone modulates plant odor responses in the antennal lobe of a moth. *Chem. Senses* 39, 451–463. doi: 10.1093/chemse/bju017

Chaffiol, A., Kropf, J., Barrozo, R. B., Gadenne, C., Rospars, J. P., and Anton, S. (2012). Plant odour stimuli reshape pheromonal representation in neurons of the antennal lobe macroglomerular complex of a male moth. *J. Exp. Biol.* 215, 1670–1680. doi: 10.1242/jeb.066662

Chapman, T. B., Veblen, T. T., and Schoennagel, T. (2012). Spatiotemporal patterns of mountain pine beetle activity in the southern Rocky Mountains. *Ecology* 93, 2175–2185. doi: 10.1890/11-1055.1

Chen, J.-Y., Marachlian, E., Assisi, C., Huerta, R., Smith, B. H., Locatelli, F., et al. (2015). Learning modifies odor mixture processing to improve detection of relevant components. *J. Neurosci.* 35, 179–197. doi: 10.1523/JNEUROSCI.2345-14.2015

Chilaka, N., Perkins, E., and Tripet, F. (2012). Visual and olfactory associative learning in the malaria vector Anopheles gambiae sensu stricto. *Malaria J.* 11:27. doi: 10.1186/1475-2875-11-27

Chou, Y.-H., Spletter, M. L., Yaksi, E., Leong, J. C. S., Wilson, R. I., and Luo, L. (2010). Diversity and wiring variability of olfactory local interneurons in the *Drosophila* antennal lobe. *Nat. Neurosci.* 13, 439–449. doi: 10.1038/nn.2489

Christensen, T. A., and Hildebrand, J. G. (1987). Male-specific, sex pheromone-selective projection neurons in the antennal lobes of the moth *Manduca sexta*. *J. Comp. Physiol. A* 160, 553–569. doi: 10.1007/BF00611929

Christensen, T. A., and Hildebrand, J. G. (1988). Frequency coding by central olfactory neurons in the sphinx moth *Manduca sexta*. *Chem. Senses* 13, 123–130. doi: 10.1093/chemse/13.1.123

Christensen, T. A., Waldrop, B. R., Harrow, I. D., and Hildebrand, J. G. (1993). Local interneurons and information processing in the olfactory glomeruli of the moth *Manduca sexta*. *J. Comp. Physiol. A* 173, 385–399. doi: 10.1007/bf00193512

Claudianos, C., Lim, J., Young, M., Yan, S., Cristino, A. S., Newcomb, R. D., et al. (2014). Odor memories regulate olfactory receptor expression in the sensory periphery. *Eur. J. Neurosci.* 39, 1642–1654. doi: 10.1111/ejn.12539

Cook, S. M., Khan, Z. R., and Pickett, J. A. (2007). The use of push-pull strategies in integrated pest management. *Annu. Rev. Entomol.* 52, 375–400. doi: 10.1146/annurev.ento.52.110405.091407

Dacks, A. M., Christensen, T. A., and Hildebrand, J. G. (2008). Modulation of olfactory information processing in the antennal lobe of *Manduca sexta*. *J. Neurophysiol.* 99, 2077–2085. doi: 10.1152/jn.01372.2007

Dacks, A. M., Riffell, J. A., Martin, J. P., Gage, S. L., and Nighorn, A. J. (2012). Olfactory modulation by dopamine in the context of aversive learning. *J. Neurophysiol.* 108, 539–550. doi: 10.1152/jn.00159.2012

Daly, K. C., Christensen, T. A., Lei, H., Smith, B. H., and Hildebrand, J. G. (2004). Learning modulates the ensemble representations for odors in primary olfactory networks. *Proc. Natl. Acad. Sci. U.S.A.* 101, 10476–10481. doi: 10.1073/pnas.0401902101

Daly, K. C., Durtschi, M. L., and Smith, B. H. (2001). Olfactory-based discrimination learning in the moth, *Manduca sexta*. *J. Insect Physiol.* 47, 375–384. doi: 10.1016/S0022-1910(00)00117-7

Davis, E. E., and Sokolove, P. G. (1976). Lactic acid-sensitive receptors on the antennae of the mosquito, *Aedes aegypti*. *J. Comp. Physiol. A* 105, 43–54. doi: 10.1007/BF01380052

Davis, R. L. (2004). Olfactory learning. *Neuron* 44, 31–48. doi: 10.1016/j.neuron.2004.09.008

de Bruyne, M., Clyne, P. J., and Carlson, J. R. (1999). Odor coding in a model olfactory organ: the *Drosophila* maxillary palp. *J. Neurosci.* 19, 4520–4532.

DeGennaro, M., McBride, C. S., Seeholzer, L., Nakagawa, T., Dennis, E. J., and Goldman, C. (2013). Orco mutant mosquitoes lose strong preference for humans and are not repelled by volatile DEET. *Nature* 498, 487–491. doi: 10.1038/nature12206

Deisig, N., Giurfa, M., Lachnit, H., and Sandoz, J. C. (2006). Neural representation of olfactory mixtures in the honeybee antennal lobe. *Eur. J. Neurosci.* 24, 1161–1174. doi: 10.1111/j.1460-9568.2006.04959.x

Deisig, N., Kropf, J., Vitecek, S., Pevergne, D., Rouyar, A., Sandoz, J.-C., et al. (2012). Differential interactions of sex pheromone and plant odour in the olfactory pathway of a male moth. *PLoS ONE* 7:e33159. doi: 10.1371/journal.pone.0033159

Devaud, J. M., Acebes, A., and Ferrus, A. (2001). Odor exposure causes central adaptation and morphological changes in selected olfactory glomeruli in *Drosophila*. *J. Neurosci.* 21, 6274–6282.

Dewhirst, S. Y., Pickett, J. A., and Hardie, J. (2010). Aphid pheromones. *Vitam. Horm.* 83, 551–574. doi: 10.1016/S0083-6729(10)83022-5

Diehl, P. A., Vlimant, M., Guerenstein, P. G., and Guerin, P. M. (2003). Ultrastructure and receptor cell responses of the antennal grooved peg sensilla of *Triatoma infestans* (Hemiptera: Reduviidae). *Arthropod. Struct. Dev.* 31, 271–285. doi: 10.1016/S1467-8039(03)00004-5

Ditzen, M., Pellegrino, M., and Vosshall, L. B. (2008). Insect odorant receptors are molecular targets of the insect repellent DEET. *Science* 319, 1838–1842. doi: 10.1126/science.1153121

Dolzer, J., Fischer, K., and Stengl, M. (2003). Adaptation in pheromone-sensitive trichoid sensilla of the hawkmoth *Manduca sexta*. *J. Exp. Biol.* 206, 1575–1588. doi: 10.1242/jeb.00302

Dolzer, J., Krannich, S., and Stengl, M. (2008). Pharmacological investigation of protein Kinase C- and cGMP-dependent ion channels in cultured olfactory receptor neurons of the hawkmoth *Manduca sexta*. *Chem. Senses* 33, 803–813. doi: 10.1093/chemse/bjn043

Dusenbery, D. B. (1992). *Sensory Ecology: How Organisms Acquire and Respond to Information.* New York, NY: Freeman.

Dweck, H. K. M., Ebrahim, S. A. M., Thoma, M., Mohamed, A. A. M., Keesey, I. W., Trona, F., et al. (2015). Pheromones mediating copulation and attraction in *Drosophila*. *Proc. Natl. Acad. Sci. U.S.A.* 112, 2829–2835. doi: 10.1073/pnas.1504527112

Faber, T., Joerges, J., and Menzel, R. (1999). Associative learning modifies neural representations of odors in the insect brain. *Nat. Neurosci.* 2, 74–78. doi: 10.1038/4576

Fahrbach, S. E. (2006). Structure of the mushroom bodies of the insect brain. *Annu. Rev. Entomol.* 51, 209–232. doi: 10.1146/annurev.ento.51.110104.150954

Fahrbach, S. E., Moore, D., Capaldi, E. A., Farris, S. M., and Robinson, G. E. (1998). Experience-expectant plasticity in the mushroom bodies of the honeybee. *Learn. Mem.* 5, 115–123.

Fernandez, P. C., Locatelli, F. F., Person-Rennell, N., Deleo, G., and Smith, B. H. (2009). Associative conditioning tunes transient dynamics of early olfactory processing. *J. Neurosci.* 29, 10191–10202. doi: 10.1523/JNEUROSCI.1874-09.2009

Fishilevich, E., and Vosshall, L. B. (2005). Genetic and functional subdivision of the drosophila antennal lobe. *Curr. Biol.* 15, 1548–1553 doi: 10.1016/j.cub.2005.07.066

Foster, S. P., and Harris, M. O. (1997). Behavioural manipulation methods for insect pest management. *Annu. Rev. Entomol.* 42, 123–146. doi: 10.1146/annurev.ento.42.1.123

Fox, A. N., Pitts, R. J., Robertson, H. M., Carlson, J. R., and Zwiebel, L. J. (2001). Candidate odorant receptors from the malaria vector mosquito *Anopheles gambiae* and evidence of down-regulation in response to blood feeding. *Proc. Natl. Acad. Sci. U.S.A.* 98, 14693–14697. doi: 10.1073/pnas.261432998

Fujiwara, T., Kazawa, T., Haupt, S. S., and Kanzaki, R. (2009). Ca^{2+} imaging of identifiable neurons labeled by electroporation in insect brains. *Neuroreport* 20, 1061–1065. doi: 10.1097/WNR.0b013e32832e7d93

Galizia, C. G., and Rössler, W. (2010). Parallel olfactory systems in insects: anatomy and function. *Annu. Rev. Entomol.* 55, 399–420. doi: 10.1146/annurev-ento-112408-085442

Galizia, C. G., and Sachse, S. (2010). "Odor coding in insects," in *The Neurobiology of Olfaction*, ed A. Menini. (Boca Raton. FL, CRC Press), 35–70.

Gaudry, Q., Nagel, K. I., and Wilson, R. I. (2012). Smelling on the fly: sensory cues and strategies for olfactory navigation in *Drosophila*. *Curr. Opinion Neurobiol.* 22, 216–222. doi: 10.1016/j.conb.2011.12.010

Geier, M., Bosch, O. J., and Boeckh, J. (1999a). Ammonia as an attractive component of host odour for the yellow fever mosquito, *Aedes aegypti*. *Chem. Senses* 24, 647–653. doi: 10.1093/chemse/24.6.647

Geier, M., Bosch, O. J., and Boeckh, J. (1999b). Influence of odour plume structure on upwind flight of mosquitoes towards hosts. *J. Exp. Biol.* 202, 1639–1648.

Geier, M., Sass, H., and Boeckh, J. (1996). "A search for components in human body odour that attract females of *Aedes aegypti*," in *Mosquito Olfaction and Olfactory-Mediated Mosquito–Host Interactions, Ciba Foundation Symposium 200*, ed G. Cardew and J. Goode (New York, NY: John Wiley & Sons Ltd), 132–144.

Glendinning, J., Foley, C., Loncar, I., and Rai, M. (2009). Induced preference for host plant chemicals in the tobacco hornworm: contribution of olfaction and taste. *J. Comp. Physiol. A* 195, 591–601. doi: 10.1007/s00359-009-0434-7

Goyret, J., Markwell, P. M., and Raguso, R. A. (2008). Context- and scale-dependent effects of floral CO_2 on nectar foraging by *Manduca sexta*. *Proc. Natl. Acad. Sci. U.S.A.* 105, 4565–4570. doi: 10.1073/pnas.0708629105

Green, C. H. (1986). Effects of colours and synthetic odours on the attraction of *Glossina pallidipes* and *G. morsitans* to traps and screens. *Physiol. Entomol.* 11, 411–421. doi: 10.1111/j.1365-3032.1986.tb00432.x

Green, C. H. (1993). The effect of odours and target colour on landing responses of *Glossina morsitans morsitans* and *G. pallidipes* (Diptera: Glossinidae). *Bull. Entomol. Res.* 83, 553–562. doi: 10.1017/S0007485300039985

Green, C. H. (1994). Bait methods for tsetse fly control. *Adv. Parasitol.* 34, 229–291. doi: 10.1016/S0065-308X(08)60140-2

Grenacher, S., Kröber, T., Guerin, P. M., and Vlimant, M. (2001). Behavioural and chemoreceptor cell responses of the tick, *Ixodes ricinus*, to its own faeces and faecal constituents. *Exp. Appl. Acarol.* 25, 641–660. doi: 10.1023/A:1016145805759

Grosse-Wilde, E., Stieber, R., Forstner, M., Krieger, J. G., Wicher, D., and Hansson, B. S. (2010). Sex-specific odorant receptors of the tobacco hornworm *Manduca sexta*. *Front. Cell. Neurosci.* 4:22. doi: 10.3389/fncel.2010.00022

Guerenstein, P. G., Christensen, T. A., and Hildebrand, J. G. (2004a). Sensory processing of ambient CO_2 information in the brain of the moth *Manduca sexta*. *J. Comp. Physiol. A* 190, 707–725. doi: 10.1007/s00359-004-0529-0

Guerenstein, P. G., and Guerin, P. M. (2001). Olfactory and behavioural responses of the blood-sucking bug *Triatoma infestans* to odours of vertebrate hosts. *J. Exp. Biol.* 204, 585–597.

Guerenstein, P. G., and Guerin, P. M. (2004). A comparison of volatiles emitted by adults of three triatomine species. *Entomol. Exp. Appl.* 111, 151–155. doi: 10.1111/j.0013-8703.2004.00160.x

Guerenstein, P. G., and Hildebrand, J. G. (2008). Roles and effects of environmental carbon dioxide in insect life. *Annu. Rev. Entomol.* 53, 161–178. doi: 10.1146/annurev.ento.53.103106.093402

Guerenstein, P. G., and Lazzari, C. R. (2009). Host-seeking: how triatomines acquire and make use of information to find blood. *Acta Trop.* 110, 148–158. doi: 10.1016/j.actatropica.2008.09.019

Guerenstein, P. G., and Lazzari, C. R. (2010). "The role of olfaction in host seeking of Triatominae bugs," in *Ecology and Control of Vector-Borne Diseases, Olfaction in Vector-Host Interactions*, *Vol 2,* ed W. Takken and B. Knols (Wageningen: Wageningen University Press), 309–325.

Guerenstein, P. G., Yepez, E. A., van Haren, J., Williams, D. G., and Hildebrand, J. G. (2004b). Floral CO_2 emission may indicate food abundance to nectar-feeding moths. *Naturwiss* 91, 329–333. doi: 10.1007/s00114-004-0532-x

Guerrieri, F., Gemeno, C., Monsempes, C., Anton, S., Jacquin-Joly, E., Lucas, P., et al. (2012). Experience-dependent modulation of antennal sensitivity and input to antennal lobes in male moths (*Spodoptera littoralis*) pre-exposed to sex pheromone. *J. Exp. Biol.* 215, 2334–2341. doi: 10.1242/jeb.060988

Guidobaldi, F., and Guerenstein, P. G. (2013). Evaluation of a CO_2-free commercial mosquito attractant to capture triatomines in the laboratory. *J. Vector Ecol.* 38, 245–250. doi: 10.1111/j.1948-7134.2013.12037.x

Guidobaldi, F., and Guerenstein, P. G. (2016). A CO_2-free synthetic host-odor mixture that attracts and captures triatomines: effect of emitted odorant ratios. *J. Med. Entomol.* doi: 10.1093/jme/tjw057. [Epub ahead of print].

Guidobaldi, F., May Concha, I. J., and Guerenstein, P. G. (2014). Morphology and physiology of the olfactory system of blood-feeding insects. *J. Physiol. Paris* 108, 96–111. doi: 10.1016/j.jphysparis.2014.04.006

Gupta, N., and Stopfer, M. (2012). Functional analysis of a higher olfactory center, the lateral horn. *J. Neurosci.* 32, 8138–8148. doi: 10.1523/JNEUROSCI.1066-12.2012

Hallem, E. A., and Carlson, J. R. (2006). Coding of odors by a receptor repertoire. *Cell* 125, 143–160. doi: 10.1016/j.cell.2006.01.050

Hansson, B. S., Almaas, T. J., and Anton, S. (1995). Chemical communication in heliothine moths. 5. Antennal lobe projection patterns of pheromone-detecting olfactory receptor neurons in the male *Heliothis virescens* (Lepidoptera, Noctuidae). *J. Comp. Physiol. A* 177, 535–543.

Hansson, B. S., Carlsson, M. A., and Kalinova, B. (2003). Olfactory activation patterns in the antennal lobe of the sphinx moth, *Manduca sexta*. *J. Comp. Physiol. A* 189, 301–308. doi: 10.1007/s00359-003-0403-5

Hansson, B. S., Christensen, T. A., and Hildebrand, J. G. (1991). Functionally distinct subdivisions of the macroglomerular complex in the antennal lobe of the male sphinx moth *Manduca sexta*. *J. Comp. Neurol.* 312, 264–278. doi: 10.1002/cne.903120209

Hansson, B. S., Larsson, M. C., and Leal, W. S. (1999). Green leaf volatile-detecting olfactory receptor neurons display very high sensitivity and specificity in a scarab beetle. *Physiol. Entomol.* 24, 121–126. doi: 10.1046/j.1365-3032.1999.00121.x

Hansson, B. S., Ljungberg, H., Hallberg, E., and Löfstedt, C. (1992). Functional specialization of olfactory glomeruli in a moth. *Science* 256, 1313–1315. doi: 10.1126/science.1598574

Hartlieb, E., Anderson, P., and Hansson, B. S. (1999). Appetitive learning of odours with different behavioral meaning in moths. *Physiol. Behav.* 67, 671–677. doi: 10.1016/S0031-9384(99)00124-9

Hartlieb, E., and Hansson, B. S. (1999). Sex or food? Appetetive learning of sex odors in a male moth. *Naturwiss* 86, 396–399. doi: 10.1007/s001140050640

Hatano, E., Saveer, A. M., Borrero-Echeverry, F., Strauch, M., Zakir, A., Bengtsson, M., et al. (2015). A herbivore-induced plant volatile interferes with host plant and mate location in moths through suppression of olfactory signalling pathways. *BMC Biol.* 13:75. doi: 10.1186/s12915-015-0188-3

Heinbockel, T., Christensen, T. A., and Hildebrand, J. G. (1999). Temporal tuning of odor responses in pheromone-responsive projection neurons in the brain of the sphinx moth *Manduca sexta*. *J. Comp. Neurol.* 409, 1–12.

Heinbockel, T., Christensen, T. A., and Hildebrand, J. G. (2004). Representation of binary pheromone blends by glomerulus-specific olfactory projection neurons. *J. Comp. Physiol. A* 190, 1023–1037. doi: 10.1007/s00359-004-0559-7

Hildebrand, J. G. (1996). King solomon lecture: olfactory control of behavior in moths: central processing of odor information and the functional significance of olfactory glomeruli. *J. Comp. Physiol. A* 178, 5–19. doi: 10.1007/BF00189586

Hildebrand, J., G., Matsumoto, S. G., Camazine, S. M., Tolbert, L. P., Blank, S., Ferguson, H., et al. (1980). "Organisation and physiology of antennal centres in the brain of the moth *Manduca sexta*," in *Insect Neurobiology and Pesticide Action* (Neurotox 79) (London: Society of Chemical Industry), 375–382.

Hillier, N. K., Kelly, D., and Vickers, N. J. (2006). A specific male olfactory sensillum detects behaviorally antagonistic hairpencil odorants. *J. Insect Sci.* 7:4. doi: 10.1673/031.007.0401

Homberg, U., Christensen, T. A., and Hildebrand, J. G. (1989). Structure and function of the deutocerebrum in insects. *Annu. Rev. Entomol.* 34, 477–501. doi: 10.1146/annurev.en.34.010189.002401

Homberg, U., Montague, R. A., and Hildebrand, J. G. (1988). Anatomy of antenno-cerebral pathways in the brain of the sphinx moth *Manduca sexta*. *Cell Tissue Res.* 254, 255–281. doi: 10.1007/BF00225800

Hoskins, S. G., Homberg, U., Kingan, T. G., Christensen, T. A., and Hildebrand, J. G. (1986). Immunocytochemistry of GABA in the antennal lobes of the sphinx moth *Manduca sexta*. *Cell Tissue Res.* 244, 243–252. doi: 10.1007/BF00219199

Huang, J., Stelinski, L. L., and Gut, L. J. (2010). Mating behaviors of *Cydia pomonella* (Lepidoptera: Tortricidae) as influenced by sex pheromone in electrostatic powder. *J. Econ. Entomol.* 103, 2100–2106. doi: 10.1603/EC10063

Huetteroth, W., Perisse, E., Lin, S., Klappenbach, M., Burke, C., and Waddell, S. (2015). Sweet taste and nutrient value subdivide rewarding dopaminergic neurons in *Drosophila*. *Curr. Biol.* 25, 751–758. doi: 10.1016/j.cub.2015.01.036

Husch, A., Paehler, M., Fusca, D., Paeger, L., and Kloppenburg, P. (2009). Calcium current diversity in physiologically different local interneuron types of the antennal lobe. *J. Neurosci.* 29, 716–726. doi: 10.1523/JNEUROSCI.3677-08.2009

Hussain, A., Zhang, M., Üçpunar, H. K., Svensson, T., Quillery, E., Gompel, N. et al. (2016). Ionotropic chemosensory receptors mediate the taste and smell of polyamines. *PLoS Biol* 14:e1002454. doi: 10.1371/journal.pbio.1002454

Ignell, R., Root, C. M., Birse, R. T., Wang, J. W., Nässel, D. R., and Winther, S. M. E. (2009). Presynaptic peptidergic modulation of olfactory receptor neurons in *Drosophila*. *Proc. Natl. Acad. Sci. U.S.A.* 106, 13070–13075. doi: 10.1073/pnas.0813004106

Ito, I., Bazhenov, M., Ong, R. C., Raman, B., and Stopfer, M. (2009). Frequency transitions in odor-evoked neural oscillations. *Neuron* 64, 692–706. doi: 10.1016/j.neuron.2009.10.004

Iwano, M., Hill, E. S., Mori, A., Mishima, T., Ito, K., and Kanzaki, R. (2010). Neurons associated with the flip-flop activity in the lateral accessory lobe and ventral protocerebrum of the silkworm moth brain. *J. Comp. Neurol.* 518, 366–388. doi: 10.1002/cne.22224

Jeanne, J. M., and Wilson, R. I. (2015). Convergence, divergence, and reconvergence in a feedforward network improves neural speed and accuracy. *Neuron* 88, 1014–1026. doi: 10.1016/j.neuron.2015.10.018

Jefferis, G. S., Potter, C. J., Chan, A. M., Marin, E. C., Rohlfing, T., Maurer, C. R. Jr., et al. (2007). Comprehensive maps of *Drosophila* higher olfactory centers: spatially segregated fruit and pheromone representation. *Cell* 128, 1187–1203. doi: 10.1016/j.cell.2007.01.040

Jhumur, U. S., Dötterl, S., and Jürgens, A. (2006). Naive and conditioned responses of *Culex pipiens pipiens* biotype molestus (Diptera: Culicidae) to flower odors. *J. Med. Entomol.* 43, 1164–1170. doi: 10.1603/0022-2585(2006)43[1164:nacroc]2.0.co;2

Jones, W. D., Cayirlioglu, P., Kadow, I. G., and Vosshall, L. B. (2007). Two chemosensory receptors together mediate carbon dioxide detection in *Drosophila*. *Nature* 445, 86–90. doi: 10.1038/nature05466

Kadohisa, M., and Wilson, D. A. (2006). Olfactory cortical adaptation facilitates detection of odors against background. *J. Neurophysiol.* 95, 1888–1896. doi: 10.1152/jn.00812.2005

Kaissling, K.-E., Hildebrand, J. G., and Tumlinson, J. H. (1989). Pheromone receptor cells in the male moth *Manduca sexta*. *Arch. Insect Biochem. Physiol.* 10, 273–279. doi: 10.1002/arch.940100403

Kanzaki, R., and Shibuya, T. (1983). Olfactory neural pathway and sexual pheromone responses in the deutocerebrum of the male silkworm moth, *Bombyx mori* (Lepidoptera: Bombycidae). *Appl. Ent. Zool.* 18, 131–133.

Kaur, J., Lai, Y., and Giger, A. (2003). Learning and memory in the mosquito *Aedes aegypti* shown by conditioning against oviposition deterrence. *Med. Vet. Entomol.* 17, 457–460. doi: 10.1111/j.1365-2915.2003.00455.x

Kent, L. B., Walden, K. O., and Robertson, H. M. (2008). The Gr family of candidate gustatory and olfactory receptors in the yellow fever mosquito *Aedes aegypti*. *Chem. Senses* 33, 79–93. doi: 10.1093/chemse/bjm067

Klun, J. A., Chapman, O. L., Mattes, K. C., Wojtkowski, P. W., Beroza, M., and Sonnet, P. E. (1973). Insect sex pheromones: minor amount of opposite geometrical isomer critical to attraction. *Science* 181, 661–663. doi: 10.1126/science.181.4100.661

Kohl, J., Huoviala, P., and Jefferis, G. S. (2015). Pheromone processing in *Drosophila*. *Curr. Opin. Neurobiol.* 34, 149–157. doi: 10.1016/j.conb.2015.06.009

Krieger, J., Gondesen, I., Forstner, M., Gohl, T., Dewer, Y., and Breer, H. (2009). HR11 and HR13 Receptor-expressing neurons are housed together in pheromone-responsive sensilla Trichodea of male *Heliothis virescens*. *Chem. Senses* 34, 469–477. doi: 10.1093/chemse/bjp012

Krockel, U., Rose, A., Eiras, A. E., and Geier, M. (2006). New tools for surveillance of adult yellow fever mosquitoes: comparison of trap catches with human landing rates in an urban environment. *J. Am. Mosq. Control Assoc.* 22, 229–238. doi: 10.2987/8756-971X(2006)22[229:NTFSOA]2.0.CO;2

Kwon, J.-Y., Dahanukar, A., Weiss, L. A., and Carlson, J. R. (2007). The molecular basis of CO_2 reception in *Drosophila*. *Proc. Natl. Acad. Sci. U.S.A.* 104, 3574–3578. doi: 10.1073/pnas.0700079104

Larsson, M. C., Domingos, A. I., Jones, W. D., Chiappe, M. E., Amrein, H., and Vosshall, L. B. (2004). Or83b encodes a broadly expressed odorant receptor essential for *Drosophila* olfaction. *Neuron* 43, 703–714. doi: 10.1016/j.neuron.2004.08.019

Leal, W. S. (2013). Odorant reception in insects: roles of receptors, binding ‘proteins, and degrading enzymes. *Annu. Rev. Entomol.* 58, 373–391. doi: 10.1146/annurev-ento-120811-153635

Leal, W. S. (2014). The enigmatic reception of DEET—the gold standard of insect repellents. *Curr. Opin. Insect Sci.* 6, 93–98. doi: 10.1016/j.cois.2014.10.007

Lee, Y., Kim, S. H., and Montell, C. (2010). Avoiding DEET through insect gustatory receptors. *Neuron* 67, 555–561. doi: 10.1016/j.neuron.2010.07.006

Lei, H., Chiu, H. Y., and Hildebrand, J. G. (2013). Responses of protocerebral neurons in *Manduca sexta* to sex-pheromone mixtures. *J. Comp. Physiol. A* 199, 997–1014. doi: 10.1007/s00359-013-0844-4

Lei, H., Christensen, T. A., and Hildebrand, J. G. (2002). Local inhibition modulates odor-evoked synchronization of glomerulus-specific output neurons. *Nat. Neurosci.* 5, 557–565. doi: 10.1038/nn0602-859

Lei, H., Christensen, T. A., and Hildebrand, J. G. (2004). Spatial and temporal organization of ensemble representations for different odor classes in the moth antennal lobe. *J. Neurosci.* 24, 11108–11119. doi: 10.1523/JNEUROSCI.3677-04.2004

Lei, H., and Hansson, B. S. (1999). Central processing of pulsed pheromone signals by antennal lobe neurons in the male moth *Agrotis segetum*. *J. Neurophysiol.* 81, 1113–1122.

Lei, H., Riffell, J. A., Gage, S. L., and Hildebrand, J. G. (2009). Contrast enhancement of stimulus intermittency in a primary olfactory network and its behavioral significance. *J. Biol.* 8, 21. doi: 10.1186/jbiol120

Lei, H., and Vickers, N. (2008). Central processing of natural odor mixtures in insects. *J. Chem. Ecol.* 34, 915–927 doi: 10.1007/s10886-008-9487-2

Levinson, H. Z., Levinson, A. R., and Maschwitz, U. (1974a). Action and composition of the alarm pheromone of the bedbug *Cimex lectularius* L. *Naturwissenschaften* 61, 684–685. doi: 10.1007/BF00606522

Levinson, H. Z., Levinson, A. R., Müller, B., and Steinbrecht, R. A. (1974b). Structure of sensilla, olfactory perception, and behaviour of the bedbug, *Cimex lectularius*, in response to its alarm pheromone. *J. Insect Physiol.* 20, 1231–1248. doi: 10.1016/0022-1910(74)90229-7

Linn, C. Jr., Nojima, S., and Roelofs, W. (2005). Antagonist effects of non-host fruit volatiles on discrimination of host fruit by *Rhagoletis* flies infesting apple (*Malus pumila*), hawthorn (*Crataegus* spp.), and flowering dogwood (*Cornus florida*). *Entomol. Exp. Appl.* 114, 97–105. doi: 10.1111/j.1570-7458.2005.00222.x

Linster, C., Henry, L., Kadohisa, M., and Wilson, D. A. (2007). Synaptic adaptation and odor-background segmentation. *Neurobiol. Learn. Mem.* 87, 352–360. doi: 10.1016/j.nlm.2006.09.011

Liu, C., Placais, P.-Y., Yamagata, N., Pfeiffer, B. D., Aso, Y., Friedrich, A. B., et al. (2012). A subset of dopamine neurons signals reward for odour memory in *Drosophila*. *Nature* 488, 512–516. doi: 10.1038/nature11304

Löfstedt, C., Herrebout, W. M., and Menken, S. B. (1991). Sex pheromones and their potential role in the evolution of reproductive isolation in small ermine moths (Yponomeutidae). *Chemoecology* 2, 20–28. doi: 10.1007/BF01240662

Logan, J. G., and Birkett, M. A. (2007). Semiochemicals for biting fly control: their identification and exploitation. *Pest Manag. Sci.* 63, 647–657. doi: 10.1002/ps.1408

Logan, J. G., Birkett, M. A., Clark, S. J., Powers, S., Seal, N. J., Wadhams, L. J., et al. (2008). Identification of human-derived volatile chemicals that interfere with attraction of *Aedes aegypti* mosquitoes. *J. Chem. Ecol.* 34, 308–322. doi: 10.1007/s10886-008-9436-0

Logan, J. G., Seal, N. J., Cook, J. I., Stanczyk, N. M., Birkett, M. A., Clark, S. J., et al. (2009). Identification of human-derived volatile chemicals that interfere with attraction of the Scottish biting midge and their potential use. *J. Med. Entomol.* 46, 208–219. doi: 10.1603/033.046.0205

Lorenzo Figueiras, A. N., Girotti, J. R., Mijailovsky, S. J., and Juárez, M. P. (2009). Epicuticular lipids induce aggregation in Chagas disease vectors. *Parasites Vectors* 2:8. doi: 10.1186/1756-3305-2-8

Lu, T., Qiu, Y.-T., Wang, G., Kwon, J. Y., Rützler, M., Kwon, H., et al. (2007). Odor coding in the maxillary palp of the malaria vector mosquito *Anopheles gambiae*. *Curr. Biol.* 17, 1533–1544. doi: 10.1016/j.cub.2007.07.062

Lyimo, I. N., and Ferguson, H. M. (2009). Ecological and evolutionary determinants of host species choice in mosquito vectors. *Trends Parasitol.* 25, 189–196. doi: 10.1016/j.pt.2009.01.005

MacKay, C. A., Sweeney, J. D., and Hillier, N. K. (2015). Olfactory receptor neuron responses of a longhorned beetle, *Tetropium fuscum* (Fabr.) (Coleoptera: Cerambycidae), to pheromone, host, and non-host volatiles. *J. Insect Physiol.* 83, 65–73. doi: 10.1016/j.jinsphys.2015.10.003

MacLeod, K., and Laurent, G. (1996). Distinct mechanisms for synchronization and temporal patterning of odor-encoding neural assemblies. *Science* 274, 976–979. doi: 10.1126/science.274.5289.976

Majeed, S., Hill, S. R., and Ignell, R. (2014). Impact of elevated CO_2 background levels on the host-seeking behaviour of *Aedes aegypti*. *J. Exp. Biol.* 217, 598–604, doi: 10.1242/jeb.092718

Manrique, G., Vitta, A. C., Ferreira, R. A., Zani, C. L., Unelius, C. R., Lazzari, C. R., et al. (2006). Chemical communication in Chagas disease vectors. Source, identity, and potential function of volatiles released by the metasternal and Brindley's glands of Triatoma infestans adults. *J. Chem. Ecol.* 32, 2035–2052. doi: 10.1007/s10886-006-9127-7

Martelli, C., Carlson, J. R., and Emonet, T. (2013). Intensity invariant dynamics and odor-specific latencies in olfactory receptor neuron response. *J. Neurosci.* 33, 6285–6297. doi: 10.1523/JNEUROSCI.0426-12.2013

Martin, J. P., Lei, H., Riffell, J. A., and Hildebrand, J. G. (2013). Synchronous firing of antennal-lobe projection neurons encodes the behaviorally effective ratio of sex-pheromone components in male *Manduca sexta*. *J. Comp. Physiol. A* 199, 963–979. doi: 10.1007/s00359-013-0849-z

Masante-Roca, I., Gadenne, C., and Anton, S. (2002). Plant odour processing in the antennal lobe of male and female grapevine moths, *Lobesia botrana* (Lepidoptera:Tortricidae). *J. Insect Physiol.* 48, 1111–1121. doi: 10.1016/S0022-1910(02)00204-4

Matthews, B. J., McBride, C. S., DeGennaro, M., Despo, O., and Vosshall, L. B. (2016). The neurotranscriptome of the *Aedes aegypti* mosquito. *BMC Genomics* 17:32. doi: 10.1186/s12864-015-2239-0

May-Concha, I., Rojas, J. C., Cruz-López, L., Millar, J. G., and Ramsey, J. M. (2013). Volatile compounds emitted by *Triatoma dimidiata*, a vector of Chagas disease: chemical analysis and behavioural evaluation. *Med. Vet. Entomol.* 27, 165–174. doi: 10.1111/j.1365-2915.2012.01056.x

Mboera, L. E. G., Takken, W., Mdira, K. Y., Chuwa, G. J., and Pickett, J. A. (2000). Oviposition and behavioral responses of *Culex quinquefasciatus* to Skatole and synthetic oviposition pheromone in Tanzania. *J. Chem. Ecol.* 26, 1193–1203. doi: 10.1023/A:1005432010721

McCall, P. J., and Kelly, D. W. (2002). Learning and memory in disease vectors. *Trends Parasitol.* 18, 429–433. doi: 10.1016/S1471-4922(02)02370-X

McMeniman, C. J., Corfas, R. A., Matthews, B., Ritchie, S. A., and Vosshal, L. B. (2014). Multimodal integration of carbon dioxide and other sensory cues drives mosquito attraction to humans. *Cell* 156, 1060–1071. doi: 10.1016/j.cell.2013.12.044

McQuate, G. T. (2014). Green light synergistally enhances male sweetpotato weevil response to sex pheromone. *Sci. Rep.* 4:4499. doi: 10.1038/srep04499

Miller, J. R., and Gut, L. J. (2015). Mating disruption for the 21st Century: matching technology with mechanism. *Environm. Entomol.* 44, 427–453. doi: 10.1093/ee/nvv052

Minoli, S., Palottini, F., Crespo, J. G., and Manrique, G. (2013b). Dislodgement effect of natural semiochemicals released by disturbed triatomines: a possible alternative monitoring tool. *J. Vector Ecol.* 38, 353–360. doi: 10.1111/j.1948-7134.2013.12051.x

Minoli, S., Palottini, F., and Manrique, G. (2013a). The main component of an alarm pheromone of kissing bugs plays multiple roles in the cognitive modulation of the escape response. *Front. Behav. Neurosc.* 7:77. doi: 10.3389/fnbeh.2013.00077

Mitsuno, H., Sakurai, T., Murai, M., Yasuda, T., Kugimiya, S., Ozawa, R., et al. (2008). Identification of receptors of main sex-pheromone components of three Lepidopteran species. *Eur. J. Neurosci.* 28, 893–902. doi: 10.1111/j.1460-9568.2008.06429.x

Montagné, N., Chertemps, T., Brigaud, I., François, A., François, M. C., and de Fouchier, A. (2012). Functional characterization of a sex pheromone receptor in the pest moth *Spodoptera littoralis* by heterologous expression in *Drosophila*. *Eur. J. Neurosci.* 36, 2588–2596. doi: 10.1111/j.1460-9568.2012.08183.x

Moore, S. J., and Lenglet, A. (2004). "Repellence and vector control," in *Traditional Medicinal Plants and Malaria*, eds M. Wilcox, G. Bodeker, and P. Rasoanaivo (London: CRC Press; Taylor and Francis), 343–363.

Mordue, A. J., Blackwell, A., Hansson, B. S., Wadhams, L. J., and Pickett, J. A. (1992). Behavioural and electrophysiological evaluation of oviposition attractants for*Culex quinquefasciatus* say (Diptera: Culicidae). *Experientia* 48, 1109–1111. doi: 10.1007/BF01947999

Mukabana, W. R. L., Mweresa, C. K., Otieno, B., Omusula, P., Smallegange, R. C., van Loon, J. J., et al. (2012). A novel synthetic odorant blend for trapping of malaria and other African mosquito species. *J. Chem. Ecol.* 38, 235–244. doi: 10.1007/s10886-012-0088-8

Murlis, J., Elkinton, J. S., and Cardé, R. T. (1992). Odor plumes and how insects use them. *Annu. Rev. Entomol.* 37, 505–532. doi: 10.1146/annurev.en.37.010192.002445

Najar-Rodriguez, A. J., Galizia, C. G., Stierle, J., and Dorn, S. (2010). Behavioral and neurophysiological responses of an insect to changing ratios of constituents in host plant-derived volatile mixtures. *J. Exp. Biol.* 213, 3388–3397. doi: 10.1242/jeb.046284

Namiki, S., Iwabuchi, S., and Kanzaki, R. (2008). Representation of a mixture of pheromone and host plant odor by antennal lobe projection neurons of the silkmoth *Bombyx mori*. *J. Comp. Physiol. A* 194, 501–515. doi: 10.1007/s00359-008-0325-3

Napper, E., and Pickett, J. A. (2008). "Alarm Pheromones of Insects" in *Encyclopedia of Entomology*, ed J. Capinera (Netherlands: Springer), 85–95.

Nässel, D., and Homberg, U. (2006). Neuropeptides in interneurons of the insect brain. *Cell Tissue Res.* 326, 1–24. doi: 10.1007/s00441-006-0210-8

Nikonov, A. A., and Leal, W. S. (2002). Peripheral coding of sex pheromone and behavioral antagonist in the Japanese beetle, *Popillia japonica*. *J. Chem. Ecol.* 28, 1075–1089. doi: 10.1023/A:1015274104626

Ochieng, S. A., Park, K. C., and Baker, T. C. (2002). Host plant volatiles synergize responses of sex pheromone-specific olfactory receptors neurons in male *Helicoverpa zea*. *J. Comp. Physiol. A* 188, 325–333. doi: 10.1007/s00359-002-0308-8

Olberg, R. M. (1983). Pheromone triggered flip-flopping interneurons in the ventral nerve cord of the silkworm moth, *Bombyx mori*. *J. Comp. Physiol. A* 152, 297–307. doi: 10.1007/BF00606236

Olsen, S. R., Bhandawat, V., and Wilson, R. I. (2010). Divisive normalization in olfactory population codes. *Neuron* 66, 287–299. doi: 10.1016/j.neuron.2010.04.009

Olson, J. F., Moon, R. D., and Kells, S. A. (2009). Off-host aggregation behavior and sensory basis of arrestment by *Cimex lectularius* (Heteroptera: Cimicidae). *J. Insect Physiol.* 55, 580–587. doi: 10.1016/j.jinsphys.2009.03.001

Papaj, D. R. (2009). "Learning," in *Encyclopedia of Insects, 2nd Edn*, ed V. H. R. T. Cardé (San Diego, CA: Academic Press), 552–555.

Papaj, D. R., and Prokopy, R. J. (1989). Ecological and evolutionary aspects of learning in Phytophagous insects. *Annu. Rev. Entomol.* 34, 315–350. doi: 10.1146/annurev.en.34.010189.001531

Pappenberger, B., Geier, M., and Boeckh, J. (1996). "Responses of antennal olfactory receptors in the yellow fever mosquito *Aedes aegypti* to human body odours," in *Olfaction in Mosquito-Host Interactions*, eds G. R. Bock and G. Cardew (Wiley; Chichester: Ciba Foundation Symposium 2000), 254–266.

Pellegrino, M., Steinbach, N., Stensmyr, M. C., Hansson, B. S., Leslie, B., and Vosshall, L. (2011). A natural polymorphism alters odour and DEET sensitivity in an insect odorant receptor. *Nature* 478, 511–514. doi: 10.1038/nature10438

Pickett, J. A., Birkett, M. A., and Logan, J. G. (2008). DEET repels ornery mosquitoes. *Proc. Natl. Acad. Sci. U.S.A.* 105, 13195–13196. doi: 10.1073/pnas.0807167105

Pickett, J. A., Wadhams, L. J., and Woodcock, C. M. (1997). Developing sustainable pest control from chemical ecology. *Agric. Ecosyst. Environ.* 64, 149–156. doi: 10.1016/S0167-8809(97)00033-9

Piñero, J., Galizia, C. G., and Dorn, S. (2008). Synergistic behavioral responses of female oriental fruit moths (Lepidoptera: Tortricidae) to synthetic host plant-derived mixtures are mirrored by odor-evoked calcium activity in their antennal lobes. *J. Insect Physiol.* 54, 333–343. doi: 10.1016/j.jinsphys.2007.10.002

Pregitzer, P., Schubert, M., Breer, H., Hansson, B. S., Sachse, S., and Krieger, J. (2012). Plant odorants interfere with detection of sex pheromone signals by male *Heliothis virescens*. *Front. Cell Neurosci.* 6:42. doi: 10.3389/fncel.2012.00042

Prokopy, R., and Papaj, D. R. (1988). Learning of apple fruit biotypes by apple maggot flies. *J. Insect Behav.* 1, 67–74. doi: 10.1007/BF01052504

Qiu, Y.-T., Smallegange, R. C., Cajo, J. F., Braak, T., Spitzen, J., Van Loon, J. J. A., et al. (2007). Attractiveness of MM-X traps baited with human or synthetic odor to mosquitoes (Diptera: Culicidae) in the Gambia. *J. Med. Entomol.* 44, 970–983. doi: 10.1093/jmedent/44.6.970

Raffa, K. F., Powell, E. N., and Townsend, P. A. (2013). Temperature-driven range expansion of an irruptive insect heightened by weakly coevolved plant defenses. *Proc. Natl. Acad. Sci. U.S.A.* 110, 2193–2198. doi: 10.1073/pnas.1216666110

Rath, L., Galizia, C. G., and Szyszka, P. (2011). Multiple memory traces after associative learning in the honey bee antennal lobe. *Eur. J. Neurosci.* 34, 352–360. doi: 10.1111/j.1460-9568.2011.07753.x

Reinhardt, K., and Siva-Jothy., M. T. (2007). Biology of the bed bugs (Cimicidae). *Annu. Rev. Entomol.* 52, 351–374. doi: 10.1146/annurev.ento.52.040306.133913

Reisenman, C., Riffell, J., Duffy, K., Pesque, A., Mikles, D., and Goodwin, B. (2013). Species-specific effects of herbivory on the oviposition behavior of the moth *Manduca sexta*. *J. Chem. Ecol.* 39, 76–89. doi: 10.1007/s10886-012-0228-1

Reisenman, C. E. (2014). Hunger is the best spice: effects of starvation in the antennal responses of the blood-sucking bug *Rhodnius prolixus*. *J. Insect Physiol.* 71, 8–13. doi: 10.1016/j.jinsphys.2014.09.009

Reisenman, C. E., Christensen, T. A., Francke, W., and Hildebrand, J. G. (2004). Enantioselectivity of projection neurons innervating identified olfactory glomeruli. *J. Neurosci.* 24, 2602–2611. doi: 10.1523/JNEUROSCI.5192-03.2004

Reisenman, C. E., Christensen, T. A., and Hildebrand, J. G. (2005). Chemosensory selectivity of output neurons innervating an identified, sexually isomorphic olfactory glomerulus. *J. Neurosci*. 25, 8017–8026. doi: 10.1523/JNEUROSCI.1314-05.2005

Reisenman, C. E., Dacks, A., and Hildebrand, J. (2011). Local interneuron diversity in the primary olfactory center of the moth *Manduca sexta*. *J. Comp. Physiol. A* 197, 653–665. doi: 10.1007/s00359-011-0625-x

Reisenman, C. E., Heinbockel, T., and Hildebrand, J. G. (2008). Inhibitory interactions among olfactory glomeruli do not necessarily reflect spatial proximity. *J. Neurophysiol.* 100, 554–564. doi: 10.1152/jn.90231.2008

Reisenman, C. E., and Riffell, J. A. (2015).The neural bases of host plant selection in a Neuroecology framework. *Front. Physiol.* 12:229. doi: 10.3389/fphys.2015.00229

Reisenman, C. E., Riffell, J. A., Bernays, E. A., and Hildebrand, J. G. (2010). Antagonistic effects of floral scent in an insect-plant interaction. *Proc. R. Soc. B* 277, 2371–2379. doi: 10.1098/rspb.2010.0163

Riffell, J. A. (2012). Olfactory ecology and the processing of complex mixtures. *Curr. Opin. Neurobiol.* 22, 236–242. doi: 10.1016/j.conb.2012.02.013

Riffell, J. A., Alarcon, L., Abrell, J. L., Bronstein, J., Davidowitz, G., and Hildebrand, J. G. (2008). Behavioral consequences of innate preferences and olfactory learning in hawkmoth-flower interactions. *Proc. Natl. Acad. Sci. U.S.A.* 105, 3404–3409. doi: 10.1073/pnas.0709811105

Riffell, J. A., Lei, H., Abrell, J. L., and Hildebrand, J. G. (2013). Neural basis of a pollinator's buffet: olfactory specialization and learning in *Manduca sexta*. *Science* 339, 200–204. doi: 10.1126/science.1225483

Riffell, J. A., Lei, H., Christensen, T. A., and Hildebrand, J. G. (2009b). Characterization and coding of behaviorally significant odor mixtures. *Curr. Biol.* 19, 335–340. doi: 10.1016/j.cub.2009.01.041

Riffell, J. A., Lei, H., and Hildebrand, J. G. (2009a). Neural correlates of behavior in the moth *Manduca sexta* in response to complex odors. *Proc. Natl. Acad. Sci. U.S.A.* 106, 19219–19226. doi: 10.1073/pnas.0910592106

Riffell, J. A., Shlizerman, E., Sanders, E., Abrell, J. L., Medina, B., Hinterwirth, A. J., et al. (2014). Flower discrimination by pollinators in a dynamic chemical environment. *Science* 344, 1515–1518. doi: 10.1126/science.1251041

Roitberg, B. D., and Prokopy, R. J. (1981). Experience required for pheromone recognition by the apple maggot fly. *Nature* 292, 540–541. doi: 10.1038/292540a0

Root, C. M., Ko, K. I., Jafari, A., and Wang, J. W. (2011). Presynaptic facilitation by neuropeptide signaling mediates odor-driven food search. *Cell* 145, 133–144. doi: 10.1016/j.cell.2011.02.008

Rospars, J. P., and Hildebrand, J. G. (2000). Sexually dimorphic and isomorphic glomeruli in the antennal lobes of the sphinx moth *Manduca sexta*. *Chem. Senses* 25, 119–129. doi: 10.1093/chemse/25.2.119

Roussel, E., Carcaud, J., Combe, M., Giurfa, M., and Sandoz, J.-C. (2014). Olfactory coding in the honeybee lateral horn. *Curr. Biol.* 24, 561–567. doi: 10.1016/j.cub.2014.01.063

Rouyar, A., Deisig, N., Dupuy, F., Limousin, D., Wycke, M. A., Renou, M., et al. (2015). Unexpected plant odor responses in a moth pheromone system. *Front. Physiol.* 6:148. doi: 10.3389/fphys.2015.00148

Rusch, C., Broadhead, G. T., Raguso, R. A., and Riffell, J. A. (2016). Olfaction in context—sources of nuance in plant–pollinator communication. *Curr. Opin. Insect Sci.* 15, 53–60. doi: 10.1016/j.cois.2016.03.007

Ryelandt, J., Noireau, F., and Lazzari, C. R. (2011). A multimodal bait for trapping blood-sucking arthropods. *Acta Trop.* 117, 131–136. doi: 10.1016/j.actatropica.2010.11.005

Rytz, R., Croset, V., and Benton, R. (2013). Ionotropic receptors (IRs): chemosensory ionotropic glutamate receptors in *Drosophila* and beyond. *Insect Biochem. Mol. Biol.* 43, 888–897. doi: 10.1016/j.ibmb.2013.02.007

Sachse, S., Rueckert, E., Keller, A., Okada, R., Tanaka, N. K., Ito, K., et al. (2007). Activity-dependent plasticity in an olfactory circuit. *Neuron* 56, 838–850. doi: 10.1016/j.neuron.2007.10.035

Sadek, M. M., Hansson, B. S., Rospars, J. P., and Anton, S. (2002). Glomerular representation of plant volatiles and sex pheromones components in the antennal lobe of the female *Spodoptera littoralis*. *J. Exp. Biol.* 205, 1363–1376.

Sanford, M. R., Olson, J. K., Lewis, W. J., and Tomberlin, J. K. (2013). The effect of sucrose concentration on olfactory-based associative learning in *Culex quinquefasciatus Say* (Diptera: Culicidae). *J. Insect Behav.* 26, 494–513. doi: 10.1007/s10905-012-9368-y

Sanford, M. R., and Tomberlin, J. K. (2011). Conditioning individual mosquitoes to an odor: sex, source, and time. *PLoS ONE* 6:e24218. doi: 10.1371/journal.pone.0024218

Sato, K., Pellegrino, M., Nakagawa, T., Nakagawa, T., Vosshall, L. B., and Touhara, K. (2008). Insect olfactory receptors are heteromeric ligand-gated ion channels. *Nature* 452, 1002–1006. doi: 10.1038/nature06850

Saveer, A. M., Kromann, S. H., Birgersson, G., Bengtsson, M., Lindblom, T., Balkenius, A., et al. (2012). Floral to green: mating switches moth olfactory coding and preference. *Proc. R. Soc. B Biol. Sci.* 279, 2314–2322. doi: 10.1098/rspb.2011.2710

Schmera, D., and Guerin, P. M. (2012). Plant volatile compounds shorten reaction time and enhance attraction of the codling moth (*Cydia pomonella*) to codlemone. *Pest Manag. Sci.* 68, 454–461. doi: 10.1002/ps.2292

Schröder, M. L., Glinwood, R., Webster, B., Ignell, R., and Krüger, K. (2015). Olfactory responses *of Rhopalosiphum padi* to three maize, potato, and wheat cultivars and the selection of prospective crop border plants. *Entomol. Exp. Appl.* 157, 241–253. doi: 10.1111/eea.12359

Schroeder, R., and Hilker, M. (2008). The relevance of background odor in resource location by insects: a behavioral approach. *Bioscience* 58, 308–316. doi: 10.1641/B580406

Seki, Y., and Kanzaki, R. (2008). Comprehensive morphological identification and GABA immunocytochemistry of antennal lobe local interneurons in *Bombyx mori*. *J. Comp. Neurol.* 506, 93–107. doi: 10.1002/cne.21528

Seki, Y., Rybak, J., Wicher, D., Sachse, S., and Hansson, B. S. (2010). Physiological and morphological characterization of local interneurons in the *Drosophila* antennal lobe. *J. Neurophysiol.* 104, 1007–1019. doi: 10.1152/jn.00249.2010

Smallegange, R. C., Qiu, Y. T., Van Loon, J. J. A., and Takken, W. (2005). Synergism between ammonia, lactic acid and carboxylic acids as kairomones in the host-seeking behaviour of the malaria mosquito *Anopheles gambiae sensu stricto* (Diptera: Culicidae). *Chem. Senses* 30, 145–152. doi: 10.1093/chemse/bji010

Sonenshine, D. E. (2006). Tick pheromones and their use in tick control. *Annu. Rev. Entomol.* 51, 557–580. doi: 10.1146/annurev.ento.51.110104.151150

Späthe, A., Reinecke, A., Haverkamp, A., Hansson, B. S., and Knaden, M. (2013). Host plant odors represent immiscible information entities-blend composition and concentration matter in hawkmoths. *PLoS ONE* 8:e77135. doi: 10.1371/journal.pone.0077135

Stanczyk, N. M., Brookfield, J. F., Ignell, R., Logan, J. G., and Field, L. M. (2010). Behavioral insensitivity to DEET in *Aedes aegypti* is a genetically determined

trait residing in changes in sensillum function. *Proc. Natl. Acad. Sci. U.S.A.* 107, 8575–8580. doi: 10.1073/pnas.1001313107

Stanczyk, N. M., Brookfield, J. F. Y., Field, L. M., and Logan, J. G. (2013). *Aedes aegypti* mosquitoes exhibit decreased repellency by DEET following previous exposure. *PLoS ONE* 8:e54438. doi: 10.1371/journal.pone.0054438

Stange, G. (1997). Effects of changes in atmospheric carbon dioxide on the location of hosts by the moth, *Cactoblastis cactorum*. *Oecologia* 110, 539–545. doi: 10.1007/s004420050192

Stange, G., Monro, J., Stowe, S., and Osmond, C. B. (1995). The CO_2 sense of the moth *Cactoblastis cactorum* and its probable role in the biological control of the CAM plant *Opuntia stricta*. *Oecologia* 102, 341–352. doi: 10.1007/BF00329801

Steib, B. M., Geier, M., and Boeckh, J. (2001). The effect of lactic acid on odour-related host preference of yellow fever mosquitoes. *Chem. Senses* 26, 523–528. doi: 10.1093/chemse/26.5.523

Stelinski, L. L., Gut, L. J., and Miller, J. R. (2005). Occurrence and duration of long-lasting peripheral adaptation among males of three species of economically important tortricid moths. *Ann. Entomol. Soc. Am.* 98, 580–586. doi: 10.1603/0013-8746(2005)098[0580:OADOLP]2.0.CO;2

Stengl, M., and Funk, N. W. (2013). The role of the coreceptor Orco in insect olfactory transduction. *J. Comp. Physiol. A* 199, 897–909. doi: 10.1007/s00359-013-0837-3

Stensmyr, M. C., Giordano, E., Balloi, A., Angioy, A. M., and Hansson, B. S. (2003). Novel natural ligands for *Drosophila* olfactory receptor neurones. *J. Exp. Biol.* 206, 715–724. doi: 10.1242/jeb.00143

Stierle, J. S., Galizia, C. G., and Szyszka, P. (2013). Millisecond stimulus onset-asynchrony enhances information about components in an odor mixture. *J. Neurosci.* 33, 6060–6069. doi: 10.1523/JNEUROSCI.5838-12.2013

Stranden, M., Rostelien, T., Liblikas, I., Almaas, T. J., Borg-Karlson, A. K., and Mustaparta, H. (2003). Receptor neurons in three heliothine moths responding to floral and inducible plant volatiles. *Chemoecology* 13, 143–154. doi: 10.1007/s00049-003-0242-4

Su, C.-Y., Menuz, K., Reisert, J., and Carlson, J. R. (2012). Non-synaptic inhibition between grouped neurons in an olfactory circuit. *Nature* 492, 66–72. doi: 10.1038/nature11712

Suh, E., Bohbot, J. D., and Zwiebel, L. J. (2014). Peripheral olfactory signaling in insects. *Curr. Opin. Insect Sci.* 6, 86–92. doi: 10.1016/j.cois.2014.10.006

Suh, G. S., Wong, A. M., Hergarden, A. C., Wang, J. W., Simon, A. F., Benzer, S., et al. (2004). A single population of olfactory sensory neurons mediates an innate avoidance behaviour in Drosophila. *Nature* 431, 854–859. doi: 10.1038/nature02980

Syed, Z., and Leal, W. S. (2008). Mosquitoes smell and avoid the insect repellent DEET. *Proc. Natl. Acad. Sci. U.S.A.* 105, 13598–13603. doi: 10.1073/pnas.0805312105

Syed, Z., Pelletier, J., Flounders, E., Chitolina, R. F., and Leal, W. S. (2011). Generic insect repellent detector from the fruit fly *Drosophila melanogaster*. *PLoS ONE* 6:e17705. doi: 10.1371/journal.pone.0017705

Szyszka, P. (2014). Follow the odor. *Science* 344, 1454. doi: 10.1126/science.1255748

Szyszka, P., Gerkin, R. C., Galizia, C. G., and Smith, B. H. (2014). High-speed odor transduction and pulse tracking by insect olfactory receptor neurons. *Proc. Natl. Acad. Sci. U.S.A.* 111, 16925–16930. doi: 10.1073/pnas.1412051111

Szyszka, P., Stierle, J. S., Biergans, S., and Galizia, C. G. (2012). The speed of smell: odor-object segregation within milliseconds. *PLoS ONE* 7:e36096. doi: 10.1371/journal.pone.0036096

Tabuchi, M., Dong, L., Inoue, S., Namiki, S., Sakurai, T., and Nakatani, K., et el. (2015). Two types of local interneurons are distinguished by morphology, intrinsic membrane properties, and functional connectivity in the moth antennal lobe. *J. Neurophysiol.* 114, 3002–3013. doi: 10.1152/jn.00050.2015

Takken, W., Van Loon, J. J. A., and Adam, W. (2001). Inhibition of host-seeking response and olfactory responsiveness in *Anopheles gambiae* following blood feeding. *J. Insect Physiol.* 47, 303–310. doi: 10.1016/S0022-1910(00)00107-4

Tanaka, N. K., Ito, K., and Stopfer, M. (2009). Odor-evoked neural oscillations in *Drosophila* are mediated by widely branching interneurons. *J. Neurosci.* 29, 8595–8603. doi: 10.1523/JNEUROSCI.1455-09.2009

Tanaka, N. K., Suzuki, E., Dye, L., Ejima, A., and Stopfer, M. (2012). Dye fills reveal additional olfactory tracts in the protocerebrum of wild-type *Drosophila*. *J. Comp. Neurol.* 520, 4131–4140. doi: 10.1002/cne.23149

Tasin, M., Bäckman, A. C., Coracini, M., Casado, D., Ioriatti, C., and Witzgall, P. (2007). Synergism and redundancy in a plant volatile blend attracting grapevine moth females. *Phytochemistry* 68, 203–209. doi: 10.1016/j.phytochem.2006.10.015

Tauxe, G., MacWilliam, D., Boyle, S. M., Guda, T., and Ray, A. (2013). Targeting a dual detector of skin and CO_2 to modify mosquito host seeking. *Cell* 155, 1365–1379. doi: 10.1016/j.cell.2013.11.013

Thom, C., Guerenstein, P. G., Mechaber, W., and Hildebrand, J. G. (2004). Floral CO_2 reveals flower profitability to moths. *J. Chem. Ecol.* 30, 1285–1288. doi: 10.1023/B:JOEC.0000030298.77377.7d

Thöming, G., Larsson, M. C., Hansson, B., and Anderson, P. (2013). Comparison of plant preference hierarchies of male and female moths and the impact of larval rearing hosts. *Ecology* 94, 1744–1752. doi: 10.1890/12-0907.1

Tomberlin, J. K., Rains, G. C., Allan, S. A., Sanford, M. R., and Lewis, W. J. (2006). Associative learning of odor with food-or blood-meal by *Culex quinquefasciatus Say* (Diptera: Culicidae). *Naturwissenschaften* 93, 551–556. doi: 10.1007/s00114-006-0143-9

Trimble, R. M., and Marshall, D. B. (2010). Differences in the relationship between sensory adaptation of antennae and concentration of aerial pheromone in the oriental fruit moth and obliquebanded leafroller (Lepidoptera: Tortricidae): implications for the role of adaptation in sex pheromone-mediated mating disruption of these species. *Environ. Entomol.* 39, 625–632. doi: 10.1603/EN09178

Trona, F., Anfora, G., Balkenius, A., Bengtsson, M., Tasin, M., Knight, A., et al. (2013). Neural coding merges sex and habitat chemosensory signals in an insect herbivore. *Proc. R. Soc. B Biol. Sci.* 280:20130267. doi: 10.1098/rspb.2013.0267

Tsitoura, P., Koussis, K., and Iatrou, K. (2015). Inhibition of *Anopheles gambiae* odorant receptor function by mosquito repellents. *J. Biol. Chem.* 290, 7961–7972. doi: 10.1074/jbc.M114.632299

Tsuchihara, K., Fujikawa, K., Ishiguro, M., Yamada, T., Tada, C., Ozaki, K., et al. (2005). An odorant-binding protein facilitates odorant transfer from air to hydrophilic surroundings in the blowfly. *Chem. Senses* 30, 559–564. doi: 10.1093/chemse/bji049

Tumlinson, J. H., Brennan, M. M., Doolittle, R. E., Mitchell, E. R., Brabham, A., and Mazomenos, B. E. (1989). Identification of a pheromone blend attractive to *Manduca sexta* (L.) males in a wind tunnel. *Arch. Insect Biochem. Physiol.* 10, 255–271. doi: 10.1002/arch.940100402

Turner, G. C., Bazhenov, M., and Laurent, G. (2008). Olfactory representations by *Drosophila* mushroom body neurons. *J. Neurophysiol.* 99, 734–746. doi: 10.1152/jn.01283.2007

Turner, S. L., Li, N., Guda, T., Githure, J., Cardé, R. T., and Ray, A. (2011). Ultra-prolonged activation of CO_2-sensing neurons disorients mosquitoes. *Nature* 474, 87–91. doi: 10.1038/nature10081

van Breugel, F., and Dickinson, M. H. (2014). Plume-tracking behavior of flying *Drosophila* emerges from a set of distinct sensory-motor reflexes. *Curr. Biol.* 24, 274–286. doi: 10.1016/j.cub.2013.12.023

van Breugel, F., Riffell, J., Fairhall, A., and Dickinson, M. H. (2015). Mosquitoes use vision to associate odor plumes with thermal targets. *Curr. Biol.* 25, 2123–2129. doi: 10.1016/j.cub.2015.06.046

van der Goes van Naters, W., and Carlson, J. R. (2006). Insects as chemosensors of humans and crops. *Nature* 444, 302–307. doi: 10.1038/nature05403

Vandermoten, S., Mescher, M. C., Francis, F., Haubruge, E., and Verheggen, F. J. (2012). Aphid alarm pheromone: an overview of current knowledge on biosynthesis and functions. *Insect Biochem. Mol. Biol.* 42, 155–163. doi: 10.1016/j.ibmb.2011.11.008

Vickers, N. J., and Baker, T. C. (1997). Chemical communication in Heliothine moths VII Correlation between diminished responses to point source plumes and single filaments similarly tainted with a behavioural antagonist. *J. Comp. Physiol. A* 180, 523–536. doi: 10.1007/s003590050069

Vickers, N. J., Christensen, T. A., and Hildebrand, J. G. (1998). Combinatorial odor discrimination in the brain: attractive and antagonist odor blends are represented in distinct combinations of uniquely identifiable glomeruli. *J. Comp. Neurol.* 400, 35–56.

Vinauger, C., Buratti, L., and Lazzari, C. R. (2011a). Learning the way to blood: first evidence of dual olfactory conditioning in a blood-sucking insect, *Rhodnius prolixus*. I. Appetitive learning. *J. Exp. Biol.* 214, 3032–3038. doi: 10.1242/jeb.056697

Vinauger, C., Buratti, L., and Lazzari, C. R. (2011b). Learning the way to blood: first evidence of dual olfactory conditioning in a blood-sucking insect, *Rhodnius prolixus*. II. Aversive learning. *J. Exp. Biol.* 214, 3039-3045. doi: 10.1242/jeb.057075

Vinauger, C., Lallement, H., and Lazzari, C. R. (2013). Learning and memory in *Rhodnius prolixus*: habituation and aversive operant conditioning of the proboscis extension response. *J. Exp. Biol.* 216, 892–900. doi: 10.1242/jeb.079491

Vinauger, C., Lutz, E. K., and Riffell, J. A. (2014). Olfactory learning and memory in the disease vector mosquito *Aedes aegypti*. *J. Exp. Biol.* 217, 2321–2330. doi: 10.1242/jeb.101279

Vogt, R. G., and Riddiford, L. M. (1981). Pheromone binding and inactivation by moth antennae. *Nature* 293, 161–163. doi: 10.1038/293161a0

Vosshall, L., Amrein, H., Morozov, P., Rzhetsky, A., and Axel, R. (1999). A spatial map of olfactory receptor expression in the *Drosophila* antenna. *Cell* 96, 725–736. doi: 10.1016/S0092-8674(00)80582-6

Vosshall, L. B., and Hansson, B. S. (2011). A unified nomenclature system for the insect olfactory coreceptor. *Chem. Senses* 36, 497–498. doi: 10.1093/chemse/bjr022

Vosshall, L. B., and Stocker, R. F. (2007). Molecular architecture of smell and taste in *Drosophila*. *Annu. Rev. Neurosci.* 30, 505–533. doi: 10.1146/annurev.neuro.30.051606.094306

Vosshall, L. B., Wong, A. M., and Axel, R. (2000). An olfactory sensory map in the fly brain. *Cell* 102, 147–159. doi: 10.1016/S0092-8674(00)00021-0

Wang, J. W., Wong, A. M., Flores, J., Vosshall, L. B., and Axel, R. (2003). Two-photon calcium imaging reveals an odor-evoked map of activity in the fly brain. *Cell* 112, 271–282. doi: 10.1016/S0092-8674(03)00004-7

Wang, X., Zhong, M., and Liu, Q. (2013). Molecular characterization of the carbon dioxide receptor in the oriental latrine fly, *Chrysomya megacephala* (Diptera: Calliphoridae). *Parasitol. Res.* 112, 2763–2771. doi: 10.1007/s00436-013-3410-7

Warren, B., and Kloppenburg, P. (2014). Rapid and slow chemical synaptic interactions of cholinergic projection neurons and GABAergic local interneurons in the insect antennal lobe. *J. Neurosci.* 34, 13039–13046. doi: 10.1523/JNEUROSCI.0765-14.2014

Watanabe, H. (2012). Spatio-temporal activity patterns of odor-induced synchronized potentials revealed by voltage-sensitive dye imaging and intracellular recording in the antennal lobe of the cockroach. *Front. Syst. Neurosci.* 6:55. doi: 10.3389/fnsys.2012.00055

Webster, B., Bruce, T., Pickett, J., and Hardie, J. (2010). Volatiles functioning as host cues in a blend become nonhost cues when presented alone to the black bean aphid. *Anim. Behav.* 79, 451–457. doi: 10.1016/j.anbehav.2009.11.028

Wertheim, B., Baalen, E.-J., Dicke, M., and Vet, L. E. (2005). Pheremone-mediated aggregation in nonsocial arthropods: an evolutionary ecological perspective. *Annu. Rev. Entomol.* 50, 321–346. doi: 10.1146/annurev.ento.49.061802.123329

White, G. B. (2007). "Chapter 2: Terminology of insect repellents," in *Insect Repellents: Principles, Methods, and Uses*, eds M. Debboun, S. P. Frances, and D. Strickman (Boca Raton, FL: CRC Press) 31–46.

Wicher, D., Schafer, R., Bauernfeind, R., Stensmyr, M. C., Heller, R., and Heinemann, S. H. (2008). *Drosophila* odorant receptors are both ligand-gated and cyclic-nucleotide-activated cation channels. *Nature* 452, 1007–1011. doi: 10.1038/nature06861

Willis, M. A., Avondet, J. L., and Zheng, E. (2011). The role of vision in odor-plume tracking by walking and flying insects. *J. Exp. Biol.* 214, 4121–4132. doi: 10.1242/jeb.036954

Wilson, D. A., and Sullivan, R. M. (2011). Cortical processing of odor objects. *Neuron* 72, 506–519. doi: 10.1016/j.neuron.2011.10.027

Wilson, J. K., Kessler, A., and Woods, H. A. (2015). Noisy communication via airborne infochemicals. *Bioscience* 65, 667–677. doi: 10.1093/biosci/biv062

Wilson, R. I., and Laurent, G. (2005). Role of GABAergic inhibition in shaping odor-evoked spatiotemporal patterns in the drosophila antennal lobe. *J. Neurosci.* 25, 9069–9079. doi: 10.1523/JNEUROSCI.2070-05.2005

Winnington, A. P., Napper, R. M., and Mercer, A. (1996). Structural plasticity of identified glomeruli in the antennal lobes of the adult worker honey bee. *J. Comp. Neurol.* 365, 479–490.

Witzgall, P., Kirsch, P., and Cork, A. (2010). Sex pheromones and their impact on pest management. *J. Chem. Ecol.* 36, 80–100. doi: 10.1007/s10886-009-9737-y

Wyatt, T. D. (2003). *Pheromones and Animal Behavior: Communication by Smell and Taste*. Cambridge: Cambridge University Press.

Xu, P., Choo, Y.-M., De La Rosa, A., and Leal, W. S. (2014). Mosquito odorant receptor for DEET and methyl jasmonate. *Proc. Natl. Acad. Sci. U.S.A.* 111, 16592–16597. doi: 10.1073/pnas.1417244111

Yao, C. A., Ignell, R., and Carlson, J. R. (2005). Chemosensory coding by neurons in the coeloconic sensilla of the *Drosophila* antenna. *J. Neurosci.* 25, 8359–8367. doi: 10.1523/JNEUROSCI.2432-05.2005

Yarnell, E., and Abascal, K. (2004). Botanical prevention and treatment of malaria, Part 1—herbal mosquito repellants. *Altern. Complement. Ther.* 10, 206–210. doi: 10.1089/1076280041580332

Zars, T., Fischer, M., Schulz, R., and Heisenberg, M. (2000). Localization of a short-term memory in *Drosophila*. *Science* 288, 672–675. doi: 10.1126/science.288.5466.672

Zavada, A., Buckley, C. L., Martinez, D., Rospars, J. P., and Nowotny, T. (2011). Competition-based model of pheromone component ratio detection in the moth. *PLosONE* 6:e16308. doi: 10.1371/journal.pone.0016308

Zermoglio, P. F., Martin-Herrou, H., Bignon, Y., and Lazzari, C. R. (2015). *Rhodnius prolixus* smells repellents: behavioural evidence and test of present and potential compounds inducing repellency in Chagas disease vectors. *J. Insect Physiol.* 8, 137–144. doi: 10.1016/j.jinsphys.2015.07.012

Zhang, J., Yan, S., Liu, Y., Jacquin-Joly, E., Dong, S., and Wang, G. (2015). Identification and functional characterization of sex pheromone receptors in the common cutworm (*Spodoptera litura*). *Chem. Senses* 40, 7–16. doi: 10.1093/chemse/bju052

Zhang, P.-J., and Liu, S.-S. (2006). Experience induces a Phytophagous insect to lay eggs on a nonhost plant. *J. Chem. Ecol.* 32, 745–753. doi: 10.1007/s10886-006-9032-0

Conflict of Interest Statement: The authors declare that the research was conducted in the absence of any commercial or financial relationships that could be construed as a potential conflict of interest.

frontiers in Physiology

ORIGINAL RESEARCH
published: 05 October 2016
doi: 10.3389/fphys.2016.00452

BdorOBP83a-2 Mediates Responses of the Oriental Fruit Fly to Semiochemicals

Zhongzhen Wu[1], *Jintian Lin*[2], *He Zhang*[2] *and Xinnian Zeng*[1]*

[1] Key Laboratory of Natural Pesticide and Chemical Biology of the Ministry of Education, College of Natural Resources and Environment, South China Agricultural University, Guangzhou, China, [2] Institute for Management of Invasive Alien Species, Zhongkai University of Agriculture and Engineering, Guangzhou, China

The oriental fruit fly, *Bactrocera dorsalis* (Diptera: Tephritidae), is one of the most destructive pests throughout tropical and subtropical regions in Asia. This insect displays remarkable changes during different developmental phases in olfactory behavior between sexually immature and mated adults. The olfactory behavioral changes provide clues to examine physiological and molecular bases of olfactory perception in this insect. We comparatively analyzed behavioral and neuronal responses of *B. dorsalis* adults to attractant semiochemicals, and the expression profiles of antenna chemosensory genes. We found that some odorant-binding proteins (OBPs) were upregulated in mated adults in association with their behavioral and neuronal responses. Ligand-binding assays further showed that one of OBP83a orthologs, BdorOBP83a-2, binds with high affinity to attractant semiochemicals. Functional analyses confirmed that the reduction in BdorOBP83a-2 transcript abundance led to a decrease in neuronal and behavioral responses to selected attractants. This study suggests that BdorOBP83a-2 mediates behavioral responses to attractant semiochemicals and could be a potential efficient target for pest control.

Keywords: ***Bactrocera dorsalis*, olfactory, odorant binding proteins, functional analysis, attractive semiochemicals**

OPEN ACCESS

Edited by:
Anders Garm,
University of Copenhagen, Denmark

Reviewed by:
Nicolas Montagné,
Pierre-and-Marie-Curie University, France
Sylvia Anton,
French National Institute for Agricultural Research (INRA), France

***Correspondence:**
Xinnian Zeng
zengxn@scau.edu.cn

Specialty section:
This article was submitted to Invertebrate Physiology, a section of the journal Frontiers in Physiology

Received: *28 June 2016*
Accepted: *21 September 2016*
Published: *05 October 2016*

Citation:
Wu Z, Lin J, Zhang H and Zeng X (2016) BdorOBP83a-2 Mediates Responses of the Oriental Fruit Fly to Semiochemicals. Front. Physiol. 7:452. doi: 10.3389/fphys.2016.00452

INTRODUCTION

In insects, olfaction plays a key role in behavior such as host-seeking, mating, and oviposition. At the molecular level, soluble binding proteins and membrane-bound receptors have crucial functions in chemical signal transduction (Pelosi et al., 2006, 2014; Zhou, 2010; Leal, 2013; Oppenheim et al., 2015). Odorant molecules penetrate into the sensilla via pore tubules and diffuse through sensillar lymph to membrane-bound receptor proteins. Activation of these proteins generates action potentials in receptor neurons. Two families of soluble binding proteins, odorant binding proteins (OBPs; Pelosi and Maida, 1995; Zhou, 2010) and chemosensory proteins (CSPs; Pelosi et al., 2005, 2006), are involved in this process.

Various functional studies support a role of insect OBPs in olfactory perception. Expression of moth pheromone receptors in heterologous systems (Grosse-Wilde et al., 2006, 2007; Forstner et al., 2009; Chang et al., 2015) and studies *in vivo* using the *Drosophila melanogaster* "empty neuron system" (Hallem et al., 2004; Syed et al., 2006) have demonstrated that the presence of a corresponding pheromone-binding protein significantly enhances the sensitivity of insects to pheromones. The OBP Lush with a mutation led to reduction in sensitivity of olfactory receptor

neuron reception to the pheromone 11-cis-vaccenylacetate in *Drosophila* (Xu et al., 2005; Laughlin et al., 2008). RNA interference (RNAi) knockdown of OBPs lead to altered olfactory behavior in *Drosophila* (Swarup et al., 2011) and decreased electrophysiological responses in mosquito antennae (Biessmann et al., 2010; Pelletier et al., 2010a,b). There are two different hypotheses regarding the mechanisms of odor receptor (OR) activation. In moths and mosquitoes, OBPs act as solubilizers and carriers for the release of ligands onto ORs, thus contributing to the sensitivity of the insect olfactory system (Syed et al., 2006; Biessmann et al., 2010; Pelletier et al., 2010a). In *D. melanogaster*, LUSH (DmelOBP76a) forms an OBP-odorant complex that activates an OR, which is required for olfaction (Xu et al., 2005; Laughlin et al., 2008).

Insect CSPs are highly expressed in the sensillar lymph and exhibit binding activity toward odorants and pheromones (Jacquin-Joly et al., 2001; Gu et al., 2012; Iovinella et al., 2013; Zhang et al., 2014). CSPs of *Locusta migratoria* in antennae are involved in the physiological shift from solitary to gregarious phase (Guo et al., 2011), and an antenna-specific CSP of *Glossina morsitans morsitans* is thought to be associated with host searching behavior (Liu et al., 2012). However, there is no direct evidence to confirm a role of CSPs in olfaction.

The oriental fruit fly, *Bactrocera dorsalis* (Diptera: Tephritidae), is one of the most important pests throughout tropical and subtropical regions in Asia (Drew and Hancock, 1994). This insect pest can damage over 117 species of fruits and vegetables (Allwood et al., 1999), suggesting that it can detect and recognize a wide range of odorants. *B. dorsalis* exhibits remarkable developmental phases in olfactory behavior. When male adults reach sexual maturity, they are strongly attracted to and compulsively feed on methyl eugenol (4-allyl-1,2-dimethoxybenzene; Tan and Nishida, 2012). During the oviposition period, gravid females become more sensitive to a wide variety of volatile compounds, which have been shown to attract and/or stimulate oviposition (Jayanthi et al., 2014). These changes in olfactory behavior provide clues to study the physiological and molecular bases of olfactory perception in this pest, and may offer the possibility to explore alternative methods for pest control. Our previous transcriptome analysis of *B. dorsalis* provided a set of chemosensory genes and their expression profiles (Wu et al., 2015). Those antenna-specific or antenna-predominant chemosensory genes could be involved in recognition of specific ligands and contribute to olfactory behavioral changes in *B. dorsalis*.

The objective of the present study is to determine if there is a correlation between olfactory behavioral changes and those OBPs that are specifically or predominantly expressed in antennae. Specifically, we conducted behavioral assays, analyzed electroantennogram (EAG) responses to selected plant volatiles, and examined expression profiles of antenna-specific or antenna-predominant chemosensory genes in sexually immature and mated *B. dorsalis* adults. Using fluorescence competitive binding assays and molecular docking (*in silico*), binding affinity of selected OBPs to selected semiochemicals was also measured. The impact of the most abundant OBP, BdorOBP83a-2, on olfactory behavior was studied through RNAi. Our results suggest a likely involvement of antenna-specific or antenna-predominant OBPs in olfaction, especially in regulating foraging and oviposition behaviors.

MATERIALS AND METHODS

Insect Rearing and Collection

B. dorsalis used in this study was reared at the Institute for Management of Invasive Alien Species, Zhongkai University of Agriculture and Engineering, Guangzhou, China. Insects were reared under a photoperiod of 14:10 h (L:D) at 28°C and 70% relative humidity (Jayanthi and Abraham, 2002).

Sexually immature individuals (2 days old) and mated individuals (mated males and gravid females of 15 days old) were collected and used for the analyses of olfactory behavioral changes, olfactory sensitivity changes, and transcriptional changes of olfactory genes that are potentially induced by mating and gravidity. To obtain mated males and gravid females, 9 days old virgin adults of each sex were introduced into a 30 × 30 × 30 cm cage for mating. Once copulating pairs were formed for at least 60 min, they were transferred to another cage and maintained there until 15 days old.

Semiochemicals

All semiochemicals used to investigate olfactory behavioral responses, EAG responses, and binding assays were purchased from Sigma-Aldrich (St. Louis, MO, USA) and with more than 95% purity (**Table S1**).

Olfactory Behavioral Assays

Olfactory attraction was tested using a modified two-choice trap system based on the body size of *B. dorsalis* (**Figure S1**; Faucher et al., 2013). Odor traps were constructed from 250 ml conical flasks to which a silicone top containing 15 ml centrifuge tube (cut for 4.5 cm) was securely placed. Each trap contained a cotton-foam plug to which either 0.2 ml of 1% semiochemicals dissolved in paraffin oil or paraffin oil alone were added. Olfactory behavioral assays were conducted for 6 h in a dark humidified room at 28°C. Testing insects were starved for 4 h (6:00–10:00) in insect rearing cages with only water. Thirty insects per assay were then transferred to a new rearing cage. A performance index (PI) was used to measure olfactory attraction, which was calculated using the following formula: Performance index (PI) = (flies in odor vial – flies in control vial)/total of flies. Each trap assay was replicated five times.

Electroantennogram (EAG) Recording

EAG recordings (Syntech, Kirchzarten, Germany) were used to investigate *B. dorsalis* antennal responses to different semiochemicals according to standard protocols (Hayase et al., 2009). Insects were again starved for 4 h (6:00–10:00) before assays. The whole antennae of males and females were excised, cut on both ends and attached to two electrodes with Spectra 360 conducting gel (Parker Lab., Inc., Hellendoorn, Netherlands). Pure chemicals were dissolved in paraffin oil and tested at a final concentration of 10^{-2} v/v. A 10 μl aliquot of paraffin oil was used as a control. The neuronal responses of antennae from five males

and five females were tested in each treatment. Five stimulations of each chemical were applied at intervals of 10 s on the antennae. EAG signals were amplified, filtered, digitized, and analyzed with an EAG Pro program (Syntech).

Olfactory Gene Expression Analysis

qRT-PCR was used to investigate the variation of the transcription levels of olfactory genes in sexually immature and mated adults. From each experiment, 100 whole antennae for each gender were excised and immediately transferred to a polypropylene tube cooled over liquid nitrogen. The frozen antennae were crushed, and total RNA was extracted with an RNeasy Mini kit (Qiagen), following the manufacturer's protocol. cDNA was synthesized from total RNA using a First strand cDNA synthesis kit (Takara). Specific primer pairs for the qRT-PCR were the same to those used in our previous study (Wu et al., 2015). The α-tublin (α-TUB; GenBank Acc. GU269902) of *B. dorsalis* was used for normalizing the target gene expression (Shen et al., 2010). qRT-PCR analysis was conducted on a LightCycler 480 system (Roche) with a SYBR Premix ExTaq kit (Takara). Negative controls without template were included in each experiment. To ensure reproducibility, each qRT-PCR reaction was performed using technical triplicates and biological triplicates. Relative gene expression data was estimated using the $2^{-\Delta\Delta CT}$ method (Livak and Schmittgen, 2001).

Bacterial Expression and Purification of BdorOBPs and BdorCSP

The sequences of BdorOBPs and BdorCSPs encoding mature proteins (without signal peptide) were amplified by PCR using specific primers carrying a restriction site EcoRI or XhoI (**Table S2**). PCR fragments were digested with both EcoRI and XhoI enzymes and the released DNA fragments were cloned into a PET-32a vector (Invitrogen), which were used to transform BL21 (DE3) *E. coli* competent cells (Invitrogen). A selected positive clone was grown overnight in 5 mL liquid LB/ampicillin medium overnight at 37°C. Protein expression was induced with 1 mM IPTG for 3 h when the culture had reached an OD_{600}-value of 0.7–0.9. Cells were then harvested by centrifugation and lysed by sonication. After sonication and centrifugation, most recombinant proteins were present in inclusion bodies. Protein extracts were dissolved in extraction buffer (8 M urea, 0.5 M NaCl, 5 mM Imidazole, 1 mM β-mercaptoethanol, and 20 mM Tris-HCl pH 7.4) and purified using HisTrap affinity columns (GE Healthcare Biosciences, Uppsala, Sweden). Renaturation of purified proteins were accomplished by gradient dilution at 4°C. His-tag was removed by digestion with recombinant enterokinase (Novagen) and the digested mixtures were passed through a HisTrap affinity column to remove any undigested protein. At each step during protein preparation and purification, protein extracts, and purified proteins were examined on 15% SDS-PAGE.

Fluorescence Competitive Binding Assay

To measure the affinity of the recombinant proteins to the fluorescent probe N-phenyl-1-naphthylamine (1-NPN), a 2 μM solution of each target protein in 50 mM Tris-HCl buffer, pH 7.4, was titrated with aliquots of 1 mM 1-NPN in methanol to final concentrations of 1–16 μM. The affinity of the proteins to other ligands was measured in competitive binding assays, where a solution of the protein and 1-NPN, both at the concentration of 2 μM, was titrated with 1 mM methanol solution containing a competitor with concentrations in the range of 5–50 μM. Fluorescence spectra were measured on an F-7000 FL Fluorescence Spectrophotometer (Hitachi) in a 10 mm light path quartz cuvette at 25°C. All were excited at 337 nm with emission and excitation slit of both 10 nm. The emission spectra were recorded between 350 and 500 nm. Data analysis and plot binding curves were accomplished in the Prism software, assuming that the target protein had a 100% activity with a stoichiometry of 1:1 protein: ligand at saturation. All measurements were performed in triplicates and mean values and standard errors are calculated. The dissociation constants of the competitors were calculated from the corresponding IC_{50}-values (the concentration of ligand halving the initial fluorescence value of 1-NPN), by the equation: $K_D = [IC_{50}]/1 + [1\text{-NPN}]/ K_{1\text{-NPN}}$, where [1-NPN] is the free concentration of 1-NPN and $K_{1\text{-NPN}}$ is the dissociation constant of the complex Protein/1-NPN.

Three-Dimensional Modeling and Molecular Docking

Two different strategies were employed to predict three-dimensional modeling of OBPs and CSP of *B. dorsalis*. Those that have more than 30% homology with the OBP or CSP templates in the Protein Database (http://www.rcsb.org/pdb) were predicted using the on-line program SWISS MODEL (Guex and Peitsch, 1997; Arnold et al., 2006; Guex et al., 2009), while others <30% were generated using an online protein threading (PHYRE 2; Kelley et al., 2015). The information of the templates was shown in **Tables S3**, **S4**. Alignments of BdorOBP83a-1, BdorOBP83a-2, BdorCSP3, BdorOBP84a-1, BdorOBP84a-2, and BdorOBP56h with the template protein are shown in **Figure S2**. Furthermore, rapid energy minimization of protein molecules was carried out using discrete molecular dynamics with an all-atom representation for each residue in the protein in Chiron (http://troll.med.unc.edu/chiron/login.php; Ramachandran et al., 2011). Molecular docking was performed using "Docking server" (Bikadi and Hazai, 2009). All compounds from previous studies were used for docking studies. Three-dimensional structures of compounds were obtained from NCBI. Docking was performed 255 times with selected OBPs and ligands. For each run, the 10 highest docking poses were saved and were further processed for molecular dynamics simulations. Free binding energies were calculated as previously described (Okimoto et al., 2009).

Phylogenetic Analysis and Sequence Alignment

Phylogenetic analyses of the newly identified *B. dorsalis* OBPs were performed in conjunction with previously identified *B. dorsalis* OBPs and OBPs from other species, including 31 OBPs from *B. dorsalis* (Wu et al., 2015), 52 OBPs from *D. melanogaster* (Hekmat-Scafe et al., 2002; Vieira et al., 2007; Vieira and Rozas,

2011), 16 OBPs from *Ceratitis capitata* (Siciliano et al., 2014a), 15 OBPs from *Rhagoletis pomonella* (Schwarz et al., 2009), 9 OBPs from *Rhagoletis suavis* (Ramsdell et al., 2010), Obp83a orthologs from *G. m. morsitans* (Liu et al., 2010; Macharia et al., 2016), *Musca domestica* (Scott et al., 2014), and *Calliphora stygia* (Leitch et al., 2015). After removal of signal peptide sequences, OBP amino acid sequences were aligned using MAFFT v6.935b (Katoh and Toh, 2010; Katoh and Standley, 2013) with the E-INS-i strategy, BLOSUM62 matrix, 1000 maxiterate and offset 0. The maximum-likelihood trees were constructed using FastTree 2.1.7 (Price et al., 2009, 2010) with 1000 bootstrap replications. The phylogenetic tree was visualized in FigTree (http://tree.bio.ed.ac.uk/software/figtree). For comparative purpose, the analyzed sequences were aligned using the E-INS-I strategy in MAFFT and visualized with Jalview 2.0.1 (Waterhouse et al., 2009).

RNA Interference and Bioassay

dsRNAs for BdorOBP83a-2 and Bdorβ-gal (Glyceraldehyde-3-phosphate dehydrogenase) were synthesized through *in vitro* transcription from PCR products generated using a MEGAscript T7 transcription kit (Ambion). Briefly, the pMD18-T vector containing the target-gene insert (constructed as described above) was used as template for PCR amplification. PCR was performed using two specific primers with a T7 promoter sequence (5′-TAATACGACTCACTATAGGG-3′) at the 5′-end of each primer (**Table S5**). Large-scale dsRNAs were purified using a MEGAclear kit (Ambion) and precipitated with 5 M ammonium acetate to yield 30–50 μg/μL dsRNA. Ten days old adults were used for all injection experiments. Individuals receiving injection were placed on a stereomicroscope and surface-sterilized with 70% ethanol. One microgram of dsRNA was injected into each individual at the suture between third and fourth abdominal segments (100 ng/mg equivalent) using an automatic microinjection apparatus (Nanoject II Auto-Nanoliter). The injected insects were then transferred to new rearing cages for continuous culture (at 25 ± 1°C, 50% humidity) until 15 days old.

Given that rapid degradation of dsRNA fragments has been observed in insect hemolymph in other studies (Garbutt et al., 2013), we performed a pre-assay for the stability of dsRNA fragments under our conditions before starting dsRNA microinjection experiment. In the pre-assay, peripheral hemolymph was extracted from thoraxes of 10 days old adults individually using a microsyringe. Hemolymph from individual insects was combined into a precooled 50 μl PCR tube containing phenylthiourea to avoid melanization (Arakawa, 1995). The BdorOBP83a-2 dsRNA (1 μg) and hemolymph (3 μl) mixture was incubated at 25°C for 0–3 h. A control was included by mixing dsRNA with DEPC-water under the same conditions. After incubation, dsRNA was re-extracted with 20 μl nuclease-free water using an RNeasy Mini Kit (Qiagen, Valencia, CA) according to the RNA Cleanup instruction. Re-extracted dsRNA (8 μl) was separated on 1% agarose gels. Our *ex vivo* experiments showed that dsRNA fragments were stable in adult hemolymph, with a residence time of at least 3 h (**Figure S3**), indicating that dsRNA is likely to be stable in *B. dorsalis* for RNAi testing.

For PCR analysis, 30 pairs of antennae from 15 days old male and female adults, were excised and used for RNA isolation. Detailed procedures for RNA isolation, cDNA synthesis, and PCR amplification were the same as described previously. An α-tubulin (α-TUB; GenBank Acc. GU269902) of *B. dorsalis* was used as an internal reference. qRT-PCR primers used for BdorOBP83a-2 and Bdorβ-gal genes were designed with the Primer 3 program (http://primer3.ut.ee/) and the primer sequences are listed in **Table S6**. Technical triplicates and three biological replicates were carried out for each treatment.

EAG recordings were used to investigate any changes in antennal responses to attractant compounds (methyl eugenol and γ-octalactone) in water-treated, β-galactosidase-dsRNA-injected, BdorOBP83a-2-dsRNA-injected adults (both male and female). EAG responses were recorded for at least five individuals of water-treated control, β-galactosidase-dsRNA-injected control, and BdorOBP83a-2-dsRNA-injected insects. Each EAG observation was recorded with 10 individuals of each sex. Behavioral phenotypes of water-treated, β-galactosidase-dsRNA-injected, BdorOBP83a-2-dsRNA-injected insects were also assessed using a wind tunnel (**Figure S4**).

A fixed setting of 300 ml/min air-flow was used during the assays. Odor molecules pass through the glass tube from the odor source to the other end of the pipe along with the air flow. In each trial, one tested fly was placed in the opposite end of the odor source as the starting point. The time needed for insects to reach the odor source from the starting point was determined. The odor source was made by dissolving the test chemicals into paraffin oil at a final concentration of 10^{-2} v/v. Twenty microliters of the resulting mixture were added onto an absorbent cotton ball, which was used immediately as odor source. The wind tunnel experiment was recorded with 10 individuals of each sex, and performed in triplicates. Both EAG and wind tunnel experiments were performed at 25°C with relative humidity 90%.

Statistical Analysis

Statistical analyses were performed using Prism 6.0 (GraphPad Software, CA, USA). Statistical significance levels were derived through ANOVA and adjusted by a Tukey multiple comparison test.

RESULTS AND DISCUSSION

OBP Gene Expression Levels and Changes in Insect Olfactory Behavior

To determine olfactory behavioral changes in different stages of *B. dorsalis*, we used traps with different attractants to measure olfactory reactions in sexually immature and mated individuals from both sexes. We conducted olfactory assays with attractants that have been previously reported effective to *B. dorsalis* adults (**Table S1**; Chiu, 1990; Hwang et al., 2002; Tan et al., 2010; Hu et al., 2012; Tan and Nishida, 2012; Kamala Jayanthi et al., 2014; Jayanthi et al., 2014; Pagadala Damodaram et al., 2014). We found that immature males and females responded relatively weakly to nearly all tested attractant compounds (left part of **Figure 1**, **Table S7**). In contrast, both mated males and females responded strongly to most of the tested attractant compounds (right part of

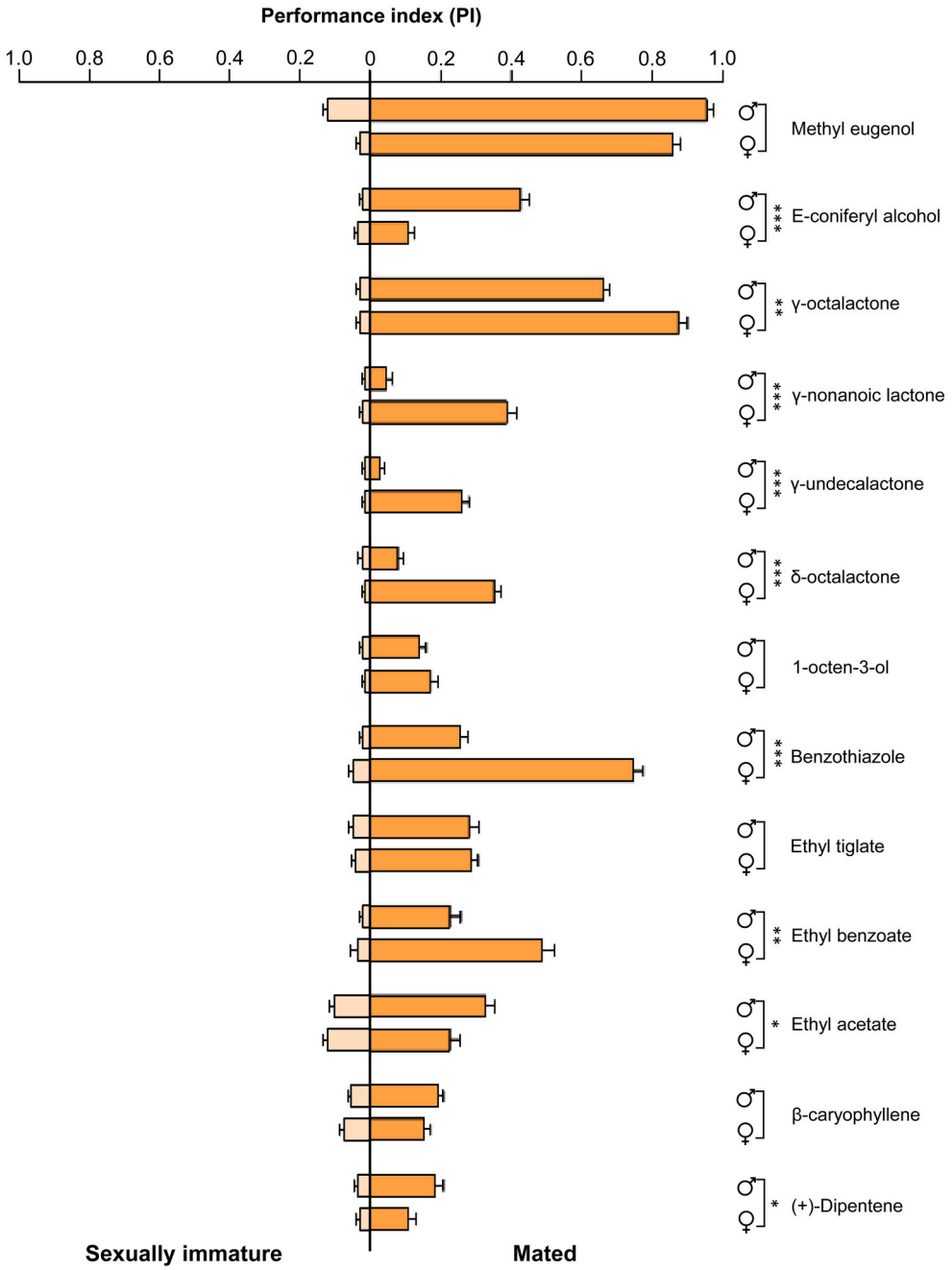

FIGURE 1 | Olfactory behavior responses of sexually immature and mated males and females of *B. dorsalis* to selected attractant chemicals. Asterisks indicate significant differences in performance index of males and females (*$P < 0.05$, **$P < 0.01$, ***$P < 0.0001$, unpaired two-tailed *t*-tests).

Figure 1). To some chemicals including E-coniferyl alcohol, γ-octalactone, and benzothiazole, mated males and females reacted differently. We also examined EAG responses on the same types of insects with the same set of chemicals. The EAG data exhibited similar differences between immature and mated flies as observed in olfactory behavior except that immature insects responded more strongly to the tested chemicals than what was observed in olfactory response assays (**Figure 2**). Mated males and females also responded differently to the attractants E-coniferyl alcohol and γ-octalactone, but reacted similarly to benzothiazole.

Previous reports indicate that expression levels of olfactory genes correlate with antennal odorant receptivity in the mosquito *Anopheles gambiae* (Rinker et al., 2013a,b), the tsetse fly *G. m. morsitans* (Liu et al., 2010, 2012), and the beet armyworm *Spodoptera exigua* (Wan et al., 2015). Here, we wanted to investigate whether expression levels of

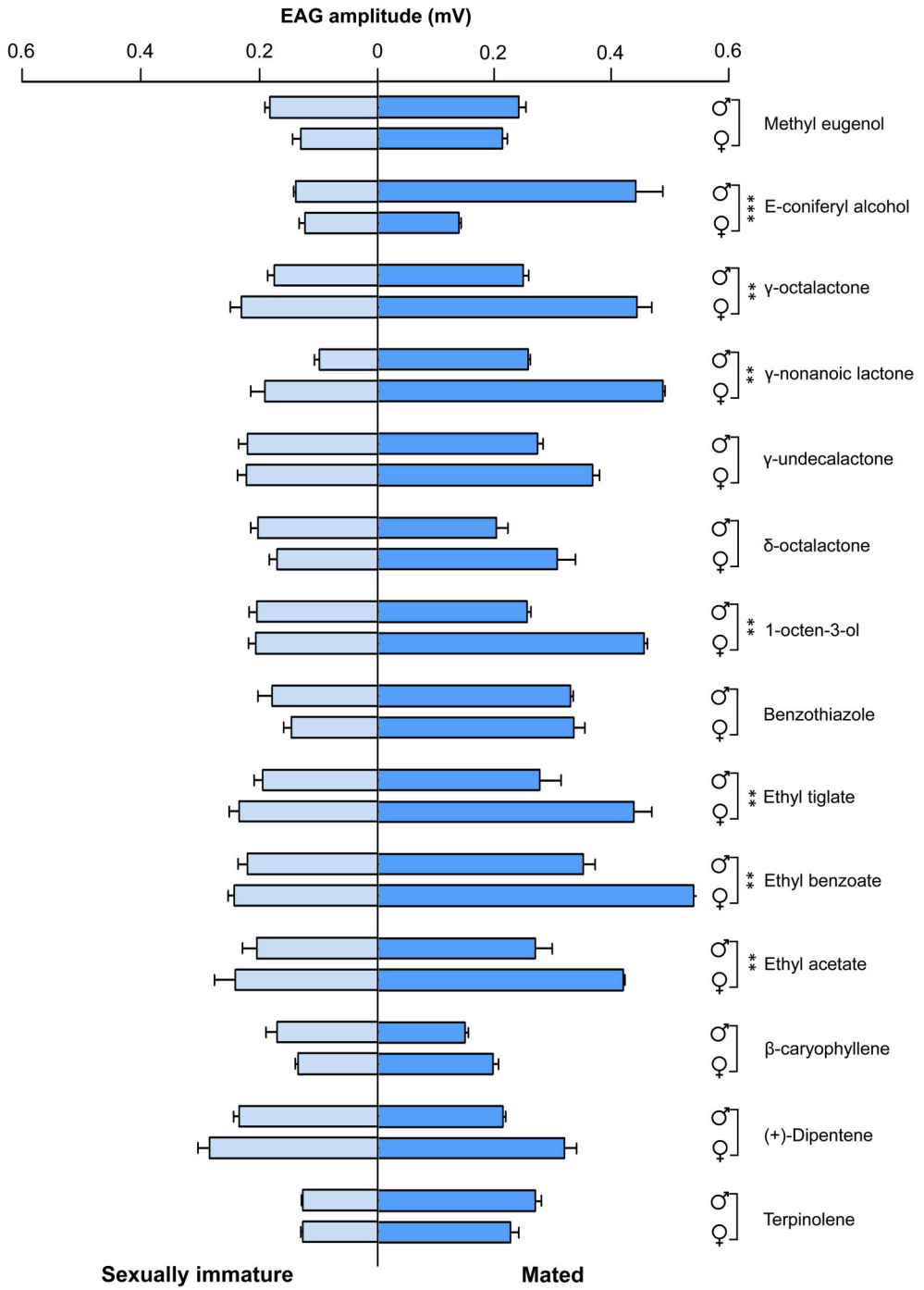

FIGURE 2 | EAG responses of sexually immature and mated males and females of *B. dorsalis* to selected chemicals. Asterisks indicate significant differences in EAG responses of males and females (**$P < 0.01$, ***$P < 0.0001$, unpaired two-tailed *t*-tests).

olfactory genes could regulate both behavioral and neuronal responses in *B. dorsalis* at different physiological status. Previously, we determined the expression profiles of individual genes (Wu et al., 2015). The following antenna-specific or antenna-predominant olfaction genes, including 10 OBPs (BdorOBPlush, BdorOBP19a, BdorOBP19d-1, BdorOBP28a, BdorOBP56h, BdorOBP69a, BdorOBP83a-1, BdorOBP83a-2, BdorOBP84a-1), one CSP (BdorCSP3), one ORco (BdorORCO), and two SNMPs (BdorSNMP1-1 and BdorSNMP1-2), are expressed exclusively or predominantly in antennae. At the present study, we further determined if these antenna-specific genes were differentially expressed in different developmental

stages of male and female adults. We found that five OBP genes were significantly upregulated in mated females during oviposition compared with immature females, whereas only one was significantly upregulated in mated males (**Figure 3**). These observations suggested that the specific upregulation of OBPs in mated adults might be involved in changes in olfactory perception. However, CSPs and ORco genes were not significantly upregulated in either mated females or males, and a significant down-regulation of SNMP1-1 in females was observed under our conditions (**Figure 4**). Expression of genes encoding antenna-specific chemosensory proteins varies in different insect species. In *G. m. morsitans*, antenna-specific CSPs (GmmCSP2), the orthologs of BdorCSP3, are up-regulated during starvation in female adults, and are thought to be linked to olfactory perception of hosts (Liu et al., 2012). In *A. gambiae,* a subset of OBP genes are upregulated post a blood feeding whereas most other chemosensory genes are not affected or even down-regulated (Rinker et al., 2013a); and such changes following blood feeding are coincident with a switch from host-seeking to oviposition behaviors. These observations suggest that different mechanisms likely exist for chemosensory perception in different insects under different conditions.

Olfactory behavior of most insects displays remarkable phase changes associated with different physiological status, such as sexually immature and mated adults. Typically, mated male fruit flies are strongly attracted to and compulsively feed on methyl eugenol, but sexually immature males showed a weak behavioral response to methyl eugenol (Mitchell et al., 1985; Tan and Nishida, 2012). In addition, various fruit volatiles attract gravid females, which lay their eggs in host fruits (Cornelius et al., 2000; Hwang et al., 2002; Siderhurst and Jang, 2006; Jayanthi et al., 2012; Kamala Jayanthi et al., 2014; Pagadala Damodaram et al., 2014). On the contrary, sexually immature females showed limited responses to food-type attractants, such as fermenting sugars, hydrolyzed protein, and yeast. In this study, the expression level of BdorOBP83a-2 along with other antenna-specific OBPs correlated with increased olfactory sensitivity, indicating that specific OBPs were likely responsible for detection of specific attractants.

Binding Assays of OBPs to Attractant Semiochemicals

To determine the roles of specific OBPs in recognition of attractants in *B. dorsalis*, recombinant proteins of selected

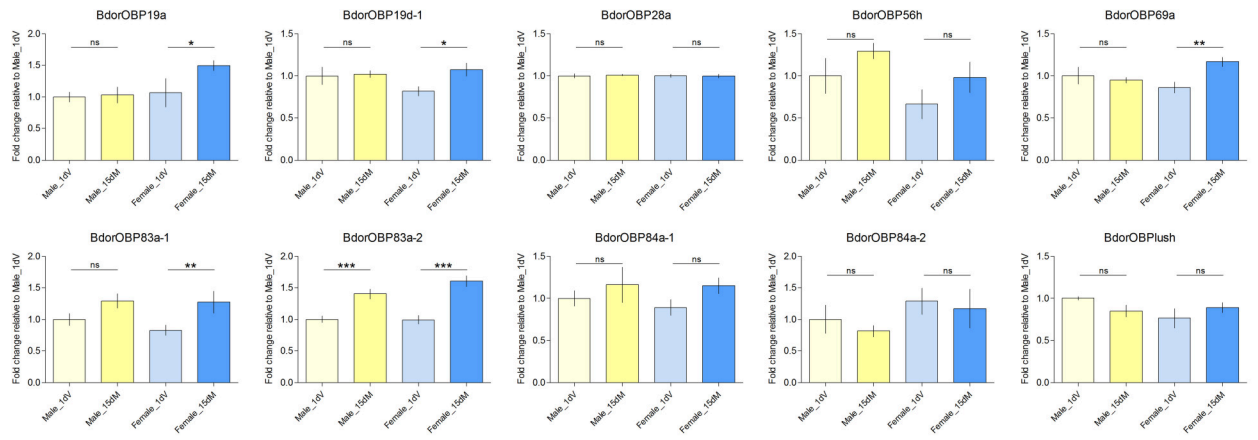

FIGURE 3 | Transcript abundance of selected OBP genes in the antennae of 1 day immature (1 dV), and 15 days old mated (15 dM) males and females. Asterisks indicate significant differences in transcript abundances (*$P < 0.05$, **$P < 0.01$, ***$P < 0.0001$, unpaired two-tailed *t*-tests).

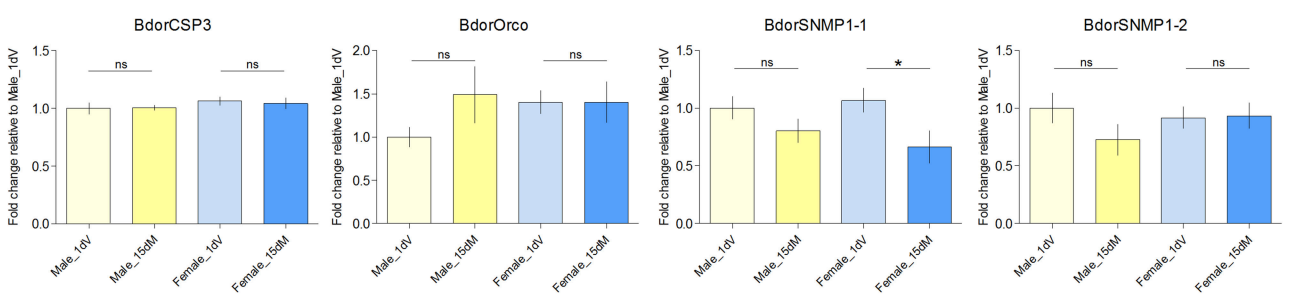

FIGURE 4 | Transcript abundance of BdorCSP3, BdorOrco, BdorSNMP1-1, BdorSNMP1-2 in the antennae of 1 day immature (1 dV), and 15 days old mated (15 dM) males and females. Asterisks indicate significant differences in transcript abundances (*$P < 0.05$, unpaired two-tailed *t*-tests).

antenna-abundant OBPs and CSPs were obtained using a prokaryotic expression system (**Figure 5**). Purified OBPs and CSPs were used to determine binding affinity of each protein via fluorescence competitive binding assays. Thirteen pure attractant compounds were tested against each recombinant protein. Six antenna-rich proteins (five OBPs and one CSP) exhibited high

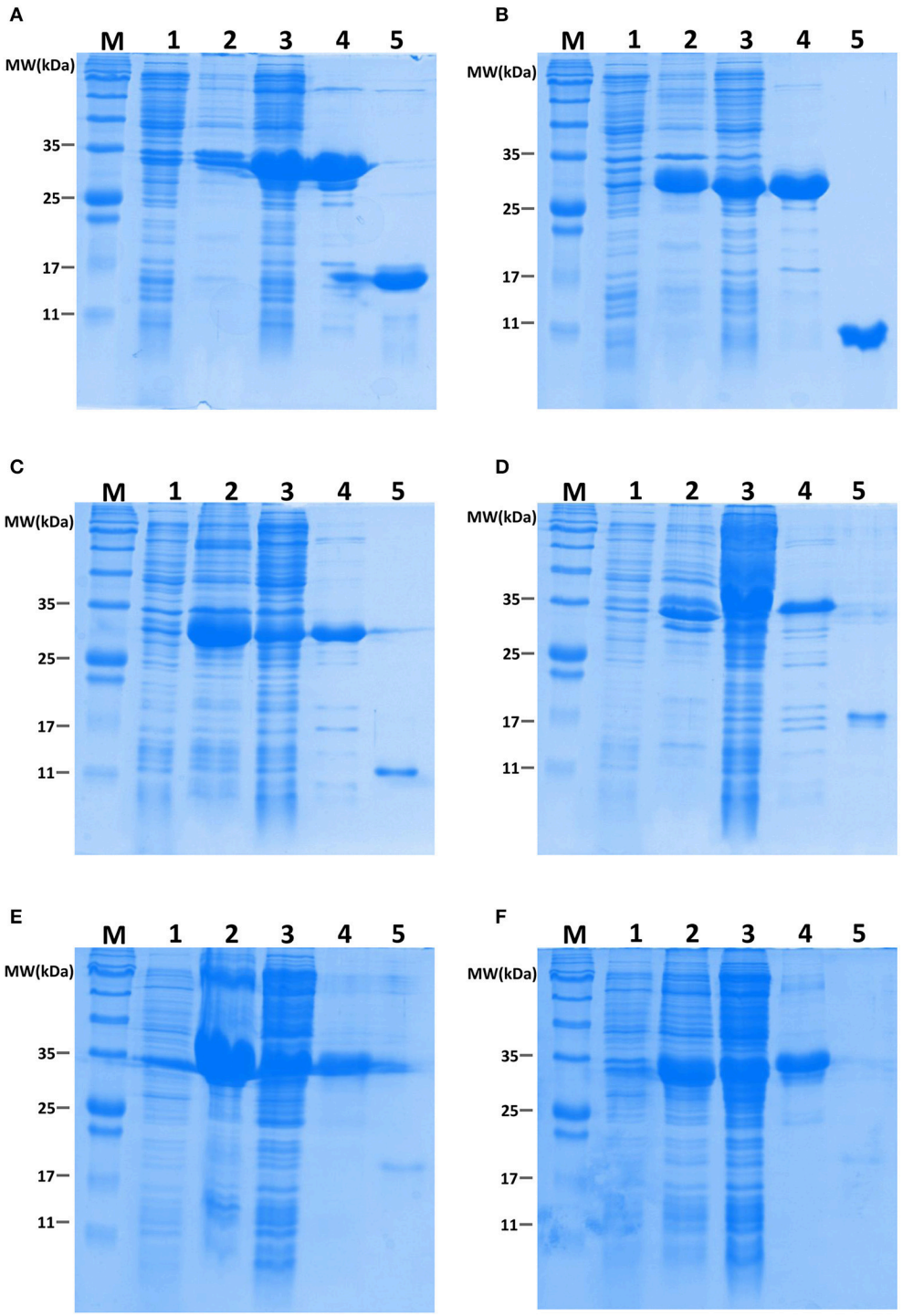

FIGURE 5 | Recombinant BdorOBPs and a BdorCSP analyzed on SDS-PAGE. M, Molecular weight marker; 1, Total protein extract from non-induced pET32a transformed BL21 (DE3) cells; 2, Protein extract from isolated inclusion body of pET32a transformed cells; 3, Supernatant of ultrasonated pET32a transformed cells; 4, Proteins purified through Ni-NTA columns; 5, Purified proteins with His-tag cleaved using recombinant enterrokinase; **(A)**, BdorCSP3; **(B)**, BdorOBP56h; **(C)**, BdorOBP83a-1; **(D)**, BdorOBP83a-2; **(E)**, BdorOBP84a-1; **(F)**, BdorOBP84a-2.

affinity to the fluorescent probe 1-NPN (**Figure 6**). Except for BdorCSP3 and BdorOBP84a-2, all remaining OBPs could bind to the tested compounds (**Figure 6**; **Table S8**). The binding inability of BdorCSP3 and BdorOBP84a-2 might suggest that other compounds could be ligands for these two proteins. Alternatively they might be involved in functions other than odor detection. Among the analyzed proteins, BdorOBP83a-1 and BdorOBP83a-2 showed higher affinity than the remaining OBPs to all tested attractant chemicals, with BdorOBP83a-2 being the highest (**Table S8**). For BdorOBP83a-2, attractants methyl eugenol and esters exhibited the lowest dissociation constants (**Figure 7**; **Table S8**). The binding affinity decreased in order for attractants methyl eugenol, γ-nonanoic lactone, δ-octalactone, γ-undecalactone, and γ-octalactone. Overall, we observed lower binding affinity with our recombinant proteins and tested attractants. As shown in **Figure 7**, the highest binding affinity was with BdorOBP83a-2, which reached approximately 40% of displacement in competitive binding assays. In other studies, much higher affinity has been reported. For example, competitive binding assays with a lepidopteran pheromone-binding protein can reach nearly 100% displacement (Hooper et al., 2009; Gu et al., 2013), and competitive binding assays with an aphid OBP (OBP7) can reach about 80% displacement with the alarm pheromone (E)-ss-farnesene (Sun et al., 2012). The biological significance of the observed lower affinity with *B. doralis* OBPs here remains to be determined. It could be due to diverse binding mechanisms between different functional OBPs and the corresponding compounds. Alternatively, BdorOBP83a-2 may interact with high affinity with other odor chemicals not yet identified.

Possible 3-dimensional structures of five OBPs and one CSP were predicted through molecular simulation (**Figure S5**), and the interactions between each of the six proteins and thirteen compounds were tested through docking (**Table S9**). Each protein displayed distinct spectra of binding affinity with the tested chemicals. Among them, BdorOBP83a-1 and BdorOBP83a-2 showed the highest affinity on average. Our overall simulation and docking data were in agreement with binding assays.

Phylogenetic analysis revealed that two OBP83a homologs, BdorOBP83a-1 and BdorOBP83a-2, clustered together with orthologous OBPs from other Dipterans (**Figure S6**), consistent

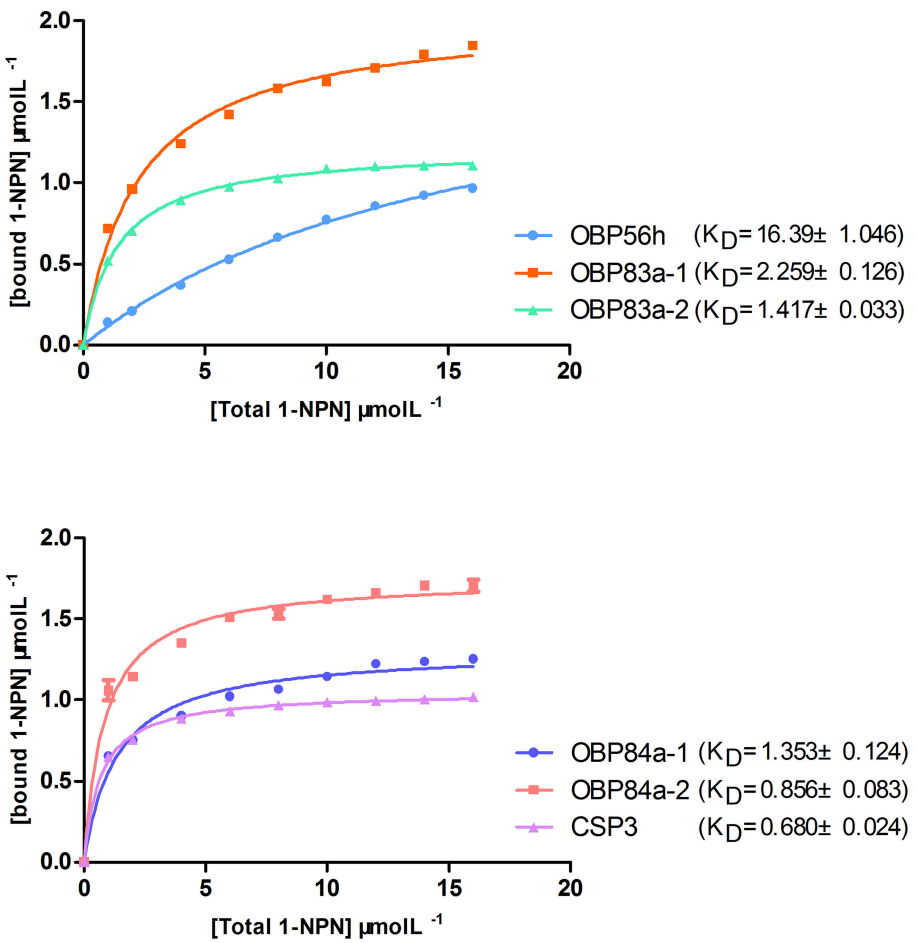

FIGURE 6 | Binding assays of recombinant OBPs and a CSP with the fluorescent probe 1-NPN. Data are means of three independent experiments.

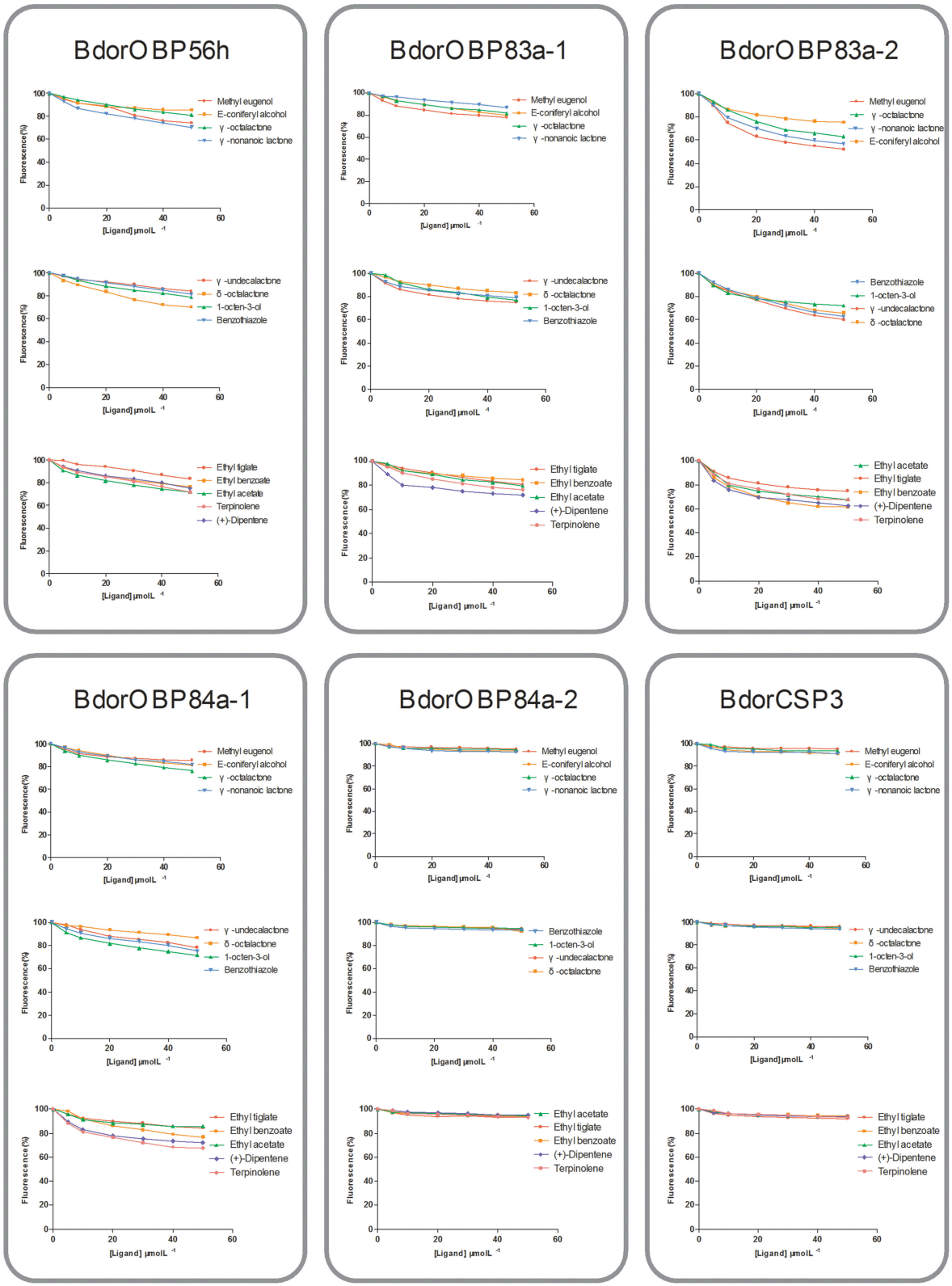

FIGURE 7 | Binding assays of recombinant OBPs and a CSP with selected ligands. Data are means of two independent experiments.

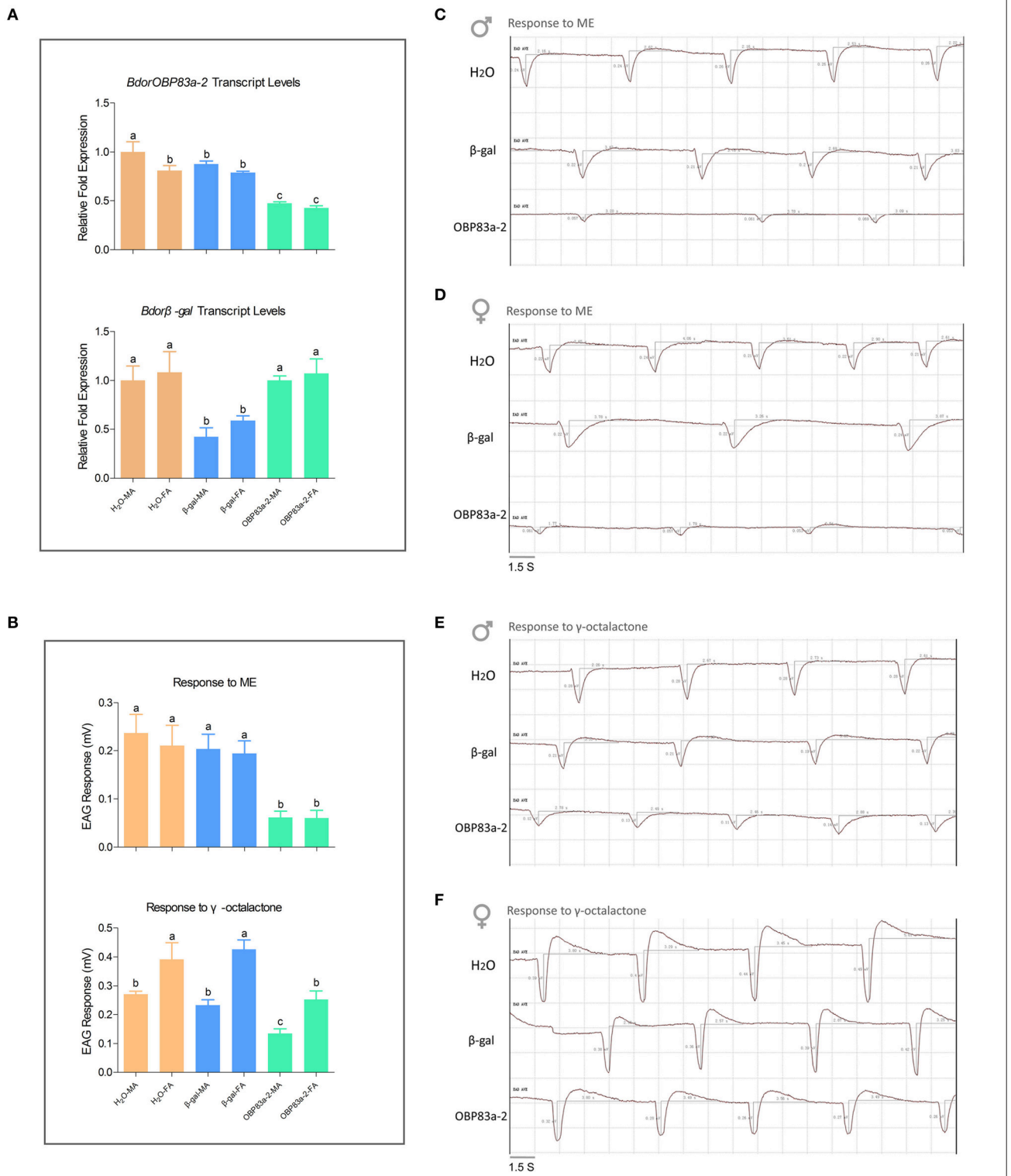

FIGURE 8 | Effect of RNAi treatments on electrophysiological responses to methyl eugenol and γ-octalactone. (A) Upper part: BdorOBP83a-2 transcript levels in water-treated (orange), β-galactosidase-dsRNA-injected (blue), and BdorOBP83a-2-dsRNA-injected the oriental fruit fly (lime); lower part: Bdorβ-gal transcript levels in water-treated (orange), β-galactosidase-dsRNA-injected (blue), and BdorOBP83a-2-dsRNA-injected the oriental fruit fly (lime); **(B)** upper part: EAG responses to methyl eugenol in water-treated (orange), β-galactosidase-dsRNA-injected (blue), and BdorOBP83a-2-dsRNA-injected; lower part: EAG responses to γ-octalactone in water-treated (orange), β-galactosidase-dsRNA-injected (blue), and BdorOBP83a-2-dsRNA-injected; EAG traces recorded from antennae of water-treated, β-galactosidase-dsRNA-injected, and BdorOBP83a-2-dsRNA-injected male and female challenged with methyl eugenol **(C,D)** and γ-octalactone (**E,F**). MA, male antennae; FA, female antennae. Different lowercase letters above each bar denote significant differences between samples ($p < 0.05$).

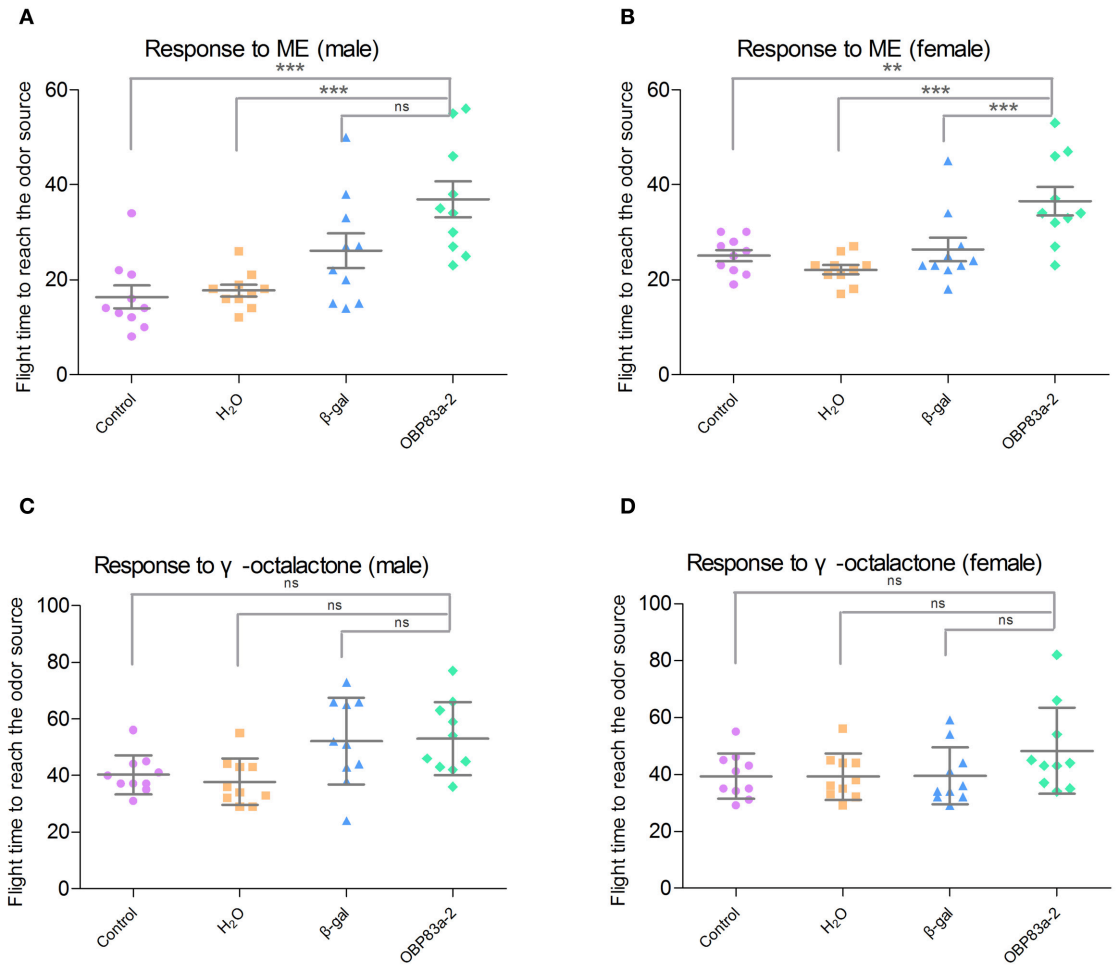

FIGURE 9 | Effect of RNAi treatments on olfactory behavior to the attractants methyl eugenol and γ-octalactone. Olfactory behavior to methyl eugenol in non-treated (purple), water-treated (orange), β-galactosidase-dsRNA-injected (blue), and BdorOBP83a-2-dsRNA-injected (green) in males **(A)** and females **(B)**; and to γ-octalactone in males **(C)** and females **(D)** (**$P < 0.01$, ***$P < 0.0001$).

with exceptional conservation in function among OBP83a orthologs from different species (**Figure S7**). OBP83a orthologs, which were exclusively expressed in antennae, have been reported to play crucial roles in olfactory perception, such as in starved females in host seeking of *G. m. morsitans* (Liu et al., 2010), and pheromone components detection in *C. capitata* (Siciliano et al., 2014a,b). These results correspond well to its specific tissue distribution within antennae which could give a functional implication that BdorOBP83a-1 and BdorOBP83a-2 would share a relatively conserved physiological function with its orthologs.

Roles of BdorOBP83a-2 in Attractant Perception

Since BdorOBP83a-2 was upregulated in both mated males and females, and exhibited the highest ligand-binding affinity, we further analyzed its potential role in olfactory perception via RNAi. Microinjection of BdorOBP83a-2 dsRNA inhibited approximately 50% expression of the gene in antennae based on qPCR analysis (**Figure 8A**). Males and females with BdorOBP83a-2 knocked down were examined for possible impact on olfactory behavior changes. As shown in **Figures 8B(upper part),C,D**, knockdown of BdorOBP83a-2 resulted in 60–70% reduction of EAG response activity to methyl eugenol. Similarly, knockdown of BdorOBP83a-2 resulted in approximately 40% reduction of EAG response activity to γ-octalatone (lower part of **Figures 8B,E,F**). In comparison, knockdown of olfactory-unrelated control genes resulted in no significant changes in EAG response activities. Males and females with BdorOBP83a-2 knocked down were also used for olfactory behavior analysis. Flight time to reach the odor source for insects with BdorOBP83a-2 knocked down increased 30–50% with methyl eugenol as attractant. Knockdown of control genes resulted in no apparent changes in flight time (**Figures 9A,B**). Our data strongly suggest that BdorOBP83a-2 contributes to the changes observed in chemosensory and behavioral function. Our observation is consistent with reports that knockdown of a single OBP gene led to a significant

decrease in the sensitivity of *C. quinquefasciatus* and *A. gambiae* adults to major oviposition attractants (Biessmann et al., 2010; Pelletier et al., 2010a). Mutations in a single OBP gene can also cause significant changes in odorant perception and courtship behavior of Drosophila adults (Xu et al., 2005; Laughlin et al., 2008).

CONCLUSIONS

We have comparatively analyzed olfactory attraction and EAG responses to semiochemicals in sexually immature and mated males and females. The expression of antenna-predominant OBPs was upregulated in the mated flies, and this increase may be related to the need for an increased ability to detect some key volatiles. Our ligand-binding assays demonstrated that OBP83a homologs exhibited the highest affinity to the attractant semiochemicals. Reduction in BdorOBP83a-2 transcript abundance led to a decrease in neuronal responses to representative attractants as well as behavioral responses. Together, these results suggest that BdorOBP83a-2 is likely to participate in mediating responses of *B. dorsalis* adults to attractant semiochemicals.

AUTHOR CONTRIBUTIONS

ZW and XZ designed the experiments. ZW and HZ performed the experiments. ZW and JL contributed reagents/materials/gene identification. ZW analyzed the data. ZW and XZ wrote and revised the paper.

ACKNOWLEDGMENTS

We thank Dr. Mingshun Chen (Kansas State University, USA), Dr. Paolo Pelosi (University of Pisa, Italy), and Dr. Guirong Wang (Chinese Academy of Agricultural Sciences, China) for comments and editorial assistance on the manuscript. This work was supported financially by Guangdong Engineering Research Center for Insect Behavior Regulation (2015B0909 03076).

SUPPLEMENTARY MATERIAL

The Supplementary Material for this article can be found online at: http://journal.frontiersin.org/article/10.3389/fphys.2016.00452

Table S1 | Detailed information of semiochemicals. IUPAC nomenclature, CAS number (CAS #), Behavioral output, Odor resource, Chemical structure, and References are shown.

Table S2 | Primers for heterologous expression of OBP and CSP proteins.

Table S3 | Three-dimensional modeling of proteins using SWISS-MODEL.

Table S4 | Three-dimensional modeling of proteins using Phyre2.

Table S5 | Primers used for producing constructs for BdorOBP83a-2 and Bdorβ-gal genes and for PCR amplification of templates for dsRNA synthesis.

Table S6 | Primers used for qRT-PCR to determine transcript levels of BdorOBP83a-2 and Bdorβ-gal genes.

Table S7 | Performance index (PI) of response to different compounds in sexual immaturity and sexual maturity.

Table S8 | Binding characteristics of four recombinant BdorOBPs with selected semiochemicals.

Table S9 | Outputs of *in silico* docking analyses of selected semiochemicals with putative OBPs and a CSP through the "Docking Server."

Figure S1 | Schematic presentation of olfactory trap assays.

Figure S2 | Alignments of BdorOBP83a-1, BdorOBP83a-2, BdorCSP3, BdorOBP84a-1, BdorOBP84a-2, and BdorOBP56h with the template protein.

Figure S3 | *Ex vivo* degradation assay of dsRNA fragments using hemolymph. H_2O: H_2O+dsRNA; 0–3 h: hemolymph plasma+dsRNA

Figure S4 | The device used for olfactory behavior assays (A), its dimensions (B) and sketches (C).

Figure S5 | Three-dimensional modeling of putative proteins BdorOBP56h, BdorOBP83a-1, BdorOBP83a-2, BdorOBP84a-1, BdorOBP83a-2, and BdorCSP3.

Figure S6 | Phylogenetic relationship of OBPs from *B. dorsalis* and other dipterans. Bars indicate branch lengths in proportion to amino acid substitutions per site. Bdor, *Bactrocera dorsalis*; Csty, *Calliphora stygia*; Dmel, *Drosophila melanogaster*; Gmm, *Glossina morsitans morsitans*; Mdom, *Musca domestica*; Rpom, *Rhagoletis pomonella*; Rsua, *Rhagoletis suavis*.

Figure S7 | An amino acid alignment of BdorOBP83a-2 with orthologs from other dipterans. Signal peptides were removed from all amino acid sequences. All conserved cysteine residues are displayed under the alignment.

REFERENCES

Allwood, A. J., Chinajariyawong, A., Kritsaneepaiboon, S., Drew, R. A. I., Hamacek, E. L., Hancock, D. L., et al. (1999). Host plant records for fruit flies (Diptera: Tephritidae) in Southeast Asia. *Raffles. B Zool.* 47, 1–92.

Arakawa, T. (1995). Phenylthiourea, an effective inhibitor of the insect haemolymph melanization reaction, interferes with the detection of lipoprotein hydroperoxide. *Appl. Entomol. Zool.* 30, 443–449.

Arnold, K., Bordoli, L., Kopp, J., and Schwede, T. (2006). The SWISS-MODEL workspace: a web-based environment for protein structure homology modelling. *Bioinformatics* 22, 195–201. doi: 10.1093/bioinformatics/bti770

Biessmann, H., Andronopoulou, E., Biessmann, M. R., Douris, V., Dimitratos, S. D., Eliopoulos, E., et al. (2010). The *Anopheles gambiae* odorant binding protein 1 (AgamOBP1) mediates indole recognition in the antennae of female mosquitoes. *PLoS ONE* 5:e9471. doi: 10.1371/journal.pone.0009471

Bikadi, Z., and Hazai, E. (2009). Application of the PM6 semi-empirical method to modeling proteins enhances docking accuracy of AutoDock. *J. Cheminform.* 1:15. doi: 10.1186/1758-2946-1-15

Chang, H., Liu, Y., Yang, T., Pelosi, P., Dong, S., and Wang, G. (2015). Pheromone binding proteins enhance the sensitivity of olfactory receptors to sex pheromones in *Chilo suppressalis*. *Sci. Rep.* 5:13093. doi: 10.1038/srep 13093

Chiu, H. T. (1990). Ethyl benzoate: an impact ovipositional attractant of the oriental fruit fly, *Dacus dorsalis* Hendel. *Chinese J. Entomol.* 10, 375–387.

Cornelius, M. L., Duan, J. J., and Messing, R. H. (2000). Volatile host fruit odors as attractants for the oriental fruit fly (Diptera: Tephritidae). *J. Econ. Entomol.* 93, 93–100. doi: 10.1603/0022-0493-93.1.93

Drew, R. A. I., and Hancock, D. L. (1994). The *Bactrocera dorsalis* complex of fruit flies (Diptera: Tephritidae: Dacinae) in Asia. *B. Entomol. Res.* 2, 1–68. doi: 10.1017/S1367426900000278

Faucher, C. P., Hilker, M., and de Bruyne, M. (2013). Interactions of carbon dioxide and food odours in Drosophila: olfactory hedonics and sensory neuron properties. *PLoS ONE* 8:e56361. doi: 10.1371/journal.pone.0056361

Forstner, M., Breer, H., and Krieger, J. (2009). A receptor and binding protein interplay in the detection of a distinct pheromone component in the silkmoth *Antheraea polyphemus*. *Int. J. Biol. Sci.* 5, 745–757. doi: 10.7150/ijbs.5.745

Garbutt, J. S., Bellés, X., Richards, E. H., and Reynolds, S. E. (2013). Persistence of double-stranded RNA in insect hemolymph as a potential determiner of RNA interference success: evidence from *Manduca sexta* and *Blattella germanica*. *J. Insect. Physiol.* 59, 171–178. doi: 10.1016/j.jinsphys.2012.05.013

Grosse-Wilde, E., Gohl, T., Bouché, E., Breer, H., and Krieger, J. (2007). Candidate pheromone receptors provide the basis for the response of distinct antennal neurons to pheromonal compounds. *Eur. J. Neurosci.* 25, 2364–2373. doi: 10.1111/j.1460-9568.2007.05512.x

Grosse-Wilde, E., Svatos, A., and Krieger, J. (2006). A pheromone-binding protein mediates the bombykol-induced activation of a pheromone receptor *in vitro*. *Chem. Senses.* 31, 547–555. doi: 10.1093/chemse/bjj059

Gu, S. H., Wang, S. Y., Zhang, X. Y., Ji, P., Liu, J. T., Wang, G. R., et al. (2012). Functional characterizations of chemosensory proteins of the alfalfa plant bug *Adelphocoris lineolatus* indicate their involvement in host recognition. *PLoS ONE* 7:e42871. doi: 10.1371/journal.pone.0042871

Gu, S. H., Zhou, J. J., Wang, G. R., Zhang, Y. J., and Guo, Y. Y. (2013). Sex pheromone recognition and immunolocalization of three pheromone binding proteins in the black cutworm moth *Agrotis ipsilon*. *Insect Biochem. Mol. Biol.* 43, 237–251. doi: 10.1016/j.ibmb.2012.12.009

Guex, N., and Peitsch, M. C. (1997). SWISS-MODEL and the Swiss-PdbViewer: an environment for comparative protein modeling. *Electrophoresis* 18, 2714–2723. doi: 10.1002/elps.1150181505

Guex, N., Peitsch, M. C., and Schwede, T. (2009). Automated comparative protein structure modeling with SWISS-MODEL and Swiss-PdbViewer: a historical perspective. *Electrophoresis* 30 (Suppl. 1), S162–S173. doi: 10.1002/elps.200900140

Guo, W., Wang, X., Ma, Z., Xue, L., Han, J., Yu, D., et al. (2011). CSP and takeout genes modulate the switch between attraction and repulsion during behavioral phase change in the migratory locust. *PLoS Genet.* 7:e1001291. doi: 10.1371/journal.pgen.1001291

Hallem, E. A., Ho, M. G., and Carlson, J. R. (2004). The molecular basis of odor coding in the Drosophila antenna. *Cell* 117, 965–979. doi: 10.1016/j.cell.2004.05.012

Hayase, S., Renou, M., and Itoh, T. (2009). Possible origin of modified EAG activity by point-fluorination of insect pheromones. *Future Med. Chem.* 1, 835–845. doi: 10.4155/fmc.09.73

Hekmat-Scafe, D. S., Scafe, C. R., McKinney, A. J., and Tanouye, M. A. (2002). Genome-wide analysis of the odorant-binding protein gene family in *Drosophila melanogaster*. *Genome Res.* 12, 1357–1369. doi: 10.1101/gr.239402

Hooper, A. M., Dufour, S., He, X., Muck, A., Zhou, J. J., Almeida, R., et al. (2009). High-throughput ESI-MS analysis of binding between the *Bombyx mori* pheromone-binding protein BmorPBP1, its pheromone components and some analogues. *Chem. Commun.* 14, 5725–5727. doi: 10.1039/b914294k

Hu, L. M., Shen, J. M., Bin, S. Y., Chen, G. F., Lin, B. Q., and Lin, J. T. (2012). Chemical constituents of the essential oils from Citrus reticulate and its influence on the oviposition of *Bactrocera dorsalis* (Diptera: Tephritidae). *J. Fruit Sci.* 29, 630–633.

Hwang, J. S., Yen, Y. P., Chang, M. C., and Liu, C. Y. (2002). Extraction and identification of volatile components of guava fruits and their attraction to oriental fruit fly, *Bactrocera dorsalis* (Hendel). *Plant Prot.* 44, 279–302.

Iovinella, I., Bozza, F., Caputo, B., Della Torre, A., and Pelosi, P. (2013). Ligand-binding study of *Anopheles gambiae* chemosensory proteins. *Chem. Senses* 38, 409–419. doi: 10.1093/chemse/bjt012

Jacquin-Joly, E., Vogt, R. G., François, M. C., and Nagnan-Le Meillour, P. (2001). Functional and expression pattern analysis of chemosensory proteins expressed in antennae and pheromonal gland of *Mamestra brassicae*. *Chem. Senses* 26, 833–844. doi: 10.1093/chemse/26.7.833

Jayanthi, K. P., Kempraj, V., Aurade, R. M., Roy, T. K., Shivashankara, K. S., and Verghese, A. (2014). Computational reverse chemical ecology: virtual screening and predicting behaviorally active semiochemicals for *Bactrocera dorsalis*. *BMC Genomics* 15:209. doi: 10.1186/1471-2164-15-209

Jayanthi, P. D. K., and Abraham, V. (2002). A simple and cost-effective mass rearing technique for the tephritid fruit fly, *Bactrocera dorsalis* (Hendel). *Curr. Sci.* 82, 266–268.

Jayanthi, P. D. K., Woodcock, C. M., Caulfield, J., Birkett, M. A., and Bruce, T. J. A. (2012). Isolation and identification of host cues from mango, *Mangifera indica*, that attract gravid female oriental fruit fly, *Bactrocera dorsalis*. *J. Chem. Ecol.* 38, 361–369. doi: 10.1007/s10886-012-0093-y

Kamala Jayanthi, P. D., Kempraj, V., Aurade, R. M., Venkataramanappa, R. K., Nandagopal, B., Verghese, A., et al. (2014). Specific volatile compounds from mango elicit oviposition in gravid *Bactrocera dorsalis* females. *J. Chem. Ecol.* 40, 259–266. doi: 10.1007/s10886-014-0403-7

Katoh, K., and Standley, D. M. (2013). MAFFT multiple sequence alignment software version 7: improvements in performance and usability. *Mol. Biol. Evol.* 30, 772–780. doi: 10.1093/molbev/mst010

Katoh, K., and Toh, H. (2010). Parallelization of the MAFFT multiple sequence alignment program. *Bioinformatics* 26, 1899–1900. doi: 10.1093/bioinformatics/btq224

Kelley, L. A., Mezulis, S., Yates, C. M., Wass, M. N., and Sternberg, M. J. (2015). The Phyre2 web portal for protein modeling, prediction and analysis. *Nat. Protoc.* 10, 845–858. doi: 10.1038/nprot.2015.053

Laughlin, J. D., Ha, T. S., Jones, D. N., and Smith, D. P. (2008). Activation of pheromone-sensitive neurons is mediated by conformational activation of pheromone-binding protein. *Cell* 133, 1255–1265. doi: 10.1016/j.cell.2008.04.046

Leal, W. S. (2013). Odorant reception in insects: roles of receptors, binding proteins, and degrading enzymes. *Annu. Rev. Entomol.* 58, 373–391. doi: 10.1146/annurev-ento-120811-153635

Leitch, O., Papanicolaou, A., Lennard, C., Kirkbride, K. P., and Anderson, A. (2015). Chemosensory genes identified in the antennal transcriptome of the blowfly *Calliphora stygia*. *BMC Genomics* 16:255. doi: 10.1186/s12864-015-1466-8

Liu, R., He, X., Lehane, S., Lehane, M., Hertz-Fowler, C., Berriman, M., et al. (2012). Expression of chemosensory proteins in the tsetse fly *Glossina morsitans morsitans* is related to female host-seeking behaviour. *Insect Mol. Biol.* 21, 41–48. doi: 10.1111/j.1365-2583.2011.01114.x

Liu, R., Lehane, S., He, X., Lehane, M., Hertz-Fowler, C., Berriman, M., et al. (2010). Characterisations of odorant-binding proteins in the tsetse fly *Glossina morsitans morsitans*. *Cell. Mol. Life Sci.* 67, 919–929. doi: 10.1007/s00018-009-0221-1

Livak, K. J., and Schmittgen, T. D. (2001). Analysis of relative gene expression data using real-time quantitative PCR and the 2(-Delta Delta C(T)) Method. *Methods* 25, 402–408. doi: 10.1006/meth.2001.1262

Macharia, R., Mireji, P., Murungi, E., Murilla, G., Christoffels, A., Aksoy, S., et al. (2016). Genome-Wide comparative analysis of chemosensory gene families in five tsetse fly species. *PLoS Negl. Trop. Dis.* 10:e0004421. doi: 10.1371/journal.pntd.0004421

Mitchell, W. C., Metcalf, R. L., Metcalf, E. R., and Mitchell, S. (1985). Candidate substitutes for methyl eugenol as attractants for the area-wide monitoring and control of the oriental fruitfly, *Dacus dorsalis* Hendel (Diptera: Tephritidae). *Environ. Entomol.* 14, 176–181. doi: 10.1093/ee/14.2.176

Okimoto, N., Futatsugi, N., Fuji, H., Suenaga, A., Morimoto, G., Yanai, R., et al. (2009). High-performance drug discovery: computational screening by combining docking and molecular dynamics simulations. *PLoS Comput. Biol.* 5:e1000528. doi: 10.1371/journal.pcbi.1000528

Oppenheim, S. J., Baker, R. H., Simon, S., and DeSalle, R. (2015). We can't all be supermodels: the value of comparative transcriptomics to the study of non-model insects. *Insect Mol. Biol.* 24, 139–154. doi: 10.1111/imb.12154

Pagadala Damodaram, K. J., Kempraj, V., Aurade, R. M., Venkataramanappa, R. K., Nandagopal, B., and Verghese, A. (2014). Oviposition site-selection by *Bactrocera dorsalis* is mediated through an innate recognition template tuned to γ-octalactone. *PLoS ONE* 9:e85764. doi: 10.1371/journal.pone.0085764

Pelletier, J., Guidolin, A., Syed, Z., Cornel, A. J., and Leal, W. S. (2010a). Knockdown of a mosquito odorant-binding protein involved in the sensitive detection of oviposition attractants. *J. Chem. Ecol.* 36, 245–248. doi: 10.1007/s10886-010-9762-x

Pelletier, J., Hughes, D. T., Luetje, C. W., and Leal, W. S. (2010b). An odorant receptor from the southern house mosquito *Culex pipiens*

quinquefasciatus sensitive to oviposition attractants. *PLoS ONE* 5:e10090. doi: 10.1371/journal.pone.0010090

Pelosi, P., Calvello, M., and Ban, L. (2005). Diversity of odorant-binding proteins and chemosensory proteins in insects. *Chem. Senses* 30(Suppl. 1), i291–i292. doi: 10.1093/chemse/bjh229

Pelosi, P., Iovinella, I., Felicioli, A., and Dani, F. R. (2014). Soluble proteins of chemical communication: an overview across arthropods. *Front. Physiol.* 5:320. doi: 10.3389/fphys.2014.00320

Pelosi, P., and Maida, R. (1995). Odorant-binding proteins in insects. *Comp. Biochem. Physiol. B Biochem. Mol. Biol.* 111, 503–514. doi: 10.1016/0305-0491(95)00019-5

Pelosi, P., Zhou, J. J., Ban, L. P., and Calvello, M. (2006). Soluble proteins in insect chemical communication. *Cell. Mol. Life Sci.* 63, 1658–1676. doi: 10.1007/s00018-005-5607-0

Price, M. N., Dehal, P. S., and Arkin, A. P. (2009). FastTree: computing large minimum evolution trees with profiles instead of a distance matrix. *Mol. Biol. Evol.* 26, 1641–1650. doi: 10.1093/molbev/msp077

Price, M. N., Dehal, P. S., and Arkin, A. P. (2010). FastTree 2–approximately maximum-likelihood trees for large alignments. *PLoS ONE* 5:e9490. doi: 10.1371/journal.pone.0009490

Ramachandran, S., Kota, P., Ding, F., and Dokholyan, N. V. (2011). Automated minimization of steric clashes in protein structures. *Proteins* 79, 261–270. doi: 10.1002/prot.22879

Ramsdell, K. M., Lyons-Sobaski, S. A., Robertson, H. M., Walden, K. K., Feder, J. L., Wanner, K., et al. (2010). Expressed sequence tags from cephalic chemosensory organs of the northern walnut husk fly, *Rhagoletis suavis*, including a putative canonical odorant receptor. *J. Insect Sci.* 10, 51. doi: 10.1673/031.010.5101

Rinker, D. C., Pitts, R. J., Zhou, X., Suh, E., Rokas, A., and Zwiebel, L. J. (2013a). Blood meal-induced changes to antennal transcriptome profiles reveal shifts in odor sensitivities in *Anopheles gambiae*. *Proc. Natl. Acad. Sci. U.S.A.* 110, 8260–8265. doi: 10.1073/pnas.1302562110

Rinker, D. C., Zhou, X., Pitts, R. J., The AGC Consortium, Rokas, A., and Zwiebel, L. J. (2013b). Antennal transcriptome profiles of anopheline mosquitoes reveal human host olfactory specialization in *Anopheles gambiae*. *BMC Genomics* 14:749. doi: 10.1186/1471-2164-14-749

Schwarz, D., Robertson, H. M., Feder, J. L., Varala, K., Hudson, M. E., Ragland, G. J., et al. (2009). Sympatric ecological speciation meets pyrosequencing: sampling the transcriptome of the apple maggot *Rhagoletis pomonella*. *BMC Genomics* 10:633. doi: 10.1186/1471-2164-10-633

Scott, J. G., Warren, W. C., Beukeboom, L. W., Bopp, D., Clark, A. G., Giers, S. D., et al. (2014). Genome of the house fly, *Musca domestica* L., a global vector of diseases with adaptations to a septic environment. *Genome Biol.* 15, 466. doi: 10.1186/s13059-014-0466-3

Shen, G. M., Jiang, H. B., Wang, X. N., and Wang, J. J. (2010). Evaluation of endogenous references for gene expression profiling in different tissues of the oriental fruit fly *Bactrocera dorsalis* (Diptera: Tephritidae). *BMC Mol. Biol.* 11:76. doi: 10.1186/1471-2199-11-76

Siciliano, P., He, X. L., Woodcock, C., Pickett, J. A., Field, L. M., Birkett, M. A., et al. (2014b). Identification of pheromone components and their binding affinity to the odorant binding protein CcapOBP83a-2 of the Mediterranean fruit fly, *Ceratitis capitata*. *Insect Biochem. Mol. Biol.* 48, 51–62. doi: 10.1016/j.ibmb.2014.02.005

Siciliano, P., Scolari, F., Gomulski, L. M., Falchetto, M., Manni, M., Gabrieli, P., et al. (2014a). Sniffing out chemosensory genes from the Mediterranean fruit fly, *Ceratitis capitata*. *PLoS ONE* 9:e85523. doi: 10.1371/journal.pone.0085523

Siderhurst, M. S., and Jang, E. B. (2006). Female-biased attraction of Oriental fruit fly, *Bactrocera dorsalis* (Hendel), to a blend of host fruit volatiles from *Terminalia catappa* L. *J. Chem. Ecol.* 32, 2513–2524. doi: 10.1007/s10886-006-9160-6

Sun, Y. F., De Biasio, F., Qiao, H. L., Iovinella, I., Yang, S. X., Ling, Y., et al. (2012). Two odorant-binding proteins mediate the behavioural response of aphids to the alarm pheromone (E)-ß-farnesene and structural analogues. *PLoS ONE* 7:e32759. doi: 10.1371/journal.pone.0032759

Swarup, S., Williams, T. I., and Anholt, R. R. (2011). Functional dissection of Odorant binding protein genes in *Drosophila melanogaster*. *Genes Brain Behav.* 10, 648–657. doi: 10.1111/j.1601-183X.2011.00704.x

Syed, Z., Ishida, Y., Taylor, K., Kimbrell, D. A., and Leal, W. S. (2006). Pheromone reception in fruit flies expressing a moth's odorant receptor. *Proc. Natl. Acad. Sci. U.S.A.* 103, 16538–16543. doi: 10.1073/pnas.0607874103

Tan, K. H., and Nishida, R. (2012). Methyl eugenol: its occurrence, distribution, and role in nature, especially in relation to insect behavior and pollination. *J. Insect Sci.* 12, 1–74. doi: 10.1673/031.012.5601

Tan, K. H., Tokushima, I., Ono, H., and Nishida, R. (2010). Comparison of phenylpropanoid volatiles in male rectal pheromone gland after methyl eugenol consumption, and molecular phylogenetic relationship of four global pest fruit fly species: *Bactrocera invadens*, *B. dorsalis*, *B. correcta*, and *B. zonata*. *Chemoecology* 21, 25–33. doi: 10.1007/s00049-010-0063-1

Vieira, F. G., and Rozas, J. (2011). Comparative genomics of the odorant-binding and chemosensory protein gene families across the Arthropoda: origin and evolutionary history of the chemosensory system. *Genome Biol. Evol.* 3, 476–490. doi: 10.1093/gbe/evr033

Vieira, F. G., Sánchez-Gracia, A., and Rozas, J. (2007). Comparative genomic analysis of the odorant-binding protein family in 12 Drosophila genomes: purifying selection and birth-and-death evolution. *Genome Biol.* 8:R235. doi: 10.1186/gb-2007-8-11-r235

Wan, X., Qian, K., and Du, Y. (2015). Synthetic pheromones and plant volatiles alter the expression of chemosensory genes in *Spodoptera exigua*. *Sci. Rep.* 5:17320. doi: 10.1038/srep17320

Waterhouse, A. M., Procter, J. B., Martin, D. M., Clamp, M., and Barton, G. J. (2009). Jalview Version 2–a multiple sequence alignment editor and analysis workbench. *Bioinformatics* 25, 1189–1191. doi: 10.1093/bioinformatics/btp033

Wu, Z., Zhang, H., Wang, Z., Bin, S., He, H., and Lin, J. (2015). Discovery of chemosensory genes in the oriental fruit fly, *Bactrocera dorsalis*. *PLoS ONE* 10:e0129794. doi: 10.1371/journal.pone.0129794

Xu, P., Atkinson, R., Jones, D. N., and Smith, D. P. (2005). Drosophila OBP LUSH is required for activity of pheromone-sensitive neurons. *Neuron* 45, 193–200. doi: 10.1016/j.neuron.2004.12.031

Zhang, Y. N., Ye, Z. F., Yang, K., and Dong, S. L. (2014). Antenna-predominant and male-biased CSP19 of *Sesamia inferens* is able to bind the female sex pheromones and host plant volatiles. *Gene* 536, 279–286. doi: 10.1016/j.gene.2013.12.011

Zhou, J. J. (2010). Odorant-binding proteins in insects. *Vitam. Horm.* 83, 241–272. doi: 10.1016/S0083-6729(10)83010-9

Conflict of Interest Statement: The authors declare that the research was conducted in the absence of any commercial or financial relationships that could be construed as a potential conflict of interest.

frontiers in Physiology

ORIGINAL RESEARCH
published: 01 June 2016
doi: 10.3389/fphys.2016.00201

The Mouthparts Enriched Odorant Binding Protein 11 of the Alfalfa Plant Bug *Adelphocoris lineolatus* Displays a Preferential Binding Behavior to Host Plant Secondary Metabolites

Liang Sun[1,2†], Yu Wei[2†], Dan-Dan Zhang[3], Xiao-Yu Ma[2], Yong Xiao[2], Ya-Nan Zhang[4], Xian-Ming Yang[2], Qiang Xiao[1], Yu-Yuan Guo[2] and Yong-Jun Zhang[2]*

[1] Key Laboratory of Tea Biology and Resources Utilization, Ministry of Agriculture, Tea Research Institute, Chinese Academy of Agricultural Sciences, Hangzhou, China, [2] State Key Laboratory for Biology of Plant Diseases and Insect Pests, Institute of Plant Protection, Chinese Academy of Agricultural Sciences, Beijing, China, [3] Department of Biology, Lund University, Lund, Sweden, [4] College of Life Sciences, Huaibei Normal University, Huaibei, China

OPEN ACCESS

Edited by:
Sylvia Anton,
Institut National de la Recherche Agronomique, France

Reviewed by:
Ewald Grosse-Wilde,
Max Planck Institute for Chemical Ecology, Germany
William Benjamin Walker,
Swedish University of Agricultural Sciences, Sweden

***Correspondence:**
Yong-Jun Zhang
yjzhang@ippcaas.cn

[†] These authors have contributed equally to this work.

Specialty section:
This article was submitted to Invertebrate Physiology, a section of the journal Frontiers in Physiology

Received: 01 February 2016
Accepted: 17 May 2016
Published: 01 June 2016

Citation:
Sun L, Wei Y, Zhang D-D, Ma X-Y, Xiao Y, Zhang Y-N, Yang X-M, Xiao Q, Guo Y-Y and Zhang Y-J (2016) The Mouthparts Enriched Odorant Binding Protein 11 of the Alfalfa Plant Bug Adelphocoris lineolatus Displays a Preferential Binding Behavior to Host Plant Secondary Metabolites. Front. Physiol. 7:201. doi: 10.3389/fphys.2016.00201

Odorant binding proteins (OBPs) are proposed to be directly required for odorant discrimination and represent potential interesting targets for pest control. In the notoriously agricultural pest *Adelphocoris lineolatus*, our previous functional investigation of highly expressed antennal OBPs clearly supported this viewpoint, whereas the findings of the current study by characterizing of AlinOBP11 rather indicated that OBP in hemipterous plant bugs might fulfill a different and tantalizing physiological role. The phylogenetic analysis uncovered that AlinOBP11 together with several homologous bug OBP proteins are potential orthologs, implying they could exhibit a conserved function. Next, the results of expression profiles solidly showed that *AlinOBP11* was predominantly expressed at adult mouthparts, the most important gustatory organ of Hemiptera mirid bug. Finally, a rigorously selective binding profile was observed in the fluorescence competitive binding assay, in which recombinant AlinOBP11 displayed much stronger binding abilities to non-volatile secondary metabolite compounds than the volatile odorants. These results reflect that *AlinOBP11*, even its orthologous proteins across bug species, could be associated with a distinctively conserved physiological role such as a crucial carrier for non-volatiles host secondary metabolites in gustatory system.

Keywords: ***Adelphocoris lineolatus*, odorant binding protein, expression profiles, phylogenetic analysis, Fluorescence competitive binding assay**

INTRODUCTION

Smell is undoubtedly the most important sensory for insects survival and reproduction (Li and Liberles, 2015; Groot et al., 2016). Olfactory system that can sensitively and selectively detect biologically active odorants attracts great attention from researchers who attempt to explore alternative environment-friendly pest management strategy. In insect olfactory signal transduction pathway, several classes of membrane-bound proteins such as odorant receptor (ORs), ionotropic receptors (IRs), and sensory neuron membrane proteins (SNMPs) have been proven to play

central roles in facilitating the conversion of the chemical message to an electrical signal, while the carrier proteins like odorant binding proteins (OBPs) or chemosensory proteins (CSPs) are proposed to bind, deliver and even recognize specific pheromones and odorants to their relevant receptors (Jacquin-Joly and Merlin, 2004; Leal, 2013). For decades, various functional studies toward important olfactory protein families such as OBPs or ORs actually lead to a quick discovering of some high-efficiency pest repellents or attractants (Tanaka et al., 2009; Sun Y. F. et al., 2012; Sun L. et al., 2013). For instance, in the alfalfa plant bug, *A. lineolatus*, behavioral active compounds were successfully screened via ligand binding assay of an antennae highly expressed AlinOBP10 (Sun L. et al., 2013). Synthetic compounds targeting OBP3 or OBP7 which was proven to be responsible for (*E*)-ß-farnesene perception elicited significantly behavioral responses in aphids (Sun Y. F. et al., 2012).

Insect OBPs which were first identified in antennal sensillum of silk moth, *Antheraea polyphemus* (Vogt and Riddiford, 1981) belong to the superfamily of small acidic soluble carrier proteins and could be recognized by six highly conserved cysteines (Leal et al., 1999; Sandler et al., 2000; Tegoni et al., 2004; Pelosi et al., 2014). Studies of both immunocytochemical localization and *in situ* hybridization revealed that OBPs were synthesized by non-neuronal auxiliary cells (trichogen and tormogen cells) and secreted into the sensillum lymph with a very high concentration (up to 10 mM) (Steinbrecht et al., 1995; Hekmat-Scafe et al., 1997; Michael, 2000; De Santis et al., 2006; Sun Y. P. et al., 2013; Sun et al., 2014a). So far, various investigations elucidated that antennal sensillum enriched OBPs indeed played essential roles in recognition of physiologically relevant odorants (Jacquin-Joly et al., 2000; Pophof, 2004; Große-Wilde et al., 2006; He et al., 2010). For example, one subclass of OBP families named pheromone binding proteins, PBPs, was highly abundant in long trichoid sensilla and showed significantly specific binding affinities to insect sex pheromones (Vogt and Riddiford, 1981; Krieger et al., 1996; Leal et al., 1999; Klusák et al., 2003; Pophof, 2004; Große-Wilde et al., 2006; De Santis et al., 2006). Sensilla basiconica expressed OBPs were proposed to be involved in terpenoids or other plant volatiles detection (Feng and Prestwich, 1997). Meanwhile, in two Lepidopteran species, the cotton leafworm *Spodoptera littoralis* (Poivet et al., 2012) and the diamondback moth *Plutella xylostella* (Zhu et al., 2016), OBPs were even demonstrated to be associated with the interesting behavior why larvae are attracted by conspecific moth sex pheromone.

However, the functions of insect OBPs may be more complicated and could not be restrict within olfactory cue recognition. In *Drosophila melanogaster*, most OBPs were detected in both gustatory and olfactory sensilla and some numbers were even expressed exclusively in taste organs (Galindo and Smith, 2001). Jeong et al. (2013) proposed that feeding behavior of *D. melanogaster* can be suppressed by a gustatory organ expressed OBP49a responding to bitter compounds. Two OBP genes, *Obp57d* and *Obp57e* in *D. sechellia* have been demonstrated to be involved in the evolution of taste perception and host-plant preference (Matsuo et al., 2007). Particularly, expressions of *Aedes aegypti* OBP22 in antennae and reproductive organs indicated its multiple functions (Li et al., 2008). Likewise, physiological roles of male reproductive organs expressed orthologous OBP10 in two sibling moth species has been proposed to act as a specific carrier for female oviposition deterrents that could help *Helicoverpa* offspring avoid cannibalism (Sun Y. L. et al., 2012).

The alfalfa plant bug, *A. lineolatus*, a typical polyphagous insect pest outbreaks frequently in cotton field since the transgenic *Bacillus thuringiensis* cotton largely cultivation in China (Lu et al., 2010). Worse still, flight behavior enable it to migrate among different host plants (Lu et al., 2009), and many other important crops like alfalfa (*Medicago sativa* L.), green bean (*Phaseolus vulgaris*), and tea plant (*Camellia sinensis*) suffer from its serious destroy (Lu and Wu, 2008). Evidence suggested that this bug heavily relies on chemical cues for host plant location and migration (Lu and Wu, 2008). Thus, studies aiming at the physiological and molecular basis of insect chemosensation may help explore an alternatively effective pest control method.

Previously, 14 OBP transcripts of *A. lineolatus* were identified (Gu et al., 2011a) and functional studies of several antennae highly expressed OBPs such as AlinOBP1, AlinOBP5, AlinOBP10, and AlinOBP13 indicated their potential olfactory roles (Gu et al., 2011b; Sun L. et al., 2013; Wang et al., 2013; Sun et al., 2014a). Subsequently, Hull et al. (2014) identified 33 putative OBP transcripts in the tarnished plant bug, *Lygus lineolaris*, and suggested that several OBP genes included *LylinOBP19* can be expressed in gustatory organs, implying they may be related to taste compound detected. However, whether OBPs could express at taste organs and fulfill potential gustatory functions in *A. lineolatus* remains largely unknown. In the current study, we mainly focus our attention on *AlinOBP11*, a putative orthologous OBP gene of *LylinOBP19* in *A. lineolatus* and our current results of tissue distribution pattern, ligand binding assay, and phylogenetic analysis would provide detail cues for its functional discussion.

MATERIALS AND METHODS

Insect Rearing and Tissue Collection

A. lineolatus adults were collected from alfalfa fields at the Langfang Experimental Station of Chinese Academy of Agricultural Sciences, Hebei Province, China. The laboratory colony was established in plastic containers (20 × 13 × 8 cm), which were maintained at 29 ± 1°C, 60 ± 5% relative humidity, and 14 h light:10 h dark cycle. The adults and newly emerged nymphs were reared on green beans and 10% honey. Different tissues from *A. lineolatus* adults of both sexes including antennae, mouthparts, heads (without antennae and mouthparts), thoraxes, abdomens, legs, and wings were collected for qRT-PCR. Each tissue was collected from three biological pools and all the specimens were immediately stored in −80°C for further process.

RNA Isolation and cDNA Synthesis

Total RNA of each sample was isolated using the Trizol reagent (Invitrogen, Carlsbad, CA, USA), and the first-strand cDNA was synthesized by FastQuant RT-kit with gDNA Eraser (TianGen, Beijing, China) according to the manufacturer's instructions.

qRT-PCR

qRT-PCR assay regarding different developmental stages and tissues were carried out using an ABI 7500 Real-Time PCR System (Applied Biosystems, Carlsbad, CA). Two house-keeping genes *Alin*β-*actin* (GenBank No.GQ477013) and *AlinElongation factor* (GenBank No.AEY99651) were used as endogenous controls to normalize the target gene expression and correct for sample-to-sample variation. Taqman primers of *Alin*β-*actin* and *AlinOBP11* cited Gu et al. (2011a) and primers of *AlinElongation factor* were designed using Primer Express 3.0 (Applied Biosystems) and listed in **Table S1**. For the qRT-PCR reaction, the cDNA was diluted to concentration of 200 ng /μL. Each reaction was performed in a 25 μL mixture of 12.5 μL of Premix Ex Taq (TaKaRa), 1 μL of each primer (10 mM), 0.5 μL probe (10 mM), 0.5 μL of Rox Reference Dye II, 1 μL of sample cDNA (200 ng), and 8.5 μL of sterilized H_2O. Negative controls were non-template reactions (H_2O instead of cDNA). The reaction cycling parameters were as follows: 95°C for 10 s, 40 cycles at 95°C for 20 s, 60°C for 34 s. For the data reproducibility, qRT-PCR reaction for each sample was performed in three technical replicates and three biological replicates. Since our preliminary experiment demonstrated that the amplification efficiency between targeted genes and reference gene was similar (data not shown), the comparative $2^{-\Delta\Delta CT}$ method was used to calculate the relative quantification between tissues (Livak and Schmittgen, 2001).

The comparative analyses of target gene among different tissues and developmental stages were determined using a one-way nested analysis of variance (ANOVA), followed by Tukey's honestly significance difference (HSD) test using the software SPSS Statistics 18.0 (SPSS Inc., Chicago, IL, USA).

Phylogenetic Construction and Selective Pressure Analysis

The 92 OBP sequences of five mirid bug species (GenBank accession numbers and references can be seen in **Table S2**) were used to infer the evolutionary history with the software MEGA 6.0 with a *p*-distance model and a pairwise deletion of gaps (Tamura et al., 2013). The bootstrap support of tree branches was assessed by re-sampling amino acid positions 1000 times. Estimation of the non synonymous (dN) to synonymous (dS) substitution rate (ω) was performed by the maximum likelihood method (Anisimova et al., 2001) using the Codeml program in the PAML 4.6 package (Yang, 1997).

Western Blot Assay

The polyclonal antiserum against the recombinant AlinOBP11 was produced by injecting robust adult rabbits subcutaneously and intramuscularly with the highly purified recombinant protein. Recombinant protein was emulsified with an equal volume of Freund's complete adjuvant (Sigma, St. Louis, MO, USA) for the first time injection (500 μg) and then with incomplete adjuvant for the three additional injections (300 mg each time). The interval between each injection was approximately half a month, and blood was collected 7 days after the last injection and centrifuged at 6000 rpm for 20 min. The serum was purified based on a MAb Trap kit (GE Healthcare) following the manufacturer's instructions. The rabbits were maintained in large cages at room temperature, and all of the operations were performed according to ethical guidelines to minimize the pain and discomfort of the animals.

Crude extracts from different tissues of female and male adult bugs included the antennae, mouthparts, legs, wings, and bodies (without aforesaid parts) were separated on 15% SDS-PAGE, respectively. Samples were transferred to a polyvinylidene fluoride membrane (PVDF, Millipore, Carrigtwohill, Ireland) at the condition of 200 mA for 50 min, and then membrane was blocked using 5% dry skimmed milk (BD Biosciences, San Jose, CA, USA) in phosphate-buffered saline (PBS) containing 0.1% Tween-20 (PBST) for 2 h at room temperature. After washing three times with PBST (10 min each time), the blocked membrane was incubated with purified rabbit anti-AlinOBP11antiserum (dilution 1:2000) for 1 h. Three times washing with PBST again, the membrane was incubated with anti-rabbit IgG horseradish peroxidase (HRP) conjugate and HRP-streptavidin complex (Promega, Madison, WI, USA) at a dilution of 1:10000 for 1 h. The membrane was then incubated with the western blot substrates of the enhanced chemiluminescence western blot kit (CoWinbiotech, China), and the bands were visualized by exposing to X-OMATBT films (Kodak, New York, USA).

Fluorescence Competitive Binding Assay

The recombinant protein expression and purification was performed according to our previous protocols (Sun L. et al., 2013; Sun et al., 2014a). Briefly, the plasmid containing *AlinOBP11* gene was constructed and transformed into *Escherichia coli* BL21 (DE3) competent cells for recombinant protein expression, and the protein was largely induced with 1 mM isopropyl ß-D-1-thiogalactopyranoside (IPTG) at 37°C for 3–6 h. The purification was performed using two rounds of Ni ion affinity chromatography (GE-Healthcare), and the His-tag was removed with recombinant enterokinase (Novagen). The highly purified proteins were desalted through extensive dialysis, and then the size and purity of the recombinant proteins were verified by 15% SDS-PAGE.

For the ligand binding assays, 45 compounds include 41 volatiles and four non-volatiles were selected based on previously reported isolation from *A. lineolatus* host plants (Meisner et al., 1977; Halloin, 1982; Aldrich, 1988; Loughrin et al., 1995; Röse and Tumlinson, 2004; Millar, 2005). The binding assay was performed on an F-380 fluorescence spectrophotometer (Tianjin, China) at room temperature (25°C) with a 1-cm light path quartz cuvette and 10-nm slits for both excitation and emission. The excitation wavelength was 337 nm, and the emission spectrum was recorded between 390 and 460 nm. Firstly, the constant of AlinOBP11 with the fluorescent probe N-phenyl-1-naphthylamine (1-NPN) was measured, a final concentration of 2 μM protein solution in 50 mM Tris-HCl (pH 7.4) was titrated with aliquots of 1 mM 1-NPN dissolved in methanol to final concentrations ranging from 1 to 16 μM. Then the affinities of other ligands were tested through competitive binding assays using 1-NPN as the fluorescent reporter at a concentration of 2 μM, and the concentration of each competitor ranged from 2 to 30 μM. The fluorescence intensities at the

maximum fluorescence emission between 390 and 460 nm were plotted against the free ligand concentration to determine the binding constants. The bound chemical was evaluated based on its fluorescence intensity with the assumption that the protein was 100% active with a stoichiometry of 1:1 (protein: ligand) saturation. The binding curves were linearized using a Scatchard plot, and the dissociation constants of the competitors were calculated from the corresponding IC_{50} values based on the following equation: Ki= $[IC_{50}]$ / (1+ [1-NPN]/K_{1-NPN}), where [1-NPN] is the free concentration of 1-NPN and K_{1-NPN} is the dissociation constant of the complex protein/1-NPN.

To evaluate potential selective pressure acting on this *OBP11* orthologous cluster, we calculated the ratio of non synonymous to synonymous substitutions (dN/dS or ω) of this cluster with branch models using PAML and compared the log likelihoods (lnL) for the one ratio model M0 (assuming one ω ratio for all branches) and the free ratio model M1 (assuming one ω ratio for each branch) in likelihood ratio tests. The results uncovered that the one ratio model (M0) could not be rejected ($p > 0.01$) and all branches shared a normalized ω ratio of 0.2954 (**Figure 1A**), implying that purifying selection was acting on this cluster and *AlinOBP11* would share a relatively conserved physiological function with its orthologous genes (Qiao et al., 2009; Zhou et al., 2010; Vandermoten et al., 2011).

RESULTS

Phylogenetic Tree Construction and Selective Pressure Analysis

A phylogenetic tree of 92 OBPs was constructed using the neighbor-joining method to analyze evolutional relationships between AlinOBP11 and other OBPs of different mirid species. **Figure 1** revealed a divergent OBP repertoire. AlinOBP11 and four other OBPs i.e., AlucOBP36, AfasOBP11, AsutOBP11, and LylinOBP19 from each bug species clustered into one same clade with bootstrap support value up to 74 (**Figure 1A**). Sequence alignment analysis showed AlinOBP11 has 94, 95, 94, and 60% identity to AsutOBP11, AlucOBP36, AfasOBP11, and LylinOBP19, respectively (**Figures 1B,C**). These results reflect AlinOBP11 and these four OBPs form a clear orthologous group across bug species.

Specific Tissue and Developmental Expression Profiles of *AlinOBP11*

The results of our western blot assay showed that clear protein bands could be found at mouthparts, legs, antennae as well as other tissues, which seems that AlinOBP11 can be ubiquitously expressed at adult tissues of both sexes (**Figure 2**). To compare the expression levels of *AlinOBP11* among different tissues, we then conducted the qRT-PCR assay. Interestingly, unlike previously reported uniformly antennae predominant expressed *AlinOBPs* (Gu et al., 2011a; Sun L. et al., 2013; Sun et al., 2014a), our current results revealed that *AlinOBP11* was strongly expressed at mouthparts, and slightly expressed at legs, antennae, and other tissues (**Figure 3**). Meanwhile, *AlinOBP11* transcript abundance varied among different developmental instars and

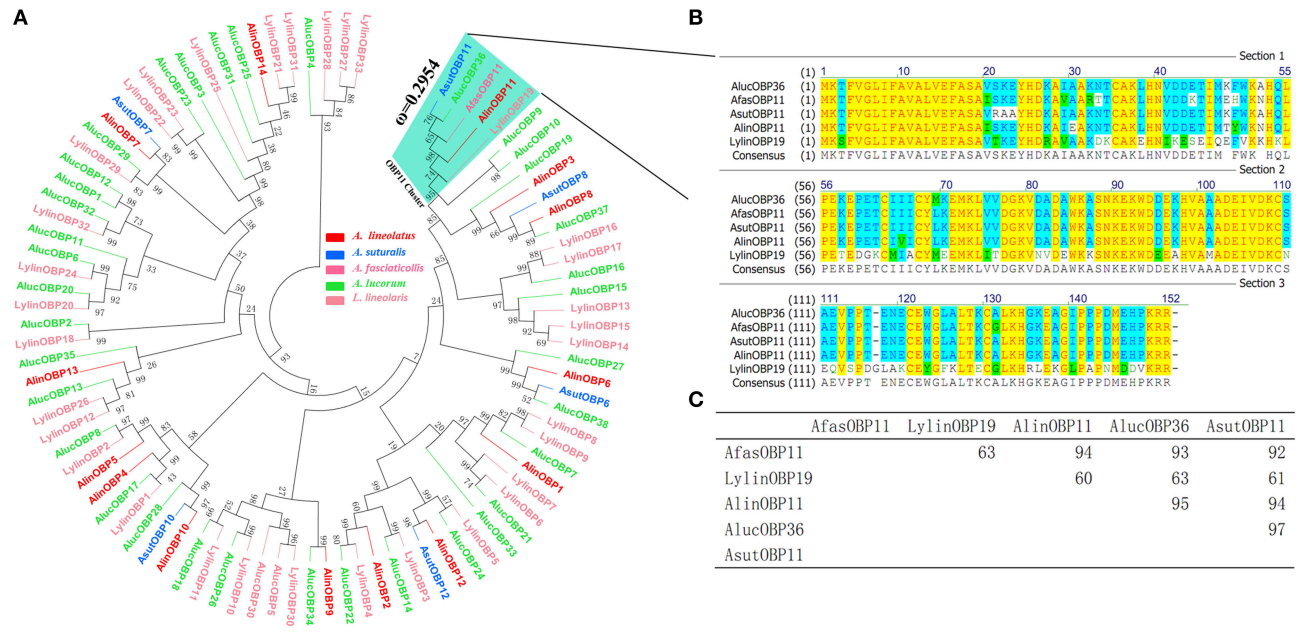

	AfasOBP11	LylinOBP19	AlinOBP11	AlucOBP36	AsutOBP11
AfasOBP11		63	94	93	92
LylinOBP19			60	63	61
AlinOBP11				95	94
AlucOBP36					97
AsutOBP11					

FIGURE 1 | Sequence alignment and phylogeny of AlinOBP11 with other OBPs identified in five bug species. (A) Neighbor-joining phylogenetic tree was constructed used MEGA 6.0 with a p-distance model and a pairwise deletion of gaps; The non-synonymous (dN) to synonymous (dS) substitution rate (ω) of OBP11 orthologs was labeled beside its cluster. **(B)** Sequence alignment was performed using the program ClustalX 2.1 with default gap penalty parameters of gap opening 10 and extension 0.2, and was edited using the GeneDoc 2.7.0 software. **(C)** The percent identity matrix of OBP11 orthologs is calculated using Vector NTI 10.0.

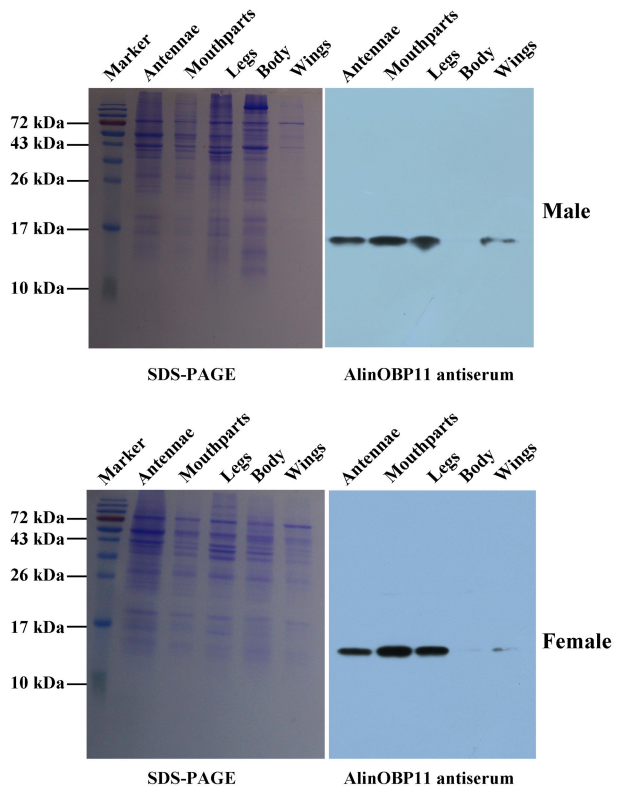

FIGURE 2 | SDS-PAGE and AlinOBP11 expression profiles among different adult tissues of both sexes assessed by western blot analysis. The results showed that AlinOBP11 was detected at both male and female adult mouthparts, legs, antennae, and weakly or even undetectably at other tissues.

significantly higher expression level was observed in adult bugs (**Figure 3**).

In vitro Expression and Purification of AlinOBP11

The recombinant AlinOBP11 was successfully expressed using a bacterial system. Induced targeted recombinant appeared at both supernatant and insoluble inclusion bodies and the former was selected to be purified using two rounds of Ni ion affinity chromatography (GE Healthcare, Little Chalfont, UK). The finally purified AlinOBP11 recombinant protein on the sodium dodecyl sulfate polyacrylamide gel electrophoresis (SDS-PAGE) analysis displayed a single band (**Figure S1**).

Ligand-Binding of Recombinant AlinOBP11

Before the ligand-binding analysis, we measured the binding affinities of fluorescence probe 1-NPN with purified AlinOBP11. The results showed AlinOBP11 could solidly bind to 1-NPN with binding affinity of 5.86 ± 0.47 μM (**Figure 4A**). Consequently, the binding properties of AlinOBP11 to compounds with different functional groups were analyzed and the results suggested it had a relatively narrow binding profile. Notably, all the tested non-volatile compounds showed strong binding abilities to AlinOBP11, and quercetin was the best ligand (K_i = 2.63 ± 0.23 μM), followed by gossypol (K_i = 3.43 ± 0.32 μM), rutin hydrate (K_i = 7.78 ± 1.23 μM), and (−)-catechin (K_i = 15.26 ± 0.70 μM). Additionally, the tested host volatiles such as aliphatic alcohols, aldehydes, ketones, esters, aromatics could hardly bind to recombinant AlinOBP11, except of three terpenoids α-phellandrene, nerolidol, and *trans, trans*-farnesol, which can bind to AlinOBP11 and their binding constant K_i was 20.07 ± 0.41, 20.76 ± 0.55, and 19.26 ± 1.78 μM, respectively (**Figures 4B,C**; **Table 1**).

DISCUSSION

Insect OBPs may serve as important molecular target for designing and screening new effectively behavioral blocking agents used in the application of eco-friendly pest management strategies as they are considered to be strongly expressed in antennal sensillum lymph and are involved in olfactory cues discrimination, binding and transduction (Qiao et al., 2009; He et al., 2011; Sun Y. F. et al., 2012; Pelosi et al., 2013, 2014; Sun L. et al., 2013; Sun et al., 2014a). However, a plenty of studies suggested that OBPs' expression patterns are not restricted in olfactory organs and thus their physiological functions would be more complex and diversified (Park et al., 2000; Foret and Maleszka, 2006; Li et al., 2008; Sun Y. F. et al., 2012; Yuan et al., 2015). To confirm whether OBPs in the Hemiptera mirid bug species could fulfill putative gustatory function, in the present study we especially focus on a putative non-olfactory organ biased OBP gene, the *OBP11* in *A. lineolatus*.

Previously, Gu et al. identified 14 putative OBP genes from the antennal cDNA library of *A. lineolatus* and suggested *AlinOBP11* was strongly expressed at adult legs of both sexes (Gu et al., 2011a). Subsequently, a large number of potential OBP genes were identified in the tarnished plant bug, *L. lineolaris* and the green plant bug, *Apolygus lucorum* via transcriptome strategy, and more OBP transcripts were found to be expressed at gustatory organs such as legs and mouthparts (Hull et al., 2014; Yuan et al., 2015). Therefore, we firstly re-confirmed the tissue expression profiles of *AlinOBP11* after taking mouthparts into account, the most important gustatory organs of Hemiptera species. The results of our western blot analysis revealed that clear single bands could be seen at mouthparts, legs as well as antennae of both male and female adult bugs (**Figure 2**). Interestingly, we found that relative mRNA level of *AlinOBP11* was extraordinarily higher at adult mouthparts of both sexes than that of previous reported legs and other tissues (**Figure 3**). In addition, higher expression level was also observed in adult bugs than different instars of nymph (**Figure 3**). If we considered the tissue distribution patterns of all the 14 identified OBP genes, according to the inference that mRNA expression is indicative of physiological function of its encoded protein, a putative functional subdivision of different OBP genes in the same species of *A. lineolatus* would occur and the mouthparts-biased *AlinOBP11* could be separated from other OBPs such as *AlinOBP1*, *10*, *13* which have been demonstrated strongly

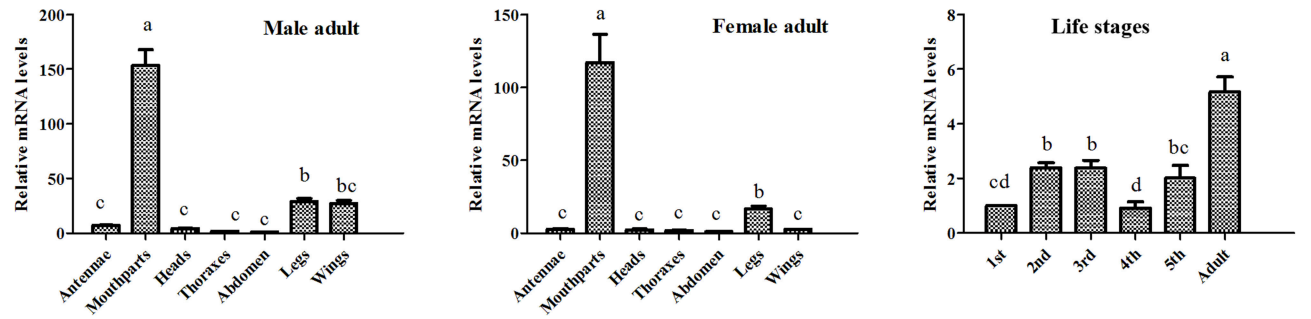

FIGURE 3 | The relative transcript levels of *AlinOBP11* at different developmental stages and adult tissues of both sexes analyzed by qRT-PCR. All data were normalized to endogenous house-keeping genes *Alinβ-actin* (GenBank No. GQ477013) and relative fold changes are normalized to transcript level of the first instar nymph or abdomen. The error bars represents the standard errors, and the different letters a, b, c, and d indicate significant differences ($p < 0.05$) among different samples. The similar results were obtained with *AlinElongation factor* (GenBank No. AEY99651) as internal control (**Figure S2**).

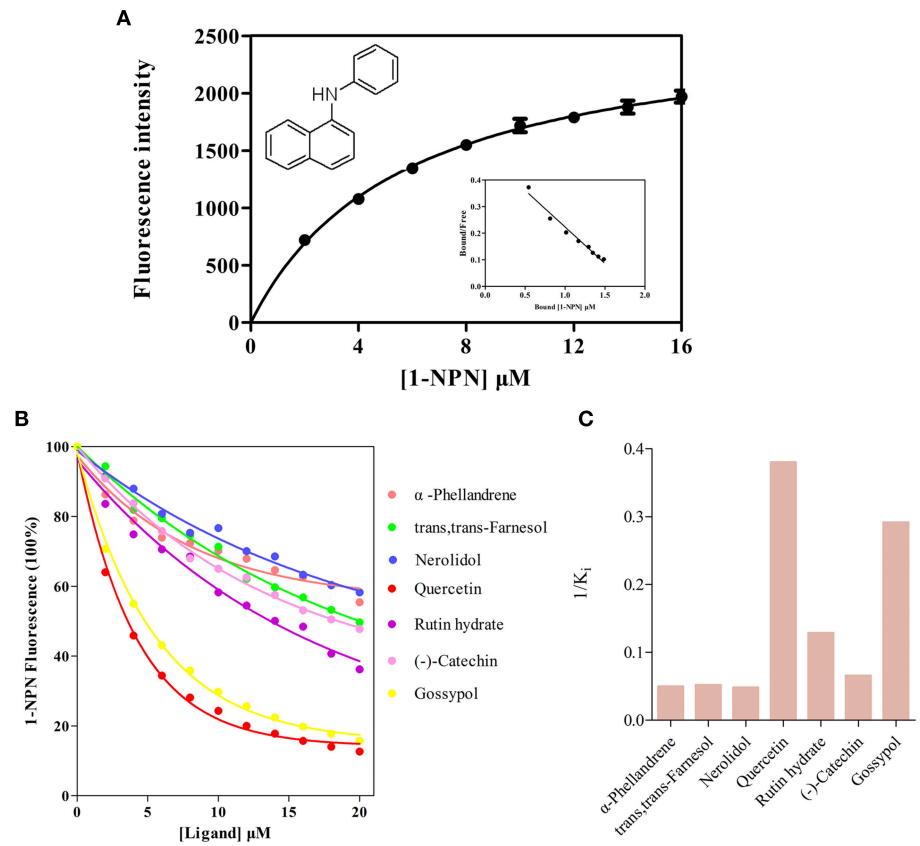

FIGURE 4 | Fluorescence competitive binding assay. (A) Binding curve and relative Scatchard plot of 1-NPN to AlinOBP11. The dissociation constant of the AlinOBP11/1-NPN complex was calculated as 5.86 ± 0.47 μM. **(B)** Competitive binding curves of selected host plant compounds to AlinOBP11. **(C)** The reverse values of the dissociation constants (Ki) measured with putative ligands of AlinOBP11. A mixture of the recombinant AlinOBP11 protein and N-phenyl-1-naphthylamine (1-NPN) in 50 mM Tris-Hcl buffer (pH 7.4) both at the concentration of 2 μM was titrated with 1 mM solutions of each competing ligand to the final concentration range of 2 to 30 μM. Fluorescence intensities are reported as percent of the values in the absence of competitor. Data are represented as means of three independent experiments.

TABLE 1 | Binding affinities of all of the selected compounds to the recombinant AlinOBP11 protein.

Ligand	CAS Number	AlinOBP11	
		IC_{50} (μM)	K_i (μM)
GENERAL ODORANTS			
2-Hexanol	626-93-7	u.d.	u.d.
Pentanol	71-41-0	u.d.	u.d.
Valeraldehyde	110-62-3	u.d.	u.d.
Hexanal	66-25-1	u.d.	u.d.
Heptanal	111-71-7	u.d.	u.d.
Octanal	124-13-0	u.d.	u.d.
Nonanal	124-19-6	u.d.	u.d.
2-Hexanone	591-78-6	u.d.	u.d.
2-Heptanone	110-43-0	u.d.	u.d.
2-Octanone	111-13-7	u.d.	u.d.
3-Hexanone	589-38-8	u.d.	u.d.
6-Methyl-5-hepten-2-one	110-93-0	u.d.	u.d.
Amyl acetate	628-637-7	u.d.	u.d.
Nonyl acetate	1143-13-5	u.d.	u.d.
Undecane	1120-21-4	u.d.	u.d.
Indole	120-72-9	u.d.	u.d.
Benzaldehyde	100-52-7	u.d.	u.d.
3,4-Dimethyl-benzaldehyde	5973-71-7	u.d.	u.d.
Acetophenone	98-86-2	u.d.	u.d.
Methyl salicylate	119-36-8	u.d.	u.d.
GREEN LEAF VOLATILES			
1-Hexanol	111-27-3	u.d.	u.d.
cis-3-Hexen-1-ol	928-96-1	u.d.	u.d.
trans-2-Hexenal	6278-26-3	u.d.	u.d.
cis-3-hexenyl acetate	3681-71-8	u.d.	u.d.
TERPENOIDS			
E-β-Ocimene	3016-19-1	u.d.	u.d.
Limonene	5989-27-5	u.d.	u.d.
α-Phellandrene	99-83-2	26.16 ± 0.52	20.07 ± 0.41
β-Pinene	18172-67-3	u.d.	u.d.
(+)-α-Pinene	7785-70-8	u.d.	u.d.
β-Ionone	79-77-6	u.d.	u.d.
Myrcene	123-35-3	u.d.	u.d.
Nerolidol	7212-44-4	27.23 ± 0.71	20.76 ± 0.55
β-Caryophyllene	87-44-5	u.d.	u.d.
α-Humulene	6753-98-6	u.d.	u.d.
trans-β-Farnesene	18794-84-8	u.d.	u.d.
trans,trans-Farnesol	106-28-5	25.21 ± 2.36	19.26 ± 1.78
PUTATIVE SEX PHEROMONES			
Hexyl butyrate	2639-63-6	u.d.	u.d.
Hexyl hexanoate	6378-65-0	u.d.	u.d.
Butyl butyrate	109-21-7	u.d.	u.d.
Ethyl butyrate	105-54-4	u.d.	u.d.
trans-2-hexenyl butyrate	53398-83-7	u.d.	u.d.
HOST PLANT SECONDARY METABOLITES			
(−)-Catechin	18829-704	19.26 ± 0.93	15.26 ± 0.70
Rutin hydrate	207671-50-9	9.89 ± 1.61	7.78 ± 1.23
Quercetin	117-39-5	3.36 ± 0.30	2.63 ± 0.23
Gossypol	303-45-7	4.45 ± 0.34	3.43 ± 0.32

U.d. means that the IC_{50} value exceeds 30 μM and thus that the binding affinities (Ki) of the candidate competitive ligand were not calculated in this study.

expressed at antennae sensillum and fulfilled vital roles in bug olfactory cue perception (Gu et al., 2011b; Sun L. et al., 2013; Sun et al., 2014a). Indeed, unlike the antennae which are equipped with various olfactory sensilla (Chinta et al., 1997; Sun et al., 2014b), mouthparts of Hemiptera bug species consist of piercing-sucking stylets and labium, the former is used to eject saliva for food ingestion and is considered to be directly related to oviposition behavior (Romani et al., 2005), while the latter has 11–12 uniporous gustatory sensilla which are responsible for assessing the suitability of food substrates (Ave et al., 1978; Hatfield and Frazier, 1980). Our current results of tissue expression pattern merely confirmed that *AlinOBP11* was preferentially expressed at *A. lineolatus* adult mouthparts. Although it is not known whether *AlinOBP11* was expressed in stylets or the gustatory sensillum of labium, we can conceivably speculate that this provocatively specific expression profile would benefit the alfalfa plant bugs, to a great extent, in many importantly behavioral performances such as egg laying, host plants selection, and even of toxic substances avoidance.

Our fluorescence competition assay provides further insight into understanding of physiological roles of AlinOBP11. The results clearly showed that recombinant AlinOBP11 protein displayed preferential binding abilities to tested non-volatile host plant secondary metabolites than all the volatile compounds (**Figures 4B,C**; **Table 1**). These results correspond well to its specific tissue distribution within mouthparts which could give a functional implication that AlinOBP11 could function as carrier in gustatory system for non-volatile compounds detection when plant bugs begin to search suitable food substrates by using the mouthparts to rub or tap on plant surfaces or insert plant tissues. Additionally, plant secondary compounds play key roles in the long-term evolution of plant-herbivore interactions (Elsayed, 2011; Mithöfer and Boland, 2012), and the content level variation of quercetin, gossypol, and rutin hydrate, three AlinOBP11 best ligands, over the course of host plant maturation have been demonstrated to be involved in herbivore defense. In particular, gossypol and rutin hydrate were proposed to increase the resistance of cotton plants in response to mirid bug feeding, while the content of quercetin in cotton tended to perform a negatively correlation between their interactions (Lin et al., 2011). Thus, *A. lineolatus* might employ the mouthparts-biased expressed AlinOBP11 to perceive and discriminate these functional different non-volatile secondary metabolites; however, this speculation still needs to be supported by more evidences.

Gene duplication was pointed to be the main mechanism underlying the fast expansion and functional evolution of chemosensory genes (Zhou et al., 2010; Zhang and Löfstedt, 2013); nevertheless, physiological functions of putative orthologs also attract great interest. In aphid species, the distribution of orthologous *OBP* genes may reflect their life styles and host relationships. As an example, homologous OBP3 proteins of different aphid species were proved to be associated with recognition of alarm pheromone (*E*)-ß-farnesene (Qiao et al., 2009; Vandermoten et al., 2011; Sun Y. F. et al., 2012). We re-constructed the phylogenetic trees used reported OBPs of several bug species (**Figure 1**) and the results clearly suggest AlinOBP11 and AsutOBP11, AlucOBP36, AfasOBP11, and LylinOBP19 fall

into the same clade and support they are potential orthologs across bug species which was consistent with Hull's assumption (Hull et al., 2014). Selective pressure assess by calculation of dN/dS or $\omega = 0.295$ (**Figure 1**) also indicates that genes in this cluster are under purifying selection and would perform conserved functions (Qiao et al., 2009; Zhou et al., 2010; Vandermoten et al., 2011). Meanwhile, we found the *AlinOBP11* was predominately expressed at mouthparts similar to tissue expression profiles of previous reported *LylinOBP19* (Hull et al., 2014) and our further studies of *AfasOBP11* and *AsutOBP11* (data not shown here). However, Hua et al. (2012) suggested that *AlucOBP36* (named as *AlucOBP3* in their study) was antennae-biased expressed. This could be explained by different genetic relationships and evolutionary processes of these bugs. *A. lineolatus*, *A. suturalis*, and *A. fasciaticollis* belong to the same genus *Adelphocoris*, while *A. lucorum* belongs to the other genus *Apolygus*. Notably, the *in vitro* functional studies of antennae expressed AlucOBP36 resembled our results of AlinOBP11, which also showed better binding abilities to non-volatile host plant secondary compounds of rutin hydrate, but not to quercetin and gossypol (Hua et al., 2012), and this could be attributed to the mutations of several amino acids in these two proteins' binding pockets.

In conclusion, this study characterizes a mouthparts enriched *OBP11* protein in *A. lineolatus* which preferentially binds to non-volatile plant secondary compounds; to our current knowledge, AlinOBP11 represents the first physiological function of mouthparts highly expressed OBP in Hemiptera species. As putative orthologous genes probably exhibited conserved physiological function, orthologous OBP11 could be involved in mirid bug feeding behaviors and serve as potential molecular targets for the development of eco-friendly pest management strategies against mirid bugs' outbreaks.

AUTHOR CONTRIBUTIONS

LS and YZ conceived and designed the experimental plan. LS, XM, and YX preformed the experiments. LS, YW, DZ, YZ, XY, QX, and YG analyzed the data. LS and DZ drafted the manuscript.

ACKNOWLEDGMENTS

This work was supported by China National "973" Basic Research Program (2012CB114104), the National Natural Science Foundation of China (31272048, 31321004, 31471778, and 31501652) and Research Foundation of State Key Laboratory for Biology of Plant Diseases and Insect Pests (SKLOF201514).

SUPPLEMENTARY MATERIAL

The Supplementary Material for this article can be found online at: http://journal.frontiersin.org/article/10.3389/fphys.2016.00201

Figure S1 | SDS-PAGE analyses of AlinOBP11 expression and purification. Protein markers are shown in the left side; −, crude bacterial extract before induction with IPTG; + crude bacterial extracts after induction with IPTG; Sup, supernatant of disrupted PET/AlinOBP11; Pel, inclusion body of disrupted PET/AlinOBP11; P/His-tag, purified AlinOBP11 protein with His-tag; P, finally purified AlinOBP11 protein obtained after two rounds of purification.

Figure S2 | The relative transcript levels of *AlinOBP11* at different developmental stages and adult tissues of both sexes evaluated by qRT-PCR with *AlinElongation factor* (GenBank No.AEY99651) as internal control. The results clearly showed *AlinOBP11* was strongly expressed at adult mouthparts.

Table S1 | The primers used in this article.

Table S2 | The protein names, GenBank accession numbers, and references of OBPs used in the phylogenetic analysis.

REFERENCES

Aldrich, J. R. (1988). Chemical ecology of the Heteroptera. *Annu. Rev. Entomol.* 33, 211–238. doi: 10.1146/annurev.en.33.010188.001235

Anisimova, M., Bielawski, J. P., and Yang, Z. H. (2001). Accuracy and power of the likelihood ratio test in detecting adaptive molecular evolution. *Mol. Biol. Evol.* 18, 1585–1592. doi: 10.1093/oxfordjournals.molbev.a003945

Ave, D., Frazier, J. L., and Hatfield, L. D. (1978). Contact chemoreception in the tarnished plant bug *Lygus lineolaris*. *Entomol. Exp. Appl.* 24, 217–227. doi: 10.1111/j.1570-7458.1978.tb02776.x

Chinta, S., Dickens, J. C., and Baker, G. T. (1997). Morphology and distribution of antennal sensilla of the tarnished plant bug, *Lygus lineolaris* (Palisot de beauvois) (Hemiptera: Miridae). *Inter. J. Insect Morphol. Embryol.* 26, 21–26. doi: 10.1016/S0020-7322(96)00022-0

De Santis, F., Francois, M.-C., Merlin, C., Pelletier, J., Maibeche-Coisne, M., Conti, E., et al. (2006). Molecular cloning and in situ expression patterns of two new pheromone-binding proteins from the corn stemborer *Sesamia nonagrioides*. *J. Chem. Ecol.* 32, 1703–1717. doi: 10.1007/s10886-006-9103-2

Elsayed, G. (2011). Plant secondary substances and insects behaviour. *Arch. Phytopathol. Plant Prot.* 44, 1534–1549. doi: 10.1080/03235408.2010.507957

Feng, L., and Prestwich, G. D. (1997). Expression and characterization of a Lepidopteran general odorant binding protein. *Insect Biochem. Mol. Biol.* 27, 405–412. doi: 10.1016/S0965-1748(97)00012-X

Foret, S., and Maleszka, R. (2006). Function and evolution of a gene family encoding odorant binding-like proteins in a social insect, the honey bee (*Apis mellifera*). *Genome Res.* 16, 1404–1413. doi: 10.1101/gr.5075706

Galindo, K., and Smith, D. P. (2001). A large family of divergent drosophila odorant-binding proteins expressed in gustatory and olfactory sensilla. *Genetics* 159, 1059–1072.

Groot, A. T., Dekker, T., and Heckel, D. G. (2016). The genetic basis of pheromone evolution in moths. *Annu. Rev. Entomol.* 61, 99–117. doi: 10.1146/annurev-ento-010715-023638

Große-Wilde, E., Svatoš, A., and Krieger, J. (2006). A pheromone-binding protein mediates the bombykol-induced activation of a pheromone receptor *in vitro*. *Chem. Senses* 31, 547–555. doi: 10.1093/chemse/bjj059

Gu, S. H., Wang, S. P., Zhang, X. Y., Wu, K. M., Guo, Y. Y., Zhou, J. J., et al. (2011a). Identification and tissue distribution of odorant binding protein genes in the lucerne plant bug *Adelphocoris lineolatus* (Goeze). *Insect Biochem. Mol. Biol.* 41, 254–263. doi: 10.1016/j.ibmb.2011.01.002

Gu, S.-H., Wang, W.-X., Wang, G.-R., Zhang, X.-Y., Guo, Y.-Y., Zhang, Z. D., et al. (2011b). Functional characterization and immunolocalization of odorant binding protein 1 in the lucerne plant bug, *Adelphocoris lineolatus* (Goeze). *Arch. Insect Biochem. Physiol.* 77, 81–99. doi: 10.1002/arch.20427

Halloin, J. M. (1982). Localization and changes in catechin and tannins during development and ripening of cottonseed. *New Phytol.* 90, 651–657. doi: 10.1111/j.1469-8137.1982.tb03274.x

Hatfield, L. D., and Frazier, J. L. (1980). Ultrastructure of the labial tip sensilla of the tarnished plant bug, *Lygus lineolaris* (P. de Beauvois) (Hemiptera: Miridae). *Inter. J. Insect Morphol. Embryol.* 9, 59–66. doi: 10.1016/0020-7322(80)90036-7

He, P., Zhang, J., Liu, N. Y., Zhang, Y. N., Yang, K., and Dong, S. L. (2011). Distinct expression profiles and different functions of odorant binding proteins in *Nilaparvata lugens* Stål. *PLoS ONE* 6:e28921. doi: 10.1371/journal.pone.0028921

He, X., Tzotzos, G., Woodcock, C., Pickett, J. A., Hooper, T., Field, L. M., et al. (2010). Binding of the general odorant binding protein of *Bombyx mori* BmorGOBP2 to the moth sex pheromone components. *J. Chem. Ecol.* 36, 1293–1305. doi: 10.1007/s10886-010-9870-7

Hekmat-Scafe, D. S., Steinbrecht, R. A., and Carlson, J. R. (1997). Coexpression of two odorant-binding protein homologs in *Drosophila*: implications for olfactory coding. *J. Neurosci.* 17, 1616–1624.

Hua, J. F., Zhang, S., Cui, J. J., Wang, D. J., Wang, C. Y., Luo, J. Y., et al. (2012). Identification and binding characterization of three odorant binding proteins and one chemosensory protein from *Apolygus lucorum* (Meyer-Dür). *J. Chem. Ecol.* 38, 1163–1170. doi: 10.1007/s10886-012-0178-7

Hull, J. J., Perera, O. P., and Snodgrass, G. L. (2014). Cloning and expression profiling of odorant-binding proteins in the tarnished plant bug, *Lygus lineolaris*. *Insect Mol. Biol.* 23, 78–97. doi: 10.1111/imb.12064

Jacquin-Joly, E., Bohbot, J., Francois, M. C., Cain, A. H., and Nagnan-Le Meillour, P. (2000). Characterization of the general odorant-binding protein 2 in the molecular coding of odorants in *Mamestra brassicae*. *Eur. J. Biochem.* 267, 6708–6714. doi: 10.1046/j.1432-1327.2000.01772.x

Jacquin-Joly, E., and Merlin, C. (2004). Insect olfactory receptors: contributions of molecular biology to chemical ecology. *J. Chem. Ecol.* 30, 2359–2397. doi: 10.1007/s10886-004-7941-3

Jeong, Y. T., Shim, J., Oh, S. R., Yoon, H. I., Kim, C. H., Moon, S. J., et al. (2013). An odorant-binding protein required for suppression of sweet taste by bitter chemicals. *Neuron* 79, 725–737. doi: 10.1016/j.neuron.2013.06.025

Klusák, V., Havlas, Z., RulìŠek, L. R., Vondrášek, J., and Svatoš, A. (2003). Sexual attraction in the silkworm moth: nature of binding of bombykol in pheromone binding protein—an ab initio study. *Chem. Biol.* 10, 331–340. doi: 10.1016/S1074-5521(03)00074-7

Krieger, J., Von Nickisch-Rosenegk, E., Mameli, M., Pelosi, P., and Breer, H. (1996). Binding proteins from the antennae of *Bombyx mori*. *Insect Biochem. Mol. Biol.* 26, 297–307. doi: 10.1016/0965-1748(95)00096-8

Leal, W. S. (2013). Odorant reception in insects: roles of receptors, binding proteins, and degrading enzymes. *Annu. Rev. Entomol.* 58, 373–391. doi: 10.1146/annurev-ento-120811-153635

Leal, W. S., Nikonova, L., and Peng, G. (1999). Disulfide structure of the pheromone binding protein from the silkworm moth, *Bombyx mori*. *FEBS Lett.* 464, 85–90. doi: 10.1016/S0014-5793(99)01683-X

Li, Q., and Liberles, S. D. (2015). Aversion and attraction through olfaction. *Curr. Biol.* 25, R120–R129. doi: 10.1016/j.cub.2014.11.044

Li, S., Picimbon, J. F., Ji, S., Kan, Y., Chuanling, Q., Zhou, J. J., et al. (2008). Multiple functions of an odorant-binding protein in the mosquito *Aedes aegypti*. *Biochem. Biophy. Res. Commun.* 372, 464–468. doi: 10.1016/j.bbrc.2008.05.064

Lin, F., Wu, D., Lu, Y., Zhang, Y., Wang, M., and Wu, K. (2011). The relationship between the main secondary metabolites and the resistance of cotton to *Apolygus lucorum*. *Acta Phytophy. Sin.* 38, 202–208.

Livak, K. J., and Schmittgen, T. D. (2001). Analysis of relative gene expression data using real-time quantitative PCR and the $2^{-\Delta\Delta CT}$ method. *Methods* 25, 402–408. doi: 10.1006/meth.2001.1262

Loughrin, J., Manukian, A., Heath, R., and Tumlinson, J. (1995). Volatiles emitted by different cotton varieties damaged by feeding beet armyworm larvae. *J. Chem. Ecol.* 21, 1217–1227. doi: 10.1007/BF02228321

Lu, Y. H., and Wu, K. M. (2008). *Biology and Control of Cotton Mirids*. Beijing: Golden Shield Press.

Lu, Y. H., Wu, K. M., Jiang, Y. Y., Xia, B., Li, P., Feng, H. Q., et al. (2010). Mirid bug outbreaks in multiple crops correlated with wide-scale adoption of Bt cotton in China. *Science* 328, 1151–1154. doi: 10.1126/science.1187881

Lu, Y., Wu, K., Wyckhuys, K., and Guo, Y. (2009). Comparative flight performance of three important pest *Adelphocoris* species of Bt cotton in China. *B. Entomol. Res.* 99, 543–550. doi: 10.1017/S000748530800655X

Matsuo, T., Sugaya, S., Yasukawa, J., Aigaki, T., and Fuyama, Y. (2007). Odorant-binding proteins OBP57d and OBP57e affect taste perception and host-plant preference in *Drosophila sechellia*. *PLoS Biol.* 5:e118. doi: 10.1371/journal.pbio.0050118

Meisner, J., Zur, M., Kabonci, E., and Ascher, K. (1977). Influence of gossypol content of leaves of different cotton strains on the development of *Spodoptera littoralis* larvae. *J. Econom. Entomol.* 70, 714–716. doi: 10.1093/jee/70.6.714

Michael, L. (2000). Immunolocalization of general odorant-binding protein in antennal sensilla of moth caterpillars. *Arthropod Struct. Dev.* 29, 57–73. doi: 10.1016/S1467-8039(00)00013-X

Millar, J. G. (2005). Pheromones of true bugs. *Top Curr. Chem.* 240, 37–84. doi: 10.1007/b98315

Mithöfer, A., and Boland, W. (2012). Plant defense against herbivores: chemical aspects. *Annu. Rev. Plant Biol.* 63, 431–450. doi: 10.1146/annurev-arplant-042110-103854

Park, S. K., Shanbhag, S. R., Wang, Q., Hasan, G., Steinbrecht, R. A., and Pikielny, C. W. (2000). Expression patterns of two putative odorant-binding proteins in the olfactory organs of *Drosophila melanogaster* have different implications for their functions. *Cell Tissue Res.* 300, 181–192. doi: 10.1007/s004410050059

Pelosi, P., Iovinella, I., Felicioli, A., and Dani, F. R. (2014). Soluble proteins of chemical communication: an overview across arthropods. *Front. Physiol.* 5:320. doi: 10.3389/fphys.2014.00320

Pelosi, P., Mastrogiacomo, R., Iovinella, I., Tuccori, E., and Persaud, K. (2013). Structure and biotechnological applications of odorant-binding proteins. *Appl. Microbiol. Biotechnol.* 98, 61–70. doi: 10.1007/s00253-013-5383-y

Poivet, E., Rharrabe, K., Monsempes, C., Glaser, N., Rochat, D., Renou, M., et al. (2012). The use of the sex pheromone as an evolutionary solution to food source selection in caterpillars. *Nat. Commun.* 3, 1047. doi: 10.1038/ncomms2050

Pophof, B. (2004). Pheromone-binding proteins contribute to the activation of olfactory receptor neurons in the silkmoths *Antheraea polyphemus* and *Bombyx mori*. *Chem. Senses* 29, 117–125. doi: 10.1093/chemse/bjh012

Qiao, H., Tuccori, E., He, X., Gazzano, A., Field, L., Zhou, J. J., et al. (2009). Discrimination of alarm pheromone (*E*)-β-farnesene by aphid odorant-binding proteins. *Insect Biochem. Molecul. Biol.* 39, 414–419. doi: 10.1016/j.ibmb.2009.03.004

Romani, R., Salerno, G., Frati, F., Conti, E., Isidoro, N., and Bin, F. (2005). Oviposition behaviour in *Lygus rugulipennis*: a morpho-functional study. *Entomol. Experiment. Appl.* 115, 17–25. doi: 10.1111/j.1570-7458.2005.00268.x

Röse, U. R., and Tumlinson, J. (2004). Volatiles released from cotton plants in response to *Helicoverpa zea* feeding damage on cotton flower buds. *Planta* 218, 824–832. doi: 10.1007/s00425-003-1162-9

Sandler, B. H., Nikonova, L., Leal, W. S., and Clardy, J. (2000). Sexual attraction in the silkworm moth: structure of the pheromone-binding-protein-bombykol complex. *Chem. Biol.* 7, 143–151. doi: 10.1016/S1074-5521(00)00078-8

Steinbrecht, R., Laue, M., and Ziegelberger, G. (1995). Immunolocalization of pheromone-binding protein and general odorant-binding protein in olfactory sensilla of the silk moths *Antheraea* and *Bombyx*. *Cell Tissue Res.* 282, 203–217. doi: 10.1007/BF00319112

Sun, L., Gu, S. H., Xiao, H. J., Zhou, J. J., Guo, Y. Y., Liu, Z. W., et al. (2013). The preferential binding of a sensory organ specific odorant binding protein of the alfalfa plant bug *Adelphocoris lineolatus* AlinOBP10 to biologically active host plant volatiles. *J. Chem. Ecol.* 39, 1221–1231. doi: 10.1007/s10886-013-0333-9

Sun, L., Xiao, H. J., Gu, S. H., Guo, Y. Y., Liu, Z. W., and Zhang, Y. J. (2014b). Perception of potential sex pheromones and host-associated volatiles in the cotton plant bug, *Adelphocoris fasciaticollis* (Hemiptera: Miridae): morphology and electrophysiology. *Appl. Entomol. Zool.* 49, 43–57. doi: 10.1007/s13355-013-0223-1

Sun, L., Xiao, H. J., Gu, S. H., Zhou, J. J., Guo, Y. Y., Liu, Z. W., et al. (2014a). The antenna-specific odorant-binding protein AlinOBP13 of the alfalfa plant bug *Adelphocoris lineolatus* is expressed specifically in basiconic sensilla and has high binding affinity to terpenoids. *Insect Mol. Biol.* 23, 417–434. doi: 10.1111/imb.12089

Sun, Y. F., De Biasio, F., Qiao, H. L., Iovinella, I., Yang, S. X., Ling, Y., et al. (2012). Two odorant-binding proteins mediate the behavioural response of aphids to the alarm pheromone *E*-ß-farnesene and structural analogues. *PLoS ONE* 7:e32759. doi: 10.1371/journal.pone.0032759

Sun, Y. L., Huang, L. Q., Pelosi, P., and Wang, C. Z. (2012). Expression in antennae and reproductive organs suggests a dual role of an odorant-binding protein in two sibling *Helicoverpa* species. *PLoS ONE* 7:e30040. doi: 10.1371/journal.pone.0030040

Sun, Y. P., Zhao, L. J., Sun, L., Zhang, S. G., and Ban, L. P. (2013). Immunolocalization of odorant-binding proteins on antennal chemosensilla of the peach aphid *Myzus persicae* (Sulzer). *Chem. Senses* 38, 129–136. doi: 10.1093/chemse/bjs093

Tamura, K., Stecher, G., Peterson, D., Filipski, A., and Kumar, S. (2013). MEGA6: Molecular Evolutionary Genetics Analysis Version 6.0. *Mol. Biol. Evol.* 30, 2725–2729. doi: 10.1093/molbev/mst197

Tanaka, K., Uda, Y., Ono, Y., Nakagawa, T., Suwa, M., Yamaoka, R., et al. (2009). Highly selective tuning of a silkworm olfactory receptor to a key mulberry leaf volatile. *Curr. Biol.* 19, 881–890. doi: 10.1016/j.cub.2009.04.035

Tegoni, M., Campanacci, V., and Cambillau, C. (2004). Structural aspects of sexual attraction and chemical communication in insects. *Trends Biochem. Sci.* 29, 257–264. doi: 10.1016/j.tibs.2004.03.003

Vandermoten, S., Francis, F., Haubruge, E., and Leal, W. S. (2011). Conserved odorant-binding proteins from aphids and eavesdropping predators. *PLoS ONE* 6:e23608. doi: 10.1371/journal.pone.0023608

Vogt, R. G., and Riddiford, L. M. (1981). Pheromone binding and inactivation by moth antennae. *Nature* 293, 161–163. doi: 10.1038/293161a0

Wang, S. Y., Gu, S. H., Han, L., Guo, Y. Y., Zhou, J. J., and Zhang, Y. J. (2013). Specific involvement of two amino acid residues in *cis*-nerolidol binding to odorant-binding protein 5 AlinOBP5 in the alfalfa plant bug, *Adelphocoris lineolatus* (Goeze). *Insect Mol. Biol.* 22, 172–182. doi: 10.1111/imb.12012

Yang, Z. H. (1997). PAML: a program package for phylogenetic analysis by maximum likelihood. *Comput. Appl. Biosci.* 13, 555–556. doi: 10.1093/bioinformatics/13.5.555

Yuan, H. B., Ding, Y. X., Gu, S. H., Sun, L., Zhu, X. Q., Liu, H. W., et al. (2015). Molecular characterization and expression profiling of odorant-binding proteins in *Apolygus lucorum*. *PLoS ONE* 10:e140562. doi: 10.1371/journal.pone.0140562

Zhang, D. D., and Löfstedt, C. (2013). Functional evolution of a multigene family: orthologous and paralogous pheromone receptor genes in the turnip moth, *Agrotis segetum*. *PLoS ONE* 8:e77345. doi: 10.1371/journal.pone.0077345

Zhou, J. J., Vieira, F. G., He, X. L., Smadja, C., Liu, R., Rozas, J., et al. (2010). Genome annotation and comparative analyses of the odorant-binding proteins and chemosensory proteins in the pea aphid *Acyrthosiphon pisum*. *Insect Mol. Biol.* 19(Suppl. 2), 113–122. doi: 10.1111/j.1365-2583.2009.00919.x

Zhu, J., Ban, L., Song, L. M., Liu, Y., Pelosi, P., and Wang, G. (2016). General odorant-binding proteins and sex pheromone guide larvae of *Plutella xylostella* to better food. *Insect Biochem. Mol. Biol.* 72, 10–19. doi: 10.1016/j.ibmb.2016.03.005

Conflict of Interest Statement: The authors declare that the research was conducted in the absence of any commercial or financial relationships that could be construed as a potential conflict of interest.

frontiers in Physiology

ORIGINAL RESEARCH
published: 28 October 2015
doi: 10.3389/fphys.2015.00305

Flight control and landing precision in the nocturnal bee *Megalopta* is robust to large changes in light intensity

Emily Baird[1]*, *Diana C. Fernandez*[2], *William T. Wcislo*[3] and *Eric J. Warrant*[1]

[1] Department of Biology, Lund University, Lund, Sweden, [2] Department of Biological Sciences, University of Lethbridge, Lethbridge, AB, Canada, [3] Smithsonian Tropical Research Institute, Panama City, Republic of Panama

Like their diurnal relatives, *Megalopta genalis* use visual information to control flight. Unlike their diurnal relatives, however, they do this at extremely low light intensities. Although *Megalopta* has developed optical specializations to increase visual sensitivity, theoretical studies suggest that this enhanced sensitivity does not enable them to capture enough light to use visual information to reliably control flight in the rainforest at night. It has been proposed that *Megalopta* gain extra sensitivity by summing visual information over time. While enhancing the reliability of vision, this strategy would decrease the accuracy with which they can detect image motion—a crucial cue for flight control. Here, we test this temporal summation hypothesis by investigating how *Megalopta's* flight control and landing precision is affected by light intensity and compare our findings with the results of similar experiments performed on the diurnal bumblebee *Bombus terrestris*, to explore the extent to which *Megalopta's* adaptations to dim light affect their precision. We find that, unlike *Bombus*, light intensity does not affect flight and landing precision in *Megalopta*. Overall, we find little evidence that *Megalopta* uses a temporal summation strategy in dim light, while we find strong support for the use of this strategy in *Bombus*.

Keywords: flight control, light intensity, neural summation, *Megalopta*, *Bombus*

OPEN ACCESS

Edited by:
Sylvia Anton,
Institut National de la Recherche Agronomique, France

Reviewed by:
Natalie Hempel De Ibarra,
University of Exeter, UK
Jake Socha,
Virginia Tech, USA

***Correspondence:**
Emily Baird
emily.baird@biol.lu.se

Specialty section:
This article was submitted to Invertebrate Physiology, a section of the journal Frontiers in Physiology

Received: *21 July 2015*
Accepted: *12 October 2015*
Published: *28 October 2015*

Citation:
Baird E, Fernandez DC, Wcislo WT and Warrant EJ (2015) Flight control and landing precision in the nocturnal bee Megalopta *is robust to large changes in light intensity. Front. Physiol. 6:305. doi: 10.3389/fphys.2015.00305*

INTRODUCTION

As light intensities fall, visual information becomes increasingly unreliable and nocturnal animals compensate for this by having eyes that are extremely sensitive to light (Warrant, 2008a,b). Many nocturnal insects, for example, possess superposition compound eyes, a design that greatly increases light capture compared to the apposition compound eye, which is better suited to fast vision in bright environments and is therefore more typical of diurnal insects (Land, 1981). Nonetheless, the nocturnal neotropical sweat bee *Megalopta genalis*, which relies heavily on visual information to control flight (Baird et al., 2011) and locate its nest stick (Warrant et al., 2004) in dim light, possesses apposition compound eyes. So how are these insects able to see at night? *Megalopta* elevate their photon capture by having unusually wide, light-sensitive rhabdoms, and very large facet lenses (Warrant et al., 2004; Greiner et al., 2004a). Although this increases the sensitivity of their eyes quite significantly, theoretical calculations indicate that it does not allow them to capture enough light to reliably control flight and to locate a small nest stick under the dense rainforest canopy at night (Warrant et al., 2004; Greiner et al., 2004a). Anatomical investigations suggest

that *Megalopta* most likely enhances visual reliability in dim light by neurally summing visual information in the spatial domain (Greiner et al., 2004b). In addition, theoretical analyses also suggest that they may also sum this information in the temporal domain (Theobald et al., 2006), although neither possibility has been tested behaviorally.

While improving the reliability of visual information, temporal neural summation comes at the cost of decreasing sensitivity to image motion (Sponberg et al., 2015), a crucial requirement for flight control and landing in many flying insects (for a review, see: Taylor and Krapp, 2007). To maintain the precision of flight control in dim light despite a loss of temporal resolution, the insect would need to reduce the overall speed of image motion by flying slower as light levels decline. This strategy has been observed in hornets (Spiewok and Schmolz, 2006), honeybees (Menzel, 1981), and bumblebees (Reber et al., 2015). Interestingly, *Megalopta* does not seem to change ground speed in response to decreasing light intensities but instead appears to sacrifice flight performance: when returning to their nest in dim light, they fly with significantly more convoluted trajectories than when returning in brighter light, sometimes even making unsuccessful approach and landing attempts (Theobald et al., 2007). One explanation for the increased tortuosity in their flight paths is that the bees are losing temporal resolution without making any compensatory decreases in speed, something that would likely limit the precision with which *Megalopta* could control its flight and land. If *Megalopta* does indeed use temporal summation to enhance visual reliability in dim light without flying slower, we would expect flight control and landing accuracy to be significantly compromised as light levels fall. But is this the case? Here, we aim to answer this question by investigating experimentally the effect of light intensity on position control and landing in *Megalopta* and compare this with similar experiments performed on the diurnal bumblebee, *Bombus terrestris*, which most likely uses temporal summation in dim light (Reber et al., 2015).

MATERIALS AND METHODS

Animals

M. genalis create nests (otherwise referred to as nest sticks) by burrowing holes and tunnels into dead, broken branches, lianas and vines [typically 30–50 mm in diameter (Eickwort, 1969)], in the rainforest understory. The entrance holes to these nest tunnels are ∼5 mm in diameter (Eickwort, 1969). *Megalopta* nest sticks were collected and transferred to an experimental site in the rainforest of Barro Colorado Island in Panama. The experiments were conducted in March and April 2013 (with the exception of the natural nest stick landings, which were performed in 2009, see below for details). A light meter (IL1700, International Light, USA) placed at the experimental location (2 m from the nest stick) recorded light intensity (illuminance in lux) at 1 s intervals using an electronic data logger built in-house. The time stamp of the light meter recordings was then carefully matched to the time stamp of the recordings from the camera. Trajectories of *Megalopta* returning to the nest in both experimental conditions (see below for details) were filmed under infrared illumination at 25 fps (using a Sony Handycam HDR-HC5E, Sony Corporation, Japan) during their normal foraging times, approximately 40 min both before sunrise and after sunset. The light intensities at which the flights were filmed depended on when the bees returned and were therefore not under experimental control. In some cases, more than one bee inhabited the nest stick so that two or more individual flights were recorded per session. Because we could not identify the individual bees, we therefore report the approximate number of individuals included in the data set as well as the absolute number of nest sticks.

B. terrestris experiments used a commercial hive (Koppert, UK) and were performed at Lund University in an indoor flight cage (2.3 m long × 2 m wide × 2 m high) during their peak activity period (between 08:00 and 14:00) at light intensities of either 19 or 190 lux. Bees returning to the nest were recorded in 30 min sessions interspersed with 30 min control periods to allow for habituation to the test condition and light intensity. For both experimental conditions (see below for details) only the first 10 flights to the nest were recorded in each session because they often occurred in quick succession—we could thus be confident that they represented 10 different individuals. Otherwise, experiments were conducted as for *Megalopta*.

For both species, different individuals were used for the two different experiments (described below).

Statistics

Non-parametric Wilcoxon rank sum tests (z statistic) and Spearman's rank-order correlations at the 5% significance level were used for all statistical comparisons. The r_s statistic of the correlation test indicates the strength and sign of the relationship between -1 (perfect negative correlation), 0 (no correlation), and 1 (perfect positive correlation). Values are reported as the median and 25–75% interquartile range (iqr). Linear regression analyses were performed using the "fitlm" function in Matlab 2015a (Mathworks), which provided the F-statistic vs. constant model value and associated *P*-value.

The Effect of Light Intensity on Flight Control

The experimental apparatus consisted of a clear acrylic tunnel, 14 cm wide × 14.5 cm high × 50 cm long, mounted 65 cm above the ground (**Figure 1A**). The nest was placed at an opening in one end of the tunnel at least 2 days before recording began to ensure that the bees were accustomed to flying along the tunnel to exit and enter their nest. The tunnel remained in this position for the duration of the experiment. After 2 days of habituation to the tunnel, all of the bees that flew made direct trajectories through the tunnel to the nest. The nest entrance was covered with a 5 cm diameter white disk (which had a low contrast against the sandblasted Perspex back wall) having a central 1 cm diameter hole aligned with the entrance hole of the nest. The walls of the tunnel were lined with a pattern composed of randomly distributed black and white 3 × 3 cm squares. The top panel of the tunnel was sandblasted. Flights to the nest were recorded at 25 Hz using a camera (Sony Handycam

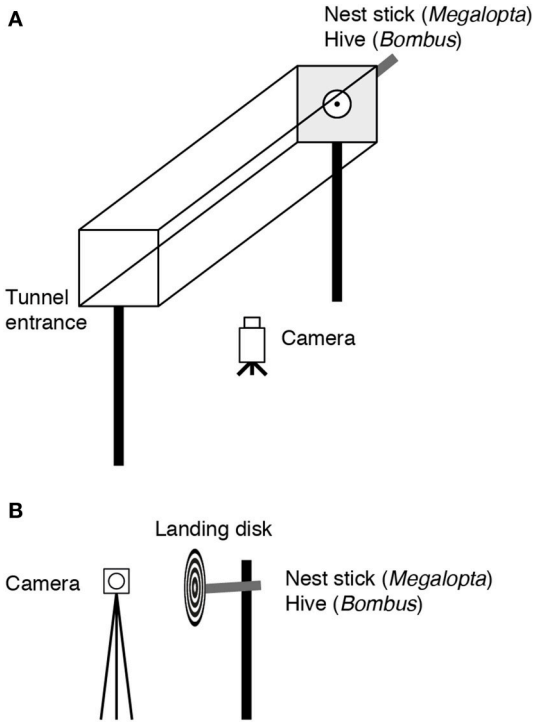

FIGURE 1 | The experimental apparatus. (A) The experimental tunnel used to investigate the effect of light intensity on flight control in *Megalopta* and *Bombus*. Flights from the tunnel entrance to the nest were recorded using a camera mounted underneath the tunnel. **(B)** The experimental apparatus used to investigate the effect of light intensity on landing in *Megalopta* and *Bombus*. Approaches to and landings on the disk were recorded using a camera mounted to the side.

HDR-HC5E, Sony Corporation, Japan) mounted beneath the tunnel. The trajectories were analyzed over the first 25 cm of the tunnel to avoid including landing maneuvers at the nest. Fifty-one flights from 19 individuals from 11 nest sticks were recorded for *Megalopta* and 51 flights (23 flights at 19 lux and 28 flights at 190 lux) from approximately 20 individuals were recorded for *Bombus*.

Ground speed was calculated as the average of the two-dimensional distance traveled between successive frames divided by the time step between the frames (0.04 s). Accuracy of position control was calculated by finding the average lateral distance from the midline of the tunnel as well as the variance in lateral position (the iqr of lateral positions) for each flight.

The Effect of Light Intensity on Landing

In these experiments, the flights of bees landing on either patterned disks or natural nest sticks (*Megalopta* only) were recorded (**Figure 1B**). Black-and-white concentric ring or radial patterns (*Megalopta* only) were printed on paper and attached to plastic disks, 10 cm in diameter with a 1 cm diameter hole at the center. The radial pattern provided strong expansion cues for bees approaching the disk while these cues were minimized in the sector pattern. In these experiments, the entrance to the nest was not placed in a tunnel but was surrounded by clear space. The disks were fitted over the nest entrance such that bees returning to their nest would have to approach and land on them. A camera mounted to the side of the disks, parallel to the trajectories of the bees, recorded the landings. Leg extension was defined as the moment when the bees began to extend their front or middle legs prior to making contact with the disk (depending on which came first). Time to contact (TC) was calculated as the time between leg extension and contact with the disk. Sixty-one landings (27 for the ring pattern, 34 for the radial pattern) from 10 individuals from four nest sticks were recorded for *Megalopta*, 58 landings from approximately 20 individuals were recorded for *Bombus*.

The natural nest stick landings for *Megalopta* were performed in March and April 2009. In these experiments, light intensity measurements (recorded in cd/m^2) were made every 5 min using a Kodak 18% gray card reflecting incident downwelling daylight and a light meter (IL1700, International Light, USA), at a location about 2 m from the nest (as for the other *Megalopta* measurements). The nest sticks sticks were between 30 and 50 mm in diameter with a ∼5 mm diameter hole that has approximately 72% contrast with the surrounding wood (Warrant et al., 2004). For the purpose of consistency and ease of comparison, these light intensity measurements were exchanged for careful intensity measurements in lux that were taken under similar conditions and at the same time of year for identical pre- and post-sunset times in later years. It is important to note that we performed statistical tests using both units and they both indicated that light intensity had no significant effect on landing precision in this experiment.

RESULTS

Changes in Light Intensity Affect Flight Control in *Bombus* But not in *Megalopta*

To investigate the effect of light intensity on flight control in *Megalopta* and *Bombus*, we recorded the trajectories of bees flying through an experimental tunnel at different light intensities. Flights of *Megalopta* were recorded over a range of light intensities between 0.0014 and 40.4 lux (this could not be experimentally controlled as it was determined by when the bees chose to return to their nest after a foraging trip). Despite the four log units of difference, light intensity did not have a strong effect on ground speed ($r_s = 0.24$, $P = 0.09$, $n = 51$; **Figure 2A**) nor the absolute lateral position ($r_s = -0.06$, $P = 0.69$; **Figure 2B**). There is a suggestion, however, that the within-flight variance of lateral position is weakly affected by light intensity ($r_s = 0.26$, $p = 0.06$; **Figure 2C**). This result is also reflected in the linear regression analyses of the data and the statistical comparison with a constant relationship between the variables (details of these analyses are provided in each subplot of **Figure 2**). In contrast to *Megalopta*, the ground speed of *Bombus* flying at higher light intensities of 190 or 19 lux (the bumblebees were reluctant to fly in lower light intensities) was significantly affected by light intensity ($r_s = 0.46$, $P < 0.001$, $n = 50$; **Figure 2A**), although

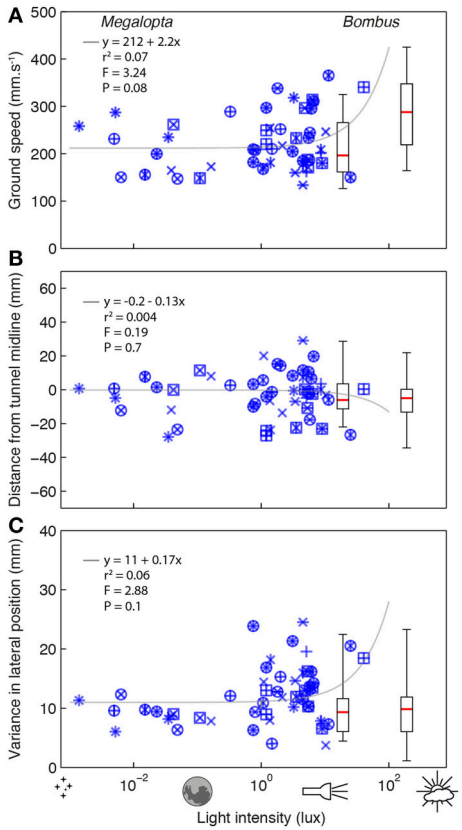

FIGURE 2 | The effect of light intensity on flight control in *Megalopta* and *Bombus*. The effect of light intensity on ground speed **(A)**, median lateral position **(B),** and variance (inter-quartile range) in lateral position **(C)** of *Megalopta* (blue stars; 51 flights, 19 individuals, 15 nests—different symbols indicate data from different nests) and *Bombus* [box plots; 23 flights (19 lux), 28 flights (190 lux), ~20 individuals] flying along an experimental tunnel (140 mm wide) at different light intensities. The boxes indicate the 25–75% quartile of the data, the red line indicates the median and the whiskers show the extent of the data. Gray lines indicate a linear regression analysis of the *Megalopta* data; details of the analysis and the statistical comparison (*F*-value) against a constant model are provided in each plot.

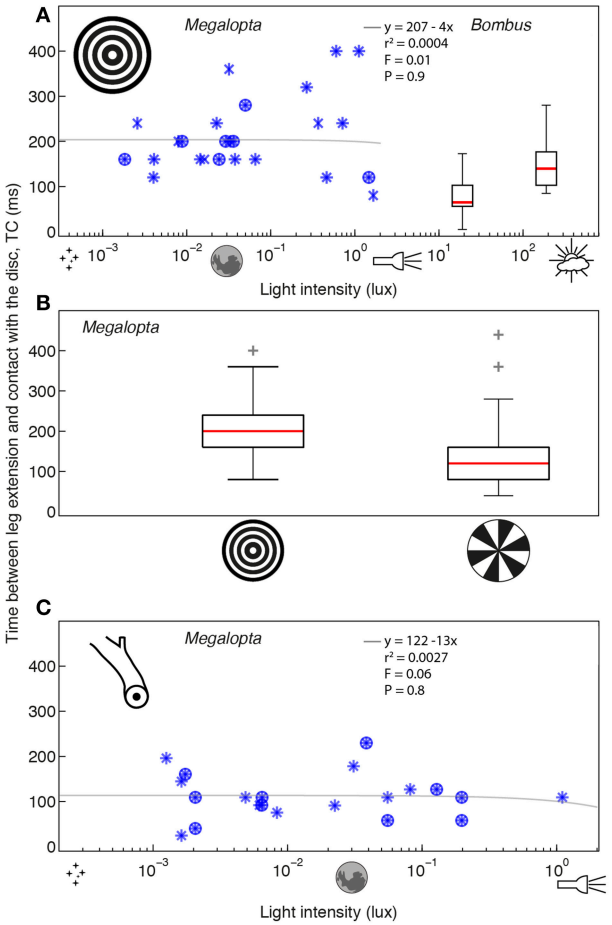

FIGURE 3 | The effect of light intensity on the timing of leg extension when landing in *Megalopta* and *Bombus*. (A) The effect of light intensity on the time between leg extension and contact (TC) with a concentric ring pattern (inset) in *Megalopta* (blue stars, 27 landings, 10 individuals, 4 nests—different symbols indicate data from different nests) and *Bombus* [box plots, details as in **Figure 1**; 21 landings (19 lux), 37 landings (190 lux), ~20 individuals]. **(B)** The effect of visual expansion cues on TC in *Megalopta* [ring pattern (inset): 27 landings, radial pattern (inset): 34 landings]. Box plot details as in **Figure 1** indicate the distance between the lower and upper quartile values, red lines indicate the median, whiskers indicate the entire spread of the data and red crosses indicate outliers. **(C)** The effect of light intensity on TC for a natural nest stick (inset) in *Megalopta* (23 landings, 4 individuals, 2 nests—different symbols indicate data from different nests). Gray lines indicate a linear regression analysis of the *Megalopta* data; details of the analysis and the statistical comparison (*F*-value) against a constant model are provided in each plot.

the absolute lateral position ($r_s = 0.07$, $P = 0.63$; **Figure 2B**) and the variance in lateral position was not ($r_s = 0.05$, $p = 0.76$; **Figure 2C**).

Changes in Light Intensity Affect Landing Control in *Bombus* But not in *Megalopta*

To investigate the effect of light intensity on the precision of landing (measured in terms of the timing of the leg extension response), we recorded the final stage of return flights to the nest in *Megalopta* and *Bombus* under different light intensities. *Megalopta* landings on a concentric ring pattern (which provides strong visual expansion cues) were recorded over a range of light intensities between 0.0018 and 3.58 lux (once again, this was not under experimental control but rather determined by when the bees returned to their nest after a foraging trip). Over this range, light intensity did not affect the time between leg extension and contact with the surface, TC ($r_s = -0.02$, $P = 0.91$, $n = 27$; see also details of the linear regression analysis in **Figure 3A**). In contrast, a single order of magnitude change in light intensity from 190 to 19 lux was sufficient to significantly affect TC in *Bombus* landing on the same pattern ($r_s = 0.4$, $p = 0.0016$, $n = 58$; **Figure 3A**). Because only light intensity varied in this experiment, this result suggests that visual information is important for initiating the leg extension response in *Bombus* but that it may not play such an important role in *Megalopta*.

To examine if visual cues are used to regulate the timing of the leg extension response in *Megalopta*, we compared TC for a concentric ring pattern, which provides strong visual expansion cues, with TC for a radial pattern, which provides only weak expansion cues over a similar range of light intensities (0.00094–19.94 lux). If the bees use visual expansion cues to initiate a leg extension, we expect that it will be initiated later (that is, TC will be reduced) for the radial pattern because the bees will receive little information about the distance to the surface. A TC lower than that obtained for the ring pattern (which we assume to represent optimal timing for landing) would indicate that landing has become less precise. Our results showed that TC was affected by the visual pattern (Wilcoxon rank sum, $z = 3.3$, $P < 0.0001$, $n = 61$; see also details of the linear regression analysis in **Figure 3B**), with leg extension occurring earlier for the ring compared to the radial pattern (ring: 200 [80] ms; radial: 120 [80] ms, median [iqr]). This decrease in TC for the radial pattern indicates that *Megalopta* becomes less precise when visual expansion cues are removed, suggesting that these cues are important for coordinating the timing of leg extension during landing.

To investigate if TC in *Megalopta* is robust to light intensity under more natural conditions, we filmed landings on unmodified nest over a range of light intensities between 0.0007 and 0.95 lux. Again, we found no effect of light intensity on TC ($r_s = -0.05$, $p = 0.81$, **Figure 3C**), although the average of 116 [46] ms is lower than the value of 200 [80] ms recorded for the much larger ring pattern, suggesting that the size and visual saliency of the landing surface is another factor that affects the timing of leg extension in *Megalopta*.

DISCUSSION

In this study, we investigate the effect of light intensity on flight control and landing in a nocturnal (*Megalopta*) and diurnal (*Bombus*) bee species. Overall, we find that flight control and landing precision in *Megalopta* is not strongly affected by light intensity, even over a five orders of magnitude decrease from twilight down to illumination levels approaching starlight. In contrast, ground speed and landing precision in *Bombus* decrease significantly over just a single order of magnitude decrease in light intensity, from illumination levels similar to an overcast day to those experienced just before twilight.

The finding that light intensity does not have a strong effect on ground speed in *Megalopta* is consistent with previous findings (Theobald et al., 2007), despite the large methodological differences between analysing natural return flights in the earlier study and analysing flights in an experimental tunnel in the present study. Does this lack of dependence of ground speed on light intensity come at the cost of flight performance in *Megalopta*? Surprisingly, we found that flight accuracy, at least in terms of positioning between the walls of a tunnel, does not worsen even over a five orders of magnitude decrease in light intensity. Despite the increased sensitivity afforded by their optical specializations (Greiner et al., 2004a), the ability to maintain the same level of flight control precision over such a broad range of intensities strongly suggests that *Megalopta* rely on neural summation strategies to improve visual reliability in dim light. The lack of a change in ground speed in combination with a negligible effect on precision makes it unlikely that *Megalopta* rely heavily on temporal neural summation strategies to control flight in dim light but that they more likely rely heavily on spatial summation strategies to do this.

In contrast to *Megalopta*, we observe a strong effect of light intensity on flight control in *Bombus*, even over a single log unit change in light intensity. These findings are consistent with previous work (Reber et al., 2015) and suggest that, as light intensities fall, *Bombus* use neural temporal summation to improve visual reliability and that they compensate for the subsequent loss of temporal resolution by flying more slowly, as hornets (Spiewok and Schmolz, 2006) and honeybees (Menzel, 1981) also appear to do. This compensatory decrease in ground speed allows them to obtain enough visual information to continue to control their position accurately.

To date, all investigations into the effect of light intensity on flight control in insects have focussed primarily on how light intensity affects ground speed. However, insects must control more than their speed to be able to fly safely in dim light. One of the most challenging behaviors that flying insects must perform is landing. To orchestrate a safe and efficient landing, flying insects need to determine the moment when they will contact the surface so that they can extend their legs in time. One cue that stimulates this leg extension response in tethered flies is the apparent rate of image expansion generated by the surface, which is used to measure the relative distance to the surface and the TC (Goodman, 1960; Wehrhahn et al., 1981; Borst, 1986; Borst and Bahde, 1986)—once this apparent rate of expansion reaches a certain threshold value, the leg extension reflex is initiated. To investigate if changes in light intensity affect landing precision in *Megalopta* and *Bombus*, we analyzed the effect of light intensity on the timing of the leg extension reflex.

As with the other parameters of flight control discussed above, the timing of the leg extension reflex is not affected by light intensity in *Megalopta*, while in *Bombus* precision is clearly lost and they extend their legs much later (i.e., closer to the nest) when light intensity decreases. One possible explanation for the lack of observeable effect of light intensity on TC in *Megalopta* is that the leg extension response is not mediated by visual cues. However, when we tested the effect of removing expansion cues from the landing surface, we find that *Megalopta* extend their legs later, suggesting that visual cues do indeed play an important role in the control of landing and that the neural summation mechanisms they employ do not affect their ability to measure the rate of expansion of optic flow cues generated by the landing surface, despite a four orders of magnitude decrease in light intensity (note that the bees in the tunnel experiments flew over five orders of magnitude difference in light intensity while in the landing experiments the flights were distributed over four orders of magnitude).

Although our results show that the timing of the leg extension response in *Megalopta* is not affected by light intensity, the patterns that we used in the experiment were not representative of the natural landing surface of an unmodified nest stick, for

which the only strong contrast cues are provided by the edge of the stick and the dark entrance. Although the timing of the leg extension was reduced for landings at the nest stick in comparison to landings on the disk, suggesting that the size and visual saliency of the landing surface might be an important cue, we find no effect of light intensity in this situation either. This result further supports our finding that flight control and landing precision in *Megalopta* is extraordinarily robust to large changes in light intensity.

Considered together, the results of this study reveal that the visual control of flight and landing in *Megalopta* is not affected by large changes in light intensity, even at intensities similar to a moonless clear night sky ($\sim 10^{-3}$ lux, according to our own measurements). Under similar experimental conditions (but under much brighter limiting light levels), *Bombus* fly more slowly and the time between leg extension and landing decreases—elevating their risk of colliding with the landing surface (an event that was frequently observed at low light levels)—even for a decline in light intensity of just a single order of magnitude. These findings suggest that the neural summation strategies employed by these two species are fundamentally different. The reduction in ground speed and landing precision observed in *Bombus* as light levels fall strongly supports the hypothesis that they rely on neural temporal summation mechanisms to obtain enough visual information to see in dim light. In contrast, *Megalopta* do not fly more slowly and nor does their flight accuracy appear to suffer, even over a very large range of light intensities. This strongly implies that their temporal resolution does not vary with light intensity and that spatial summation is instead employed to ensure sufficient visual reliability to control flight at night. At first glance, these findings appear to contradict those of Theobald et al. (2007), who showed that flight trajectories become more tortuous as light intensity decreases, suggesting a loss of precision. Our results suggest, however, that the apparent loss of accuracy is not due to a decrease in the accuracy of flight control *per se* but rather to a decrease in the ability of *Megalopta* to accurately locate the nest stick due to increased spatial summation (as evidenced by the shorter time between leg extension and landing at a natural nest, **Figure 2C**). Nonetheless, these bees could use coarser spatial landmarks in the rainforest to systematically home in on the general vicinity of their nest stick, thus eventually allowing them to locate it.

Here, we show that the neural summation strategies of *Megalopta* are adequate for the fine control of flight and landing while also enabling them to navigate over large distances back to their nest across a broad range of light intensities, which change rapidly and somewhat unpredictably in their equatorial habitat (Endler, 1993). An improved understanding of how *Megalopta* increase their visual sensitivity without sacrificing flight precision will not only be important for understanding how animals use neural adaptations to optimize sensory information when signal-to-noise ratios are low but also for the development of artificial visual guidance systems that are effective in dim light.

FUNDING

Air Force Office of Scientific Research/European Office for Aerospace Research and Development (grant numbers FA8655-07-C-4011, FA8655-08-C-4004). The Swedish Foundation for Strategic Research (2014-4762).

ACKNOWLEDGMENTS

We would like to thank the staff at the Smithsonian Tropical Research Institute for logistical support.

REFERENCES

Baird, E., Kreiss, E., Wcislo, W., Warrant, E., and Dacke, M. (2011). Nocturnal insects use optic flow for flight control. *Biol. Lett.* 7, 499–501. doi: 10.1098/rsbl.2010.1205

Borst, A. (1986). Time course of the housefly's landing response. *Biol. Cybern.* 54, 379–383. doi: 10.1007/BF00355543

Borst, A., and Bahde, S. (1986). What kind of movement detector is triggering the landing response of the housefly? *Biol. Cybern.* 55, 59–69. doi: 10.1007/BF00363978

Eickwort, G. C. (1969). A comparative morphological study and generic revision of the augochlorine bees (Hymenoptera: Halictidae). *Kansas Univ. Sci. Bull.* 48, 325–524.

Endler, J. A. (1993). The color of light in forests and its implications. *Ecol. Monogr.* 63, 2–27. doi: 10.2307/2937121

Goodman, L. J. (1960). The landing responses of insects: I. The landing response of the fly, Lucilia sericata, and other Calliphorinae. *J. Exp. Biol.* 37, 854–878.

Greiner, B., Ribi, W. A., and Warrant, E. J. (2004a). Retinal and optical adaptations for nocturnal vision in the halictid bee *Megalopta genalis*. *Cell Tissue Res.* 316, 377–390. doi: 10.1007/s00441-004-0883-9

Greiner, B., Ribi, W. A., Wcislo, W. T., and Warrant, E. J. (2004b). Neural organisation in the first optic ganglion of the nocturnal bee *Megalopta genalis*. *Cell Tissue Res.* 318, 429–437. doi: 10.1007/s00441-004-0945-z

Land, M. F. (1981). "Optics and vision in invertebrates," in *Vision in Invertebrates*. Handbook of sensory physiology, Vol. VII/6B, ed H. Autrum (Springer; New York: Berlin Heidelberg), 471–592.

Menzel, R. (1981). Achromatic vision in the honeybee at low light intensities. *J Comp Physiol* 141, 389–393. doi: 10.1007/BF00609941

Reber, T., Vähäkainu, A., Baird, E., Weckström, M., Warrant, E., and Dacke, M. (2015). Effect of light intensity on flight control and temporal properties of photoreceptors in bumblebees. *J. Exp. Biol.* 218, 1339–1346. doi: 10.1242/jeb.113886

Spiewok, S., and Schmolz, E. (2006). Changes in temperature and light alter the flight speed of hornets (*Vespa crabro* L.). *Physiol. Biochem. Zool.* 79, 188–193. doi: 10.1086/498181

Sponberg, S., Dyhr, J. P., Hall, R. W., and Daniel, T. (2015). Luminance-dependent visual processing enables moth flight in low light. *Science* 348, 1245–1248. doi: 10.1126/science.aaa3042

Taylor, G. K., and Krapp, H. G. (2007). Sensory systems and flight stability: what do insects measure and why? *Adv. Insect Physiol.* 34, 231–316. doi: 10.1016/s0065-2806(07)34005-8

Theobald, J. C., Coates, M. M., Wcislo, W. T., and Warrant, E. J. (2007). Flight performance in night-flying sweat bees suffers at low light levels. *J. Exp. Biol.* 210, 4034–4042. doi: 10.1242/jeb.003756

Theobald, J. C., Greiner, B., Weislo, W. T., and Warrant, E. J. (2006). Visual summation in night-flying sweat bees: a theoretical study. *Vision Res.* 46, 2298–2309. doi: 10.1016/j.visres.2006.01.002

Warrant, E. J. (2008a). Seeing in the dark: vision and visual behaviour in nocturnal bees and wasps. *J. Exp. Biol.* 211, 1737–1746. doi: 10.1242/jeb.015396

Warrant, E. J. (2008b). "Nocturnal vision," in *The Senses: A Comprehensive Reference*, Vol. 2, eds T. D. Albright and R. H. Masland (Oxford: Academic Press), 55–86. doi: 10.1016/b978-012370880-9.00297-8

Warrant, E. J., Kelber, A., Gislén, A., Greiner, B., Ribi, W., and Wcislo, W. T. (2004). Nocturnal vision and landmark orientation in a tropical halictid bee. *Curr. Biol.* 14, 1309–1318. doi: 10.1016/j.cub.2004.07.057

Wehrhahn, C., Hausen, K., and Zanker, J. M. (1981). Is the landing response of the housefly driven by motion of a flowfield? *Biol. Cybern.* 41, 91–99. doi: 10.1007/BF00335364

Conflict of Interest Statement: The authors declare that the research was conducted in the absence of any commercial or financial relationships that could be construed as a potential conflict of interest.

frontiers in Physiology

ORIGINAL RESEARCH
published: 30 March 2016
doi: 10.3389/fphys.2016.00099

Hunting in Bioluminescent Light: Vision in the Nocturnal Box Jellyfish *Copula sivickisi*

Anders Garm[1]*, *Jan Bielecki*[2], *Ronald Petie*[1] and *Dan-Eric Nilsson*[3]

[1] Marine Biological Section, Department of Biology, University of Copenhagen, Copenhagen, Denmark, [2] Department of Ecology evolution and Marin Biology, University of California, Santa Barbara, Santa Barbara, CA, USA, [3] Vision Group, Department of Biology, Lund University, Lund, Sweden

Cubomedusae all have a similar set of six eyes on each of their four rhopalia. Still, there is a great variation in activity patterns with some species being strictly day active while others are strictly night active. Here we have examined the visual ecology of the medusa of the night active *Copula sivickisi* from Okinawa using optics, morphology, electrophysiology, and behavioral experiments. We found the lenses of both the upper and the lower lens eyes to be image forming but under-focused, resulting in low spatial resolution in the order of 10–15°. The photoreceptor physiology is similar in the two lens eyes and they have a single opsin peaking around 460 nm and low temporal resolution with a flicker fusion frequency (fff) of 2.5 Hz indicating adaptions to vision in low light intensities. Further, the outer segments have fluid filled swellings, which may concentrate the light in the photoreceptor membrane by total internal reflections, and thus enhance the signal to noise ratio in the eyes. Finally our behavioral experiments confirmed that the animals use vision when hunting. When they are active at night they seek out high prey-concentration by visual attraction to areas with abundant bioluminescent flashes triggered by their prey.

Keywords: cubozoa, night active, eyes, spectral sensitivity, foraging

OPEN ACCESS

Edited by:
Robert Huber,
Bowling Green State University, USA

Reviewed by:
Netta Cohen,
University of Leeds, UK
Rhanor Gillette,
University of Illinois at Urbana-Champaign, USA

***Correspondence:**
Anders Garm
algarm@bio.ku.dk

Specialty section:
This article was submitted to Invertebrate Physiology, a section of the journal Frontiers in Physiology

Received: *17 October 2015*
Accepted: *01 March 2016*
Published: *30 March 2016*

Citation:
Garm A, Bielecki J, Petie R and Nilsson D-E (2016) Hunting in Bioluminescent Light: Vision in the Nocturnal Box Jellyfish Copula sivickisi. Front. Physiol. 7:99. doi: 10.3389/fphys.2016.00099

INTRODUCTION

Within Cnidaria a small group, the cubozoans, have diverged to evolve an elaborate visual apparatus along with an according expansion of their nervous systems (Satterlie, 1979; Garm et al., 2007). The cubomedusae, or box jellyfish, all possess a similar set of 24 eyes distributed on four sensory structures called rhopalia. Each rhopalium holds eyes of four morphologically distinct types, the upper lens eye, the lower lens eye, the pit eyes, and the slit eyes, and offer a clear example of special purpose eyes (Yamasu and Yoshida, 1976; Pearse and Pearse, 1978; Matsumoto, 1995; Nilsson et al., 2005; Garm et al., 2008). The optics have been investigated only in two species, *Tripedalia cystophora* and *Chiropsella bronzie*. In these species, the lens eyes provide low spatial resolution in the order of 10° or worse (Nilsson et al., 2005; O'Connor et al., 2009). This does not allow visually guided hunting for prey. Instead they use vision to seek out habitats with high prey densities. This is best understood for the Caribbean species, *T. cystophora*, which feed on copepods accumulating in light shafts between the mangrove prop roots (Buskey, 2003; Garm et al., 2011). They avoid the dark roots but are attracted to the light shafts where the positively phototactic copepods gather. Once in the right habitat they hunt passively with extended and trailing tentacles and the actual prey capture is no different from the typical scypho- and hydromedusa which rely on the prey accidentally contacting a tentacle.

The small eyes (pupil diameter <100 μm) of *T. cystophora* agree with their diurnal activity pattern: they are only found hunting between the prop roots during the day and rest on the bottom at night (Garm et al., 2012). Still, in all other examined species it seems to be different. Several species are found actively swimming both day and night, but unfortunately most of the data originates from tank experiments which might induce artificial behaviors (Yatsu, 1917; Satterlie, 1979). In one case, the Australian *Chironex fleckeri,* individuals have been tagged in the wild, and the tracking revealed that this species has great variations between individuals but at least some were just as active during dark hours as during the day (Gordon and Seymour, 2009). Whether they hunt and capture prey during the night is still unknown though. Interestingly, one species, *Copula sivickisi*, from the Indo Pacific is strictly night active and sits inactive and attached to the substrate during the day (Garm et al., 2012). This species is predominantly associated with coral reefs where it hunts a variety of planktonic crustaceans in the surface waters at night. Like *T. cystophora* they have internal fertilization and mating happens in the dark only (Hartwick, 1991; Lewis and Long, 2005; Garm et al., 2012, 2015). Despite the strictly nocturnal behavior, they still have the same set of small eyes (**Figure 1**) as the day active *T. cystophora*. How they locate each other or prey items in the dark is unknown and could in principle be governed by random swimming and accidental encounters. But this would be rather inefficient, unless prey, and mate densities are very high. In a recent paper we suggested an alternative method (Garm et al., 2012). At least at Okinawa, Japan, *C. sivickisi* are co-localized with the bioluminescent dinoflagellate *Pyrocystis noctiluca* which is constantly triggered to emit light by encounters with a variety of planktonic crustaceans (Garm et al., 2012). We hypothesized that the medusa of *C. sivickisi* are attracted by the flashes of blue light and thereby aggregate in areas with high prey densities.

Here we test the hypothesis that *C. sivickisi* locate areas of high prey densities using the bioluminescent signals from *P. noctiluca.* We focused on the lens eyes since they are the only image forming eyes and examined their optics and used electroretinograms (ERGs) to investigate their receptor physiology, including spectral sensitivity and temporal resolution. Further, we conducted behavioral experiments to test if they are attracted by the flashes emitted by *P. noctiluca*. All the results clearly support the hypothesis.

MATERIALS AND METHODS

Experimental Organisms

Medusa of *C. sivickisi* were collected using light traps in the harbor at Akajima, Okinawa, Japan, and brought back to Akajima Marine Science Laboratory (AMSL) where they were kept in 40–80 l tanks with seawater at 29°C and 33 psu, and fed *Artemia* or copepods daily. The traps attracted medusae of both sexes and all sizes (1.5–8 mm in diameter). The electrophysiological experiments on the temporal resolution was carried out at AMSL using 10 adult animals of both sexes, but for spectral sensitivity measurements, 15 juvenile medusae were brought back to University of Copenhagen and raised to mature size during 4–5 weeks. They were raised in a 50 l tank at 29°C and 33 psu and fed SELCO enriched *Artemia* daily. Circulation in the tank was created by aeration and half the water was exchanged every other week. The behavioral experiments were conducted at AMSL using adult males and females (bell diameter 8–10 mm) within 3 days of capture. The dinoflagellate, *P. noctiluca*, was caught at nighttime in the harbor using a 100 μm plankton net. After manually sorting them from the rest of the plankton samples they were kept in a 60 l tank under natural light conditions at AMSL.

Anatomical Model

As a basis for our analyses of visual optics, a geometrically accurate model was made of the two lens eyes and their position in the rhopalium. The model was based on histological sections as well as fresh rhopalia photographed from the front, the side and from above. The shape of excised fresh lenses, together with histological sections, were used to determine the position and dimensions of all optically relevant structures. The model was based on five rhopalia from five fully-grown medusae.

Focal-Length Measurements in the Lens Eyes

Fresh lenses from the lens eyes were excised from the eye by tearing the retinal cup with two needles, one on either side of the lens. Roughly 50% of the attempts delivered seemingly intact lenses. The isolated lenses were placed in seawater on a microscope slide and covered by a cover-slip, which was supported to form a 1 mm deep cavity. The lens was arranged such that the longest axis was perpendicular to the incoming light, as would be the case in an intact eye. The microscope condenser was removed and a pinhole of 0.5 mm was placed 10 cm below the preparation. Images were then taken through a high numeric aperture objective (x50), focusing first at the lens equator and then at every 10 μm to a distance well below the depth of best focus. Measurements were performed on five lenses from lower lens eyes and three lenses from upper lens eyes.

Electrophysiology

For measurements of the dynamic range and spectral sensitivity, extracellular ERG recordings were obtained from seven lower lens eyes and seven upper lens eyes originating form 11 adult individuals of both sexes. A maximum of two rhopalia were used per animal and only one eye from each rhopalium. Rhopalia were dissected from the animals by cutting the rhopalial stalk and afterwards they were transfered to a petri dish in the electrophysiological setup containing seawater (29°C, salinity 33 psu). A custom made glass suction electrode was placed on the edge of either the upper or the lower lens eye and suction was applied until a slight migration of pigment into the electrode was observed. The diameter of the electrode tip was 1–3 μm resulting in an impedance of 2–5 MOhm. Recordings were amplified 1000 times and filtered (0.1 Hz high pass, 1000 Hz low pass, and 50 Hz notch filter) via a differential AC amplifier (1700, A-Msystems Inc., WA) and recorded using a custom made program for Labview (Labview 8.5, National Instruments, TX). The light stimulus was provided by an ultra-bright white LED (Luxeon III

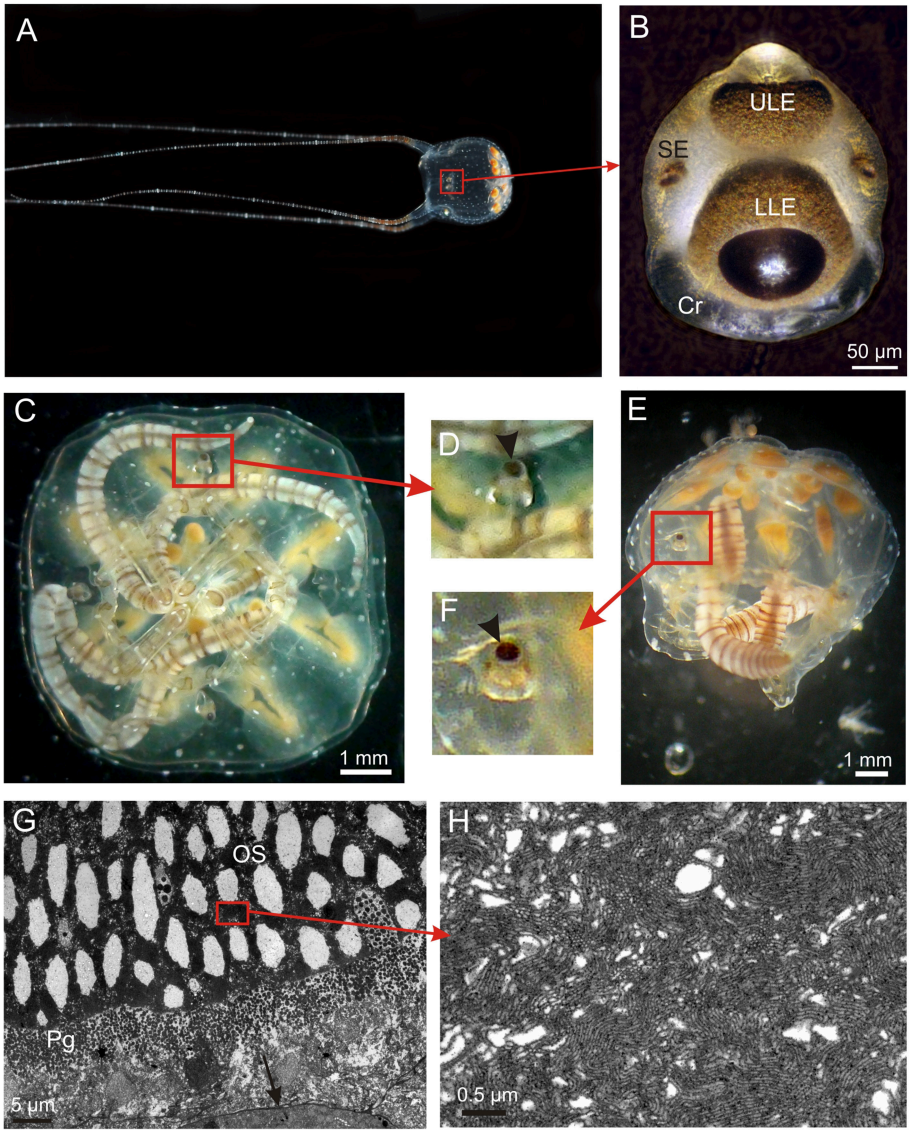

FIGURE 1 | The visual system of *Copula sivickisi*. **(A)** An adult male fishing with outstretched tentacles. Framed area indicates location of one of the rhopalia. **(B)** Close up of a rhopalium showing four of the six eyes. Note the large crystal (Cr) distally. **(C)** Resting medusae lying upside down but the rhopalia still orient with the upper lens eye pointing straight upwards due to the heavy crystal. **(D)** Close up of framed area in **(C)** showing upright rhopalium, arrowhead indicates upper lens eye. **(E)** Medusa laying on the side still having upright rhopalia. **(F)** Close up of framed area in **(E)** showing upright rhopalium, arrowhead indicates upper lens eye. **(G)** TEM micrograph of photoreceptors in the lower lens eye. The outer segments (OS) are modified cilia, and the photoreceptors also contain screening pigment (Pg). Note apparent holes in the outer segments. **(H)** Close up of OS showing the cilia projecting densely packed microvilli. LLE, lower lens eye; SE, slit eye; ULE, upper lens eye.

star, Philips, San Jose, CA) placed in a Linos microbench system (Linos, Goettingen, Germany). The microbench was equipped with a series of neutral density filters and interference color filters (half width = 12 nm, CVI laser, Bensheim, Germany). The stimulus was presented to the eye using a 1 mm light guide close to the pupil to create a close to even illumination of the entire visual field.

The experimental protocol started with 15 min of dark adaptation. Then an intensity series was presented covering four log units in steps of 0.3 or 0.7 log units starting at the low intensity end (1.1×10^{1}W/sr/m^2). This was followed by an equal quanta (6×10^{18} photons/s/sr/m^2) spectral series covering 410–680 nm in 20 steps and the protocol ended with a 2nd intensity series to ensure that the sensitivity had not changed during the experiment. Each stimulus lasted 25 ms and the stimuli were presented with 1 1/2 min in between. Only data from eyes lasting a full protocol, where the 2nd intensity series differed <15% from the 1st, were used for the analysis. This similarity between the two V-log I curves also shows that the initial dark adaptation, stimulus duration, and inter stimulus times were long enough to avoid a change in adaptational state during the experiments. The data were analyzed manually in the program Igor Pro 6.12A

(Wavematrics, Lake Oswego, Oregon). The spectral data were transformed by the V-log I curve to obtain the relative sensitivity (see Coates et al., 2006 for details on this procedure).

The temporal resolution of the lens eyes was examined using flicker fusion frequency (fff) experiments. Five upper lens eyes and five lower lens eyes were presented with a sinusoidal stimulus for 10 s covering the frequency spectrum 0.5–20 Hz in 0.5 Hz steps while recording the ERG as described above. Initially, the eyes were adapted for 10 min to the mid intensity of the stimulus, which was followed by the sinusoidal stimuli starting at the low frequency end with 2 min at mid intensity between. A full protocol thus lasted 90 min. The recordings were analyzed using a fast forward fourier transformation on what equals five stimulus cycles. The returned value at the principle frequency was normalized and used to create an fff curve.

Behavioral Experiments

Nine fully grown medusae were placed in a 20 l tank with seawater at 29°C and 33 psu and without circulation. The experiment was conducted within the natural activity period of the medusae at 10 p.m. and the medusae had last been fed the night before. The tank was kept in a fully darkened room and the animals were left for 30 min to adjust to the tank. A similar tank next to the medusa tank with the same conditions held ∼300 *P. noctiluca* caught between 24 and 48 h prior to the experiments. The two tanks were separated by 0.5 cm to minimize possible transfer of vibrations. After the 30 min, aeration was started in the *P. noctiluca* tank and continued for 2 min. The bubbling had a frequency of 2–3 Hz and triggered the bioluminescence immediately. The behavioral response to the bioluminescence was recorded using a Sony handycam (Sony DCR-HC44) under infrared light (IR-65LED, Loligo Systems, Denmark; peak wavelength = 850 nm, intensity at surface = 27.5 $W/m^2/sr$). The video was analyzed in a custom made program for Matlab 2013b (Mathwork, Inc., Natick, MA, USA) which tracked the position of the medusae from 2 min before the onset of the bioluminescence to 2 min after with a 2 s time resolution. In a further analysis of the video recording the tank was divided in four equally sized horizontal sectors (#1 closest to the bioluminescence, #4 the furthest away) and it was noted in which sector each of the medusae were positioned again with a time resolution of 2 s.

RESULTS

Morphology

In *C. sivickisi* the rhopalia carry the six eyes, as typical for cubozoans (**Figures 1A,B**). The rhopalia hang in the rhopalial niche suspended on a flexible stalk. Along with the heavy crystal in the distal end, this results in the rhopalium always keeping the same vertical orientation with the upper lens eye pointing straight upwards (**Figures 1C–F**). The sections of the lens eyes show that they have the same structure with a thin cornea, a slightly elliptic lens, a thin vitreous space, upright ciliary photoreceptors also holding the brown screening pigment, and retinal associated neurons (**Figure 1G**). The lens cells appear dead and devoid of organelles in the center while the peripheral cells facing the retina have nuclei and other organelles. The photoreceptors of the two lens eyes are very similar and have outer segments of 40–70 μm depending on the area of the retina, with the central ones being the longest. The outer segments form dense layers of microvilli arising from a single cilium (**Figures 1G,H**). Interestingly, the outer segments in both lens eyes have large empty swellings along the central axis appearing like holes in the retina (**Figure 1G**).

Optics

Isolated fresh lenses were slightly ellipsoidic with the longer axes in the pupil plane (**Figures 2A,B**). Using a compound microscope to project parallel light through the lens we determined the focusing properties of the lens by measuring the width of the beam as a function of distance behind the lens. Lenses from both the upper and lower eyes brought light to a focus at a surprisingly short distance—approximately 100 μm. At the plane of best focus, the beam was converged to a diameter of 15–20% of the lens diameter. To account for the variation in eye size and lens size (about ± 25%) we normalized all measurements to units of lens diameter and plotted the beam profile in an anatomical model of the eye (**Figures 2A–E**). This demonstrated that the plane of best focus is at the base of the retina in both the upper and lower lens eyes. Even though the f-number (focal ratio) is lower than that found in the related jellyfish *T. cystophora*, we estimate that the spatial resolution will be roughly the same, i.e., 10–20° in both upper and lower lens eyes (compare **Figures 2A,B,F–H**).

Dynamic Range

The electrophysiologically recorded dynamic range was very similar in the upper and lower lens eyes, and flashes of light with varying intensity resulted in graded impulse responses typically biphasic (**Figure 3A**). The dynamic range covered at least four log units from 1.1 × 10 to 1.1 × 10^5 $W/m^2/sr$ (**Figures 3A**, **4A**). It might well be broader tough, since the V-Log I curves showed no sign of saturation in the high intensity end (**Figure 4A**).

Spectral Sensitivity

The spectral sensitivity curves were also very similar in the two lens eyes. They had a single peak in the deep blue part of the visual spectrum around 460 nm (**Figure 5**). Using the least square of the mean method to fit the spectral sensitivity curve of the lens eyes to theoretical absorption curves of opsins (Govardovskii et al., 2000), returned the best match in both lens eyes to a single opsin peaking at 458 nm (**Figure 5**). In contrast to linear models where the R^2 is commonly used, the goodness of fit for non-linear models is best described by Akaike's Information Criterion (AIC). The AIC for the opsin fit was −53.7 and −35.9 for the upper and lower lens eye, respectively. Note that more negative values reflect a better model fit.

Temporal Resolution

The temporal resolution of the two lens eyes was tested using two different methods, a direct and an indirect. In the indirect method the width at half height of the impulse response was measured, indicating a difference between the two eyes. The upper lens eye showed a decreasing half width with increasing

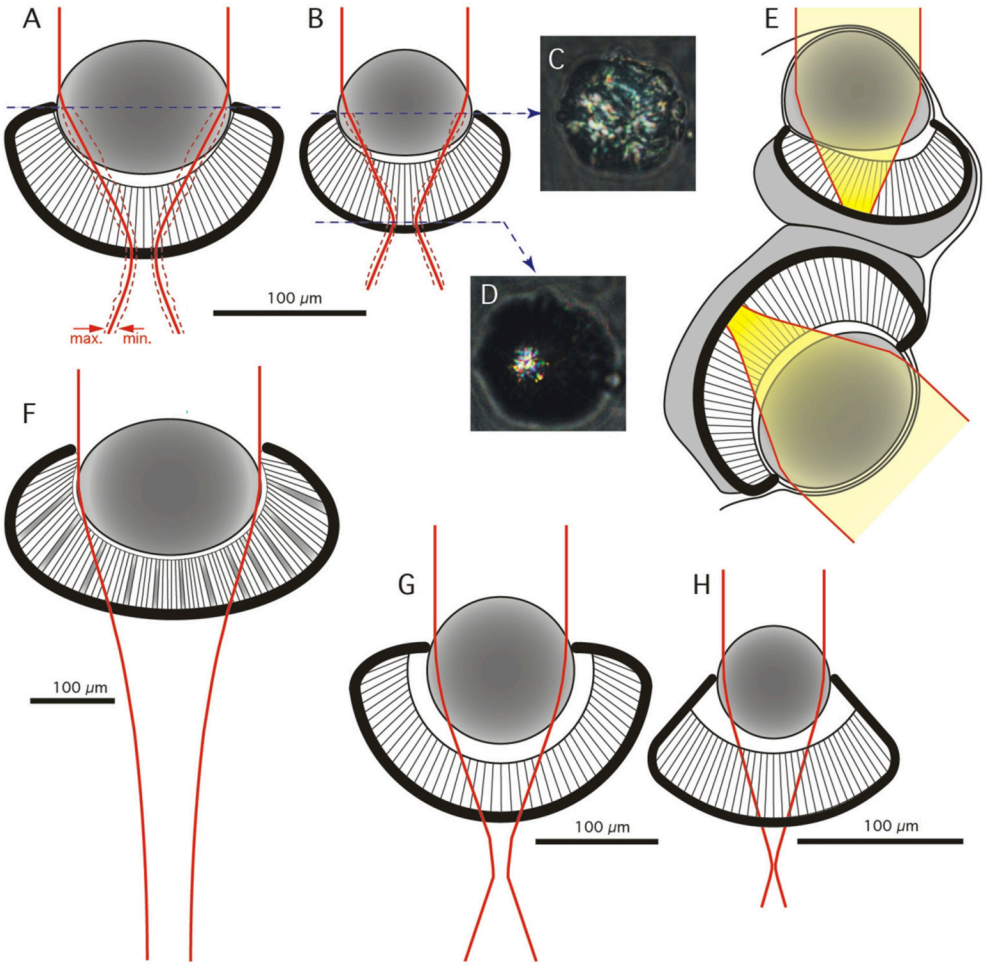

FIGURE 2 | Geometrical model and optics of the lens eyes. (A,B) Frontal view of anatomical models of the lower **(A)** and upper (**B**) lens eye of *C. sivickisi*. Red line indicates average beam width of a distant point light source, broken red lines indicate maximum and minimum beam width ($N = 5$ in **A** and $N = 3$ in **B**). **(C,D)** Examples of the appearance of beam cross-sections behind a lens of the upper lens eye photographed at the lens equator and at the focal plane. **(E)** The average beam profilers from **(A,B)** plotted in the sagittal plane of the rhopalium. The yellow field highlights beam width for a point source and thus the blur spot in the retina. **(F)** Optical model of the lower lens eye of *Chiropsella bronzie* for comparison (modified from O'Connor et al., 2009). **(G,H)** Optical models of the lower and upper lens eyes of *Tripedalia cystophora* respectively (modified from Nilsson et al., 2005).

light intensity of the 25 ms flashes, and at the highest intensity the half width was 29 ± 0.5 ms (mean ± SEM; **Figure 4B**). The lower lens eye was slower at all tested intensities and had a minimal half width of 42 ± 4 ms (mean ± SEM; **Figure 4B**). The flicker fusion frequency (fff) experiments provided stable responses to the sinusoidal stimulus throughout the entire stimulation period (**Figure 3B**). Interestingly, when measuring the temporal resolution with this direct method the difference between the upper and lower lens eyes disappeared. Both eyes were very slow and showed a close to linear decline in the response to a sinusoidal flicker going from 0.5 to 2.5 Hz (**Figures 3B**, **4C**). Above 2.5 Hz no response was seen and the fff is thus ∼2.5 Hz for both eyes. At low frequencies, <1.5 Hz the response peak preceded the stimulus peak putatively due to build in temporal filters. The same is seen for *T. cystophora* (O'Connor et al., 2010).

Response to Bioluminescence from *Pyrocystis noctiluca*

When the tank holding the nine medusae was kept in darkness, the medusae displayed what we consider to be a natural foraging behavior, swimming slowly with their tentacles fully or partly extended near the surface. They did not distribute evenly but preferred the ends of the tank over the middle part (**Figures 6A**, **7**), which is a natural consequence of random exploratory behavior. Importantly, they spent the same amount of time in the two ends (two-sided unpaired student t-test, $p = 0.88$). There was a marked change in behavior soon after the aeration was turned on and the bioluminescence initiated (**Figure 6B**). Some medusae swam directly to the end of the tank toward the bioluminescence and stayed there throughout the 2 min. Others took 10–20 s before swimming toward the light but all medusae spend most of the 2 min in zone 1 close closest to the bioluminescence

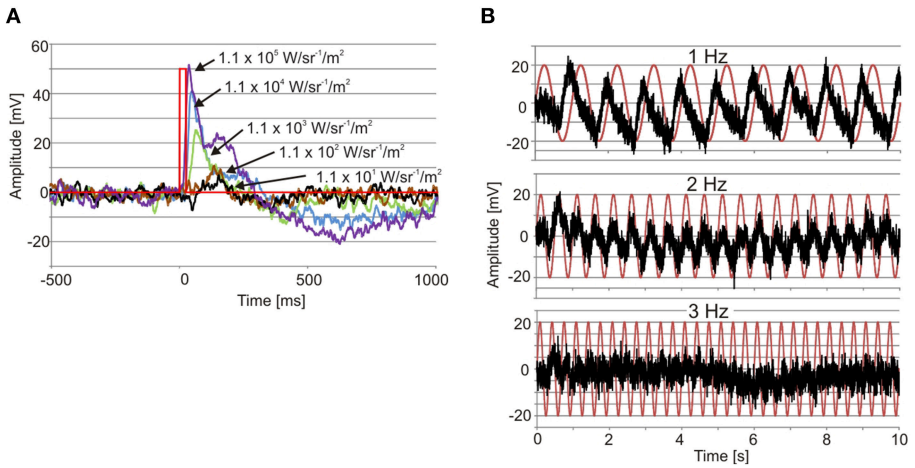

FIGURE 3 | Examples of ERGs. (A) Recordings from an upper lens eye showing the graded impulse response to 25 ms flashes of light (red line) covering four log units. Note also the longer time to peak with declining light intensity. **(B)** Recording from a lower lens eye showing the responses to 1, 2, and 3 Hz sinusoidal light stimuli (red traces). Note that the response peaks before max intensity at 1 Hz.

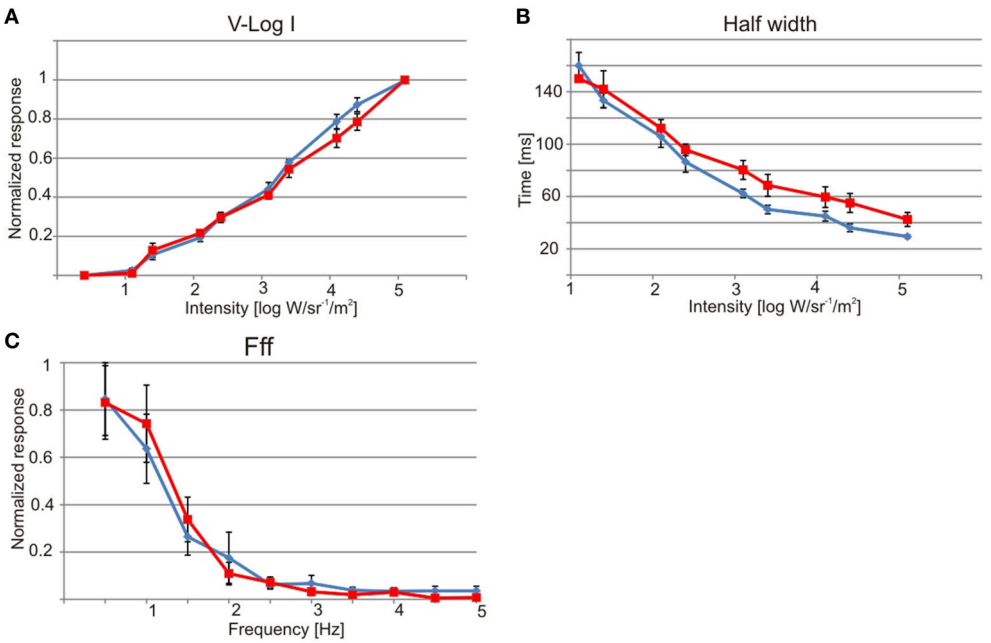

FIGURE 4 | Physiology of the lens eyes. Upper lens eye (ULE) in blue and lower lens eye (LLE) in red. **(A)** V-log I curve showing a dynamic range of about four log units from ~10 to 1 × 10^5 W/sr/m^2. **(B)** The half width of the impulse response decrease with increasing intensity. At max intensity the half width was 29 ms for ULE and 42 ms for LLE. **(C)** Both lens eyes are very slow and had flicker fusion frequencies (fff) of about 2.5 Hz. All curves are showing mean ± S.E.M. $N = 7$, except for **(C)** where $N = 5$.

flashes (**Figure 6B**). In the 2 min with bioluminescence the medusae spent significantly more time in zone 1 than any of the other zones of the tank (two-sided unpaired student *t*-test, $p > 0.0001$). They also spent significantly more time in zone 1 during activation of the bioluminescence than in darkness and less time in zone 4 (two-sided unpaired student *t*-test, $p = 0.027$ and 0.028, respectively). At the end of the 2 min, two medusae started mating (**Figure 6B**, parallel blue and green trace).

DISCUSSION

Our results show that the lenses of both lens eyes of *C. sivickisi* form under-focused images on the retinae, generating poor spatial resolution with large blur spots in the range of 10–20° depending on retinal location. Further, the eyes are color-blind, having a single opsin with peak sensitivity in the blue part of the spectrum close to 460 nm. Both lens eyes have very low temporal

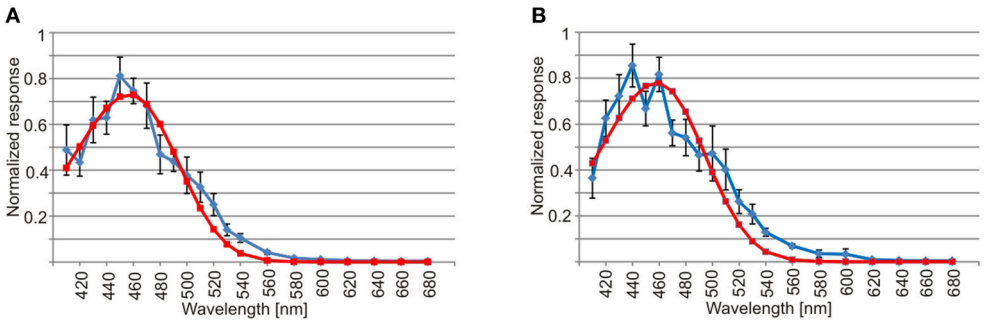

FIGURE 5 | Spectral sensitivity of the lens eye. (A) The spectral sensitivity curve of the upper lens eye (blue line) has a single peak in the deep blue part of the spectrum and has a good match with the absorption curve of a 458 nm opsin (red line, AIC = −53.7). **(B)** Similar to the upper lens eye the spectral sensitivity of the lower lens eye (blue line) peaks in the deep blue part of the spectrum and had a best match with a single opsin peaking a 458 nm (red line, AIC = −35.9). The curves are showing mean ± S.E.M., $N = 7$.

resolution with fff's around 2.5 Hz. We also show that under dark conditions the medusae are attracted to bioluminescent flashes produced by the dinoflagellate *P. noctiluca*, which is occurring in high densities in their natural habitat. In conclusion all data support our hypothesis, that the medusae use vision to find parts of the habitat where hunting will be most successful. They are unlikely, however, to use vision to directly spot or pursue individual prey items due to their low spatial resolution.

Low Intensity Vision for Spotting Bioluminescence

So far *C. sivickisi* is the only cubomedusa known to be strictly night active (Garm et al., 2012). Still, they have a visual system similar to all other examined cubomedusae. Our morphological data show that the lens eyes of *C. sivickisi* are structurally similar to other box jellyfish eyes (Claus, 1878; Berger, 1900; Yamasu and Yoshida, 1976; Pearse and Pearse, 1978; Nilsson et al., 2005). Fully grown, the upper and lower lens eyes have a diameter of about 150 and 200 µm, respectively. In general, small eyes with pupils in the order of 100 µm provide only low spatial resolution, especially at the low light intensities present at night. But our results also point to several features, both in the morphology and in the physiology, which will enhance the photon capture. The outer segments are relatively long and have very dense membrane stacking when compared to other box jellyfish (Laska and Hündgen, 1982; Martin, 2004; O'Connor et al., 2010). Assuming that this implies more photopigment, it will enhance the photon capture, and can thus be interpreted as adaptation for a nocturnal life-style. If there is more opsin per photoreceptor cell it will also result in additional dark noise, which will set a limit to the dimmest stimulus that can be discriminated from noise (Barlow, 1956).

The photon capture is further optimized by a long integration time shown by the very low temporal resolution with flicker fusion frequencies of about 2.5 Hz. Such long integration time is typically found in night active or deep sea animals and are adaptations for vision in low light intensities (Warrant, 2004; Warrant and Locket, 2004). The long integration times has the obvious disadvantage of causing motion blur of objects moving across the visual field. The large acceptance angles of the photoreceptors, estimated to be 10–20°, will also enhance photon capture but reduce the ability to spot individual bioluminescent flashes. This supports the notion that the lens eye of *C. sivickisi* are tuned for finding the direction toward the densest population of bioluminescent organisms rather than guiding behavior toward single bioluminescent flashes. Detection of bioluminescence is further supported by the spectral sensitivity of the lens eyes peaking close to 460 nm which is a fairly good match with the peak emission of 473–478 nm from *P. noctiluca* (Hastings and Morin, 1991). Further, the flashes typically have a duration between 100 and 200 ms which is slightly faster than the temporal resolution we find for both lens eye and this ensures a maximum photon capture from each flash (Hastings and Morin, 1991).

The slight mismatch between the spectral sensitivity of the photoreceptors and the *P. noctiluca* emission is probably hinting at another important visual task for the medusae. At dawn the medusae come to a rest and anchor themselves to the underside of stony corals (Garm et al., 2012). This means that they have to seek out the coral in the morning light and having a spectral sensitivity in the deep blue part of the spectrum will optimize the contrast between the reef structures and the surrounding ocean water. Clear ocean water peaks at about 450 nm (McFarland and Munz, 1975) whereas coral reef structures, though varying, typically reflect very little blue light and much more in the green and red part of the spectrum (Schalles et al., 2000; Hochberg et al., 2004). The peak sensitivity at about 460 nm could thus be seen as a compromise allowing both habitat recognition and prey detection.

Retinal Cavities for Noise Reduction

As mentioned above, dark noise is a major problem for vision at low light intensities. Interestingly, the retinal structure with a large fraction (about 50%) of empty spaces found in *C. sivickisi* might be a unique way to minimize this problem. In the closely related diurnal species *T. cystophora* the lens eyes have very similar shapes and sizes, but there is much less empty space in the retina (<10–15%; Nilsson et al., 2005). There is a possibility that the retinal cavities are part of the adaptation to a nocturnal

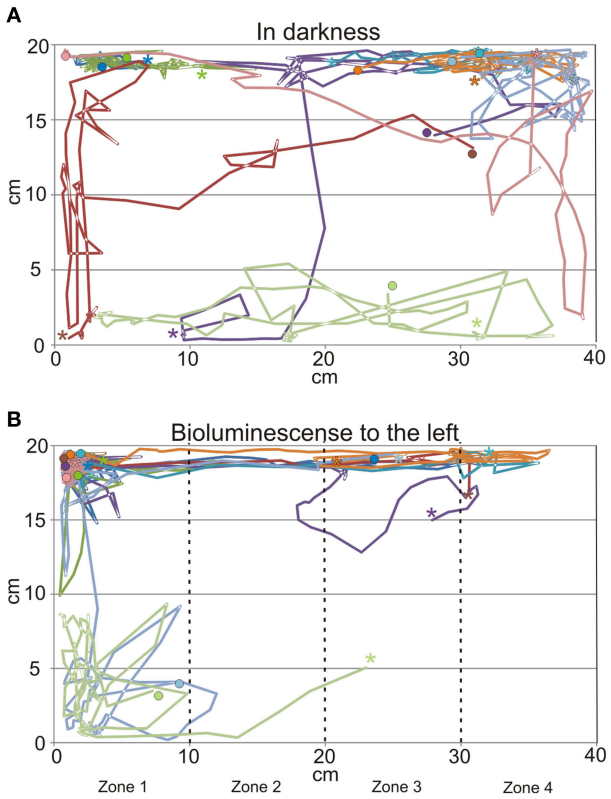

FIGURE 6 | Swim trajectories from behavioral experiments. (A) In darkness the medusae swim in most of the tank but had a preference for the corners of the tank. **(B)** When the dinoflagellate *Pyrocystis noctiluca* is emitting bioluminescent light to the left of the tank the medusae spend most of the time in the left side of the tank. Each trace represents 2 min with 2 s time resolution and each color represents a single medusa ($N = 9$). It is the same nine medusae in **(A,B)** and timewise the trajectories from **(A)** continues in **(B)**. See also **Figure 7**. Note the parallel run of the blue and green trance in the bottom left where a mating started. * indicates start of trajectory, • end.

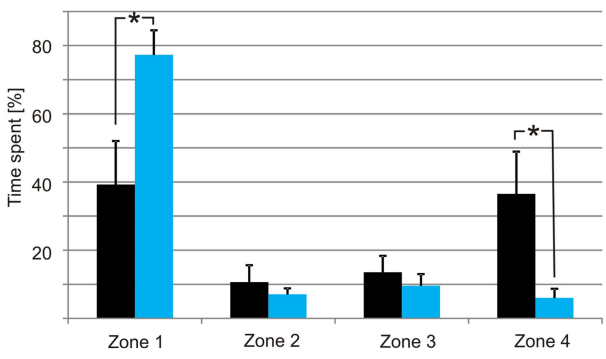

FIGURE 7 | Distribution of the medusae in darkness (black bars) and with bioluminescence (light blue bars). The tank was divided into four zones with zone 1 closest to the tank with *P. noctiluca* and zone 4 the furthest away. In darkness the medusae spend most time at the ends of the tank but with no significant difference between zone 1 and zone 4. When the bioluminescence of the algae is activated the medusae spend most of the time in zone 1. Asterisks indicate significant difference at the 0.05 level. Bars are means ± S.E.M., $N = 9$.

life-style. The longitudinal structure of the empty spaces will concentrate light to the microvillar sections between the spaces, because these have a higher refractive index and will trap some light by total internal reflections. This will boost absorption in the photopigment. The spaces will also reduce the microvillar volume of the retina, and if this means fewer rhodopsin molecules it will lead to less thermal noise. We thus hypothesize that the pronounced cavities in the *C. sivickisi* retina is yet another adaptation for a nocturnal life style, providing both a better signal and less noise. However, without modeling the ray path in the retina and measuring both density and thermal instability of the rhodopsin, it is not possible to assess to which degree the retinal spaces will improve the signal to noise ratio.

Visually Guided Hunting in *C. sivickisi*

Like many other cnidarian medusae, the medusa of *C. sivickisi* is a predator feeding for a large part on pelagic crustaceans (Larson, 1976; Mackie, 1980; Buskey, 2003; Colin et al., 2003; Garm et al., 2012). While most medusae behave as plankton organisms following the currents, cubomedusae are agile swimmers actively choosing their location. Even though a higher number of test animals than used here would be needed to understand the full details of the hunting behavior of *C. sivickisi*, the statistical significance of our results show that they use vision to place themselves in areas with maximum prey density. This they do using the bioluminescence emitted when their crustacean prey contact the dinoflagellate *P. noctiluca* which can be present in high densities in the habitat. The observed mating during the experiments indicates that the results could be influenced by a group effect (tendency to aggregate). Since the medusae in general displayed natural behavior (including mating) in the tank and since they are also found in close vicinity to conspecifics when hunting in the natural habitat we trust that even though a group effect might have been present it has not resulted in unnatural behavior during the experiments.

The hunting behavior of *C. sivickisi* is similar to the diurnal box jellyfish *T. cystophora*, which is visually attracted to light shafts produced by gaps in the mangrove canopy. These light shafts also attract their crustacean prey, and when these occur in large numbers, their light scattering effect makes the light shafts much more visible. The role of vision in *C. sivickisi* and *T. cystophora* is not to spot individual prey animals, which is typically implied by the term "visually guided predation." But both species are clearly engaged in visually guided foraging, and it may be the passive mode of prey capture in medusae that have prevented the evolution of high resolution vision in box jellyfish. In principle terms, the foraging mode of *C. sivickisi* and *T. cystophora* is an important example of a visual task that may drive evolution from low resolution to high resolution vision. It can be seen, therefore, as an important intermediate between simple low resolution vision for habitat selection and the high resolution vision which putatively drove the evolution of large eyes and brains in vertebrates, cephalopods and arthropods (Nilsson, 2009, 2013).

AUTHOR CONTRIBUTIONS

AG designed the experiments, conducted some of the experiments, wrote the initial draft of the MS incl the figures, and financed most of the work. JB conducted some of the experiments. RP conducted some of the experiments. DN conducted some of the experiments and financed part of the work. All authors helped finalize the MS.

ACKNOWLEDGMENTS

The authors greatly appreciate the technical assistance of Lis M. Frederiksen, University of Copenhagen and Eva Landgren, Lund University. We also acknowledge the financial support from the Villum Foundation (to AG, grant# VKR022162), The Danish Research Council (to RP grant# DFF – 4002-00284) and from the Swedish Research Council (to D-EN, grant 2011-4768).

REFERENCES

Barlow, H. B. (1956). Retinal noise and absolute threshold. *J. Opt. Soc. Am.* 46, 634–639. doi: 10.1364/JOSA.46.000634

Berger, E. W. (1900). *Physiology and Histology of the Cubomedusae, including Dr. F.S. Conant's Notes on the Physiology*. Memoirs from the Biological Laboratory of the Johns Hopkins University, Vol. 4 (Baltimore: The Johns Hopkins Press), 1–83.

Buskey, E. J. (2003). Behavioral adaptations of the cubozoan medusa *Tripedalia cystophora* for feeding on copepod (*Dioithona oculata*) swarms. *Mar. Biol.* 142, 225–232. doi: 10.1007/s00227-002-0938-y

Claus, C. (1878). *Ueber Charybdea Marsupialis*. *Arbeiten aus dem Zoologischen Institut Universität Wien*.

Coates, M. M., Garm, A., Theobald, J. C., Thompson, S. H., and Nilsson, D. E. (2006). The spectral sensitivity in the lens eyes of a box jellyfish, *Tripedalia cystophora*. *J. Exp. Biol.* 209, 3758–3765. doi: 10.1242/jeb.02431

Colin, S. P., Costello, J. H., and Klos, E. (2003). *In situ* swimming and feeding behavior of eight co-occurring hydromedusae. *Mar. Ecol. Prog. Ser.* 253, 309. doi: 10.3354/meps253305

Garm, A., Anderson, F., and Nilsson, D. E. (2008). Unique structure and optics of the lesser eyes of the box jellyfish *Tripedalia cystophora*. *Vision Res.* 48, 1061–1073. doi: 10.1016/j.visres.2008.01.019

Garm, A., Bielecki, J., Petie, R., and Nilsson, D. E. (2012). Opposite patterns of diurnal activity in the box jellyfish *Tripedalia cystophora* and *Carybdea sivickisi*. *Biol. Bull.* 222, 35–45. doi: 10.2307/23188035

Garm, A., Lebouvier, M., and Duygu, T. (2015). Mating in the box jellyfish *Copula sivickisi* - novel function of cnidocytes. *J. Morphol.* 276, 1055–1064. doi: 10.1002/jmor.20395

Garm, A., Oskarsson, M., and Nilsson, D. E. (2011). Box jellyfish use terrestrial visual cues for navigation. *Curr. Biol.* 21, 798–803. doi: 10.1016/j.cub.2011.03.054

Garm, A., Poussart, Y., Parkefelt, L., and Nilsson, D. E. (2007). The ring nerve of the box jellyfish *Tripedalia cystophora*. *Cell Tissue Res.* 329, 147–157. doi: 10.1007/s00441-007-0393-7

Gordon, M. C., and Seymour, J. (2009). Quantifying movement of the tropical Australian cubozoan *Chironex fleckeri* using acoustic telemetry. *Hydrobiologia* 616, 87–97. doi: 10.1007/s10750-008-9594-7

Govardovskii, V. I., Fyhrquist, N., Reuter, T., Kuzmin, D. G., and Donner, K. (2000). In search of the visual pigment template. *Vis. Neurosci.* 17, 509–528. doi: 10.1017/S0952523800174036

Hartwick, R. F. (1991). Observations on the anatomy, behaviour, reproduction and life cycle of the cubozoan *Carybdea sivickisi*. *Hydrobiologia* 216/217, 171–179. doi: 10.1007/BF00026459

Hastings, J. W., and Morin, J. G. (1991). "Bioluminescence," in *Neural and Integrative Animal Physiology*, ed C. L. Prosser (New York, NY: Wiley-Liss, Inc.), 131–170.

Hochberg, E. J., Atkinsonn, M. J., and Apprill, A. A. (2004). Spectral reflectance of coral. *Coral Reefs* 23, 84–95. doi: 10.1007/s00338-003-0350-1

Larson, R. J. (1976). "Cubomedusae: feeding, functional morphology, behaviour, and phylogenetic position," in *Coelanterate Ecology and Behaviour*, ed G. O. Mackie (New York, NY: Plenum Press), 237–245.

Laska, G., and Hündgen, M. (1982). Morphologie und ultrastruktur der lichtsinnesorgane von *Tripedalia cystophora* conant (Cnidaria, Cubozoa). *Zool. Jb. Anat.* 108, 107–123.

Lewis, C., and Long, T. A. F. (2005). Courtship and reproduction in *Carybdea sivickisi* (Cnidaria: Cubozoa). *Mar. Biol.* 147, 477–483. doi: 10.1007/s00227-005-1602-0

Mackie, G. O. (1980). Slow swimming and cyclical "fishing" behavior in *Aglantha digitale* (Hydromedusae: Trachylina). *Can. J. Fish. Aquat. Sci.* 37, 1550–1556. doi: 10.1139/f80-200

Martin, V. J. (2004). Photoreceptors of cubozoan jellyfish. *Hydrobiologia* 530/531, 135–144. doi: 10.1007/s10750-004-2674-4

Matsumoto, G. I. (1995). Observations on the anatomy and behaviour of the cubozoan *Carybdea rastonii* Haacke. *Mar. Freshw. Behav. Physiol.* 26, 139–148. doi: 10.1080/10236249509378935

McFarland, W. N., and Munz, F. W. (1975). Part II The photic environment of clear tropical seas during the day. *Vision Res.* 15, 1063–1070. doi: 10.1016/0042-6989(75)90002-4

Nilsson, D. E. (2009). The origin of eyes and visually guided behaviour. *Proc. R. Soc. Lond. B Biol. Ser.* 364, 2833–2847. doi: 10.1098/rstb.2009.0083

Nilsson, D. E. (2013). Eye evolution and its functional basis. *Vis. Neurosci.* 30, 5–20. doi: 10.1017/S0952523813000035

Nilsson, D. E., Gislén, L., Coates, M. M., Skogh, C., and Garm, A. (2005). Advanced optics in a jellyfish eye. *Nature* 435, 201–205. doi: 10.1038/nature03484

O'Connor, M., Garm, A., and Nilsson, D. E. (2009). Structure and optics of the eyes of the box jellyfish *Chiropsella bronzie*. *J. Comp. Physiol. A* 195, 557–569. doi: 10.1007/s00359-009-0431-x

O'Connor, M., Nilsson, D.-E., and Garm, A. (2010). Temporal properties of the lens eyes of the box jellyfish *Tripedalia cystophora*. *J. Comp. Physiol. A* 196, 213–220. doi: 10.1007/s00359-010-0506-8

Pearse, J. S., and Pearse, V. B. (1978). Vision in cubomedusan jellyfish. *Science* 199, 458. doi: 10.1126/science.22934

Satterlie, R. A. (1979). Central control of swimming in the cubomedusan jellyfish *Carybdea rastonii*. *J. Comp. Physiol. A* 133, 357–367. doi: 10.1007/BF00661138

Schalles, J. F., Maeder, J. A., Rundquist, D. C., Narumalani, S., and Keck, J. (2000). "Close range, hyperspectral reflectance measurements of corals and other reef substrates" *Proceedings 9th International Coral Reef Symposium, Vol. 2*, ed M. K. Moosa (Bali: Indonesian Institute of Sciences), 1017–1024.

Warrant, E. J. (2004). Vision in the dimmest habitats on Earth. *J. Comp. Physiol. A* 190, 765–789. doi: 10.1007/s00359-004-0546-z

Warrant, E. J., and Locket, A. N. (2004). Vision in the deep sea. *Biol. Rev.* 79, 671–712. doi: 10.1017/S1464793103006420

Yamasu, T., and Yoshida, M. (1976). Fine structure of complex ocelli of a cubomedusan, *Tamoya bursaria* Haeckel. *Cell Tissue Res.* 170, 325–339. doi: 10.1007/BF00219415

Yatsu, N. (1917). Notes on the physiology of *Charybdea rastonii*. *J. Coll. Sci. Tokyo* 40, 1–12.

Conflict of Interest Statement: The authors declare that the research was conducted in the absence of any commercial or financial relationships that could be construed as a potential conflict of interest.

frontiers in Physiology

ORIGINAL RESEARCH
published: 25 November 2015
doi: 10.3389/fphys.2015.00316

Heat Perception and Aversive Learning in Honey Bees: Putative Involvement of the Thermal/Chemical Sensor AmHsTRPA

Pierre Junca and Jean-Christophe Sandoz *

Evolution, Genomes, Behavior and Ecology, CNRS, Univ. Paris-Sud, IRD, Université Paris-Saclay, Gif-sur-Yvette, France

The recent development of the olfactory conditioning of the sting extension response (SER) has provided new insights into the mechanisms of aversive learning in honeybees. Until now, very little information has been gained concerning US detection and perception. In the initial version of SER conditioning, bees learned to associate an odor CS with an electric shock US. Recently, we proposed a modified version of SER conditioning, in which thermal stimulation with a heated probe is used as US. This procedure has the advantage of allowing topical US applications virtually everywhere on the honeybee body. In this study, we made use of this possibility and mapped thermal responsiveness on the honeybee body, by measuring workers' SER after applying heat on 41 different structures. We then show that bees can learn the CS-US association even when the heat US is applied on body structures that are not prominent sensory organs, here the vertex (back of the head) and the ventral abdomen. Next, we used a neuropharmalogical approach to evaluate the potential role of a recently described Transient Receptor Potential (TRP) channel, HsTRPA, on peripheral heat detection by bees. First, we applied HsTRPA activators to assess if such activation is sufficient for triggering SER. Second, we injected HsTRPA inhibitors to ask whether interfering with this TRP channel affects SER triggered by heat. These experiments suggest that HsTRPA may be involved in heat detection by bees, and represent a potential peripheral detection system in thermal SER conditioning.

Keywords: insects, thermoreception, nociception, aversive learning, AmHsTRPA

OPEN ACCESS

Edited by:
Sylvia Anton,
Institut National de la Recherche Agronomique, France

Reviewed by:
Andre Fiala,
Georg-August-Universität Göttingen, Germany
Tatsuhiko Kadowaki,
Nagoya University, Japan

***Correspondence:**
Jean-Christophe Sandoz
sandoz@egce.cnrs-gif.fr

Specialty section:
This article was submitted to Invertebrate Physiology, a section of the journal Frontiers in Physiology

Received: *17 July 2015*
Accepted: *20 October 2015*
Published: *25 November 2015*

Citation:
Junca P and Sandoz JC (2015) Heat Perception and Aversive Learning in Honey Bees: Putative Involvement of the Thermal/Chemical Sensor AmHsTRPA. Front. Physiol. 6:316. doi: 10.3389/fphys.2015.00316

INTRODUCTION

In associative learning, animals associate sensory stimuli or their own behavioral responses with particular outcomes, possessing a positive or negative hedonic value for the animal. In classical (or Pavlovian) learning, an initially neutral stimulus such as an odor, sound or color (conditioned stimulus–CS) is associated with a salient appetitive or aversive outcome, like the presence of food or of a noxious stimulus (unconditioned stimulus—US; Pavlov, 1927). Learning success critically depends on the salience of the involved stimuli for the animal, especially on the subjective intensity of the US (Rescorla, 1988; Hammer, 1993; Scheiner et al., 2005). Understanding Pavlovian conditioning therefore implies a careful analysis of how a particular US is detected at the sensory

level and how its information is processed within the animal brain.

In honeybees, both appetitive and aversive conditioning can be studied in laboratory conditions thanks to two dedicated protocols (Giurfa and Sandoz, 2012; Tedjakumala and Giurfa, 2013). The conditioning of the proboscis extension response (PER), in which bees associate an odor CS with a sucrose US, is a well-established assay that mimics the final part of bees' foraging behavior, when they experience a floral aroma together with nectar. It has been used for decades for unraveling the neural mechanisms of appetitive learning (Bitterman et al., 1983; Menzel, 1999; Giurfa and Sandoz, 2012). In this paradigm, data are already available about how the sucrose US is detected and processed in the bee brain. Sucrose is detected by dedicated sugar receptors (AmGr1) on gustatory neurons within specific sensilla on the bees' antennae, mouthparts and tarsi (de Brito Sanchez, 2011; Jung et al., 2015). These neurons project to the subesophageal ganglion, where they are thought to directly or indirectly contact a single octopaminergic neuron, VUM-mx1 (ventral unpaired median neuron 1 of the maxillary neuromere), which represents the appetitive reinforcement in the bee brain (Hammer, 1993). It converges at multiple sites with the olfactory pathway, allowing the formation of the odor-sucrose association (Menzel, 1999, 2012).

By contrast, very little information is yet available concerning US detection and perception in aversive conditioning. The most influential aversive learning paradigm is based on the bees' sting extension response (SER). This response represents the final stage of bees' aggressive response to the presence of a potential intruder in front of the hive (Breed et al., 2004), classically elicited by many sensory stimuli (dark colors, moving objects, etc., Free, 1961) and by honeybees' alarm pheromones (Free, 1987). In fixed bee in the laboratory, SER is triggered by noxious stimuli, such as an electric shock (Núñez et al., 1983) or a strong tactile contact (Zhang and Nieh, 2015). In the initial version of the aversive conditioning, bees learned to associate an odor CS with an electric shock US (Vergoz et al., 2007; Roussel et al., 2009). As the electric shock is an unnatural stimulus for bees, a recent study proposed a modified version of SER conditioning, in which the electric shock is replaced by a thermal stimulation with a heated probe as US (Junca et al., 2014). Heat is a natural stimulus for bees and temperature variations play an important role in the life of honeybees. At the colony level, bees strictly regulate the hives' temperature, as deviations from normal brood temperature results in increased mortality as well as in morphological and behavioral defects (Himmer, 1927; Koeniger, 1978; Tautz et al., 2003; Groh et al., 2004; Jones et al., 2005). High temperatures are critical, and in summer, when temperatures rise above the thermal optimum of the hive (∼34°C), workers stand at the hive entrance and fan their wings to decrease in-hive temperature. Foragers also bring water inside the hive, thereby cooling air temperature (Lindauer, 1954). At the individual level, bees strictly avoid temperatures above 44°C and respond with a sting extension to heat stimulations (Junca et al., 2014). They thus perceive a high temperature as an aversive stimulus, and can associate an odorant with such a heat stimulus.

Changing the nature of the aversive reinforcement has opened new possibilities for studying US detection and processing. Contrary to the electric shock, which requires using EEG gel and does not easily allow topical applications, the heated probe can be used for precisely stimulating particular parts of the bees' body. In the appetitive modality, US perception varies according to which structure is stimulated with sucrose: mouthparts, antennae and foreleg tarsi (Marshall, 1935; Scheiner et al., 2004; de Brito Sanchez et al., 2008). Several studies have dissected the differential contributions of these potential USs in appetitive olfactory learning (Bitterman et al., 1983; Sandoz et al., 2002; Scheiner et al., 2005; Wright et al., 2007; de Brito Sanchez et al., 2008). First, these studies showed that all three locations support some level of conditioning, although sucrose solution applied to the proboscis leads to higher acquisition success compared to antennal or tarsal USs. This effect is thought to be related to the mouthparts' higher sensitivity to sucrose compared for instance to the tarsi (de Brito Sanchez et al., 2008). In addition, the location of the sucrose US can have an effect on the duration of memory retention and the types of memories produced (Wright et al., 2007). PER conditioning with an antenna-only US supports, shorter memory retention (<24 h) than when bees receive the US on the mouthparts (>96 h; Wright et al., 2007). Thus, different US locations may support different learning and/or retention performances. Sucrose detection is limited to a few structures on the bee body, which have evolved to arbor gustatory sensory organs involved in appetitive behaviors. In aversive learning, by contrast, bees learn to associate an odor with a noxious stimulus, potentially leading to an injury. Contrary to the detection of food stimuli, animals must be able to avoid injuries on their whole body. Until now, we showed that thermal stimulation of the antennae, mouthparts and foreleg tarsi all trigger SER and can act as aversive US, yielding a similar learning success (Junca et al., 2014). In the present study, we asked if in bees, the aversive thermal US must be detected by dedicated sensory organs to act as US (as in appetitive conditioning) or if thermal detection is a more general sensory ability and heat applied anywhere on their body may act as US.

The use of heat as US may also allow searching for the involved peripheral receptors. In the animal kingdom, a wide range of receptors belonging to very different families have been shown to be responsible for temperature detection, from cold to extreme heat (Clapham et al., 2001). Among them, Transient Receptor Potential (TRP) channels seem to be especially important (Montell et al., 1985; Clapham, 2003; Voets et al., 2005). In invertebrates, Drosophila possesses several types of TRP channels involved in high temperature detection. Among them, members of the TRPA subfamily are essential for responding to heat, like Painless and dTRPA1 (Tracey et al., 2003; Hamada et al., 2008; Kwon et al., 2010; Neely et al., 2011). Unfortunately, no *TRPA1* receptor is known in honeybees and *AmPain* is poorly described (Matsuura et al., 2009). However, honey bees express HsTRPA, a Hymenoptera-specific non-selective cationic channel belonging to the TRPA subfamily and activated by temperatures above 34°C (honeybee gene: *AmHsTRPA*, Kohno et al., 2010). When expressed in a heterologous system, this channel's current response increases rather monotonically with

increasing temperature without showing any maximum at least until 42°C (it was not tested for higher temperatures). Such response is reminiscent of the SER probability increase observed from room temperature until 65°C in worker bees (Junca et al., 2014). To this day, *HsTRPA* thus represents the best candidate for thermal detection involved in aversive thermal conditioning. This TRP channel is a joint thermal and chemical sensor, being also triggered by exogenous activators like AITC (allyl isothiocyanate), CA (cinnamaldehyde) and camphor (Kohno et al., 2010). Two exogenous inhibitors, Ruthenium Red (RuR) and menthol have also been isolated (Kohno et al., 2010). The existence of both activators and inhibitors for this receptor provides us with the opportunity to test whether HsTRPA is necessary and/or sufficient for thermal detection assessed through SER.

In this study, we first mapped thermal responsiveness all over the honeybee body, by measuring workers' SER after applying heat on 41 different structures. We, then, assessed the aversive olfactory conditioning performances of bees when applying the thermal US on body structures that are not prominent sensory interfaces, the vertex (back of the head) and the ventral abdomen. We next used a neuropharmalogical approach to evaluate the role of HsTRPA for heat detection. First, we performed topical applications of HsTRPA activators on the bee to assess if it is sufficient for triggering SER. Second, we injected HsTRPA inhibitors to ask whether interfering with this TRP channel affects SER triggered by heat.

MATERIALS AND METHODS

Animals

Experiments were performed on honey bees caught on the landing platform of several hives on the CNRS campus of Gif-sur-Yvette, France. After chilling on ice, bees were harnessed in individual holders so that both sting- and proboscis extension could be clearly monitored in the same harnessed position. Bees were fed with 5 µl of sucrose solution (50% w/w) every morning to standardize satiety levels and were conserved in a dark and humid box between experiments.

Stimulations

Thermal stimulations were provided for 1 s by means of a pointed copper cylinder (widest diameter: 6 mm; length: 13 mm), mounted onto the end of a minute soldering iron running at low voltage (HQ-Power, PS1503S). Temperature at the end of the cylinder was controlled using a contact thermometer (Voltcraft, Dot-150). Sucrose stimulations were provided for 1 sec with a soaked toothpick to the bees' antennae.

Thermal Sensitivity Map of the Bee Body

We first aimed at determining whether noxious thermal stimulation of the bees' different body parts triggers a SER and if thermal sensitivity varies among them. Thermal stimulations (65°C for 1 s) were applied on 41 different areas of the bees' body (see **Figure 1A**). Although, bees' encounters with such a high temperature would be very rare in natural conditions, this stimulation was chosen in order to study bees' thermal nociceptive system. Recent studies in Drosophila have shown that insects possess a nociceptive system which quickly and strongly responds to potentially deadly temperatures and allows them to avoid such stimuli (Tracey et al., 2003; Neely et al., 2011). Our previous work already showed that a short (1 s) stimulation at this temperature triggers clear SER responses when applied on the antennae, the mouthparts or the forelegs of the bees, without inducing any long-lasting effect on bees (Junca et al., 2014). Eleven median unpaired structures were tested: labrum, clypeus, back of the head, mesoscotum, mesosternum, 1-2, 3-4 sternites, 5-6 sternites, 1-2 tergites, 3-4 tergites, 5-6 tergites. Fifteen paired body parts were also tested on the left or right side independently: antenna flagellum, antenna scape, compound eye, mandible, proximal forewing, distal forewing, protarsus, protibia, profemur, mesotarsus, mesotibia, mesofemur, metatarsus, metatibia, metafemur. To avoid any fatigue of the bees, only four structures were tested per bee. In addition to thermal stimulations, tactile controls were applied on the same structures to verify that sting extension was a consequence of thermal stimulation. Tactile stimulations were performed with a duplicate copper probe which remained at ambient temperature. For each bee, the order of stimulation of the different structures, as well as whether each stimulation was performed with the heated or with the control probe, were determined randomly prior to starting the experiment. The eight stimulations were performed at 10 min intervals. In this experiment, two groups of 20 bees were tested each day.

SER Conditioning with a Thermal US on the Vertex and the Ventral Abdomen

To assess whether or not bees are able to perform aversive olfactory conditioning with a thermal US on body parts that do not correspond to sensory organs, SER conditioning experiments were carried out with a thermal stimulus (65°C) on 3-4 sternites or on the back of the head as reinforcement. In a differential aversive conditioning procedure, one odorant (the CS+) was associated with a thermal reinforcement (the US), while another odorant was presented without reinforcement (the CS−). The odor CSs were 2-octanone and nonanal (Sigma Aldrich, Deisenhofen, Germany). Five microliters of pure odorant were applied onto a 1 cm^2 piece of filter paper which was transferred into a 20 ml syringe (Terumo, Guyancourt, France) allowing odorant delivery to the antennae. Half of the honeybees received thermal reinforcement when 2-octanone (odor A) was presented and no reinforcement when nonanal (odor B) was presented, while the reversed contingency was used for the other half of the bees. Both groups were conditioned along 16 trials (8 reinforced and 8 non-reinforced) in which odorants were presented in a pseudo-random sequence (e.g., ABBABAAB) starting with odorant A or B in a balanced way across animals. The inter-trial interval (ITI) was 10 min. Each conditioning trial lasted 36 s. The bee was placed in the stimulation site in front of the air extractor, and left for 18 s before being exposed to the odorant paired with the US. Each odorant (CS+ or CS−) was delivered manually for 4 s. The thermal stimulus started 3 s after odorant onset and finished with the odorant (1 s temperature

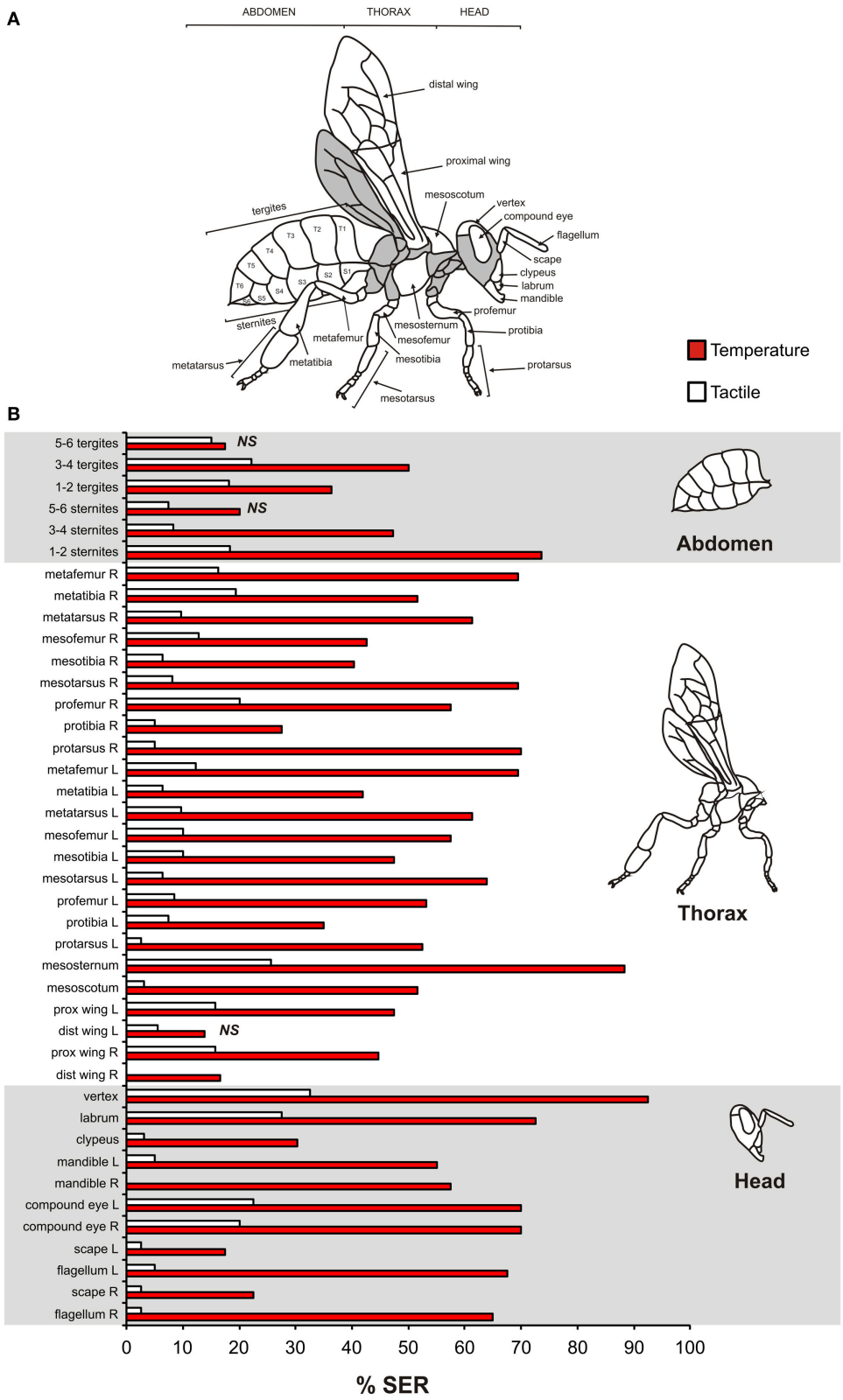

FIGURE 1 | Impact of thermal stimulation of 41 structures of the honeybee body on sting extension responses (SER). (A) Map of the bee body showing the names of the tested structures. Gray areas were not accessible in our holding setups and were thus not tested. **(B)** Percentage of SER observed for thermal stimulations on the 41 different body parts using a heated copper probe ($n = 555$, four structures tested per bee). As control, tactile stimulations with an unheated probe were given. Prox, proximal; dist, distal; L, Left; R, Right.

stimulation). The bee was then left in the setup for 14 s and was then removed. The temperature of 65°C was chosen for the US because this stimulation induced a high rate of SER in the previous experiments. One group of 16 bees was tested daily.

HsTRPA Involvement in Thermal Sting Extension Response

We investigated the putative involvement of the thermal/chemical sensor HsTRPA in heat sensitivity as measured by sting extension. To this end, we evaluated the effects of known HsTRPA activators and inhibitors. We focused on the SER triggered by thermal stimulation on the mouthparts, as this is the US commonly used for aversive thermal conditioning (Junca et al., 2014; Cholé et al., 2015).

In a first experiment, we asked if topical application of a chemical HsTRPA activator on the mouthparts directly triggers SER, as a thermal stimulation does. Kohno et al. (2010) isolated three exogenous molecules able to activate this channel: allyl isothiocyanate (AITC), cynnalmaldehyde (CA), and camphor (Sigma Aldrich, Deisenhofen, Germany). These compounds were applied with a soaked toothpick at two concentrations per drug in distilled water: AITC (1 mM and 100 mM), CA (1 mM and 100 mM), camphor (3 and 300 mM). As controls, thermal stimulation (65°C) as above and a toothpick soaked with distilled water (vehicle) were applied to the mouthparts. Activator solutions and controls were provided in a randomized order with a 10 min interval. Two groups of 18 bees divided in three subgroups for each activator were tested each day.

We also evaluated the effect of injections of HsTRPA inhibitors on SER triggered by heat. A small hole was pricked into the cornea of the median ocellus to allow the insertion of a 1 µl microsyringe (Hamilton company, Reno, Nevada, USA). Different groups of bees were injected with 1 µl Ringer solution, menthol in Ringer, or ruthenium red (RuR) in Ringer (Sigma Aldrich, Deisenhofen, Germany). Two concentrations were tested for each drug: menthol (0.5 and 5 mM), RuR (0.1 and 1 mM). One hour after the injections (Kohno et al., 2010), bees received a thermal stimulation (65°C) and a tactile control on the mouthparts, in a randomized order for each bee. Stimulations were performed at 10 min intervals. In a further experiment, bees were injected with the highest inhibitor concentrations (RuR 5 mM or menthol 1 mM) or Ringer and were then subjected to a thermal responsiveness experiment (Junca et al., 2014). One hour after inhibitor injection, bees received a succession of six stimulations of increasing temperature (from ambient temperature ∼25 to 75°C), in steps of 10°C. Thermal stimulations alternated with tactile controls, provided as above with an identical unheated probe. Stimulations were applied during 1 s and the bees' SER was noted.

We also verified that the application of HsTRPA inhibitors did not have any non-specific deleterious effects on bees' behavioral responsiveness. We thus chose to assess their potential effect on bees' PER responses to sucrose. After injections with the inhibitors (RuR 5 mM, menthol 1 mM) or Ringer, we performed a typical sucrose responsiveness protocol as described in Scheiner et al. (2004). Bees were presented sucrose solutions of increasing concentration, following an exponential progression (0, 0.1, 0.3, 1, 3, 10, 30% w/w). Sucrose stimulations were alternated with water controls. Sucrose and water stimulations were provided with a soaked toothpick to the bees' two antennae simultaneously, and the PER (extension or not of the proboscis) was noted.

Each trial lasted 38 s. One bee at a time was placed in the setup, and left for 20 s before stimulus application started. The stimulation lasted for 1 s. The bee was then left in the setup for 17 s before being removed. For a given bee, all stimulations were performed at 10 min intervals.

Statistical Analysis

All recorded data were dichotomous, with a sting or proboscis extension being recorded as 1 and a non-extension as 0. When comparing the responses of the same bees to thermal and tactile stimulations on the different structures composing the heat sensory map, pairwise McNemar comparisons were used. Differences in thermal or in tactile responses among body structures were assessed using a Chi^2 test. When comparing responses to thermal or tactile stimuli across wider areas (lateralization, core/periphery, body parts), Chi^2 tests were used. For pairwise comparisons, as body parts were composed of three structures (head, thorax, abdomen), each structure was involved in two comparisons. A Bonferroni correction for multiple comparisons was thus applied, and the significance threshold was $\alpha_{corr} = 0.05/2 = 0.025$. When analyzing within group the effect of topical applications of HsTRPA activators, McNemar tests were used to compare drug application to water control. To compare between groups the responses of bees injected with HsTRPA inhibitors or vehicle, Fisher's exact test were used. As three groups were involved, the significance threshold was corrected for multiple comparisons as $\alpha_{corr} = 0.025$. To analyze thermal and sucrose responsiveness curves or aversive conditioning curves, we used repeated measure ANOVAs with stimulus (thermal vs. tactile, sucrose vs. water or CS+ vs. CS−) and trial as repeated factors. For aversive conditioning, following standard procedures, only bees which responded to the US at least three times in the course of acquisition were kept for analysis (vertex: 2%; 3-4 sternites: 29%). To test the effect of inhibitors on thermal and sucrose responsiveness, thermal, or sucrose response curves were compared using repeated measure ANOVAs with drug as a between-group factor. Monte Carlo studies have shown that it is permissible to use ANOVA on dichotomous data only under controlled conditions, which are met in these experiments (Lunney, 1970). Statistical tests were performed with STATISTICA 5.5 (Statsoft, Tulsa, USA).

RESULTS

Thermosensory Map of the Bee Body Assessed by Sting Extension

We first aimed to map the heat sensitivity of the different parts of the honeybee body, by applying a heated probe and measuring sting extension responses (SER). Heat was applied for 1 s, and heat stimulations were alternated with tactile controls in a pseudo-randomized order. In total, 41 different structures were tested (**Figure 1A**, four structures tested per bee, $n = 555$ bees).

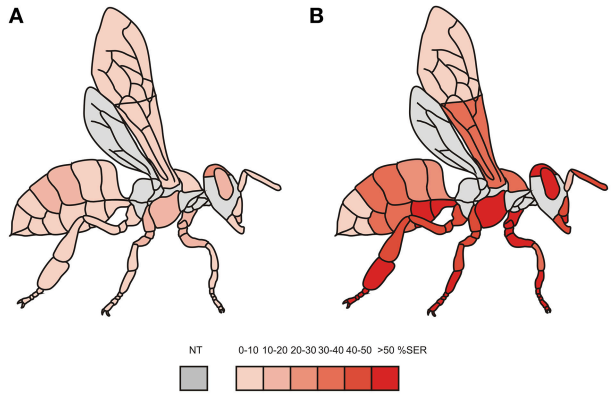

FIGURE 2 | Tactile and heat sensitivity maps obtained by measuring sting extension responses. The maps represent the percentage of SER observed after tactile **(A)** or thermal **(B)** stimulation of each structure of the bee body, using a color scale from light red (0–10% of SER) to dark red (>50% of SER). Gray areas were not accessible in our holding setups and were thus not tested (NT). Sting extensions are mainly due to thermal input as seen from the comparison of both maps.

Figure 1B presents the percentage of responses obtained for each structure to heat and to the tactile control. The proportion of SER to heat stimulation varied among tested structures (Chi^2 test: $Chi^2 = 235.7$, $P < 0.001$, 40 df, from 13.9% SER for the left distal wing to 92.5% SER for the dorsal part of the head (vertex)). Likewise, responses to tactile control stimulations varied according to the tested structure (Chi^2 test: $Chi^2 = 104.8$, $P < 0.001$), from 0% SER (right mandible and right distal wing) to 32% SER (vertex). Overall, 38 out of the 41 tested structures exhibited significantly higher responses to heat than to the tactile control (McNemar test: $Chi^2 > 4.17$, $p < 0.05$; exceptions: left distal wing, 5.6 sternites, 5.6 tergites: $Chi^2 < 1.78$, NS).

Figure 2 presents the same data on a schematic individual, using a color scale from light red (0–10% of SER) to dark red (>50% of SER). This map shows strong variations in the responses of the different body parts to heat stimulations, more so than for tactile stimulations. To evaluate this observation statistically, we next analyzed the responses of different body parts according to their localization (**Figure 3**). First, we asked whether bees' tactile and heat sensitivities are lateralized (**Figure 3A**). We found that responses to tactile and to heat stimuli were identical between the bees' left and right appendages (tactile: $Chi^2 = 0.10$, 1 df, NS; temperature: $Chi^2 = 0.04$, 1 df, NS). Second, we asked if a difference in sensitivity exists between the honeybees' body and its different appendages (**Figure 3B**). We found that SER were significantly more frequent when stimulating the body than when stimulating the appendages, both for thermal stimulation ($Chi^2 = 10.1$, 1 df, $p < 0.01$) and for tactile stimulation ($Chi^2 = 35.4$, 1 df, $p < 0.001$). Lastly, we examined tactile and heat sensitivity according to the bees' antero-posterior axis (**Figure 3C**). A significant heterogeneity appeared among body parts (head, thorax, abdomen) in the bees' responses to thermal stimuli ($Chi^2 = 14.4$, 2 df, $p < 0.001$) but not to tactile stimuli ($Chi^2 = 5.40$, 2 df, NS). Thermal responses were highest for the head (56.8% SER) and lowest for the abdomen (40.4% SER), and all body parts differed from the others (head/thorax: $Chi^2 = 5.99$, $p < \alpha_{corr} = 0.025$; head/abdomen: $Chi^2 = 15.9$, $p < \alpha_{corr} = 0.025$; thorax/abdomen: $Chi^2 = 6.39$, $p < \alpha_{corr} = 0.025$). We thus conclude that although the whole honeybee body is sensitive to thermal stimuli, differences in thermal sensitivity appear among body parts.

Thermal Aversive Reinforcement on Main Body Structures

If honey bees are able to detect heat on their whole body and to respond with a SER, one may then wonder whether such stimulations may also act as an aversive reinforcement in a conditioning procedure. Our previous work showed that heat application on the antennae, the mouthparts or the front legs may operate as aversive reinforcement in olfactory SER conditioning (Junca et al., 2014). These structures are however all known sensory organs, acting as interfaces between the animal and its environment. Here, we chose two structures, the rear part of the head (vertex) and the ventral abdomen (3-4 sternites), which are not dedicated sensory structures, and asked whether 65°C stimulations of these structures can act as reinforcement in a differential olfactory conditioning procedure. In this protocol, bees had to differentiate between an odor associated with the thermal stimulation (CS+) and an explicitly non-reinforced odor (CS−).

Bees learned the task efficiently in both situations (**Figure 4**). When the vertex was stimulated (**Figure 4A**, $n = 37$), bees' SER to the CS+ increased significantly (from 6 to 54%, ANOVA for repeated measurements—RM-ANOVA, $F_{(7, 238)} = 4.13$, $p < 0.001$), while their responses to the CS- remained low and stable ($F_{(7,238)} = 0.27$, NS). Consequently, bees' responses to the CS+ and CS− developed differently in the course of training (stimulus × trial interaction: $F_{(7, 238)} = 3.89$, $p < 0.001$). When the 3-4 sternites were stimulated (**Figure 4B**, $n = 57$), bees' SER to the CS+ increased along trials (from 9 to 49%, $F_{(7, 392)} = 5.99$, $p < 0.001$) while responses to the CS− did not change throughout the experiment ($F_{(7, 392)} = 1.81$, NS). Accordingly, bees' responses to the CS+ and CS− developed differently in the course of training (stimulus × trial interaction: $F_{(7, 392)} = 7.66$, $p < 0.001$). These results, obtained on the vertex and the ventral abdomen, suggest a general ability of bees to associate odorants (CS) with thermal stimulations on their body (US).

Impact on SER of Topical Applications of HsTRPA Activators

The previous experiments showed that bees perceive a heat stimulus on their whole body and can use this information in the context of aversive conditioning. But how does heat detection take place at the peripheral level? We focused on HsTRPA, so far the only well-described thermal receptor in the honey bee. As a previous study isolated chemical activators of this receptor *in vitro* (Kohno et al., 2010), we first wondered if topical application of these chemicals is sufficient for triggering a SER. We thus evaluated the effect caused by the application on the bees' mouthparts of a toothpick soaked with AITC (allyl

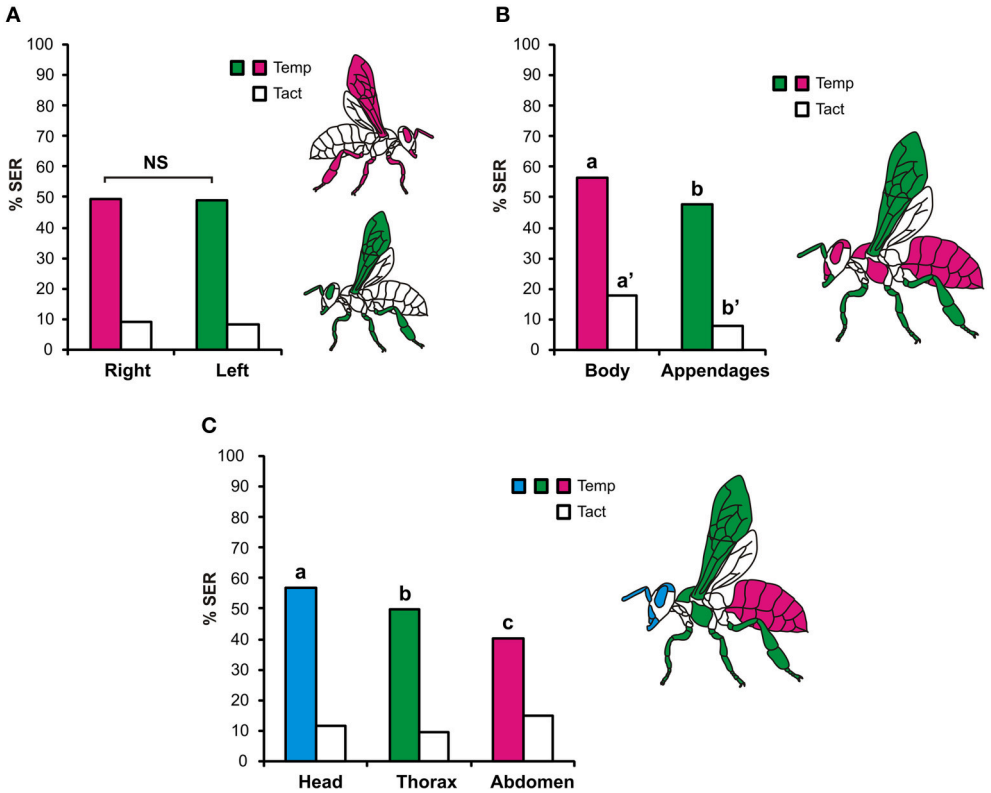

FIGURE 3 | Tactile and heat sensitivity according to the location of the structures. (A) Bilateral symmetry: responses of left (green) or right (magenta) structures were pooled and compared. Stimulations on both sides induced similar SER rates. **(B)** Body/appendages: data were pooled for all appendages (green: antennae, mouthparts, legs, wings) and for main body parts (magenta). Body structures responded significantly more than appendages to both tactile and heat stimulations. **(C)** Heat sensitivity according to the antero-posterior axis: data were pooled separately for head (blue), thorax (green), and abdomen (magenta). A gradient of thermal response intensity was found from head to abdomen. Different letters indicate significant differences in Chi^2 tests.

isothiocyanate), CA (cinnamaldehyde) or camphor, in three groups of animals. We focused here on the mouthparts because thermal stimulation of this structure is routinely used in our aversive conditioning experiments (Junca et al., 2014; Junca et al. in preparation). As controls, identical stimulations with a water-soaked toothpick (solvent control) and a heated copper probe (65°C, positive control) were applied. Stimulations were given at 10 min intervals in a randomized order. Two concentrations of each drug were tested.

At the lower concentrations (**Figure 5A**; 1 mM AITC, $n = 39$; 1 mM CA, $n = 39$; 3 mM camphor, $n = 41$), no effect of the drugs was observed. As expected, honey bees exhibited high SER to the heated probe and low responses to the water control stimulation, with a clear difference between both stimulations (Mc Nemar test, $Chi^2 > 24.04$, $p < \alpha_{corr} = 0.025$). However, drugs generally induced low response rates, which were not statistically higher than the water control (Mc Nemar test, $Chi^2 < 3.20$, NS). At the 100 times higher concentrations (**Figure 5B**; 100 mM AITC, $n = 37$; 100 mM CA, $n = 36$; 300 mM camphor, $n = 36$), one of the three drugs was effective in triggering SER. As above, in all groups, thermal stimulation led to strong responses but the water control did not (Mc Nemar test, $Chi^2 > 24.04$, $p < 0.025$). While CA and camphor application did not elicit any clear response (Mc Nemar test, $Chi^2 < 1.50$, NS), AITC induced 32% SER, which was significantly higher than the water control (Mc Nemar test, $Chi^2 = 8.10$, $p < 0.025$). We thus conclude that only one HsTRPA activator was effective when applied topically on the bees' mouthparts, and only at a very high concentration.

Impact of HsTRPA Inhibitors on Heat Sensitivity

We then asked whether HsTRPA is necessary for bees to detect heat and respond with a sting extension. We focused here on SER triggered by thermal stimulation on the mouthparts, the US commonly used for aversive thermal conditioning (Junca et al., 2014; Cholé et al., 2015). Two chemical inhibitors of HsTRPA have been identified *in vitro* (Kohno et al., 2010), menthol and ruthenium red (RuR). If drug injections provoke a decrease in SER triggered by heat, it would position HsTRPA as a good candidate for high temperature detection. To test this hypothesis, three groups of bees received an injection of 1 µl menthol, RuR, or Ringer (vehicle) as a control, in the median ocellus. After 1 h, bees were then subjected to a thermal stimulation (65°C) to the mouthparts and a tactile control at 10 min intervals in a randomized order. Two concentrations of each drug were tested.

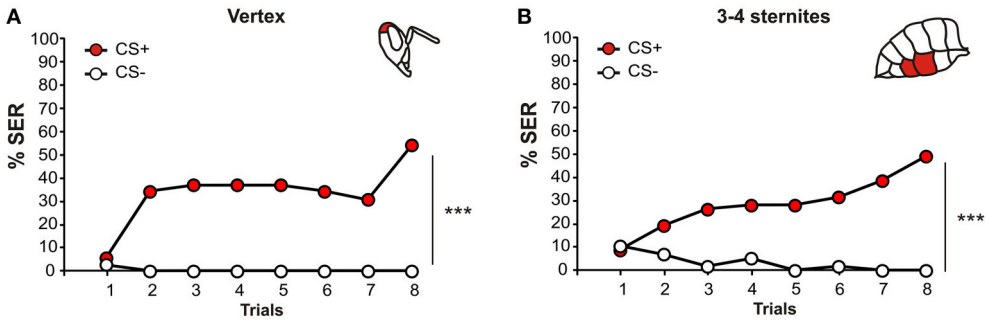

FIGURE 4 | Thermal aversive conditioning with US application on the head and the abdomen. Differential olfactory SER conditioning with a US consisting in thermal stimulation of **(A)** the rear of the head (vertex) or **(B)** the ventral abdomen (3-4 sternites). In both cases, honey bees managed to differentiate between the CS+ (red dots) and the CS− (white dots) along the 8 trials (***$p < 0.001$).

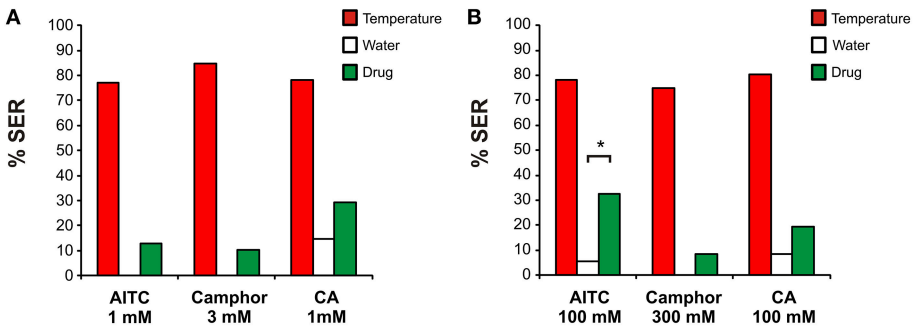

FIGURE 5 | Effect of topical application of HsTRPA activators on sting extension responses. The bees' mouthparts were stimulated with AITC (allyl isothiocyanate), CA (cinnamaldehyde) or camphor at two concentrations, **(A)** 1–3 mM or **(B)** 100–300 mM (all drugs in green). A thermal stimulation (red) or a water control (white) were used as controls. Only 100 mM AITC led to significant SER compared to the water control (*$p < \alpha_{corr} = 0.025$).

When the lower concentrations of inhibitors were tested (**Figure 6A**; 0.5 mM menthol, $n = 40$; 0.1 mM RuR, $n = 39$; Ringer $n = 43$), no effect was observed. In all three groups, honey bees exhibited high SER to the heated probe and low responses to the tactile control, with a clear difference between these stimulations (Mc Nemar test, $Chi^2 > 20.0$, $p < 0.001$). No difference was observed among groups in SER to the thermal stimulation ($Chi^2 = 1.13$, 2 df, NS) or to the tactile control ($Chi^2 = 1.86$, 2 df, NS). At the 10 times higher concentration (**Figure 6B**; 5 mM menthol, $n = 64$; 1 mM RuR, $n = 61$; Ringer $n = 62$), both drugs were effective in blocking SER. Although, in all three groups responses induced by thermal stimuli were still significantly higher than responses to tactile controls (Mc Nemar test, $Chi^2 > 26.0$, $p < 0.001$), SER to the heat stimulus was different among groups ($Chi^2 = 17.4$, 2 df, $p < 0.001$). In particular, responses to heat were lower in both drug-injected groups compared to the Ringer control group (Fisher's exact test, RuR: $Chi^2 = 8.95$, $p < \alpha_{corr} = 0.025$; menthol: $Chi^2 = 17.3$, $p < 0.025$). RuR- and menthol-injected groups displayed comparable rates of SER to the thermal stimulus (Fisher's exact test, $Chi^2 = 1.5$, NS). No difference appeared among groups in SER to the tactile stimulus ($Chi^2 = 0.14$, 2 df, NS).

Thus, HsTRPA inhibitors appear to inhibit SER to heat. We next aimed to confirm and expand this result by characterizing the impact of HsTRPA inhibitors on thermal sensitivity along an increasing temperature gradient, as usually tested for measuring bees' aversive responsiveness (Junca et al., 2014; Junca et al. in preparation). Bees were thus injected with the higher dose of each inhibitor or with Ringer, as above, but were then subjected to a series of thermal stimulations at increasing temperatures on the mouthparts alternated with tactile controls (**Figures 7A–C**). All stimulations were applied at 10 min intervals.

Bees' SER increased significantly with increasing temperature in all three groups (RM-ANOVA, trial effect: Ringer: $n = 40$, $F_{(5, 195)} = 21.6$, $p < 0.001$; RuR: $n = 38$, $F_{(5, 185)} = 10.8$, $p < 0.001$; menthol: $n = 40$, $F_{(5, 195)} = 9.84$, $p < 0.001$). By contrast, responses to alternated tactile stimuli did not increase, and even decreased in the Ringer group, throughout the experiment (RM-ANOVA: ringer: $F_{(5, 195)} = 2.46$, $p < 0.05$; RuR: $F_{(5, 185)} = 1.22$, NS; menthol: $F_{(5, 195)} = 1.05$, NS). Accordingly, in all three groups, responses to the temperature stimulus evolved differently from those triggered by tactile controls (RM-ANOVA, stimulus × trial interaction: Ringer: $F_{(5, 195)} = 24.6$, $p < 0.001$; RuR: $F_{(5, 185)} = 10.2$, $p < 0.001$; menthol: $F_{(5, 195)} = 9.17$, $p < 0.001$]. However, responses to heat were significantly different in the three groups (**Figure 7D**, RM-ANOVA, stimulus effect: $F_{(2, 115)} = 5.47$, $p < 0.01$; stimulus × trial interaction: $F_{(10, 575)} =$

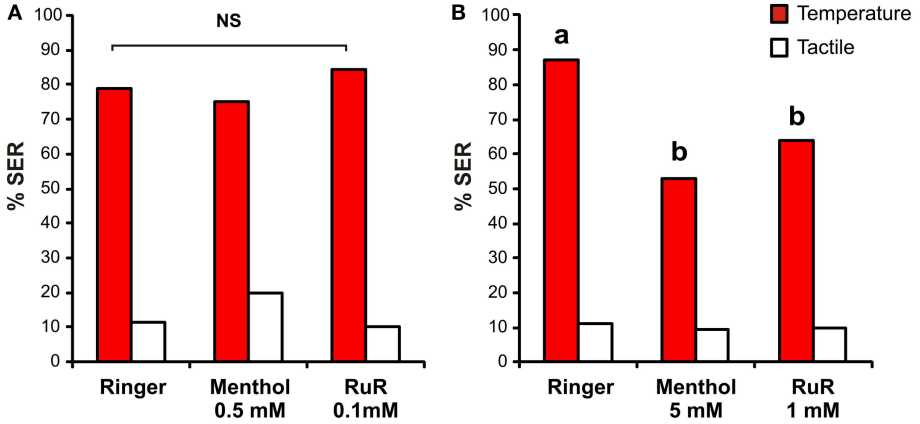

FIGURE 6 | Impact of HsTRPA inhibitors on SER to thermal stimulations. Bees were injected in the median ocellus with menthol, ruthenium red (RuR) or Ringer as control. Sting extensions were recorded in response to 1 sec thermal stimulation (65°C; red) and tactile stimulation (white). **(A)** At low concentration (0.5 mM menthol and 0.1 mM RuR), no effect of the inhibitors appeared. **(B)** At 10 times higher concentrations (5 mM menthol and 1 mM RuR) both drugs significantly inhibited SER responses to heat. Different letters indicate significant differences among groups ($p < \alpha_{corr} = 0.025$).

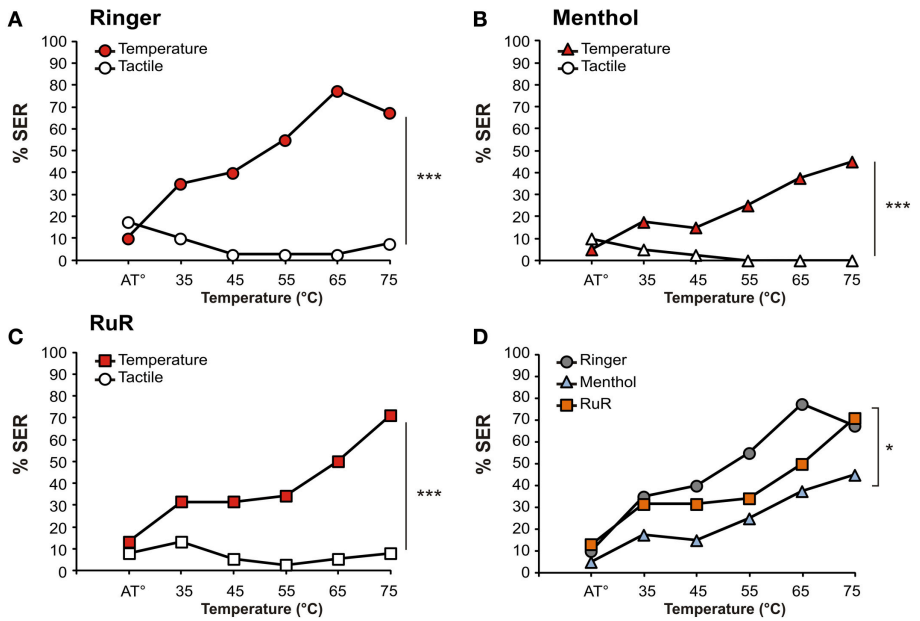

FIGURE 7 | Effect of HsTRPA inhibitors on thermal responsiveness. Different groups of bees were injected with Ringer as control (**A**) or with an HsTRPA inhibitor, either menthol (5 mM; **B**) or ruthenium red (RuR, 1 mM; **C**) SER was measured in response to increasing temperatures (red) alternated with tactile controls (white). **(D)** Comparison of thermal response curves among the three groups (Ringer: gray circles; menthol: light blue triangles; RuR: orange squares). Both inhibitors decreased heat responsiveness (*$p < 0.05$; ***$p < 0.001$).

2.03, $p < 0.05$). In particular, weaker responses were observed in the RuR- and menthol-injected groups compared to the Ringer control (RM-ANOVA, stimulus × trial interaction, Ringer/RuR: $F_{(5, 380)} = 2.59$, $p < 0.05$; Ringer/menthol: $F_{(5, 390)} = 2.78$, $p < 0.05$). No difference appeared between the groups injected with HsTRPA inhibitors (RuR/menthol: $F_{(5, 380)} = 0.73$, NS). Lastly, no difference appeared among groups in the responses to the tactile controls (RM-ANOVA, stimulus effect: $F_{(2, 115)} = 1.29$, NS; stimulus × trial interaction: $F_{(10, 575)} = 0.74$, NS).

The previous experiment confirmed that HsTRPA inhibitors affect thermal responsiveness measured by means of SER. Most probably, this result is due to the effect of the inhibitors on HsTRPA receptors. However, theoretically, it could also be due to a non-specific detrimental effect of the drugs on the bees' physiological state, even though no such effect was apparent by simple observation. In the next experiment, we thus checked the possible effect of HsTRPA inhibitors in another context and another hedonic modality—the appetitive

modality. To this end, we measured bees' PER in a typical sucrose responsiveness protocol (Scheiner et al., 2004). After Ringer or HsTRPA inhibitor injections as above, bees were thus subjected to a series of stimulations on the antennae with sucrose solutions at increasing concentrations alternated with water controls (**Figures 8A–C**). All stimulations were applied at 10 min intervals.

Bees' PER increased significantly with increasing sucrose concentrations in all three groups (RM-ANOVA, trial effect: Ringer: $n = 39$, $F_{(6, 228)} = 21.9$, $p < 0.001$; RuR: $n = 38$, $F_{(6, 234)} = 24.1$, $p < 0.001$; menthol: $n = 40$, $F_{(6, 222)} = 21.9$, $p < 0.001$). Responses to the control water stimulations remained stable for Ringer and menthol but slightly increased for RuR (ringer: $F_{(6, 228)} = 1.63$, NS; RuR: $F_{(6, 234)} = 2.20$, $p < 0.05$; menthol: $F_{(6, 222)} = 1.45$, NS). In all groups, sucrose responses evolved differently from responses to water controls (RM-ANOVA, stimulus × trial interaction: Ringer: $F_{(6, 228)} = 8.03$, $p < 0.001$; RuR: $F_{(6, 234)} = 6.50$, $p < 0.001$; menthol: $F_{(6, 222)} = 10.0$, $p < 0.001$). However, responses evolved similarly in the three groups both for sucrose stimulations (**Figure 8D**; RM-ANOVA, stimulus effect: $F_{(2, 114)} = 1.44$, NS; stimulus × trial interaction: $F_{(12, 684)} = 0.68$, NS) and for the water controls (stimulus effect: $F_{(2, 114)} = 0.85$, NS; stimulus × trial interaction, $F_{(12, 684)} = 0.68$, NS). We conclude that HsTRPA inhibitors have no effect on bees' PER responses to sucrose, suggesting that their effect on heat-evoked SER is not due to a general behavioral impairment.

DISCUSSION

Our study provides the first heat sensitivity map of the honeybee, measured using heat-induced SER. This map reveals that responses are symmetrical between body sides, that body structures are more sensitive than the appendages and it shows a gradual decrease in thermal sensitivity from the head to the abdomen. We then demonstrated that heat application does not need to be located on specific structures (mouthparts, antennae or protarsi) to serve as an aversive US in SER conditioning. Indeed, bees learned successfully when the US was provided on the vertex or on the ventral abdomen (3-4 sternites). Lastly, we observed that HsTRPA activators (AITC, CA, camphor) applied topically on the bees' mouthparts did not easily induce SER (only AITC at the higher dose) whereas inhibitor injections (RuR, menthol) significantly decreased SER to heat. This impact of HsTRPA inhibitors was specific of SER to heat, since no effect was observed on PER responses to sucrose.

Thermal Body Map

We observed that bees' heat sensitivity, as measured by the induced SER, varied among body structures. Control tactile stimulations also led to variations in responses among body structures but on a much smaller scale compared to heat-triggered responses. Thus, most of the observed SER were due to heat application. The map showed clearly that heat detection is a general phenomenon and is not restricted to a few dedicated sensory structures, like the antennae, mouthparts or tarsi (Junca et al., 2014). A possible explanation for this observation may originate from the high temperature (65°C) used for thermal stimulation, which may have induced activation of nociceptive pathways responsible for preserving the animals' physical integrity. Such system should be differentiated from fine-tuned thermosensory pathways which detect temperatures in the physiological range and employ dedicated thermosensitive sensilla (coelocapitular sensilla) on the bee antenna (Lacher, 1964; Yokohari et al., 1982; Yokohari, 1983). The existence of nociceptive pathways in insects has been recently demonstrated in Drosophila larvae, in which the detection and avoidance of noxious heat, bright light, or strong mechanical stimuli is operated by class IV multidendritic neurons that express a range of nocisensor proteins (Im and Galko, 2012). These neurons extend their dendrites within the derma and are widely distributed along the body surface (Hwang et al., 2007). Although, strongly remodeled, they survive through metamorphosis and may play a similar role in adults (Kuo et al., 2005; Shimono et al., 2009). The wide field heat sensitivity we have found in this study would fit with the existence of an analogous neuron family in honeybees. To this day, however, they have not yet been described. Alternately, thermosensation may also involve some of the many sensory hairs present on the bee body. Only a few structures of the bee body did not elicit more SER when they were thermally stimulated than with the tactile control: the tip of the abdomen and the distal part of the forewings. A possible lack of nociceptive neurons in the wings may explain this observation. At the tip of the abdomen, it would seem rather unlikely that nocisensor neurons are utterly absent. Rather, the proximity between the heat stimulus and the sting chamber might have prevented any sting extension, the animal attempting to avoid any internal injuries.

Responses to heat were compared among body parts. First, we did not find any lateralization bias on the paired appendages. The opposite would have been surprising. Indeed, organisms expressing such an asymmetrical perception would suffer from obvious disadvantages (Corballis, 1998). The physical world is indifferent to left and right, and any lateralized deficit might leave an animal vulnerable to attacks on one side or unable to attack prey or competitors appearing on one side (Vallortigara and Rogers, 2005). Second, peripheral structures appeared less sensitive than body structures. This difference was mostly due to a lower sensitivity of appendages to tactile stimuli, which could be related to the fact that appendages are more likely to come in contact with mechanical substrates than the body. Lastly, we observed a gradient of decreasing thermal responsiveness from the head to the abdomen. The brain located in the head capsule contains neuropils essential for processing and integrating information from many sensory modalities (gustatory, olfactory, visual, tactile, etc) as well as for motor control, navigation, learning, and memory processes among others (Menzel, 1999, 2012). Therefore, physical integrity of the head is crucial for bees to be able to assess their environment and exhibit adapted behaviors, and noxious simulations located close to the head should trigger stronger responses.

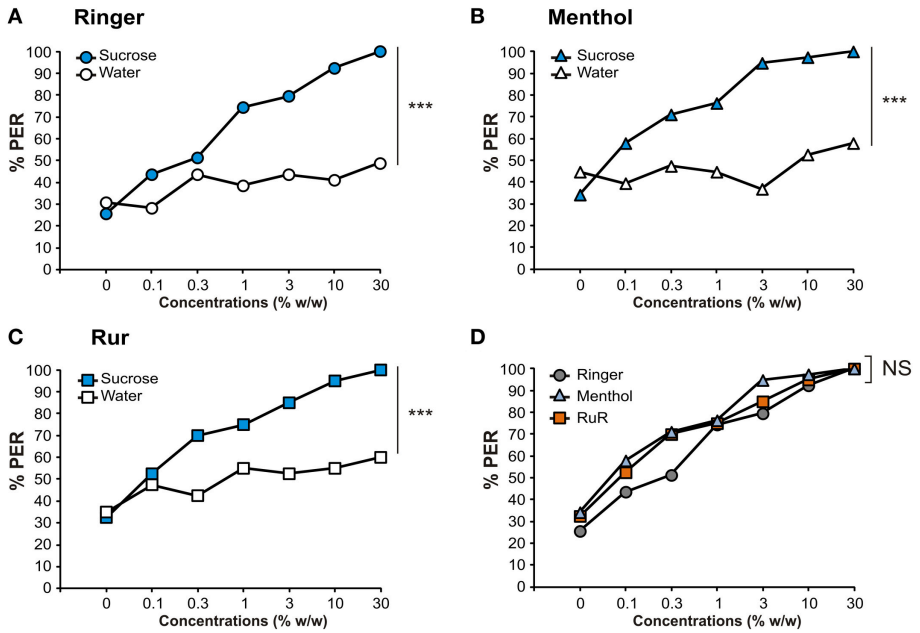

FIGURE 8 | Effect of HsTRPA inhibitors on sucrose responsiveness. Different groups of bees were injected with Ringer as control **(A)** or with a HsTRPA inhibitor, either **(B)** menthol (5 mM) or **(C)** Ruthenium red (RuR, 1 mM). Proboscis extension responses (PER) were measured in response to sucrose solutions at increasing concentrations (blue) alternated with water controls (white). **(D)** Comparison of sucrose response curves among the three groups (Ringer: gray circles; menthol: light blue triangles; RuR: orange squares). Inhibitor injections did not impact sucrose responsiveness (NS: Non Significant; $^{***}p < 0.001$).

SER Learning on the Vertex and the Ventral Abdomen

In a previous study, we demonstrated that thermal SER conditioning is successful with a heat US on the mouthparts, the antennae and the tarsi of the forelegs (Junca et al., 2014). Such structures are well known sensory organs (Hammer, 1993; de Brito Sanchez et al., 2008; Giurfa and Sandoz, 2012; Jung et al., 2015). We show here that heat stimulation on body structures that are not dedicated sensory organs (vertex, ventral abdomen) can also act as US in SER conditioning. This observation supports our current putative neural model of thermal aversive conditioning in honeybees (**Figure 9**). Associative learning relies on the convergence of CS and US information at one or several locations in the brain. The olfactory (CS) pathway is well known in bees (Menzel, 1999; Giurfa, 2007; Sandoz, 2011): axons of olfactory receptor neurons (ORN) located on each antenna project to the antennal lobes (AL) where they synapse with approximately 4000 local interneurons (not shown) and 800 projection neurons (PN). Projection neurons then convey processed information to higher-order brain structures, the mushroom bodies (MB) and the lateral horn (not shown). For aversive learning, the US pathway is mostly unknown, but our results may provide some new clues. Except for the case in which an antenna heat US is used (Junca et al., 2014), and for which thermo-sensory neurons from the antenna are thought to project to the antennal lobe (Yokohari, 1983; Nishino et al., 2009), all other heat stimulations probably rely on thermal detection by the above-mentioned putative multidendritic neurons. It is unlikely that this information also projects to the antennal lobe. Rather, it can be expected from neuroanatomical work in other insects (for instance on the mechanosensory system, Pflüger et al., 1988; Newland and Burrows, 1997) that such putative thermo-sensitive/nociceptive neurons would first project to the respective ganglia of the ventral nerve cord, i.e., to sub-esophageal, thoracic or abdominal ganglia depending on the location of the stimulation (SEG, TG, and AG in **Figure 9**). From there, information could be conveyed by ascending interneurons toward the brain, possibly to a thermal/nociceptive integration center (TNC in **Figure 9**), as suggested by several observations. In the Asian bee *Apis cerana*, immediate early gene (Acks) expression mapping showed that exposure to a high temperature (46°C) induces neural activity in several brain regions: within the mushroom body, intrinsic neurons (class I and II Kenyon cells), and in a region of the protocerebrum located between the dorsal and the optic lobe (Ugajin et al., 2012). Thus, stimulation with a high temperature presumably induces activity in one thermo-sensitive center and in the mushroom bodies, a well-known multimodal integration and association center of the bee brain. Our working hypothesis is that neurons from the putative thermo-sensory center could then activate aversive reinforcement circuits, which would converge with the olfactory pathway and induce learning-associated plasticity, in particular in the mushroom bodies. Previous work on SER conditioning indicated that dopaminergic neurons (dopN in **Figure 9**) are involved in aversive reinforcement, because pharmacological blockade of dopamine receptors disrupts aversive learning (Vergoz et al., 2007). Dopamine neurotransmission is also necessary for aversive learning in other insects (Drosophila,

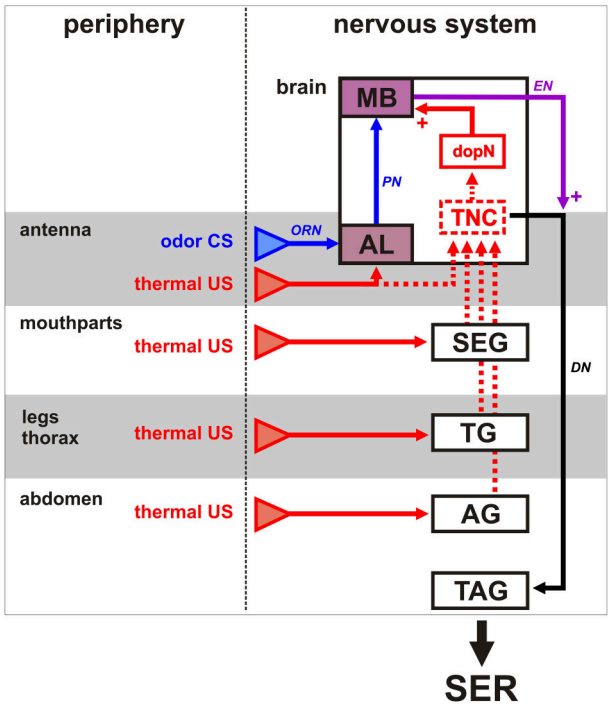

FIGURE 9 | Working model of aversive olfactory conditioning of SER using a thermal US. Putative pathways involved in **(A)** the expression of SER after thermal stimulation, **(B)** the acquired SER after learning a CS-US association, are shown. **(A)** At the periphery, stimulation of the different structures with a high temperature is thought to activate thermosensitive neurons (possibly class IV multidendritic neurons), which would first project to the respective relays on the ventral nerve cord, the subesophageal ganglion (SEG), thoracic ganglia (TG), or abdominal ganglia (AG). As a second step, interneurons would project to a thermal/nociceptive center (TNC) in the brain. Antennal thermal stimulation induces activity in the antennal lobe (AL) but possibly also activates the TNC. Activation of this center would stimulate premotor descending neurons (DN) which would in turn trigger stinging motor patterns in the terminal abdominal ganglion (TAG), producing SER (Ogawa et al., 1995). **(B)** Olfactory learning: odorants are detected on the antenna by olfactory receptor neurons (ORNs) projecting to the AL. Then information is prominently conveyed to the mushroom bodies (MB) by projection neurons (PN). Activation of dopaminergic neurons (dopN) by the TNC would inform the olfactory pathway of the aversive thermal reinforcement. Associative plasticity at the level of MB extrinsic neurons (EN) feeding onto the sting premotor descending neurons would allow the CS to elicit SER after learning.

Schwarzel et al., 2003; Schroll et al., 2006; crickets, Unoki et al., 2005). The bee brain contains a complex arrangement of many dopamine-immunoreactive neurons (Schäfer and Rehder, 1989; Schürmann et al., 1989). Among dopamine neurons, three clusters are especially interesting as they contain processes that project to the mushroom body calyces and lobes (especially the α-lobe), and may thus provide aversive reinforcement information (Tedjakumala and Giurfa, 2013). Co-activation of CS and US pathways could modify the strength of synapses between the specific Kenyon cells representing the learned odorant and mushroom body extrinsic neurons (EN in **Figure 9**) feeding onto the sting extension premotor system. After learning, presentation of the odor CS alone would trigger SER thanks to this modification. Further work is needed to confirm the different putative elements of this working model. The present study started this task by evaluating potential receptors detecting temperature at the periphery (see below).

Putative Involvement of HsTRPA in Heat Perception

We assessed the possible involvement of HsTRPA in heat-triggered SER using topical applications of activators and injections of inhibitors. We observed that topical application of HsTRPA activators is not sufficient for triggering SER, except when a very high concentration (100 mM) of AITC was used as stimulus. This result might appear surprising since all three tested drugs were potent activators of the channel *in vitro* (Kohno et al., 2010). However, if thermosensation is carried out by a similar class of class IV multidendritic neurons as in Drosophila (Im and Galko, 2012), it is likely that the thermal channels are located in the epidermis, i.e., below the cuticle, so that direct contact of the activators with the channel is not possible, or at least difficult. Heat could diffuse through the cuticle to activate the channel, but chemical activators would not. In our view, therefore, this result does not invalidate a potential role of HsTRPA in thermal sensitivity and nociception in bees. Concerning the SER increase observed with AITC stimulation, we cannot be sure at this stage that it is not related to a possible aversive gustatory effect of this compound when presented to the mouthparts, because AITC was found to inhibit PER responses when added to sucrose solution (Kohno et al., 2010). However, in the same study, the effect of AITC was reversed by RuR, suggesting a possible involvement of HsTRPA. Until now no SER in response to bitter or repellent gustatory stimuli has been reported. It will be necessary to test the effect on SER of AITC application on other locations of the bee body, while also checking if known aversive gustatory stimuli (salt or bitter compounds) can trigger SER when applied on the mouthparts. This will be addressed in more details in the future.

Injections of HsTRPA inhibitors produced significant blocking of SER in response to heat. This effect is similar to the reversal of the suppression of PER by heat in previous work (Kohno et al., 2010). In this study, heating a sucrose solution to 70°C was found to decrease bees' PER to sucrose, compared to an unheated solution. Both RuR and menthol restored normal PER responses in the presence of the heated sucrose solution, presumably by blocking HsTRPA activity (Kohno et al., 2010). The effective inhibitor concentrations in our study were about 10 times higher than the concentrations that significantly modified bees' warmth (36.5°C) avoidance in a thermal gradient (0.1 mM RuR and 0.5 mM menthol, Kohno et al., 2010). It is possible that inhibition of the highly-sensitive stinging response requires higher inhibitor concentrations (i.e., more general blocking of HsTRPA channels) than a fine-tuned behavior like warmth avoidance. Alternately, the mode of injection performed in the two studies (ocellar injection in the present study, injection between the antennae in Kohno et al., 2010) might be involved. Performing both experiments in the same conditions may clarify this question. As a control for the effect of the drugs on thermally-induced SER, we tested the effective concentrations on bees' PER to sucrose and found that neither RuR nor menthol

had any effect. If indeed both compounds act on HsTRPA, as we suppose, such a result could have been expected since responses to sucrose are mediated by dedicated gustatory receptors, mostly AmGr1 (Jung et al., 2015). This confirms, however, that RuR and menthol did not reduce SER to heat through a non-specific effect on bees' general responsiveness to stimuli, but rather specifically inhibited their responses to heat.

For the moment, we need to remain cautious about the involvement of HsTRPA in bees' heat sensitivity, as a neuropharmalogical approach alone is not sufficient for demonstrating the role of this TRP channel *per se*. Indeed, the chemical activators and inhibitors we have used are also known to be inhibitors/activators of other members of the TRP family in other species. For instance, in mammals, menthol is able to activate TRPM8 (cold, Behrendt et al., 2004), while RuR is a non-specific inhibitor of TRPM8 (Story et al., 2003) and all four TRPV channels (fine temperature deviation to extreme heat, Clapham et al., 2001; Clapham, 2003). It would thus be especially important in the future to use a technique for blocking HsTRPA more specifically, for instance using RNA interference (Farooqui et al., 2003; Louis et al., 2012), especially because bees express other TRP channels. In invertebrates, channels belonging to the TRPA subfamily are more specifically involved in thermal detection (Matsuura et al., 2009). Most prominently, TRPA1 and Painless have been well described in Drosophila and were shown to be crucial for thermal nociception (Tracey et al., 2003; Hamada et al., 2008; Kohno et al., 2010; Neely et al., 2011). In addition, Pyrexia, another TRP channel, plays a significant part in heat detection and tolerance in this species (Lee et al., 2005). The honeybee genome, as that of other Hymenoptera, does not contain any TRPA1 channel. It is thought that *HsTRPA*, which has evolved from the duplication of an ancestral hygrosensor (*Wtrw*), has gained thermoresponsive properties, which may have resulted in the loss of *TRPA1* in Hymenoptera (Matsuura et al., 2009). Consequently, HsTRPA is considered as a prominent thermosensor in bees and our results suggest it is involved in heat sensitivity leading to SER. However, homologs of the Drosophila genes painless and pyrexia have been described in the honey bee genome, and named *AmPain* and *AmPyr* respectively (Matsuura et al., 2009). It would thus be important to evaluate next the possible involvement of these two channels in heat sensitivity and thermal aversive conditioning. Thanks to the thermal sensitivity map we have established, future studies will be able to compare the relative sensitivity of the different body parts with the expression patterns of *AmHsTRPA*, *AmPain* and *AmPyr* in the bee body. In addition, SER triggered by heat stimulation, coupled to the use of RNA interference will allow testing the involvement of each channel.

In conclusion, this study constitutes a first step for understanding heat perception and aversive SER conditioning in honey bees. Our current results suggest that a RuR- and menthol-sensitive thermal receptor, possibly HsTRPA, is involved in heat sensitivity leading to sting extension and may represent the peripheral US detector in our aversive conditioning protocol.

ACKNOWLEDGMENTS

We are thankful to Hanna Cholé for helpful comments on this manuscript, and to all members of the Evolbee team at CNRS Gif-sur-Yvette for insightful discussions. PJ thanks the French Research Ministry and JCS the CNRS for funding.

REFERENCES

Behrendt, H. J., Germann, T., Gillen, C., Hatt, H., and Jostock, R. (2004). Characterization of the mouse cold-menthol receptor TRPM8 and vanilloid receptor type-1 VR1 using a fluorometric imaging plate reader (FLIPR) assay. *Br. J. Pharmacol.* 141, 737–745. doi: 10.1038/sj.bjp.0705652

Bitterman, M. E., Menzel, R., Fietz, A., and Schäfer, S. (1983). Classical conditioning of proboscis extension in honeybees (*Apis mellifera*). *J. Comp. Psychol.* 97:107. doi: 10.1037/0735-7036.97.2.107

Breed, M. D., Guzman-Novoa, E., and Hunt, G. J. (2004). Defensive behavior of honey bees: organization, genetics, and comparisons with other bees. *Annu. Rev. Entomol.* 49, 271–298. doi: 10.1146/annurev.ento.49.061802.123155

Cholé, H., Junca, P., and Sandoz, J. C. (2015). Appetitive but not aversive olfactory conditioning modifies antennal movements in honeybees. *Learn. Mem.* 22, 604–616. doi: 10.1101/lm.038448.115

Clapham, D. E., Runnels, L. W., and Strübing, C. (2001). The TRP ion channel family. *Nat. Rev. Neurosci.* 2, 387–396. doi: 10.1038/35077544

Clapham, D. E. (2003). TRP channels as cellular sensors. *Nature* 426, 517–524. doi: 10.1038/nature02196

Corballis, M. C. (1998). Cerebral asymmetry: motoring on. *Trends Cogn. Sci.* 2, 152–157. doi: 10.1016/S1364-6613(98)01156-5

de Brito Sanchez, M. G., Chen, C., Li, J., Liu, F., Gauthier, M., and Giurfa, M. (2008). Behavioral studies on tarsal gustation in honeybees: sucrose responsiveness and sucrose-mediated olfactory conditioning. *J. Comp. Physiol. A* 194, 861–869. doi: 10.1007/s00359-008-0357-8

de Brito Sanchez, M. G. (2011). Taste perception in honey bees. *Chem. Senses* 36, 675–692. doi: 10.1093/chemse/bjr040

Farooqui, T., Robinson, K., Vaessin, H., and Smith, B. H. (2003). Modulation of early olfactory processing by an octopaminergic reinforcement pathway in the honeybee. *J. Neurosci.* 23, 5370–5380. Available online at: http://www.jneurosci.org/content/23/12/5370

Free, J. B. (1961). The stimuli releasing the stinging response of honeybees. *Anim. Behav.* 9, 193–196. doi: 10.1016/0003-3472(61)90008-2

Free, J. B. (1987). *Pheromones of Social Bees.* London: Chapman & Hall.

Giurfa, M., and Sandoz, J. C. (2012). Invertebrate learning and memory: fifty years of olfactory conditioning of the proboscis extension response in honeybees. *Learn. Mem.* 19, 54–66. doi: 10.1101/lm.024711.111

Giurfa, M. (2007). Behavioral and neural analysis of associative learning in the honeybee: a taste from the magic well. *J. Comp. Physiol. A* 193, 801–824. doi: 10.1007/s00359-007-0235-9

Groh, C., Tautz, J., and Rössler, W. (2004). Synaptic organization in the adult honey bee brain is influenced by brood-temperature control during pupal development. *Proc. Natl. Acad. Sci. U.S.A.* 101, 4268–4273. doi: 10.1073/pnas.0400773101

Hamada, F. N., Rosenzweig, M., Kang, K., Pulver, S. R., Ghezzi, A., Jegla, T. J., et al. (2008). An internal thermal sensor controlling temperature preference in *Drosophila*. *Nature* 454, 217–220. doi: 10.1038/nature07001

Hammer, M. (1993). An identified neuron mediates the unconditioned stimulus in associative olfactory learning in honeybees. *Nature* 366, 59. doi: 10.1038/366059a0

Himmer, A. (1927). Ein Beitrag zur Kenntnis des Wärmehaushalts im Nestbau sozialer Hautflügler. *J. Comp. Physiol. A* 5, 375–389.

Hwang, R. Y., Zhong, L., Xu, Y., Johnson, T., Zhang, F., Deisseroth, K., et al. (2007). Nociceptive neurons protect *Drosophila* larvae from parasitoid wasps. *Curr. Biol.* 17, 2105–2116. doi: 10.1016/j.cub.2007.11.029

Im, S. H., and Galko, M. J. (2012). Pokes, sunburn, and hot sauce: drosophila as an emerging model for the biology of nociception. *Dev. Dynam.* 241, 16–26. doi: 10.1002/dvdy.22737

Jones, J. C., Helliwell, P., Beekman, M., Maleszka, R., and Oldroyd, B. P. (2005). The effects of rearing temperature on developmental stability and learning and memory in the honey bee, *Apis mellifera*. *J. Comp. Physiol. A* 191, 1121–1129. doi: 10.1007/s00359-005-0035-z

Junca, P., Carcaud, J., Moulin, S., Garnery, L., and Sandoz, J. C. (2014). Genotypic influence on aversive conditioning in honeybees, using a novel thermal reinforcement procedure. *PLoS ONE* 9:e97333. doi: 10.1371/journal.pone.0097333

Jung, J. W., Park, K. W., Ahn, Y. J., and Kwon, H. W. (2015). Functional characterization of sugar receptors in the western honeybee, *Apis mellifera*. *J. Asia Pac. Entomol.* 18, 19–26. doi: 10.1016/j.aspen.2014.10.011

Koeniger, N. (1978). Das Wärmen der Brut bei der Honigbiene (*Apis mellifera* L.). *Apidologie* 9, 305–320. doi: 10.1051/apido:19780404

Kohno, K., Sokabe, T., Tominaga, M., and Kadowaki, T. (2010). Honey bee thermal/chemical sensor, AmHsTRPA, reveals neofunctionalization and loss of transient receptor potential channel genes. *J. Neurosci.* 30, 12219–12229. doi: 10.1523/JNEUROSCI.2001-10.2010

Kuo, C. T., Jan, L. Y., and Jan, Y. N. (2005). Dendrite-specific remodeling of Drosophila sensory neurons requires matrix metalloproteases, ubiquitin-proteasome, and ecdysone signaling. *Proc. Natl. Acad. Sci. U.S.A.* 102, 15230–15235. doi: 10.1073/pnas.0507393102

Kwon, Y., Shen, W. L., Shim, H. S., and Montell, C. (2010). Fine thermotactic discrimination between the optimal and slightly cooler temperatures via a TRPV channel in chordotonal neurons. *J. Neurosci.* 30, 10465–10471. doi: 10.1523/JNEUROSCI.1631-10.2010

Lacher, V. (1964). Elektrophysiologische untersuchungen an einzelnen rezeptoren für geruch, kohlendioxyd, luftfeuchtigkeit und tempratur auf den antennen der arbeitsbiene und der drohne (*Apis mellifica* L.). *Z. Vergl. Physiol.* 48, 587–623. doi: 10.1007/BF00333743

Lee, Y., Lee, Y., Lee, J., Bang, S., Hyun, S., Kang, J., et al. (2005). Pyrexia is a new thermal transient receptor potential channel endowing tolerance to high temperatures in *Drosophila melanogaster*. *Nat. Genet.* 37, 305–310. doi: 10.1038/ng1513

Lindauer, M. (1954). Temperaturregulierung und Wasserhaushalt im Bienenstaat. *Z. Vergl. Physiol.* 36, 391–432. doi: 10.1007/BF00345028

Louis, T., Musso, P. Y., de Oliveira, S. B., Garreau, L., Giurfa, M., Raymond, V., et al. (2012). Amelα8 subunit knockdown in the mushroom body vertical lobes impairs olfactory retrieval in the honeybee, *Apis mellifera*. *Eur. J. Neurosci.* 36, 3438–3450. doi: 10.1111/j.1460-9568.2012.08261.x

Lunney, G. H. (1970). Using analysis of variance with a dichotomous dependent variable: an empirical study. *J. Educ. Meas.* 7, 263–269. doi : 10.1111/j.1745-3984.1970.tb00727.x.

Marshall, J. (1935). On the sensitivity of the chemoreceptors on the antenna and fore-tarsus of the honey-bee, *Apis mellifica* L. *J. Exp. Biol.* 12, 17–26.

Matsuura, H., Sokabe, T., Kohno, K., Tominaga, M., and Kadowaki, T. (2009). Evolutionary conservation and changes in insect TRP channels. *BMC Evol. Biol.* 9:228. doi: 10.1186/1471-2148-9-228

Menzel, R. (1999). Memory dynamics in the honeybee. *J. Comp. Physiol. A* 185, 323–340. doi: 10.1007/s003590050392

Menzel, R. (2012). The honeybee as a model for understanding the basis of cognition. *Nat. Rev. Neurosci.* 13, 758–768. doi: 10.1038/nrn3357

Montell, C., Jones, K., Hafen, E., and Rubin, G. (1985). Rescue of the Drosophila phototransduction mutation trp by germline transformation. *Science* 230, 1040–1043. doi: 10.1126/science.3933112

Neely, G. G., Keene, A. C., Duchek, P., Chang, E. C., Wang, Q. P., Aksoy, Y. A., et al. (2011). TrpA1 regulates thermal nociception in Drosophila. *PLoS ONE* 6:e24343. doi: 10.1371/journal.pone.0024343

Newland, P. L., and Burrows, M. (1997). Processing of tactile information in neuronal networks controlling leg movements of the locust. *J. Insect Physiol.* 43, 107–123. doi: 10.1016/S0022-1910(96)00081-9

Nishino, H., Nishikawa, M., Mizunami, M., and Yokohari, F. (2009). Functional and topographic segregation of glomeruli revealed by local staining of antennal sensory neurons in the honeybee *Apis mellifera*. *J. Comp. Neurol.* 515, 161–180. doi: 10.1002/cne.22064

Núñez, J., Maldonado, H., Miralto, A., and Balderrama, N. (1983). The stinging response of the honeybee: effects of morphine, naloxone and some opioid peptides. *Pharmacol. Biochem. Behav.* 19, 921–924. doi: 10.1016/0091-3057(83)90391-X

Ogawa, H., Kawakami, Z., and Yamaguchi, T. (1995). Motor pattern of the stinging response in the honeybee *Apis mellifera*. *J. Exp. Biol.* 198, 39–47. Available online at: http://jeb.biologists.org/content/198/1/39

Pavlov, I. P. (1927). *Conditioned Reflexes: An Investigation of the Physiological Activity of the Cerebral Cortex*. London: Oxford University Press

Pflüger, H. J., Braunig, P., and Hustert, R. (1988). The organization of mechanosensory neuropiles in locust thoracic ganglia. *Philos. Trans. R. Soc. Lond. B Biol. Sci.* 321, 1–26. doi: 10.1098/rstb.1988.0090

Rescorla, R. A. (1988). Pavlovian conditioning: it's not what you think it is. *Am. Psychol.* 43:151. doi: 10.1037/0003-066X.43.3.151

Roussel, E., Carcaud, J., Sandoz, J. C., and Giurfa, M. (2009). Reappraising social insect behavior through aversive responsiveness and learning. *PLoS ONE* 4:e4197. doi: 10.1371/journal.pone.0004197

Sandoz, J. C., Hammer, M., and Menzel, R. (2002). Side-specificity of olfactory learning in the honeybee: US input side. *Learn. Mem.* 9, 337–348. doi: 10.1101/lm.50502

Sandoz, J. C. (2011). Behavioral and neurophysiological study of olfactory perception and learning in honeybees. *Front. Sys. Neurosci.* 5:98. doi: 10.3389/fnsys.2011.00098

Schäfer, S., and Rehder, V. (1989). Dopamine−like immunoreactivity in the brain and suboesophageal ganglion of the honeybee. *J. Comp. Neurol.* 280, 43–58. doi: 10.1002/cne.902800105

Scheiner, R., Kuritz-Kaiser, A., Menzel, R., and Erber, J. (2005). Sensory responsiveness and the effects of equal subjective rewards on tactile learning and memory of honeybees. *Learn. Mem.* 12, 626–635. doi: 10.1101/lm.98105

Scheiner, R., Page, R. E., and Erber, J. (2004). Sucrose responsiveness and behavioral plasticity in honey bees (*Apis mellifera*). *Apidologie* 35, 133–142. doi: 10.1051/apido:2004001

Schroll, C., Riemensperger, T., Bucher, D., Ehmer, J., Völler, T., Erbguth, K., et al. (2006). Light-induced activation of distinct modulatory neurons triggers appetitive or aversive learning in Drosophila larvae. *Curr. Biol.* 16, 1741–1747. doi: 10.1016/j.cub.2006.07.023

Schürmann, F. W., Elekes, K., and Geffard, M. (1989). Dopamine-like immunoreactivity in the bee brain. *Cell Tissue Res.* 256, 399–410. doi: 10.1007/BF00218898

Schwarzel, M., Monastirioti, M., Scholz, H., Friggi-Grelin, F., Birman, S., and Heisenberg, M. (2003). Dopamine and octopamine differentiate between aversive and appetitive olfactory memories in *Drosophila*. *J. Neurosci.* 23, 10495–10502. Available online at: http://www.jneurosci.org/content/23/33/10495

Shimono, K., Fujimoto, A., Tsuyama, T., Yamamoto-Kochi, M., Sato, M., Hattori, Y., et al. (2009). Multidendritic sensory neurons in the adult Drosophila abdomen: origins, dendritic morphology, and segment-and age-dependent programmed cell death. *Neural Dev.* 4, 10–1186. doi: 10.1186/1749-8104-4-37

Story, G. M., Peier, A. M., Reeve, A. J., Eid, S. R., Mosbacher, J., Hricik, T. R., et al. (2003). ANKTM1, a TRP-like channel expressed in nociceptive neurons, is activated by cold temperatures. *Cell* 112, 819–829. doi: 10.1016/S0092-8674(03)00158-2

Tautz, J., Maier, S., Groh, C., Rossler, W., and Brockmann, A. (2003). Behavioral performance in adult honey bees is influenced by the temperature experienced during their pupal development. *Proc. Natl. Acad. Sci. U.S.A.* 100, 7343–7347. doi: 10.1073/pnas.1232346100

Tedjakumala, S. R., and Giurfa, M. (2013). Rules and mechanisms of punishment learning in honey bees: the aversive conditioning of the sting extension response. *J. Exp. Biol.* 216, 2985–2997. doi: 10.1242/jeb.086629

Tracey, W. D., Wilson, R. I., Laurent, G., and Benzer, S. (2003). painless, a Drosophila gene essential for nociception. *Cell* 113, 261–273. doi: 10.1016/S0092-8674(03)00272-1

Ugajin, A., Kiya, T., Kunieda, T., Ono, M., Yoshida, T., and Kubo, T. (2012). Detection of neural activity in the brains of Japanese honeybee workers during the formation of a "hot defensive bee ball". *PLoS ONE* 7:e32902. doi: 10.1371/journal.pone.0032902

Unoki, S., Matsumoto, Y., and Mizunami, M. (2005). Participation of octopaminergic reward system and dopaminergic punishment system in insect olfactory learning revealed by pharmacological study. *Eur. J. Neurosci.* 22, 1409–1416. doi: 10.1111/j.1460-9568.2005.04318.x

Vallortigara, G., and Rogers, L. J. (2005). Survival with an asymmetrical brain: advantages and disadvantages of cerebral lateralization. *Behav. Brain Sci.* 28, 575–588. doi: 10.1017/S0140525X05000105

Vergoz, V., Roussel, E., Sandoz, J. C., and Giurfa, M. (2007). Aversive learning in honeybees revealed by the olfactory conditioning of the sting extension reflex. *PLoS ONE* 2:e288. doi: 10.1371/journal.pone.0000288

Voets, T., Talavera, K., Owsianik, G., and Nilius, B. (2005). Sensing with TRP channels. *Nat. Chem. Biol.* 1, 85–92. doi: 10.1038/nchembio0705-85

Wright, G. A., Mustard, J. A., Kottcamp, S. M., and Smith, B. H. (2007). Olfactory memory formation and the influence of reward pathway during appetitive learning by honey bees. *J. Exp. Biol.* 210, 4024–4033. doi: 10.1242/jeb.006585

Yokohari, F., Tominaga, Y., and Tateda, H. (1982). Antennal hygroreceptors of the honey bee, *Apis mellifera* L. *Cell Tissue Res.* 226, 63–73. doi: 10.1007/BF00217082

Yokohari, F. (1983). The coelocapitular sensillum, an antennal hygro- and thermoreceptive sensillum of the honey bee, *Apis mellifera* L. *Cell Tissue Res.* 233, 355–365. doi: 10.1007/BF00238302

Zhang, E., and Nieh, J. C. (2015). A neonicotinoid, imidacloprid, impairs honey bee aversive learning of simulated predation. *J. Exp. Biol.* 218, 3199–3205. doi: 10.1242/jeb.127472

Conflict of Interest Statement: The authors declare that the research was conducted in the absence of any commercial or financial relationships that could be construed as a potential conflict of interest.

frontiers in Physiology

HYPOTHESIS AND THEORY
published: 21 December 2015
doi: 10.3389/fphys.2015.00391

Concept of an Active Amplification Mechanism in the Infrared Organ of Pyrophilous *Melanophila* Beetles

Erik S. Schneider[1†], *Anke Schmitz*[2†] *and Helmut Schmitz*[2*†]

[1] *Institute of Zoology, University of Graz, Graz, Austria,* [2] *Institute of Zoology, University of Bonn, Bonn, Germany*

Jewel beetles of the genus *Melanophila* possess a pair of metathoracic infrared (IR) organs. These organs are used for forest fire detection because *Melanophila* larvae can only develop in fire killed trees. Several reports in the literature and a modeling of a historic oil tank fire suggest that beetles may be able to detect large fires by means of their IR organs from distances of more than 100 km. In contrast, the highest sensitivity of the IR organs, so far determined by behavioral and physiological experiments, allows a detection of large fires from distances up to 12 km only. Sensitivity thresholds, however, have always been determined in non-flying beetles. Therefore, the complete micromechanical environment of the IR organs in flying beetles has not been taken into consideration. Because the so-called photomechanic sensilla housed in the IR organs respond bimodally to mechanical as well as to IR stimuli, it is proposed that flying beetles make use of muscular energy coupled out of the flight motor to considerably increase the sensitivity of their IR sensilla during intermittent search flight sequences. In a search flight the beetle performs signal scanning with wing beat frequency while the inputs of the IR organs on both body sides are compared. By this procedure the detection of weak IR signals could be possible even if the signals are hidden in the thermal noise. If this proposed mechanism really exists in *Melanophila* beetles, their IR organs could even compete with cooled IR quantum detectors. The theoretical concept of an active amplification mechanism in a photon receptor innervated by highly sensitive mechanoreceptors is presented in this article.

Keywords: ***Melanophila*, pyrophilous insect, infrared receptor, photomechanic receptor, fire detection, active amplification**

OPEN ACCESS

Edited by:
Sylvia Anton,
Institut National de la Recherche Agronomique, France

Reviewed by:
Maria Hellwig,
University of Vienna, Austria
Daniel Robert,
University of Bristol, UK

***Correspondence:**
Helmut Schmitz
h.schmitz@uni-bonn.de

† *These authors have contributed equally to this work.*

Specialty section:
This article was submitted to Invertebrate Physiology, a section of the journal Frontiers in Physiology

Received: *09 October 2015*
Accepted: *30 November 2015*
Published: *21 December 2015*

Citation:
Schneider ES, Schmitz A and Schmitz H (2015) Concept of an Active Amplification Mechanism in the Infrared Organ of Pyrophilous Melanophila Beetles. Front. Physiol. 6:391. doi: 10.3389/fphys.2015.00391

INTRODUCTION

With 13 recent species jewel beetles of the genus *Melanophila* mainly can be found in the boreal and temperate forests of the holarctic zone (Bellamy, 2008). According to the current state of knowledge, males and females approach forest fires because their larvae can only develop in wood of freshly burnt trees (Linsley, 1943; Apel, 1988, 1989, 1991). As an adaptation to the pyrophilous way of life the 1 cm long black beetles (**Figure 1A**) are equipped with special antennal smoke receptors (Schütz et al., 1999) and one pair of metathoracic IR organs (Evans, 1964; Vondran et al., 1995; Schmitz et al., 1997). An IR organ consists of a little array of dome-shaped sensilla which is situated at the bottom of a little pit (**Figures 1B**, **2A,B**). The inner spherule of each sensillum is innervated by a ciliary mechanosensitive cell (**Figure 2C**; Vondran et al., 1995; Schmitz et al., 2007). Thus, the

IR sensilla do not only respond to IR radiation but also to mechanical stimuli. A bimodality has already been demonstrated by electrophysiological experiments: single sensilla respond to weak vibratory stimuli with distinct action potentials (see Figure 3C in Schmitz and Bleckmann, 1998).

There are several hints in the literature that beetles are not only able to detect forest fires but also fires and heat sources of anthropogenic origin from distances of 30 km, 60 km, and even more than 100 km (Van Dyke, 1926; Linsley, 1943; Linsley and Hurd, 1957). Currently it seems not very likely that beetles use the smell of smoke to detect fires from greater distances. It could not be demonstrated that *Melanophila* beetles could be lured by the smell of smoke (Evans, 1964) or that beetles resting at temperatures of 25°C could be aroused by smoke (unpublished data). A recent study, however, shows that beetles can be attracted by certain volatiles emitted by burning or smoldering wood (Paczkowski et al., 2013). In the study crawling beetles were tested in a two arm olfactometer at a temperature of 30°C. No information about the sex and mating state of the beetles is provided in this study. So these data are more likely suited to show that beetles (e.g., mated females?), once having landed on a burnt tree, can detect a suitable spot for oviposition by olfactory cues. Evaluations of satellite images very often yielded the result that the large smoke plume from a forest fire initially is driven away from the fire by the wind in a narrow angle over distances of many kilometers and finally gradually ascends to higher altitudes. So only beetles inside the smoke plume have a chance to become aware of the fire by olfactory cues. In contrast, beetles that are already close to the fire but outside the smoke plume most probably can see the plume but are not able to smell the smoke. Also the light of the flames—generally only visible at night—may not play an important role, because *Melanophila* beetles, as nearly all jewel beetles, are diurnal (Evans et al., 2007).

All threshold sensitivities published so far were measured in non-flying beetles (highest sensitivity 60 $\mu W/cm^2$, see **Table 1**).

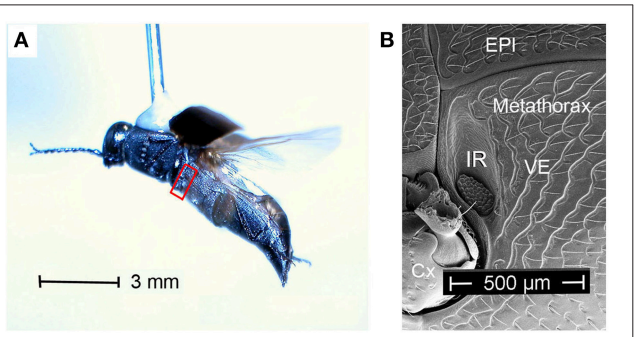

FIGURE 1 | (A) *Melanophila cuspidata* dorsally glued to a needle flying in front of a wind tunnel. Red box encircles area shown in **(B)**. **(B)** Boundary between meso- and metathorax. Cx, coxa; EPI, episternite; VE, ventrite with IR organ (IR) close to the boundary to the mesothorax.

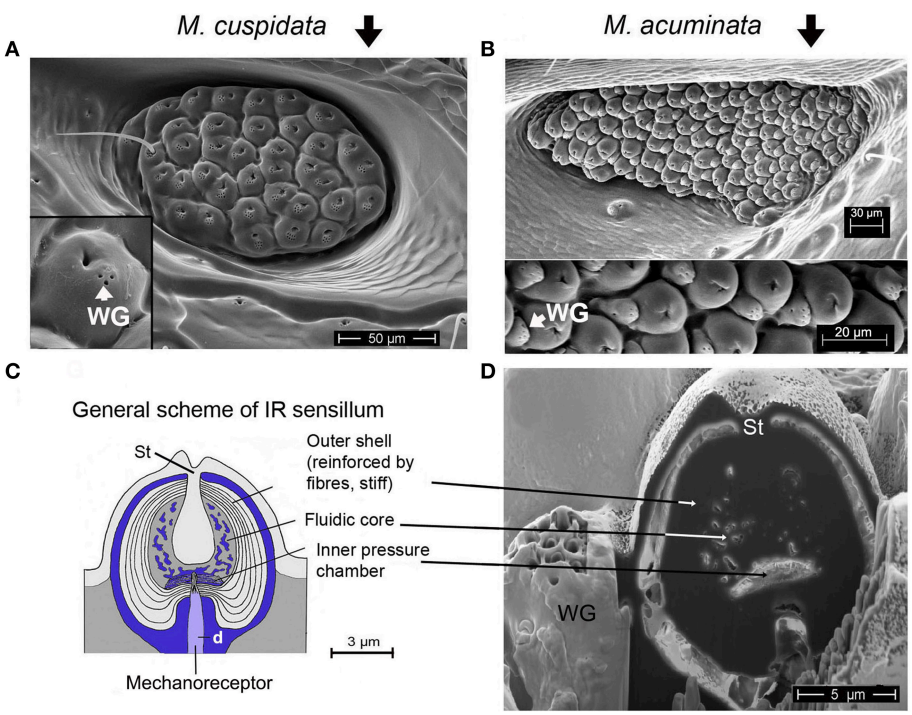

FIGURE 2 | (A) IR organ of *Melanophila cuspidata*. About 40 sensilla are inside the pit organ. Sensilla belong to a more basic type because wax glands (WG) are still intergrated into the domes of the IR sensilla (inset shows single sensillum). On the left a not fully differentiated sensillum can be seen which still has a bristle. **(B)** IR organ of *Melanophila acuminata*. The pit organ contains more than 80 sensilla of a more specialized type (wax glands clearly separated from the domes, see lower part of the image). Image modified after Schmitz et al. (2007). **(C)** General scheme of a *Melanophila* sensillum. d, dendrite; St, stalk. Image modified after Schmitz et al. (2007). **(D)** Air dried sensillum opened up in the center with a focused ion beam (FIB). WG, wax gland; St, stalk.

TABLE 1 | Sensitivity thresholds of biological and technical IR sensors.

	Threshold	Source/Explanation
Melanophila Behavioral experiments	60 μW/cm^2	Evans, *Ecology* (1966); Determined by behavioral experiments with non-flying beetles
Pyroelectric sensor (room temperature) (DIAS 256 LTI)	8.4 μW/cm^2	Sensorarray DIAS Infrared, Dresden
Rattlesnake *Crotalus atrox*	3.3 μW/cm^2	Ebert and Westhoff, *JCP A* (2006)
Microbolometer (room temperature)	2.3 μW/cm^2	Sensorarray Information provided by Dr. N. Hess, DIAS Infrared GmbH, Dresden. Compiled after: annual SPIE-Conferences "Infrared Technology," Orlando, USA, 1999–2011
Cooled quantum detector (AIM HgCdTe)	79 nW/cm^2	Sensorarray AIM Infrarotmodule GmbH, Heilbronn AIM Data Sheet 2nd-3rd-Generation
Melanophila Coalinga-Simulation	40 nW/cm^2	Schmitz and Bousack, *PLoS ONE* (2012)
Cryogenic cooled quantum detector (Hamamatsu P5274 Serie)	250 pW/cm^2	High sensitivity single element quantum detector Hamamatsu MCT photoconductive detectors Data sheet P2748/P5274 series

Theoretical calculations, however, show that these sensitivities only allow a detection of a large fire from a distance of about 12 km (Evans, 1966; Schmitz and Bleckmann, 1998).

The results of a simulation of a huge man-made fire provide further evidence that *Melanophila* beetles might be able to detect IR radiation emitted by remote fires from much larger distances (Schmitz and Bousack, 2012). In this study a big oil-tank fire was modeled that burnt in 1925 for 3 days in Coalinga (California) and attracted "untold numbers" of *Melanophila consputa*. This event has also been documented in the entomological literature (Van Dyke, 1926). The site of the fire in the woodless Central Valley of California suggests that most beetles detected the fire by IR radiation from distances of 130 km. This would imply a threshold sensitivity of only 40 nW/cm^2 (**Table 1**), corresponding to an energy at a single sensillum of 1.3×10^{-17} J. If the threshold of the *Melanophila* IR organ should really be in this range, the biological IR receptor would be two orders of magnitude more sensitive than all current uncooled technical IR sensors and would be able to compete with much more expensive cooled quantum detectors (cf. **Table 1**).

However, a sensitivity three orders of magnitude higher than the highest sensitivity ever published (**Table 1**) is only explainable by active amplification mechanisms. Until now, active amplification of very weak input signals has only be reported in the context of hearing: in the cochlear amplifier in the inner ear of vertebrates (Hudspeth, 1989, 1997; Gillespie and Müller, 2009), in antennal ears of mosquitoes and the fly *Drosophila* (Göpfert and Robert, 2001, 2003; Göpfert et al., 2005, 2006; Mhatre, 2015) and recently discovered also in the tympanal ears of a tree cricket (Mhatre and Robert, 2013). An amplification of 1000-fold can be achieved by electromotile outer hair cells in the mammalian cochlea (Robles and Ruggero, 2001; Ashmore et al., 2010). Like hair cells and scolopidia in vertebrate and insect ears, respectively, the mechanosensitive sensory cells that innervate the IR sensilla in *Melanophila* are ciliary mechanoreceptors. Therefore, the search for active amplification mechanisms appears highly challenging.

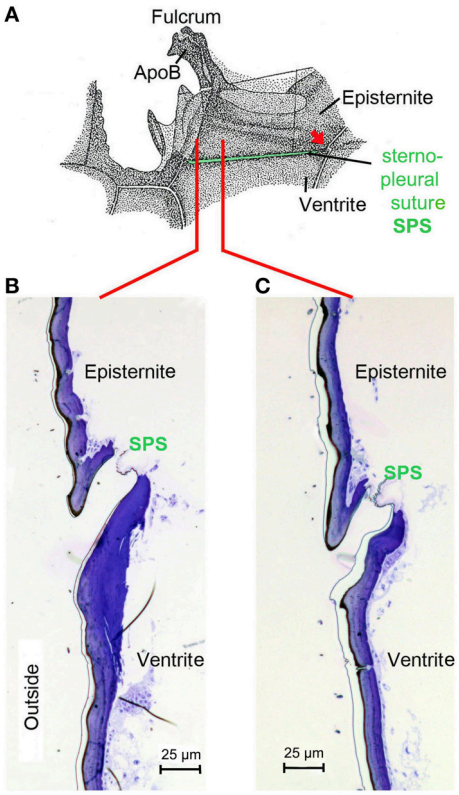

FIGURE 3 | (A) Morphology of the pleural region of the metathorax in beetles shown here for the rhinoceros beetle *Oryctes rhinoceros* (after Darwin and Pringle, 1959). The episternite with the fulcrum and the apodem of the basalar muscle (ApoB) are connected by a posterior hinge (red arrow) to the ventrite. In the region of the sternopleural suture (SPS, green) a hinge membrane allows movement of the episternite against the ventrite (Pringle, 1957). **(B)** Dorsoventrally oriented section through episternite and ventrite in the anterior region (indicated by red line in **A**) in the buprestid beetle *Chrysobothris solieri*. **(C)** Corresponding section about 150 μm in posterior direction.

MORPHOLOGICAL PREREQUISITES

Starting point for the development of the concept was the consideration that the IR organs are situated on the metathorax just below the wing hinges (fulcra) of the alae (**Figures 1A**, **4A,B**). Thus, the IR organs are located at a site strongly subjected to vibrations during flight. Additionally, a detail so far not understood was considered: the sphere of a sensillum is attached by a little stalk to the outer cuticular dome (**Figures 2C,D**). These stalks are missing in the photomechanic IR sensilla of pyrophilous *Aradus* bugs which are quite similar to the *Melanophila* IR sensilla but are not enclosed in a pit organ (Schmitz et al., 2010). By this constellation, vibrations of the spheres in flying *Melanophila* beetles can be proposed to affect the receptor potentials of the mechanosensory cells.

To realize genuine amplification, however, a mechanism has to be implemented permitting a precise regulation of the depolarization amplitude. The morphological prerequisites for such a regulation mechanism were found in the two hitherto investigated species *Melanophila acuminata* and *M. cuspidata*. The structural preadaptation for the evolution of an adjustable beat mechanism most probably was a special feature of the metathoracic pleural region in beetles: the sternopleural suture (SPS, **Figures 3A–C**). Episternite and ventrite are tightly connected only by a posterior hinge and thus can be moved against each other—especially at their anterior edges (Pringle, 1957). Amongst other purposes this mechanism mainly serves for lifting the fulcrum during flight. When the basalar muscle contracts, the episternite is pulled against the ventrite and the leading edge of the wing is pronated during the downstroke (Darwin and Pringle, 1959). The opposing edges of the episternite and the ventrite are formed in a manner so that the episternite can glide over the ventrite (as in the non IR-sensitive jewel beetle *Chrysobothris solieri,* closely related to the *Melanophila*-species, **Figures 3B,C**).

It turned out that in IR-sensitive *Melanophila*-species especially the morphology of the opposing anterior edges of episternite and ventrite has been modified. The slim ventral edge of the episternite can be beaten in a trench on the dorsal edge of the ventrite, thus a kind of impact edge is realized (**Figures 4D**, **5A–C**). According to the current conception beating of the two sclerites against one another is accomplished by contractions of the basalar muscle, which extends from the dorsal apodeme (ApoB; shown in **Figure 4B**) posteriorly to the basal region of the ventrite. By regulating the power of the muscle contractions during a search flight sequence (see below), the vibrations of the spheres caused by the proposed mechanism can be controlled. Therefore, also the magnitude of receptor depolarizations could be regulated.

In this context it is of great importance that the IR sensilla are innervated by ciliary mechanoreceptors. Specialized arthropod mechanoreceptors innervated by ciliary mechanosensory cells are the most sensitive receptors known. This could be shown for trichobothria in spiders, where energies of 1.5×10^{-19} J to 2.5×10^{-20} J are still sufficient for a suprathreshold stimulation of the receptors (Humphrey et al., 2003; Barth, 2004) and also for filiform hairs in insects (Thurm, 1982). Filiform hairs in crickets serving for detection of faint airflows can already generate an action potential if energies are still in the range of k_BT (k_B: Boltzmann constant; T: temperature), i.e., about 4×10^{-21} J (Shimozawa et al., 2003).

At the threshold, these ultrasensitive mechanoreceptors already work within the range of thermal noise of Brownian

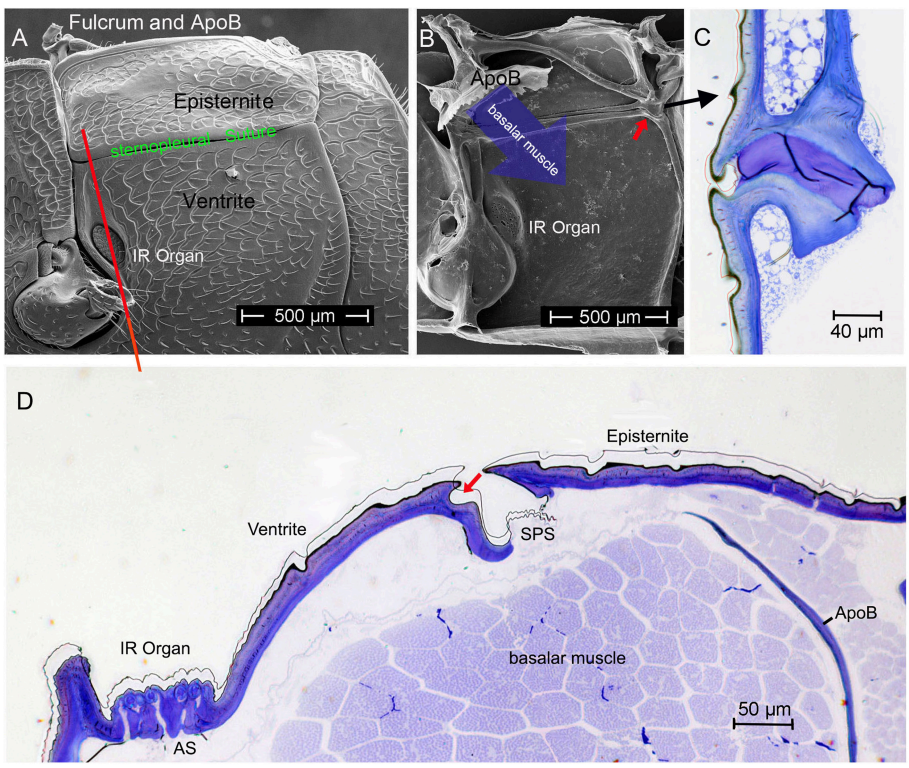

FIGURE 4 | (A) Outer and **(B)** inner view of the pleural metathorax of *Melanophila cuspidata*. The ventral anterior region of the episternite is developed as impact edge which can be beaten in a furrow of the ventrite. In **(B)** the apodeme of the basalar muscle (ApoB) is shown which is connected to the fulcrum (tissue removed). Red arrow points to posterior hinge shown in **(C)**. **(C)** Section through hinge in dorso-ventral direction, outside on the left). **(D)** Dorso-ventral section through the pleural metathorax (indicated in **A** by red line). By contraction of the basalar muscle the edge of the episternite is beaten in the dorsal furrow of the ventrite (red arrow). Vibrations caused by the beats most probably are conducted to the IR sensilla. AS, air sac below IR organ; SPS, sternopleural suture.

molecular motion and therewith close to the physical limit (Barth, 2004). It can be concluded that for a subthreshold depolarization of the mechanosensitive sensory cell innervating the IR sensilla most probably vibration amplitudes of the spheres of less than one nanometer are already sufficient.

In the two *Melanophila* species investigated so far, *M. acuminata* and *M. cuspidata*, morphological differences were found. It appears that the IR detection system (i.e., IR-organ plus the structures used for the proposed beat mechanism) in *M. cuspidata* is more ancient and relatively simple: IR organs contain less sensilla into which the wax glands are fully integrated (**Figure 2A**). So an unrestrained vibration of the sphere most probably may be somewhat hampered and less precise. An explanation could be that *M. cuspidata* is distributed in the Mediterranean region where fires are more frequent than in northern Europe (San-Miguel and Camia, 2009). Thus, the necessity to detect fires also from very large distances seems not to be predominant. In contrast, *M. acuminata* is distributed in the boreal forests of the northern hemisphere (in Europe northern distribution up to Fennoscandia; Horion, 1955), where forest fires are less frequent. Accordingly, a higher evolutionary pressure with respect to the sensitivity of the IR organs can be proposed. In *M. acuminata,* the IR organs contain significantly more IR sensilla from which wax glands are clearly separated (**Figures 2B–D**). It can be concluded that unobstructed vibrations of the spheres are possibles. Furthermore, an additional damping system obviously has developed. This system may allow a precise "fine tuning" of the depolarizations of the IR sensilla caused by the beat mechanism. By a system of at least two muscles of hitherto unknown origin a damping cushion of about 300 µm lengths can be brought down into the inner trench of the ventrite (**Figures 5A–D**). Thus, at a given contraction power of the basalar muscle a very precise adjustment of the beat intensity and consequently of the evoked pre-depolarizations could be adjusted. Despite intense search in two further specimens such a damping cushion could not be found in the Mediterranean *M. cuspidata* (cf. **Figure 4**).

HOW IT COULD WORK

According to the present idea how *Melanophila* beetles may be able to become aware of a fire from large distances, beetles use a combination of visual cues (view of a big cloud against the horizon) and IR radiation. To make sure that a smoke plume and not a cloud bank is approached over distances of many kilometers a zone of IR emission has to exist at the base of the cloud above tree top level. IR sensitive *Melanophila* beetles, therefore, will conduct search flights for fire

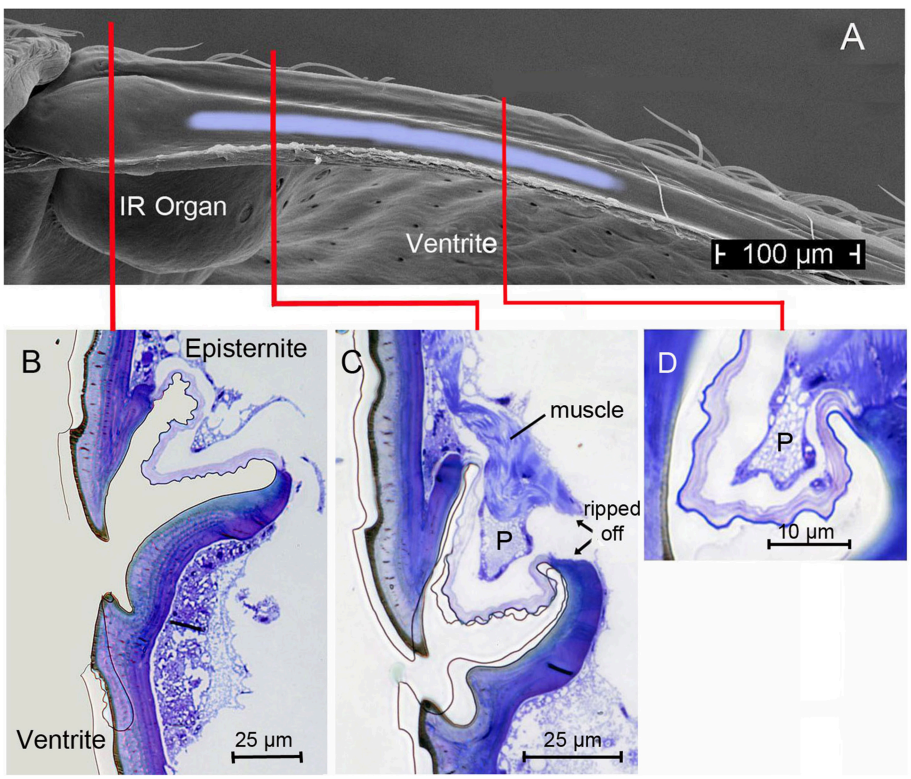

FIGURE 5 | (A) Top view (SEM micrograph) onto the furrow at the dorsal edge of the ventrite in *Melanophila acuminata* (all tissue removed). Light-blue area indicates region in which the proposed damping cushion (pad) can be brought into contact with the ventrite. **(B)** Section through region marked with red line in **(A)** showing the beating edge of the episternite and the narrow furrow in the ventrite. Same orientation as in **Figure 4A**. **(C)** Section through region marked in **(A)** with red line: here the damping pad (P) with its musculature is shown. **(D)** Section through the pad about 150 µm posteriorly. Pad becomes smaller toward its posterior end. After about 300 µm the pad is not longer present.

detection. While doing so, beetles especially examine potential smoke plumes in view of additional IR emission. By the beat mechanism a cyclic depolarization of the IR sensilla with wing beat frequency appears possible (**Figures 6A,B**). In beetles, the basalar muscle serves as a well-developed direct wing depressor, which, together with the indirect dorso-longitudinal muscles (main muscle for propulsion), is used for wing downstroke. In principle the basalar muscle can be classified as a steering muscle (Nachtigall, 2003). By adjusting the contraction power of the basalar muscle, the wing inclination angle during the downstroke of the wing (pronation) and in this way propulsion and buoyancy is adjusted. During a supposed search flight sequence, which may last for a few seconds only, the beetles could tune the contractions of the basalar muscles exactly so that the peak amplitudes of the oscillatory receptor potential almost reach the spike-triggering threshold. At the same time a slight reduction in propulsion and buoyancy would not be disadvantageous. To tune the IR organs to maximal sensitivity in anticipation of arriving IR radiation, the beetles should be able to adjust the intensity of the beat mechanism and therewith the probability of impulse generation by sensory feedback. As a result only a certain, most probably very low, percentage of sensilla in both organs generate action potentials.

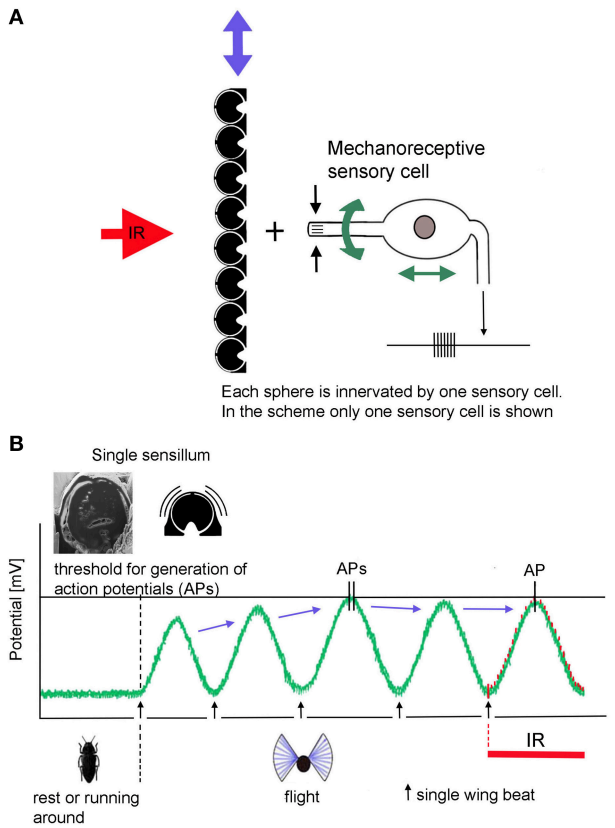

FIGURE 6 | Schematic depiction of the proposed beating mechanism. **(A)** Coupling in muscular energy (blue double arrows) from the flight motor results in vibration of the cuticular spheres. This in turn causes the stimulation of the mechanoreceptive sensory cells by which the spheres are innervated. By sensory feedback the sensory cells can be systematically depolarized with wing beat frequency. In contrast, energy for active amplification in hearing organs is generated by molecular motors of the sensory cells itself (green double arrows at the sensory cells). **(B)** In non-flying beetles the receptor potential of the IR sensilla is set at about −70 mV. Slight fluctuations are caused by thermal and mechanical noise. When the beetles take off, IR sensilla become depolarized by the beating mechanism: (1) by increasing beat intensity, the beetle is able to release action potentials in the absence of IR radiation. (2) by tuning the beat intensity and—in *Melanophila acuminate*—by additional fine tuning of the damping system, depolarization can be adjusted in a way that the generator potentials of most sensilla remain just below the threshold. (3) in turn IR radiation superimposed to the thermal noise at the peaks of the receptor potentials causes the generation of (additional) action potentials in exposed sensilla.

With respect to symmetry the inputs of both IR organs could be permanently compared by central comparator neurons. Such central units enable acoustically communicating insects to approach, e.g., a sound source by paired hearing organs (von Helversen and von Helversen, 1995; Stumpner and von Helversen, 2001). A mechanical prestimulation of only a few sensilla in the *Melanophila* IR organ could be explainable by the fact that the sensilla show minute differences in their dimensions (cf. **Figures 2A,B**). In case of an oscillatory mechanical stimulation with constant intensity some sensilla will already generate first action potentials whereas most others will remain just below the threshold. At the peak of a given subthreshold depolarization additional IR radiation will slightly increase the height of the amplitude (**Figure 6B**). This will result in a few more spiking sensilla in the organ exposed to IR radiation. The asymmetry in the inputs of both organs immediately could be detected by comparator neurons. Therewith the beetle gets information about the spatial direction from which IR radiation arrives. This information could be combined with visual cues (e.g., a smoke plume) and the beetle should be able to directly approach a fire.

Based on theoretical considerations it seems essential that the vibrations of the spheres caused by the proposed beat mechanism have to be strongly damped. By appropriate damping an uncontrolled soaring up of the system can be suppressed and it can be ensured that the spheres all are in a defined initial state before the next impact impulse arrives. Ideally a creeping case (i.e., damping so strong that no oscillation can arise) or at least an aperiodic limit case (i.e., strong damping ensures oscillation of the sphere with only one zero crossing) has to be proposed. In this way beat impulses of constant intensity will always cause monotonic depolarization amplitudes. Most probably damping is realized by a slender margin of fluid surrounding each sphere (**Figure 2C**). This margin with a thickness of about 0.3 μm consists of the apical extensions of the two outer enveloping cells (Vondran et al., 1995). By this specific feature a fluidic damping system is build. Subthreshold depolarizations of the receptors most probably are already evoked by sub-nanometer vibrations of the spheres. The necessary small scale dislocation of water is allowed by compensatory air sacs below the IR organ (**Figure 4D**, AS).

Provided that the cuticular apparatus (i.e., mainly the spheres) is able to convert the energies of absorbed IR photons effectively into mechanical energy (so-called photomechanic mechanism

of IR reception, Schmitz and Bleckmann, 1998) it could be possible that the sensitivity threshold of a *Melanophila* IR organ is about thousand fold lower (analogous to the mammalian cochlear amplifier) than the hitherto published lowest threshold of 60 $\mu W/cm^2$.

CLOSING REMARKS

Among biological IR sensory systems it is a unique feature of *Melanophila* beetles that IR sensilla serve as photon receptors although they are innervated by mechanosensitive neurons. The cuticular apparatus absorbs incoming IR radiation and transforms photon energy into a micromechanical event measured by a dedicated mechanoreceptor. In principle this constellation provides the possibility of active amplification of faint mechanical input signals. As mentioned in the Introduction active amplification has been shown in the context of hearing: for the hair cells in the cochlear amplifier in vertebrates (Hudspeth, 1997; LeMasurier and Gillespie, 2005; Fettiplace and Hackney, 2006; Ashmore et al., 2010) but also for the chordotonal organs in the ears of certain flies (Göpfert and Robert, 2001; Göpfert et al., 2005; Nadrowski et al., 2008) and a tree cricket (Mhatre and Robert, 2013). In hearing, however, the energy required for amplification is expended by the sensory cells themselves whereas in the proposed active IR receptors in *Melanophila* beetles the energy originates from the flight motor. Thus, in principle, the proposed mechanism to achieve a high sensitivity in a receptor for electromagnetic radiation is new. We further suggest that three different mechanisms are involved: (i) as proposed active signal amplification, (ii) active sensing which means that activity of the sensor system already starts in anticipation of a stimulus (Nelson and MacIver, 2006), and (iii) stochastic resonance: noise—in this case self-generated—is used for better signal detection (Harmer et al., 2002; Moss et al., 2004; McDonnell and Abbott, 2009).

The proposed beat mechanism, however, shows some marked differences compared to the mechanisms mentioned. No energy used for target analysis is emitted into the surrounding (difference to conventional *active sensing*), muscular energy is used for signal amplification (fundamental difference to the cellular molecular motors of the sensory cells in ears) and the crucial part of the "noise" is produced by self-generated oscillations. For the purpose of ultrasensitive stimulus detection the probability of action potential generation can be adjusted by altering the overall noise amplitude (difference to stochastic resonance that only works at an optimal noise intensity, which can hardly be influenced by the sensor system).

If the proposed high sensitivity of the IR organ could be demonstrated, the biological IR sensor would advance into the sensitivity gap currently existing between relatively cheap uncooled thermal IR sensors and expensive cooled quantum detectors requiring much more effort during operation and also more costly service (see **Table 1**). Thus, the demonstration of the postulated amplification mechanism would also be of technical interest for the development of new active IR sensors.

ACKNOWLEDGMENTS

We are indebted to Horst Bleckmann for useful discussion and improvements of the manuscript.

REFERENCES

Apel, K.-H. (1988). Befallsverteilung von *Melanophila acuminata* DEG., *Phaenops cyanea* F. und *Ph. formaneki* JACOB. (*Col., Buprestidae*) auf Waldbrandflächen. *Beitr. Forstwirtschaft* 22, 45–48.

Apel, K.-H. (1989). Zur Verbreitung von *Melanophila acuminata* DEG. (*Col., Buprestidae*). *Entomol. Nach. Ber.* 33, 278–280.

Apel, K.-H. (1991). *Die Kiefernprachtkäfer*. Eberswalde: Forschungsanstalt für Forst- und Holzwirtschaft Eberswalde, Merkblatt Nr. 50, 1–30.

Ashmore, J., Avan, P., Brownell, W. E., Dallos, P., Dierkes, K., Fettiplace, R., et al. (2010). The remarkable cochlear amplifier. *Hear. Res.* 266, 1–17. doi: 10.1016/j.heares.2010.05.001

Barth, F. G. (2004). Spider mechanoreceptors. *Curr. Opin. Neurobiol.* 14, 415–422. doi: 10.1016/j.conb.2004.07.005

Bellamy, C. L. (2008). *A World Catalogue and Bibliography of the Jewel Beetels* (*Coleoptera*: *Buprestidae*). Pensoft Series Faunistica No. 78.

Darwin, F. W., and Pringle, J. W. S. (1959). The physiology of insect fibrillar muscle. I. Anatomy and innervation of the basalar muscle of lamellicorn beetles. *Proc. R. Soc. London B* 151, 194–203. doi: 10.1098/rspb.1959.0059

Evans, H. F., Moraal, L. G., and Pajares, J. A. (2007). "Biology, ecology and economic importance of Buprestidae and Cerambycidae," in *Bark and Wood Boring Insects in Living Trees in Europe, A Synthesis,* eds K. R. D. F. Lieutier, A. Battisti, J.-C. Grégoire, and H. F. Evans (Dordrecht: Springer), 447–474.

Evans, W. G. (1964). Infrared receptors in *Melanophila acuminata* De Geer. *Nature* 202, 211. doi: 10.1038/202211a0

Evans, W. G. (1966). Perception of infrared radiation from forest fires by *Melanophila acuminata* De Geer (*Buprestidae, Coleoptera*). *Ecology* 47, 1061–1065. doi: 10.2307/1935658

Fettiplace, R., and Hackney, C. M. (2006). The sensory and motor roles of auditory hair cells. *Nat. Rev. Neurosci.* 7, 19 –29. doi: 10.1038/nrn1828

Gillespie, P. G., and Müller, U. (2009). Mechanotransduction by hair cells: models, molecules, and mechanisms. *Cell* 139, 33–44. doi: 10.1016/j.cell.2009.09.010

Göpfert, M. C., Albert, J. T., Nadrowski, B., and Kamikouchi, A. (2006). Specification of auditory sensitivity by *Drosophila* TRP channels. *Nat. Neurosci.* 9, 999–1000. doi: 10.1038/nn1735

Göpfert, M. C., Humphris, A. D. L., Alber, J. T., Robert, D., and Hendrich, O. (2005). Power gain exhibited by motile mechanosensory neurons in *Drosophila* ears. *Proc. Natl. Acad. Sci. U.S.A.* 102, 325–330. doi: 10.1073/pnas.0405741102

Göpfert, M. C., and Robert, D. (2001). Active auditory mechanics in mosquitoes. *Proc. R. Soc. Lond. B* 268, 333–339. doi: 10.1098/rspb.2000.1376

Göpfert, M. C., and Robert, D. (2003). Motion generation by *Drosophila* mechanosensory neurons. *Proc. Natl. Acad. Sci. U.S.A.* 100, 5514–5519. doi: 10.1073/pnas.0737564100

Harmer, G. P., Davis, B. R., and Abbott, D. (2002). A review of stochastic resonance: circuits and measurement. *IEEE Trans. Instrum. Meas.* 51, 299–309. doi: 10.1109/19.997828

Horion, A. (1955). *Faunistik der mitteleuropäischen Käfer, Bd. 4: Sternoxia (Buprestidae), Fossipedes, Macrodactylia, Brachymera.* Entomol. Arb. Mus. Frey, Tutzing, Sonderband.

Hudspeth, A. J. (1989). How the ear's works work. *Nature* 341, 397–404. doi: 10.1038/341397a0

Hudspeth, A. J. (1997). Mechanical amplification of stimuli by hair cells. *Curr. Opin. Neurobiol.* 7, 480–486. doi: 10.1016/S0959-4388(97)80026-8

Humphrey, J. A. C., Barth, F. G., Reed, M., and Spak, A. (2003). "The physics of arthropod medium-flow sensitive hairs: biological models for artificial sensors," in *Sensors and Sensing in Biology and Engineering,* eds J. H. FG Barth, and T. W. Secomb (Wien; New York, NY: Springer-Verlag), 129–144.

LeMasurier, M., and Gillespie, P. G. (2005). Hair-cell mechanotransduction and cochlear amplification. *Neuron* 48, 403–415. doi: 10.1016/j.neuron.2005.10.017

Linsley, E. G. (1943). Attraction of *Melanophila* beetles by fire and smoke. *J. Econ. Entomol.* 36, 341–342. doi: 10.1093/jee/36.2.341

Linsley, E. G., and Hurd, P. D. (1957). *Melanophila* beetles at cement plants in southern California (*Coleoptera, Buprestidae*). *Coleopt. Bull.* 11, 9–11.

McDonnell, M. D., and Abbott, D. (2009). What is stochastic resonance? Definitions, misconceptions, debates, and its relevance to biology. *PLoS Computat. Biol.* 5:e1000348. doi: 10.1371/journal.pcbi.1000348

Mhatre, N. (2015). Active amplification in insect ears: mechanics, models and molecules. *J. Comparat. Physiol. A* 201, 19–37. doi: 10.1007/s00359-014-0969-0

Mhatre, N., and Robert, D. (2013). A tympanal insect ear exploits a critical oscillator for active amplification and tuning. *Curr. Biol.* 23, 1–6. doi: 10.1016/j.cub.2013.08.028

Moss, F., Ward, L. M., and Sannita, W. G. (2004). Stochastic resonance and sensory information processing: a tutorial and review of application. *Clin. Neurophysiol.* 115, 267–281. doi: 10.1016/j.clinph.2003.09.014

Nachtigall, W. (2003). *Insektenflug.* Berlin; Heidelberg: Springer-Verlag.

Nadrowski, B., Albert, J. T., and Göpfert, M. C. (2008). Transducer-based force generation explains active process in *Drosophila* hearing. *Curr. Biol.* 18, 1365–1372. doi: 10.1016/j.cub.2008.07.095

Nelson, M. E., and MacIver, M. A. (2006). Sensory acquisition in active sensing systems. *J. Comp. Physiol. A* 192, 573–586. doi: 10.1007/s00359-006-0099-4

Paczkowski, S., Paczkowska, M., Dippel, S., Schulze, N., Schutz, S., Sauerwald, T., et al. (2013). The olfaction of a fire beetle leads to new concepts for early fire warning systems. *Sens. Actuators. B. Chem.* 183, 273–282. doi: 10.1016/j.snb.2013.03.123

Pringle, J. W. S. (1957). *Inset Flight.* London: Cambridge University Press.

Robles, L., and Ruggero, M. A. (2001). Mechanics of the mammalian cochlea. *Physiol. Rev.* 81, 1305–1352. Available online at: http://physrev.physiology.org/content/81/3/1305.short

San-Miguel, J., and Camia, A. (2009). "Forest fires at a glance: facts, figures and trends in the EU," in *Living with Wildfires: What Science Can Tell Us. EFI Discussion Paper 15,* ed Y. Birot (European Forest Institute), 11–18.

Schmitz, A., Schätzel, H., and Schmitz, H. (2010). Distribution and functional morphology of photomechanic infrared sensilla in flat bugs of the genus Aradus (Heteroptera, Aradidae). *Arthropod Struct. Dev.* 39, 17–25. doi: 10.1016/j.asd.2009.10.007

Schmitz, A., Sehrbrock, A., and Schmitz, H. (2007). The analysis of the mechanosensory origin of the infrared sensilla in *Melanophila acuminata* (*Coleoptera; Buprestidae*) adduces new insight into the transduction mechanism. *Arthropod Struct. Dev.* 36, 291–303. doi: 10.1016/j.asd.2007.02.002

Schmitz, H., and Bleckmann, H. (1998). The photomechanic infrared receptor for the detection of forest fires in the buprestid beetle *Melanophila acuminata*. *J. Comp. Physiol. A* 182, 647–657. doi: 10.1007/s0035900 50210

Schmitz, H., and Bousack, H. (2012). Modelling a historic oil-tank fire allows an estimation of the sensitivity of the infrared receptors in pyrophilous *Melanophila* beetles. *PLoS ONE* 7:e37627. doi: 10.1371/journal.pone.0037627

Schmitz, H., Mürtz, M., and Bleckmann, H. (1997). Infrared detection in a beetle. *Nature* 386, 773–774. doi: 10.1038/386773a0

Schütz, S., Weissbecker, B., Hummel, H. E., Apel, K.-H., Schmitz, H., and Bleckmann, H. (1999). Insect antennae as a smoke detector. *Nature* 398, 298–299. doi: 10.1038/18585

Shimozawa, T., Murakami, J., and Kumagai, T. (2003). "Cricket wind receptors: Thermal noise for the highest sensitivity known," in *Sensors and Sensing in Biology and Engineering,* eds F. G. Barth, J. A. C. Humphrey, and T. W. Secomb (New York, NY: Springer), 145–157.

Stumpner, A., and von Helversen, D. (2001). Evolution and function of auditory systems in insects. *Naturwissenschaften* 88, 159–170. doi: 10.1007/s001140100223

Thurm, U. (1982). "Grundzüge der Transduktionsmechanismen," in *Sinneszellen. Mechano-elektrische Transduktion*, eds W. Hoppe, W. Lohmann, H. Markl, and H. Ziegler (Berlin: Springer), 681–696.

Van Dyke, E. C. (1926). Buprestid swarming. *Pan-Pac. Ent.* 3, 41.

Vondran, T., Apel, K. H., and Schmitz, H. (1995). The infrared receptor of *Melanophila acuminata* De Geer (*Coleoptera: Buprestidae*): ultrastructural study of a unique insect thermoreceptor and its possible descent from a hair mechanoreceptor. *Tissue Cell* 27, 645–658. doi: 10.1016/S0040-8166(05) 80020-5

von Helversen, D., and von Helversen, O. (1995). Acoustic pattern recognition and orientation in orthopteran insects: parallel or serial processing? *J. Comp. Physiol. A* 177, 767–774. doi: 10.1007/BF00187635

Conflict of Interest Statement: The authors declare that the research was conducted in the absence of any commercial or financial relationships that could be construed as a potential conflict of interest.

frontiers in Physiology

REVIEW
published: 25 February 2016
doi: 10.3389/fphys.2016.00046

Sequential Filtering Processes Shape Feature Detection in Crickets: A Framework for Song Pattern Recognition

Berthold G. Hedwig *

Department of Zoology, University of Cambridge, Cambridge, UK

Intraspecific acoustic communication requires filtering processes and feature detectors in the auditory pathway of the receiver for the recognition of species-specific signals. Insects like acoustically communicating crickets allow describing and analysing the mechanisms underlying auditory processing at the behavioral and neural level. Female crickets approach male calling song, their phonotactic behavior is tuned to the characteristic features of the song, such as the carrier frequency and the temporal pattern of sound pulses. Data from behavioral experiments and from neural recordings at different stages of processing in the auditory pathway lead to a concept of serially arranged filtering mechanisms. These encompass a filter for the carrier frequency at the level of the hearing organ, and the pulse duration through phasic onset responses of afferents and reciprocal inhibition of thoracic interneurons. Further, processing by a delay line and coincidence detector circuit in the brain leads to feature detecting neurons that specifically respond to the species-specific pulse rate, and match the characteristics of the phonotactic response. This same circuit may also control the response to the species-specific chirp pattern. Based on these serial filters and the feature detecting mechanism, female phonotactic behavior is shaped and tuned to the characteristic properties of male calling song.

Keywords: feature detection, calling song, onset activity, reciprocal inhibition, delay line, coincidence detector, post-inhibitory rebound, modulation

OPEN ACCESS

Edited by:
Hadley Wilson Horch,
Bowdoin College, USA

Reviewed by:
Jens Herberholz,
University of Maryland, USA
Ralf Heinrich,
University of Göttingen, Germany

***Correspondence:**
Berthold G. Hedwig
bh202@cam.ac.uk

Specialty section:
This article was submitted to Invertebrate Physiology, a section of the journal Frontiers in Physiology

Received: *15 September 2015*
Accepted: *01 February 2016*
Published: *25 February 2016*

Citation:
Hedwig BG (2016) Sequential Filtering Processes Shape Feature Detection in Crickets: A Framework for Song Pattern Recognition. Front. Physiol. 7:46. doi: 10.3389/fphys.2016.00046

INTRODUCTION

In many species of insects, intraspecific signaling systems have evolved to allow mate attraction over long distances, including systems based on sex pheromones in moths and butterflies (Jacobsen, 1972), light patterns in fireflies (Carlson and Copeland, 1985; Lewis and Cratsley, 2008) and acoustic signals in orthoptera and hemiptera (Busnel, 1963; Alexander, 1967; Hedwig, 2014). These specialized communication systems are shaped by evolution so that both the signal generation and recognition processes are selective to a species-specific pattern. As intraspecific communication is crucial for the animals' mating success it requires reliable performance at the sender and the receiver side. The species-specific signals emitted by a sender require matched detection and recognition mechanisms by the receiver. Signal generation and signal recognition processes in insects are implemented in rather simple nervous systems and therefore provide a chance to unravel the underlying neural mechanisms at a cellular level.

The acoustic behavior of crickets is an established model system to analyse the neurobiological basis of auditory processing. Females approach singing males by phonotaxis, using only acoustic cues for pattern recognition and subsequent orientation. Considerable research in this field is aimed to understand how the temporal pattern of male calling song is recognized by the female nervous system (Popov et al., 1974; Hoy, 1978; Huber, 1978). As outlined in different hypothesis (review by Kostarakos and Hedwig, 2015), for pattern recognition to occur single neurons or networks of neurons should selectively respond to the species-specific characteristics of a signaling pattern. These are known as "feature detector" neurons or networks (Bullock, 1961; Hoy, 1978). Revealing the cellular and network mechanisms that lead to the selectivity of these neurons provides the opportunity to understand how a sensory system has been shaped during evolution to specifically process behaviorally relevant stimuli (Konishi, 1991).

In crickets, phonotaxis toward a species-specific calling song requires that its salient features are reliably detected, processed, and transformed into an appropriate motor response by the nervous system. Here a framework is outlined that calling song pattern recognition is organized in a set of serial filters, with each filter selectively responding to a particular characteristic of the song. At each level of auditory processing, a different feature of the calling song is extracted from the overall original signal leading eventually to the very specific activity of feature-detecting neurons in the brain.

This outline for song pattern recognition is mainly based on data in the sister species of *G. bimaculatus* and *G. campestris,* which have similar sound patterns and auditory preferences (Thorson et al., 1982). It however should provide a framework for different species of crickets as well as for the processing of communication signals in other specialized sensory pathways. Note, that data regarding auditory thresholds and tuning may slightly vary in papers cited, as different experimental procedures and recording methods were used.

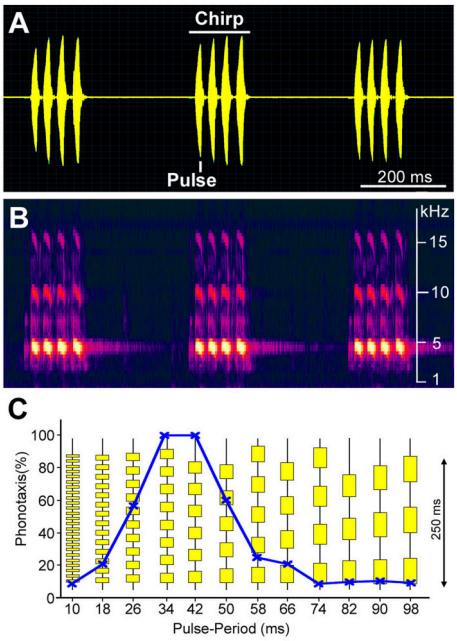

FIGURE 1 | Sound pattern of a male *G. bimaculatus* calling song in the temporal (A) and frequency domain (B). Chirps with four sound pulses are repeated at a rate of 3 per second. The main carrier frequency of the sound is around 4.8 kHz, with corresponding higher harmonics. **(C)** Tuning of female phonotactic behavior toward different temporal patterns of sound pulses as revealed in trackball experiments (Hedwig and Poulet, 2005). Test patterns of chirps with different pulse durations and intervals are vertically arranged. Each pattern was presented for 30 s from the left and right hand side while the cricket's phonotactic steering toward the stimulus was recorded.

THE MALE CALLING SONG AND THE FEMALE AUDITORY CHALLENGE

Only male crickets sing, which they achieve by the rhythmic opening and closing of their elevated front wings, with sound generated only on the closing movements. Males of different species produce different species-specific patterns of sound pulses in the contexts of mate attraction, courtship and rivalry behavior (Alexander, 1962; Otte, 1992). During calling song in *Gryllus bimaculatus* (**Figures 1A,B**), sound pulses are 15–20 ms long, separated by 15–20 ms silent intervals; and grouped into chirps of 3–5 pulses, which are repeated at a rate of 3–4 chirps/s (Doherty, 1985). Sound pulses rise to a maximum intensity of about 100 dB Sound Pressure Level (SPL) within a few milliseconds, and have a carrier frequency of around 4.8 kHz. Thus, the typical calling song of *G. bimaculatus* is characterized by four features: carrier frequency, pulse duration, pulse repetition rate, and chirp structure, which is given by the number of pulses per chirp and the interchirp interval. In male-male interactions, variable short rivalry songs are generated with chirps comprising 6–12 pulses. When courting a female, males generate single sound pulses at the chirp rate of the calling song, but with carrier frequencies of 11–16 kHz (Libersat et al., 1994). As compared to the more episodic courtship and rivalry song, which are accompanied by other sensory signals, e.g., antennal contact, and emitted in close male-female and male-male encounters, the stereotypic calling song is a long distance communication signal which may be emitted continuously for many hours to attract females.

Sexually-receptive females walk or fly toward a singing male, using only the male's acoustic cues as guidance for their phonotactic orientation. The tuning of their phonotactic behavior matches the temporal pattern of the male calling song (**Figure 1C**). They prefer pulse patterns similar to calling song, and are not attracted by short pulses repeated at a high repetition rate or by long pulses repeated at a lower rate (Thorson et al., 1982; Hedwig, 2006). Female *G. bimaculatus* and *G. campestris* therefore show a band-pass tuning of their phonotactic behavior based on pulse duration and pulse interval. Sound pulses also need to be at the species' typical carrier frequency to be attractive.

SERIAL FILTER PROCESSES UNDERLYING CALLING SONG RECOGNITION

Current data indicate that the properties of the peripheral and central auditory pathway are specifically adapted to process the male calling song. This process is organized in a set of serially arranged filter mechanisms (**Figure 2**) that finally leads to a highly selective response of feature detecting brain neurons and the tuned phonotactic behavior. First, at the level of the hearing organ a peripheral filter is selective for the song carrier frequency; second is a neural filter mechanism of phasic afferent and interneuronal activity which enhances the response to the onset of sound pulses; and third is a neural network in the brain with a delay line and coincidence detector feeding into feature detecting neurons which are tuned to a specific pulse repetition rate. The detection of the species-specific pulse rate may also control the phonotactic steering responses to the chirp pattern. All these filters together contribute to and shape the band-pass tuning of the cricket phonotactic orientation behavior.

Processing of the Calling Song Carrier Frequency

In all auditory systems, frequency processing starts at the biophysical level. Due to the mechanical filtering properties of the peripheral transduction mechanism, frequency components are separated and forwarded to spatially distinct structures of the hearing organ in a frequency-specific way as revealed in the ears of moths, locusts, and cicada (Windmill et al., 2005, 2007; Sueur et al., 2006). Oscillations of these structures then drive the activity of afferent neurons in the hearing organs. In the field cricket *G. bimaculatus* the carrier frequencies of calling songs cover a range of 4.3–5.2 kHz (Kostarakos et al., 2009), and courtship songs are in the range of 11–16 kHz (Libersat et al., 1994). The biophysics of the peripheral auditory system allows for selective responses at the level of the auditory afferents to these low and high frequency components of the communication signals (Oldfield et al., 1986). The afferent activity is then carried forward to the central nervous system where it sets the limits for the subsequent frequency tuning of central interneurons, and finally the categorical phonotactic responses (Wyttenbach et al., 1996; **Figures 2**, **3**).

The Peripheral Auditory System: Tuning of Tympanic Membrane Vibrations

The peripheral auditory system in crickets is characterized by a small frontal and a large posterior tympanic membrane, which are located on the tibia of each front leg. The hearing organ is positioned behind the posterior tympanum where a row of 40–60 auditory afferents is arranged in a structure known as the crista acustica. The organ is attached to the auditory trachea (Michel, 1974), which extends from the front tibia to the first thoracic segment where it ends with a lateral opening at the auditory spiracle (Nocke, 1972; Huber and Thorson, 1985). Sound enters the auditory system via the spiracles of the auditory trachea, and also via the posterior tympanic membrane in the tibia. For directional coding, the efficiency of the different sound pathways depends on the carrier frequency and the angle of incidence (Michelsen et al., 1994; Seagraves and Hedwig, 2014). The peripheral auditory pathway also provides the essential step of frequency filtering. Movements of the posterior tympanal membrane are necessary for hearing in crickets (Kleindienst et al., 1983) and mirror the frequency tuning of the auditory system. Laser vibrometry measurements of the mechanical oscillations of the posterior tympanic membrane in *G. bimaculatus* (Larsen, 1981) revealed the best response at 5.3 kHz (**Figure 3A**); the velocity response drops toward 2 kHz and decreases toward 14 kHz. Like in other species of crickets (Johnstone et al., 1970; Paton et al., 1977), these data indicate that the mechanical response of the peripheral auditory system matches the calling song carrier frequency (**Figure 1B**). Since these early measurements, the oscillation properties of tympanic membranes in field cricket have not been studied any further; using more recent laser technology refined tuning curves may be recorded or even active hearing mechanisms like those in tree crickets (Mhatre and Robert, 2013) may be revealed.

Frequency Tuning of Auditory Afferents

The biophysical and neurophysiological basis for frequency tuning of the auditory afferents are not yet resolved in detail. They may depend on the opening state of the spiracles (Kostarakos et al., 2009), the properties of the tracheal tubes, and also on intrinsic properties of the sensory neurons. The 40–60 afferent neurons are linearly arranged over a distance of 300 μm in the tonotopically organized crista acustica, in which sensory

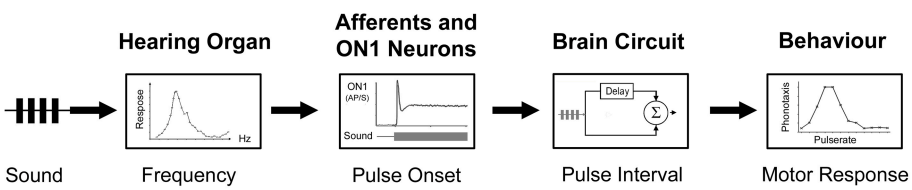

FIGURE 2 | Schematic diagram of serial filter processes in the cricket auditory pathway. At each stage, the response specificity is enhanced. Left to right: frequency tuning of the tympanic membrane response is based on biophysical filter mechanisms in the hearing organ; the detection of sound pulses is supported by the phasic-tonic response properties of auditory afferents and by reciprocal inhibition at the level of thoracic interneurons; the pulse rate is processed in the brain by a delay line coincidence detecting circuit, driving feature detector neurons that preferentially respond to the species-specific pulse rate. In addition, the feature detection circuit may modulate a reactive non-selective steering pathway at the time scale of the chirp rate (not shown). Finally, phonotactic walking behavior is tuned to sound pulses of the calling song carrier frequency presented at the species-specific pulse duration and pulse interval.

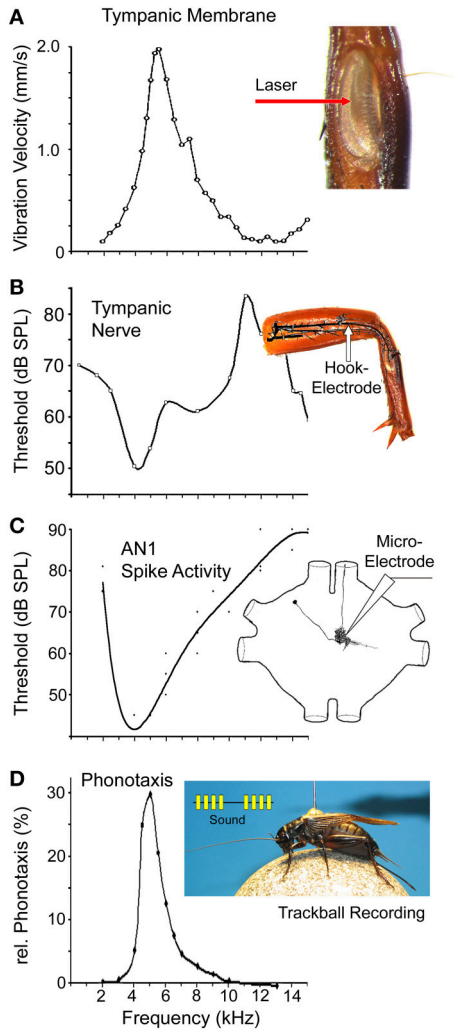

FIGURE 3 | Frequency tuning at different processing stages in the auditory pathway of field crickets. (A) Vibration velocity amplitude of the posterior tympanic membrane in *G. bimaculatus* as measured with laser vibrometry at a constant sound amplitude of 94 dB SPL while acoustic spiracles were blocked. Redrawn from Larsen (1981). Inset shows the posterior tympanal membrane in the tibia. **(B)** Frequency tuning of the auditory organ. Threshold of the summed activity of the tympanal nerve in *G. campestris*. Redrawn on a linear frequency scale, after Nocke (1972). Inset shows the recording site of the auditory nerve in the femur. **(C)** Threshold for frequency tuning of AN1 spike activity in *G. bimaculatus*. Data pooled and redrawn from Rheinlaender et al. (1976); Schildberger et al. (1989), and Horseman and Huber (1994). Inset shows structure of AN1. **(D)** Frequency tuning of phonotactic behavior in *G. bimaculatus* based on auditory steering responses of tethered females walking on a trackball system. Calling song pattern presented at 75 dB SPL with varying carrier frequency. Data based on seven tests. Inset shows sound pattern and cricket on a trackball.

neurons responding to low frequencies are located proximally and neurons responding to high frequencies are located distally (Oldfield et al., 1986). The sensory neurons are positioned right on the surface of the anterior branch of the auditory trachea while their dendrites project into a attachment cells of systematically varying size, which are linked to the lateral cuticle of the tibia (Michel, 1974). The auditory sensory neurons may be activated in a frequency-specific way by sound-induced traveling waves in the auditory trachea, mechanically stimulating the dendrites and opening mechanically gated ion channels. Frequency-specific traveling waves within the auditory trachea of bushcrickets have recently been described (Montealegre-Z et al., 2012; Udayashankar et al., 2012); the waves preferably elicit oscillations of the auditory trachea in a tonotopically arranged gradient along the crista acustica and appear to establish the tuning of the auditory afferents.

At the afferent population level, the summed activity of the auditory nerve in *G. campestris*, shows the lowest threshold for hearing to be around 50 dB SPL for sound pulses of 4.0–4.5 kHz, i.e., in the range of male calling song (**Figure 3B**; Nocke, 1972). The hearing threshold sharply increases toward 2 kHz, but toward higher frequencies, a secondary broad-threshold minimum at 65 dB SPL occurs for sound of 7–9 kHz. The system becomes increasingly less sensitive toward 10–12 kHz, but sensitivity subsequently increases, with the threshold dropping to 60 dB SPL at 14 kHz. Overall, in the range of 4–6 kHz the threshold curve corresponds well with the velocity response of the tympanic membrane (**Figure 3A**). The summed activity of the auditory nerve comprises the response of many auditory afferents, each of which has a lowest threshold of around 45 dB SPL (Esch et al., 1980; Oldfield et al., 1986). The tuning of the individual auditory afferents shows a discontinuous distribution of best frequencies, with about 75% of afferents responding to the carrier frequency of male calling song (Zaretsky and Eibl, 1978; Esch et al., 1980; Imaizumi and Pollack, 1999), and with the remaining to high frequencies that represent the male courtship song with dominant frequencies of 11–16 kHz (Libersat et al., 1994) and ultrasound sonar calls of echolocating bats above 20 kHz. This discontinuous distribution of best frequencies may reflect the frequencies of the most behaviorally relevant sounds for females, as they must respond with positive phonotaxis to the signals of conspecific males and with negative phonotaxis to the calls of predatory bats (Wyttenbach et al., 1996; Imaizumi and Pollack, 1999).

The activity of the auditory afferents is carried toward the prothoracic ganglion where their axons terminate in the anterior ventral neuropil (Eibl and Huber, 1979; Wohlers and Huber, 1985). Axonal arborizations are tonotopically arranged with afferents tuned to calling song projecting more medially, and afferents tuned to sounds of higher frequencies projecting more laterally (Imaizumi and Pollack, 2005). In *Teleogryllus oceanicus*, and likely also in *G. bimaculatus*, the bifurcating axons of afferents tuned to calling song project more posteriorly. They may connect to descending interneurons like the DN1 neurons, which forward signals in the frequency range of the calling song to the posterior thoracic ganglia (Esch et al., 1980; Wohlers and Huber, 1982; Imaizumi and Pollack, 2005). Details of auditory processing in these ganglia are, however still not well analyzed.

Tuning of Thoracic Interneurons

In the prothoracic ganglion, afferents make synaptic contact to bilateral pairs of local (ON1, ON2), descending (DN1), ascending (AN1, AN2), and T-shaped (TN1) auditory interneurons (Wohlers and Huber, 1982; Imaizumi and Pollack, 2005). The

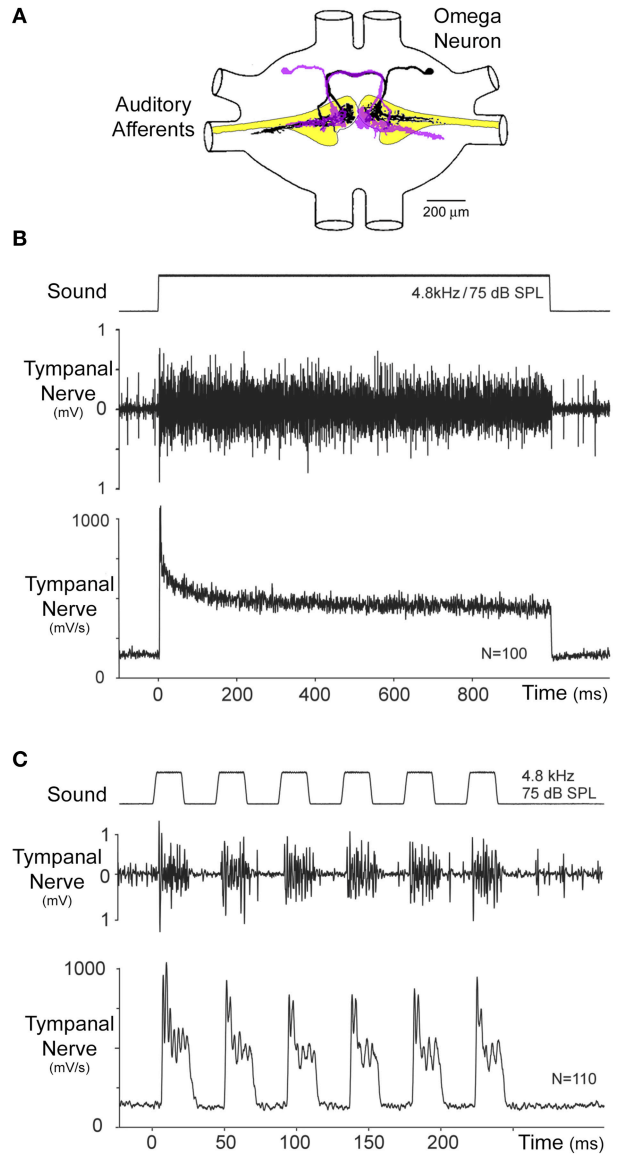

FIGURE 4 | (A) Arrangement of auditory afferents (yellow) and the mirror image ON1 neurons in the prothoracic ganglion, redrawn from Wohlers and Huber (1985). **(B)** Phasic-tonic response of the auditory afferents as revealed by a summed recording of the tympanal nerve in the distal femur. Stimulation with a 1000 ms pulse demonstrates the phasic synchronized onset response of the auditory afferents, which adapts to a tonic activity level. The phasic response is clearly revealed by averaging the rectified neural signal. **(C)** Acoustic stimulation with the species-specific pulse pattern shows the phasic onset and representation of the pulse pattern in the summed afferent activity. Modified from Nabatiyan et al. (2003).

local omega shaped ON1 neurons (see **Figure 4A**) respond most strongly to the carrier frequency of the calling song, but also respond to the high frequency components of courtship songs or bat calls (Marsat and Pollack, 2004). The two pairs of bilateral ascending interneurons forward information from the thoracic auditory neuropil toward the brain. AN1 (**Figure 3C**) is tuned to the male calling song (Rheinlaender et al., 1976; Schildberger et al., 1989; Horseman and Huber, 1994). It has its lowest threshold of about 43 dB SPL at around 5 kHz, and matches the best tuning of both the posterior tympanal membrane and the auditory nerve. The threshold of AN1 increases sharply to 80 dB SPL from 2 to 5 kHz and increases gradually to 80 dB SPL from 5 to 12 kHz (**Figure 3C**). AN1 is the only neuron that carries information about the calling song toward the brain. Schildberger and Hörner (1988) provided an experimental proof for the close link of AN1 activity and phonotaxis. Manipulation of the AN1 spike activity by intracellular current injection in phonotactic walking crickets changed the female's walking direction and performance. AN2 and TN1, the only other interneurons with an ascending axon, are tuned to high frequencies and do not reliably copy the calling song pattern (Wohlers and Huber, 1982). The tuning to high frequency sounds may relate to courtship song or the calls of bats (Libersat et al., 1994). Therefore, high frequency signals alone are not sufficient to reliably indicate a courting male or an echolocating bat.

Frequency Tuning of the Phonotactic Behavior in *G. bimaculatus*

The frequency tuning of the auditory pathway closely corresponds to the frequency tuning of female phonotactic behavior (**Figure 3D**). If female *G. bimaculatus* crickets walking on a trackball (Hedwig and Poulet, 2005) are exposed to 75 dB SPL calling song patterns with systematic alteration of the carrier frequency, phonotactic steering toward the sound source is strongest at 4.5–5.0 kHz. From this maximum response, phonotactic behavior decreases sharply toward 3 kHz and becomes gradually weaker toward 12 kHz. There is a good match between the frequency tuning of phonotactic behavior and the tuning of AN1, which was also established by direct comparison of AN1 activity and lateral steering (Kostarakos et al., 2008). A similar match has also been indicated for the carrier frequency and the tuning of the AN1 interneuron in *Teleogryllus commodus* (Hill, 1974).

Neural Representation of Sound Pulses

Patterns of sound pulses and silent intervals are a characteristic element of cricket songs. Sensory processing at the level of auditory afferents and first order interneurons may therefore be adapted to respond specifically to the temporal structure of the sounds and to represent it in patterns of neural activity.

Phasic-Tonic Responses of Auditory Afferents

The primary auditory neurons are scolopidial mechanoreceptors (Michel, 1974), and show phasic-tonic response characteristics (Nocke, 1972; Oldfield et al., 1986; Nabatiyan et al., 2003). They project into the prothoracic ganglion and activate first order interneurons like ON1 (**Figure 4A**). When stimulated with a 1000 ms sound pulse at the carrier frequency of calling song (**Figure 4B**), summed recordings from the auditory nerve show a salient response of the afferents to the onset of the pulse. It is best revealed by averaging the rectified (i.e., the negative signal components have been made positive) nerve recording; this procedure preserves the tonic activity component, which otherwise is lost when the signal is directly processed. The phasic onset of the auditory nerve is in the range of twice the

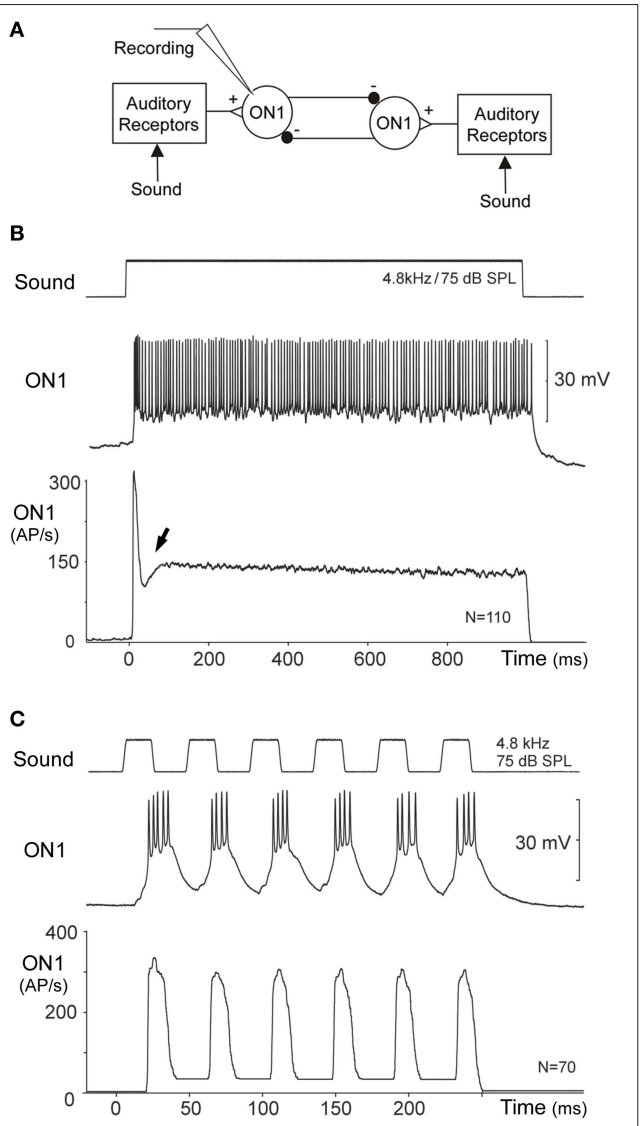

FIGURE 5 | (A) Diagram of the reciprocal inhibitory connection between ON1 neurons. **(B)** Intracellularly recorded activity of an ON1 neuron in response to a 1000 ms acoustic stimulus presented simultaneously to both ears. Averaging the instantaneous spike rate of ON1 reveals a pronounced phasic onset response to the pulse, followed by a reduced spike rate after the onset response (arrow) with a subsequent tonic activity level. **(C)** During acoustic stimulation with the species-specific pulse pattern, ON1 activity mirrors the temporal pattern of the signal in its spike activity and the instantaneous spike rate.

amplitude of the subsequent tonic response. The onset response rapidly decays within 10–20 ms and then gradually to the lower level of the tonic response. Intracellular recordings from single auditory afferents showed a high spike-rate activity at the sound onset (Oldfield et al., 1986). During stimulation with a repetitive pulse pattern corresponding to the *G. bimaculatus* calling song (**Figure 4C**), the phasic component of the afferent activity reliably encodes the sound pulses, generating a peak response at the beginning of each pulse, even for pulse repetition rates higher than the pulse rate of the calling song (Nabatiyan et al., 2003). Thus, the phasic-tonic response properties of the population of auditory afferents allow the temporal structure of the pulse pattern to be forwarded reliably to the central nervous system. Based on the spike response of single afferents in *T. oceanicus*, Marsat and Pollack (2004) calculated the information transfer rates as bits/s transmitted by the spike patterns at different amplitude modulation frequencies. The information transfer rate of the afferents broadly represented a spectrum of amplitude-modulated sounds up to 150 Hz. Therefore, the response range of the afferents is not specifically tuned to the species-specific pulse pattern of the calling song; the filtering for the temporal pattern rather must be achieved in the central nervous system.

Sharpening Sound Onset Responses by Reciprocal Inhibition in Thoracic ON1 Neurons

The time course of the afferent response is mirrored in the response pattern of the local ON1 neurons (**Figures 4A**, **5A**), a bilateral pair of first order interneurons (Casaday and Hoy, 1977; Popov et al., 1978; Wohlers and Huber, 1978, 1982). Each ON1 neuron receives synaptic input from the auditory afferents of the ear ipsilateral to its dendritic field while its axon projects to the contralateral side. As the auditory phasic onset response sums across all afferents tuned to the calling song (Ronacher and Römer, 1985; Pollack and Faulkes, 1998), the onset of sound pulses also leads to a pronounced phasic response in these interneurons.

The bilateral pair of ON1 neurons is coupled by reciprocal inhibition (**Figure 5A**; Selverston et al., 1985), which has been suggested to contribute to temporal filtering of the species-specific pulse pattern (Wiese and Eilts, 1985; Wiese and Eilts-Grimm, 1985) and may play an important role for their auditory response properties. When a 1000 ms acoustic stimulus at 75 dB SPL and 4.8 kHz is presented from the anterior, the ON1 neurons generate a transient onset response with a burst of spikes reaching instantaneous spike rates in excess of 300 AP/s. Thereafter, they rapidly stabilize to a tonic spike rate of about 150 AP/s (**Figure 5B**). At first sight, the time course of this response appears to be similar to the summed afferent response (**Figure 4B**). However, immediately following the phasic onset response of ON1, a pronounced drop in spike rate occurs, by about 50 AP/s (arrow **Figure 5B**), which transiently reduces the neuron's activity even below the subsequent level of tonic activity. This transient drop therefore enhances/sharpens the phasic onset activity relative to the tonic response. The fast drop in ON1 spike activity is not typical for the decline of a phasic response and it is not expected by the time course of the afferent activity. This peculiar feature may rather indicate that the neural representation of the onset of sound pulses becomes more salient at the level of ON1 neurons due to their reciprocal inhibitory connection. Upon simultaneous acoustic stimulation of both ears each ON1 neuron will be driven by afferent activity and also by the inhibition from the contralateral ON1. Due to synaptic delay and conduction time between the neurons the inhibition reaches an ON1 just after its initial peak spiking response (Selverston et al., 1985; Wiese and Eilts, 1985; see also Römer et al., 1981 for similar processing in locusts). Without substantially changing its phasic onset response, the

reciprocal inhibition will have its greatest impact immediately after the onset activity and then during the tonic activity. The reciprocal inhibition, if strong enough, thereby can enhance the representation of pulse-like acoustic signals in ON1. This can be demonstrated directly: the onset response of an ON1 to sound becomes less pronounced when the contralateral hearing organ is removed and the contralateral inhibition abolished. Recording ON1, while presenting calling song like pulse patterns, reveals that the phasic onset response reliably mirrors each sound pulse with a burst of spikes (**Figure 5C**). Thus, following the phasic onset response of the auditory afferents, which drives the excitation of ON1, the reciprocal inhibition between the ON1 neurons can act as a mechanism that further sharpens the onset response to sound, and thereby provides an additional way to represent sequences of short sound pulses.

Selective Attention to the Louder Signal

Another mechanism on a slower time scale that supports reliable coding of sound pulses is described as "selective attention" (Pollack, 1988). Continuous repetitive acoustic stimulation elicits spike activity in ON1, which causes a gradual increase in its cytosolic calcium concentration and subsequently triggers a hyperpolarizing potassium current (Sobel and Tank, 1994; Baden and Hedwig, 2007). This leads to a suppression of the ON1 neuron's spike response to low amplitude sound pulses e.g., 60 dB SPL, when they are interspersed with a louder signal of 80 dB SPL (Pollack, 1988). Due to the build-up of hyperpolarization, the response to the low intensity sound signal gradually becomes subthreshold and the ON1 spike pattern is dominated by its response to the louder signal. In a non-competitive situation with only one signal source, the mechanisms will suppress any non-specific background noise and will enhance the neural representation of the sound pattern. In a situation of competing signalers the selective attention mechanism will ensure that when a female approaches a singing male the signal from this loudest/nearest male will dominate the spike pattern of its central auditory pathway. Behavioral experiments (Simmons, 1988; Harrison et al., 2013) indicate that females orient preferentially to the calls of louder males.

The Detection of Pulse Periods by a Delay Line and Coincidence Detector Circuit in the Brain

As the simple opening and closing movements of the wings underlying sound production do not allow for a complex amplitude modulation, it is the temporal pattern of the signals that convey the male cricket's message, similar to the pulses in Morse code. Detecting the specific temporal sequence of sound pulses, i.e., the pulse period and the chirp pattern, is not achieved at the level of the auditory afferents, and so requires more complex processing in the central nervous system. Only the bilateral pair of AN1 interneurons forwards auditory signals in the range of calling song to the brain; another pair of neurons (AN2) responds to high frequency signals. AN1 is not tuned to the temporal pattern of the calling song (Wohlers and Huber, 1982; Schildberger, 1984b) and reliably responds to different temporal patterns of sound pulses, although, the spike rate of the response decreases at high pulse repetition rates. Therefore, besides some pre-filtering that occurs at the thoracic level, the final processing and selective detection of the species-specific pulse rate must occur in the brain. Furthermore, crickets in which the connectives to the brain have been severed do not show any positive or negative phonotactic responses (Pollack and Hoy, 1981).

Circuit Structure

Several different mechanisms have been proposed to underlie the processing of the species-specific pulse rates, such as internal templates, band-pass filtering, resonant networks, and delay line coincidence detection (Hoy, 1978; Schildberger, 1984b; Weber and Thorson, 1989; Bush and Schul, 2006; Kostarakos and Hedwig, 2015). Current data provide strong support for a circuit comprising a delay line and a coincidence detector (**Figure 6A**; Schöneich et al., 2015), a similar circuit design was originally proposed for directional auditory processing (Jeffress, 1948) and outlined as a concept of resonant networks by Reiss (1964). Corresponding to the delay line coincidence detection concept the response to sound pulses is split into two parallel pathways. The activity in one pathway is directly forwarded to the coincidence detector whereas the activity in the parallel pathway is delayed by the species-specific pulse period before reaching the detector. Consequently, a single sound pulse will only weakly activate the coincidence detector, but when the pulse-interval of the stimulus pattern corresponds to the internal delay, the direct input, and the delayed input from the previous pulse coincide and the response of the detector will be significantly enhanced. The delay in the cricket brain cannot be achieved by axonal delay-lines as proposed for binaural processing by Jeffress (1948) and which in owls allow only microsecond delays (Carr, 1993). As processing of communication signals in the cricket brain requires delays of about 40 ms the delay rather needs to be based on an inhibitory mechanism.

The axonal projections of AN1 (**Figures 3C**, **6B**) terminate in the frontal protocerebrum and form a ring-like arborization. A set of four local auditory interneurons (LN2–LN5) closely match this arborization pattern and form a similarly-shaped ring-like auditory neuropil in the brain (**Figure 6B**; Kostarakos and Hedwig, 2012); the structure of LN5 (Schöneich et al., 2015) is similar to LN2. Like AN1, these local neurons are also tuned to the carrier frequency of calling song (Schöneich et al., 2015). The response properties of these neurons together constitute a delay line coincidence detection circuit as outlined in **Figure 6C**. This conclusion is supported by increasing latencies for auditory processing in the circuit and very specific synaptic responses of the neurons (Schöneich et al., 2015). Together these indicate one particular flow of activity in the circuit and allow only one most parsimonious interpretation for the function of the local circuitry (**Figures 6D,E**), which matches a previous hypothesis on pattern recognition (Weber and Thorson, 1989).

Functional Properties of the Delay Line Coincidence Detector Circuit

A delay line coincidence detector requires two parallel pathways; a direct pathway and a delayed pathway. In the cricket brain,

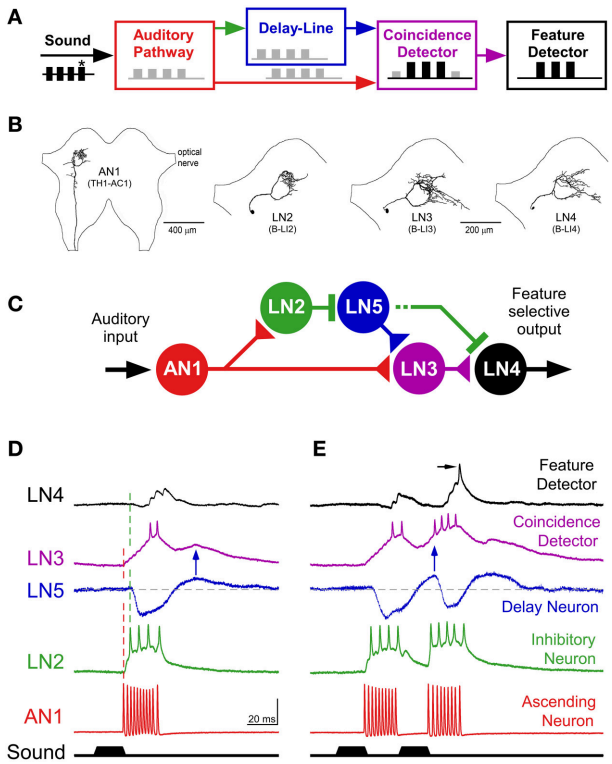

FIGURE 6 | Feature detection in the cricket brain. (A) Delay line coincidence detector circuitry proposed for feature detection of the species-specific pulse rate, after Weber and Thorson (1989). **(B)** Axonal arborizations of AN1 and local auditory brain neurons LN2–LN4 in the anterior protocerebrum, neurons are labeled as "B-LI" neurons in Kostarakos and Hedwig (2012). **(C)** Proposed feature detecting circuitry in the brain with the ascending neuron AN1, the delay line neurons LN2 and LN5, the coincidence detecting neuron LN3 and the feature detector neuron LN4. The coincidence detector neuron integrates activity directly forwarded from AN1 and delayed activity forwarded via the delay line with the non-spiking neuron LN5. **(D)** In response to a single sound pulse, AN1 generates a burst of spikes, which directly drives the activity of the coincidence detector neuron LN3. AN1 also activates the delay line via LN2, which tightly follows the activity of AN1, and subsequently inhibits the non-spiking interneuron LN5. At the end of a sound pulse, when released from inhibition, LN5 generates a post-inhibitory rebound, which reaches its maximum amplitude after about 40 ms and elicits a delayed gradual depolarization in the coincidence detector neuron LN3 (blue arrow). In response to the first sound pulse, the response of the feature detector neuron LN4 is dominated by the inhibition via LN2, and shows minor excitation via LN3. **(E)** In response to a second sound pulse presented at the species-specific pulse interval, the coincidence detector integrates the delayed response from LN5 (blue arrow) and the direct response from AN1. The second response of the coincidence detector LN3 is boosted, now its excitatory input to LN4 overcomes the inhibition, causing the feature detector neuron to spike (arrow). **(A,C–E)** from Schöneich et al. (2015); **(B)** modified after Kostarakos and Hedwig (2012).

the direct pathway is based on the connection between AN1 and the coincidence detector neuron, LN3 (**Figure 6C**). The delayed pathway appears to be set up via two neurons, an inhibitory neuron, LN2, which closely follows the activity of AN1, and a non-spiking interneuron, LN5 (Schöneich et al., 2015), which is inhibited for the 20 ms duration of a single sound pulse. At the end of a sound pulse, and so release of inhibition from LN2, neuron LN5 generates an excitatory post-inhibitory rebound response which reaches its maximum about 40 ms after the end of the sound pulse, corresponding to the duration of the pulse period (**Figure 6D**). This post-inhibitory rebound response can also be induced experimentally by applying a hyperpolarizing current pulse, and is produced upon the offset of the current pulse, i.e., when the hyperpolarization is removed. The post-inhibitory rebound has the same amplitude for stimulus intensities in the range of 50–80 dB SPL and thus provides a mechanism for intensity-independent auditory processing, which is a fundamental property of pattern recognition processes. The rebound response is also independent of stimulus duration, in the range of 10 to about 50 ms. For a delay line coincidence detector network, a coincidence detecting neuron should only respond when the direct and delayed pathways coincide, and one of the local brain neurons, LN3 exhibits response properties characteristic of a coincidence detector. Intracellular recordings of its synaptic activity indicate that the direct input to this neuron is provided by AN1, and the delayed input, based on the post-inhibitory rebound by the non-spiking interneuron, LN5. The response of LN3 to a single sound pulse is low (**Figure 6D**). However, if two pulses are presented at the species-specific pulse period of about 40 ms, its synaptic input and spike activity considerably increase, by a factor of 2.3 (**Figure 6E**). At lower pulse rates the direct and the delayed excitation to the coincidence detector are out of sync, and at higher pulse rates AN1 spike activity does not properly represent the sound pulses (see Schöneich et al., 2015 for details). Therefore, from the properties of this network, the neural circuitry responds best to the species-specific pulse rate (**Figure 6E**). The final element in this circuitry is the LN4 neuron. Its spike response to single sound pulses is subthreshold (**Figure 6D**) but it responds with 1–2 spikes if a second pulse arrives at the right interval (**Figure 6E**). This neuron integrates excitatory and inhibitory inputs, and its tuning toward different temporal patterns becomes more specific than the response of the coincidence detector neuron. This is due to the inhibition that suppresses spiking responses toward single sound pulses, and allows only sound pulses with the right interval to elicit spikes. Therefore, the LN4 is selectively only activated by the species-specific pulse pattern and acts like a feature detector for calling song. The neuron shows a band-pass tuning curve in its spike activity that very closely matches the tuning of female phonotactic behavior (Kostarakos and Hedwig, 2012). The evidence demonstrates that processing of the pulse rate occurs within the local network of ring-like brain neurons, which form a close association with the arborizations of AN1. This neural network may therefore represent the filter mechanism or feature detector circuit for the pulse pattern of calling song in crickets like *G. bimaculatus*. The auditory activity of other neurons in the brain with band-pass tuning curves similar to LN4 may be a consequence of this early processing mechanism (Schildberger, 1984b; Zorovič and Hedwig, 2011).

Interestingly, the overall auditory response within the circuit i.e., the number of spikes elicited per chirp, decreases at different levels of processing from AN1 to LN4 by about 90% (Kostarakos and Hedwig, 2012). This points toward sparse coding of the stimulus pattern (Olshausen and Field, 2004), which shifts the

representation of the stimulus features from a temporal code to a neuron-specific place code. Sparse coding appears to be an efficient way for simple nervous systems to ensure a robust representation of stimulus patterns.

PROCESSING AT THE CHIRP LEVEL: INSIGHTS FROM PATTERN RECOGNITION AND AUDITORY STEERING

In addition to the pulse pattern of calling song, in many species of crickets (Alexander, 1962; Otte, 1992) sound pulses are grouped into chirps, which in *G. bimaculatus* are repeated at a rate of 3–4/s. In phonotactic experiments, females tolerate a range of chirp periods and respond even when chirps are presented only at a rate of 1/s (Doherty, 1985). The chirp pattern may require an additional filter mechanism on a longer time scale than the pulse repetition rate (Grobe et al., 2012). Some insights into possible mechanisms of processing at the chirp time scale can be derived from female phonotactic steering responses. When exposed to an attractive calling song signal presented from above, female crickets will have no directional cue and cannot orient toward the sound source. However, when a non-attractive sound pattern is additionally interleaved and presented from the side, a female will steer toward the non-attractive pattern. This indicates that steering is under control of the pattern recognition process and that pattern recognition and phonotactic steering are organized in a serial manner (Doherty, 1991); a pattern apparently has been recognized before the steering process is permitted.

More details can be revealed with a trackball system that measures the fast steering responses during phonotaxis. Female *G. bimaculatus* will not orient to non-attractive sounds like chirps with long sound pulses or oval-shaped amplitude-modulated sound signals presented at the natural chirp rate, whereas they readily respond toward the species-specific pulse pattern (**Figures 7A,B**). The females however, do steer to non-attractive chirps when these are interspersed into an ongoing calling song (Poulet and Hedwig, 2005), or in some animals even when presented just after single normal chirps, interspersed into a sequence of non-attractive chirps (**Figure 7C**). The readiness to orient toward non-attractive chirps gradually decays over several seconds after listening to a sequence of calling song (Poulet and Hedwig, 2005). This steering response to non-attractive patterns indicates that a modulation process on a longer time scale is initiated which modulates the auditory motor response when the species-specific pattern is processed.

Once female *G. bimaculatus* have been exposed to the calling song, they no longer evaluate the complete temporal pattern of chirps during phonotaxis, but instead steer to the first sound pulse of a chirp. They even rapidly orient toward individual sound pulses, when these are presented in a split-song paradigm, with alternating pulses on the left and the right hand side of the animals' length axis; the steering responses occur with a latency of only 55–60 ms (Hedwig and Poulet, 2004, 2005). As the recognition for the pulse rate requires at least two sound pulses (see above) the pattern recognition network can not directly provide the commands for phonotactic steering. The

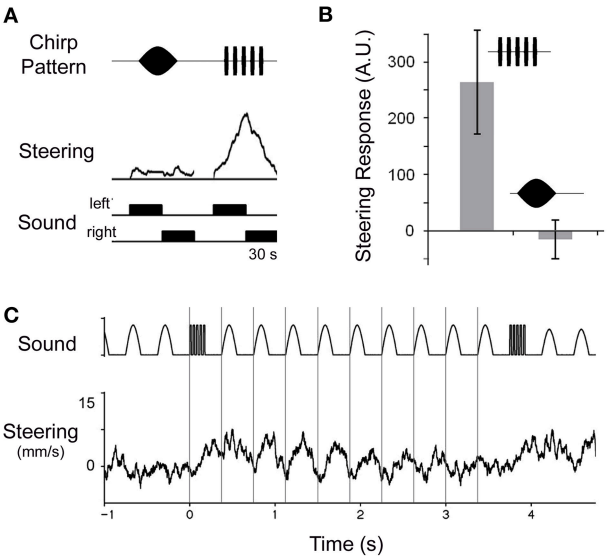

FIGURE 7 | Modulation of steering and pattern selectivity during phonotaxis. (A) Female crickets do not steer toward an oval-shaped amplitude-modulated chirp, but respond to the normal chirp pattern when walking on a trackball. Each pattern is presented for 30 s from the left and right hand side. **(B)** Quantitative analysis of phonotactic steering in four animals demonstrates the relative attractiveness of both patterns. **(C)** When a single normal chirp pattern is interspersed into a sequence of non-attractive oval-shaped amplitude-modulated chirps; this female transiently steers toward the non-attractive pattern, indicating that processing a normal chirp modulates the subsequent processing of acoustic signals. Steering responses averaged over 15 trials.

sparse coding at the level of the feature detector neuron LN4 (Kostarakos and Hedwig, 2012; Schöneich et al., 2015) further makes it difficult to envisage how its spike pattern might drive rapid auditory steering responses. Steering may rather involve a form of low level reactive processing which however is controlled and modulated on a longer time scale by the pattern recognition process in the brain (Poulet and Hedwig, 2005). The time-scale of this modulatory process is sufficient to explain phonotactic processing at the chirp level and could be the basis for trade-off phenomena of different song parameters as observed before (Stout et al., 1983; Doherty, 1985). A modulatory effect on phonotactic steering will be useful under natural conditions and will allow females to pursue their phonotactic approach to a calling male, even when the signal is temporally degraded due to diffraction or obstacles.

A specific neural circuitry for temporal filtering on the time scale of the chirp rate may not be required; processing at the chirp level may rather emerge from the modulatory properties of the pulse processing network. The upper limit for tolerated chirp periods could be set by the time constant of the gradually decreasing modulation effect and its lower limit may be reached when the pulse rate filter becomes ineffective, as very short chirp intervals will lead to an adaptation of the network and prevent its recovery. Whether the modulatory effect occurs within the thoracic ganglia or within the brain is unknown. The more posterior projection pattern of auditory afferents tuned

to the calling song may point toward a thoracic pathway that nonetheless will be under descending control from the pattern recognition process in the brain. Processing at the level of the thoracic ganglia could provide an advantage because the auditory signals for steering could be directly forwarded to the walking motor control system with a short latency, avoiding a long loop via the brain.

DISCUSSION: FRAMEWORK AND OPEN QUESTIONS

"Deciphering the brain's codes" (Konishi, 1991) is a central ongoing topic in neuroscience. In relation to sensory pattern recognition, ideas of a "single central integrator" (Barlow, 1961; Bullock, 1961), or "feature detectors" (Hoy, 1978) that represent complex sensory input at the highest level have been central, and have shaped our thinking and concepts (Martin, 1994). Experimental approaches aiming to identify such higher order feature detecting neurons and their response properties have fostered an understanding of the way that sensory systems operate when processing behaviorally relevant stimuli (Konishi, 1991). Even simple acoustic communication signals require a combination of sensory filters for a selective behavioral response. These sensory filters, such as for the amplitude, duration, or frequency of a signal, could be arranged in parallel, to finally feed into a feature detector similar to the combination-sensitive neurons in vertebrate auditory processing (Bullock, 1961; Rauschecker and Tian, 2006). Alternatively, pattern recognition may be broken down into a sequential process of autonomous stages (Barlow, 1961). The latter may be more specific, and adaptive in "simple" insect nervous systems, in which the capacity for neural processing is more restricted (Wehner, 1987). Auditory feature detection underlying cricket mate attraction points toward such a sequential solution. Otherwise, in the insect CNS and brain also multimodal neurons integrate information from different sensory pathways (Pearson et al., 1980; Schildberger, 1984a) a process which at a higher level of behavioral control may be essential for selecting and initiating adaptive motor responses (Wessnitzer and Webb, 2006).

In *G. bimaculatus* the problem of recognizing the conspecific calling song can be described as a sequence of filter processes that gradually sharpen the neuronal responses to be more selective, which eventually lead to a species-specific phonotactic motor response (**Figure 2**). In this sequence, only the final stage of signal processing may be regarded as a "feature detector," whereas the lower levels provide "filtering processes." An important functional difference between the filtering processes and the feature detector is that only the feature detector activity should be coupled to a behavioral decision that may be initiated once the detector is activated; none of the preceding filter processes should have such an impact. Several filtering steps contribute to calling song feature detection in the cricket brain, with a similar organization of sensory processing in other sensory systems.

Processing of Sound Frequency

The conserved frequency tuning at different levels of the auditory pathway demonstrates that peripheral biomechanical filtering provides the essential basis for the tuning of phonotactic behavior. The frequency selectivity of female phonotactic behavior is already determined at the level of the hearing organ, and the tuning of the hearing organ defines the tuning of the auditory afferents. The detailed basis of frequency tuning in the cricket hearing organ is however not yet revealed. Auditory filter mechanisms, which tune hearing organs to the frequencies of the communication signal, are found in many other species, which depend on acoustic signals for mate attraction (grasshoppers: Meyer and Elsner, 1996, 1997), predator avoidance (moths: Schiolten et al., 1981; Fullard, 1984), and host detection (parasitic flies: Robert et al., 1992; Oshinsky and Hoy, 2002). These systems represent examples of a peripheral "matched filter," which limits the information received by the nervous system, but simplifies the way it can be processed (Wehner, 1987).

Comparing the tuning curve of AN1 with the tuning of the auditory nerve may suggest that some additional central neural processing may sharpen the response of AN1 or rather that AN1 is selectively activated by the low frequency afferents. The data nonetheless indicate that the best mechanical response of the auditory organ drives the tuning of the majority of auditory afferents and finally the tuning of the AN1 interneuron, which matches phonotaxis (Kostarakos et al., 2008) and is crucial for phonotaxis as it provides the auditory information to the brain (Schildberger and Hörner, 1988). The response of the AN1 neuron subsequently determines the frequency tuning of brain neurons in the delay line coincidence detector network (Schöneich et al., 2015) and the tuning of the behavioral response. Like in other insect auditory systems the frequency filter in crickets is already established at the most peripheral level and provides the first filter in the calling song recognition process.

Onset Responses to Sound Pulses

Phasic responses of afferents and interneurons are a common feature of insect mechanoreceptive neurons (Field and Matheson, 1998). In auditory sensory neurons, they enhance the response to the onset of sound pulses (Nabatiyan et al., 2003) and are therefore suited to reliably code the timing of song patterns (Machens et al., 2003). The pool of afferent neurons with synchronously activated spike patterns (Ronacher and Römer, 1985) provides the nervous system with a robust temporal representation of regularly repeated communication signals. The prevalence of phasic responses in auditory neurons may indicate that evolution has shaped the call of male crickets into a series of regularly-repeated sound pulses in order to exploit the phasic response of the auditory afferents of females. This is in-keeping with the concept of sensory exploitation; as communication signals may evolve by the signaler exploiting pre-existing sensory biases in receivers (Ryan and Rand, 1993).

Reciprocal inhibition at the level of thoracic ON1 neurons enhances and sharpens the response to the onset of sound, and thereby is suited to especially represent short sound pulses in the activity pattern of the neurons. The dynamics of spike activity in ON1 at sound onset is in agreement with the reciprocal inhibition functioning as a temporal filter (Wiese and Eilts, 1985; Wiese and Eilts-Grimm, 1985). Based on the time constants of the transmission delay between the neurons, these authors had

suggested that the tuning of the cricket auditory pathway to the calling song pattern may be due to the reciprocal inhibition, which follows the intervals of the sound pattern. However, such a filter had not yet been clearly demonstrated experimentally, as cricket auditory systems have rarely been analyzed under symmetrical stimulus conditions, like during phonotaxis when the auditory signal arrives from the front. As the strength of the inhibitory coupling may vary in different animals, the significance of this bilateral processing mechanism remains to be substantiated; it certainly is not the pattern recognition mechanism for the calling song. However, the mechanism may contribute to the enhanced information transfer, i.e., the number of bits coded by the spike patterns, in ON1 neurons for species-specific pulse rates as described in *T. oceanicus* (Marsat and Pollack, 2004). The excitatory and inhibitory inputs to ON1 neurons depend on the directionality of the ears, therefore processing at the level of the ON1 neurons may form a type of spatially selective filter for the crickets' communication signal (Marsat and Pollack, 2004). This filter mechanism would be especially important whenever the insects face a frontal signal source, such as during the approach of a singing male. As a spatially selective filter, it should play a crucial part in hyper-acute auditory orientation that allows females to steer to signal sources which are just 1–2 degree off their length axis (Schöneich and Hedwig, 2010).

The combination of the phasic-tonic response properties of the auditory afferents and the onset-enhancing mechanisms of some first order interneurons allow for an efficient neural representation of the cricket's acoustic communication pulses. Together, they can be regarded an important filtering step for the processing of calling song pulses which occurs at the thoracic level. To what degree this processing at the level of the ON1 also influences auditory activity ascending to the brain will need further elucidation.

Detecting Pulse Rate—A Feature Detector of Calling Song

The recordings from brain neurons provide strong support for a circuit comprising a delay line and a coincidence detector (Schöneich et al., 2015), as outlined in a general concept of resonant network design (Reiss, 1964; Weber and Thorson, 1989; for a discussion of concepts for cricket pattern recognition such as internal templates, band-pass filtering, resonant networks see Kostarakos and Hedwig, 2015). Based on the initial filter processes, the delay line coincidence detection circuitry in the brain allows a feature detecting neuron (LN4) to selectively respond to the pulse rate of the calling song. It provides a robust description of the pulse-rate filter at a circuit and cellular level. The pulse rate tuning of the LN4 neuron matches the band-pass tuning of phonotactic behavior, as well as its frequency dependence (Kostarakos and Hedwig, 2015; Schöneich et al., 2015). The neuron therefore is a higher order neuron that can be classified as a feature detector for the cricket's calling song (Hoy, 1978).

The function of this circuitry depends on two essential processes: generation of a delay line via a post-inhibitory rebound and coincidence detection. A computational model for temporal selectivity in the acoustically communicating fish *Pollimyrus adspersus* based on a post-inhibitory rebound mechanisms, shows that temporal selectivity of the network can be tuned by the delayed time course of the post-inhibitory and by the subsequent excitatory input that coincides with the intrinsic rebound excitation (Crawford, 1997; Large and Crawford, 2002). By systematic changing the timing of the post-inhibitory rebound, this model network allows to tune output neurons to different click rates of the fish communication signal. Post-inhibitory rebound also occurs in the mouse auditory pathway where neurons in the superior olivary nucleus generate a pronounced post-inhibitory rebound underlying their selectivity for periodic low frequency amplitude modulations of sound signals (Felix et al., 2011). Post-inhibitory rebound is furthermore widely involved in precisely timed auditory processing (Koch and Grothe, 2003; Kopp-Scheinpflug et al., 2011). Delay lines and coincidence detectors covering time scales of many milliseconds are also implicated in the processing of echolocating signals in bats where they lead to topographic maps for echo delays (Suga, 1990; Kössl et al., 2014). In general they may represent a fundamental neural mechanism for processing the temporal structure of sound signals.

The feature detecting circuits are present at both sides of the protocerebrum and are coupled via local bilateral projecting neurons (Kostarakos and Hedwig, 2012), two bilateral song recognizers had been proposed by Pollack (1986). If and how the bilateral circuits interact, is not yet resolved; in acoustically communicating grasshoppers the auditory information from both sides is added in support of pattern recognition (von Helversen and von Helversen, 1995).

The field cricket *G. bimaculatus* may only need an auditory feature detecting mechanism for the pulse pattern of the calling song as rivalry and courtship signals are embedded in more complex close up encounters of mates. As the timing of sound pulses during calling and rivalry song is quite similar, the discussed filter mechanisms likely are also activated during rivalry song; whereas the high pitch courtship signals may require a different line of processing. The modulatory component in the auditory pathway, which allows for transient steering to non-attractive signals, may provide the basis for temporal filtering at the chirp level. For females, it will be sufficient to employ one neural circuit for pulse rate recognition and use a modulatory effect based on the pattern recognition process to also control responses at the time scale of the chirps.

Control of Phonotactic Behavior

Female phonotaxis gradually develops and appears with sexual maturation 6–7 days after the last molt in *G. bimaculatus* (Loher et al., 1993) and 10–13 days in *G. assimilis* (Pacheco et al., 2013); it is strongly reduced after mating and upon female contact to males (Cade, 1979; Loher et al., 1993); and in *T. oceanicus* it may even depend on social experience of the larvae (Bailey and Zuk, 2009). The quality and strength of phonotaxis varies among females. Only 25–50% perform phonotaxis reliable under experimental conditions (Weber et al., 1981) and the probability that a female shows phonotaxis changes over time

(Bailey, 2011). The physiological background for the maturation and variation in the strength of phonotaxis over periods of days is not yet resolved; however juvenile hormone may not play a role (Loher et al., 1992). Understanding the physiological background and moreover having neurochemical tools available to control phonotactic behavior would be a decisive advance for the neurophysiological analysis.

On a short time scale females steer to non-attractive patterns which are interspersed into calling song (Doherty, 1991; Poulet and Hedwig, 2005). This change in phonotactic behavior will be adaptive under natural conditions, when the acoustic signal quality transiently deteriorates (Forrest, 1994) and needs to be considered when interpreting behavioral data.

The location of the delay line coincidence detector circuit in the anterior protocerebrum raises a central question of how the pulse rate recognition circuit may finally initiate the phonotactic motor response. The central control mechanisms for phonotaxis is likely embedded in more general brain control architecture for insect behavior involving the central body complex (Strausfeld, 1999; Wessnitzer and Webb, 2006). Cricket auditory behavior is controlled by the circadian clock; medulla bilateral neurons project toward the neuropil dorsal to the central body and the stalk of the mushroom body (Yukizane et al., 2002). Neuropil areas in the vicinity of the central complex and the mushroom bodies are implicated in the control of singing (Huber, 1962; Otto, 1971; Hedwig, 2006; see Hoffmann et al., 2007 for grasshoppers). In flies and cockroaches the central body complex is involved in the control of walking (Strausfeld, 1999; Strauss, 2002; Bender et al., 2010). Like in some other insects in crickets it provides a compass like map for spatial orientation to polarized light (Sakura et al., 2008); yet so far we do not know to what degree it may contribute to auditory orientation during phonotaxis. The dendrites of local and descending auditory responsive brain neurons are found in the lateral accessory lobes, which generally are implicated in the control of insect motor activity and are regarded as a pre-motor region of the insect brain (Zorovič and Hedwig, 2011). Ipsilateral descending brain neurons controlling walking have also been identified in the dorsal protocerebrum (Böhm and Schildberger, 1992). However, recordings of descending brain neurons during robust phonotactic walking are still lacking; so far the reported auditory responses of such interneurons (Staudacher and Schildberger, 1998; Zorovič and Hedwig, 2013) are not sufficient to identify neural commands as required for fast and precise phonotactic steering.

The modulatory effect of pattern recognition on phonotactic steering may control auditory-motor integration at the level of thoracic networks involving posteriorly branching auditory afferents and DN1 interneurons which are tuned to the cricket calling song (Imaizumi and Pollack, 2005; Poulet and Hedwig, 2005). In such a scenario precise descending motor commands would not be required and direct reflex-like responses to auditory signals could be integrated into the walking motor pattern at the thoracic level once the modulation kicks in. How auditory steering is incorporated into the walking motor output adds another complexity to signal processing, which we just begin to understand at the behavioral level using high speed video recordings (Baden and Hedwig, 2008; Witney and Hedwig, 2011; Petrou and Webb, 2012).

Animals with specialized behavior provide model systems to analyse adapted neural processing. Particularly, insects with their "simple" nervous systems allow a detailed study of neural mechanisms at the level of identified neurons, to unravel how the system is designed to process relevant stimuli. This review focussed on data in the crickets *G. campestris* and *G. bimaculatus.* From this a comprehensive picture starts to emerge outlining the functional properties and neural basis of auditory signal processing. Pattern recognition is based on a sequence of filter mechanisms in the auditory pathway, which selectively respond to a characteristic property of the calling song and gradually sharpen the response of a neural feature detector in the brain. Based on these findings a most interesting comparative approach could reveal the filter and feature detecting mechanisms in other species, which signal with different pulse patterns for mate attraction (Alexander, 1962). Will these species use functional similar filter mechanisms and a neural circuit in the brain as a feature detector network, and in which way will the properties of the component neurons and the networks be adapted to the species-specific signals? Computational approaches based on Gabor filters have addressed this question and predict different temporal filter properties (Hennig et al., 2014; Ronacher et al., 2015). However, physiological experiments are required to reveal the actual species-specific adaptations in the neuronal mechanisms for pattern recognition that have been adapted and shaped during evolution.

ETHIC STATEMENT

Experiments in the Hedwig lab complied with the principles of Laboratory Animal Care.

AUTHOR CONTRIBUTIONS

The author confirms being the sole contributor of this review and approved it for publication.

FUNDING

Supported by the Biotechnology and Biological Sciences Research Council (BB/J01835X/1) and the Isaac Newton Trust (Trinity College, Cambridge).

ACKNOWLEDGMENTS

I thank Kostas Kostarakos and Stefan Schöneich for their contribution to the analyses of the feature detector network; Tim Bayley and Pedro Jacob for their constructive comments on the MS, Julie Sarmiente-Ponce for the frequency tuning data of phonotaxis, Oliver Bock-Brown and Jack Stockdale for the data on the modulation of phonotactic steering, and Leonie Remm for images and sound recordings.

REFERENCES

Alexander, R. D. (1962). Evolutionary change in cricket acoustical communication. *Evolution* 16, 443–467. doi: 10.2307/2406178

Alexander, R. D. (1967). Acoustical communication in arthropods. *Ann. Rev. Entomol.* 12, 495–526. doi: 10.1146/annurev.en.12.010167.002431

Baden, T., and Hedwig, B. (2007). Neurite-specific Ca^{2+} dynamics underlying sound processing in an auditory interneurone. *J. Neurobiol.* 67, 68–80. doi: 10.1002/neu.20323

Baden, T., and Hedwig, B. (2008). Front leg movements and tibial motoneurons underlying auditory steering in the cricket (*Gryllus bimaculatus* deGeer). *J. Exp. Biol.* 211, 2123–2133. doi: 10.1242/jeb.019125

Bailey, N. W. (2011). Mate choice plasticity in the field cricket *Teleogryllus oceanicus*: effects of social experience in multiple modalities. *Behav. Ecol. Soc.* 65, 2269–2278. doi: 10.1007/s00265-011-1237-8

Bailey, N. W., and Zuk, M. (2009). Field crickets change mating preferences using remembered social information. *Biol. Lett.* 5, 449–451. doi: 10.1098/rsbl.2009.0112

Barlow, H. B. (1961). "Possible principles underlying the transformation of sensory messages," in *Sensory Communication*, ed W. A. Rosenblith (Cambridge, MA: MIT Press), 217–234.

Bender, J. A., Pollack, A. J., and Ritzmann, R. E. (2010). Neural activity in the central complex of the insect brain is linked to locomotor changes. *Curr. Biol.* 20, 921–926. doi: 10.1016/j.cub.2010.03.054

Böhm, H., and Schildberger, K. (1992). Brain neurones involved in the control of walking in the cricket *Gryllus bimaculatus*. *J. Exp. Biol.* 166, 113–130.

Bullock, T. H. (1961). "The problem of recognition in an analyzer made of neurons," in *Sensory Communication*, ed W. A. Rosenblith (Cambridge, MA: MIT Press), 717–724.

Bush, S. L., and Schul, J. (2006). Pulse-rate recognition in an insect: evidence of a role for oscillatory neurons. *J. Comp. Physiol. A* 192, 113–121. doi: 10.1007/s00359-005-0053-x

Busnel, R. G. (1963). *Acoustic Behaviour of Animals.* Amsterdam; London: Elsevier.

Cade, W. H. (1979). Effect of male-deprivation on female phonotaxis in field crickets (Orthoptera: Gryllidae; Gryllus). *Can. Entomol.* 111, 741–744. doi: 10.4039/Ent111741-6

Carlson, A. D., and Copeland, J. (1985). Flash communication in fireflies. *Q. Rev. Biol.* 60, 415–436. doi: 10.1086/414564

Carr, C. E. (1993). Delay line models of sound localization in the barn owl. *Am. Zool.* 33, 79–85. doi: 10.1093/icb/33.1.79

Casaday, G. B., and Hoy, R. R. (1977). Auditory interneurons in the cricket Teleogryllus oceanicus: physiological and anatomical properties. *J. Comp Physiol. A.* 121, 1–13. doi: 10.1007/BF00614177

Crawford, J. D. (1997). Feature-detecting auditory neurons in the brain of a sound-producing fish. *J. Comp. Physiol. A.* 180, 439–450. doi: 10.1007/s003590050061

Doherty, J. A. (1985). Trade-off phenomena in calling song recognition and phonotaxis in the cricket, *Gryllus bimaculatus* (Orthoptera, Gryllidae). *J. Comp. Physiol. A.* 156, 787–801. doi: 10.1007/BF00610831

Doherty, J. A. (1991). Song recognition and localization in the phonotaxis behavior of the field cricket, *Gryllus bimaculatus* (Orthoptera: Gryllidae). *J. Comp. Physiol. A.* 168, 213–222. doi: 10.1007/BF00218413

Eibl, E., and Huber, F. (1979). Central projections of tibial sensory fibers within the three thoracic ganglia of crickets (*Gryllus campestris* L., *Gryllus bimaculatus* DeGeer). *Zoomorphology* 92, 1–17. doi: 10.1007/BF00999832

Esch, H., Huber, F., and Wohlers, D. W. (1980). Primary auditory neurons in crickets: physiology and central projections. *J. Comp. Physiol. A.* 137, 27–38. doi: 10.1007/BF00656914

Felix, R. A., Fridberger, A., Leijon, S., Berrebi, A. S., and Magnusson, A. K. (2011). Sound rhythms are encoded by postinhibitory rebound spiking in the superior paraolivary nucleus. *J. Neurosci.* 31, 12566–12578. doi: 10.1523/jneurosci.2450-11.2011

Field, L. H., and Matheson, T. (1998). Chordotonal organs of insects. *Adv. Ins. Physiol.* 27, 1–56. doi: 10.1016/S0065-2806(08)60013-2

Forrest, T. (1994). From sender to receiver: propagation and environmental effects on acoustic signals. *Am. Zool.* 34, 644–654. doi: 10.1093/icb/34.6.644

Fullard, J. H. (1984). External auditory structures in two species of neotropical notodontid moths. *J. Comp. Physiol. A.* 155, 625–632. doi: 10.1007/BF00610848

Grobe, B., Rothbart, M. M., Hanschke, A., and Hennig, R. M. (2012). Auditory processing at two time scales by the cricket *Gryllus bimaculatus*. *J. Exp. Biol.* 215, 1681–1690. doi: 10.1242/jeb.065466

Harrison, S. J., Thomson, I. R., Grant, C. M., and Bertram, S. M. (2013). Calling, courtship, and condition in the fall field cricket, *Gryllus pennsylvanicus*. *PLoS ONE* 8:e60356. doi: 10.1371/journal.pone.0060356

Hedwig, B. (2006). Pulses, patterns and paths: neurobiology of acoustic behaviour in crickets. *J. Comp. Physiol. A.* 192, 677–689. doi: 10.1007/s00359-006-0115-8

Hedwig, B. (2014). *Insect Hearing and Acoustic Communication*. Berlin; Heidelberg: Springer Verlag.

Hedwig, B., and Poulet, J. F. A. (2004). Complex auditory behaviour emerges from simple reactive steering. *Nature* 430, 781–785. doi: 10.1038/nature02787

Hedwig, B., and Poulet, J. F. A. (2005), Mechanisms underlying phonotactic steering in the cricket *Gryllus bimaculatus* (de Geer) revealed with a fast trackball system. *J. Exp. Biol.* 208, 915–927. doi: 10.1242/jeb.01452

Hennig, R. M., Heller, K.-G., and Clemens, J. (2014). Time and timing in the acoustic recognition system of crickets. *Front. Physiol.* 5:286. doi: 10.3389/fphys.2014.00286

Hill, K. G. (1974). Carrier frequency as a factor in phonotactic behaviour of female crickets (*Teleogryllus commodus*). *J. Comp. Physiol. A.* 93, 7–18. doi: 10.1007/BF00608756

Hoffmann, K. Wirmer, A., Kunst, M., Gocht, D. and Heinrich, R. (2007). Muscarinic excitation in grasshopper song control circuits is limited by acetylcholinesterase activity. *Zoolog. Sci.* 24, 1028–1035. doi: 10.2108/zsj.24.1028

Horseman, G., and Huber, F. (1994). Sound localisation in crickets I. Contralateral inhibition of an ascending auditory interneuron (AN1) in the cricket *Gryllus bimaculatus*. *J. Comp. Physiol. A.* 175, 399–413.

Hoy, R. R. (1978). Acoustic communication in crickets: a model system for the study of feature detection. *Fed. Proc.* 37, 2316–2323.

Huber, F. (1962). Central nervous control of sound production in crickets and some speculations on its evolution. *Evolution* 16, 429–442. doi: 10.2307/2406177

Huber, F. (1978). The insect nervous system and insect behaviour. *Anim. Behav.* 26, 969–981. doi: 10.1016/0003-3472(78)90085-4

Huber, F., and Thorson, J. (1985). Cricket auditory communication. *Sci. Am.* 253, 46–54. doi: 10.1038/scientificamerican1285-60

Imaizumi, K., and Pollack, G. S. (1999). Neural coding of sound frequency by cricket auditory receptors. *J. Neurosci.* 19, 1508–1516.

Imaizumi, K., and Pollack, G. S. (2005). Central projections of auditory receptor neurons of crickets. *J. Comp. Neurol.* 493, 439–447. doi: 10.1002/cne.20756

Jacobsen, M. (1972). *Insect Sex Pheromones*. New York, NY; London: Academic Press.

Jeffress, L. A. (1948). A place theory of sound localization. *J. Comp. Physiol. Psychol.* 41, 35–39.

Johnstone, B., Saunders, J. C., and Johnstone, J. R. (1970). Tympanic membrane response in the cricket. *Nature* 227, 625–626. doi: 10.1038/227625a0

Kleindienst, H. U., Wohlers, D. W., and Larsen, O. N. (1983). Tympanal membrane motion is necessary for hearing in crickets. *J. Comp. Physiol. A.* 151, 397–400. doi: 10.1007/BF00605455

Koch, U., and Grothe, B. (2003). Hyperpolarization-activated current (Ih) in the inferior colliculus: distribution and contribution to temporal processing. *J. Neurophysiol.* 90, 3679–3687. doi: 10.1152/jn.00375.2003

Konishi, M. (1991). Deciphering the brain's codes. *Neur. Comp.* 3, 1–18. doi: 10.1162/neco.1991.3.1.1

Kopp-Scheinpflug, C., Tozer, A. J. B., Robinson, S. W., Tempel, B. L., Hennig, M. H., and Forsythe, I. D. (2011). The sound of silence: ionic mechanisms encoding sound termination. *Neuron* 71, 911–925. doi: 10.1016/j.neuron.2011.06.028

Kössl, M., Hechavarria, J. C., Voss, C., Macias, S., Mora, E. C., and Vater, M. (2014). Neural maps for target range in the auditory cortex of echolocating bats. *Curr. Opin. Neurobiol.* 24, 68–75. doi: 10.1016/j.conb.2013.08.016

Kostarakos, K., Hartbauer, M., and Römer, H. (2008). Matched filters, mate choice and the evolution of sexually selected traits. *PLoS ONE* 3:e3005. doi: 10.1371/journal.pone.0003005

Kostarakos, K., and Hedwig, B. (2012). Calling song recognition in female crickets: temporal tuning of identified brain neurons matches behavior. *J. Neurosci.* 32, 9601–9612. doi: 10.1523/JNEUROSCI.1170-12.2012

Kostarakos, K., and Hedwig, B. (2015). Pattern recognition in field crickets: concepts and neural evidence. *J. Comp. Physiol. A*. 201, 73–85. doi: 10.1007/s00359-014-0949-4

Kostarakos, K., Hennig, M. R., and Römer, H. (2009). Two matched filters and the evolution of mating signals in four species of cricket. *Front. Zool.* 6:22. doi: 10.1186/1742-9994-6-22

Large, E. W., and Crawford, J. D. (2002). Auditory temporal computation: interval selectivity based on post-inhibitory rebound. *J. Comp. Neurosci.* 13, 125–142. doi: 10.1023/A:1020162207511

Larsen, O. N. (1981). Mechanical time resolution in some insect ears. *J. Comp. Physiol. A*. 143, 297–304. doi: 10.1007/BF00611165

Lewis, S. M., and Cratsley, C. K. (2008). Flash signal evolution, mate choice, and predation in fireflies. *Annu. Rev. Entomol.* 53, 293–321. doi: 10.1146/annurev.ento.53.103106.093346

Libersat, F., Murray, J., and Hoy, R. R. (1994). Frequency as a releaser in the courtship song of two crickets, *Gryllus bimaculatus* (de Geer) and *Teleogryllus oceanicus*: a neuroethological analysis. *J. Comp. Physiol. A*. 174, 485–494. doi: 10.1007/BF00191714

Loher, W., Weber, T., and Huber, F. (1993). The effect of mating on phonotactic behaviour in *Gryllus bimaculatus* (De Geer). *Physiol. Entomol*. 18, 57–66. doi: 10.1111/j.1365-3032.1993.tb00449.x

Loher, W., Weber, T., Rembold, H., and Huber, F. (1992). Persistence of phonotaxis in females of four species of crickets following allatectomy. *J. Comp. Physiol. A*. 171, 325–341. doi: 10.1007/BF00223963

Machens, C. K., Schütze, H., Franz, A., Kolesnikova, O., Stemmler, M. B., Ronacher, B., et al. (2003). Single auditory neurons rapidly discriminate conspecific communication signals. *Nat. Neurosci.* 6, 341–342. doi: 10.1038/nn1036

Marsat, G., and Pollack, G. S. (2004). Differential temporal coding of rhythmically diverse acoustic signals by a single interneuron. *J. Neurophysiol*. 92, 939–948. doi: 10.1152/jn.00111.2004

Martin, K. A. (1994). A brief history of the "feature detector." *Cereb. Cortex* 4, 1–7.

Meyer, J., and Elsner, N. (1996). How well are frequency sensitivities of grasshopper ears tuned to species-specific song spectra? *J. Exp. Biol.* 199, 1631–1642.

Meyer, J., and Elsner, N. (1997). Can spectral cues contribute to species separation in closely related grasshoppers? *J. Comp. Physiol. A*. 180, 171–180. doi: 10.1007/s003590050038

Mhatre, N., and Robert, D. (2013). A tympanal insect ear exploits a critical oscillator for active amplification and tuning. *Curr. Biol.* 23, 1952–1957. doi: 10.1016/j.cub.2013.08.028

Michel, K. (1974). Das Tympanalorgan von *Gryllus bimaculatus* Degeer (Saltatoria, Gryllidae). *Z. Morphol. Tiere.* 77, 285–315. doi: 10.1007/BF00298805

Michelsen, A., Popov, A., and Lewis, B. (1994). Physics of directional hearing in the cricket *Gryllus bimaculatus*. *J. Comp. Physiol. A*. 175, 153–164. doi: 10.1007/BF00215111

Montealegre-Z, F., Jonsson, T., Robson-Brown, K. A., Postles, M., and Robert, D. (2012). Convergent evolution between insect and mammalian audition. *Science* 338, 968–671. doi: 10.1126/science.1225271

Nabatiyan, A., Poulet, J., de Polavieja, G., and Hedwig, B. (2003). Temporal pattern recognition based on instantaneous spike rate coding in a simple auditory system. *J. Neurophysiol.* 90, 2484–2493. doi: 10.1152/jn.00259.2003

Nocke, H. (1972). Physiological aspects of sound communication in crickets (*Gryllus campestris* L.). *J. Comp. Physiol. A* 80, 141–162. doi: 10.1007/BF00696487

Oldfield, B., Kleindienst, H., and Huber, F. (1986). Physiology and tonotopic organization of auditory receptors in the cricket *Gryllus bimaculatus* DeGeer. *J. Comp. Physiol. A*. 159, 457–464. doi: 10.1007/BF00604165

Olshausen, B. A., and Field, D. J. (2004). Sparse coding of sensory inputs. *Curr. Opin. Neurobiol.* 14, 481–487. doi: 10.1016/j.conb.2004.07.007

Oshinsky, M. L., and Hoy, R. R. (2002). Physiology of the auditory afferents in an acoustic parasitoid fly. *J. Neurosci*. 22, 7254–7763.

Otte, D. (1992). Evolution of cricket songs. *J. Orthop. Res.* 1, 25–49. doi: 10.2307/3503559

Otto, D. (1971). Untersuchungen zur zentralnervösen Kontrolle der Lauterzeugung von Grillen. *J. Comp. Physiol. A*. 74, 227–271.

Pacheco, K., Dawson, J. W., Jutting, M., and Bertram, S. M. (2013). How age influences phonotaxis in virgin female Jamaican field crickets (*Gryllus assimilis*). *PeerJ* 1:e130. doi: 10.7717/peerj.130

Paton, J. A., Capranica, R. R., Dragsten, P. R., and Webb, W. W. (1977). Physical basis for auditory frequency analysis in field crickets (Gryllidae). *J. Comp. Physiol. A*. 119, 221–240. doi: 10.1007/BF00656635

Pearson, K., Heitler, W., and Steeves, J. (1980). Triggering of locust jump by multimodal inhibitory interneurons. *J. Neurophysiol*. 43, 257–278.

Petrou, G., and Webb, B. (2012). Detailed tracking of body and leg movements of a freely walking female cricket during phonotaxis. *J. Neurosci. Meth.* 203, 56–68. doi: 10.1016/j.jneumeth.2011.09.011

Pollack, G., and Faulkes, Z. (1998). Representation of behaviorally relevant sound frequencies by auditory receptors in the cricket *Teleogryllus oceanicus*. *J. Exp. Biol.* 201, 155–163.

Pollack, G. S. (1986). Discrimination of calling song models by the cricket, *Teleogryllus oceanicus*: the influence of sound direction on neural encoding of the stimulus temporal pattern and on phonotactic behavior. *J. Comp. Physiol. A*. 158, 549–561. doi: 10.1007/BF00603799

Pollack, G. S. (1988). Selective attention in an insect auditory neuron. *J. Neurosci*. 8, 2635–2639.

Pollack, G. S., and Hoy, R. R. (1981). Phonotaxis in flying crickets: neural correlates. *J. Insect Physiol.* 27, 41–45. doi: 10.1016/0022-1910(81)90030-5

Popov, A., Markovich, A., and Andjan, A. (1978). Auditory interneurons in the prothoracic ganglion of the cricket, *Gryllus bimaculatus* DeGeer I. The large Segmental auditory neuron (LSAN). *J. Comp. Physiol. A*. 126, 183–192. doi: 10.1007/BF00666372

Popov, A., Shuvalov, V., Svetlogorskaya, I., and Markovich, A. (1974). "Acoustic behaviour and auditory system in insects," in *Mechanoreception, Abhandlungen der Rheinisch-Westfälischen Akademie der Wissenschaften Symposium,* Vol. 53, ed J. Schwartzkopff (Opladen: Westdeutscher Verlag), 281–306.

Poulet, J. F. A., and Hedwig, B. (2005). Auditory orientation in crickets: pattern recognition controls reactive steering. *Proc. Natl. Acad. Sci. U.S.A.* 102, 15665–15669. doi: 10.1073/pnas.0505282102

Rauschecker, J., and Tian, B. (2006). "Hierarchic processing of communication sounds in primates," in *Behavior and Neurodynamics for Auditory Communication*, eds J. S. Kanwal and G. Ehret (Cambridge: Cambridge University Press), 205–223.

Reiss, R. (1964). "A theory of resonant networks," in *Neural Theory and Modeling,* ed R. F. Reiss (Stanford, CA: Stanford University Press), 105–137.

Rheinlaender, J., Kalmring, K., Popov, A. V., and Rehbein, H. (1976). Brain projections and information processing of biologically significant sounds by two large ventral-cord neurons of *Gryllus bimaculatus* DeGeer (Orthoptera, Gryllidae). *J. Comp. Physiol. A*. 110, 251–269. doi: 10.1007/BF00659143

Robert, D., Amoroso, J., and Hoy, R. R. (1992). The evolutionary convergence of hearing in a parasitoid fly and its cricket host. *Science* 258, 1135–1135. doi: 10.1126/science.1439820

Römer, H., Rheinlaender, J., and Dronse, R. (1981). Intracellular studies on auditory processing in the metathoracic ganglion of the locust. *J. Comp. Physiol. A*. 144, 305–312. doi: 10.1007/BF00612562

Ronacher, B., Hennig, R. M., and Clemens, J. (2015). Computational principles underlying recognition of acoustic signals in grasshoppers and crickets. *J. Comp. Physiol. A*. 201, 1–11. doi: 10.1007/s00359-014-0966-3

Ronacher, B., and Römer, H. (1985). Spike synchronization of tympanic receptor fibres in a grasshopper (*Chorthippus biguttulus* L., Acrididae). *J. Comp. Physiol. A*. 157, 631–642. doi: 10.1007/BF01351357

Ryan, M. J., and Rand, A. S. (1993). Sexual selection and signal evolution: the ghost of biases past. *Phil. Trans. R. Soc. Lond. B* 340, 187–195. doi: 10.1098/rstb.1993.0057

Sakura, M., Lambrinos, D., and Labhart, T. (2008). Polarized skylight navigation in insects: model and electrophysiology of e-vector coding by neurons in the central complex. *J. Neurophysiol.* 99, 667. doi: 10.1152/jn.00784.2007

Schildberger, K. (1984a). Multimodal interneurons in the cricket brain: properties of identified extrinsic mushroom body cells. *J. Comp. Physiol. A*. 154, 71–79.

Schildberger, K. (1984b). Temporal selectivity of identified auditory neurons in the cricket brain. *J. Comp. Physiol. A*. 155, 171–185.

Schildberger, K., and Hörner, M. (1988). The function of auditory neurons in cricket phonotaxis I. Influence of hyperpolarization of identified neurons on sound localization. *J. Comp. Physiol. A*. 163, 621–631. doi: 10.1007/BF00603846

Schildberger, K., Huber, F., and Wohlers, D. (1989). "Central auditory pathway: neuronal correlates of phonotactic behavior," in *Cricket Behaviour and*

Neurobiology, eds F. Huber, T. E. Moore, and W. Loher (London: Cornell University Press), 423–458.

Schiolten, P., Larsen, O. N., and Michelsen, A. (1981). Mechanical time resolution in some insect ears. *J. Comp. Physiol. A*. 143, 289–295. doi: 10.1007/BF00611164

Schöneich, S., and Hedwig, B. (2010). Hyperacute directional hearing and phonotactic steering in the cricket (*Gryllus bimaculatus* deGeer). *PLoS ONE* 5:e15141. doi: 10.1371/journal.pone.0015141

Schöneich, S., Kostarakos, K., and Hedwig, B. (2015). An auditory feature detection circuit for sound pattern recognition. *Sci. Adv.* 1:e1500325. doi: 10.1126/sciadv.1500325

Seagraves, K., and Hedwig, B. (2014). Phase shifts in binaural stimuli provide directional cues for sound localization in the field cricket *Gryllus bimaculatus*. *J. Exp. Biol.* 217, 2390–2398. doi: 10.1242/jeb.101402

Selverston, A. I., Kleindienst, H. U., and Huber, F. (1985). Synaptic connectivity between cricket auditory interneurons as studied by selective photoinactivation. *J. Neurosci.* 5, 1283–1292.

Simmons, L. (1988). Male size, mating potential and lifetime reproductive success in the field cricket, *Gryllus bimaculatus* (DeGeer). *Anim. Behav.* 36, 372–379. doi: 10.1016/S0003-3472(88)80008-3

Sobel, E. C., and Tank, D. W. (1994). *In vivo* Ca^{2+} dynamics in a cricket auditory neuron: an example of chemical computation. *Science* 263:823. doi: 10.1126/science.263.5148.823

Staudacher, E., and Schildberger, K. (1998). Gating of sensory responses of descending brain neurones during walking in crickets. *J. Exp. Biol.* 201, 559–572.

Stout, J. F., DeHaan, C. H., and McGhee, R. W. (1983). Attractiveness of the male *Acheta* domesticus calling song to females. *J. Comp. Physiol. A*. 153, 509–521. doi: 10.1007/BF00612605

Strausfeld, N. J. (1999). A brain region in insects that supervises walking. *Prog. Brain Res.* 123, 273–284. doi: 10.1016/S0079-6123(08)62863-0

Strauss, R. (2002). The central complex and the genetic dissection of locomotor behaviour. *Curr. Opin. Neurobiol.* 12, 633–638. doi: 10.1016/S0959-4388(02)00385-9

Sueur, J., Windmill, J. F. C., and Robert, D. (2006). Tuning the drum: the mechanical basis for frequency discrimination in a *Mediterranean cicada*. *J. Exp. Biol.* 209, 4115–4128. doi: 10.1242/jeb.02460

Suga, N. (1990). Cortical computational maps for auditory imaging. *Neural Netw.* 3, 3–21. doi: 10.1016/0893-6080(90)90043-K

Thorson, J., Weber, T., and Huber, F. (1982). Auditory behavior of the cricket II. Simplicity of calling-song recognition in Gryllus, and anomalous phonotaxis at abnormal carrier frequencies. *J. Comp. Physiol. A*. 146, 361–378. doi: 10.1007/BF00612706

Udayashankar, A. P., Kössl, M., and Nowotny, M. (2012). Tonotopically arranged traveling waves in the miniature hearing organ of bushcrickets. *PLoS ONE* 7:e31008. doi: 10.1371/journal.pone.0031008

von Helversen, D., and von Helversen, O. (1995). Acoustic pattern recognition and orientation in orthopteran insects: parallel or serial processing? *J. Comp. Physiol. A*. 177, 767–774. doi: 10.1007/BF00187635

Weber, T., and Thorson, J. (1989). "Phonotactic behavior of walking crickets," in *Cricket Behaviour and Neurobiology,* eds F. Huber, T. E. Moore, and W. Loher (Ithaca, NY: Cornell University Press), 310–339.

Weber, T., Thorson, J., and Huber, F. (1981). Auditory behavior of the cricket I. Dynamics of compensated walking. *J. Comp. Physiol. A*. 141, 215–232. doi: 10.1007/BF01342668

Wehner, R. (1987). "Matched filters"- neural models of the external world. *J. Comp. Physiol. A*. 161, 511–531. doi: 10.1007/BF00603659

Wessnitzer, J., and Webb, B. (2006). Multimodal sensory integration in insects—towards insect brain control architectures. *Bioinsp. Biomim.* 1, 63–75. doi: 10.1088/1748-3182/1/3/001

Wiese, K., and Eilts-Grimm, K. (1985). "Functional potential of recurrent lateral inhibition in cricket audition," in *Acoustic and Vibrational Communication in Insects*, eds K. Kalmring and N. Elsner (Berlin; Hamburg: Parey), 33–40.

Wiese, K., and Eilts, K. (1985). Evidence for matched frequency dependence of bilateral inhibition in the auditory pathway of *Gryllus bimaculatus*. *Zool. Jahrb. Physiol.* 89, 181–201.

Windmill, J. F. C., Göpfert, M. C., and Robert, D. (2005). Tympanal travelling waves in migratory locusts. *J. Exp. Biol.* 208, 157–168. doi: 10.1242/jeb.01332

Windmill, J., Fullard, J., and Robert, D. (2007). Mechanics of a "simple" ear: tympanal vibrations in noctuid moths. *J. Exp. Biol.* 210, 2637–2648. doi: 10.1242/jeb.005025

Witney, A. G., and Hedwig, B. (2011). Kinematics of phonotactic steering in the walking cricket *Gryllus bimaculatus* (de Geer). *J. Exp. Biol.* 214, 69–79. doi: 10.1242/jeb.044800

Wohlers, D. W., and Huber, F. (1978). Intracellular recording and staining of cricket auditory interneurons (*Gryllus campestris* L., *Gryllus bimaculatus* DeGeer). *J. Comp. Physiol. A*. 127, 11–28. doi: 10.1007/BF00611922

Wohlers, D. W., and Huber, F. (1982). Processing of sound signals by six types of neurons in the prothoracic ganglion of the cricket, *Gryllus campestris* L. *J. Comp. Physiol. A*. 146, 161–173. doi: 10.1007/BF00610234

Wohlers, D. W., and Huber, F. (1985). Topographical organization of the auditory pathway within the prothoracic ganglion of the cricket *Gryllus campestris* L. *Cell Tiss. Res.* 239, 555–565. doi: 10.1007/BF00219234

Wyttenbach, R. A., May, M. L., and Hoy, R. R. (1996). Categorical perception of sound frequency by crickets. *Science* 273, 1542–1544. doi: 10.1126/science.273.5281.1542

Yukizane, M., Kaneko, A., and Tomioka, K. (2002). Electrophysiological and morphological characterization of the medulla bilateral neurons that connect bilateral optic lobes in the cricket, *Gryllus bimaculatus*. *J. Insect Physiol.* 48, 631–641. doi: 10.1016/S0022-1910(02)00091-4

Zaretsky, M. D., and Eibl, E. (1978). Carrier frequency-sensitive primary auditory neurons in crickets and their anatomical projection to the central nervous system. *J. Insect Physiol.* 24, 87–95. doi: 10.1016/0022-1910(78)90016-1

Zorovič, M., and Hedwig, B. (2011). Processing of species-specific auditory patterns in the cricket brain by ascending, local, and descending neurons during standing and walking. *J. Neurophysiol.* 105, 2181–2194. doi: 10.1152/jn.00416.2010

Zorovič, M., and Hedwig, B. (2013). Descending brain neurons in the cricket *Gryllus bimaculatus* (de Geer): auditory responses and impact on walking. *J. Comp. Physiol. A*. 199, 25–34. doi: 10.1007/s00359-012-0765-7

Conflict of Interest Statement: The author declares that the research was conducted in the absence of any commercial or financial relationships that could be construed as a potential conflict of interest.

frontiers in Physiology

ORIGINAL RESEARCH
published: 28 October 2016
doi: 10.3389/fphys.2016.00506

Encoding of Tactile Stimuli by Mechanoreceptors and Interneurons of the Medicinal Leech

Jutta Kretzberg[1,2]*, *Friederice Pirschel*[1,3], *Elham Fathiazar*[1] and *Gerrit Hilgen*[1,4]

[1] Computational Neuroscience, Department of Neuroscience, University of Oldenburg, Oldenburg, Germany, [2] Cluster of Excellence Hearing4all, University of Oldenburg, Oldenburg, Germany, [3] Department of Organismal Biology and Anatomy, University of Chicago, Chicago, IL, USA, [4] Faculty of Medical Sciences, Institute of Neuroscience, Newcastle University, Newcastle upon Tyne, UK

For many animals processing of tactile information is a crucial task in behavioral contexts like exploration, foraging, and stimulus avoidance. The leech, having infrequent access to food, developed an energy efficient reaction to tactile stimuli, avoiding unnecessary muscle movements: The local bend behavior moves only a small part of the body wall away from an object touching the skin, while the rest of the animal remains stationary. Amazingly, the precision of this localized behavioral response is similar to the spatial discrimination threshold of the human fingertip, although the leech skin is innervated by an order of magnitude fewer mechanoreceptors and each midbody ganglion contains only 400 individually identified neurons in total. Prior studies suggested that this behavior is controlled by a three-layered feed-forward network, consisting of four mechanoreceptors (P cells), approximately 20 interneurons and 10 individually characterized motor neurons, all of which encode tactile stimulus location by overlapping, symmetrical tuning curves. Additionally, encoding of mechanical force was attributed to three types of mechanoreceptors reacting to distinct intensity ranges: T cells for touch, P cells for pressure, and N cells for strong, noxious skin stimulation. In this study, we provide evidences that tactile stimulus encoding in the leech is more complex than previously thought. Combined electrophysiological, anatomical, and voltage sensitive dye approaches indicate that P and T cells both play a major role in tactile information processing resulting in local bending. Our results indicate that tactile encoding neither relies on distinct force intensity ranges of different cell types, nor location encoding is restricted to spike count tuning. Instead, we propose that P and T cells form a mixed type population, which simultaneously employs temporal response features and spike counts for multiplexed encoding of touch location and force intensity. This hypothesis is supported by our finding that previously identified local bend interneurons receive input from both P and T cells. Some of these interneurons seem to integrate mechanoreceptor inputs, while others appear to use temporal response cues, presumably acting as coincidence detectors. Further voltage sensitive dye studies can test these hypotheses how a tiny nervous system performs highly precise stimulus processing.

Keywords: mechanoreception, somatosensory system, touch, pressure, skin stimulation, voltage sensitive dye, local bend, hirudo

OPEN ACCESS

Edited by:
Sylvia Anton,
French National Institute for Agricultural Research (INRA), France

Reviewed by:
Harald Tichy,
Univerity Vienna, Austria
Daniel A. Wagenaar,
California Institute of Technology, USA

***Correspondence:**
Jutta Kretzberg
jutta.kretzberg@uni-oldenburg.de

Specialty section:
This article was submitted to Invertebrate Physiology, a section of the journal Frontiers in Physiology

Received: *26 June 2016*
Accepted: *14 October 2016*
Published: *28 October 2016*

Citation:
Kretzberg J, Pirschel F, Fathiazar E and Hilgen G (2016) Encoding of Tactile Stimuli by Mechanoreceptors and Interneurons of the Medicinal Leech. Front. Physiol. 7:506. doi: 10.3389/fphys.2016.00506

INTRODUCTION

A simple neuronal system produces a basic behavior with a surprisingly high precision: The leech bends away locally from a light touch (Stuart, 1970; Kristan, 1982; Lockery and Sejnowski, 1992; Lewis and Kristan, 1998a; Zoccolan et al., 2002; Baca et al., 2005; Thomson and Kristan, 2006) with a spatial precision of approximately 1 mm (Baca et al., 2005); similar to that of the human fingertip (Johnson, 2001). The different leech mechanoreceptor types show similar spiking patterns to primate and human mechanoreceptor types (Lewis and Kristan, 1998b; Baca et al., 2005; Johansson and Flanagan, 2009; Smith and Lewin, 2009), and mechanoreceptor responses were shown to depend on common stimulus properties like touch location, mechanical force, duration, and speed (leech: Carlton and McVean, 1995; Zoccolan et al., 2002; Baca et al., 2005; Pirschel and Kretzberg, 2016; primate reviews: Johansson and Flanagan, 2009; Abraira and Ginty, 2013; Saal and Bensmaia, 2014). However, the number of mechanoreceptor cells in the leech skin is an order of magnitude lower than in the human fingertip, which is innervated by more than 200 mechanoreceptors per cm^2 (Vallbo and Johansson, 1984). Nevertheless, the complex innervation structure of the leech skin enables the highly accurate and reproducible local bend response to avoid being stimulated with minimal muscle movement. Hence, the small and simple neuronal system of the leech raises a fundamental computational question on sensory processing: How can such a precise behavior be performed with a nervous system consisting of so few cells?

The leech nervous system is a rigorously segmented, highly repetitive ventral nerve cord with one ganglion per segment. Each ganglion contains about 400 neurons of approximately 200 types (Kristan et al., 2005). The leech local bend behavior was suggested to be controlled by a three-layered feed-forward network consisting of mechanoreceptors, interneurons, and motor neurons (Kristan, 1982; Lockery and Kristan, 1990b; Lewis and Kristan, 1998a; Kristan et al., 2005), which are found in each segment of the animal.

The input layer of the local bend network consists of mechanoreceptors. The three types of leech mechanoreceptors were classically associated with tactile stimuli of distinct intensities, resulting in the names of these neurons: T cells for light touch, P cells for stronger pressure, and N cells for noxious, very strong squeeze (Nicholls and Baylor, 1968). In computational terms, these distinct functions refer to a labeled line code. Moreover, spike patterns in response to tactile skin stimulation differ characteristically between receptor types. T cells produce transient, fast adapting responses to stimulus on- and offset, while P cells respond with sustained, regular spiking throughout the stimulation and N cells produce only few spikes separated by long interspike intervals (Nicholls and Baylor, 1968; Carlton and McVean, 1995; Lewis and Kristan, 1998b; Pirschel and Kretzberg, 2016). In each segment the total population of mechanoreceptors consists of only 14 cells (6 T, 4 P, 4 N) innervating the skin at different depths with their processes (Blackshaw, 1981; Blackshaw et al., 1982) and sending information about tactile stimuli toward their cell bodies in the segmental ganglion. Skin regions innervated by several cells lead to widely overlapping receptive fields between mechanoreceptors. For example, tactile stimulation applied to the ventral midline cause spike responses in two P, two T, and two N cells (see **Figure 1A** bottom for a sketch of overlapping receptive fields at ventral midline). In all mechanoreceptors the inhomogeneous distribution of dendritic branches and nerve endings in the skin (Blackshaw, 1981; Blackshaw et al., 1982) cause spatially structured receptive fields. Stimulation close to the most densely innervated receptive field center triggers highest spike counts and shortest spike latencies (Nicholls and Baylor, 1968; Thomson and Kristan, 2006; Pirschel and Kretzberg, 2016).

Since P cell responses were found to influence muscle movements more strongly than T cells, previous studies assumed that P cells elicit the local bend reflex (Kristan, 1982; Lewis and Kristan, 1998b; Zoccolan et al., 2002). Therefore, a prior study aiming at the identification of interneurons involved in the local bend network was limited to neurons responding to presynaptic P cell spikes (Lockery and Kristan, 1990b). Based on a huge number of double recordings this study identified one unpaired and eight paired interneurons to be involved in the local bend network. Most of these interneurons responded with postsynaptic potentials to spikes from all four P cells suggesting very extended receptive fields. Substantial lateral synaptic connections between interneurons were not found in this study except for electrical connections between the pair of interneurons of the same type (Lockery and Kristan, 1990b). In contrast, identified motor neurons were found to be laterally connected. In addition to inhibiting longitudinal muscles, inhibitory motor neurons also suppress excitatory motor neurons, which cause contraction of the antagonistic muscles (Granzow and Kristan, 1986; Lockery and Kristan, 1990a; Kristan et al., 2005; Baca et al., 2008). This antagonistic inhibition leads to a stronger bending movement to one side.

Based on these results, Lewis and Kristan (1998a) developed a computational model of the local bend network. The model consists of three layers of cells with evenly spaced cosine shaped tuning curves, implementing a population vector paradigm as optimal decoding scheme from one layer to the next. Using the spike rates of the four P cells as input, this model predicted the behaviorally observed direction of local bending. While the cell numbers of the input and output layers were fixed to 4 P cells and 10 motor neurons, the number of the much less-known interneurons was varied, revealing that the number of 17 previously identified local bend interneurons (Lockery and Kristan, 1990b) was compatible with the modeled network structure.

Despite the elegant plainness of this model, recent results require to revise the hypothesized structure and computations of the local bend network. Stimulus-estimation studies revealed that latency differences between two P cell responses carry more information about tactile stimulus position on the skin than spike counts (Thomson and Kristan, 2006; Pirschel and Kretzberg, 2016). Hence, temporal response features might play an important role in the network. Moreover, latency differences between T cell pairs allowed an even more exact estimation of stimulus location (Pirschel and Kretzberg, 2016).

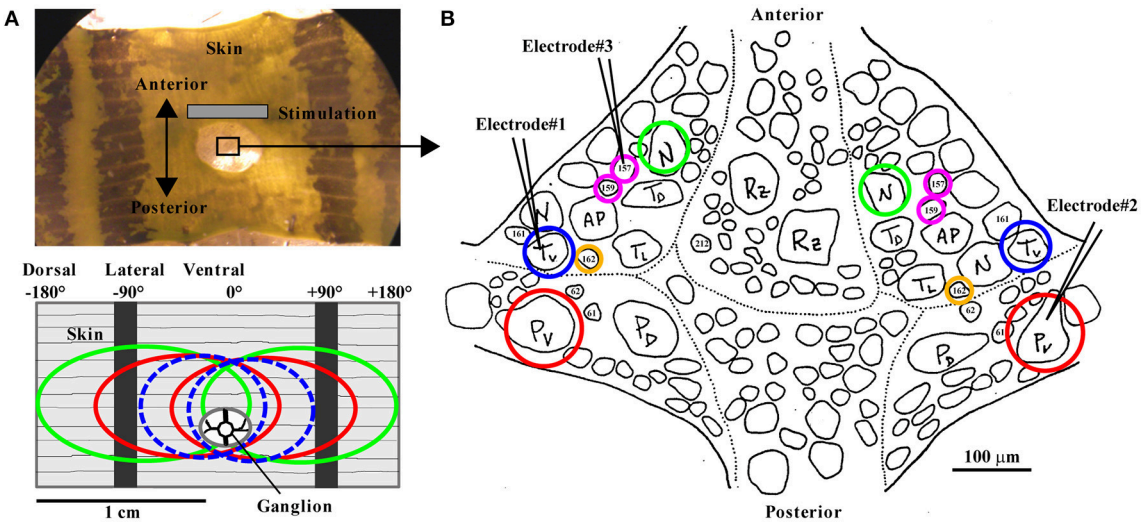

FIGURE 1 | The body-wall preparation with receptive fields of mechanoreceptors and standard ganglion map. (**A**, top) Photograph of the body-wall preparation with the ganglion (sketch in **B**), which is pulled slightly posterior for better access through a hole in the skin. The gray bar indicates the main area used for tactile stimulation. The center of the preparation between the two dark stripes on the skin, called the ventral midline, was defined as 0°. The skin was touched at the third annulus of segment 10, identified by the sensilla positions. Touch locations to the left were denoted as negative numbers of degrees (left end of the preparation: −180°) and to the right as positive numbers (right end: +180°). The black stripes are located approximately at −90° and +90°. (**A**, bottom) Receptive fields of all mechanoreceptors responding to tactile stimulation at the ventral midline are shown in a sketch of the body wall preparation: Left and right T_V cells (dashed blue ovals), left and right P_V cells (red), and left and right N cells (green). **(B)** Sketch of the leech ganglion with cell body positions of bilateral mechanoreceptor pairs of P_V (red), T_V (blue), N (green), corresponding to the receptive fields shown in **(A)**, and of interneurons 157, 159 (magenta), 162 (yellow). Electrodes (symbolized by black pointed angles) were used for intracellular recordings of up to 3 neurons (combinations of T_V, P_V, N, 157, 159, and 162; the electrode positions shown here refer to the data shown in **Figures 5A,B**), while the skin was stimulated mechanically (see section Methods).

Therefore, P cell spikes might not be the only relevant input to the network, but the role of T cells—and maybe also N cells—in the network should be reconsidered. Another aspect not covered by the classical local bend model is the fact that the behavioral response to a tactile stimulus depends on a combination of stimulus properties like location, mechanical force intensity and duration (Baca et al., 2005), as well as velocity (Carlton and McVean, 1995). On the mechanoreceptor level, the finding that several response features, including spike count and latency, depend on more than one stimulus property leads to the fundamental question how complex stimuli are encoded by the nervous system. For example, stimulus location and mechanical force intensity influence the neuronal responses of the mechanoreceptor types in an ambiguous way. A mechanoreceptor response with a high spike count and a short response latency could be elicited either by a relatively weak stimulus close to the cell's receptive field center, or by a stronger stimulus at a less preferred position (Pirschel and Kretzberg, 2016). How does the leech distinguish between these stimuli based on such ambiguous responses?

Our hypothesis is that a population of interneurons solves this task by means of multiplexing, simultaneous encoding of different stimulus properties with different response features. The population of T and P cells provides multiplexed information about combinations of e.g., stimulus location and intensity by encoding them simultaneously with temporal and spike count features (Pirschel and Kretzberg, 2016). The first aim of this study is to investigate if interneurons respond specifically to one mechanoreceptor type—indicating a labeled line code, as it was classically assumed for intensity encoding—or if they integrate inputs from multiple receptor types. The second question is, which mechanoreceptor response features determine interneuron responses. Are all of them integrators as it was assumed in the spike rate-based computational network model (Lewis and Kristan, 1998a), or are some of them specialized for temporal processing?

In the first part of this study, responses of all three types of mechanoreceptors (T, P, and N cells) to tactile skin stimulation are revisited. Our recent results (Pirschel and Kretzberg, 2016) are extended by adding N cell responses and the analysis of two-dimensional tuning to combinations of different stimulus locations and intensities. In the second part, intracellular electrophysiology, anatomical studies and voltage sensitive dye recordings are performed as complementary experimental approaches to study interneurons on the next network layer. In particular, we aim to identify interneurons responding to input from P and/or T cells and to find out which mechanoreceptor response features determine their postsynaptic responses. In this way, we try to identify general computational principles of sensory information processing, which are not limited to the leech, but could be implemented also by other sensory systems.

METHODS

Animals and Preparations

All experiments were performed on adult, hermaphrodite medicinal leeches (Hirudo verbana), weighing 1–2 g. According to German regulations, no ethics approval is needed for the work on these invertebrates. Leeches were obtained from Biebertaler Leech Breeding Farm (Biebertal, Germany) and were kept in tanks with Ocean Sea Salt 1:1000 diluted with purified water. Animals were kept at room temperature and anesthetized with ice-cold saline (Muller and Scott, 1981) before and during dissection. Experiments were performed at room temperature.

For the body-wall preparation (**Figure 1A**; detailed description is given in Pirschel and Kretzberg, 2016), segments 9–11 were dissected and innervations of segment 10 remained unscathed, while the ganglion was accessible through a hole in the skin (**Figure 1A**). The middle annulus of the 10th segment, which was identified by the location of the sensilla (Blackshaw et al., 1982), was used for the skin stimulation.

Voltage sensitive dye (VSD) experiments (section Voltage Sensitive Dye Experiments and Analysis) and cell fills (section Dye Injection and Cell Labeling) were performed on isolated ganglia dissected from segment 10.

Tactile Stimulation and Intracellular Electrophysiology

In the skin preparation, the skin was stimulated by the Dual-Mode Lever Arm System (Aurora Scientific, Ontario, Canada, Model 300B; poker tip size: 1 mm^2; see Baca et al., 2005; Thomson and Kristan, 2006; Pirschel and Kretzberg, 2016). The stimulus was applied as an instantaneous step function of 200 ms length. At stimulus onset, the poker moved down at very high speed, reached the desired pressure within 2 ms, fluctuated slightly for less than 10 ms and stayed at a constant position, until moving up at very high speed again. Poker speed and duration of skin indentation were the same in all experiments. Touch locations were set relative to the ventral midline (set as 0°) of the preparation: Locations to the left are denoted as negative and to the right as positive numbers of degrees (**Figure 1A**). The stimulus was varied in mechanical force intensity (5–200 mN) and location (−20° to +20°, relative to the ventral midline, in 5° steps) (see Lewis and Kristan, 1998b; Baca et al., 2005; Pirschel and Kretzberg, 2016). Other parameters like shape or indentation depth were not varied. All combinations of stimulus properties force intensity and location were presented 8–15 times in pseudo-randomized order.

While stimulating the skin mechanically, intracellular recordings from one to three cells at the same time were performed with sharp glass micropipettes (resistances between 20 and 40 MΩ) filled with 3 M potassium acetate (for detailed description of the experimental rig, see Pirschel and Kretzberg, 2016). Varied combinations of the three types of mechanosensory cells (T_v and P_v, N) and three types of interneurons (157, 159, and 162) were obtained. Numbers of preparations used for analyses are given in the figure legends. Mechanosensory cell types were easily identifiable based on their electrical properties (Nicholls and Baylor, 1968). In tactily stimulated preparations, the receptive field of recorded mechanoreceptors was confirmed prior to experiments, yielding the standard map shown in **Figure 1B**. In most ganglia, cell bodies of T_v and P_v (the mechanoreceptors with ventral receptive fields) were located most laterally. But since in particular T cells sometimes switch their positions, we specify in this manuscript subtypes of T and P cells only for experiments with attached skin. The interneurons (INs) were identified according to the results and descriptions by Lockery and Kristan (1990b).

To physiologically identify synaptic connections, intracellular double recordings of INs and a simultaneous recording of a mechanosensory cell were obtained, while stimulating the mechanosensory cell by constant current pulses of 1.5 nA, lasting 50 ms.

Dye Injection and Cell Labeling

To study cell morphologies and putative points of contact, interneurons, and mechanosensory cells were filled in isolated ganglia by means of sharp glass electrodes (20–40 MΩ) with 10 mM Alexa-dyes (Alexa Fluor 488/546/633, Invitrogen, Karlsruhe, Germany) and/or 2% Neurobiotin (Vector Labs, Peterborough, UK) solved and backfilled with 200 mM KCl. Cells were iontophoretically injected either with positive (Neurobiotin) or negative (Alexa) currents (2–4 nA, 500 ms, 1 Hz, 30–60 min). Neurobiotin-filled samples were allowed to settle for 1 h after injection before further processing. All samples were fixated in 4% PFA (Sigma, Munich, Germany) for 1 h and rinsed 6 × 10 min in 0.1 M PBS. Neurobiotin-filled samples were afterwards incubated in 1:1000 Streptavidin DyLight 488 (Vector Labs)/PBS/0.5% Triton-X overnight at 4°C. Samples were rinsed afterwards (6 × 10 min) in PBS and embedded with VectaShield (Vector Labs) on a microscope slide for high resolution microscopy. Fluorescent image acquisition and analysis were performed as previously described (Meyer et al., 2014). Briefly, filled cells were scanned with a Leica TCS SP2 (Leica, Nussloch, Germany) Confocal Microscope with an HCX PL APO 40.0 × 1.25 OIL UV objective to obtain confocal stacks with a voxel dimension of 0.366 × 0.366 × 0.200 μm. The scanned sequential images were trimmed for the desired z-depth and a maximal projection of the images was calculated with ImageJ (NIH, Bethesda, MD). Channel overlay and gentle adjustment of contrast and brightness were done with Photoshop CS3 (Adobe, San Jose, CA). An animation of the confocal stack underlying **Figure 6B** is provided in the Supplemental Material.

Voltage Sensitive Dye Experiments and Analysis

Voltage sensitive dye (VSD) recording was performed in isolated leech midbody ganglia simultaneously to a double intracellular recording from a P and a T cell. Both mechanosensory cells were stimulated with intracellular current injection, while the activities of all visible cells on the ventral side of the ganglion were monitored through a microscope [Zeiss Examiner.D1, objective plan-apochromat 20 x/1.0 DIC (UV)] with a CCD camera (Photometrics QuantEM:512SC), using bath-applied VF2.1.CL dye (λ_{max} = 522 nm, λ_{em} = 535 nm, see Miller et al., 2012). Imaging was performed with a temporal sampling frequency of

94 Hz and a spatial resolution of 64 × 128 pixels. Prior to the recording, a snap shot was taken with the full spatial resolution of the camera, 512 × 512 pixels (**Figure 2A**), based on which regions of interest (ROIs) representing individual cell bodies were selected manually (Fathiazar et al., 2016; see **Figure 7B** for an example). In this manuscript, data from one representative VSD recording is presented. Similar results were obtained in seven additional preparations.

Electrical stimulation, consisting of 10 ms long pulses of 2 nA (T cell) or 3 nA (P cell), was designed to mimic these cells' spiking patterns in response to tactile stimulation of 70 mN in the ventral midline of the skin in a semi-intact preparation (Pirschel and Kretzberg, 2016). Four different stimulus conditions were compared (see **Figure 7**): In the PT-stimulated condition, both sensory cells were electrically stimulated in a pattern that reproduces natural responses to tactile stimulation. In the P-stimulated and the T-stimulated condition only one of the cells was stimulated, while the other cell remained unstimulated. In control condition, both cells were not stimulated. In our experiments, responses to 7 repetitions of each condition (trials) were recorded.

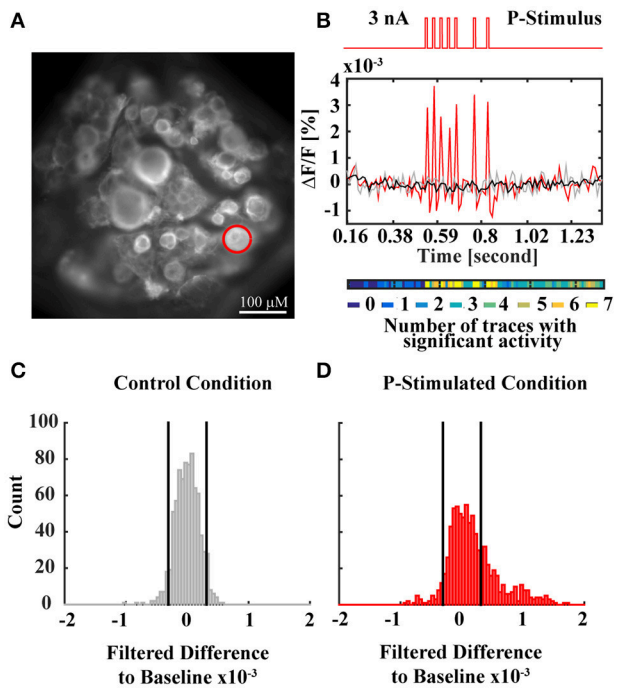

FIGURE 2 | VSD data analysis method. (A) Snapshot of a ganglion with full resolution. The red circle indicates the cell body of the P cell, which was stimulated by intracellular current injection into the soma during the experiment. **(B)** Time course of the electrical P cell stimulation, applied through an intracellular electrode (top red trace) and corresponding single VSD response of the P cell (red spikes) in comparison to a single P cell response to control condition (not stimulated, gray) and baseline (averaged P cell responses to 7 traces of control condition, black). The activity map (colored line below) indicates for each recording frame in how many of 7 response traces the activity differed significantly from control condition. **(C)** Histogram of filtered differences between P cell responses to control condition (7 traces with 110 frames each) and baseline. Black vertical lines indicate thresholds of the $p < 0.05$ criterion for activity differing significantly from baseline. **(D)** Histogram of filtered differences between P cell responses to stimulated condition (7 traces with 110 frames each) and baseline. Black vertical lines indicate the significance thresholds determined in **(C)**, showing that the activity differs significantly from baseline more often than in control condition. The activity map in **(B)** depicts in which frames the significant deviations from baseline occurred, indicating consistent activation during current stimulation.

For data analysis, 55 ROIs corresponding to visible cell bodies were drawn over the first frame of the VSD recording presented in this manuscript. VSD signals of the cells were extracted by averaging and normalizing the brightness of the pixels in the corresponding ROIs. Movement and bleaching artifacts were corrected as described in Fathiazar and Kretzberg (2015). For each cell, baseline (black line in **Figure 2B**) was calculated as an average of the seven trials of control condition. Baseline was subtracted from all VSD signals obtained for all four stimulus conditions. To reduce the noise level, the difference signal was filtered with a moving average filter of three frames window size.

Statistical analysis to identify stimulus-activated cells was performed as described in Fathiazar et al. (2016). In short, the histogram of the filtered VSD difference signals in control conditions was calculated for each cell. Applying a statistical significance level of $\alpha = 0.05$ on this histogram, we defined the thresholds of activity differing significantly from baseline (black vertical lines in **Figure 2C**), indicating very strong de- or hyperpolarization of the cell's membrane potential. These thresholds (quantiles 2.5 and 97.5% of control response distribution) were applied to the filtered VSD difference signals obtained for the three conditions of mechanoreceptor stimulation (**Figure 2D**: P-stimulated condition) to discriminate which individual cells were activated at each time frame (activation map of the P cell in **Figure 2B**). The activation maps I(i,j) in **Figures 7C–F** show the pooled activity for all seven trials of each condition, where $I(i,j) \in \{0, ...,7\}$ and $i \in \{1, ...,55\}$ indicates the cell number (chosen by the sequence of cells' activations after stimulus onset, not corresponding to the cell numbers in the standard ganglion map shown e.g., in Lockery and Kristan, 1990b) and $j \in \{1, ...,110\}$ is the frame (referring to times $0.16 < t < 1.36$ in s). I(i,j) has the value of 0 (shown in dark blue) if the cell i in frame j was not activated in any of the seven trials. If cell i was found to be activated in all the trials in frame j, I(i,j) has the value of seven (shown in yellow). A cell i was classified as a "stimulus-activated" cell for a specific stimulus condition (PT-, P-, or T-stimulated), if at least six of the seven trials revealed significantly increased or decreased activity compared to baseline in at least one time frame in the period $0.53 < t < 0.87$ s (from stimulus onset to offset plus five frames).

RESULTS

Encoding of Tactile Information by Mechanoreceptors

The three types of leech mechanoreceptors were classically associated with tactile stimuli of different intensities, as reflected in their notation: T cells for light touch, P cells for stronger pressure, and N cells for noxious, very hard mechanical

stimulation (Nicholls and Baylor, 1968). However, simultaneous recordings of different mechanoreceptor types responding to skin stimulation revealed a different picture: Both T and P cells responded reliably to a large range of stimulus intensities, from very light touch (5 mN) to strong pressure (200 mN), and even N cell responses started at a moderate touch intensity of 50 mN (**Figure 3**). These strongly overlapping sensitivity ranges clearly contradicted the classical idea of a labeled line code with different cell types, signaling the presence of stimuli in distinct force intensity ranges. Instead, this finding suggested that the tiny population of leech mechanoreceptors (6 T cells, 4 P cells, 4 N cells in each ganglion) uses a different strategy for encoding the intensity of tactile stimuli. As shown in **Figure 3A**, response patterns to tactile stimulation at the ventral midline differed considerably between cell types, in accordance with many previous publications (Nicholls and Baylor, 1968; Carlton and McVean, 1995; Lewis and Kristan, 1998b; Pirschel and Kretzberg, 2016). T_v cells typically produced transient, rapidly adapting responses, both at stimulus onset and offset, while P_v cells usually responded with sustained sequences of regularly occurring spikes within the entire duration of tactile stimulation. N cells were not very active when the skin was stimulated with relatively weak pressure, leading to responses consisting of only one or two spikes. Despite these differences in spike timing patterns, all three types of mechanoreceptors shared similar dependencies of standard response features on stimulus intensity. All cells responded to increasing pressure intensity with increasing spikes counts and decreasing response latencies, both of which saturated for high intensities (100–200 mN) in T and P cell responses. In a preceding study (Pirschel and Kretzberg, 2016), we showed for the intensity range of 5–100 mN that summed spike counts of mechanoreceptor pairs yielded the best estimation performance for stimulus intensity. In particular the sustained P_v cell responses allowed a reliable estimation.

When stimulus location was varied, P_v and T_v cells showed the same effects as were reported in previous studies (Thomson and Kristan, 2006; Pirschel and Kretzberg, 2016). Spike rates decreased and latencies increased with increasing distance from the center of the cell's receptive field (**Figures 4A,C,D**). A similar tendency was also visible for N cell responses (**Figure 4B**), although the low spike counts (between 0 and 2 spikes in 200 ms), induced by the range of stimulus intensities applied in this study, made results more difficult to interpret. In Pirschel and Kretzberg (2016) it was shown that for a tactile stimulation with 50 mN, the latency differences between pairs of mechanoreceptors, in particular the fast responses of T_v cells, led to the best location-estimation performance. Here, we extended the analysis of P_v and T_v cell responses by varying combinations of stimulus location and force intensity, while keeping velocity and all other stimulus parameters constant across experiments. Stimuli of all intensities yielded similar dependencies of spike counts and latencies on stimulus location, with higher mechanical force triggering more and earlier spikes, resulting in virtually parallel curves for both response features (**Figures 4C,D**). For T_v cells similar response characteristics of spike counts and latencies were found even for strong pressure stimuli of 100 mN (**Figure 4D**),

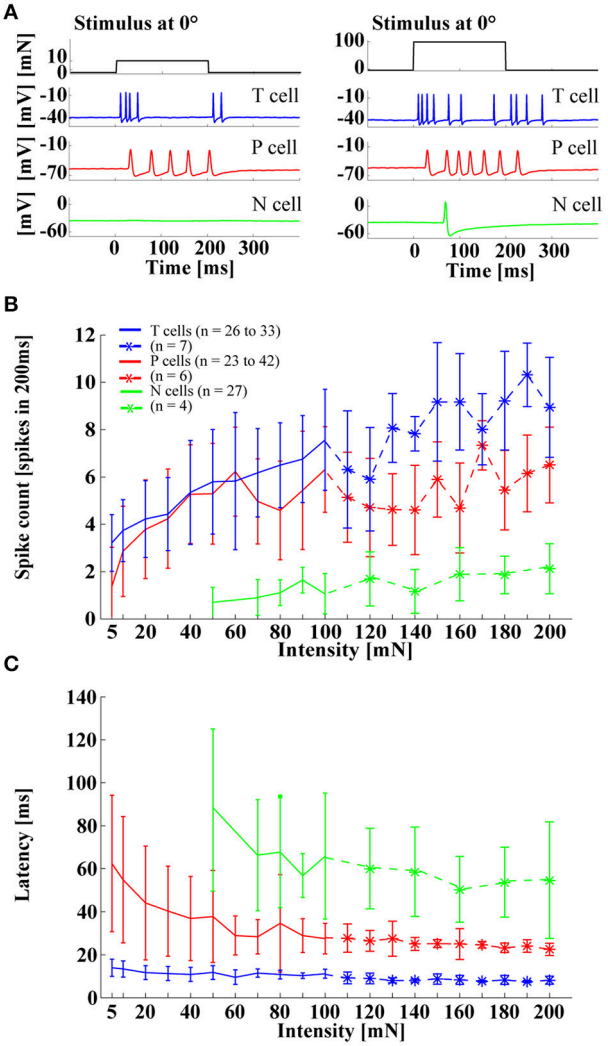

FIGURE 3 | Influences of stimulus intensity on mechanoreceptor responses. (A) Example responses of an intracellular triple recording of a left T_v cell (blue), a left P_v cell (red), and a right N cell (green) responding to a tactile stimulus of 10 mN (left) and 100 mN (right) applied for 200 ms at 0° (ventral midline). **(B)** Spike count and **(C)** response latency (mean and STD) for T_v cells (blue), P_v cells (red) and N cells (green) responding to tactile stimuli with intensities of 5–200 mN applied at 0°. Stronger pressure intensities (> 100 mN) were tested with fewer cells (see legend).

giving further evidence against a labeled line coding of stimulus intensities.

Since T_v cells also responded to the offset of a constant tactile stimulation (**Figures 3A**, **4A**, **5A–C**), stimulus force intensity and location dependencies of these off-responses were also analyzed (**Figure 4E**). Only strong pressure stimuli (100 mN) close to the receptive field center triggered large numbers of off spikes in T_v cells. These off response spike counts decreased steeply with distance (**Figure 4E** left, Supplementary Figure 1C). For light and moderate tactile stimulation, off-response spike counts were lower then spike counts at stimulus onset. These off-response spike counts depended mainly on stimulus intensity, while

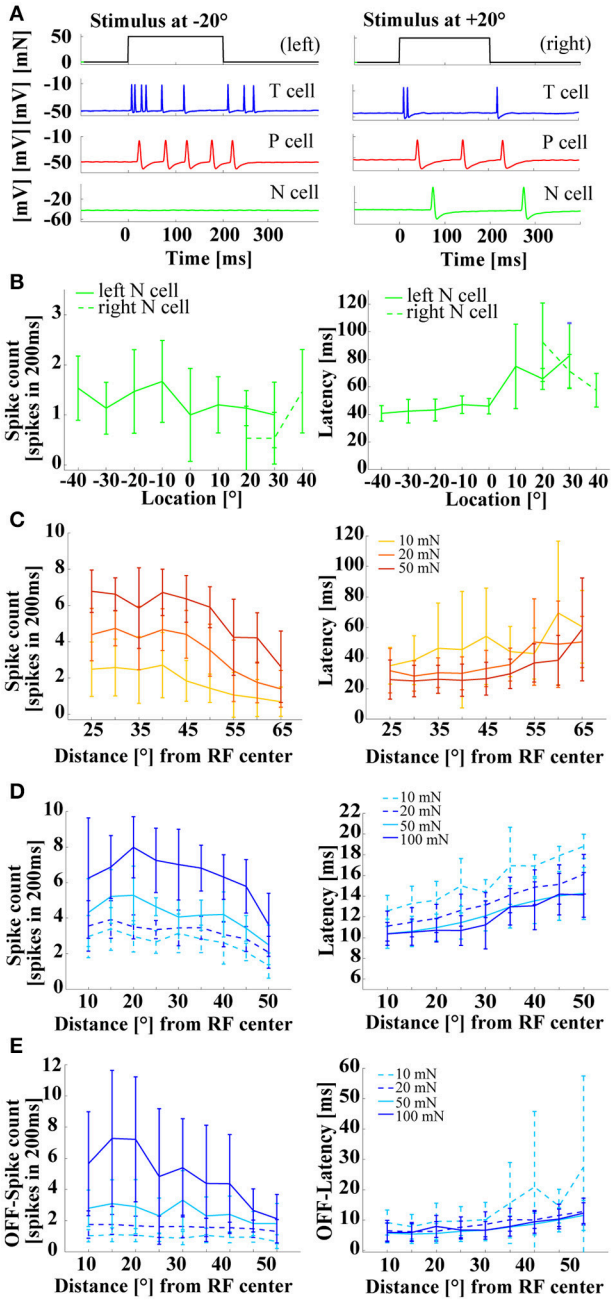

FIGURE 4 | Influences of stimulus location on mechanoreceptor responses. (A) Example responses of an intracellular triple recording of a left T_V cell (blue), a left P_V cell (red), and a right N cell (green) responding to a tactile stimulus of 50 mN for 200 ms at locations −20° (left) and +20° (right). Ventral midline is defined as 0°, stimulus locations to the right as positive and to the left as negative numbers of degrees. **(B)** Example for the dependency of N cell spike count and response latency on stimulus location. Spike count and response latency (mean and STD) are shown for one representative double recording of two N cells with 15 repeated stimulus presentations and a stimulus intensity of 100 mN. **(C)** Dependency of spike count and response latency (mean and STD) of P_V cells ($N = 10$, each 8–10 stimulus presentations; pooled responses of left and right cells) on stimulus location. Responses at different locations [displayed as distance from receptive field center in (°)] are *(Continued)*

FIGURE 4 | Continued
shown for three stimulus intensities of 10 mN (yellow), 20 mN (orange), and 50 mN (red). **(D)** Dependency of spike count and latency (Mean and STD) of T_V cells ($N = 10$, each 8–10 repeated stimulus presentations; pooled responses of left and right cells) on stimulus location. Responses at different locations [displayed as distance from receptive field center in (°)] are shown for four stimulus intensities of 10 mN (dashed-cyan), 20 mN (dashed blue), 50 mN (solid-cyan), and 100 mN (solid-blue) ($N = 8$ cells). **(E)** Dependency of off-spike count and off-spike latency (Mean and STD) of T_V cells on stimulus location (same recordings and figure conventions as in **D**). Linear fits for the stimulus response curves shown in **(D,E)** are provided in the Supplementary Material.

stimulus location had virtually no effect, resulting in the parallel flat curves shown in the left panel of **Figure 4E**. Consequently, linear regression revealed shallower decreases and smaller y-intercepts of spike counts at stimulus offset (Supplementary Figure 1C) than at stimulus onset (Supplementary Figure 1A, see also Table 1 in Supplementary Material for comparison). In contrast, the latency of off-responses triggered by moderate and high mechanical force depended almost exclusively on stimulus location (**Figure 4E** right panel, Supplementary Figure 1D). The virtually identical off latency response curves obtained for intensities between 20 and 100 mN rose at least as steeply with increasing distance from the center of the receptive field as for the latencies observed at stimulus onset (Supplementary Figures 1B,D, Supplementary Table 1) and showed similarly low variability (**Figures 4D,E** right panels). Only very soft touch stimuli of 10 mN, which often failed to trigger off-responses at all, caused highly variable off response latencies, which were not approximated well by linear regression (Supplementary Figure 1D). In conclusion, these results suggest that T cell responses occurring at the offset of skin stimulation could play an additional role for tactile encoding.

Interneurons Involved in Tactile Information Processing

After studying the encoding of tactile stimulus properties at the mechanoreceptor level, the main questions arising from these results are: Which mechanoreceptors provide input to which of the cells at the next network level? And which mechanoreceptor response features shape the responses of which interneurons involved in processing tactile information?

To tackle these questions, we performed a combination of three experimental approaches: Simultaneous intracellular double recordings from a mechanoreceptor and an interneuron, anatomical examination revealing potential contact points, and voltage sensitive dye recordings providing access to mechanoreceptor-induced responses of many cells simultaneously.

In the first step, responses of three different interneurons were characterized by the classical electrophysiological approach: Intracellular double and triple recordings of mechanoreceptor(s) and an interneuron (**Figure 5**). The three interneurons 157, 159, and 162 (see **Figure 1B** for cell body positions in the ganglion) were previously identified as members of the local bend network according to the criteria that they responded to presynaptic P

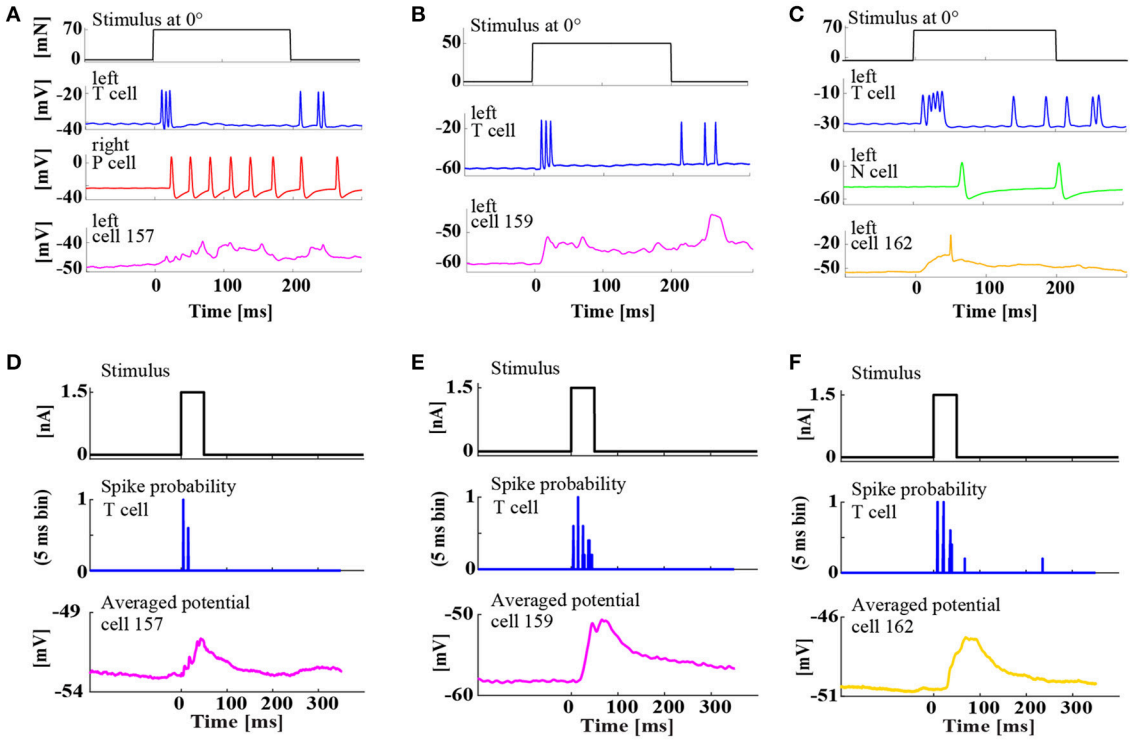

FIGURE 5 | Simultaneous, intracellular recordings of three different interneurons and ipsilateral mechanoreceptors. (A–C) Example responses of mechanoreceptors and three types of interneurons to tactile skin stimulation for 200 ms at 0° (ventral midline). **(A)** Triple recording of left T_V cell (blue), right P_V cell (red), and left cell 157 (magenta) responding to a tactile stimulus of 70 mN. **(B)** Double recording of left T_V cell (blue) and left cell 159 (magenta) responding to a tactile stimulus of 50 mN. **(C)** Triple recording of left T_V cell (blue), a left N cell (green), and left cell 162 (yellow) responding to a tactile stimulus of 70 mN. **(D–F)** Responses of the same interneurons of types **(D)** cell 157, **(E)** cell 159, **(F)** cell 162 to constant current injection of 1.5 nA for 50 ms (upper trace) applied intracellularly to the ipsilateral T_V cell, which responded reproducibly with regular spike patterns (see spike probability in 5 ms bins) in the same double or triple recording as shown in the corresponding upper panel **(A–C)**. Cell responses were averaged over 20–50 repetitions.

cell stimulation and influenced the activity of motor neuron 3 (Lockery and Kristan, 1990b). Here, our recordings showed that these three interneuron types also receive synaptic input from an ipsilateral T_V cell. Intracellular injection of a constant current step reproducibly triggered rhythmic spike patterns in T_V cells, which elicited clear excitatory postsynaptic potentials (EPSPs) in all three types of interneurons (**Figures 5D–F**).

Additionally, intracellular recordings of interneurons 157, 159, and 162 during tactile stimulation provided direct evidence that these cell types are involved in the processing of tactile information (**Figures 5A–C**). The recordings revealed their distinctly different response characteristics: Cell 157 displayed a sustained graded response, resembling integrated EPSPs lasting for the entire duration of stimulation (**Figure 5A**), while the other two cell types responded more transiently. Cell 159 produced large EPSPs both at tactile stimulus on- and offset (**Figure 5B**). Cell 162 responded mainly with a very large EPSP at stimulus onset, sometimes triggering a single postsynaptic spike (**Figure 5C**).

The second step of the network analyses provided anatomical evidence for network connections (**Figure 6**). Simultaneous dye injections into T cells and interneurons revealed cell morphology and prospective points of contacts. Potential locations of contacts with a T cell (cyan) were found for all three types of interneurons 157 (magenta, arrowheads in **Figure 6B**), 159 (magenta, arrowheads in **Figure 6C**), and 162 (yellow, arrows in **Figure 6B**). Interestingly, the triple staining of T, 157, and 162 (see also stack animation in Supplementary Material) additionally identified putative contacts of interneurons 157 and 162 suggesting potential lateral network connections at the interneuron level (circles in **Figure 6B**). However, since the study by Lockery and Kristan (1990b) did not find synaptic responses in double recordings of this cell pair, additional electrophysiological tests are needed.

Neurobiotin injection into a T cell (**Figure 6D**) led to staining of five additional cell bodies suggesting electrical coupling. For one of them, the location of the cell body matched the location of cell 159 (labeled c in **Figure 6D**), fitted very well with the electrophysiological finding of this cell type's responses following the time course of T cell responses (**Figures 5B,E**). Judging from the cell body location one of the other cells could be cell 212 (labeled d in **Figure 6D**), which was also identified as local bend interneuron by Lockery and Kristan (1990b). Two more cells were stained in the posterior-lateral package of the ganglion. By location these cells could be numbers 61 and 62 (b and a in **Figure 6D**) in the standard ganglion map (**Figure 1B**). At a larger

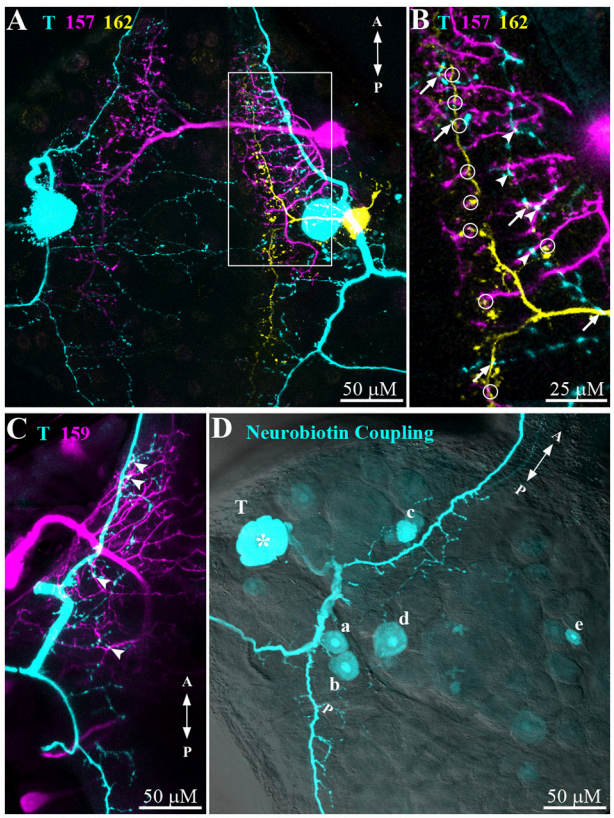

FIGURE 6 | Morphological connections of T cells and interneurons. (A) Dye injections (Alexa Fluor 488/546/633) were performed to reveal the morphology and putative cell-cell contact zones of a T cell (cyan), interneuron 157 (magenta), and 162 (yellow). Z-depth 70 µm. **(B)** Magnification of the area indicated in **(A)** (white box) shows putative contacts between T cell and interneuron 157 (arrowheads), T cell and interneuron 162 (arrows), and interneuron 157 and 162 (circles). Z-depth 10 µm. See Supplementary Material for an animation of the confocal image stack underlying this figure. **(C)** Visualized morphology of an Alexa-dye injected T cell (cyan) and a Neurobiotin injected interneuron 159 (magenta). Arrowheads indicate putative contacts. Z-depth 30 µm. **(D)** Neurobiotin (cyan) was injected into a T cell (indicated by asterisk) to reveal electrically coupled cells. Putative cell types: (a) and (b) interneurons 62 and 61, (c) 159, (d) 212, and (e) unknown. Z-depth 110 µm. Confocal microscope transmission image overlayed with 40% transparency for cell location identification. In all panels letters A and P indicate anterior to posterior direction of the ganglion.

distance from the T cell an additional cell body (e in **Figure 6D**) was also clearly stained, but remained to be identified.

The third step of our analyses aimed to identify interneurons involved in tactile processing using voltage sensitive dye (VSD) recordings. In these experiments, intracellular double recordings of a T and a P cell were performed, while the activity of the ventral side of the ganglion was imaged. After VSD bath application, graded de- and hyperpolarization of all neurons could be estimated based on the emitted light of the corresponding pixels in the camera image (Miller et al., 2012). Individual spikes could only be identified in VSD traces of some cell types with large and slow spikes, otherwise the temporal resolution of the camera (94 Hz at a spatial resolution of 64 × 128 pixels) and the signal to noise ratio were too low. In the recording shown in **Figure 7**, 55 ROIs representing individual cell bodies were selected for analysis (**Figure 7B**). Four different conditions of electrical stimulation were used during VSD recordings: (1) Control condition without stimulation (**Figure 7C**), used to determine baseline spontaneous network activity, (2) PT-stimulated condition (**Figures 7D,G**) with short current pulses injected into the cell bodies of the T cell and the P cell, which elicited spike trains reproducing typical mechanoreceptor responses to a touch stimulation (Pirschel and Kretzberg, 2016), (3) P-stimulated condition (**Figures 7E,H**) with the same spike train elicited in the P cell as in the PT-stimulated condition, while the T cell remained unstimulated, and the corresponding (4) T-stimulated condition (**Figures 7F,I**) with only T cell stimulation.

For the statistical analysis to identify interneurons activated by mechanoreceptor responses the control condition was used to calculate the normal range of spontaneous activity for each cell. The upper and the lower thresholds of this range were defined as percentiles 2.5 and 97.5% of the empirically determined distribution of VSD values (leading to a significance level of $\alpha = 0.05$, see Section Methods, **Figure 2C**, and Fathiazar et al., 2016) These thresholds were applied to the same cell's responses during the three different stimulated conditions to find if and when the cell was more de- or hyperpolarized than during control condition (see **Figure 2**). **Figures 7D–F** show for each cell at each time frame how many of the seven trials deviated significantly from baseline, with a color code ranging from dark blue (no deviations from baseline) to yellow (deviation from baseline in this time frame in all seven stimulus presentations). In **Figure 7** cells were numbered according to the timing of their first activation (significant deviation from baseline in at least six of seven stimulus presentations) after stimulus onset in the PT-stimulated condition (**Figure 7D**). Hence, cell numbers in **Figure 7** differ from the cell identity numbers used in the standard ganglion map, e.g., in **Figure 1B** and in Lockery and Kristan (1990b). In **Figure 7** cell number 1 is the stimulated T cell, cell number 2 the stimulated P cell. Cells showing consistent deviations from the baseline during stimulation in at least six out of seven presentations were classified as stimulus-activated (see Section voltage sensitive dye experiments and analysis). These cells are indicated by colored borders in **Figures 7G–I**.

Comparison of different stimulation conditions revealed that electrical stimulation of T and P cell together (**Figure 7D**) as well as activation of P cell alone (**Figure 7E**) activated 22 of the 55 analyzed cells, while T cell stimulation alone elicited significant activation only in 10 cells. However, populations of activated cells were not identical for PT-stimulated and for P-stimulated conditions. One cell (number 24, magenta in **Figure 7G**) reached activation threshold exclusively when it received input from both the P and the T cell. Since it was located in the posterior package and was not activated by P cell input alone, this cell did not correspond to any of the known local bend interneurons (Lockery and Kristan, 1990b). In addition to the T cell (number 1) itself one cell (number 18, blue in **Figures 7G,I**), putatively interneuron 161, needed T cell but no P cell stimulation for activation. Interestingly, three cells [numbers

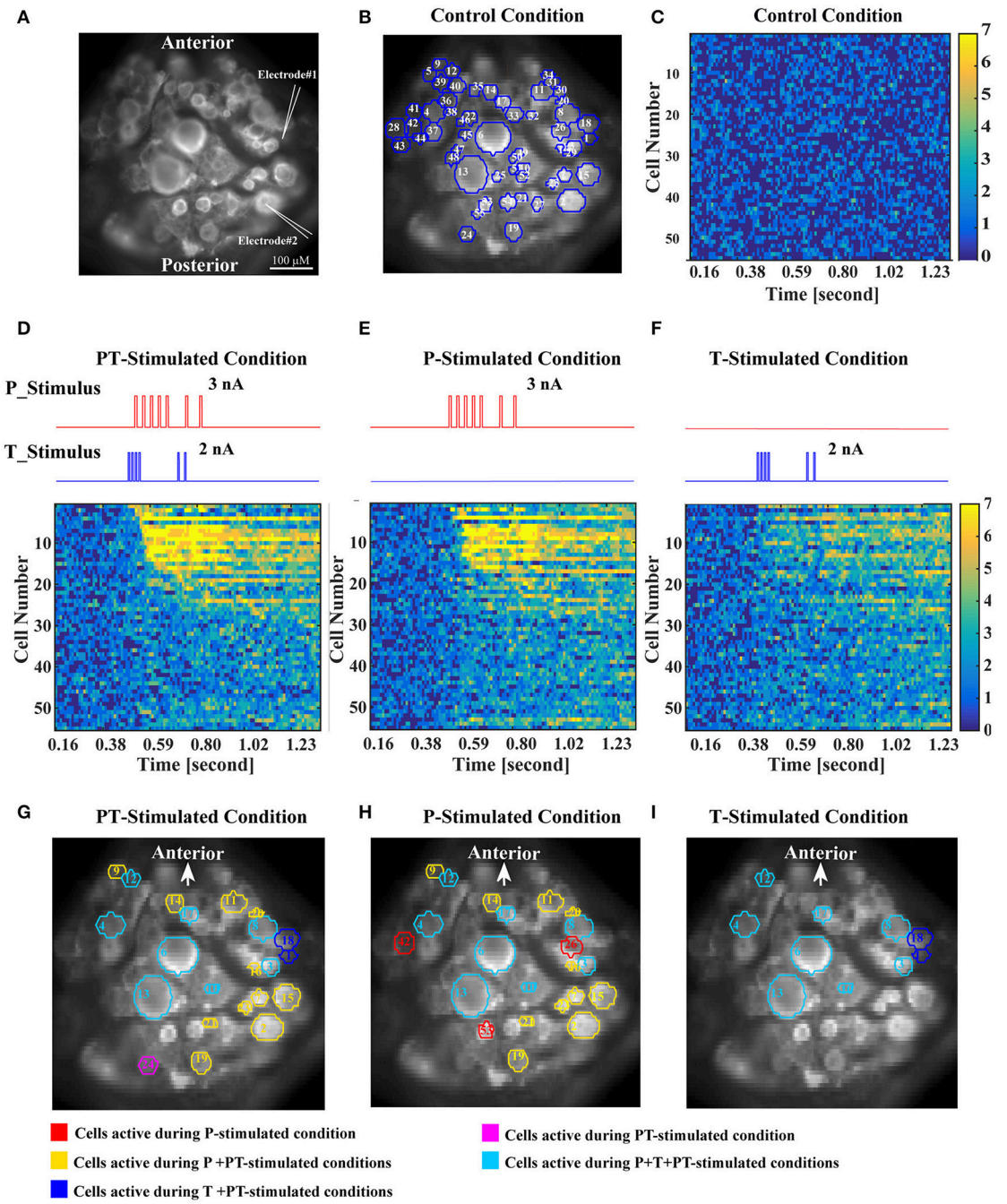

FIGURE 7 | Identification of interneurons involved in the processing of tactile stimuli based on VSD recordings. (A) High resolution image of VSD labeled cells in the leech ganglion. For typical positions of the cell bodies located on the ventral surface of the ganglion, refer to **Figure 1B**. Intracellular electrodes (symbolized by white pointed angles) were used for electrical stimulation of a T cell (Electrode #1) and a P cell (Electrode #2). **(B)** One frame of the VSD recorded ganglion with superimposed blue cell borders showing all 55 ROIs used for analysis. White numbers refer to the order of cells' activation determined in **(D)**, not to the cell identity numbers commonly used in the standard ganglion map. **(C)** Activity map of all 55 recorded cells in response to control condition (no stimulation). The color of each pixel indicates in how many of the seven control trials the activity of a specific cell (row) at a specific recording frame (column) deviated significantly from baseline. Colors range from dark blue (0 deviations) to yellow (7 deviations). The absence of bright colors indicates that no consistent deviation from baseline occurred for any of the cells. Cell numbers correspond to **(B,D)**. **(D)** Activity map in response to intracellular current stimulation of a P cell and a T cell (stimulus time courses shown above in red and blue). Cells were sorted and numbered by the timing of the first occurrence of consistent significant deviation (>5 of 7 trials) from baseline in this condition after stimulus onset (T cell is #1, P cell is #2). Cells not activated by the PT-stimulated condition remained in random order. For cell body locations see **(B)**. **(E,F)** Activity maps in response to intracellular current stimulation of only the P cell **(E)** or the T cell **(F)**. Cell numbers correspond to **(B,D)**. **(G–I)** Cells activated by the specific stimulus conditions, P and T cell stimulation **(G)**, only P cell stimulation **(H)**, and only T cell stimulation **(I)**. A cell was defined as stimulus activated, if its activity deviated significantly from baseline in more than 5 of 7 trials, in at least one time frame after stimulus onset (see Methods). Red ROIs show cells activated only during P stimulated condition, yellow ROIs during P and PT conditions, blue during T and PT conditions, magenta only during PT condition, cyan during all three conditions.

26, 32, 42 (**Figure 7H** red), cell types remained to be identified] showed significant activity during P cell stimulation, but not in response to the combined PT-stimulated condition. This finding could indicate nonlinear interaction of inputs from different mechanoreceptors or inhibition by the T cell.

According to our classification criterion, eight cells responded with consistent significant activation to all three stimulated conditions (cyan borders in **Figures 7G–I**). Some of them were easy to identify by soma positions and sizes and by their characteristic response patterns: Both Retzius cells (numbers 6 and 13 in **Figure 7**) and both AP cells (numbers 4 and 8 in **Figure 7**) could be identified unambiguously across different preparations. The fastest postsynaptic responding cell, marked with number 3, could be the ipsilateral interneuron 162 (compare **Figures 5**, **6**). The cell labeled with number 10 could putatively be interneuron 212 (compare **Figure 6D** and the ganglion map in **Figure 1B**). Cells labeled 12 and 17, which also were activated in all three stimulated conditions, still remained to be identified.

Some of the interneurons identified by the study of Lockery and Kristan (1990b) could correspond to the cells activated by PT- and P-stimulated conditions (cyan borders in **Figures 7G,H**). In particular, judging by position, the cells labeled with numbers 11 and 20 could correspond to the interneurons 157 and 159 analyzed in this study. These cells were not found in the map of the activated cells in the T-stimulated condition shown in **Figure 7I** even though the connection to a T cell was demonstrated both electrophysiologically (**Figure 5**) as well as anatomically (**Figure 6**). However, this discrepancy seemed to be due to the very strict criterion for the classification of T-condition activated cells requiring precisely timed and strong deviation from baseline activity in at least six of the seven trials. Since interneuron response amplitudes were small and VSD signal-to-noise ratio was low this criterion provided a conservative estimate of cells showing very clear responses. When this criterion was relaxed by a lower significance level or a lower number of significant trials used as threshold, more cells, including the interneurons under study, were classified as activated (results not shown). In future studies, network activation patterns obtained for varied classification criteria need to be compared across different preparations to reveal all members in the network and the interaction of different types of mechanosensory inputs.

DISCUSSION

After more than 30 years of research on the local bend reflex of the leech (Kristan, 1982), the perspective on the neuronal network controlling this seemingly simple behavior still gains complexity. In line with other recent findings (Gaudry and Kristan, 2009; Palmer et al., 2014; Baljon and Wagenaar, 2015; Pirschel and Kretzberg, 2016) the results of this study indicate that the model of the local bend network needs to be revised regarding the input signals provided by mechanoreceptors and the computation performed by interneurons.

Encoding of Tactile Information by Mechanoreceptors

On the level of mechanoreceptors our results suggest that three dogmata of leech tactile information processing should be revised:

Contrary to the common belief (and the cell's names), the three types of mechanoreceptors—touch, pressure and noxious cells—do not implement a labeled line code for tactile stimulus intensities. The ranges of constant pressure intensities encoded by these cell types overlapped quite substantially, with longer stimulus durations leading to higher spike counts (Pirschel and Kretzberg, 2016). T and P cells both reacted to the entire range of tested intensities from very light touch (5 mN) to moderate pressure (200 mN) with increasing spike counts and decreasing response latencies. In both cell types N cells generated spikes in response to moderate stimulus intensities. Even though the relatively weak tactile stimuli used in this study were clearly not in the optimal range for N cell stimulation, they elicited weak but reliable N cell responses. Indeed, a large range of intensities triggered spikes in all three cell types and also N cells might contribute to the local bend network by providing additional input to interneurons.

Despite the finding that T cell spikes increase muscle tension during the local bend response reported already in the first publication on leech local bending (Kristan, 1982) their contribution to the network was disregarded in most studies. Electrical stimulation of a single P cell was sufficient to elicit a local bend response, while a single T cell often failed to trigger an obvious muscle movement. It was therefore concluded that the local bend network relies on P cell rather than T cell input (Kristan, 1982; Lewis and Kristan, 1998b). However, recent results suggest that T cells encode tactile stimulus properties by relative response features of a cell pair with overlapping receptive fields (Pirschel and Kretzberg, 2016). Thus, electrical stimulation of a single T cell triggers a response that would not occur in natural situations. Each patch of skin is innervated by a pair of T cells and a pair of P cells with overlapping receptive fields. They all respond to tactile stimulation at this location (see **Figure 1A** bottom for a sketch of overlapping receptive field at ventral midline). Hence, even if spikes of a single stimulated cell fail to elicit the local bend response it cannot be concluded that this cell is not important for the response. Carlton and McVean (1995) pointed out that T cells provide behaviourally important input to the leech nervous system, in particular when acting as velocity detectors in exploration behavior. In a study comparing T and P cell encoding (Pirschel and Kretzberg, 2016), T cell responses were shown to allow higher percentages of tactile stimulus location estimation than P cell responses. Moreover, mixed populations of P and T cells considerably improved the combined estimation of stimulus location and intensity compared to each cell type separately. Here, we showed with three complementary methods that T cells provide synaptic input to several previously identified local bend interneurons (**Figures 5**–**7**). Hence, T cells should be considered as additional members of the local bend network.

As in most neuronal systems, the analysis of leech mechanoreceptor responses was restricted to spike counts of single cells for many decades. However, more recent studies showed that combining responses of two cells with overlapping receptive fields drastically improves stimulus estimation and that temporal response features contain more information about stimulus location than spike counts (Thomson and Kristan, 2006; Pirschel and Kretzberg, 2016). This study confirmed that spike counts and response latencies depended both on stimulus intensity and location for T_v and P_v cells and showed similar dependencies also for N cell responses (**Figures 3**, **4**). Moreover, combined variation of stimulus location and intensities revealed that the dependency of both response features on stimulus location stayed the same for different stimulus intensities, leading to parallel shifted tuning curves in **Figures 4C,D**. Since T_v cells produced transient responses at stimulus on- and offset, encoding properties of off-responses occurring after stimulus offset were additionally analyzed. Interestingly, the off-response spike count showed a much stronger dependency on stimulus force intensity than on location—at least for light and moderate tactile stimulation. In contrast, off-response latency depended almost exclusively on stimulus location. This finding suggests that T cell off-spikes could play an additional role in tactile information encoding that should be considered in future studies. For primate afferents, on-off-response patterns were proposed to play a role in the encoding of object contact and release during active touching (Johnson, 2001; Johansson and Flanagan, 2009). Hence, the importance of T cells during exploration (Carlton and McVean, 1995)—actively touching the environment—might indicate a general mechanism of tactile stimulus encoding shared by man and worm.

Taken together, these results suggest that encoding of tactile stimulation on the mechanoreceptor level can be explained neither by a labeled line of different cell types encoding distinct ranges of mechanical force, nor by symmetrical spike count tuning curves representing stimulus location. Instead, we propose a mixed-type population of mechanoreceptors performing simultaneous encoding of stimulus location and intensity by multiplexing temporal response features and spike counts. Since mixed-type combination of multiple afferent classes and multiplexed encoding of several stimulus properties were also proposed as underlying mechanisms of touch perception in primates (Saal and Bensmaia, 2014), these encoding principles might be fundamental mechanisms of tactile information processing. For the leech, future studies are needed to investigate how additional stimulus properties like probe shape and velocity are represented in this mixed-type, multiplexed coding scheme.

Interneurons Involved in Tactile Information Processing

Any sensory system relies on receptors conveying all available information about the stimulus to the next network level. In many systems, including the mechanoreceptors of primates (Saal and Bensmaia, 2014) and leeches (Nicholls and Baylor, 1968; Carlton and McVean, 1995), this input layer of the sensory processing network contains different receptor types (Smith and Lewin, 2009), which specifically react to certain types of stimulation. However, for exploiting the information about the stimulus encoded by receptors, this information must be transferred to and processed by the next network layers. While it is difficult to study directly connected pre- and postsynaptic cells in complex sensory systems in vertebrates like the primate, the individually characterized cells in the simple nervous system of the leech are optimally suited for this question.

As discussed in section Encoding of Tactile Information by Mechanoreceptors, our hypothesis is that the individual sensory cells send multiplexed signals, containing a combination of temporal response features and spike rate, which simultaneously represent multiple stimulus properties. The ensemble of interneurons has the task to integrate and process these ambiguous signals coming from the 10 mechanoreceptors (6 T, 4 P, 2 N), which are present in each ganglion. Our preliminary results suggest that the individual interneurons have spatial receptive fields as was also found by Lockery and Kristan (1990b), but additionally differ in their integration properties. At least one type of interneuron (cell 157, **Figure 5A**) seemed to act as slow integrator, presumably reacting mainly to the spike count of all presynaptic cells. The membrane potentials of other interneurons (cells 159 and 162, **Figures 5B,C**) showed more complex temporal response structures, suggesting temporal information processing, e.g., as coincidence detectors. Furthermore, these results indicate that responses of individual interneurons could be influenced to different extents by responses of the three mechanosensory cell types. While the responses of slow integrators probably follow mainly the sustained P cell spikes, the more complex interneuron response patterns could stem from the transient T cell responses to stimulus changes and the sparse N cell spikes.

Interneuron responses found in this study matched and complemented previous findings. The three interneurons considered here in more detail, cells 157, 159, 162, were identified as local bend interneurons, receiving P cell input and influencing motor neuron activity (Lockery and Kristan, 1990b). Judging by locations of cells' somata, all of these three interneurons also significantly changed their membrane potentials when a P cell was stimulated in our voltage sensitive dye recordings (**Figures 7G,H**). Furthermore, our physiological and anatomical results (**Figures 5**, **6**) showed that these three cells also receive input from T cells.

In addition to these three interneurons, which we chose to study in detail, our results showed several other cells receiving mechanoreceptor inputs, confirming results from previous studies. Judging by location of their cell bodies, our VSD experiments yielded at least two more previously identified local bend interneurons, cells 161 and 212 (Lockery and Kristan, 1990b), reacting to T-cell stimulation (**Figure 7I**). Cell 212 might also be one of the cells visible in the Neurobiotin staining of a T cell, indicating electrical coupling (**Figure 6D**). Another interneuron, cell 61, for which we found a putative electrical coupling to the Neurobiotin-filled T cell and an activation in the VSD experiments, also was reported before to receive mechanoreceptor input (Nusbaum and Kristan, 1986). Activity of this serotonin-containing cell was associated with modification of the local bend behavior and initiation of swimming (Nusbaum and Kristan, 1986; Kristan et al., 1988; Lockery and Kristan, 1991). Moreover, the activation of Retzius and AP cell pairs in

our VSD experiments (**Figures 7G–I**) was also consistent with previous findings that both cell types react to mechanoreceptor responses and pressure applied to the skin (Zhang et al., 1990; Lockery and Kristan, 1991; Zhang et al., 1995; Jin and Zhang, 2002; Fathiazar et al., 2016).

Despite this updated list of candidate cells revealed in this study, we assume that not all interneurons involved in processing of tactile information showed up as stimulus activated cells in the VSD experiments (**Figures 7G–I**), because of three technical reasons: (1) the restricted visibility of cells in preparations, (2) the statistical selection criterion, and (3) the type of stimulation used in this study.

Firstly, visibility of cells in VSD recordings varies from preparation to preparation. VSD experiments require removal of the glia sheath from the ganglion to ensure that the dye reaches all neuronal membranes. However, this procedure led to displacement of the cell bodies. Some cell bodies moved out of focus of the microscope. Proximate cells, which are usually well visible in the ganglion before de-sheathing, might overlap or even completely occlude each other after that dissection procedure. These effects led to a lower number of ROIs (55 in **Figure 7B**) visible in the VSD images than cells located at the ventral side of the ganglion (approximately 200). Moreover, even though the positions of cell bodies in the ganglion are relatively fixed, they sometimes switch positions, requiring additional physiological or anatomical evidence for definite cell type classification. Hence, it is of general concern that not all stimulus-activated interneurons can be found in all VSD preparations.

The second reason for the low number of interneurons classified as stimulus-activated (in particular for separate T-cell stimulation, **Figures 7F,I**) is the strict criterion we applied. A cell's activity needed to deviate significantly ($\alpha = 0.05$) from baseline activity in at least in six out of seven stimulated trials in exactly the same frame. Hence, in this time frame the cell had to be consistently more depolarized or more hyperpolarized than 97.5% of the values obtained under control conditions. Relaxing this criterion led to a higher number of cells classified as stimulus-activated. Example, for a level of $\alpha = 0.1$ and the same threshold (six out of seven active trials), 40 cells were marked as stimulus-activated in the PT-activated condition, 30 cells in the P-activated and 28 in the T-activated conditions (results not shown). Judged by location, these populations included the three interneurons 157, 159, 162 that we studied in more detail and also several other interneurons previously identified as members of the local bend network (Lockery and Kristan, 1990b). However, since many additional cells were also classified as activated, we decided to present strictly restricted populations of clearly stimulus-activated cells in this study. In future studies, effects of statistical selection criteria should be compared across preparations to optimize the detection of stimulus-activated cells, which would lead to a more consistent picture of the network for tactile information processing.

The third reason for the incomplete activation maps could be the stimulation used in the experiments presented here. Even though the electrical stimulation of the P and/or T cell elicited spike trains mimicking typical responses to tactile skin stimulation (Pirschel and Kretzberg, 2016), the network received inputs from only one or two mechanoreceptors. In contrast, tactile stimulation always elicits responses of at least four mechanoreceptors, because each patch of the skin is covered by the overlapping receptive fields of two P cells and two T cells. For higher stimulus intensities, at least one N cell will react additionally. Since our VSD setup was limited to two intracellular electrodes, a complete simulation of the natural input to the tactile network by intracellular stimulation of four (or five) mechanoreceptors was not possible. Hence, if some interneurons are specifically tuned to relative temporal features of mechanoreceptor spike trains, e.g., coincidence detection they would not (or at least not optimally) respond to electrical stimulation of one P and one T cell, even though the timing of their spikes matches realistic skin stimulation. Hence, additional VSD experiments are needed with the skin attached to the ganglion to reveal a more complete network structure. Comparison of activity maps obtained for tactile stimulation to electrical stimulation of mechanoreceptor pairs or single mechanoreceptors can test our hypothesis of temporal processing on the level of interneurons.

Once these issues will be settled, combined electrophysiological, anatomical, and VSD studies applied to this small nervous system consisting of individually characterized cells can yield conclusive answers to fundamental questions of neural coding including the roles of spike counts versus spike timing, population coding and multiplexing. In particular, the analysis of combined encoding of multiple stimulus properties should be extended to a larger space of stimulus dimensions (e.g., velocity, shape, application angle, indentation depth, vibration, duration additionally to location and intensity). Moreover, the local bend response was reported to be modulated by feedback-loops in the network (Baljon and Wagenaar, 2015), by neuromodulators (Lockery and Kristan, 1991; Gaudry and Kristan, 2009), as well as by feeding status and environmental factors like water depth (Palmer et al., 2014). Hence, despite the low number of neurons involved in this seemingly so hard-wired network, the leech tactile system is also well suited for studies on general mechanisms underlying the flexibility of neural activity and behavior.

AUTHOR CONTRIBUTIONS

All authors contributed to data analysis, interpretation of results, writing the manuscript and designing the figures. In addition, JK designed and coordinated the studies and drafted the text; FP performed intracellular recordings and skin stimulation, EF and GH performed VSD experiments, GH performed cell staining and confocal microscopy.

FUNDING

Funding was provided by "Professorinnenprogramm" of Bundesministerium für Bildung und Forschung/ Niedersächsisches Ministerium für Wissenschaft und Kultur (JK, GH, FP), by a fellowship of the graduate school "Neurosenses" of Niedersächsisches Ministerium für Wissenschaft und Kultur (FP), and by a fellowship of German Academic Exchange Service (EF).

ACKNOWLEDGMENTS

We thank William Kristan and Paxon Frady for teaching how to perform VSD experiments and leech skin preparation to FP and GH and Daniel Wagenaar for sharing his construction plans and software for the VSD setup, as well as Evan Miller for providing the dye. Thanks to Go Ashida and all members of the computational neuroscience group for critically reading the manuscript and to Lena Koepcke for literally fruitful discussions.

SUPPLEMENTARY MATERIAL

The Supplementary Material for this article can be found online at: http://journal.frontiersin.org/article/10.3389/fphys.2016.00506/full#supplementary-material

REFERENCES

Abraira, V. E., and Ginty, D. D. (2013). The sensory neurons of touch. *Neuron* 79, 618–639. doi: 10.1016/j.neuron.2013.07.051

Baca, S. M., Marin-Burgin, A., Wagenaar, D. A., and Kristan, W. B. Jr. (2008). Widespread inhibition proportional to excitation controls the gain of a leech behavioral circuit. *Neuron* 57, 276–289. doi: 10.1016/j.neuron.2007.11.028

Baca, S. M., Thomson, E. E., and Kristan, W. B. Jr. (2005). Location and intensity discrimination in the leech local bend response quantified using optic flow and principal components analysis. *J. Neurophysiol.* 93, 3560–3572. doi: 10.1152/jn.01263.2004

Baljon, P. L., and Wagenaar, D. A. (2015). Responses to conflicting stimuli in a simple stimulus-response pathway. *J. Neurosci.* 35, 2398–2406. doi: 10.1523/JNEUROSCI.3823-14.2015

Blackshaw, S. E. (1981). Morphology and distribution of touch cell terminals in the skin of the leech. *J. Physiol.* 320, 219–228. doi: 10.1113/jphysiol.1981.sp013945

Blackshaw, S. E., Nicholls, J. G., and Parnas, I. (1982). Physiological responses, receptive fields and terminal arborizations of nociceptive cells in the leech. *J. Physiol.* 326, 251–260. doi: 10.1113/jphysiol.1982.sp014189

Carlton, T., and McVean, A. (1995). The role of touch, pressure and nociceptive mechanoreceptors of the leech in unrestrained behaviour. *J. Comp. Physiol. A* 177, 781–791. doi: 10.1007/BF00187637

Fathiazar, E., Anemüller, J., and Kretzberg, J. (2016). "Statistical identification of stimulus-activated network nodes in multi-meuron moltage-sensitive dye optical recordings," in *38th Annual International Conference of the IEEE Engineering in Medicine and Biology Society* (Orlando, FL), 3899–3903. doi: 10.1109/EMBC.2016.7591580

Fathiazar, E., and Kretzberg, J. (2015). "Estimation of neuronal activity based on voltage-sensitive dye imaging in a moving preparation," *Conference Proceeding of IEEE Engineering Medicine and Biology Society* (Milan), 6285–6288. doi: 10.1109/EMBC.2015.7319829

Gaudry, Q., and Kristan, W. B. Jr. (2009). Behavioral choice by presynaptic inhibition of tactile sensory terminals. *Nat. Neurosci.* 12, 1450–1457. doi: 10.1038/nn.2400

Granzow, B., and Kristan, W. B. Jr. (1986). Inhibitory connections between motor neurons modify a centrally generated motor pattern in the leech nervous system. *Brain Res.* 369, 321–325. doi: 10.1016/0006-8993(86)90543-3

Jin, W., Zhang, R.-J. (2002). Pressure sensation by an anterior pagoda neuron population distributed in multiple ganglia in the leech, *Whitmania pigra*. *J. Comp. Physiol. A* 188, 165–171. doi: 10.1007/s00359-002-0283-0

Johansson, R. S., and Flanagan, J. R. (2009). Coding and use of tactile signals from the fingertips in object manipulation tasks. *Nat. Rev. Neurosci.* 10, 345–359. doi: 10.1038/nrn2621

Johnson, K. O. (2001). The roles and functions of cutaneous mechanoreceptors. *Curr. Opin. Neurobiol.* 11, 455–461. doi: 10.1016/S0959-4388(00)00234-8

Kristan, W. B. Jr. (1982). Sensory and motor neurones responsible for the local bending response in leeches. *J. Exp. Biol.* 96, 161–180.

Kristan, W. B. Jr., Calabrese, R. L., and Friesen, W. O. (2005). Neuronal control of leech behavior. *Prog. Neurobiol.* 76, 279–327. doi: 10.1016/j.pneurobio.2005.09.004

Kristan, W. B. Jr., Wittenberg, G., Nusbaum, M. P., and Stern-Tomlinson, W. (1988). Multifunctional interneurons in behavioral circuits of the medicinal leech. *Experientia* 44, 383–389. doi: 10.1007/BF01940531

Lewis, J. E., and Kristan, W. B. Jr. (1998a). A neuronal network for computing population vectors in the leech. *Nature* 391, 76–79. doi: 10.1038/34172

Lewis, J. E., and Kristan, W. B. Jr. (1998b). Representation of touch location by a population of leech sensory neurons. *J. Neurophysiol.* 80, 2584–2592.

Lockery, S. R., and Kristan, W. B. Jr. (1990a). Distributed processing of sensory information in the leech. I. Input-output relations of the local bending reflex. *J. Neurosci.* 10, 1811–1815.

Lockery, S. R., and Kristan, W. B. Jr. (1990b). Distributed processing of sensory information in the leech. II. Identification of interneurons contributing to the local bending reflex. *J. Neurosci.* 10, 1816–1829.

Lockery, S. R., and Kristan, W. B. Jr. (1991). Two forms of sensitization of the local bending reflex of the medicinal leech. *J. Comp. Physiol. A* 168, 165–177. doi: 10.1007/BF00218409

Lockery, S. R., and Sejnowski, T. J. (1992). Distributed processing of sensory information in the leech. III. A dynamical neural network model of the local bending reflex. *J. Neurosci.* 12, 3877–3895.

Meyer, A., Hilgen, G., Dorgau, B., Sammler, E. M., Weiler, R., Monyer, H., et al. (2014). AII amacrine cells discriminate between heterocellular and homocellular locations when assembling connexin36-containing gap junctions. *J. Cell Sci.* 127, 1190–1202. doi: 10.1242/jcs.133066

Miller, E. W., Lin, J. Y., Frady, E. P., Steinbach, P. A., Kristan, W. B. Jr., and Tsien, R. Y. (2012). Optically monitoring voltage in neurons by photo-induced electron transfer through molecular wires. *Proc. Natl. Acad. Sci. U.S.A.* 109, 2114–2119. doi: 10.1073/pnas.1120694109

Muller, K. J., and Scott, S. A. (1981). Transmission at a "direct" electrical connexion mediated by an interneurone in the leech. *J. Physiol.* 311, 565–583. doi: 10.1113/jphysiol.1981.sp013605

Nicholls, J. G., and Baylor, D. A. (1968). Specific modalities and receptive fields of sensory neurons in CNS of the leech. *J. Neurophysiol.* 31, 740–756.

Nusbaum, M. P., and Kristan, W. B. Jr. (1986). Swim initiation in the leech by serotonin-containing interneurones, cells 21 and 61. *J. Exp. Biol.* 122, 277–302.

Palmer, C. R., Barnett, M. N., Copado, S., Gardezy, F., and Kristan, W. B. Jr. (2014). Multiplexed modulation of behavioral choice. *J. Exp. Biol.* 217, 2963–2973. doi: 10.1242/jeb.098749

Pirschel, F., and Kretzberg, J. (2016). Multiplexed population coding of stimulus properties by leech mechanosensory cells. *J. Neurosci.* 36, 3636–3647. doi: 10.1523/JNEUROSCI.1753-15.2016

Saal, H. P., and Bensmaia, S. J. (2014). Touch is a team effort: interplay of submodalities in cutaneous sensibility. *Trends Neurosci.* 37, 689–697. doi: 10.1016/j.tins.2014.08.012

Smith, E. S. J., and Lewin, G. R. (2009). Nociceptors: a phyogenetic view. *J. Comp. Physiol. A Neuroethol. Sens. Neural. Behav. Physiol.* 195, 1089–1106. doi: 10.1007/s00359-009-0482-z

Stuart, A. E. (1970). Physiological and morphological properties of motoneurones in the central nervous system of the leech. *J. Physiol.* 209, 627–646. doi: 10.1113/jphysiol.1970.sp009183

Thomson, E. E., and Kristan, W. B. Jr. (2006). Encoding and decoding touch location in the leech CNS. *J. Neurosci.* 26, 8009–8016. doi: 10.1523/JNEUROSCI.5472-05.2006

Vallbo, A. B., and Johansson, R. S. (1984). Properties of cutaneous mechanoreceptors in the human hand related to touch sensation. *Hum. Neurobiol.* 3, 3–14.

Zhang, R.-J., Zhu, L., Wang, D. B., Zhang, F., and Zou, D.-J. (1990). Positional discrimination and re-development of synapses in the leech (*Whitmania pigra*). *J. exp. Biol.* 153, 47–60.

Zhang, R.-J., Zou, D.-J., and Zheng, J. (1995). Correlation of receptive field position of mechanosensory neurons and the strength of their connections to AP neurons in the CNS of the leech (*Whitmania pigra*). *Invertebrate Neurosci.* 1, 249–254. doi: 10.1007/BF02211026

Zoccolan, D., Pinato, G., and Torre, V. (2002). Highly variable spike trains underlie reproducible sensorimotor responses in the medicinal leech. *J. Neurosci.* 22, 10790–10800.

Conflict of Interest Statement: The authors declare that the research was conducted in the absence of any commercial or financial relationships that could be construed as a potential conflict of interest.

Advantages of publishing in Frontiers

OPEN ACCESS
Articles are free to read, for greatest visibility

COLLABORATIVE PEER-REVIEW
Designed to be rigorous – yet also collaborative, fair and constructive

FAST PUBLICATION
Average 85 days from submission to publication (across all journals)

COPYRIGHT TO AUTHORS
No limit to article distribution and re-use

TRANSPARENT
Editors and reviewers acknowledged by name on published articles

SUPPORT
By our Swiss-based editorial team

IMPACT METRICS
Advanced metrics track your article's impact

GLOBAL SPREAD
5'100'000+ monthly article views and downloads

LOOP RESEARCH NETWORK
Our network increases readership for your article

Frontiers
EPFL Innovation Park, Building I • 1015 Lausanne • Switzerland
Tel +41 21 510 17 00 • Fax +41 21 510 17 01 • info@frontiersin.org
www.frontiersin.org

Find us on